

Evaluation of Organic Waste Materials as Bio-Polymeric Admixtures in Cement Based Composite Mortars

Submitted to the Graduate School of Natural and Applied Sciences
in partial fulfillment of the requirements for the degree of

Doctor of Philosophy

in Civil Engineering

by

Şevket Onur KALKAN

ORCID 0000-0003-0250-8134

June, 2022

This is to certify that we have read the thesis **Evaluation of Organic Waste Materials as Bio-Polymeric Admixtures in Cement Based Composite Mortars** submitted by **Şevket Onur Kalkan**, and it has been judged to be successful, in scope and in quality, at the defense exam and accepted by our jury as a DOCTORAL THESIS.

APPROVED BY:

Advisor:

Prof. Dr. Lütfullah Gündüz
İzmir Kâtip Çelebi University

Committee Members:

Prof. Dr. Şemsi Yazıcı
Ege University

Prof. Dr. Halit Yazıcı
Dokuz Eylül University

Prof. Dr. Ali Uğur Öztürk
Manisa Celal University

Assoc. Prof. Dr. Mutlu Seçer
İzmir Kâtip Çelebi University

Date of Defense: June 30, 2022

Declaration of Authorship

I, **Şevket Onur Kalkan**, declare that this thesis titled **Evaluation of Organic Waste Materials as Bio-Polymeric Admixtures in Cement Based Composite Mortars** and the work presented in it are my own. I confirm that:

- This work was done wholly or mainly while in candidature for the Doctoral degree at this university.
- Where any part of this thesis has previously been submitted for a degree or any other qualification at this university or any other institution, this has been clearly stated.
- Where I have consulted the published work of others, this is always clearly attributed.
- Where I have quoted from the work of others, the source is always given. This thesis is entirely my own work, with the exception of such quotations.
- I have acknowledged all major sources of assistance.
- Where the thesis is based on work done by myself jointly with others, I have made clear exactly what was done by others and what I have contributed myself.

Date: 30.06.2022

Evaluation of Organic Waste Materials as Bio-Polymeric Admixtures in Cement Based Composite Mortars

Abstract

In this study, the effect of a new generation bio-polymeric admixture on the physical and mechanical properties of cement mortars is examined in detail. The bio-polymeric admixture is prepared by grinding egg shells, apricot kernel shells, hazelnut kernel shells, walnut kernel shells, and olive seeds in micronized sizes. The evaluation of the bio-polymeric admixtures, which are produced as wastes, among high production materials such as concrete and mortar derivative products, provides an opportunity for better disposal and management of these wastes. The bio-polymeric admixture materials have been ground to be in the range of 0/45 μm , 0/125 μm , and 125/250 μm within the scope of this study and are used as bio-polymeric admixture in cement mortars, at different rates, i.e., 0, 0.2, 0.35, 0.5, 1 and 1.5 % of total weight. The characteristics of hydration products were analyzed by SEM, EDS and XRD investigations. It has been observed that in the mortar samples produced based on constant W/C ratio, the 28 days compressive strength values of the mortars decreased due to the increase of biopolymer. However, the increase in the bio-polymeric admixture ratio had a declining effect on the water absorption capacity and capillarity values of the samples. In other words, bio-polymeric admixture improves the hydrophobicity property of the hardened mortar samples. Another important effect of

the bio-polymeric admixture contribution was also observed on the flowability property of the cement mortars. As the bio-polymeric admixture ratio added to the cement mortar increased, the flow diameter values of the mortar were also significantly increased. It has been determined that each component of the bio-polymeric admixtures in composite structure consisting of extractive, lignin, hemicellulose, and cellulose affects different properties of cementitious mortars. At the end of the study, when the physical and mechanical properties of the mortars were examined, an optimization study was carried out to determine the appropriate biopolymeric admixture type, usage rate and particle size. In addition, mathematical equations representing the 28-day compressive strength, 28-day flexural strength, 150-day compressive strength, flow diameter, initial and final setting times, and mass and capillary water absorption values of the mortars were produced by regression analysis.

Keywords: Bio-polymeric admixture, cement mortar, microstructure, chemical admixture, waste

Organik Atık Malzemelerin Biyo-polimerik Katkı Olarak Çimento Bağlayıcılı Kompozit Harçlarda Değerlendirilmesi

ÖZ

Bu çalışmada, yeni nesil biyopolimerik katkının çimento harçlarının fiziksel ve mekanik özelliklerine etkisi detaylı olarak incelenmiştir. Biyopolimerik katkı, yumurta kabukları, kayısı çekirdekleri, fındık çekirdekleri, ceviz kabukları ve zeytin çekirdeklerinin mikronize boyutlarda öğütülmesiyle hazırlanmıştır. Atık olarak üretilen biyopolimerik katkıların beton ve harç türevi ürünler gibi üretimi yüksek malzemeler arasında değerlendirilmesi, bu atıkların daha iyi bertarafı ve yönetimi için fırsat sunmaktadır. Biyopolimerik katkı malzemeleri bu çalışma kapsamında 0/45 µm, 0/125 µm ve 125/250 µm tane boyut dağılımlarında öğütülmüş ve çimento harçlarında biyopolimerik katkı olarak kullanılmıştır. Katkı kullanım oranları toplam ağırlığın %0, 0,2, 0,35, 0,5, 1 ve 1,5'i olacak şekilde belirlenmiştir. Hidrasyon ürünlerinin özellikleri SEM, EDS ve XRD araştırmaları ile analiz edilmiştir. Sabit s/ç oranı esas alınarak üretilen harç numunelerinde, biyopolimerik katkı artışına bağlı olarak harçların 28 günlük basınç dayanım değerlerinin düştüğü gözlemlenmiştir. Özellikle ekstraktif oranı yüksek biyopolimerik katkıların hidrasyon sürecinde matris yapıda hidrate olmamış çimento tanelerini arttırdığı tespit edilmiştir. Ancak, biyopolimerik katkı oranındaki artış numunelerin su emme kapasitesini ve kapilarite değerlerini düşürücü etki yapmıştır. Başka bir deyişle, biyo-polimerik katkı, sertleştirilmiş harç

numunelerinin hidrofobiklik özelliğini iyileştirmektedir. Biyopolimerik katkı katkısının bir diğer önemli etkisi de çimento harçlarının akışkanlık özelliği üzerinde gözlenmiştir. Çimento harcına eklenen biyopolimerik katkı oranı arttıkça harcın akış çapı değerleri de önemli ölçüde artmıştır. Ekstraktif, lignin, hemiselüloz ve selülozdan oluşan kompozit yapıdaki biyopolimerik katkıların herbir bileşenin çimentolu harçların farklı özelliklerine etki ettiği tespit edilmiştir. Çalışmanın sonunda, harçların fiziksel ve mekanik özellikleri irdelendiğinde uygun biyopolimerik katkı tipi, kullanım oranı ve tane boyutunun tespiti için optimizasyon çalışması yapılmıştır. Ayrıca, harçların 28 günlük basınç dayanımı, 28 günlük eğilme dayanımı, 150 günlük basınç dayanımı, yayılma çapı, ilk ve son priz süreleri ve kütlece ve kapriler su emme değerlerini temsil eden matematiksel denklemler regresyon analizleri ile üretilmiştir.

Anahtar Kelimeler: Biyo-polimerik katkı, çimento harcı, mikroyapı, kimyasal katkı, atık

To my family,

Acknowledgment

I would like to thank my advisor Prof. Dr. Lütfullah GÜNDÜZ, who endlessly helped me on any issue from the very beginning of my thesis and my five year doctoral degree with his extensive knowledge and experience. I would like to thank Prof. Dr. Ali Uğur ÖZTÜRK and Assoc. Prof. Dr. Mutlu SEÇER for their great support in the thesis monitoring committee.

I would like to thank Research Assistant Ayberk AYDOĞMUŞ, who helped me with some laboratory studies. Also, I would like to thank Prof. Dr. Nihat Sami ÇETİN, who helped me use their laboratory infrastructure. I would like to thank Research Assistant Saadet GÜLER and Research Assistant Ahmet YAVAŞ, who helped me analyze and interpret some experimental studies.

I would like to thank my mother, Nuriye KALKAN, my father, Bektaş KALKAN, my brother, Murat KALKAN, and of course other family members, especially my grandfather, without their continuous support and encouragement I never would have been able to achieve my goals. Thanks for always being there for me, believing in me, and motivating me to set out on my own path.

I am very thankful to BEŞTEPE Family, who helped my family in growing me and my brother over thirty years, for their goodness without expecting anything.

Lastly, I would like to thank my great friends in our laboratory for motivational contributions for this thesis project.

This thesis study was funded by Scientific Research Projects Coordination Unit of Izmir Katip Celebi University. Project number: 2019-TDR-FEBE-0014.

Table of Contents

Declaration of Authorship.....	ii
Abstract.....	iii
Öz.....	v
Acknowledgment.....	viii
Table of Contents.....	ix
List of Figures.....	xiii
List of Tables.....	xxvi
Abbreviations.....	xxix
1 Introduction.....	1
1.1 Topic.....	4
1.2 Aim.....	4
1.3 Scope.....	4
2 Previous Studies.....	6
2.1 Classification of Biopolymers.....	6
2.2 Use of Biopolymers in Construction Industry.....	16
2.2.1 Use of Biopolymers/Bio-polymeric admixtures in Lime Mortar.....	18
2.2.2 Use of Biopolymers in Concrete and Cement-Based Products.....	19
2.2.2.1 Lignosulfonates.....	19
2.2.2.2 Cellulose.....	20
2.2.2.3 Starch.....	23
2.2.2.4 Gums.....	25
2.2.2.5 Chitin and Chitosan.....	29
2.2.2.6 Vegetable Oils.....	31
2.2.2.7 Plant Extracts.....	33
2.2.2.8 Others.....	34

2.2.3	Use of Biopolymers in Other Construction Areas.....	36
2.3	Literature Evaluation.....	37
3	Materials and Methods	39
3.1	Materials	39
3.1.1	Cement.....	39
3.1.2	Sand.....	41
3.1.3	Mixing Water.....	42
3.1.4	Chemical Admixtures.....	42
3.1.4.1	Polycarboxylate Type Superplasticizer.....	43
3.1.4.2	Sulfonated Melamine-Formaldehyde Type Superplasticizer.....	43
3.1.4.3	Water-Repellent Admixture.....	44
3.1.4.4	Set Retarder.....	45
3.1.5	Bio-Polymeric Admixtures	46
3.1.5.1	Egg Shell.....	46
3.1.5.2	Apricot Kernel Shell	49
3.1.5.3	Hazelnut Kernel Shell	51
3.1.5.4	Walnut Kernel Shell.....	53
3.1.5.5	Olive Seed.....	55
3.2	Methods	58
3.2.1	Preliminary Study	59
3.2.1.1	Preparation of the Bio-polymeric Admixtures.....	60
3.2.1.2	Mix Design.....	61
3.2.1.3	Flexural Strength.....	62
3.2.1.4	Compressive Strength	65
3.2.2	Characterization of the Bio-polymeric Admixtures	66
3.2.2.1	Chemical Analysis of AKS, HKS, WKS and OS	68
3.2.2.1.1	Determination of Extractive Content	68

3.2.2.1.2	Determination of Lignin Content (Delignification).....	69
3.2.2.1.3	Determination of Hemicellulose and Alpha Cellulose Contents	71
3.2.2.2	XRD Analysis of Bio-polymeric Admixtures.....	73
3.2.2.3	FT-IR Analysis of Bio-polymeric Admixtures	73
3.2.2.4	SEM Analysis of Bio-polymeric Admixtures	74
3.2.3	Effect of Bio-polymeric Admixtures on Composite Cement Mortars and Comparison with Some Chemical Admixture.....	75
3.2.3.1	Mix Design.....	76
3.2.3.2	Fresh and Hardened Unit Volume Mass of Mortars	79
3.2.3.3	Flowability of Fresh Mortars	80
3.2.3.4	Setting Times of the Mortars.....	80
3.2.3.5	Water Absorption of the Mortars	81
3.2.3.6	Flexural Strength of the Mortars	82
3.2.3.7	Compressive Strength of the Mortars	82
3.2.4	Mineralogical Development and Microstructural Analysis of Mortars.....	82
3.2.5	Durability of the Mortars.....	83
3.2.6	Optimization and Regression Analysis	86
4	Results and Discussions.....	92
4.1	Test Results of Preliminary Study	92
4.1.1	Evaluation of Test Results of Preliminary Study	93
4.2	Experimental Results of Characterization Analysis	95
4.2.1	Chemical Structure of AKS, HKS, WKS and OS.....	95
4.2.2	XRD Results of Bio-polymeric Admixtures	96
4.2.3	FT-IR Results of Bio-polymeric Admixtures.....	99
4.2.4	SEM Image Results of Bio-polymeric Admixtures	103
4.2.5	Evaluation of the Characterization of Bio-polymeric Admixtures	108

4.3	Effect of Bio-polymeric Admixtures on Composite Cement Mortars and Comparison with Some Chemical Admixtures.....	110
4.3.1	Fresh and Hardened Unit Weight of Mortars.....	110
4.3.2	Flowability of Mortars	114
4.3.3	Setting Time of Mortars	123
4.3.4	Water Absorption of Mortars	139
4.3.5	Compressive Strength of Mortars	154
4.3.6	Flexural Strength of Mortars	174
4.3.7	Evaluation.....	181
4.4	Microstructural Analysis and Mineralogical Development of Mortars....	188
4.5	Durability of Cement Mortars.....	215
4.5.1	Resistance to Sulfate Effect.....	215
4.5.2	Resistance to Acid Effect	223
4.5.3	Resistance to Freeze-Thaw.....	226
4.5.4	Evaluation of Durability of Cement Mortars	236
4.6	Optimization and Regression Analysis of Test Results.....	242
4.6.1	Grey Relational Grade.....	242
4.6.2	Regression Analysis	277
5	Conclusion.....	285
	References.....	289
	Appendices.....	324
	Appendix A.....	325
	Appendix B.....	346
	Appendix C.....	366
	Curriculum Vitae.....	371

List of Figures

Figure 2.1 Biopolymer classification [7]	8
Figure 2.2 The classification of biopolymers.....	9
Figure 2.3 Structure of chitin, chitosan and cellulose [15]	12
Figure 2.4 Repeating chain alignment of lignosulfonate [33].....	20
Figure 2.5 Molecular structure of cellulose [46].....	21
Figure 2.6 Structure of amylose [63]	24
Figure 2.7 Structure of amylopectin [63].....	24
Figure 2.8 Chemical structure of welan gum [71]	26
Figure 2.9 Chemical structure of guar gum [74].....	26
Figure 2.10 Chemical structure of xanthan gum [79]	27
Figure 2.11 Chemical structure of gum Arabic [83]	28
Figure 2.12 Chemical structure of chitin [91].....	29
Figure 2.13 Chemical structure of chitosan [91].....	30
Figure 2.14 Chemical structure of stearic acid [101].....	31
Figure 2.15 Chemical structure of oleic acid [101].....	31
Figure 2.16 Chemical structure of linoleic acid [100]	32
Figure 2.17 Chemical structure of linolenic acid [100]	32
Figure 2.18 Chemical structure of polylactic acid [118].....	35
Figure 2.19 Chemical structure of casein [125].....	35
Figure 2.20 Biopolymer consumption according to different markets [130].....	36
Figure 3.1 CEM I 42.5R Portland cement	39
Figure 3.2 CEN standard sand used in the mixtures of mortar specimens.	41
Figure 3.3 PCE superplasticizer	43
Figure 3.4 SMF superplasticizer	44
Figure 3.5 Calcium stearate water-repellent admixture	45
Figure 3.6 Tartaric acid setting retarder admixture.....	46

Figure 3.7 SEM image of cross-fractured chicken eggshell [144].....	47
Figure 3.8 0/45 μm ES (a), 0/125 μm ES (b), 125/250 μm ES (c).....	49
Figure 3.9 0/45 μm AKS (a), 0/125 μm AKS (b), 125/250 μm AKS (c).....	51
Figure 3.10 0/45 μm HKS (a), 0/125 μm HKS (b), 125/250 μm HKS (c).....	53
Figure 3.11 0/45 μm WKS (a), 0/125 μm WKS (b), 125/250 μm WKS (c).....	55
Figure 3.12 0/45 μm WKS (a), 0/125 μm WKS (b), 125/250 μm WKS (c).....	58
Figure 3.13 Blade mill	61
Figure 3.14 Sieve shaker	61
Figure 3.15 Automatic test press for compression and flexure.....	63
Figure 3.16 Three point flexural testing apparatus	64
Figure 3.17 40x40x160 mm prismatic specimens for flexural strength test.....	65
Figure 3.18 Automatic test press for compression and flexure.....	66
Figure 3.19 40 mm x 40 mm compressive strength testing apparatus.....	66
Figure 3.20 Drying OS, AS, HS and WS samples	68
Figure 3.21 Extraction process of OS, AS, HS and WS samples	69
Figure 3.22 Experiment setup for the delignification process.	70
Figure 3.23 Filtration process of delignification.....	70
Figure 3.24 Samples prepared for cellulose content determination.....	71
Figure 3.25 Filtration of alpha cellulose	72
Figure 3.26 Drying of alpha cellulose.....	72
Figure 3.27 Alpha cellulose of AKS (a), HKS (b), WKS (c), OS (d).....	73
Figure 3.28 The X-diffraction (XRD) instrument.....	73
Figure 3.29 Fourier transform infrared (FT-IR) device	74
Figure 3.30 Scanning electron microscope	75
Figure 3.31 Fresh unit volume mass measurement setup	79
Figure 3.32 Flow table apparatus.....	80
Figure 3.33 Vicat apparatus for setting time.....	81
Figure 3.34 An example image of the capillary water absorption test.....	82
Figure 3.35 Some of test specimens for durability analysis.....	84
Figure 3.36 Sulfate effect test with capillary action.	85
Figure 3.37 Determination of pH value of acid solutions.....	86
Figure 4.1 Deformed specimens.	93
Figure 4.2 XRD patterns of OS, AKS, HKS and WKS.	97
Figure 4.3 XRD pattern of ES.....	99

Figure 4.4 FT-IR spectrums of OS, AS, HS and WS.....	100
Figure 4.5 FT-IR spectrums of ES	102
Figure 4.6 SEM micrograph of ES.....	103
Figure 4.7 SEM micrograph of AKS	104
Figure 4.8 SEM micrograph of HKS	104
Figure 4.9 SEM micrograph of WKS	105
Figure 4.10 SEM micrograph of OS	105
Figure 4.11 SEM micrographs of (a) limestone powder [274], (b) ES at 5000x magnification	106
Figure 4.12 SEM micrographs of (A) apricot shell [275], (B) AKS at 5000x magnification	107
Figure 4.13 SEM micrographs of (A) hazelnut shell [276], (B) HKS at 5000x magnification	107
Figure 4.14 SEM micrographs of (A) lignin [277], (B) WKS at 5000x magnification	107
Figure 4.15 SEM micrographs of (A) hazelnut shell [278], (B) HKS at 5000x magnification	108
Figure 4.16 Flow diameters of ES admixed cement mortars.....	116
Figure 4.17 Flow diameters of AKS admixed cement mortars.....	116
Figure 4.18 Flow diameters of HKS admixed cement mortars.....	117
Figure 4.19 Flow diameters of WKS admixed cement mortars.....	117
Figure 4.20 Flow diameters of OS admixed cement mortars.....	118
Figure 4.21 Relationship between chemical contents of 0/45 μm bio-polymeric admixture and flow diameter	120
Figure 4.22 Relationship between chemical contents of 0/125 μm bio-polymeric admixture and flow diameter	120
Figure 4.23 Relationship between chemical contents of 125/250 μm bio-polymeric admixture and flow diameter	121
Figure 4.24 Flow diameters of PCE and SMF admixed cement mortars.....	122
Figure 4.25 Initial setting times of ES admixed cement mortars.....	125
Figure 4.26 Initial setting times of AKS admixed cement mortars.....	125
Figure 4.27 Initial setting times of HKS admixed cement mortars.....	126
Figure 4.28 Initial setting times of WKS admixed cement mortars.....	126
Figure 4.29 Initial setting times of OS admixed cement mortars	127

Figure 4.30 Relationship between chemical contents of 0/45 μm bio-polymeric admixture and initial setting time	128
Figure 4.31 Relationship between chemical contents of 0/125 μm bio-polymeric admixture and initial setting time	129
Figure 4.32 Relationship between chemical contents of 125/250 μm bio-polymeric admixture and initial setting time	129
Figure 4.33 Initial setting times of TA admixed cement mortars	131
Figure 4.34 Final setting times of ES admixed cement mortars	132
Figure 4.35 Final setting times of AKS admixed cement mortars.....	132
Figure 4.36 Final setting times of HKS admixed cement mortars.....	133
Figure 4.37 Final setting times of WKS admixed cement mortars	133
Figure 4.38 Final setting times of OS admixed cement mortars.....	134
Figure 4.39 Relationship between chemical contents of 0/45 μm bio-polymeric admixture and final setting time	135
Figure 4.40 Relationship between chemical contents of 0/125 μm bio-polymeric admixture and final setting time	136
Figure 4.41 Relationship between chemical contents of 125/250 μm bio-polymeric admixture and final setting time	136
Figure 4.42 Final setting times of TA admixed cement mortars.....	138
Figure 4.43 Capillary water absorption of ES admixed cement mortars	141
Figure 4.44 Capillary water absorption of AKS admixed cement mortars.....	141
Figure 4.45 Capillary water absorption of HKS admixed cement mortars.....	142
Figure 4.46 Capillary water absorption of WKS cement mortars.....	142
Figure 4.47 Capillary water absorption of OS admixed cement mortars.....	143
Figure 4.48 Relationship between chemical contents of 0/45 μm bio-polymeric admixture and capillary water absorption.....	144
Figure 4.49 Relationship between chemical contents of 0/125 μm bio-polymeric admixture and capillary water absorption.....	145
Figure 4.50 Relationship between chemical contents of 125/250 μm bio-polymeric admixture and capillary water absorption.....	145
Figure 4.51 Capillary water absorption of CS admixed cement mortars.....	147
Figure 4.52 Mass water absorption of ES admixed cement mortars.....	148
Figure 4.53 Mass water absorption of AKS admixed cement mortars	149
Figure 4.54 Mass water absorption of HKS admixed cement mortars	149

Figure 4.55 Mass water absorption of WKS admixed cement mortars	150
Figure 4.56 Mass water absorption of OS admixed cement mortars	150
Figure 4.57 Relationship between chemical contents of 0/45 μm bio-polymeric admixture and mass water absorption.....	152
Figure 4.58 Relationship between chemical contents of 0/125 μm bio-polymeric admixture and mass water absorption.....	152
Figure 4.59 Relationship between chemical contents of 125/250 μm bio-polymeric admixture and mass water absorption.....	153
Figure 4.60 Capillary water absorption of CS admixed cement mortars.....	154
Figure 4.61 28-days compressive strength of ES admixed cement mortars	156
Figure 4.62 28-days compressive strength of AKS admixed cement mortars.....	156
Figure 4.63 28-days compressive strength of HKS admixed cement mortars.....	157
Figure 4.64 28-days compressive strength of WKS admixed cement mortars	157
Figure 4.65 28-days compressive strength of OS admixed cement mortars.....	158
Figure 4.66 Relationship between chemical contents of 0/45 μm bio-polymeric admixture and 28-days compressive strength.....	160
Figure 4.67 Relationship between chemical contents of 0/125 μm bio-polymeric admixture and 28-days compressive strength.....	161
Figure 4.68 Relationship between chemical contents of 125/250 μm bio-polymeric admixture and 28-days compressive strength.....	161
Figure 4.69 Relation between unit volume mass and 28-days compressive strength of mortars (0/45 μm)	163
Figure 4.70 Relation between unit volume mass and 28-days compressive strength of mortars (0/125 μm)	163
Figure 4.71 Relation between unit volume mass and 28-days compressive strength of mortars (125/250 μm)	164
Figure 4.72 150-days compressive strength of ES admixed cement mortars	165
Figure 4.73 150-days compressive strength of AKS admixed cement mortars.....	166
Figure 4.74 150-days compressive strength of HKS admixed cement mortars.....	167
Figure 4.75 150-days compressive strength of WKS admixed cement mortars	168
Figure 4.76 150-days compressive strength of OS admixed cement mortars.....	168
Figure 4.77 Relationship between chemical contents of 0/45 μm bio-polymeric admixture and 150-days compressive strength.....	170

Figure 4.78 Relationship between chemical contents of 0/125 μm bio-polymeric admixture and 150-days compressive strength.....	171
Figure 4.79 Relationship between chemical contents of 125/250 μm bio-polymeric admixture and 150-days compressive strength.....	171
Figure 4.80 Compressive strength change of chemical admixed cement mortars...	173
Figure 4.81 Flexural strength of ES admixed cement mortars.....	175
Figure 4.82 Flexural strength of AKS admixed cement mortars	176
Figure 4.83 Flexural strength of HKS admixed cement mortars	177
Figure 4.84 Flexural strength of WKS admixed cement mortars	177
Figure 4.85 Flexural strength of OS admixed cement mortars	178
Figure 4.86 Relationship between chemical contents of 0/45 μm bio-polymeric admixture and flexural strength	179
Figure 4.87 Relationship between chemical contents of 0/125 μm bio-polymeric admixture and flexural strength	180
Figure 4.88 Relationship between chemical contents of 125/250 μm bio-polymeric admixture and flexural strength	180
Figure 4.89 SEM micrograph of reference mortar.....	189
Figure 4.90 SEM micrograph of 0.2 wt.% ES admixed cement mortar	190
Figure 4.91 SEM micrograph of 0.35 wt.% ES admixed cement mortar	190
Figure 4.92 SEM micrograph of 0.5 wt.% ES admixed cement mortar	191
Figure 4.93 SEM micrograph of 1.0 wt.% ES admixed cement mortar	191
Figure 4.94 SEM micrograph of 1.5 wt.% ES admixed cement mortar	192
Figure 4.95 SEM micrograph of 0.2 wt.% AKS admixed cement mortar.....	193
Figure 4.96 SEM micrograph of 0.35 wt.% AKS admixed cement mortar.....	193
Figure 4.97 SEM micrograph of 0.5 wt.% AKS admixed cement mortar.....	194
Figure 4.98 SEM micrograph of 1.0 wt.% AKS admixed cement mortar.....	194
Figure 4.99 SEM micrograph of 1.5 wt.% AKS admixed cement mortar.....	195
Figure 4.100 SEM micrograph of 0.2 wt.% HKS admixed cement mortar.....	196
Figure 4.101 SEM micrograph of 0.35 wt.% HKS admixed cement mortar.....	197
Figure 4.102 SEM micrograph of 0.5 wt.% HKS admixed cement mortar.....	197
Figure 4.103 SEM micrograph of 1.0 wt.% HKS admixed cement mortar.....	198
Figure 4.104 SEM micrograph of 1.5 wt.% HKS admixed cement mortar.....	198
Figure 4.105 SEM micrograph of 0.2 wt.% WKS admixed cement mortar	199
Figure 4.106 SEM micrograph of 0.35 wt.% WKS admixed cement mortar	200

Figure 4.107 SEM micrograph of 0.5 wt.% WKS admixed cement mortar	200
Figure 4.108 SEM micrograph of 1.0 wt.% WKS admixed cement mortar	201
Figure 4.109 SEM micrograph of 1.5 wt.% WKS admixed cement mortar	201
Figure 4.110 SEM micrograph of 0.2 wt.% OS admixed cement mortar	202
Figure 4.111 SEM micrograph of 0.35 wt.% OS admixed cement mortar	203
Figure 4.112 SEM micrograph of 0.5 wt.% OS admixed cement mortar	203
Figure 4.113 SEM micrograph of 1.0 wt.% OS admixed cement mortar	204
Figure 4.114 SEM micrograph of 1.5 wt.% OS admixed cement mortar	204
Figure 4.115 Shell fibers of OS (a) and AKS (b).....	205
Figure 4.116 An example for EDS analysis (125OS0.5 specimen).....	207
Figure 4.117 Relationship between Compressive strength and Si/Ca ratio of ES added cement mortars.....	208
Figure 4.118 Relationship between compressive strength and Si/Ca ratio of AKS added cement mortars.	208
Figure 4.119 Relationship between compressive strength and Si/Ca ratio of HKS added cement mortars.	209
Figure 4.120 Relationship between compressive strength and Si/Ca ratio of WKS added cement mortars	209
Figure 4.121 Relationship between compressive strength and Si/Ca ratio of OS added cement mortars.....	210
Figure 4.122 X-Ray Diffraction of 0.2 wt.% bio-polymeric admixture used cements pastes hydrated at 28-day.....	211
Figure 4.123 X-Ray Diffraction of 0.35 wt.% bio-polymeric admixture used cements pastes hydrated at 28-day.....	212
Figure 4.124 X-Ray Diffraction of 0.5 wt.% bio-polymeric admixture used cements pastes hydrated at 28-day.....	212
Figure 4.125 X-Ray Diffraction of 1.0 wt.% bio-polymeric admixture used cements pastes hydrated at 28-day.....	213
Figure 4.126 X-Ray Diffraction of 1.5 wt.% bio-polymeric admixture used cements pastes hydrated at 28-day.....	213
Figure 4.127 MgSO ₄ bloom in reference cement mortar samples	215
Figure 4.128 Salts formed on the surface of the reference mortar specimens after wetting-drying cycle, 0 cycle (a), 10 cycle (b), 20 cycle (c), 30 cycle (d)	215

Figure 4.129 Salts formed on the surface of the 125ES mortar specimens after wetting-drying cycle.....	216
Figure 4.130 Salts formed on the surface of the 125AKS mortar specimens after wetting-drying cycle	217
Figure 4.131 Salts formed on the surface of the 125HKS mortar specimens after wetting-drying cycle	218
Figure 4.132 Salts formed on the surface of the 125WKS mortar specimens after wetting-drying cycle	219
Figure 4.133 Salts formed on the surface of the 125WKS mortar specimens after wetting-drying cycle	220
Figure 4.134 Rate of change in compressive strength relative to compressive strength before sulfate exposure	222
Figure 4.135 Rate of change in compressive strength relative to compressive strength before acid exposure	225
Figure 4.136 Reference specimens' appearance before and after freeze-thaw cycles	227
Figure 4.137 125ES specimens' appearance before and after freeze-thaw cycles ..	227
Figure 4.138 125AKS specimens' appearance before and after freeze-thaw cycles	228
Figure 4.139 125HKS specimens' appearance before and after freeze-thaw cycles	229
Figure 4.140 125WKS specimens' appearance before and after freeze-thaw cycles	230
Figure 4.141 125OS specimens' appearance before and after freeze-thaw cycles..	231
Figure 4.142 Freeze-thaw cracking on the surface of reference mortar	232
Figure 4.143 Freeze-thaw cracking on the surface of 125ES02 mortar.....	232
Figure 4.144 Freeze-thaw cracking on the surface of 125ES0.5 mortar.....	233
Figure 4.145 Freeze-thaw cracking on the surface of 125ES1.5 mortar.....	233
Figure 4.146 Rate of change in compressive strength relative to compressive strength before freeze-thaw cycles	235
Figure 4.147 Compressive strength changes of cement mortars with ES admixture under different deteriorating effects	237
Figure 4.148 Compressive strength changes of cement mortars with AKS admixture under different deteriorating effects	238
Figure 4.149 Compressive strength changes of cement mortars with HKS admixture under different deteriorating effects	239

Figure 4.150 Compressive strength changes of cement mortars with WKS admixture under different deteriorating effects	240
Figure 4.151 Compressive strength changes of cement mortars with OS admixture under different deteriorating effects	241
Figure 4.152 Gray relations grades for the multiperformance	261
Figure 4.153 Gray relations grades for the multiperformance of fresh properties...	266
Figure 4.154 Gray relations grades for the multiperformance of hardened properties	271
Figure 4.155 Gray relations grades for the multiperformance of durability properties	276
Appendix A.1 Mineralogical development of reference paste.....	325
Appendix A.2 Mineralogical development of 125ES0.2	326
Appendix A.3 Mineralogical development of 125ES0.35	326
Appendix A.4 Mineralogical development of 125ES0.5	327
Appendix A.5 Mineralogical development of 125ES1.0	327
Appendix A.6 Mineralogical development of 125ES1.5	328
Appendix A.7 Mineralogical development of 125AKS0.2.....	328
Appendix A.8 Mineralogical development of 125AKS0.35.....	329
Appendix A.9 Mineralogical development of 125AKS0.5.....	329
Appendix A.10 Mineralogical development of 125AKS1.0.....	330
Appendix A.11 Mineralogical development of 125AKS1.5.....	330
Appendix A.12 Mineralogical development of 125HKS0.2.....	331
Appendix A.13 Mineralogical development of 125HKS0.35.....	331
Appendix A.14 Mineralogical development of 125HKS0.5.....	332
Appendix A.15 Mineralogical development of 125HKS1.0.....	332
Appendix A.16 Mineralogical development of 125HKS1.5.....	333
Appendix A.17 Mineralogical development of 125WKS0.2.....	333
Appendix A.18 Mineralogical development of 125WKS0.35.....	334
Appendix A.19 Mineralogical development of 125WKS0.5.....	334
Appendix A.20 Mineralogical development of 125WKS1.0.....	335
Appendix A.21 Mineralogical development of 125WKS1.5.....	335
Appendix A.22 Mineralogical development of 125OS0.2.....	336
Appendix A.23 Mineralogical development of 125OS0.35.....	336
Appendix A.24 Mineralogical development of 125OS0.5.....	337

Appendix A.25 Mineralogical development of 125OS1.0.....	337
Appendix A.26 Mineralogical development of 125OS1.5.....	338
Appendix A.27 XRD patterns of test pastes with 0.2 wt.% bio-polymeric admixtures at 3-days of curing	338
Appendix A.28 XRD patterns of test pastes with 0.35 wt.% bio-polymeric admixtures at 3-days of curing	339
Appendix A.29 XRD patterns of test pastes with 0.5 wt.% bio-polymeric admixtures at 3-days of curing	339
Appendix A.30 XRD patterns of test pastes with 1.0 wt.% bio-polymeric admixtures at 3-days of curing	340
Appendix A.31 XRD patterns of test pastes with 1.5 wt.% bio-polymeric admixtures at 3-days of curing	340
Appendix A.32 XRD patterns of test pastes with 0.2 wt.% bio-polymeric admixtures at 7-days of curing	341
Appendix A.33 XRD patterns of test pastes with 0.35 wt.% bio-polymeric admixtures at 7-days of curing	341
Appendix A.34 XRD patterns of test pastes with 0.5 wt.% bio-polymeric admixtures at 7-days of curing	342
Appendix A.35 XRD patterns of test pastes with 1.0 wt.% bio-polymeric admixtures at 7-days of curing	342
Appendix A.36 XRD patterns of test pastes with 1.5 wt.% bio-polymeric admixtures at 7-days of curing	343
Appendix A.37 XRD patterns of test pastes with 0.2 wt.% bio-polymeric admixtures at 150-days of curing	343
Appendix A.38 XRD patterns of test pastes with 0.35 wt.% bio-polymeric admixtures at 150-days of curing	344
Appendix A.39 XRD patterns of test pastes with 0.5 wt.% bio-polymeric admixtures at 150-days of curing	344
Appendix A.40 XRD patterns of test pastes with 1.0 wt.% bio-polymeric admixtures at 150-days of curing	345
Appendix A.41 XRD patterns of test pastes with 1.5 wt.% bio-polymeric admixtures at 150-days of curing	345
Appendix B.1 28-day compressive strength versus 0/45 μm bio-polymeric admixture usage	346

Appendix B.2 28-day compressive strength versus 0/125 μm bio-polymeric admixture usage	347
Appendix B.3 28-day compressive strength versus 125/250 μm bio-polymeric admixture usage	347
Appendix B.4 150-day compressive strength versus 0/45 μm bio-polymeric admixture usage	348
Appendix B.5 150-day compressive strength versus 0/125 μm bio-polymeric admixture usage	348
Appendix B.6 150-day compressive strength versus 125/250 μm bio-polymeric admixture usage	349
Appendix B.7 Compressive strength development of 45ES series.....	349
Appendix B.8 Compressive strength development of 125ES series.....	350
Appendix B.9 Compressive strength development of 125250ES series.....	350
Appendix B.10 Compressive strength development of 45AKS series	351
Appendix B.11 Compressive strength development of 125AKS series	351
Appendix B.12 Compressive strength development of 125250AKS series	352
Appendix B.13 Compressive strength development of 45HKS series	352
Appendix B.14 Compressive strength development of 125HKS series	353
Appendix B.15 Compressive strength development of 125250HKS series	353
Appendix B.16: Compressive strength development of 45WKS series	354
Appendix B.17 Compressive strength development of 125WKS series.....	354
Appendix B.18 Compressive strength development of 125250WKS series.....	355
Appendix B.19 Compressive strength development of 45OS series	355
Appendix B.20 Compressive strength development of 125OS series	356
Appendix B.21 Compressive strength development of 125250OS series	356
Appendix B.22 28-day flexural strength versus 0/45 μm bio-polymeric admixture usage	357
Appendix B.23 28-day flexural strength versus 0/125 μm bio-polymeric admixture usage	357
Appendix B.24 28-day flexural strength versus 125/250 μm bio-polymeric admixture usage	358
Appendix B.25 Flow diameters versus 0/45 μm bio-polymeric admixture usage...	358
Appendix B.26 Flow diameters versus 0/125 μm bio-polymeric admixture usage.	359

Appendix B.27 Flow diameters versus 125/250 μm bio-polymeric admixture usage	359
Appendix B.28 Initial setting times versus 0/45 μm bio-polymeric admixture usage	360
Appendix B.29 Initial setting times versus 0/125 μm bio-polymeric admixture usage	360
Appendix B.30 Initial setting times versus 125/250 μm bio-polymeric admixture usage	361
Appendix B.31 Final setting times versus 0/45 μm bio-polymeric admixture usage	361
Appendix B.32 Final setting times versus 0/125 μm bio-polymeric admixture usage	362
Appendix B.33 Final setting times versus 125/250 μm bio-polymeric admixture usage	362
Appendix B.34 Capillary water absorption versus 0/45 μm bio-polymeric admixture usage	363
Appendix B.35 Capillary water absorption versus 0/125 μm bio-polymeric admixture usage	363
Appendix B.36 Capillary water absorption versus 125/250 μm bio-polymeric admixture usage	364
Appendix B.37 Mass water absorption versus 0/45 μm bio-polymeric admixture usage	364
Appendix B.38 Mass water absorption versus 0/125 μm bio-polymeric admixture usage	365
Appendix B.39 Mass water absorption versus 125/250 μm bio-polymeric admixture usage	365
Appendix C.1 Experimental versus predicted values of 28-days compressive strength	366
Appendix C.2 Experimental versus predicted values of 150-days compressive strength	367
Appendix C.3 Experimental versus predicted values of 28-days flexural strength	367
Appendix C.4 Experimental versus predicted values of flow diameter	368
Appendix C.5 Experimental versus predicted values of initial setting time	368
Appendix C.6 Experimental versus predicted values of final setting time	369

Appendix C.7 Experimental versus predicted values of capillary water absorption 369

Appendix C.8 Experimental versus predicted values of mass water absorption 370

List of Tables

Table 2.1 Biopolymers found in nature, their monomers, and functions [3].....	7
Table 2.2 Important groups of biopolymers used in construction sector [33]	17
Table 2.3 Cellulose ethers and applications for cement-based products	21
Table 3.1 Chemical composition of PC	40
Table 3.2 Physical and mechanical properties of PC	40
Table 3.3 Particle size distribution of CEN Reference sand.....	41
Table 3.4 Chemical analysis of mixing water.....	42
Table 3.5 Top 5 hazelnut producer countries.....	52
Table 3.6 Composite cement mortar mixture combinations with bio-polymeric admixtures	76
Table 3.7 Composite cement mortar mixture combinations with chemical admixtures	78
Table 3.8 Multiple regression models including linear, quadratic, trigonometric, logarithmic, and their rational forms.....	90
Table 4.1 Test results of preliminary study.....	92
Table 4.2 The chemical contents of AKS, HKS, WKS, and OS.....	95
Table 4.3 Extractive contents of AKS, HKS, WKS, and OS.....	96
Table 4.4 Crystallinity Index of bio-polymeric materials.....	98
Table 4.5 Composite cement mortar mixture combinations with 0/45 μm grain size bio-polymeric admixtures	110
Table 4.6 Composite cement mortar mixture combinations with 0/125 μm grain size bio-polymeric admixtures	111
Table 4.7 Composite cement mortar mixture combinations with 125/250 μm grain size bio-polymeric admixtures	112
Table 4.8 Composite cement mortar mixture combinations with chemical admixtures	113
Table 4.9 Flow diameter values of test specimens.....	115
Table 4.10 Initial and final setting times of test specimens	123

Table 4.11 Water absorption values of test specimens	139
Table 4.12 Compressive strength values of test specimens	155
Table 4.13 Compressive strength property of cement mortars with the use of chemical admixtures	172
Table 4.14 Flexural strength values of test specimens.....	174
Table 4.15 Comparison of superplasticizers and bio-polymeric admixtures on flowability	184
Table 4.16 Comparison of set retarder and bio-polymeric admixtures on initial setting time.....	185
Table 4.17 Comparison of set retarder and bio-polymeric admixtures on final setting time.....	186
Table 4.18 Comparison of water repellent agent and bio-polymeric admixtures on capillary water absorption	186
Table 4.19 Comparison of water repellent agent and bio-polymeric admixtures on mass water absorption	187
Table 4.20 EDS analysis of tested cement mortars.....	206
Table 4.21 Compressive strength of mortar specimens after sulfate effect	221
Table 4.22 Compressive strength of mortar specimens after acid effect	223
Table 4.23 Compressive strength of mortar specimens after freeze-thaw effect.....	234
Table 4.24 Test factors and levels.....	242
Table 4.25 Experimental design.....	243
Table 4.26 Experimental test results	246
Table 4.27 Comparability sequence of experimental test results.....	249
Table 4.28 Deviation sequence of experimental test results	252
Table 4.29 Grey relation coefficient of experimental test results	255
Table 4.30 Gray relational grades and rankings for 8 different responses.....	258
Table 4.31 Average grey relational grade by level wise	262
Table 4.32 Gray relational grades and rankings for fresh properties.....	263
Table 4.33 Average grey relational grade by level wise for fresh properties	266
Table 4.34 Gray relational grades and rankings for hardened properties	267
Table 4.35 Average grey relational grade by level wise for hardened properties....	271
Table 4.36 Gray relational grades and rankings for durability properties	272
Table 4.37 Average grey relational grade by level wise for durability properties...	276

Table 4.38 R-squares of regression models for 28-days compressive and flexural strength, 150-days compressive strength and flow diameter	278
Table 4.39 R-squares of regression models for initial and final setting times, and capillary and mass water absorption values	279
Table 4.40 Regression equations for 28-days compressive strength and mass water absorption.....	280
Table 4.41 Regression equations for 28-days flexural strength and 150-days compressive strength.....	281
Table 4.42 Regression equations for capillary water absorption and final setting time	282
Table 4.43 Regression equations for initial setting time and flow diameter.....	283

Abbreviations

AKS	Apricot Kernel Shell
ASTM	American Society for Testing and Materials
CMC	Na-Carboxymethyl Cellulose
DNA	Deoxyribonucleic Acid
EDS	Energy Dispersive Spectroscopy
EIS	Electrochemical Impedance Spectroscopy
EN	European Norm
ES	Egg Shell
FT-IR	Fourier-Transform Infrared Spectroscopy
GRG	Grey Relational Grade
HEC	Hydroxyethyl Cellulose
HKS	Hazelnut Kernel Shell
MC	Methyl Cellulose
MHEC	Methyl Hydroxyethyl Cellulose
MHPC	Methyl Hydroxypropyl Cellulose
OS	Olive Seed
PA	Polyamide
PAC	Polyanionic Cellulose
PBS	Polybutylene Succinate
PC	Portland Cement
PCA	Polycarbonates
PCL	Polycaprolactone

PDS	Polydioxo-None
PE	Polyethylene
PEA	Poly(Ethylene Adipate)
PGA	Polyglycolide
PHA	Polyhydroxy-Alkanoates
PHB	Polyhydroxybutyrate
PHBV	Poly(3-Hydroxybutyrate-Co-3-Hydroxyvalerate)
PCE	Polycarboxylate Ether
PCM	Phase Change Material
PLA	Poly lactide
PMA	Polymethacrylates
PP	Polypropylene
PPF	Polypro-Pylene Fumigates
PTFE	Polytetra-Fluoroethylene
PU	Polyurethane
PUR	Polyurethane
PVA	Polyvinyl Alcohol
PVC	Polyvinyl Chloride
RNA	Ribonucleic Acid
SEM	Scanning Electron Microscope
SMF	Sulfonated Melamine-Formaldehyde
TSE	Turkish Standard Institute
WKS	Walnut Kernel Shell
XRD	X-Ray Diffraction

Chapter 1

Introduction

The increasing environmental concern and awareness of industrial pollution have forced the construction and manufacturing industries to search for innovative materials that are reliable, sustainable and can replace conventional synthetic chemicals and polymers in concrete and cement-based products. Natural polymers, such as polysaccharides, proteins and polynucleotides have already been considered as potential alternatives, given their environmental friendliness and ready availability in polymeric form and the fact that they can be extracted from natural sources. Natural polymers also offer environmental advantages such as reduced dependence on non-renewable energy/material sources, lower pollutant emissions, lower greenhouse gas emissions, enhanced energy recovery, and biodegradability.

In food factories, large amounts of food waste, called by-products, are produced as a result of the process, and many of these are immediately destroyed (which leads to environmental pollution), or used to produce products with low economic value (animal feed, fertilizer, etc.) using lower technologies. The effective evaluation of waste generated during food processing is important not only for the prevention of environmental pollution, but also for the creation of added value and diversification of products. With the assumption that the number of food processing factories will continue to increase with the increasing population in the coming periods, it can be said that the amount of food waste and waste problems will increase accordingly. Therefore, the collection of wastes and their use in the production of new products are important for human health, environmental pollution, and the national economy.

The building industry is a sector that provides the development of our country's economy with its great contribution to national income as well as the potential of its

labor force and strengthens our economy with each passing day. In addition, construction sector is one of the sectors that will live continuously in terms of meeting the needs of human beings as long as they exist. Although continuous increase of human population in recent years ensures that construction sector remains alive, sector must keep up with rapidly changing and developing technology.

It is not possible to achieve the level of performance required in major structural applications with concrete mixtures produced with conventional components. Many studies conducted in recent years have suggested that various chemical and mineral additives can be used easily to solve the problem. In addition to chemical and mineral admixtures, which enable structural elements to perform better both in strength and durability, various admixtures can be used to improve the performance of cement-based materials. In particular, the use of polymer admixtures has become widespread in order to improve the mechanical and physical properties of concrete whose tensile strength is much smaller than compressive strength. However, in view of environmental influences, the use of such synthetic polymers, insoluble in nature, can sometimes be considered as harmful. In recent years, the search for natural additives that can replace such chemicals and polymers and provide similar technical added value has come to the fore.

In this thesis study, hazelnut, walnut, egg, olive, and apricot wastes produced in our country will be evaluated as alternative products to cement chemicals and polymers in cement-based products. These eating products are produced extensively in our country and the seeds and shells of these products are deposited as waste. Most of these solid wastes are incinerated and form carbon dioxide again. In this study, it is aimed to re-evaluate these solid wastes with the most harmless and cheapest way. In particular, it is envisaged that such wastes can increase the physical and mechanical properties of cementitious products by at least as much as chemicals and synthetic polymers. In addition, the bio-polymeric materials used in the study were compared in terms of performance with some chemicals that are already concrete admixtures.

In the first stage of the study, it was aimed to improve some of the properties of composite cement mortar by using different materials such as ground and sized corn cob, egg shell, walnut kernel shell, apricot kernel shell, olive pomace, mallow, hazelnut kernel shell, rice husk and olive seed. In the beginning of the experimental

work, it was tried as a preliminary study that which or which of these waste materials could be used in harmony with cement mortar. Among these waste bio-polymeric materials, it has been determined that egg shell, apricot kernel shell, hazelnut kernel shell, walnut kernel shell and olive seed can be used in cement mortars.

In the second stage of the study, the characterization of olive seed, hazelnut kernel shell, apricot kernel shell and walnut kernel shell bio-polymeric materials to be evaluated in cement mortars were carried out by SEM, XRD and FT-IR analyzes.

In the third stage, these bio-polymeric admixtures were sized at 0/45, 0/125 and 125/250 μm grain sizes and evaluated at 0.25, 0.35, 0.50, 1, 1.5% of the total weight in cementitious mortars. The effects of bio-polymeric admixtures on the flowability, setting time, water absorption, 28-day flexural strength and 7-, 28-, and 150-day compressive strength of cement mortars were investigated in detail. As a result of the analysis, the most effective particle size was determined. Then, the physical and mechanical properties of cement mortars using the selected grain size bio-polymeric admixtures and commercially available cement chemicals were analyzed comparatively. It has been investigated whether bio-polymeric admixtures can be used instead of cement chemicals.

In the fourth stage, the microstructure and hydration process of cement mortars, in which bio-polymeric materials with the most effective particle size were used as admixtures, were determined by SEM/EDS and XRD analyzes, respectively.

In the fifth stage, durability properties such as sulfate attack, acid attack and freeze-thaw were determined on the test specimens.

In the sixth and last stage of the study, the optimization of the use of bio-polymeric admixtures in composite cement mortars was carried out. For the optimization study, Gray Relational Grade (GRG) method was used. Wolfram Mathematica 12 software was used for regression analysis.

According to the thesis flow, Chapter 2 focus on the literature review of classification of biopolymers, biopolymer types that can be used in construction sector, and bio-polymeric admixtures for cementitious materials. Chapter 3 deals with the materials and methods used in this study. Chapter 4 focus on the results achieved, their

interpretation and discussion. Finally, chapter 5 deals with the conclusion and recommendations for future research.

1.1 Topic

Construction sector is one of the most widely resource of material user industry. Therefore, more effective materials should be investigated and used in producing construction materials. The use of recycling materials and/or reusable materials as admixture is an effective way to produce sustainable construction products. One of these admixtures is bio-polymeric admixture.

This experimental investigation was conducted as a PhD thesis work at İzmir Kâtip Çelebi University Graduate School of Natural and Applied Sciences and it has the subject of the examination of different types of food waste, which can be considered as bio-polymeric admixtures, for the use in composite cement mortars.

1.2 Aim

Because increasing the use of waste materials in the construction industry, it was foreseen that their advanced engineering properties should be examined deeply. The experimental work presented in this thesis aims to investigate the effect of food wastes on the physical and mechanical behavior, and the microstructure of the cement mortars. After the wastes were ground and brought to the desired grain size, a new bio-polymeric admixture was recommended, and it is used in cement mortar combinations at certain ratios. The effect of the new bio-polymeric admixture on the physical and mechanical properties of the mortar has been investigated. With this study, an environmentally friendly product is developed, and waste disposal is also provided.

1.3 Scope

The work presented in this thesis is an investigation on the behavior of new generation composite mortar produced by mixing ASTM C 150 Type 1 (42.5 N/mm²) Ordinary Portland Cement (OPC), CEN standard sand in accordance with EN 196-1 standard, and bio-polymeric admixtures having various ratios. The physical, mechanical,

microstructural and durability properties of the produced test specimens were investigated experimentally. In this study, 5 different bio-polymeric materials were tested. These are apricot kernel shell, olive seed, hazelnut kernel shell, walnut kernel shell and egg shell. These bio-polymeric admixtures were investigated in terms of 3 different particle sizes, which are 0/125 μm , 0/250 μm , and 125/250 μm . 5 different bio-polymeric admixture usage rates were determined in each particle size trial. In addition, 4 different cement chemicals (two of them were superplasticizers, one was set retarder, and last one was water repellent) were tested in cement mortar to compare biopolymeric materials with cement chemicals. In this work, a total of 110 different mixture combination were designed. A total of 1365 hardened test specimens were produced in order to carry out mechanical, physical and durability tests. 190 fresh test samples were investigated for fresh state properties. For microstructural investigations, 100 samples were analyzed with XRD, and 75 samples were analyzed with SEM/EDS.

Effect of biopolymers on new generation composite cement mortars is a new research area and there is very limited information about this subject existing in the literature. Furthermore, this investigation can be interesting from technical point of view because of waste recycling and can be challenging from environmental point of view because of using completely natural admixtures instead of those cement admixtures produced by chemical processes.

Chapter 2

Previous Studies

A comprehensive review of the literature on the use of biopolymers and bio-polymeric admixtures as admixture in cementitious products is made. In the literature, it has been observed that the number of studies on the use of food waste directly in cementitious products, as in this study, is quite limited.

In this section, biopolymers are briefly introduced. Also, a broad classification of biopolymers has been made by the author. The use of biopolymers and bio-polymeric materials in the field of building materials and other construction areas has been researched and summarized in detail.

2.1 Classification of Biopolymers

Biopolymers are environmentally friendly materials that are produced from renewable natural sources and are generally biodegradable and do not contain toxic substances. Biopolymers are polymers that are created in nature throughout the life cycle of all organisms; hence they are also called natural polymers. They can be produced by biological systems such as plants, animals, or microorganisms, or can be chemically synthesized from biological starting material (sugar, starch, natural oil, or oils, etc.). Synthesis of biopolymers is usually carried out during complex metabolic processes in the chain growth polymerization reaction of activated monomers formed in the cell and an enzyme catalyst [1]. The main types of biopolymers are fats, carbohydrates, proteins, nucleic acids and bio-polyesters [2]. The most abundant biopolymers in the world are cellulose and alginate, respectively. Stevens [3] divides biopolymers into three main groups as polysaccharides, polypeptides and polynucleotides. Biopolymers found in nature, their monomers and functions are shown in Table 2.1.

Table 2.1: Biopolymers found in nature, their monomers, and functions [3]

Biopolymer	Monomer	Containing
Polysaccharides	Simple sugar	In plants and some higher organisms (cellulose, chitin), structural materials, energy storage materials (starch, glycogen), molecular identification (blood types), bacterial secretion
Polypeptides	Amino acid	Biological catalysts (enzymes), growth factors, receptors, structural materials (wool, leather, silk, hair, connective tissue), hormones (insulin), toxins
Polynucleotides	Nucleotides	Genetic information carriers (DNA, RNA) that are commonly identified in all organisms

Many different classifications of biopolymers can be found in the literature. The polysaccharide, polypeptide and polynucleotides can also be subdivided. In addition to these main groups, there are also semi-artificial biopolymers. Such polymers should also be added to the classification.

Lalit et al. [4] divided the biopolymers into three groups: polymers directly extracted from biomass (polysaccharides, proteins, lipids), polymers classically synthesized from bio derived monomers (Poly lactic acid (PLA), other polyesters), and polymers produced directly by microorganisms (polyhydroxy ikonates, bacterial cellulose, xanthan, curdlan , pullulan). Mohan et al. [5] expanded the classification by dividing the biopolymers into four groups. They classified biopolymers according to their biodegradability (biodegradable, non-biodegradable), bio-base (bio based, non-biobased), based on polymer backbone (polyesters, polysaccharides, polycarbonates, polyamides, vinyl polymers), based on repeating units (polysaccharides, proteins, nucleic acids). Similarly, Hassan et al. [6] brought a classification systematic especially on the biodegradability of biopolymers in their study. According to them, two different criteria underline the definition of a “biopolymer”: (1) the source of the raw materials and (2) polymer biodegradation. Ekiert et al. [7], unlike other researchers, proposed a fairly simple classification. They divided biopolymers into two classes, as natural and synthetic. Proteins such as collagen, fibrinogen and soy protein, and polysaccharides such as cellulose, chitin are called natural biopolymers. On the other hand, nondegradable materials such as PE, PP, PA, PU, PC, PVC, PMMA, PTFE

and degradable materials such as PGA, PLA, PDS, PLC, PHB, PPF are called synthetic biopolymers by them (Figure 2.1). Othman [8] also classified biopolymers under two groups as natural and synthetic. While carbohydrates (cellulose, starch, chitosan) and proteins (gelatin, gluten, alginate) form natural biopolymers, biopolymers produced by microbial fermentation (PHA, PHB, PHBV) and produced by chemical synthesis (PLA, PCL, PVA, PGA) constitute synthetic biopolymers, according to the researcher. Jaskiewicz and Bledzki [9] also divided biopolymer into two main groups; (1) from renewable raw materials (vegetable origin, microbial, animal origin), (2) from crude oil (e.g. PVA).

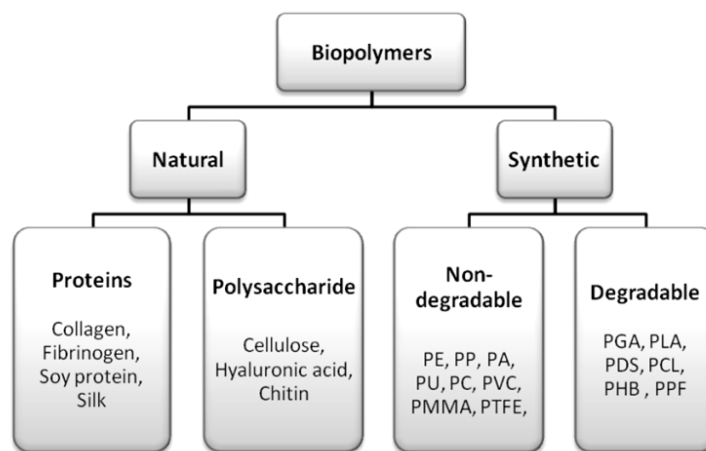


Figure 2.1: Biopolymer classification [7]

In order to understand and classify the character of natural materials to be used in this experimental work, the classification of biopolymers has been made by the author within the scope of this thesis study. The classification of biopolymers is given in Figure 2.2.

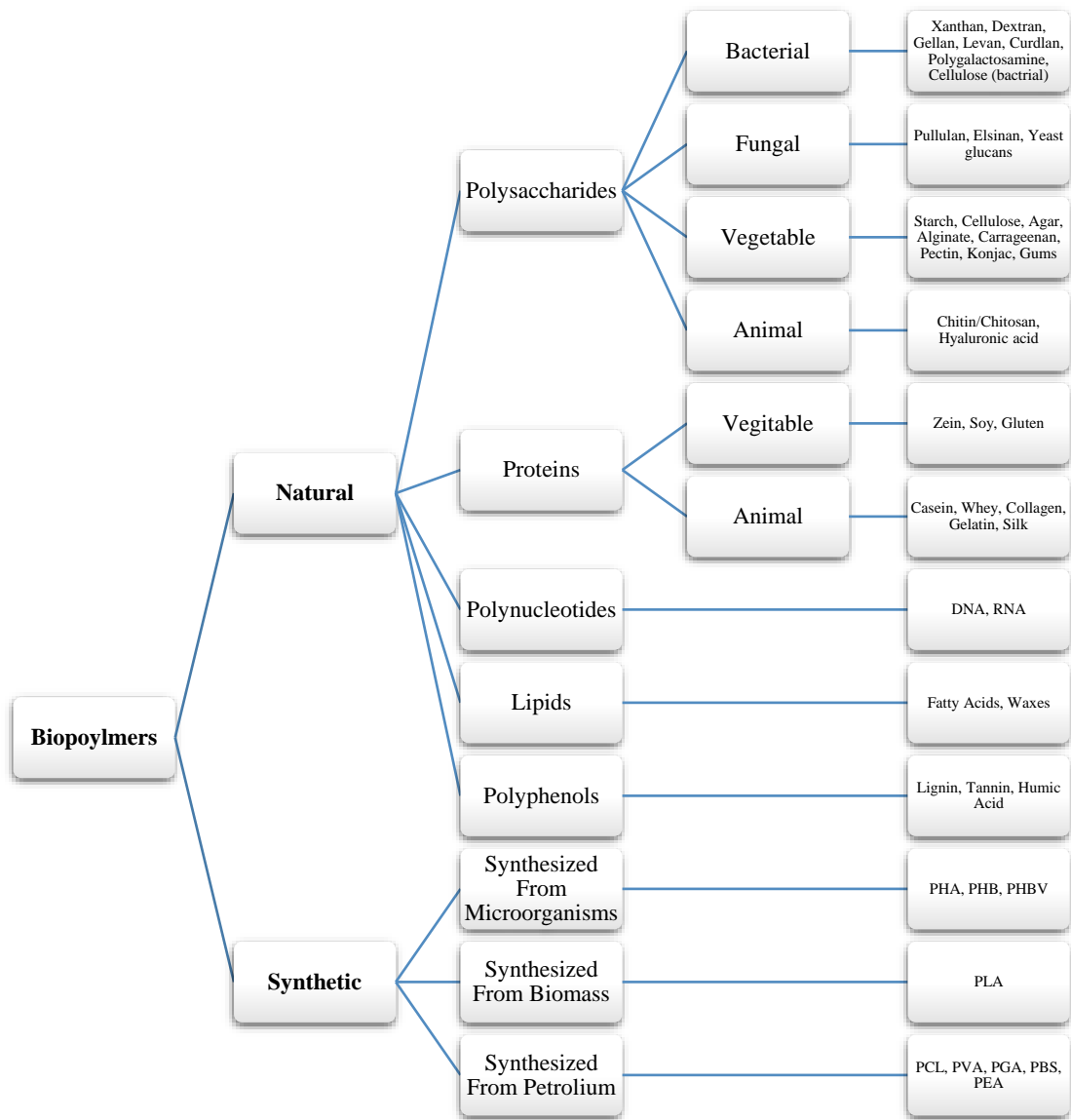


Figure 2.2: The classification of biopolymers

It is possible to reach different biopolymer classifications in the literature. However, some of them were found to be simple to reach the category of desired material, while others were quite complex. Therefore, a new biopolymer classification systematic is proposed, as can be seen in Figure 2.2. It is possible to expand to this classification, but in this case, it becomes quite complex and irregular. This systematic classification has been tried to be prepared in a simple and understandable structure as much as possible. When Figure 2.2 is examined, biopolymers are grouped under two main headings: *natural biopolymers and synthetic biopolymers*.

Natural biopolymers are produced as structural components of tissues in living organisms. These mainly include polysaccharides and proteins. In addition,

polynucleotides, lipids, and polyphenols, also found in living organisms, are among the natural biopolymers.

Polysaccharides are chemicals formed by combining multiple and separate (non-combined) monosaccharides with the glycoside bond. Connecting glucose units differently results in different properties between polysaccharides. They are large molecule compounds that are formed when many (n) monosaccharides lose “n-1” water molecules. It is also called complex sugars. Polysaccharides can be found in four different sources: bacterial, fungal, vegetable, animal. Bacterial polysaccharides are usually produced by some types of bacteria by fermentation. Bacterial cellulose and xanthan could be cited as the most common example. Bacterial cellulose can be produced by some types of bacteria by fermentation, giving a very pure cellulose product with unique properties. The most common applications of bacterial cellulose are based on very large surface area and liquid absorption ability. Very low concentrations of bacterial cellulose can be used to create the perfect binder, thickener and coating agent. It also has end uses in oil and gas recovery, mining, paints, adhesives and cosmetics [2]. Xanthan gum, a complex copolymer produced by a bacterium, is one of the first commercially successful bacterial polysaccharides for fermentation production. Xanthan producing bacteria *Xanthomonas campestris* is one of the first bacterial polysaccharide production systems targeted in genetic engineering. Industrial applications; oil recovery, viscosity control in drilling mud fluids, mineral ore process (biocide), paper production (modifier), agricultural area (plant growth stimulator), pharmaceutical field (drug release system) and cosmetics. It is used as a gelling agent for cheese, ice cream, pudding and other desserts in food applications [2]. Fungal polysaccharides are cell wall components of fungus which may act as antigens or as structural substrates. These polysaccharides found in various kinds of fungus are produced by fermentation as a biopolymer [10]. Polysaccharide biopolymers produced from fungi are used in coatings, cosmetics, lotions and shampoos [11,12]. In addition to these applications, recently, its suitability in various biomedical applications such as medicines, tissue engineering, wound healing, human health and diagnostic imaging has been investigated [13,14]. Starch and cellulose are the most commonly known vegetable polysaccharides. Starch is the main carbohydrate store for higher organisms. Starch refers to a class of materials in a wide range of structure and properties. Starch polymers can be extracted from corn, potatoes, rice,

barley, sorghum, and wheat. Corn is the main source of starch for industry and food purposes. Starch: It is a mixture of two glucan polymers, amylose, and amylopectin. This polymer is deposited in plants as water-insoluble energy storage granules with each granule containing two polymer mixtures. Plant breeding techniques are used to produce new species with varying amylose amylopectin ratio. Starch was used in various products due to its low cost and wide availability. The chemical modification of the starch polymer has caused many useful derivatives. It is used as an adhesive for use in the paper industry and related industries. Since starch can absorb up to 1000 times the weight of moisture, it is used in disposable diapers, as a cure for burns, and as a water remover in fuel filters. Corn starch polymer is also used as thickener, stabilizer, and soil conditioning and even as de-icing for roads. Cellulose is the most abundant component of biological substances. It is the main component of plant cell walls. Cotton fiber is the purest among vegetable cellulose with a 90% cellulose content. On the other hand, wood contains about 50% cellulose. Cellulose serves as an important raw material for many industries. Chemically modified vegetable cellulose is used in quite different application areas. Cellulose derivatives are used for fibers in various forms, thickener solutions, and gels. For example, carboxymethylcellulose (CMC) is used as thickener, binder, stabilizer, and flow control agent. The major markets of CMC are detergents, textiles, food, toothpastes, shampoos, skin lotions, paper, adhesives, ceramics, and latex paints [2]. The most widely known and used of animal-derived polysaccharides are chitin and chitosan. Chitin, a polysaccharide; It is a polymer abundant in nature and has similar chemical and structural properties of cellulose (Figure 2.3). Earlier, it was designated "animal cellulose" because it is structurally similar to cellulose. Although polysaccharides are simply sugar, minor modifications can result in significantly different chemical and physical properties. The only difference between cellulose and chitosan is that the hydroxy group (OH) of cellulose has replaced the amino (NH₂) group for chitosan. Chitin contains acetylated amine groups.

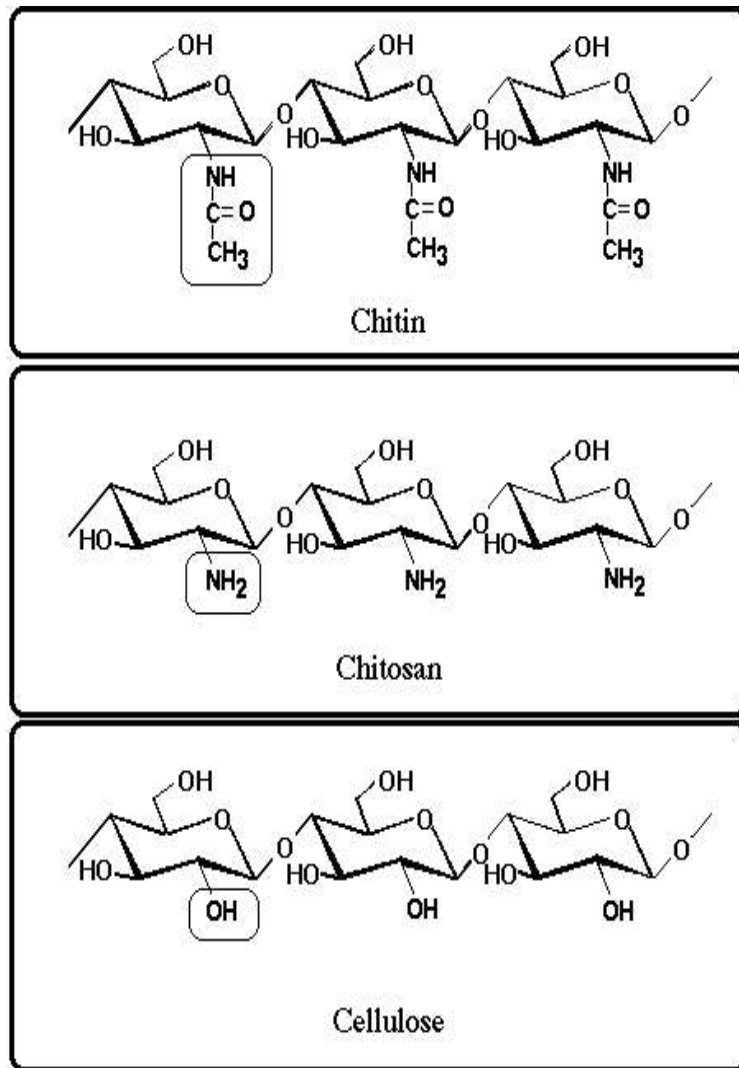


Figure 2.3: Structure of chitin, chitosan and cellulose [15]

Chitin is an important structural component of the exoskeleton of many organisms such as insects and shellfish. It also serves as the cell wall component of fungi and many plankton and other small organisms in the ocean. The chitin family of polymers is widely used in medicine, manufacturing, agricultural and waste treatment. It is used in bandage and surgical threads in chitosan wound treatment in biomedical field. Because chitosan creates a durable, water-absorbing, oxygen-permeable biocompatible film. Chitosan can be used for accelerated tissue repair and can be applied directly as an aqueous solution to treat burns. Due to its high oxygen permeability, chitosan is used as a material for contact and intraocular lenses. Chitosan can also be used to speed up blood clotting. Due to edible and biodegradable properties, chitosan has attracted notable interest in food packaging area [16]. The chitin compound is actually biodegradable (breaks down human blood chitin into simple carbohydrates, carbon dioxide and water), which makes it particularly suitable

for use in drug delivery systems. Chitosan carrier slowly releases the drug. This is particularly important in cancer chemotherapy [2].

Proteins are large biomolecules, or macromolecules, consisting of one or more long chains of amino acid residues. protein-based biopolymers can be evaluated under two main subtitles; these are vegetable-based and animal-based. Zein, soy and gluten are examples of vegetable-based protein biopolymers. This type of vegetable protein-based biopolymers is used extensively as a coating and film material in food packages, and as a coating material in the paper industry due to their hydrophilic, insolubility, viscoelastic, etc. properties [16]. Casein, whey, collagen, gelatin, silk are examples of animal-based protein biopolymers. Gelatin is an animal product produced from animal protein. Gelatin is produced by the partial hydrolysis of collagen, which is obtained from animal skin, bones, and tissues. It is used to improve air quality and shorten recovery after exercise and sports injuries. In production, gelatin is used for the preparation of foods, cosmetics and medicines, too [5]. Collagen is the most common protein in human. It is found in muscles, skin, bones, and tendons, where it forms a pier to provide strength and structure. Collagen is widely used in the medicine industry [7,17].

Lipid is a macro biomolecule that is soluble in nonpolar solvents. Non-polar solvents are typically hydrocarbons used to dissolve other naturally occurring hydrocarbon lipid molecules that do not (or do not easily) dissolve in water, including fatty acids, waxes, sterols, fat-soluble vitamins (such as vitamins A, D, E, and K), monoglycerides, diglycerides, triglycerides, and phospholipids. The functions of lipids include storing energy, signaling, and acting as structural components of cell membranes [18,19]. Lipids have applications in the cosmetic and food industries as well as in nanotechnology [20]. In chemistry, particularly in biochemistry, a fatty acid is a carboxylic acid with a long aliphatic chain, which is either saturated or unsaturated. Most naturally occurring fatty acids have an unbranched chain of an even number of carbon atoms, from 4 to 28. Fatty acids are usually not found in organisms, but instead as three main classes of esters: triglycerides, phospholipids, and cholesteryl esters. In any of these forms, fatty acids are both important dietary sources of fuel for animals and they are important structural components for cells. Fatty acids are mainly used in the production of soap, both for cosmetic purposes and, in the case of metallic soaps,

as lubricants. Fatty acids are also converted, via their methyl esters, to fatty alcohols and fatty amines, which are precursors to surfactants, detergents, and lubricants [21]. Other applications include their use as emulsifiers, texturizing agents, wetting agents, anti-foam agents, or stabilizing agents. Esters of fatty acids with simpler alcohols (such as methyl-, ethyl-, n-propyl-, isopropyl- and butyl esters) are used as emollients in cosmetics and other personal care products and as synthetic lubricants. Esters of fatty acids with more complex alcohols, such as sorbitol, ethylene glycol, diethylene glycol, and polyethylene glycol are consumed in food, or used for personal care and water treatment, or used as synthetic lubricants or fluids for metal working. Waxes are a diverse class of organic compounds that are lipophilic, malleable solids near ambient temperatures. They include higher alkanes and lipids, typically with melting points above about 40 °C (104 °F), melting to give low viscosity liquids. Waxes are insoluble in water but soluble in organic, nonpolar solvents. Natural waxes of different types are produced by plants and animals and occur in petroleum. Waxes are synthesized by many plants and animals. Those of animal origin typically consist of wax esters derived from a variety of fatty acids and carboxylic alcohols. In waxes of plant origin, characteristic mixtures of unesterified hydrocarbons may predominate over esters [22]. The composition depends not only on species, but also on geographic location of the organism. The best-known animal wax is beeswax used in constructing the honeycombs of honeybees, but other insects secrete waxes. A major component of the beeswax is myricyl palmitate which is an ester of triacontanol and palmitic acid. Plants secrete waxes into and on the surface of their cuticles as a way to control evaporation, wettability and hydration. The epicuticular waxes of plants are mixtures of substituted long-chain aliphatic hydrocarbons, containing alkanes, alkyl esters, fatty acids, primary and secondary alcohols, diols, ketones and aldehydes [22]. From the commercial perspective, the most important plant wax is carnauba wax; a hard wax obtained from the Brazilian palm *Copernicia prunifera*.

Polyphenols, known as polyhydroxyphenols, are a structural class of mainly natural, organic chemicals characterized by the presence of large multiples of phenol structural units. The number and characteristics of these phenol structures underlie the unique physical, chemical, and biological (metabolic, toxic, therapeutic, etc.) properties of particular members of the class. Examples include lignin, tannic acid and ellagitannin. The historically important chemical class of tannins is a subset of the polyphenols

[23,24]. Lignin; found in woody and herbaceous plants. Its main function is to provide structural support to the cell wall of the plant. It consists of lignin phenylpropane monomer and belongs to the polyphenol family of polymers. Together with cellulose and hemicellulose, lignin is one of three chemically different components that make up the plant tissue. Typically, woody, and herbaceous biomass contains 50% cellulose, 25% hemicellulose and 25% lignin. Wood is a complex lignocellulosic composite. Lignin polymers are highly amorphous and have a three-dimensional structure combined with hemicellulose and play a key role in preventing rotting of lignocellulosic material. Lignin wood was created in large quantities by the pulping process and as a result is relatively inexpensive. The most common commercial form of lignin is lignosulfonate, a compound derived from sulfite pulping. In addition, it is used as a binder for powder control on roads, as a binder in molding applications and animal foods, and as a phenolic adhesive by replacing formaldehyde-based compounds in applications such as industrial packaging and tape. It is used as dispersing agent in pesticide powders, concrete mixture, and thinning agent in oil drilling mud. The development of special lignin components, such as electrical conductive polymers and engineering plastics, is an important area of research [2].

Synthetic biopolymers are synthetically derived, or modified polymers designed for various applications. Synthetic biopolymers can be examined under three different types; synthesized from microorganisms, synthesized from biomass, and synthesized from petroleum. The engineering of the production of new biopolymers in plants provides a truly bio-renewable way for their synthesis. Like all polymer industries, these polymers are produced in bulk and then shaped for a specific end use. Also, microorganisms play an important role in the production of a wide variety of biopolymers such as polysaccharides, polyesters, and polyamides, ranging from viscous solutions to plastic. The main ones from synthetic biopolymers produced through microorganisms; PHA is PHB and PHBV. Polyhydroxyalkanoates or PHA is a type polyester produced in nature by numerous microorganisms (e.g. *Cupriavidus necator*), including through bacterial fermentation of sugars or lipids [25]. Thanks to its biodegradability and its potential to create bioplastics with unique properties, a great interest exists to develop the use of PHA-based plastics. PHA fits into the green material production as a means to create green plastics from fossil fuel free sources. With its biocompatibility feature, PHAs is recommended for several medical

applications such as drug release systems, surgical threads, bone layers, wound care, and personal care products such as paper and film coatings, packaging applications and cosmetic containers. PHB and PHBV are polyhydroxyalkanoate-type polymers. They are produced for similar purposes with PHA. Plant based monomers could also play an important role in the production of a wide variety of biopolymers, such as PLA. PLA is one of the highest consumption volumes of bioplastic of the world. Besides, PLA is one of the most widely used plastic filament material in 3D printing works. The two main monomers of PLA, which are lactic acid and lactide, are typically made from plant starch such as from corn, cassava, sugarcane or sugar beet pulp via fermentation [26]. PLA is consumed in medical implants in the form of screws, anchors, rods, mesh, pins and plates [27]. PLA could also be used in production of decomposable packaging materials, either cast, injection-molded, spun, cups or bags. In addition, studies are also carried out on the production of PLA matrix composites reinforced with natural fibers, which can be considered almost environmentally friendly green composites [4,28]. The last group of synthetic biopolymers is those conventionally and chemically synthesized from petroleum-based products (e.g., PCL, PVA, PGA). Such materials could often be called biodegradable polymers [29]. PVA is a water-soluble synthetic polymer. It is produced by hydrolysis of polyvinyl acetate. It is generally used in papermaking, textiles industry, and a variety of coatings and packing in food and paper industry. PCL is also a biodegradable polymer which is generally evaluated for preparing scaffolds for various biomedical and tissue engineering applications [5,30].

2.2 Use of Biopolymers in Construction Industry

Biopolymers could be used in a wide variety of industrial fields, such as biosensors, biocompatible medical materials, agriculture, drug release systems, packaging, cosmetics, food additives, textiles, high strength structural materials, wastewater treatment compounds to prevent corrosion and mineral growth, industrial plastics, absorbents, adhesives, lubricants, soil conditioners [31,32]. The use of alternative biopolymers that are environmentally compatible, usually biodegradable, and eliminate dependence on petroleum-based products, is being investigated for a wide range of industrial processes, rather than petroleum-based synthetic polymers. The construction industry continues to work on natural polymers that can be called

environmentally friendly with similar environmental concerns. These types of biodegradable polymers, obtained from natural resources, are explored extensively, especially in the production of concrete and its derivatives [33]. An overview of the important groups of biopolymers used in construction sector is given in Table 2.2.

Table 2.2: Important groups of biopolymers used in construction sector [33]

Biopolymer	Source	Chemically Modification	Primary Function	Secondary Function	Major Applications
Lignosulfonate	Wood lignin	Yes	Dispersant/ Thinner	Retarder	Concrete, plasterboards, oil well construction
Humic acid	Soil	Yes	Water retention	Dispersant	Oil well construction
Lignite	Coal	Yes	Dispersant/ Thinner	Water retention	Oil well construction
Vegetable oils	Plants	Yes & No	Carrier Fluid	-	Oil well construction; concrete
Waxes	Plants, Insects	No	Coating	-	Paints & Coatings
Bitumen	Coal, Petroleum	Yes & No	Coating	Water repellent	Road construction
Asphalt	Petroleum	Yes & No	Coating	Lubricant	Road construction; oil well construction
Casein	Milk	No	Dispersant	-	Grouts, paints
Protein extract	Animal hair, hides, hoofs	Yes	Air entraining agent	-	Concrete, mortar
Starch	Corn, potato	Yes & No	Viscosifier	Water retention	Grouts, plasters, oil well construction
Cellulose	Cotton, wood	Yes	Water retention	Viscosifier	Grouts, plasters, oil well construction
Guar gum	Guar plant	Yes & No	Viscosifier	Water retention	Plaster, oil well construction
Xanthan gum	Bacterium	No	Viscosifier	Anti settling agent	Oil well construction, floor screeds, paints

Welan gum	Bacterium	No	Viscosifier	Anti settling agent	Concrete, oil well construction
Scleroglucan	Fungus	No	Viscosifier	Anti settling agent	Oil well construction
Succinoglycan	Bacterium	No	Viscosifier	Anti settling agent	Self leveling compounds
Curdlan	Bacterium	No	Viscosifier	Anti settling agent	Concrete
Rhamsan	Bacterium	No	Viscosifier	Anti settling agent	Grouts
Chitosan	Chitin	Yes	Viscosifier	Anti settling agent	Oil well construction
Polyaspartic acid	Synthetic	Yes	Dispersant	Retarder	Gypsum retarder
Polyester	Synthetic	Yes	Dispersant	-	Grouts, plaster

2.2.1 Use of Biopolymers/Bio-polymeric admixtures in Lime Mortar

Lime mortar is simply a mixture of lime as a binder, sand as an aggregate and water. Since very ancient times, lime mortars have been used in buildings as one of the oldest building materials. Very early examples of lime mortars have been found in Turkey and Palestine 12,000 B.C. Later examples of lime mortars are found in ancient Greece and the Roman Empire. [34]. They are still used today. Due to this type of disadvantage, it has been tried to improve the characteristics of lime mortar by using various organic admixtures since ancient times. Beans, flowers, fruit pulps and different leaves soaked in different oils ancient India [35], milk, lard and blood in ancient Romans, egg white in middle age Europa, rice paste, lacquer, tung oil, molasses and boiled bananas in ancient China, cactus juice and latex in ancient Peru, bark extracts in ancient Mayans, and fruit juice, keratin, casein and egg white in ancient Egypt are some examples of natural admixture used in ancient lime mortars [36]. As can be easily noticed from these examples, it was used as a large amount of polysaccharide and protein additives in ancient lime mortars. Today, polysaccharides and proteins of similar origin are still used to improve the physical and mechanical

properties of lime mortar. In general, natural oils are used to give hydrophobic properties to the mortar [37], to bond as proteins are hydrolyzed in an alkaline medium [38], and polysaccharides are used as water retention and viscosity modifying [36].

2.2.2 Use of Biopolymers in Concrete and Cement-Based Products

Biopolymers are generally used as admixtures to improve physical and mechanical properties of fresh and hardened cement mortar and concrete. Two biopolymer sources for mortar and concrete are due to the extraction of agricultural resources and biotechnology through microorganism fermentation and conventional synthesis. Extraction of natural materials or agricultural resources produce biopolymers such as chitin, chitosan, cellulose, starch, other polysaccharides and alginates [39]. Alginates are extracted polysaccharides from brown algae and used as a self-healing agent for the repair of concrete cracks without reducing their strength [40]. Polyhydroxyalkanoates are produced by microorganism fermentation. Biopolymers to be used in concrete works can be used in both ways, which can be powder (chitin, chitosan, starch, etc.) or liquid (xanthan, rubber, guar, etc.). Biopolymers used in cement-based products are briefly explained in the following subsections.

2.2.2.1 Lignosulfonates

Lignosulfonates are also known as first generation water reducers. Their function is dispersion of cement particles and improvement of concrete flowability. Superplasticizers can disperse cement particles by two main dispersing mechanisms: electrostatic repulsion and steric hindrance. In electrostatic repulsion, molecules of the admixture neutralize cement particles and cause all surfaces to carry uniform charges of same sign. The particles having the same charge repel each other. In steric hindrance, long polymer chains adsorbed on the surface of the cement particles prevent them to come closer to each other. Lignosulfonates can disperse cement particles by both steric hindrance and electrostatic repulsion [41]. They are used to increase the strength by reducing w/c (for same consistency), to save cement by reducing both cement and water contents (w/c and consistency are same), and to increase the consistency (strength is similar and no change in the amounts of the ingredients).

Lignosulfonates contain some sugar and because of this, they may act as also retarders. Furthermore, they increase the entrapped air content in the fresh concrete, this action may also cause a reduction in strength and durability of the concrete. Therefore, purified lignosulfonates are preferred in practice. For concrete applications, desugarification and sulfomethylation are the most important purification steps to avoid undesirable effects on concrete. Besides, lignosulfonates have relatively low water reducing capability (compared to second and third generation water reducers). They can reduce the water content between 5% and 15% [33].

Lignosulfonates are produced from lignin raw material via chemical processing. Lignin is a natural biopolymer, which occurs in wood and grass. The wood is mostly composed of lignin and cellulose. Therefore, these two substances must be separated from each other in lignosulfonate production. Lignin and cellulose are dissolved with hot calcium bisulfite solution. Then, the sulfite liquor produced is cleaned from sugar and made suitable for use as a concrete admixture. Even if sugar completely removed from the liquor, lignosulfonates' retarding effect partly remains because of phenolic hydroxyl group that lignosulfonate ingredient [42]. Repeating chain alignment of lignosulfonate is given in the Figure 2.4.

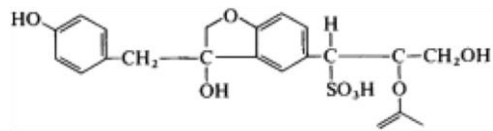


Figure 2.4: Repeating chain alignment of lignosulfonate [33]

Colombo et al. [43] investigated the rheological effects of lignosulfonate on cement mortars by using two different types of cement. As a result of their study, both yield stress and viscosity of the mortars decreased. Thus, workability has increased.

2.2.2.2 Cellulose

Cellulose is first molecularly determined as $C_6H_{10}O_5$ by French plant scientist Anselme Payen in 1838 [44] and then named in 1839 by French Academy [45], respectively. Cellulose generally contains 44.44% carbon, 6.17% hydrogen, and 49.39% oxygen, and generated from repeating β -D-gluco-pyranose molecules that are covalently linked through acetal functions between the equatorial OH groups (Figure

2.5). Therefore, cellulose is an extensive, linear-chain biopolymer with a large number of hydroxy groups [46,47].

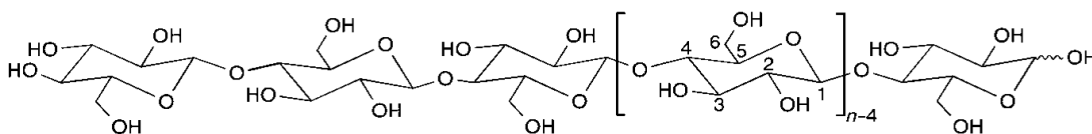


Figure 2.5: Molecular structure of cellulose [46]

Cellulose ethers gain industrial significance with derivatives such as ethylcellulose, methylcellulose, carboxymethylcellulose, hydroxyethylcellulose and benzylcellulose. Cellulose ethers are commercially prepared in alkali medium (usually NaOH) by interaction of an appropriate alcohol with sulfate or chlorine salts. Alkali cellulose is formed as an intermediate product. The degree of ethering depends on the reaction temperature, as well as the proportional properties of cellulose, alkali, water, and other variables. Cellulose ether is an environmentally friendly, natural polymer of wood or cotton cellulose, water-soluble, with a 30-65% crystalline hydrogen bond between its molecules. It is a chemical product that is formed by the conversion of cellulose hydroxyl groups to methyl and/or hydroxypropyl groups, after the chemical process, also called eterification, to be converted into water-soluble nonionic cellulose ether [48]. There are different cellulose ether derivatives according to production processes and intended uses (Table 2.3).

Table 2.3: Cellulose ethers and applications for cement-based products

Cellulose Ether	Application Field	Function
MC	Concrete, mortar	Water retention
MHEC	Gypsum plaster	Anti-sagging properties
MHPC	Lime plaster	Adhesiveness
CMC, PAC	Cement plaster	Workability
HEC	Tile adhesive	Pigment suspension
MHEC	Joint fillers	Thickener, brushability
MHPC	Cementing	Binder

The main reason why cellulose ethers are valuable in the building materials industry is their superior solubility and high chemical stability and toxicological harmlessness. Cellulose ether can be used in all areas where thickening, gelling, emulsification,

stabilization processes and water retention and good workability are required. Cellulose ethers, with many typical properties such as thickeners, water retention aids, binders, dispersion aids, lubricants, colloids, or stabilizers are cement chemicals. The main feature of this pure and/or modified biopolymer, which has different types such as MC, MHPC, MHEC, MHEC, CMC, PAC and HEC on the market, is high range water retention. They absorb water in their environment and trap a certain amount of water for a certain period of time, thereby allowing the working time of the mortar/concrete to be adjusted. Cellulose and hemicelluloses may contain a large number of polar hydroxyl groups. The polar hydroxyl groups are mostly responsible for hydrogen bonds with polar water molecules. The water absorption and water retention of cellulose and hemicelluloses can be mainly interrelated with hydrogen bonding of water molecules to the free hydroxyl groups in cellulose and hemicelluloses [49]. MHPC and MHEC cellulose ethers are mostly used in cement and plaster-based powder mortar additive systems. It is possible to work for a longer time during the application with cellulose added cement-based products. They improve the consistency of the mortar and facilitate the carding process. If different viscosity values are taken into account due to the modification coming from the production according to the need, the shear resistance of the concrete/mortar can be increased. They are especially preferred due to checking the working time and tensile test results. Generally, low viscosity cellulose ethers are preferred in plaster mortars and joints. However, high viscosity cellulose ether uses could also be faced to improve adhesion in practice.

The generally accepted viscosity classification in cellulose ether uses can be defined as follows [50–53]:

- Viscosity values between 5 mPas and 15 mPas are very low viscosity,
- Viscosity values between 20 mPas and 1500 mPas are low viscosity,
- Viscosity values between 1500 mPas and 4000 mPas are medium viscosity,
- Viscosity value between 4000 mPas and 15000 mPas are high viscosity,
- Viscosity value between 15000 mPas and 150000 mPas are very high viscosity.

Among all the polysaccharides used in the construction industry, cellulose ethers are commonly included in mortar formulations to provide many necessary properties for fresh and hardened mortar in the building materials industry [54]. However, it has been demonstrated by researchers that cellulose ethers can cause slowing and inadequate hydration of cement, besides its positive effects on water retention and workability [55–59]. Also, the addition of cellulose ether increases the consistency of the mortar [48,60]. Patural et al. [61] found that MHEC, MHPC and HEC can have water retention up to 98.8%, in their study to investigate the effect of cellulose ethers on cementitious mortars.

2.2.2.3 Starch

Starch is a water-insoluble, complex carbohydrate. It is used by plants to store excess glucose. It is used in industry for making glue, paper, and textile. It is used as a thickener in the food industry and to thicken liquids in cooking. It is an unpleasant and odorless powder obtained mostly from grains and potatoes. Chemically, it is a combination of two polymeric carbohydrates (polysaccharides), amylose and amylopectin. Amylose consists of adding glucose monomer units end-to-end with alpha-1,4 linkages. Unlike amylose, there is branching in the amylopectin, one side chain begins with an alpha-1,6 connection in one of the main 24–30 glucose monomers [62].

Amylose (Figure 2.6) is a linear molecule but forms a helix due to the tendency of the consecutive glucose units to be acylated. The two amylose molecules can be wound together to form a double helix. Since the inner surface of this spiral is hydrophobic, the water molecules in it can easily be replaced by more hydrophobic molecules. Due to the hydrogen bonds formed between the amylose coils, a dense structure with very little water is formed [63].

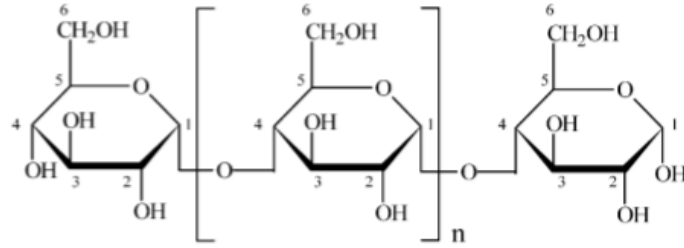


Figure 2.6: Structure of amylose [63]

In the amylopectin (Figure 2.7), after the branching points, two chains parallel to each other form one double helix. Amylopectin has a shape that expands as it branches from a center, like a bush. At the branching points, the molecule is irregular, and between the two branching points, the double helixes are stacked neatly, forming a crystal structure; therefore, these regular and irregular regions appear as growth rings in starch particles under a microscope [63].

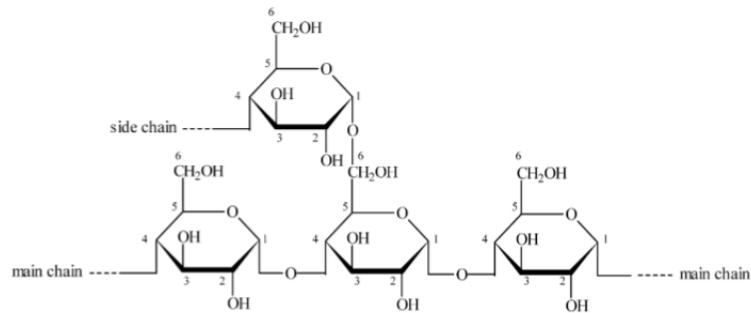


Figure 2.7: Structure of amylopectin [63]

Due to this molecular structure, amylopectin has a spiral shape that allows it to be stored as starch grains. Both amylopectin and amylose are polymers of glucose, and a typical amylose polymer is made up of 500-20,000 glucose molecules, and an amylopectin molecule is formed in about one million glucoses. Starch mostly consists of amylopectin about 75 to 80% by weight and the rest is amylose (20 to 25% by weight) depending on the plant origin [64].

In order to use in construction industry, carboxymethyl and hydroxypropyl starch are the most important starch derivatives among starch ethers [33]. Starch ethers are produced by the reaction of alkyl groups with etherifying agents [61]. The functions of starches in cement-based products are instant high viscosity, increasing water retention, reducing mortar stickiness on the trowel, ensuring surface viscosity when the mortar is first flattened and smoothed, enhance workability and improve the

application properties. Patural et al. [61] in their study, they found that as the viscosity coefficient ($\text{Pa}\cdot\text{s}^n$) of starch ether added mixtures decreased, the water retention ability of the mixtures increased. They conclude that water retention ability of a fresh mortar with starch ether increases, when viscosity decreases, unlike other polysaccharides. Also, starch widely used as biodegradable additives in cement mortar [65] and biodegradable cement [66]. Another common use of starch is to develop starch-based water-reducing agents and hydration heat-regulating materials [67,68]. Tan et al. [65] found that all corn starch and starch ethers have the effects of increasing the apparent viscosity, reducing the fluid loss and prolonging the setting time on alkali-activated cement paste. Zhang et al. [69] tried to prevent thermal crackings by controlling heat of hydration. In their study, they found that starch-based admixture reduced heat of hydration by slowing C-S-H formation. Besides, there is no loss in 28 days compressive strength values.

2.2.2.4 Gums

Gums are natural origin polysaccharides. They are capable of causing a large increase in a solution's viscosity, even at small concentrations. They are mostly botanical gums, found in the woody elements of plants or in seed coatings. The classification of natural gums can be made by their origin. Agar, alginic acid, sodium alginate and carrageenan are obtained from seaweeds; gum arabic from the sap of Acacia trees, gum ghatti from the sap of Anogeissus trees, gum tragacanth from the sap of Astragalus shrubs, karaya gum from the sap of Sterculia trees, guar gum from guar beans, locust bean gum from the seeds of the carob tree, beta-glucan from oat or barley bran, dammar gum, from the sap of Dipterocarpaceae trees, glucomannan from the konjac plant, psyllium seed husks from the Plantago plant and tara gum from the seeds of the tara tree are obtained from non-marine botanical resources. Gellan gum and xanthan gum are produced by bacterial fermentation [70].

Gums are used in concrete and derivative materials as self-leveling, set retardant, water reducing, viscosity modifier, durability enhancer, strength enhancer, pumpability improver, anti-corrosion, and concrete coating material. The main gum types commonly used in the mix designs of concrete derivative materials are gum arabic, guar gum, welan gum, gellan gum and xanthan gum [33].

Welan gum (Figure 2.8) is an exopolysaccharide. It is produced by fermentation of sugar by bacteria of the genus *Alcaligenes*. It is commonly used as a viscosity modifier in cement applications and it is very successful in stabilizing fluidity of concrete [71].

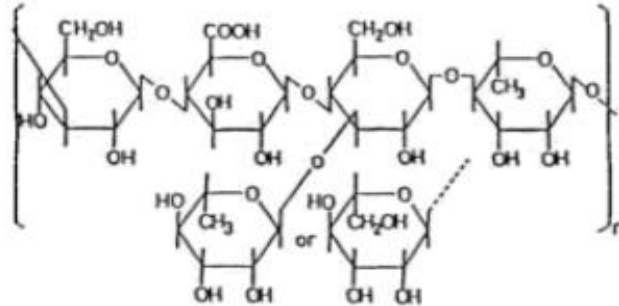


Figure 2.8: Chemical structure of welan gum [71]

Connors et al. [72] used natural gums in wall and concrete coverings materials. Annaamalai et al. [73] reported that welan gum and neem gum addition to concrete design markedly inhibited the corrosion of reinforcing steel in the concrete in NaCl solution. They explain why the corrosion in steel is reduced by the fact that the gums form a protective film, which is supported by SEM and EIS analysis.

Guar gum (see Figure 2.9) is a galactomannan polysaccharide extracted from guar beans. Guar gum consists of D-mannose monomer units linked to each other by β -(1 \rightarrow 4) linkage, thus it forms the main chain with D-galactose branches joined by α -(1 \rightarrow 6) bonds [74]. It is useful for cement product applications because of water retention, thickening and stabilizing properties.

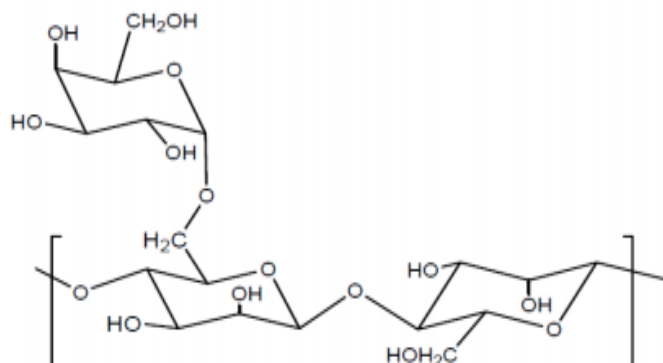


Figure 2.9: Chemical structure of guar gum [74]

Govin et al. [75] found in their study that guar gum derivatives improve water retention in cement mortars and increase the shear strength and consistency of the mortar.

Similar results were found in another study by researchers [76]. According to the results of their study, hydroxypropyl units of guar gum derivatives increase the water retention of mortars. Also, another result showed that guar gum can increase mechanical properties of concrete up to 0.4 % usage level, but decrease when used more [77].

Xanthan gum is the natural component of the cell wall of *Xanthomonas* species bacteria. Xanthan is a natural polysaccharide with high molecular weight containing mainly glucose, mannose and glucuronic acid in its structure. The commercial xanthan gum in the form of yellowish powder gives high viscosity to the solution it is added to even in low concentrations. Commercial xanthan gum is produced by microbial fermentation of *Xanthomonas campestris*. Bacteria produce xanthan gum by breaking down sugar in an aerobic fermentation medium containing simple sugar (glucose or fructose), a nitrogen source, and various minerals. When the fermentation is completed, after the bacteria are killed by heat treatment, the xanthan gum is precipitated using isopropanol. The xanthan scale obtained is then dried, milled and packaged [78]. Chemical structure of xanthan gum is given in Figure 2.10.

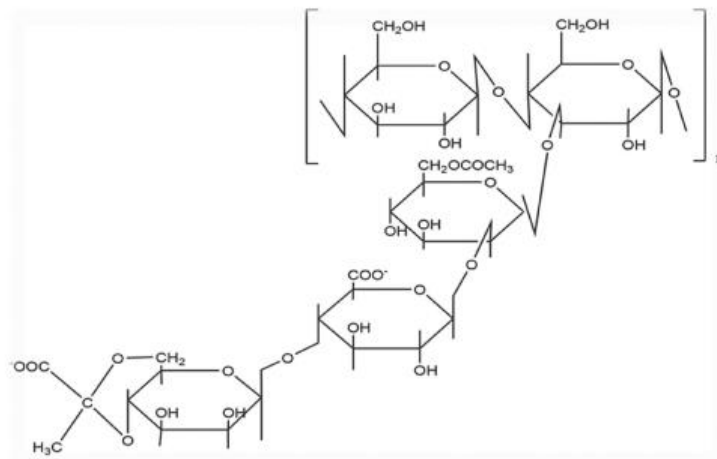


Figure 2.10: Chemical structure of xanthan gum [79]

Zhang et al. [80] examined the effect of fluidity modifying agents on the air gap structure of vibrated concrete. According to the findings obtained from the study, it has been revealed that xanthan gum increases the yield stress and viscosity of cement mortar, besides, it can stabilize trapped air retention. Increase in yield stress or the plastic viscosity generally related with hydrophilic groups of xanthan gum. They can adsorb and associate water molecules via hydrogen bond. Another reason is Van der

Waals attractive forces produced by adjacent xanthan chains. They can retard the free motion of water therein and even block water molecules if the chains are intertwined, thus presenting a network or gel-like structure at high concentration. Dursun [81] investigated the effects of different types of biopolymers on durability and mechanical properties of cement mortar. According to the test result, xanthan gum decreases the flowability of the cement mortar.

Gum arabic is a natural gum consisting of the hardened sap of two species of the acacia (*Sensum lato*) tree, the *Acacia senegal* (now known as *Senegalia senegal*) and *Vachellia* (*Acacia*) *seyal*. It also known as gum sudani, acacia gum, arabic gum, gum acacia, acacia, Senegal gum and Indian gum [82]. Gum arabic is a complex mixture of glycoproteins and polysaccharides predominantly consisting of arabinose and galactose. Chemical structure of xanthan gum is given in Figure 2.11.

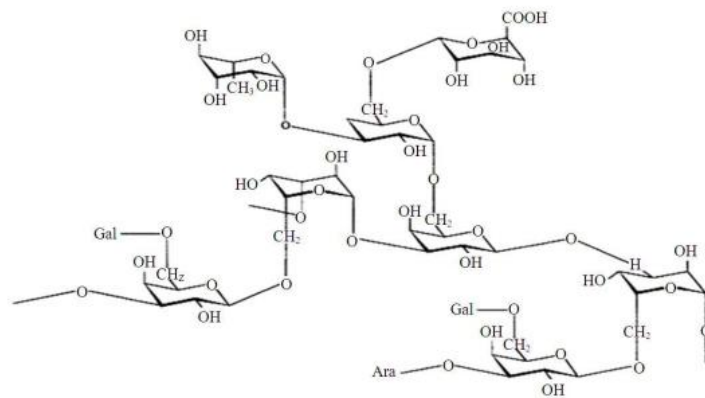


Figure 2.11: Chemical structure of gum Arabic [83]

Gum Arabic has a potential to utilize for application in the construction and building industries as a viscosity-enhancing admixture. This material also has a dispersing effect of cement particles by steric hindrance coupled with low viscosity and emulsifying characteristics [84]. It is characterized by long polymer chains called the functional groups of carboxyl acids (COOH). These have the ability to adsorb to particle surfaces by hydrogen bonding, electrostatic bonding or Van der Waals bonds [85]. In addition, it was found that the compressive strength increased with the addition of gum Arabic in the studies conducted by the researchers. It is stated that the reason for increase in compressive strength is the dispersing effect of gum Arabic on cement particles [85]. Gum Arabic also suggested as a viable ecological plasticizer as well as a very good viscosity modifying agent [86]. It could be used as a cheap plasticizer in

self-compacting concrete. Gum Arabic delays the setting time of self-compacted concrete and make it an ideal plasticizer for concrete in situations where delayed setting time is required. Elinwa et al. [87] stated that increase in compressive strength in gum Arabic concrete related with especially osumulite and tobermorite formation during cement hydration. Also, the formation of osumulite increases the density of test specimens. Palygorskite and Mordenite minerals formed in cement hydration of concrete samples containing arabic gum content showed that their test specimens were more porous. Furthermore, the slump values of the concrete test specimens increased due to the good dispersion of cement particles. Gum Arabic also recommended as a water reducer in concrete and cement mortar mix designs in the literature [88,89].

2.2.2.5 Chitin and Chitosan

Chitin was first identified in 1811 by detecting it in the structure of the fungus. It is known as the most abundant natural biopolymer on earth after cellulose. These polymers are obtained from the exoskeletal structures of crustaceans such as crab, lobster and shrimp, insects and cell walls of fungi. After processing of seafood, the exoskeletal structures of the crustaceans, which became waste as a by-product, have become an important source that can obtain chitin [90]. While the insects have about 23.5% chitin in their shells, this ratio varies between 17% and 32% in crab and shrimp, respectively. Chitin is mainly in the structure of poly- [β - (1,4) -2-acetamide-2-deoxy- β -D-glucopyranose] and contains very low rate of 2-amino-2-deoxy- β -glucopyranose monomers (see Figure 2.12). Chitin and chitosan polysaccharides are chemically similar to cellulose but differ among themselves. The cellulose contains the hydroxyl (-OH) group bound to the second carbon atom, while the chitin contains acetamide (-NHCOCH₃) and the chitosan contains the amine (-NH₂) group (see Figure 2.3) [15].

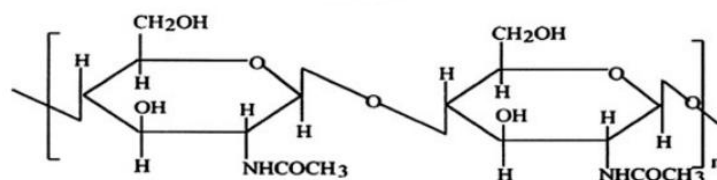


Figure 2.12: Chemical structure of chitin [91]

Although the kit has many variants, the most important of these is chitosan. Chitosan was first discovered in 1811 by Henri Bracannot. Bracannot tried to dissolve chitin

found in mushrooms in sulfuric acid but failed. In 1894, Hoppe-Seyler processed chitin at 180°C in potassium hydroxide (deacetylation) and obtained chitosan, a product with reduced acetyl content. In 1934, two patents were obtained from chitosan for film production and fiber production. The same year, Chitosan fiber production, which was very well-orientated by Clark and Smith, was also successfully carried out [92]. Chitosan production stages are as follows; deproteinization, washing, demineralization, deacetylation, washing, decolouration, drying and milling [91]. Chitosan is simply obtained by deacetylation of chitin. It consists of D-glucosamine linked to N-acetyl D-glucosamine by β -1,4-glycosidic bond (see Figure 2.13).

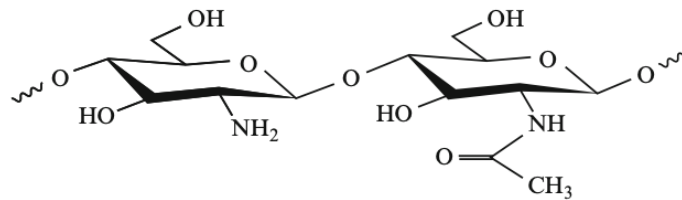


Figure 2.13: Chemical structure of chitosan [91]

In terms of applicability in building materials, the insolubility of the chitosan in alkaline media makes it more applicable in cement mixtures [93–95].

Lasheras-Zubiate et al. [95] reported the effect of the addition of chitosan to cement mortar. According to the research findings, chitosan biopolymer has been detected to increase viscosity. Thus, it has an effect of decreasing on the fluidity of the mortar mixture. This effect is found related with the chitosan biopolymer dosage. Also, when molecular weight increases, the thickening effect increases, as caused by increased entanglement and cross-linking between chains in a calcium-rich system. Additionally, set-retarding effect of chitosan in cement mortars is revealed. Ustinova and Nikiforova [96] studied on effect of chitosan on cement mortar. According to their test results, chitosan biopolymer addition in the cement compositions effected as reduction on the total volume of pores and pore distribution effected positively. Compared to polyethylhydrosiloxane synthetic polymer, it was found that there is no decrease in strength values on cement mortars with chitosan addition. The optimum chitosan amount to be added to the mortar was found between 0.6% and 1% by cement mass in order to achieve the desired freeze-thaw resistance. In addition, another important result obtained in this study is the decrease in fungal growth in chitosan added cement

mortars. Another usage area of the chitin in the building materials sector is concrete crack maintenance and remediation [97,98]. Kaplan et al. [99] examined the effects of chitin biopolymer replacement with cement on cement mortar. According to their test results, increase of the chitin ratio has a decreasing effect on the viscosity of fresh cement mortar. Thus, they suggested that use of chemical additives with chitin biopolymer was necessary. Although usage of chitin effects the compressive strength negatively, this phenomenon can be decreased by again using superplasticizer chemical additives. They explained the decrease in compressive strength with the decrease in fluidity; thus, void ratio in mortar increases.

2.2.2.6 Vegetable Oils

Vegetable oils are extracted from plants. They are mainly lipids. They consist of triglyceride molecules comprising of a glycerol molecules attached to three fatty acid chains [100]. In chemistry and biochemistry, fatty acid is usually a long, aliphatic-tailed carboxylic acid. Of the long carboxylic fatty acids, 4 carbons (butyric acid) and longer chains are counted as fatty acids. When talking about the fatty acids that make up natural oils (triglycerides), they can be assumed to be at least 8 carbons (such as caprylic acid). Most natural fatty acids have even numbered carbon atoms, because their biological synthesis uses acetate with two carbon atoms. In industrial production, fatty acids are obtained by hydrolysis of the ester bond in oils (triglycerides) and separation of glycerol. The unsaturation in the long fatty acid tail introduces a “kink” which decreases the strength of van der Waals forces between molecules. Thus, while stearic acid (see Figure 2.14) is a solid, oleic acid (see Figure 2.15) is a liquid at room temperature [101]. Some of other unsaturated fatty acids are linoleic (Figure 2.16) and linolenic acids (Figure 2.17) [101].

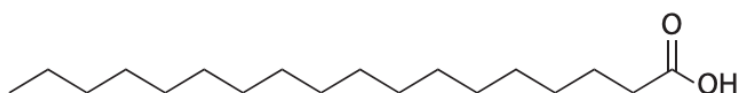


Figure 2.14: Chemical structure of stearic acid [101]

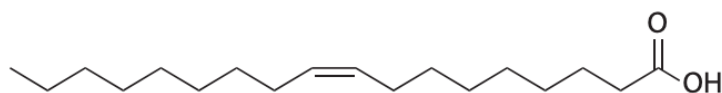


Figure 2.15: Chemical structure of oleic acid [101]

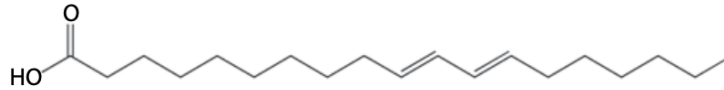


Figure 2.16: Chemical structure of linoleic acid [100]

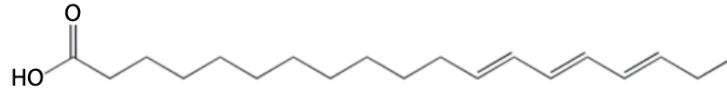


Figure 2.17: Chemical structure of linolenic acid [100]

In the building materials industry, fatty acids and their soaps/esters are especially used in the design of concrete and derivative materials thanks to their water repellent, energy storage auxiliary and air entraining properties. Oleates and stearates produced from renewable and natural source salts are hydro-repellent additives. They have ability of water solubility depending on the cations type, presence of unsaturated bonds and length of the organic chain [102]. Lagazzo et al [102] found that sodium oleate had an air entraining effect on cement mortar. They were also found that the water absorbed by the capillary effect decreased significantly compared to the control specimen. Albayrak et al. [103] have studied a different use of fatty acids in the building materials industry. They investigated the effect of fatty acids on the fineness of cement after grinding by adding different types of fatty acids to cement clinker. Test results showed that fatty acids using increased the fineness, when compared with the control cement. Oleic acid decreased the strength significantly, while Stearic acid increased it comparing with the control cement. Karaipekli and Sarı [104] stated that fatty acid ester/building PCM material composites have good thermal reliability and chemical stability even after 1000 heating and cooling cycling process. They have the ability to change their state with a defined temperature range (21.6–32.3 °C for melting and 14.5-29.5 °C for freezing) and can store and release large amounts of energy during phase change process. Cellat et al. [105] used fatty acids such as capric acid, myristic acid, lauric acid, and palmitic acid as PCMs by adding them directly to specific concrete mixtures. They claimed that PCMs developed in their work can be used for passive solar energy storage in buildings. However, some decrease in the compressive strength of concrete specimens was recorded. Cellat et al. [106] in another experimental work stated after SEM examinations on test specimens that the corrosion behavior of reinforcing bars was not affected by directly adding a fatty acid PCM in concrete. Thus, fatty acid PCM can be utilized safely for thermal energy storage in

reinforced concrete elements, according to them. There are other studies in the literature that fatty acids can be used effectively as PCMs because of their ability to easily change form from solid to liquid and liquid to solid [107–109]. Liu et al. [110] modified fly ash with oleic acid to improve hydrophobicity. They used modified fly ash in cement paste. According to contact angle photographs water contact angle of specimens increased as 39°, 65°, and 87°, respectively, with the increase of modified fly ash content.

2.2.2.7 Plant Extracts

Extracting some plants and using them in cement mortar has gained importance in recent years as environmental concerns and orientation towards natural materials. Examples of them could be given as okra extract and cactus extract. These types of natural materials are used in cementitious materials as low-cost and sustainable eco-friendly viscose biopolymer. Hazarika et al. [111] prepared biopolymers by extracting from 1 g vegetable using 10 mL water (1:10), 1 g vegetable using 20 mL water (1:20), 1:30, 1:40 and 1:50. They evaluated these materials with different concentrations in concrete and cement mortar. They concluded that the investigated bio-admixture has water retention capacity; they attributed this to the increase of the viscosity of the biopolymer and thus the cement mortar. In FT-IR examinations, they found the major polymeric constituents in the biopolymer as pectin, which is a vegetable polysaccharide. The biopolymer had a decreasing effect on slump value of concrete mixes due to the viscosity enhancing property of the bio-admixture. The bio-admixture addition drastically lowers the setting times of cement paste due to the formation of more amounts of hydration products. Also, bio-admixture decreased setting times due to an increase on hydration rate of cement particles. FTIR spectroscopic investigation indicates that the addition of bio-admixture enhances cement hydration rate; they explained the increase on the hydration rate with the interactions of pectin in bio-admixture with Ca^{2+} ions of cement paste. They also stated that compressive strength and durability performance of the tested specimens were enhanced. Chandra et al. [112] tested cactus extract from Mexico in cement mortar. They cut cactus leaves into thin pieces and were mixed with water in the proportion of 1:3 by mass. After two days, solid particles were eliminated from solution and gel-like solution was remained. From FT-IR analysis, they found that

cactus extract generally containing both proteins and polysaccharides. The workability of the mortar mix with cactus extract was found to be better than control mixture. According to them, this effect is provided by the polysaccharide from the extract, which reduces friction and increases smoothness. It was stated that cactus extract addition has an increasing effect on compressive strength of the specimens. According to XRD test results of their study, calcium hydroxide was consumed it has chemically reacted with some of the component of cactus extract and has made some calcium complexes. It was also observed that the water absorption values decreased significantly with the increase of cactus extract amount. Woldemariam et al. [113] made a research work to determine the suitability of plant extract (Blue Gum extract) as shrinkage reducing admixture for concrete. They prepare the extracts from the bark of blue gum tree by boiling the bark in water. They used 1kg of the bark boiled under pressure with four liters of water for two hours. They found that the use of plant extract reduced excessive loss of the moisture from the surface of the concrete by its ability of reducing surface tension. Also, the plant extract was effective in reducing the movement of water to surface by decreasing the surface tension in the capillary tube. They concluded that the plant extract has a capability of reducing early age cracks and hence, it can be used as shrinkage reducing admixture in concrete to reduce cracks.

2.2.2.8 Others

Poly-lactic acid is a bio-plastic material. It is preferred as a proper alternative to petroleum based chemical polymers such as PE, PP and PS due to its low-cost, non-petroleum polymer production and its accessibility [114]. PLA is derived from agricultural renewable resources such as cornstarch and sugar cane [115]. PLA is a semi-crystalline bio-polyester with biodegradable, hydrolysable aliphatic properties. It is formed by the direct condensation reaction of its lactic acid monomer, as the oligomer and followed by a ring opening polymerization of the cyclic lactide dimer [116,117]. Chemical structure of polylactic acid is given in Figure 2.18.

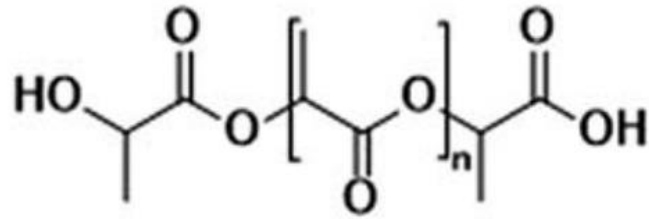


Figure 2.18: Chemical structure of polylactic acid [118]

Aliakbar Sayadi et al. have done a lot of experimental work in recent years on PLA's evaluation on lightweight and ultra-lightweight concrete as a lightweight aggregate [119–123]. They used expanded polylactic acid aggregate with 5 mm diameter and 35–43.5 kg/m³ bulk density. According to their studies results, interface bond between cement paste and PLA aggregate is relatively low. PLA aggregates are sensitive to alkaline environment and reduce PH value of concrete. Moist curing is an inappropriate way for concrete curing with PLA aggregates. However, very low concrete densities can be achieved (260–290 kg/m³) with PLA aggregates. Also, PLA addition has a positive effect on concrete thermal conductivity values. PLA aggregate was found as hydrophobic aggregates by them, hence water absorption of concrete specimens decreased with increase of PLA aggregate content.

Casein is a protein found in milk. It is a family of related phosphoproteins. It is obtained by acid precipitation from milk. It has high anionic charge density in alkaline environment because of de-protonation of amino acid molecules [124]. Casein includes amino groups, ketones, and hydrazine groups. Its chemical structure is shown in Figure 2.19.

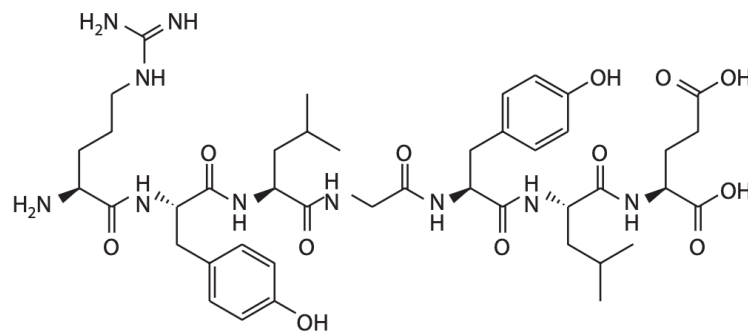
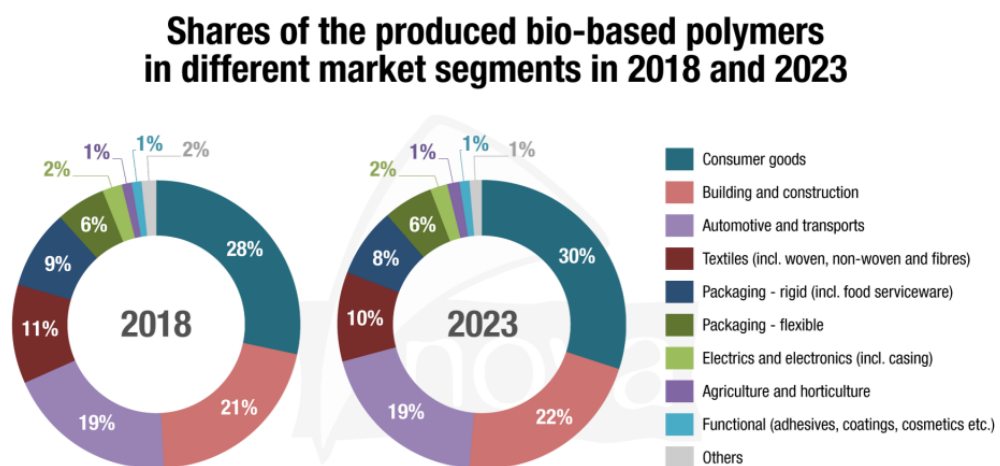


Figure 2.19: Chemical structure of casein [125]

Jagannathan and Parameswaran [124] added casein to concrete mix designs with a proportion of 0.25% and 0.75% weight of cement. According to test results, casein and fly ash gave higher strength and workability to the concrete specimens. They attribute the reason for this improvement in physical and mechanical properties to Chandra and Aavik [35] research finds that proteins bring hydrophobic properties to the concrete and also has a dispersion effect. Jasiczak and Zielinski [126] concluded that the powdered red blood cells protein industrially processed from pig's and cow's blood could be used as air entraining in cement mortars. Furthermore, there are studies on the usability of proteins in the literature as a foaming agent in foam concrete [127–129].

2.2.3 Use of Biopolymers in Other Construction Areas

Figure 2.20 shows the biopolymer consumption according to different markets. As can easily be seen in the figure, 21% of the worldwide biopolymers produced in 2018 have been used in the construction industry. However, most of them are epoxy resins, PA and PUR [130]. According to the observations obtained from the literature study, although biopolymers are mostly used in concrete and derivative products in the construction industry, there are other consumption areas, such as soil stabilization [131], soil strengthening [132] and additive for earthen materials [133].



All figures available at www.bio-based.eu/markets

© NOVA-Institute.eu | 2019

Figure 2.20: Biopolymer consumption according to different markets [130]

2.3 Literature Evaluation

In this study, a comprehensive literature research was conducted. Majority of existing literature shows that some biopolymers such as lignosulfonates, cellulose ethers, starch, etc. have been used in the cement matrix composites for a long time. However, these types of biopolymers are produced with some chemical processes. This can be considered as a separate financial burden. Recently, with the concern of sustainability and environmental protection, the use of waste or residue materials has gained an importance in the composite products. The literature review shows that the use of natural and/or bio-origin waste/residue materials rapidly increasing besides the traditional ones. Particularly, in the sector where concrete and its derivative cement products are used intensively today, the evaluation of waste materials provides a very effective waste control and recycling. According to the results of the literature study, it was observed that the majority of biopolymers evaluated in cementitious products were produced by chemical processes. It has been determined that some lignocellulosic materials are used in large sizes after pyrolysis, some are used after surface treatment, and sometimes extractives are used after extraction. Studies in which the shells of kernels of especially hard-shelled fruits are used are very limited. It has also been observed that these shells were pyrolyzed and then used in large sizes in studies carried out. Similarly, the use of olive pits in large-size cementitious products has been studied by some researchers. There is not enough literature information about the use of biopolymeric materials to be used in this thesis in fine-size, which can be an alternative to cement chemicals, and their effects on the physical and mechanical properties of the cement mortars.

The internal components of lignocellulosic materials examined in this thesis study are lignin, cellulose, hemicellulose, and extractive substances. These each substance are generally called biopolymer and it has been observed that they are used in cementitious products after the etherification process. The *biopolymeric* name is given to the material form after the material is converted into powder form without removing any of its lignin, cellulose, hemicellulose, or extractive components from the lignocellulosic materials. In the literature, there is a lack of studies that contain detailed information about the effects of materials in this form on cement mortar.

Moreover, with this study, very low cost, completely natural admixtures are proposed as an alternative to cement chemicals. Furthermore, formulaic approaches that simulate the change of physical and mechanical properties of cement mortars according to lignin, hemicellulose, cellulose, and extractive amounts of bio-polymeric admixtures (which are in composite structure consisting of lignin, cellulose, hemicellulose and extractives) are also presented in this study.

In this thesis, use bio-polymeric admixtures from waste materials as an alternative to cement chemicals in cementitious composite mortars was investigated. The effect of bio-polymeric admixtures on cement matrix composite mortar is a new research topic and there is very limited information about this subject in literature. For all these reasons, this thesis study is a pioneering research on the subject and will provide significant scientific added value to building materials technology and shed light on the development of innovative materials.

Chapter 3

Materials and Methods

3.1 Materials

3.1.1 Cement

TS EN 197-1 CEM I 42.5 R (42.5 N/mm²) Portland Cement (PC) was used as a binder throughout this study (Figure 3.1). Chemical composition of the cement is given in Table 3.1. X-ray Fluorescence (XRF) analysis was used to analyze the chemical content of the cement used [134]. By using the small pycnometer method, the specific gravity of cement was determined according to the ASTM C188 [135] standard. The fineness of the cement was determined by conducting the Blaine surface area test according to TS EN 196-6 [136] and given in Table 3.2.

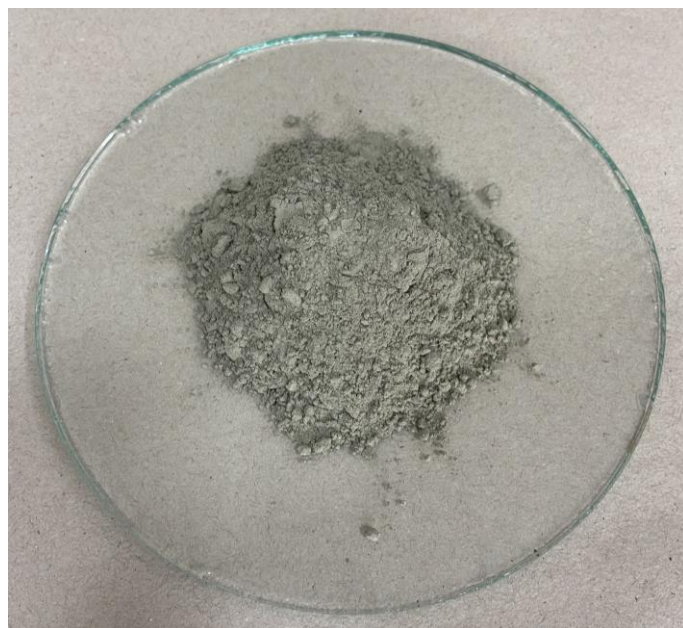


Figure 3.1: CEM I 42.5R Portland cement

Table 3.1: Chemical composition of PC

Major component	PC (%)
SiO ₂	20.05
Al ₂ O ₃	5.18
Fe ₂ O ₃	3.38
CaO	64.01
Na ₂ O	0.53
K ₂ O	0.84
MgO	1.55
LOI	2.01

Table 3.2: Physical and mechanical properties of PC

Specific gravity (g/cm ³)	3.12
Blaine specific surface area (cm ² /g)	3195
Initial setting time (min)	155
Final setting time (min)	245
Volume expansion (mm)	0.87
Compressive strength (MPa)	
2 days	20.8
7 days	33.4
14 days	39.3
28 days	43.4

3.1.2 Sand

The CEN (The European Committee for Standardization) standard sand in accordance with TS EN 196-1 [137] was used in cement mortar mixtures. Standard sand was supplied from the market in 1350 gr packages (Figure 3.2). Sieve analysis of the standard sand was given in Table 3.3.



Figure 3.2: CEN standard sand used in the mixtures of mortar specimens.

Table 3.3: Particle size distribution of CEN Reference sand.

Property	Grain size (mm)					
	0.08	0.16	0.50	1.00	1.60	2.00
Cumulative Retain (%)	98.4	87.8	68.4	33.7	7.5	0
Limit (%) [137]	99 ± 1	87 ± 5	67 ± 5	33 ± 5	7 ± 5	0

3.1.3 Mixing Water

To provide the hydration of cement based composite mortars prepared in this thesis, tap water in İzmir Katip Çelebi University Construction Materials Laboratory was used. Chemical analysis of the mixing water used is given in the Table 3.4. In the chemical analysis of the mixed water, it was seen that the water complies with the mixed water qualities in TS 1247 [138] and TS EN 1008 [139].

Table 3.4: Chemical analysis of mixing water

Parameters	Unit	Amount
pH		7.32
Chloride (Cl ⁻)	mg/L	27.21
Sulfate (SO ₄)	mg/L	41.91
Sodium (Na)	mg/L	28.32
Aluminum (Al)	mg/L	4.98
Magnesium (Mg)	mg/L	6.95
Calcium (Ca)	mg/L	48.49
Zinc (Zn)	mg/L	-
Copper (Cu)	mg/L	1.81
Iron (Fe)	mg/L	48.15
Lead (Pb)	mg/L	0.25
Nitrate (NO ₃ -N)	mg/L	15.90
Free chlorine (ClO ₂)	mg/L	0.4
Total chlorine (ClO ₂)	mg/L	0.51

3.1.4 Chemical Admixtures

In this study, in order to compare the effects of bio-polymeric admixtures on the physical and mechanical properties of cement mortars, water-repellent, superplasticizers and set retarder chemical admixtures currently used in cementitious

products were supplied and used separately in cement mortars and their effects on the physical and mechanical properties of cement mortar were examined.

3.1.4.1 Polycarboxylate Type Superplasticizer

The polycarboxylate type superplasticizer used in the study was commercially available and in powder form. This superplasticizer is polycarboxylate ether (PCE) powder, soluble and flowable powder, and formaldehyde free. The PCE type superplasticizer used in the study is presented in the Figure 3.3. The main function of PCE is to disperse the cement particles. Also, these admixtures reduce the surface tension of the water so that water can travel around the cement particles more easily thereby improving the consistency of the cement mortar.

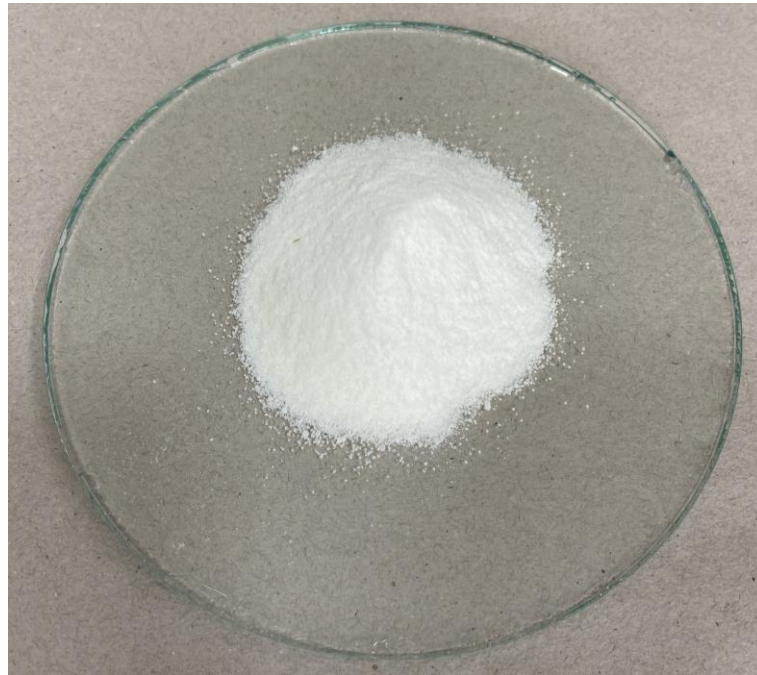


Figure 3.3: PCE superplasticizer

3.1.4.2 Sulfonated Melamine-Formaldehyde Type Superplasticizer

The dispersing agent sulfonated melamine-formaldehyde (SMF) is a powder product based on sulfonated melamine. The SMF type superplasticizer used in the study is white powder form and its general view is presented in the Figure 3.4. Although the efficiency level of SMF type superplasticizers is not as much as PCE's, they also provide a good consistency level to the cement mortar by ensuring the dispersion of cement particles, similar to the working system of PCEs.

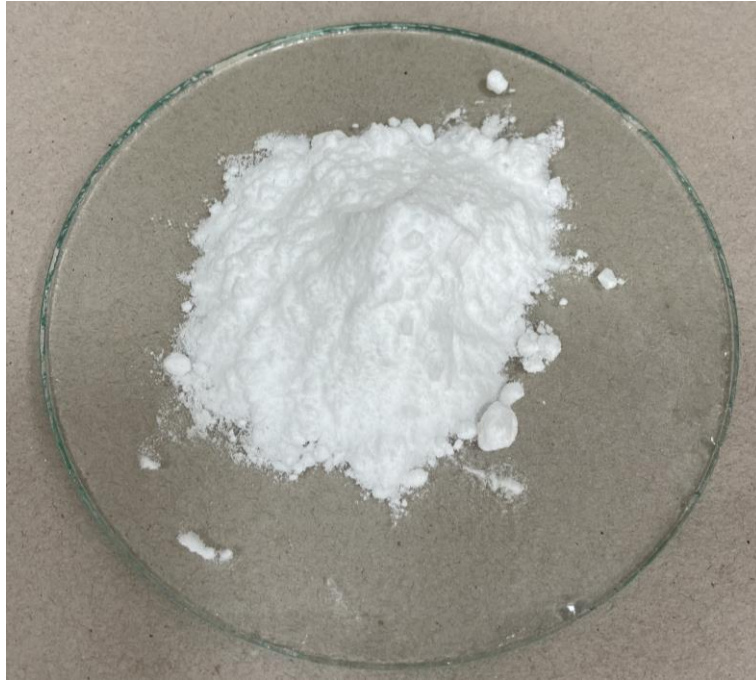


Figure 3.4: SMF superplasticizer

3.1.4.3 Water-Repellent Admixture

Hydrophobicity of the cement mortar after hardening was investigated by adding a water-repellent chemical admixture in certain proportions to the mortar mixtures. Calcium stearate was used as the water-repellent agent (Figure 3.5). It is commercially available and in white powder form. Calcium stearate is a water-proofing admixture which can provide a water-repellent layer along the capillary pores. As a result, it can reduce permeability of cementitious products.

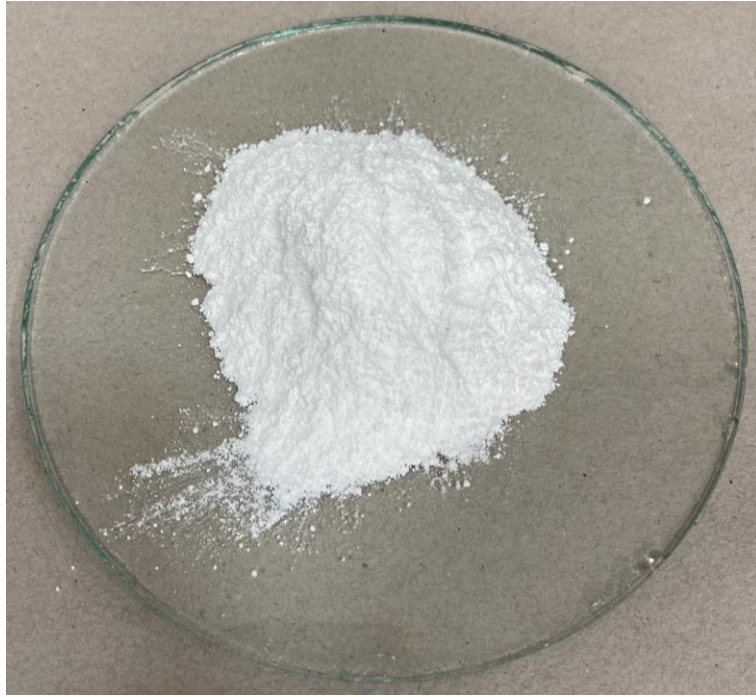


Figure 3.5: Calcium stearate water-repellent admixture

3.1.4.4 Set Retarder

Set retarders are chemicals that generally slow down the rate of early hydration of C_3S and C_3A . Therefore, the rate of heat liberation is reduced. In this study, tartaric acid was used as a setting retarder chemical. Tartaric acid is the most effective at retarding C_3A hydration and ettringite formation [140]. The tartaric acid used in this study is in the form of white, fine granule, crystalline powder. It is odorless, tastes like acid and stable in air. Its general view is represented in the Figure 3.6.

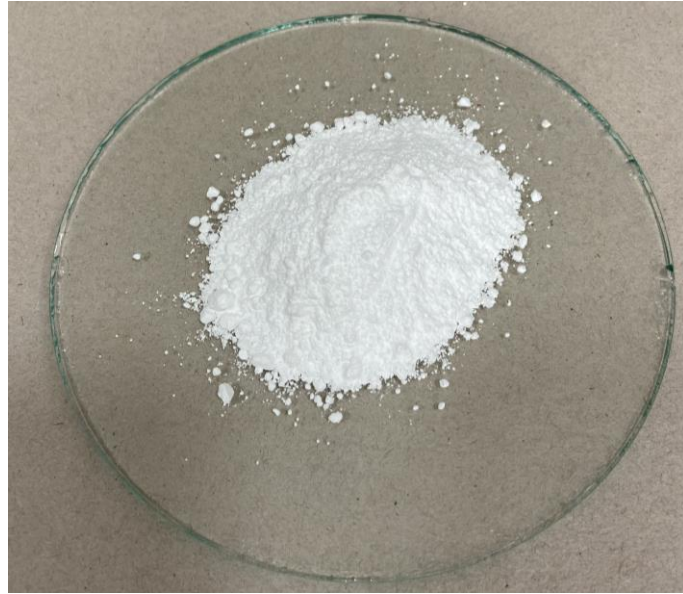


Figure 3.6: Tartaric acid setting retarder admixture

3.1.5 Bio-Polymeric Admixtures

In this thesis, the shells of four different fruit kernels that are known to contain mostly *extractives*, *lignin*, *hemicellulose*, and *cellulose* are used. These lignocellulosic materials are olive seed, apricot kernel shell, hazelnut shell and walnut kernel shell. In addition, eggshell consisting of high levels of calcium carbonate, which are also known to contain protein, is also included as a bio-polymeric admixture due to its protein content in the study. These materials occur quite frequently as waste in food processing plants and household consumption. In addition, the proteins, extractives, lignin, and cellulose in the content of these waste materials are frequently used as biopolymers in the building materials sector. However, with one difference, these types of biopolymers are used in the composition of cementitious products after being separated from the main material and passed through some chemical processes. These components were actually used in certain proportions in the cement mortars, without separating them from each other (in a way that can be considered as a composite structure). The composite structure consisting of these biopolymers is called as “*bio-polymeric admixture*” in this thesis study.

3.1.5.1 Egg Shell

The bird egg is a fertilized gamete located on the yolk surface and surrounded by albumen (i.e., egg white). Egg white is surrounded by two shell membranes (inner and

outer membranes), and above them is the shell. The chicken eggshell consist of 95-97% [141] calcium carbonate crystals, which are stabilized by a protein matrix [141–143]. The crystal structure of egg shell would be too brittle to keep its form without the protein. The protein matrix consists of proteins, glycoproteins, and proteoglycans [144]. SEM image of cross-fractured chicken eggshell is shown in Figure 3.7.

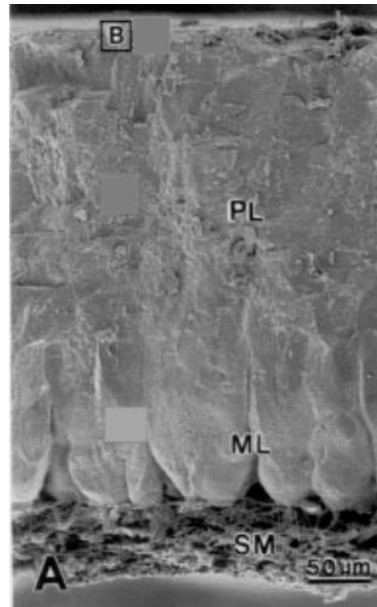


Figure 3.7: SEM image of cross-fractured chicken eggshell [144]

Shell membranes (SM) consist of inner shell membrane and outer shell membrane. There is mammillary layer (ML) on it. There is also palisade layer (PL) on the mammillary, and the surface consists of cuticle (B) [144]. Lysozym and ovocalyxin-32 protein are found in the cuticle layer of the shell. Collagens are found in the shell membranes layer of the shell. Some ovocleidin and ovocalyxin derivative proteins, and serum albumin are found in the mammillary and palisade layers [141].

The egg is one of the most consumed foods in the world. Depending on this, too much waste eggshell is generated. Therefore, the effectiveness of transforming the eggshells into useful products becomes an idea to explore. In the literature, eggshells have been used in various applications in concrete and in soil improvement applications. The studies in the literature on use of eggshells in construction sector are as follows:

Gowsika et al. [145] investigated the partial replacement of cement with eggshell powder in concrete. They tried to replace the cement with eggshell powder as 5% and they use saw dust ash, fly ash and micro silica admixtures.

Dhanalakshmi et al. [146] investigated the mechanical properties of eggshell concrete with partial replacement of cement. Eggshell powder replacement with cement was varied up to 12.5% in their experimental research. In 2.5% and 5% eggshell use, the compressive, tensile, and splitting tensile strengths of the samples were lower than those of the control samples. However, when using 7.5% eggshell, these strength values were higher than control strength. In the case of using eggshell beyond this value, the strength values showed a decreasing tendency again.

Karthick et al. [147] made a study on partial replacement of eggshell with sand in concrete. They used replacement ratios as from 10% to 50%. They observed a decreasing trend on flexural and splitting tensile strengths of the concrete samples, while eggshell amount was increasing. However, compressive strength of the concrete samples with 20% of eggshell replacement passed slightly the compressive strength of control concrete sample. Thereafter, a decrease in the compressive strength was observed.

Beraldo [148] used eggshell particles on partial replacement with sand in cementitious composite mortar. He detected a decreasing ratio on compressive strength parameter, while sand/eggshell ratio was increasing.

Sivakumar and Mahendran [149] used fly ash, rice husk ash and eggshell powder in concrete and they determined the strength and permeability properties of this concrete.

Kalkan and Gündüz [150] used powdered egg shells and acrylic esters terpolymer to improve physical and mechanical performance of composite cement mortars. According to their test results, up to 0.75% ESP and 0.75% acrylic esters terpolymer usage ratio, densities, compressive strength, and ultrasonic pulse velocities of the samples increased. In the microscopic scale studies, it was determined that the porosity in the matrix structure decreased due to the increase in the amount of admixtures.

According to Yerramala [151], cement replacement with 5% eggshell powder (max. grain size of 90 μm) has an increasing effect on mechanical properties of normal weight concrete. The reason for this is explained by the author as; the formation of calcium mono-carboaluminate hydrate phase as a result of the combination of calcium, which is abundant in the eggshell, and the alumina in cement.

Yu et al. [152] replaced cement with eggshell powder (max. grain size of 90 μm). They concluded that up to 15% replacement of cement with eggshell powder in concrete increased the compressive strength of the concrete specimens. Also, they compared air curing and water curing effects on eggshell concrete, and they found that water curing increased the compressive strength values of specimens higher than air curing. Also, they explained the reason of compressive strength enhancement with addition of eggshell as the filler effect of the eggshell and extra calcium hydroxide for the formation of the secondary C-S-H gel.

In this study, three different sizes of ground eggshell (ES) were used and the appearance of the material in each grain size is given in Figure 3.8.

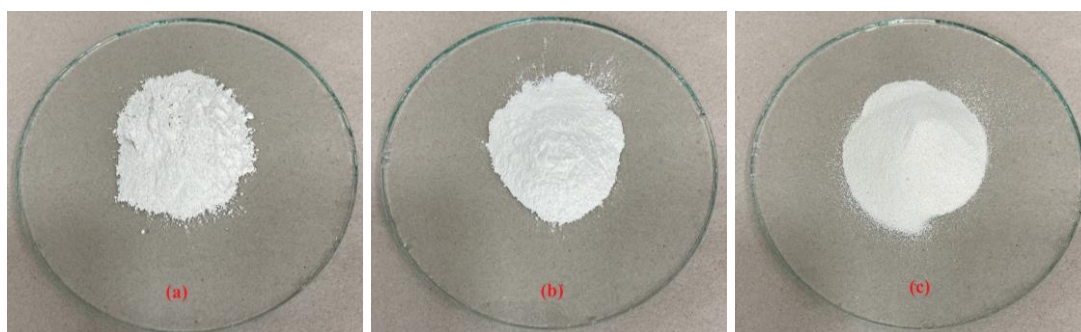


Figure 3.8: 0/45 μm ES (a), 0/125 μm ES (b), 125/250 μm ES (c)

3.1.5.2 Apricot Kernel Shell

The majority of apricots grown in the world are *Prunus armeniaca* type apricots. Central Asia, Afghanistan, Kashmir, Iran, Turkey, and the Trans-Caucasus has been established with seedlings grown from seed, apricot orchards are spread over large areas of valuable genetic resources available in these regions. According to 2019 data [153] there are 17.27 million apricot trees in Turkey. 846,6 thousand tons of apricot fruit was produced from these trees in 2019 in Turkey. Flesh-stone ratio ranges from 11/1 to 15/1 of apricot fruit grown in Turkey [154]. This account for approximately 10% of the total fruit mass [155]. Apricot kernel shell consists of hemicellulose (21.76 %), lignin (38.30 %), cellulose (34.60 %) and a small amounts of 2.80 % extractives [156].

Apricot shells are commonly considered as waste and burnt as fuel in the region where apricot are cultivated [157]. At present, apricot shells are mainly used as raw materials

for soil amendment, biomass fuel and activated carbon [158]. They used for bio fuel and clean gas suitable for power generation [159–161]. In addition, apricot shells are used to develop new adsorbents such as the activated carbon to remove pollution from water [162–164]. Using this waste material is to make something discarded valuable. An alternative way to use apricot shells would be the production of new composites by blending it with concrete or cementitious products [165].

Wu et al. [158] studied the mechanical and creep performance of apricot shell added concrete specimens. They used grain size distribution of apricot shell between 2.75 mm and 4.75 mm as lightweight aggregate and replaced normal aggregate with the lightweight aggregate. They observed that the slump values decreased with the increase in apricot shell due to a larger flakiness of apricot shell aggregate. The density values of concrete specimens also showed a decreasing trend as expected. They also observed that strength values of test samples decreased. They attribute the reason for this decrease to both low strength apricot shell aggregate and weak bond between apricot shell aggregate and cement matrix in interfacial transition zone. When the apricot shell content increased gradually, the strain of concrete containing apricot shell also increased. Wu et al. [166] in another study, they used the mixture of peach kernel and apricot kernel, they obtained similar results with Wu et al [158]. Also, Yıldız et al. [165] carried out an investigation about replacement of coarse aggregate with apricot shells in concrete. They also get similar findings with Wu et al. [158].

Wu et al. [167] investigated the effect of different surface treatment of apricot shell on performance characteristics of lightweight bio-concrete. They made five different surface treatments to apricot shells: with cement solution, waterproof agent, sodium silicate, white latex and wood oil. They stated that the purpose of the surface treatment process is to improve the mechanical properties and resistance to chemical attack of concrete by forming a film layer on the surface of aggregates, which could reduce the moisture transfer through porous organic aggregates and prevents the leaching of sugar. According to the test results, when the apricot shell aggregate was treated with waterproof agent, it had better surface characteristics and a good bond to the cement matrix interface, and no microcracks were observed between the aggregate and the cement matrix. Therefore, the waterproof treatment is a good method to improve the surface characteristics of apricot shell aggregate, according to the authors. The authors

concluded that waterproof and calcium silicate treatments reduced the porosity of concrete. Thus, they blocked the capillary pores, which reduced the uptake of water and therefore, reduced the magnesium sulfate attack in magnesium sulfate solution.

Wu et al. [158] utilized carbonized peach shell, carbonized apricot shell, peach shell and apricot shell on physical and mechanical properties of lightweight aggregate concrete (LWAC). Results showed that the replacement of raw aggregates peach shell and apricot shell with carbonized aggregates reduced the density, water absorption and open porosity. Also, the mechanical properties with carbonized organic aggregate presence were significantly enhanced, and the carbonized apricot shell mixture obtained the highest mechanical strength.

In this study, three different sizes of ground apricot kernel shell (AKS) were used and the appearance of the material in each grain size is given in Figure 3.9.

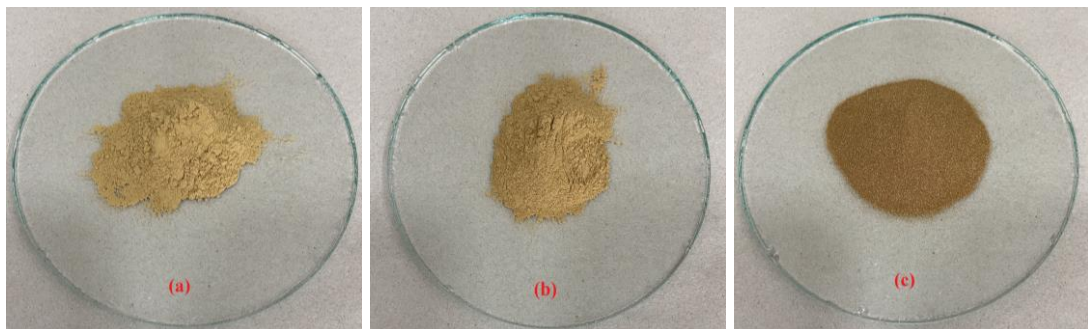


Figure 3.9: 0/45 μm AKS (a), 0/125 μm AKS (b), 125/250 μm AKS (c)

3.1.5.3 Hazelnut Kernel Shell

Hazelnut tree can be grown particularly in the Black Sea Region. Hazelnut is an important nutrient source for human life because of its nutritional value. Hazelnut shell consists of 36 % cellulose, 12.66 % hemicellulose, 40.14 % lignin, 7.86 % extractives and 3.11 % proteins [168]. According to the average of the last ten years, the Black Sea Region provides about 70 % of world production with 550.000 tons/year of hazelnut production [169]. In Turkey, Giresun has 60.3 %, Ordu 57.8 %, Trabzon 32.1 %, Bolu 24.3 %, Sakarya 17.6 %, Zonguldak 9.2%, Artvin 7.3 % and Samsun 6.2 % of total crop hazelnut production value. Table 3.5 shows the distribution of the world hazelnut production based on the producer countries for year 2016 [170].

Table 3.5: Top 5 hazelnut producer countries.

Country	Hazelnut Production (Tones)
Turkey	420000
Italy	120572
United States of America	34473
Azerbaijan	33941
Georgia	29500
Others	104969

With such a large amount of production, similar large amount of waste hazelnut shells accumulates every year. The use of biomass, which can be considered as waste hazelnut shell remaining from hazelnut production, is generally burning the waste shells for electricity or heat energy production purposes. In developed countries such as Italy, Germany and USA, hazelnut shells are used in contralite products and paint industry. In addition, the pentosan in which furfural and furfuryl alcohol are obtained in petrochemicals is found in hazelnut shell in 25-30%. Briquette charcoal, activated charcoal and industrial charcoal are obtained from the hazelnut shell by means of charring method [171]. In addition, researchers from different countries have explored the different possibilities of using hazelnut shells in the construction sector, particularly in terms of building materials.

Khushnood et al. [172] investigated the effect of pyrolyzed peanut and hazelnut shells on the mechanical properties and electromagnetic interference shielding of cementitious materials. They found that 1 wt.% addition of carbonized peanut shell or hazelnut shell to cement paste increased the cement matrix's flexural strength and toughness. Also, 0.5 wt.% addition gave better electromagnetic radiation shielding effect than reported in the literature for carbon nanotubes. In the literature, there are also sources provided by other researchers that the pyrolyzed hazelnut shell increases the strength of the cement [172,173].

Gürü et al. [174] investigated the improvement of fire and water resistance of urea-formaldehyde-based particleboard from grained hazelnut shells.

Demirbaş and Aslan [175] reported the experimental research findings about the use of ground hazelnut shells in a cement mortar. According to the research findings, they

concluded that hazelnut shell addition (2.0, 5.0, 7.5 and 10.0 wt.%) decreased the compressive and flexural strength of the cement mortar. The developing idea of evaluating natural materials and/or natural waste materials at the production stages around the world has led to the idea that vegetable wastes with different origins can be used in cement-based products.

In this study, three different sizes of ground hazelnut kernel shell (HKS) were used and the appearance of the material in each grain size is given in Figure 3.10.

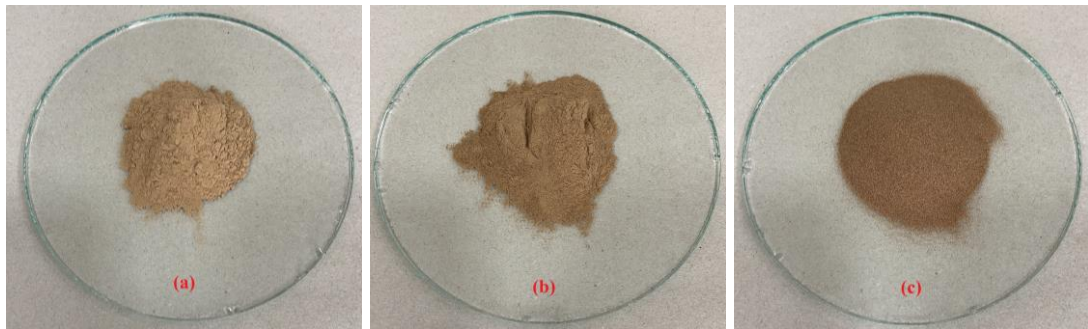


Figure 3.10: 0/45 μm HKS (a), 0/125 μm HKS (b), 125/250 μm HKS (c)

3.1.5.4 Walnut Kernel Shell

Turkey has an important place in walnut production in the world. According to data from 2019 [176], there are 11.25 million walnut trees in Turkey. 225 thousand tons of walnut fruits are produced from these trees in 2019. The walnut fruit mainly consists of four parts, which are the kernel, the skin, the shell, and the green husk. Walnut shell comprises 67 % of the total weight of the fruit [177]. Based on this information, it could be emphasized that approximately 150 thousand tons of waste walnut shells appear every year in Turkey. Walnut shell is an annual agricultural waste, which is the ligno-cellulosic material forming the thin endocarp of the walnut fruit. Farmers harvest the kernel of fruit and burn or otherwise dispose the residues (shell, husk, stalks, etc.). Also, burning agricultural residues causes serious environmental problems [178]. Shell of the walnut kernel is formed by basically four substances, cellulose (23.9%), hemicellulose (22.4 %), lignin (50.3 %) and ash (3.4 %) [179]. Walnut shell is an abundant agricultural waste with good stability, large specific surface area, high mechanical strength, good chemical stability and easy regeneration [180]. Because of the lower quantities of hygroscopic (cellulose and hemicellulose) components and higher quantities of hydrophobic (lignin) components in walnut shells, polymer-based

composite materials containing walnut shell fillers have significant commercial benefits in outdoor products with high environmental resistance, such as flooring or fencing [49]. Also, walnut shell has been successfully used in the removal of heavy metals in wastewater such as cesium, copper, chromium (VI), zinc and mercury by adsorption [181–183]. Besides, walnut shell media can be used to remove oil from wastewaters due to its good adsorption capability [184].

Hilal et al. [185] studied walnut shell (max. size of 12.5 mm) replacement with coarse aggregate at different ratios (5 %, 10 %, 15 %, 20 %, 25 %, 30 %, 35 %, 40 %, 45 % and 50 %) by volume in lightweight self-compacting concrete. According to their test results, walnut shell caused to reduce slump flow diameter of self-compacting lightweight concrete specimens. The main reason of this reduction was attributed to the irregular shape and absorption ability of Walnut shells by the authors. Compressive strength values reduced from 57 MPa at reference mixture at 0 % to 26 MPa at mixture at 50 % of walnut shell. The reason in this reduction was attributes to weak bond between WKS particles and surrounding cement matrix.

Cheng et al. [186] investigated replacement of normal coarse aggregate with walnut shell (5/10 mm) in production of lightweight wet-mix shotcrete. The more reduction in compressive and splitting strengths was observed and the decrease in slump and pressure drop by increasing the amount of walnut. However, it is also observed that shootability of fresh concrete with low rebound rate and larger build-up thickness were improved.

Kamal et al. [187] studied walnut shell for partial replacement of fine aggregate in concrete. They concluded that up to 30% walnut shell could replace with fine aggregate in concrete that results acceptable compressive strength, lower density and water absorption compared to Portland cement concrete.

In this study, three different sizes of ground walnut kernel shell (WKS) were used and the appearance of the material in each grain size is given in Figure 3.11.

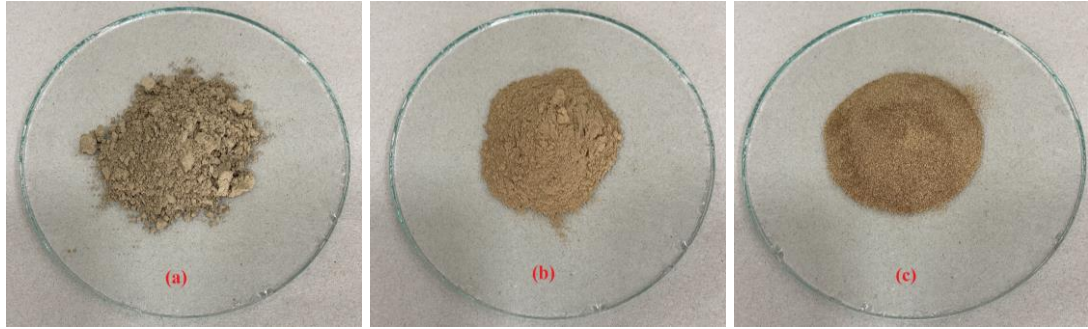


Figure 3.11: 0/45 μm WKS (a), 0/125 μm WKS (b), 125/250 μm WKS (c)

3.1.5.5 Olive Seed

Olive (*olea europea L.*), a Mediterranean vegetable, has the potential to spread in almost all the countries surrounding the Mediterranean. Olive, which can be grown even in the worst soil conditions, is also called the first tree of the nature. As a fruit, olives first become green, then it gets a shiny black color after it matures. The olive fruit consists of stem, 1-3% shell (epicarp), 70-80% fruit flesh (mesocarp), 18-22% stone (endocarp) and 2-6% seed. The epicarp layer forming the olive shell area is composed of chlorophyll, carotenoid and anthocyanin that determine the olive color. Effective part, in other words mesocarp is an important source of food consumed by people in daily life. The stone part of the olive, which is the endocarp, is the woody and the fibrous part which also covers the inside of the core that is seed [12].

Olive is a very important food source for human life. According to the 2015 data, 98% of the olive trees, reaching 900 million in the whole world, are located in the Mediterranean region, where Turkey is also located [188]. According to TurkStat data, in 2019 [189], from a total of 182 million olive trees in Turkey, 1.52 million tons of olives is produced for the same year. This production was used for the production of 415 thousand tons of table olives and 1.11 million tons for the production of olive oil [189]. Therefore, it can be observed that at least two different solid wastes are produced from olive consumption in Turkey as in the any other olive producer country. From the consumption of table olives, olive stone is produced as waste, and olive pomace is produced by the olive oil production plants as a waste material. Approximately 40-55% of an olive fruit is olive juice, 18-32% is fat and 14-22% is stone [190]. Based on this information, each year only at homes in Turkey, at least between 60 thousand and 95 thousand tons of waste olive stone is produced.

Olive pit is a lignocellulosic material which is composed by cellulose (37.5 wt.%), hemicelluloses (26 wt.%) and lignin (21.5 wt.%) and other components include moisture (8 wt.%), minerals (1 wt.%), proteins, pectins and tannins, etc. [191]

There are number of studies in the literature about the use of olive pomace formed by the pelletization of waste olive, olive stone, and olive leaves remaining in olive oil production in various sectors and products. The use of this biomass, which can be described as olive stone and/or olive pomace remaining in the production of olive oil, is generally burned with electricity or heat energy production purposes. Researchers have also conducted studies on other potential uses of this waste material, such as activated carbon, furfural production, fillers in plastics production, abrasives, cosmetics, biosorbents, animal feed and resin formation [191,192].

There are a few studies in the literature about the use of olive wastes in construction sector and building materials products:

Alkheder et al. [193] have conducted a study on the use of waste olive ash produced by burning of the waste from the production of olive oil in cement paste. In this study, waste olive ash was replaced as ratio of 3%, 6%, 9%, 12% and 15% by weight with cement. It was observed at the end of the study that the mortar's initial and final setting times were extent, as the amount of waste olive ash in the cement paste increased. In addition, the increase in the amount of waste olive ash has caused the compression strength to decrease and the flexural strength to decrease.

La Rubia-Garcia et al. [194] conducted a study on the use of crushed and wet olive wastes from the operation of two-phase olive oil production plants as pore-forming agent in the production of heat-insulated bricks. In this study, olive wastes containing approximately 62% moisture were added directly to the brick mortar as 5%, 10%, 15%, 20% and 25%. As a result of the research, olive oil process wastes in the wet state formed pores in the brick mortar and the unit weight of the mortar decreased with the increase in the waste rate. Furthermore, as the waste rate increased, a significant decrease in the thermal conductivity value of the hardened mortar was recorded.

In their work, Barreca and Fichera [195] have used the residual and relatively low-moisture olive wastes from the three-phase olive oil production process to improve the thermal insulation properties of the waste in the cementitious mortar after natural

methods of drying of the wastes. As a result of the study, it was concluded that the use of olive waste significantly reduced the thermal conductivity of the mortar.

Cuenca et al. [196] carried out a study on the use of olive fly ash that is produced by burning of the waste olive pellets, as a filling material in the production of self-compacting concrete. In their work, they compared the fly ash produced from waste olive pellets with conventional filler materials. According to the laboratory test results, the compressive strength values of olive fly ash filled concrete were determined to be the same or slightly higher than the compressive strength value of the reference sample. The self-compacting characteristics of olive fly ash filled concrete specimens gave similar results to the self-compacting characteristics of reference samples.

Eisa [197] studied the effects of replacing silica fume, fly ash, olive stone ash and corn cob ash with cement on concrete in separate mixtures. As a result of the study, they have observed that the olive stone ash has greatly increased the workability of the concrete. Compared to the reference sample, they found a 200% increase in the slump values of the concrete samples containing olive stone ash. However, the olive stone ash has a negative effect on the compressive strength values of the concrete specimens, thus reducing the compressive strength values up to 75%.

As can be observed from the literature review, there are various uses of olive stone ash, which is obtained by burning olive waste, in the production of cementitious products in the construction sector. However, the effect of the olive stone ash on concrete and/or mortar's compressive strength does not reach the desired levels since the olive wastes has low pozzolanic value due to low silica content [197]. If the sum of iron oxide (Fe_2O_3), Silicon dioxide (SiO_2) and Aluminum oxide (Al_2O_3) is more than 70% after chemical analysis according to ASTM [198], the material can be named as a pozzolanic material. As can easily be calculated from the Alkheder et al.'s work [193], the sum of iron, aluminum and silicate oxides is much less than 70%. This also indicates that the pozzolanic effect of the olive waste ash is not present.

In this study, three different sizes of ground olive seed (OS) were used and the appearance of the material in each grain size is given in Figure 3.12.

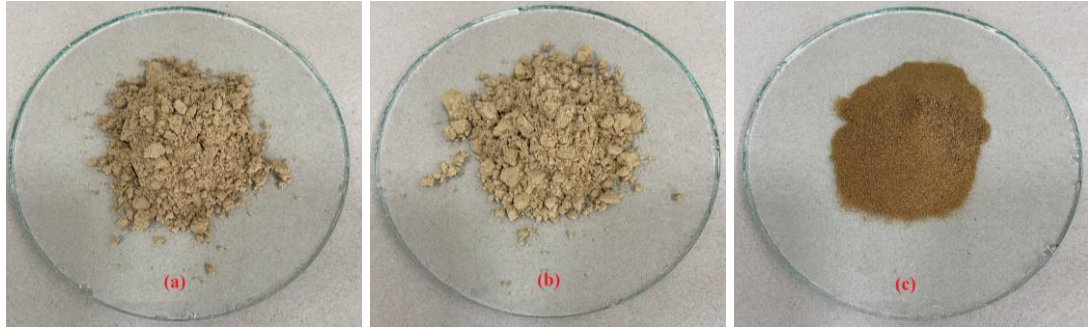


Figure 3.12: 0/45 μm WKS (a), 0/125 μm WKS (b), 125/250 μm WKS (c)

3.2 Methods

In the execution of the thesis, a work program consisting of six main stages was followed. The research content of these stages is summarized below, respectively.

In the first stage of the study, a preliminary study was carried out. It was aimed to improve compressive and flexural properties of composite cement mortar by using different materials such as ground and sized corn cob, egg shell, walnut kernel shell, apricot kernel shell, olive pomace, mallow, hazelnut kernel shell, rice husk and olive seed. It was tried to understand which or which of these waste materials could be used in harmony with cement mortar. Among these waste bio-polymeric materials, it has been determined that egg shell, apricot kernel shell, hazelnut kernel shell, walnut kernel shell and olive seed can be used in cement mortars.

In the second stage of the study, the characterization of the bio-polymeric materials was carried out by SEM, XRD and FT-IR analyzes.

In the third stage, these bio-polymeric admixtures were sized at 0/45, 0/125 and 125/250 μm grain sizes and evaluated at 0.25, 0.35, 0.50, 1, 1.5% of the total weight in cementitious mortars. The effects of bio-polymeric admixtures on flowability, setting time, water absorption, 28-day flexural strength and 7-, 28-, and 150-day compressive strength of cement mortars were investigated in detail. As a result of the analysis, the most effective particle size was determined. Also, the physical and mechanical properties of cement mortars using the selected grain size bio-polymeric admixtures and commercially available cement chemicals were analyzed comparatively. It has been investigated whether bio-polymeric admixtures can be used instead of cement chemicals.

In the fourth stage, the microstructure and hydration process of cement mortars, in which bio-polymeric materials with the most effective particle size were used as admixtures, were determined by SEM/EDS and XRD analyzes, respectively.

In the fifth stage, durability properties such as sulfate attack, acid attack and freeze-thaw were determined on the test specimens.

In the sixth and last stage of the study, an optimization of the use of bio-polymeric admixtures in composite cement mortars was carried out. Grey relation analysis was used for the optimization. Also, multiple regression analysis was carried out for mathematical representation of the effects of bio-polymeric admixtures on cement mortar performance parameters.

3.2.1 Preliminary Study

In the beginning of the study a preliminary work was planned on several different bio-polymeric admixtures. With these admixtures, the compressive and flexural strengths of the cement mortar were determined. In the preliminary study, bio-polymeric materials with more positive results were selected and the characterization of these materials, which was the second stage of the study, was performed.

Before starting the thesis research studies, the preliminary study was organized to test the compatibility of various organic materials supplied with cement mortar. In this preliminary study, cement, sand, and ground bio-polymeric materials were mixed in certain proportions, cured in water for 28 days, and finally the compressive and bending strengths of these samples were determined. As a result of physical observations during curing periods and strength results after curing, the thesis study was continued with some of these bio-polymeric materials.

In this thesis, TS EN 197-1 [199] CEM I 42.5R (42.5 N/mm²) Portland cement (PC) was used as the binder material. All specimens produced within the scope of this study were prepared using CEN standard sand in accordance with TS EN 196-1 [137] standard. In this doctoral thesis, it was aimed to improve some of the properties of composite cement mortar by using different materials such as ground and sized corn cob, egg shell, walnut kernel shell, apricot kernel shell, olive pomace, mallow, hazelnut kernel shell, rice husk and olive seed. Most of these materials are leftovers

from food production or household consumption. In the beginning of the experimental work, it was tried as a preliminary study that which or which of these waste materials could be used in harmony with cement mortar. Among these waste bio-polymeric materials, it has been determined that egg shell, apricot kernel shell, hazelnut kernel shell, walnut kernel shell and olive seed can be used in cement mortars. The mortars in which other materials were tested cracked significantly during the water curing phase after the prismatic specimens were produced and/or became unusable in terms of their 28-day compressive and flexural strength. For this reason, the studies were constructed based on five different bio-polymeric additives: egg shell, apricot kernel, hazelnut shell, walnut shell and olive kernel.

In the preliminary study, nine different organic materials were decided to select and tested. These organic materials were corn cob, egg shell, walnut kernel shell, apricot kernel shell, olive pomace, mallow, hazelnut kernel shell, rice husk, and olive seed bio-polymeric admixtures.

The cement, sand and water as introduced in Section 3.1 were used to prepare the specimens in the preliminary study.

3.2.1.1 Preparation of the Bio-polymeric Admixtures

First of all, organic materials separated from unwanted macro components. Then, all of them left to air dry for 2 weeks. All bio-polymeric admixtures were then grinded with a blade mill (Figure 3.13).



Figure 3.13: Blade mill

All organic waste types are sieved through 45, 125, and 250 μm sieve by using a sieve shaker (Figure 3.14). All bio-polymeric admixtures were ground to 0/45 μm , 0/125 μm and 125/250 μm grain size distributions.

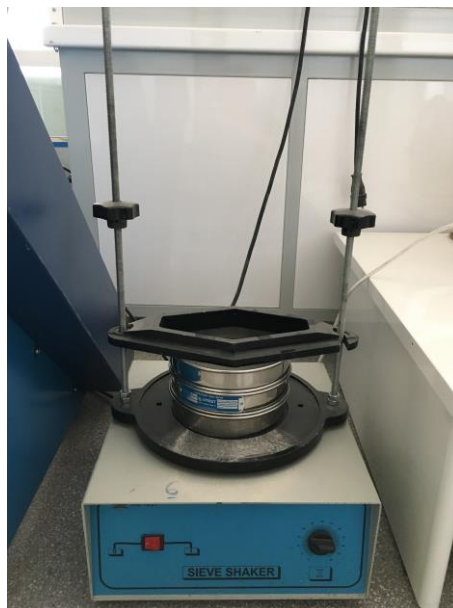


Figure 3.14: Sieve shaker

3.2.1.2 Mix Design

In this experimental preliminary study, different mixing ratios are designed to examine the effect of a bio-polymeric admixtures in cement mortars. In addition, in order to examine the effects that may arise from the use of bio-polymeric admixtures correctly,

a separate mixture without bio-polymeric admixture was designed as a control mixture. The mixing ratios are made according to the design methodology and related standards specified in TS EN 196-1 [137]. All the bio-polymeric materials used in the preliminary study were used in 0/125 μm size.

Mortars were prepared containing one part of cement to three parts of standard sand by weight. Corn cob (CC), egg shell (ES), walnut kernel shell (WKS), apricot kernel shell (AKS), olive pomace (OP), mallow (M), hazelnut kernel shell (HKS), rice husk (RH), and olive seed (OS) bio-polymeric admixtures were added to separate mix design with 0.5, 1.0, and 1.5 wt.% of total amount. The reference mortar has the required workability at w/c of 0.50. This w/c was maintained for all admixed mortars.

3.2.1.3 Flexural Strength

Flexural strength is a measure of cement based materials to resist failure in bending. The flexural strength of hardened composite mortars is determined by three point loading of the prism specimens. Size of prismatic specimens was 40x40x160 mm. The flexural strength tests were conducted according to TS EN 196-1 [137] standard. For flexural strength, prismatic specimens were tested by a 30 kN capacity flexural strength test device shown in Figure 3.15. The right part of the device shown in the figure is used for flexural strength. The automatic test device is not sufficient alone for the flexural strength test. Flexural Test Apparatus is required to perform flexural test. The testing apparatus has two supporting rollers; there is 100 mm span between two supports, and a third roller, which is the loading roller, located above the test specimen and midway between the supporting rollers. Figure 3.16 shows the three-point flexural strength apparatus. After the specimens were molded, they were kept in the molds for 24 hours, then removed from the molds and cured in water for 28 days. The curing water temperature was kept at 20 ± 1 °C throughout the curing period. After completing the curing period, the specimens were removed from the water and subjected to flexural strength test. The load was applied uniformly 50 ± 10 N/s until the prism specimen broke. Flexural strength of admixed cement mortars was calculated by taking the average of the test results measured from 3 specimens.



Figure 3.15: Automatic test press for compression and flexure



Figure 3.16: Three point flexural testing apparatus

As an image of the specimens used in the flexural strength test is given in Figure 3.17.



Figure 3.17: 40x40x160 mm prismatic specimens for flexural strength test.

3.2.1.4 Compressive Strength

Compressive strength is the ability of the material to resist the fracture under axial load impact. The compressive strength tests were conducted according to TS EN 196-1 [137] standard. The compressive strength test was carried out by loading the molded side surfaces of two half-prisms with an area of 40 mm × 40 mm obtained as a result of the flexural strength test. The test specimens to be subjected to compressive strength were cured in water for 28 days. The curing water temperature was kept at 20 ± 1 °C throughout the curing period. The compressive strengths of the specimens were tested on the 28-days cured test specimens. 303 kN capacity compressive strength test device used in the study is shown in Figure 3.18. The left part of the device shown in the figure is used for compressive strength. Compressive strengths were tested with the aid of the apparatus shown in Figure 3.19. Half prisms are centered between the plates of the apparatus shown in the figure. The load was applied smoothly at a speed of 2400 ± 200 N/s until the prism broke. Compressive strength of admixed cement mortars was calculated by taking the average of the test results measured from 3 specimens.



Figure 3.18: Automatic test press for compression and flexure



Figure 3.19: 40 mm x 40 mm compressive strength testing apparatus

3.2.2 Characterization of the Bio-polymeric Admixtures

For many centuries, in the historical construction materials, bio-based materials such as animal oil, vegetable fat, fish oil, egg white, linseed oil, olive oil, and blood have been used [200]. Bio-based materials used mostly as admixtures for mortar and plaster

to improve viscosity or retarding agent for gypsum [39]. For concrete workability and waterproofing, Brazilian builders used whale oil. The Romans used blood as an air-entraining agent and the Portuguese added vegetable oil in the mortar [201,202]. Approximately 500 different bio-based admixture products have been utilized in modern building construction [201]. Biopolymers, which are popularly used in building materials such as gums, chitin, chitosan, and cellulose ether, etc. are used as an additive in concrete and derivative materials as a final product after certain production stages. The chemical content of these materials, which have turned into the final product, can also be known [141–143]. Similarly, for the components of the kernel shells, certain ranges can be given, not fixed values.

The bio-polymeric materials evaluated in this study are not subjected to any chemical processes other than mechanical grinding. Also, their contents may vary as they can be obtained as waste in a wide variety of different regions. When the literature is examined, a range of 95-97 % is specified for the calcium carbonate content of the egg shell. For example, Corbett et al. [203] determined the cellulose content in apricot kernels to be 34.31%, while Uzuner and Çekelioğlu [204] determined the cellulose content in apricot kernels to be 24.20%. However, the cellulose ratio of apricot kernels was determined by other researchers as 22.4 %–39.8 % [205–207].

For this reason, the determination of the chemical components of bio-polymeric materials gains importance. In addition, the amount of internal components in bio-polymeric materials has a very important effect on the properties of the cement mortar. This issue will also be discussed in the following sections.

The characterization of bio-polymeric materials was carried out by SEM, XRD and FT-IR analyzes. Moreover, the extractive, pectin, lignin, hemicellulose, and alpha cellulose ratios of lignocellulosic biopolymers used in this study were determined experimentally. All experimental chemical analysis studies to determine the extractive, lignin, hemicellulose, and alpha cellulose ratios of lignocellulosic biopolymers at this stage of the study were carried out using the infrastructure of the R&D laboratory of İzmir Katip Çelebi University, Faculty of Forestry.

3.2.2.1 Chemical Analysis of AKS, HKS, WKS and OS

After the grinding and sieving processes were carried out, the classified woody samples were kept in the oven for 24 hours, which was previously set at $103\pm 2^{\circ}\text{C}$, until they reached a constant weight in order to remove the moisture in it (Figure 3.20). The dried samples were then kept in a desiccator until they reached room temperature, then put in plastic bags and tightly closed so that they do not absorb moisture.



Figure 3.20: Drying OS, AS, HS and WS samples

3.2.2.1.1 Determination of Extractive Content

In order to remove the extractive substances in the wood samples, the samples were extracted for 6 hours in the Soxhlet extraction apparatus shown in Figure 3.21 with a solvent containing a toluene/acetone/ethanol mixture at a ratio of 4/1/1 by volume [208].

Subsequently, hot water extraction was performed on the same setup by a similar procedure. The total extractive substance amount of the materials was evaluated as the sum of toluene/acetone/ethanol mixture extraction and hot water extraction. With hot water extraction, pectin, which is usually present in the lignocellulosic materials, is decomposed [209].



Figure 3.21: Extraction process of OS, AS, HS and WS samples

3.2.2.1.2 Determination of Lignin Content (Delignification)

In order to determine the lignin content of the woody samples prepared within the scope of the study, the chloride method was applied [210]. 2.5 grams from each sample, which was extracted, was taken into a 250 ml flask. Then, 80 ml of distilled water, 1 gram of NaClO_2 (Sodium Chlorite) and 0.5 ml of acetic acid were added to the flask and put into a water bath at 70-80 °C. 6 portions of sodium chloride and acetic acid were added into the flask at intervals of 1 hour and the system was occasionally mixed. Experiments were carried out on 3 samples for each biopolymeric material. The experimental setup used during the lignin content determination is shown in Figure 3.22.

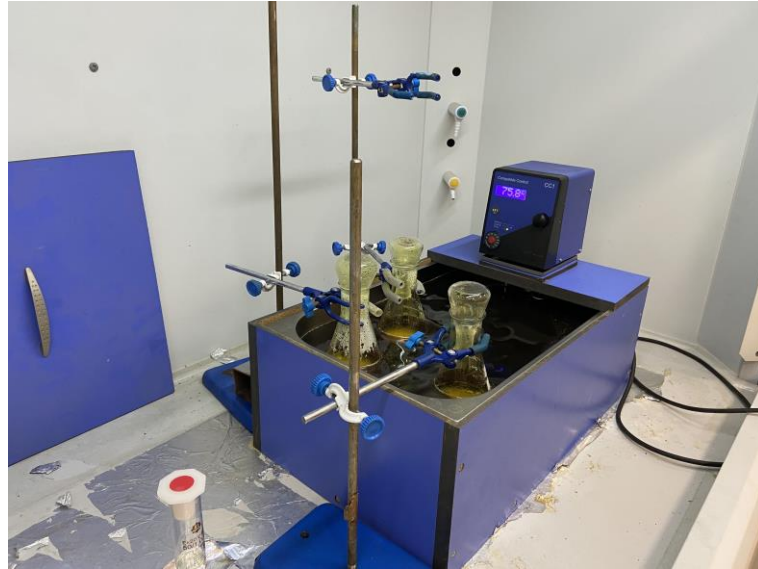


Figure 3.22: Experiment setup for the delignification process.

After the delignification process, the hot mixture was left to cool. Then, filtration with distilled water and acetone was applied through gooch crucible, which had been weighed completely dry beforehand (Figure 3.23).



Figure 3.23: Filtration process of delignification

After the delignification process, the dissolved part of the samples is evaluated as *lignin*. The remaining part after the delignification process is evaluated as *holocellulose*. Holocellulose is equal to the sum of alpha cellulose and hemicellulose.

After filtration, the filtrate was dried at 103 ± 2 °C for 24 hours until it reached a constant weight, and the percentage of lignin content was determined according to the formula below.

$$\text{Lignin (\%)} = \frac{W_1 - W_2}{W_1} * 100 \quad (3.1)$$

W1 is oven dry weight of samples before delignification process, W2 is oven dry weight of samples after delignification process.

3.2.2.1.3 Determination of Hemicellulose and Alpha Cellulose Contents

TAPPI-T203 standards [211] were applied to determine the alpha cellulose content of bio-polymeric samples prepared within the scope of the study. The remaining amount of dry samples obtained after the delignification process were used to determine alpha cellulose and hemicellulose contents. Experiments were carried out on 3 samples for each biopolymeric material. Afterwards, these samples were transferred into a 200 ml beaker and 10 ml of 17.5% sodium hydroxide (NaOH) was added into it and stirred for 5 minutes through a glass baguette (Figure 3.24). After this process, 15 ml of sodium hydroxide solution continued to be added to the samples in specified portions. After this process, 33 ml of distilled water was added to the samples and left for 1 hour.

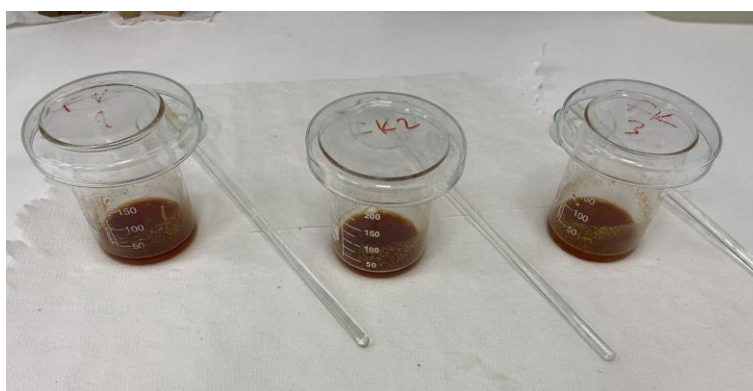


Figure 3.24: Samples prepared for cellulose content determination.

After 1 hour, the mixture was filtered through gooch crucible. The washing process was ended by pouring 100 ml of 8.3 % NaOH solution, 10 % acetic acid (CH_3COOOH) and 250 ml of distilled water on it (Figure 3.25).



Figure 3.25: Filtration of alpha cellulose

The filtrate after washing was kept in the oven at a temperature of 103 ± 2 °C for 24 hours until it reached a constant weight (Figure 3.26).

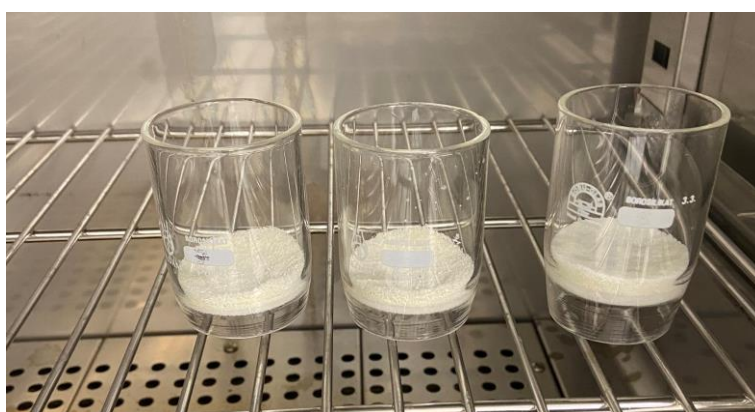


Figure 3.26: Drying of alpha cellulose

After being treated with chemicals, the dissolved part of the samples is considered as *hemicellulose*. The remainder after processing is the amount of *alpha cellulose*. The weights of the samples were taken, and the percent alpha cellulose and hemicellulose ratios were determined according to the formulas below. In Figure 3.27, the samples prepared for the determination of the amount of alpha cellulose is shown.

$$\text{Hemicellulose (\%)} = \frac{W_2 - W_3}{W_2} * 100 \quad (3.2)$$

$$\text{Alpha Cellulose (\%)} = 100 - \text{Hemicellulose (\%)} \quad (3.3)$$



Figure 3.27: Alpha cellulose of AKS (a), HKS (b), WKS (c), OS (d)

3.2.2.2 XRD Analysis of Bio-polymeric Admixtures

The X-ray diffraction (XRD) instrument (Bruker D2 Phaser) system (Figure 3.28) with Ni-filtered Cu-K alpha radiation ($k=1.54\text{\AA}$) was used to observe the microscopic crystal structure of bio-polymeric admixtures under the condition of a continuous scan angle from 5° to 90° . The step time and the increment were 0.05 and 0.024 seconds, respectively.



Figure 3.28: The X-diffraction (XRD) instrument

3.2.2.3 FT-IR Analysis of Bio-polymeric Admixtures

In order to realize the chemical structure and functional groups of bio-polymeric admixtures, Fourier transform infrared (FT-IR) spectrum analysis was applied on

powder form bio-polymeric materials. The analysis was done with Thermo Scientific model Nicoletta IS5 (Figure 3.29) with ATR mode. The analysis was done in the spectral range of 500 – 4000 cm^{-1} with absorbance mode.



Figure 3.29: Fourier transform infrared (FT-IR) device

3.2.2.4 SEM Analysis of Bio-polymeric Admixtures

A scanning electron microscope (Carl Zeiss 300VP, accelerating voltage: 1–30 kV, Magnification: up to 1,500,000x) (Figure 3.30) was used to investigate the microstructure of the cement composites. Mortar specimens produced within the scope of the thesis were dried in an oven after 28 days in water curing conditions and gold coated with QUORUM Q150 RES coating device, and SEM and EDS analysis were performed after these procedures.



Figure 3.30: Scanning electron microscope

3.2.3 Effect of Bio-polymeric Admixtures on Composite Cement Mortars and Comparison with Some Chemical Admixtures

In order to analyze the effects of bio-polymeric admixtures used in this thesis, some physical, mechanical and durability experimental studies were carried out on cement mortars. Physical tests on mortars are flowability, initial and final setting times of mortars, capillarity and water absorption. Mechanical tests on mortars are flexural and compressive strengths. Durability tests are acid attack, sulfate attack and freeze-thaw tests.

In order to better evaluate the performance of cement mortars with bio-polymeric admixtures, bio-polymeric admixtures were used in three different grain size distributions. These three different grain distributions were 0/45 μm , 0/125 μm and 125/250 μm .

This stage constitutes the third stage of the study as stated in Chapter 1. Considering the physical and mechanical properties of cement mortars produced by using bio-polymeric admixtures with different grain sizes, the most effective grain size

distribution was determined in line with the test results. Then, cement mortars were produced by using four different chemical admixtures instead of bio-polymeric admixtures in the same mixture design, and the same tests were repeated on these specimens. Thus, the effects of chemical admixtures on cement mortars and the effects of bio-polymeric admixtures on cement mortars could be compared and it was experimentally interpreted whether bio-polymeric admixtures could be used instead of chemical admixtures in mortars.

3.2.3.1 Mix Design

In initial experimental study, different mixing ratios are designed to examine the effect of bio-polymeric admixtures on cement mortars. In addition, in order to examine the effects that may arise from the use of bio-polymeric admixtures correctly, a separate mixture without bio-polymeric admixture was designed as a reference mixture. The design of the mortar combinations is given in Table 3.6, and the mixing ratios are made according to the design methodology and related standards specified in TS EN 196-1 [137].

Table 3.6: Composite cement mortar mixture combinations with bio-polymeric admixtures

Mix code	Cement (wt%)	Sand (wt%)	ES (wt%)	AKS (wt%)	HKS (wt%)	WKS (wt%)	OS (wt%)	w/c	Bio-polymeric Admixture (wt% of cement)
R	25.0	75.00	-	-	-	-	-	0.5	-
ES0.2	25.0	74.80	0.20	-	-	-	-	0.5	0.80
ES0.35	25.0	74.65	0.35	-	-	-	-	0.5	1.40
ES0.5	25.0	74.50	0.50	-	-	-	-	0.5	2.00
ES1.0	25.0	74.00	1.00	-	-	-	-	0.5	4.00
ES1.5	25.0	73.50	1.50	-	-	-	-	0.5	6.00
AKS0.2	25.0	74.80	-	0.20	-	-	-	0.5	0.80
AKS0.35	25.0	74.65	-	0.35	-	-	-	0.5	1.40
AKS0.5	25.0	74.50	-	0.50	-	-	-	0.5	2.00
AKS1.0	25.0	74.00	-	1.00	-	-	-	0.5	4.00
AKS1.5	25.0	73.50	-	1.50	-	-	-	0.5	6.00

Table 3.6 (Continued): Composite cement mortar mixture combinations with bio-polymeric admixtures

Mix code	Cement (wt%)	Sand (wt%)	ES (wt%)	AKS (wt%)	HKS (wt%)	WKS (wt%)	OS (wt%)	w/c	Bio-polymeric Admixture (wt% of cement)
HKS0.2	25.0	74.80	-	-	0.20	-	-	0.5	0.80
HKS0.35	25.0	74.65	-	-	0.35	-	-	0.5	1.40
HKS0.5	25.0	74.50	-	-	0.50	-	-	0.5	2.00
HKS1.0	25.0	74.00	-	-	1.00	-	-	0.5	4.00
HKS1.5	25.0	73.50	-	-	1.50	-	-	0.5	6.00
WKS0.2	25.0	74.80	-	-	-	0.20	-	0.5	0.80
WKS0.35	25.0	74.65	-	-	-	0.35	-	0.5	1.40
WKS0.5	25.0	74.50	-	-	-	0.50	-	0.5	2.00
WKS1.0	25.0	74.00	-	-	-	1.00	-	0.5	4.00
WKS1.5	25.0	73.50	-	-	-	1.50	-	0.5	6.00
OS0.2	25.0	74.80	-	-	-	-	0.20	0.5	0.80
OS0.35	25.0	74.65	-	-	-	-	0.35	0.5	1.40
OS0.5	25.0	74.50	-	-	-	-	0.50	0.5	2.00
OS1.0	25.0	74.00	-	-	-	-	1.00	0.5	4.00
OS1.5	25.0	73.50	-	-	-	-	1.50	0.5	6.00

In the mixture design, the letters in the front indicate which type of bio-polymeric admixture is used in the mixture and the numbers behind it indicate what percentage by weight of the bio-polymeric admixture is used in the mixture. As can be easily noticed from Table 3.6, the cement ratio was kept constant as 25 % and the w/c ratio as 0.5 in all mixtures. This mixture design is also valid for mixtures with bio-polymeric admixtures to be used in all three particle sizes (i.e. 0/45, 0/125, 125/250 μm). In the following sections, numbers describing the grain size will be placed in front of the mix codes according to the grain size (e.g. 45AKS1.0 mixture describes the use of 1 % by weight of AKS bio-polymeric admixtures with 0/45 μm grain size in the mortar design, 125250OS0.35 mixture describes the use of 0.35 wt.% of OS bio-polymeric admixtures with 125/250 μm grain size in the mortar design). In addition, cement mortars using different chemical admixtures were produced in order to compare the

effect of bio-polymeric admixtures on cement mortars and the effects of chemical admixtures on cement mortars. These chemical admixtures are calcium stearate (CS), polycarboxylate ether (PCE), sulfonated melamine formaldehyde (SMF) and tartaric acid (TA). These chemicals were chosen with the thought that they are suitable for the possible functions of bio-polymeric admixtures in cement mortars. Mortar mix combinations using chemical admixtures are given in Table 3.7.

Table 3.7: Composite cement mortar mixture combinations with chemical admixtures

Mix Code	Cement (wt%)	Sand (wt%)	CS (wt%)	PCE (wt%)	SMF (wt%)	TA (wt%)	w/c	Chemical (wt% of cement)
R	25.0	75.00	-	-	-	-	0.5	-
CS0.2	25.0	74.80	0.20	-	-	-	0.5	0.80
CS0.35	25.0	74.65	0.35	-	-	-	0.5	1.40
CS0.5	25.0	74.50	0.50	-	-	-	0.5	2.00
CS1.0	25.0	74.00	1.00	-	-	-	0.5	4.00
CS1.5	25.0	73.50	1.50	-	-	-	0.5	6.00
PCE0.01	25.0	74.99	-	0.01	-	-	0.5	0.04
PCE0.025	25.0	74.975	-	0.025	-	-	0.5	0.10
PCE0.05	25.0	74.95	-	0.05	-	-	0.5	0.20
PCE0.1	25.0	74.90	-	0.10	-	-	0.5	0.40
PCE0.2	25.0	74.80	-	0.20	-	-	0.5	0.80
SMF0.05	25.0	74.95	-	-	0.05	-	0.5	0.20
SMF0.1	25.0	74.90	-	-	0.10	-	0.5	0.40
SMF0.2	25.0	74.80	-	-	0.20	-	0.5	0.80
SMF0.35	25.0	74.65	-	-	0.35	-	0.5	1.40
SMF0.5	25.0	74.50	-	-	0.50	-	0.5	2.00
TA0.03	25.0	74.97	-	-	-	0.03	0.5	0.80
TA0.05	25.0	74.95	-	-	-	0.05	0.5	1.40
TA0.1	25.0	74.90	-	-	-	0.1	0.5	2.00
TA0.2	25.0	74.80	-	-	-	0.2	0.5	4.00
TA0.35	25.0	74.65	-	-	-	0.35	0.5	6.00

In this mixture design, the letters in the front indicate which type of chemical admixture is used in the mixture and the numbers behind it indicate what percentage by weight of the chemical admixture is used in the mixture. As can be easily noticed from Table 3.7, the cement ratio was kept constant as 25 % and the w/c ratio as 0.5 in all mixtures.

3.2.3.2 Fresh and Hardened Unit Volume Mass of Mortars

The unit volume mass of the fresh mortars was determined in accordance with the TS EN 1015-6 [212] standard. The measuring cylindrical container (1 liter) was filled with mortar overflowing from its upper surface. The full container was placed on the vibration table and vibrated until there was no further settling of the mortar. During the vibration, mortar was added on the measuring container so that the mortar level exceeded the upper limit of the container. Excess mortar was scraped off so that it was level with the upper surface of the container. The fresh unit volume mass measurement setup is shown in the Figure 3.31. The unit volume mass of fresh mortar is calculated by subtracting the mass of the empty container from the mass of the container filled with mortar and dividing by the volume of the measuring container.



Figure 3.31: Fresh unit volume mass measurement setup

The unit volume mass of the hardened mortars was determined in accordance with TS EN 1015-10 [213] standard. The determination of the unit volume mass of the hardened mortar was determined on 40x40x160 mm prismatic specimens. After 28-days of curing period, the specimens were dried in an oven set at 70 ± 5 °C until they reached a constant mass. The hardened unit volume mass of each mortar specimen was found by dividing the determined dry mass by the specimen volume.

3.2.3.3 Flowability of Fresh Mortars

In order to determine the workability properties of fresh mortars, flow table test was performed for each fresh mortar in accordance with ASTM C1437-13 [214]. Flow table apparatus is shown in Figure 3.32. Flow mold was placed at the center of flow table. A layer of mortar about 25 mm in thickness was placed in the mold and tamped 20 times with the tamper. Then, the mold filled with mortar and temped again. The surface of the mortar was finished. Then the mold lifted vertically. Finally, the table dropped 25 times in 15 seconds. The flow diameter of each mortar was calculated by taking the average of four flow diameter measurement.

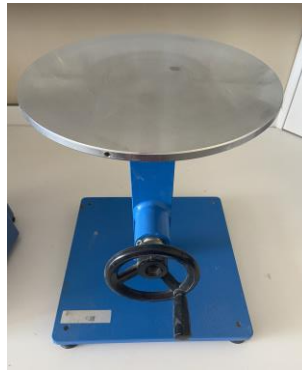


Figure 3.32: Flow table apparatus

3.2.3.4 Setting Times of the Mortars

The measurement of the setting time of fresh mortars were performed using Vicat apparatus (Figure 3.33) according to the principles stated in TS EN 196-3 standard [215]. To determine the initial and final set of the cement mortars, mortar is placed to the conical mold of the test apparatus. After that the tip of the needle is lowered until it touches the surface of the mortar, then the needle is released. This process is repeated every 5 minutes. When needle reading gives 3-5 mm on the apparatus, it means initial setting starts. When needle reading gives 39.5 mm, final setting occurs.



Figure 3.33: Vicat apparatus for setting time

3.2.3.5 Water Absorption of the Mortars

The water absorption test is the simplest method that can be considered in terms of durability in cementitious materials [14].

Capillary water absorption and water absorption by immersion tests were carried out on the specimens produced within the scope of the thesis. The prepared fresh mortars hardened in molds for 24 hours and then cured in water for 28 days. Then the specimens taken out of the water were dried in an oven until their weight stabilized. Then, water absorption tests were carried out on these specimens. Capillary water absorption tests were carried out on 3 pieces of 4x4x16 mm prismatic specimens (Figure 3.34). The water absorbed from the unit area depending on time ($\text{kg/m}^2 \cdot \text{min}^{0.5}$) was determined as the capillarity coefficient. In addition, capillary water absorptions of 5, 10, 15, 30, 60, 90, 1440 and 2880 min were measured for all specimens, and the capillary absorption characteristics of the samples were investigated. In another water

absorption experiment, the specimens were completely immersed in water and the 24-hour water absorption rates were determined as percent.



Figure 3.34: An example image of the capillary water absorption test.

3.2.3.6 Flexural Strength of the Mortars

The flexural strengths of cement mortars produced by using ES, AKS, HKS, WKS and OS bio-polymeric admixtures and CS, PCE, SMF and TA chemical admixtures were analyzed by the method described in Section 3.2.1.3.

3.2.3.7 Compressive Strength of the Mortars

The compressive strengths of cement mortars produced by using ES, AKS, HKS, WKS and OS bio-polymeric admixtures and CS, PCE, SMF and TA chemical admixtures were analyzed by the method described in Section 3.2.1.4. The compressive strengths of the mortar samples with bio-polymeric or chemical admixtures were determined on the 7th, 28th and 90th days. For the 7th and 28th day compressive strengths, the specimens were cured for 7 days and 28 days in water. After 28 days of water curing, the specimens that will be subjected to 90th day compressive strength were removed from the water and cured in air in a normal laboratory environment until the test day.

3.2.4 Mineralogical Development and Microstructural Analysis of Mortars

The mineralogical development of bio-polymeric admixed cement mortars was followed by XRD analysis. XRD analyzes were performed using the device and

method introduced in Section 3.2.2.2. For XRD analyses, cement pastes were prepared in such a way that the cement/bio-polymeric additive ratio was the same as the cement/bio-polymeric additive ratio of the mixtures used in the cement mortars given in Table 3.6. Cementitious pastes were cured in water for 28 days like cement mortars. XRD analyzes of cement pastes were designed on 3-, 7-, 28- and 150-days cured samples. At the selected hydration times, approximately 1 cm³ cementitious paste was taken and crushed. Then, crushed paste stored in isopropanol to remove the water from the paste by solvent exchange [216,217].

Microstructural investigations of cement mortars were carried out by SEM and EDS analyses. The device and method used in the analyzes are introduced in Section 3.2.2.4. SEM and EDS analyzes were performed on the samples taken from the fractured surfaces of the 28-day cured mortars.

3.2.5 Durability of the Mortars

In order to analyze the durability properties of bio-polymeric admixtures on composite cement mortars, sulfate effect, acid effect and freeze-thaw effect were applied to 5x5x5 cm cubic specimens cured in water for 28 days (Figure 3.35). In each durability analysis, 3 specimens were tested for each batch. A total of 234 cubic specimens were produced for durability tests. Durability tests were completed on cement mortars produced using bio-polymeric admixtures with 0/125 μm grain size, which was determined as the most effective particle size distribution in bio-polymeric admixtures.



Figure 3.35: Some of test specimens for durability analysis

The current test method for sulfate attack, ASTM C-1012 [218], suggests the use of a 50-g/l Na_2SO_4 solution (5 mass%, or 33,800 ppm SO_4^{2-}). It also states that other sulfate solutions, such as MgSO_4 , and other concentrations, may be used. In order to analyze the effect of sulfate in test mortars, 5 % by weight magnesium sulfate (MgSO_4) solution was prepared. The specimens, which completed the 28-day curing period, were kept in the prepared chemical solutions with capillary action for 30 cycles (Figure 3.36). Each cycle was completed by absorbing the sulphate solution by capillary action for 18 hours and drying in an oven at $110 \pm 5^\circ\text{C}$ for the following 6 hours. Mortar specimens, which were dried again at the end of the 30th period, were removed from the solution and washed with clean water. The weights of the specimens, which were dried at $110 \pm 5^\circ\text{C}$ until they reached the constant weight, were measured with a balance with a sensitivity of 0.01 g before and after the interaction with solution [219]. In addition, the strengths of the specimens at the end of 30 cycles were compared with the strengths of the specimens that were not exposed to the sulfate effect.

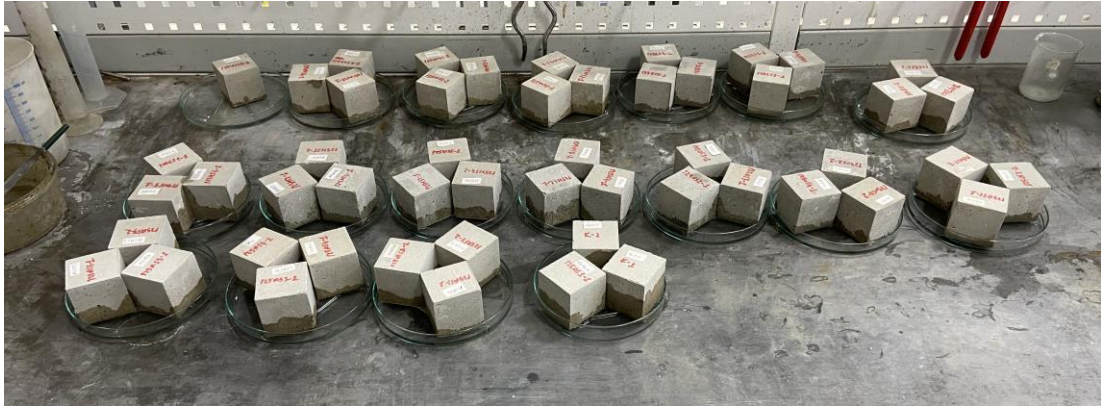


Figure 3.36: Sulfate effect test with capillary action.

Another durability feature examined within the scope of the study is the resistance of cement mortars to sulfuric acid. In the literature, prepared acid solutions in which the acid effect was examined were tested at different pH values. One of them is the severe acid solution and it is found in studies as $\text{pH}=1$ [220,221]. In this context, H_2SO_4 solution with $\text{pH}= 1\pm 0.01$ was capillary impregnated to the cubic specimens (Figure 3.37). In order to observe the effect of the prepared acid solution on the cement mortars, the specimens were capillary treated with acid solution for 18 hours and then the specimens were dried in an oven at $110 \pm 5^\circ\text{C}$ for 6 hours. This 18-hour wetting and 6 hours drying was considered as 1 cycle and the specimens were subjected to 30 wetting-drying cycles. The acid solution was renewed at the end of each cycle. After 30 cycles were completed, the specimens were dried in an oven until they reached a constant weight and then subjected to compressive strength test.

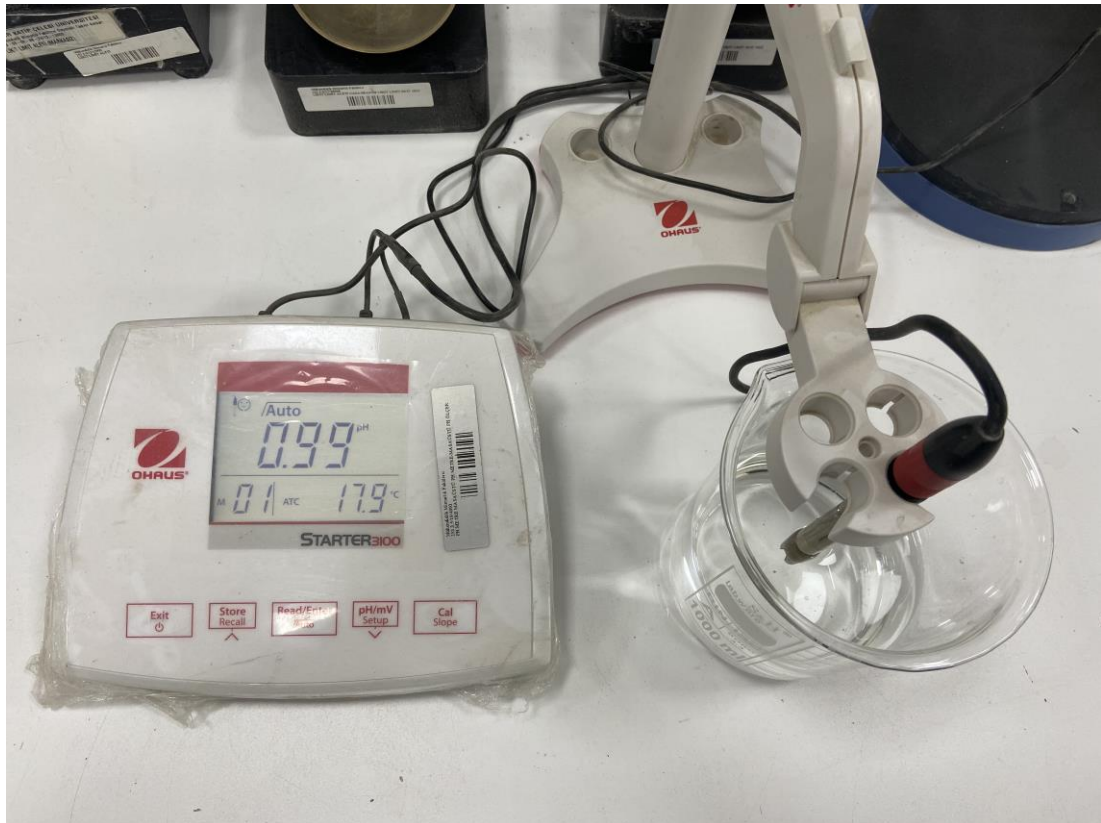


Figure 3.37: Determination of pH value of acid solutions.

The third and last durability feature of the cement mortars in the scope of the study is to determine the resistance of cement mortars against freezing-thawing. Freeze-thaw cycles were applied to the mortars to determine the freeze-thaw resistance of cement mortars containing bio-polymeric admixtures. In each cycle, the samples were frozen at $-20\text{ }^{\circ}\text{C}$ for 18 hours and then thawed in $+20\text{ }^{\circ}\text{C}$ water for the following 6 hours [222,223]. Thus, each cycle was completed in 24 hours. In total, 30 freeze-thaw cycles were applied to the test specimens. After 30 cycles were completed, the specimens were dried in an oven until they reached a constant weight and then subjected to compressive strength test.

3.2.6 Optimization and Regression Analysis

Extractive, lignin, hemicellulose, cellulose ratios of bio-polymeric admixtures, usage ratio of bio-polymeric admixture in the mortar and grain size distribution of bio-polymeric admixture, which will affect the physical and mechanical properties of cement mortars produced within the scope of this thesis, are optimized by "gray relational grade" analysis.

Gray system theory is an alternative method for quantifying uncertainty. Basically, this theory is a method that is frequently used in analysis of the relationship between systems, model building, forecasting and decision problems [224]. Gray Relational Analysis is a decision-making and analysis tool that has taken its place in the literature under the main title of Gray Theory. The gray theory was first put forward in 1982 by Professor Julong Deng, a faculty member at Hua Chung University of Science and Technology in Thailand. Gray theory; gray relational analysis, gray modelling, gray forecasting and gray decision making are applied in different areas [225]. In the gray system theory (GST), the darkness of the colors generally expresses the degree of uncertainty of the information [226]. In relational analysis, black represents having no information and white represents having all information. A gray system has a level of information between black and white. This analysis can be used to represent the degree of correlation between two sequences so that the distance between the two factors can be measured concretely. Gray correlation analysis is an effective method for analyzing the relationship between sequences with less data and can analyze many factors that can overcome the disadvantages of the statistical method [227]. Gray relational grade (GRG), one of the sub-titles of the GST, is an effective method for decision problems with complex relationships between criteria. Thanks to this feature, the applications of GRG in multi-criteria decision making problems, integrated with other methods or alone, are frequently encountered in the literature [228,229].

In a multi-response problem, the influence and relationship between different parameters is complex and unclear. This is called gray, which denotes weak and uncertain information. This proposed methodology (gray relational analysis) analyzes this complex uncertainty among multiple responses in given system and optimizes it with the help of gray relational degrees. Therefore, a multi-response optimization problem is reduced to a single-response optimization problem, which is called a single relational order [230].

When analyzing GRA, the data should be normalized to avoid different units and to reduce the variability. Normalization of data is essential because the variation of one data is different from other data. An appropriate value is derived from the original value to make the array between 0 to 1 [231]. In summary, in GRA the original data is converted into comparable data [230].

When the “lower is better” is a characteristic of the original sequence, then the original sequence should be normalized as follows [232]:

$$x_i^*(k) = \frac{\max x_i^0(k) - x_i^0(k)}{\max x_i^0(k) - \min x_i^0(k)} \quad (3.4)$$

When the “higher is better” is a characteristic of the original sequence, then the original sequence should be normalized as follows [232]:

$$x_i^*(k) = \frac{x_i^0(k) - \min x_i^0(k)}{\max x_i^0(k) - \min x_i^0(k)} \quad (3.5)$$

However, if there is a definite target value (desired value) to be achieved, the original sequence will be normalized in form [232]:

$$x_i^*(k) = 1 - \frac{|x_i^0(k) - x^0|}{\max x_i^0(k) - x^0} \quad (3.6)$$

Or, the original sequence can be simply normalized by the most basic methodology, i.e. let the values of original sequence be divided by the first value of the sequence [232]:

$$x_i^*(k) = \frac{x_i^0(k)}{\max x_i^0(1)} \quad (3.7)$$

where $i = 1, \dots, m$; $k = 1, \dots, n$. m is the number of experimental data items and n is the number of parameters. $x_i^0(k)$ denotes the original sequence, $x_i^*(k)$ the sequence after the data pre-processing, $\max x_i^0(k)$ the largest value of $x_i^0(k)$, $\min x_i^0(k)$ the smallest value of $x_i^0(k)$ and x^0 is the desired value.

After data pre-processing (normalizing) is carried out, the grey relation coefficient $\xi_i(k)$ for the k th performance characteristics in the i th experiment can be expressed as [233–235]:

$$\xi_i(k) = \frac{\Delta_{min} + \zeta\Delta_{max}}{\Delta_{0i} + \zeta\Delta_{max}} \quad (3.8)$$

$$\Delta_{0i} = \|x_0^*(k) - x_i^*(k)\| \quad (3.9)$$

$$\Delta_{min} = \min_{\forall j \in i} \min_{\forall k} \|x_0^*(k) - x_j^*(k)\| \quad (3.10)$$

$$\Delta_{min} = \max_{\forall j \in i} \max_{\forall k} \|x_0^*(k) - x_j^*(k)\| \quad (3.11)$$

where, Δ_{0i} is the deviation sequence of the reference sequence and the comparability sequence. $x_0^*(k)$ denotes the reference sequence and $x_i^*(k)$ denotes the comparability sequence. ζ is distinguishing or identification coefficient: $\zeta \in [0, 1]$ (the value may be adjusted based on the actual system requirements). A value of ζ is the smaller and the distinguished ability is the larger. $\zeta = 0.5$ is generally used. After the grey relational coefficient is derived, it is usual to take the average value of the grey relational coefficients as the grey relational grade [233,234]. The grey relational grade is defined as follows [232]:

$$\gamma_i = \frac{1}{n} \sum_{k=1}^n \xi_i(k) \quad (3.12)$$

However, in a real engineering system, the importance of various factors to the system varies. In the real condition of unequal weight being carried by the various factors, the grey relational grade in Eq. 6 was extended and defined as [233,234]:

$$\gamma_i = \frac{1}{n} \sum_{k=1}^n \omega_k \xi_i(k) \quad \sum_{k=1}^n \omega_k = 1 \quad (3.13)$$

where ω_k denotes the normalized weight of factor k .

Regression analysis is applied for modeling and analysis in the case of different variables having a relationship between one dependent variable and one or more independent variables [236]. In this thesis, also multiple regression model types including linear, quadratic, trigonometric, and logarithmic were tried to be constructed. Regression analysis was used in this thesis to calculate the equations for prediction of physical and mechanical properties of cement mortars. The regression

formulas used in the study are given in the Table 3.8 and the regression analyzes and R2 values were made in Wolfram Mathematica 12 software.

Table 3.8: Multiple regression models including linear, quadratic, trigonometric, logarithmic, and their rational forms

Model Name	Nomenclature	Formula
Multiple linear	L	$Y = \alpha_0 + \alpha_1x_1 + \alpha_2x_2 + \alpha_3x_3$
Multiple linear rational	LR	$Y = \frac{\alpha_0 + \alpha_1x_1 + \alpha_2x_2 + \alpha_3x_3}{\beta_0 + \beta_1x_1 + \beta_2x_2 + \beta_3x_3}$
Second order multiple nonlinear	SON	$Y = \alpha_0 + \alpha_1x_1 + \alpha_2x_2 + \alpha_3x_3 + \alpha_4x_1^2 + \alpha_5x_2^2 + \alpha_6x_3^2 + \alpha_7x_1x_2 + \alpha_8x_1x_3 + \alpha_9x_2x_3$
Second order multiple nonlinear rational	SONR	$Y = (\alpha_0 + \alpha_1x_1 + \alpha_2x_2 + \alpha_3x_3 + \alpha_4x_1^2 + \alpha_5x_2^2 + \alpha_6x_3^2 + \alpha_7x_1x_2 + \alpha_8x_1x_3 + \alpha_9x_2x_3) / (\beta_0 + \beta_1x_1 + \beta_2x_2 + \beta_3x_3 + \beta_4x_1^2 + \beta_5x_2^2 + \beta_6x_3^2 + \beta_7x_1x_2 + \beta_8x_1x_3 + \beta_9x_2x_3)$
First order trigonometric multiple nonlinear	FOTN	$Y = \alpha_0 + \alpha_1\sin x_1 + \alpha_2\sin x_2 + \alpha_3\sin x_3 + \alpha_4\cos x_1 + \alpha_5\cos x_2 + \alpha_6\cos x_3$
First order trigonometric multiple nonlinear rational	FOTNR	$Y = (\alpha_0 + \alpha_1\sin x_1 + \alpha_2\sin x_2 + \alpha_3\sin x_3 + \alpha_4\cos x_1 + \alpha_5\cos x_2 + \alpha_6\cos x_3) / (\beta_0 + \beta_1\sin x_1 + \beta_2\sin x_2 + \beta_3\sin x_3 + \beta_4\cos x_1 + \beta_5\cos x_2 + \beta_6\cos x_3)$
Second order trigonometric multiple nonlinear	SOTN	$Y = \alpha_0 + \alpha_1\sin x_1 + \alpha_2\sin x_2 + \alpha_3\sin x_3 + \alpha_4\cos x_1 + \alpha_5\cos x_2 + \alpha_6\cos x_3 + \alpha_7\sin^2 x_1 + \alpha_8\sin^2 x_2 + \alpha_9\sin^2 x_3 + \alpha_{10}\cos^2 x_1 + \alpha_{11}\cos^2 x_2 + \alpha_{12}\cos^2 x_3$
Second order trigonometric multiple nonlinear rational	SOTNR	$Y = (\alpha_0 + \alpha_1\sin x_1 + \alpha_2\sin x_2 + \alpha_3\sin x_3 + \alpha_4\cos x_1 + \alpha_5\cos x_2 + \alpha_6\cos x_3 + \alpha_7\sin^2 x_1 + \alpha_8\sin^2 x_2 + \alpha_9\sin^2 x_3 + \alpha_{10}\cos^2 x_1 + \alpha_{11}\cos^2 x_2 + \alpha_{12}\cos^2 x_3) / (\beta_0 + \beta_1\sin x_1 + \beta_2\sin x_2 + \beta_3\sin x_3 + \beta_4\cos x_1 + \beta_5\cos x_2 + \beta_6\cos x_3 + \beta_7\sin^2 x_1 + \beta_8\sin^2 x_2 + \beta_9\sin^2 x_3 + \beta_{10}\cos^2 x_1 + \beta_{11}\cos^2 x_2 + \beta_{12}\cos^2 x_3)$

Table 3.8 (Continued): Multiple regression models including linear, quadratic, trigonometric, logarithmic, and their rational forms

Model Name	Nomenclature	Formula
First order logarithmic multiple nonlinear	FOLN	$Y = \alpha_0 + \alpha_1 \ln x_1 + \alpha_2 \ln x_2 + \alpha_3 \ln x_3$
First order logarithmic multiple nonlinear rational	FOLNR	$Y = (\alpha_0 + \alpha_1 \ln x_1 + \alpha_2 \ln x_2 + \alpha_3 \ln x_3) / (\beta_0 + \beta_1 \ln x_1 + \beta_2 \ln x_2 + \beta_3 \ln x_3)$
Second order logarithmic multiple nonlinear	SOLN	$Y = \alpha_0 + \alpha_1 \ln x_1 + \alpha_2 \ln x_2 + \alpha_3 \ln x_3 + \alpha_4 \ln^2 x_1 + \alpha_5 \ln^2 x_2 + \alpha_6 \ln^2 x_3 + \alpha_7 \ln x_1 x_2 + \alpha_8 \ln x_1 x_3 + \alpha_9 \ln x_2 x_3$
Second order logarithmic multiple nonlinear rational	SOLNR	$Y = (\alpha_0 + \alpha_1 \ln x_1 + \alpha_2 \ln x_2 + \alpha_3 \ln x_3 + \alpha_4 \ln^2 x_1 + \alpha_5 \ln^2 x_2 + \alpha_6 \ln^2 x_3 + \alpha_7 \ln x_1 x_2 + \alpha_8 \ln x_1 x_3 + \alpha_9 \ln x_2 x_3) / (\beta_0 + \beta_1 \ln x_1 + \beta_2 \ln x_2 + \beta_3 \ln x_3 + \beta_4 \ln^2 x_1 + \beta_5 \ln^2 x_2 + \beta_6 \ln^2 x_3 + \beta_7 \ln x_1 x_2 + \beta_8 \ln x_1 x_3 + \beta_9 \ln x_2 x_3)$

Chapter 4

Results and Discussions

4.1 Test Results of Preliminary Study

The compressive and flexural strength values of the preliminary tests using different bio-polymeric admixtures are given in Table 4.1. According to the test results given in Table 4.1, egg shell, apricot kernel, hazelnut shell, walnut shell and olive kernel were selected, and the thesis study was continued with these five bio-polymeric admixtures.

Table 4.1: Test results of preliminary study

Mix	Compressive Strength (MPa)	Flexural Strength (MPa)
Reference	35.06	7.32
CC0.5	25.66	3.70
CC1.0	15.41	3.78
CC1.5	0.64	0.52
ES0.5	38.51	4.39
ES1.0	29.82	4.31
ES1.5	33.69	3.47
WKS0.5	26.78	3.25
WKS1.0	31.22	5.58
WKS1.5	34.95	6.28
AKS0.5	32.36	6.23
AKS1.0	30.11	6.41
AKS1.5	31.48	5.81
OP0.5	20.80	4.45

Table 4.1 (Continued): Test results of preliminary study

Mix	Compressive Strength (MPa)	Flexural Strength (MPa)
OP1.0	19.05	3.16
OP1.5	25.63	4.76
M0.5	23.04	4.32
M1.0	11.03	2.22
M1.5	8.05	1.21
HKS0.5	26.12	5.26
HKS1.0	26.70	5.68
HKS1.5	26.35	5.41
RH0.5	27.93	5.85
RH1.0	26.75	5.92
RH1.5	28.07	5.84
OS0.5	24.30	5.38
OS1.0	29.15	5.42
OS1.5	29.68	4.06

In Table 4.1, the letters in the mixture coding represent the admixture type and the number next to it represents the percentage amount of that admixture in the mixture by weight. As can be seen from the table, it has been observed that the 28-days strengths of composite cement mortars produced with CC and M admixtures have decreased unacceptably. Therefore, these two materials were decided to not used in further studies. In addition, it was determined that some specimens of these mixtures were deformed during water curing. This is one of the reasons why the strength values are much lower than expected. The images of deformed specimens are given in Figure 4.1. Similarly, the OP admixture was not evaluated in the study as it was below the strength expectations. RH bio-polymeric admixture, on the other hand, was not evaluated in further studies because it requires time and effort in the grinding phase.



Figure 4.1: Deformed specimens.

4.1.1 Evaluation of Test Results of Preliminary Study

The 28-days compressive and flexural strength values of 4x4x16 cm prismatic mortar specimens prepared by using several bio-polymeric admixtures were determined in

preliminary study. CC, M and OP bio-polymeric admixtures were not evaluated in this study as they reduced the compressive and flexural strength of the mortar much more than expected. In particular, cement mortars with CC and M cracked during water curing. In future studies, these materials can be investigated in different particle sizes or with different surface treatments or surface coatings as bio-polymeric admixtures in cement mortars. Although RH admixture gave similar results with other selected bio-polymeric admixtures according to the preliminary study results, it was not used in further studies due to the need for too much effort during grinding of this material. In future studies, these bio-polymeric admixtures can be ground with different grinding processes and its effect on cementitious products can be examined.

Within the scope of the preliminary study, it was determined that the compressive strength of the mortars with 0.5 % eggshell by weight gave better results than the compressive strength of the reference mixture. In addition, it has been observed that the strength properties of the mixtures, which AKS and WS admixtures are used, are close to the strength of the reference mixture. And finally, the strength properties of the mixtures with HKS and OS admixtures were found to be sufficient, and further studies continued with these materials.

Beyond these reasons, it has been experienced those substances such as extractive, lignin, cellulose and hemicellulose, especially found in the composition of the kernel shells, can contribute to different properties in cement mortar. For example, it has been experienced that olive seed and walnut kernel shells, which have high extractive and lignin content, can increase the workability of the mortar, and reduce water absorption. It is thought that materials with high cellulose content can contribute to the strength values of the mortar. At this stage of the study, the selection was made by considering the chemical composition of the bio-polymeric materials to be used in further studies, in line with the information obtained from the literature about the chemical contents of the bio-polymeric admixtures.

4.2 Experimental Results of Characterization Analysis

4.2.1 Chemical Structure of AKS, HKS, WKS and OS

The extractive, lignin, hemicellulose, and alpha cellulose contents of lignocellulosic materials to be used as bio-polymeric admixtures within the scope of experimental studies were determined proportionally by means of the experimental methods described earlier. The chemical contents of these materials are given in the Table 4.2.

Table 4.2: The chemical contents of AKS, HKS, WKS, and OS

Bio-polymeric Admixture	Extractive (%)	Lignin (%)	Hemicellulose (%)	Alpha Cellulose (%)
AKS	3.81 ± 0.11	27.07 ± 0.19	31.19 ± 0.33	37.92 ± 0.18
HKS	4.67 ± 0.19	31.79 ± 2.32	31.73 ± 1.78	33.29 ± 0.64
WKS	16.16 ± 0.21	41.23 ± 1.14	20.58 ± 4.24	22.03 ± 3.14
OS	18.39 ± 0.26	32.45 ± 2.42	29.67 ± 1.68	19.48 ± 1.22

When Table 4.2 is examined, the highest extractive content is found in olive stones with 18.39 %, followed by walnut shell with 16.16 %. The lowest extractive content was found in apricot kernel shell with 3.81 %. Considering the lignin content of bio-polymeric materials, the highest amount of lignin is in walnut kernel shells with 41.23 ± 1.14 %, followed by olive stones with 32.45 ± 2.42 %. When the amount of extractive substance and the amount of lignin were evaluated together, the bio-polymeric materials with the highest total of these two components were determined as olive stone and walnut shell. On the contrary, bio-polymeric materials with the highest total cellulose content (holocellulose) were determined as apricot kernel shell with 69.11 % and hazelnut kernel shell with 65.02 %. However, lignocellulosic materials are known to be damaged by the alkaline environment in the cement matrix [237–239]. The components most damaged by the alkaline environment are known as lignin and then hemicellulose [239]. In this context, when Table 4.2 is examined, when it is considered as the sum of lignin and hemicellulose content, the highest value is found in olive stone with 62.12 % and then in walnut shell with 61.81 %. The material found to be the richest in terms of alpha cellulose content is the apricot kernel with 37.92 ± 0.18 %. On the other hand, the lowest amount of alpha cellulose was found in the olive seed

with 19.48 ± 1.22 %. In addition, pectin is also included in the values given as the extractive substance ratio. The contents of extractive substances are also given in Table 4.3.

Table 4.3: Extractive contents of AKS, HKS, WKS, and OS

Bio-polymeric Admixture	Extractive (%)	
	Waxes, fats, proteins	Pectins
AKS	1.36	2.45
HKS	3.47	1.20
WKS	5.89	10.27
OS	7.76	10.63

4.2.2 XRD Results of Bio-polymeric Admixtures

XRD analyzes were carried out to characterize the bio-polymeric admixtures used in this thesis. The results of these analyzes are shown in Figure 4.2 and Figure 4.3.

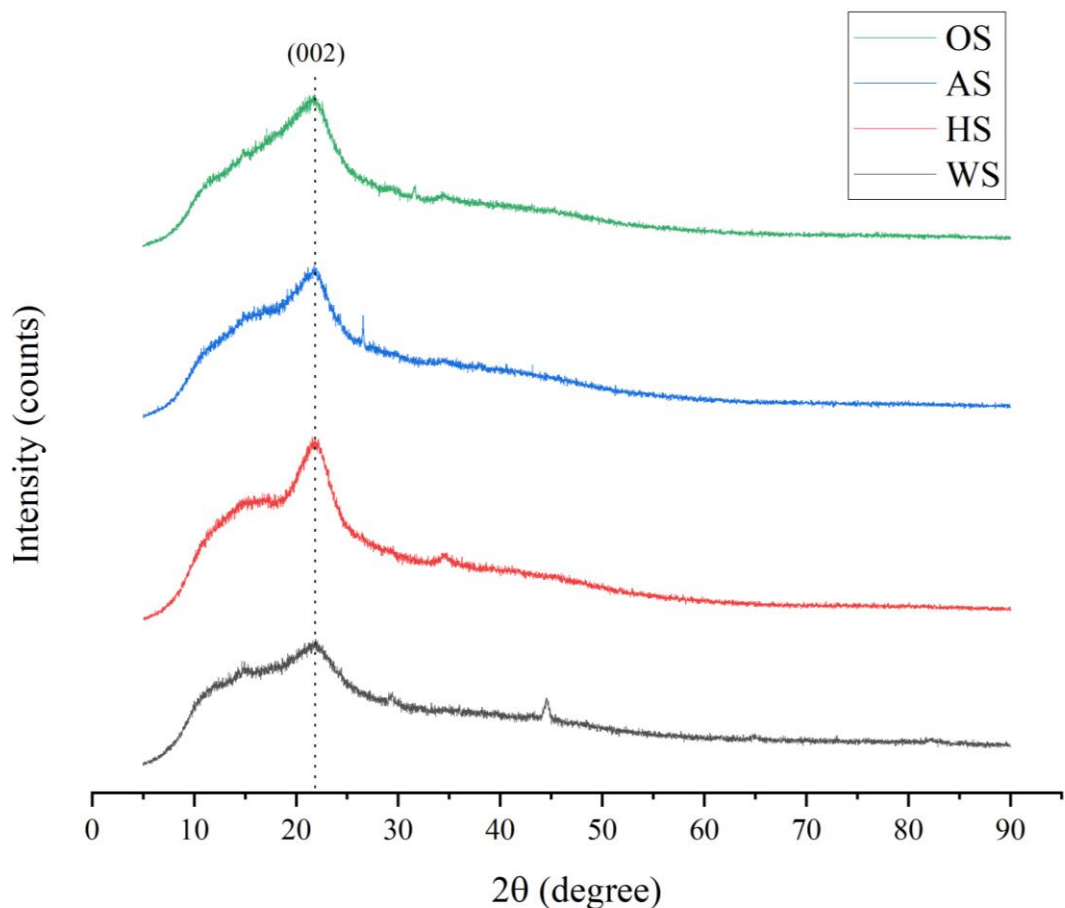


Figure 4.2: XRD patterns of OS, AKS, HKS and WKS.

Figure 4.2 shows that all lignocellulosic bio-polymeric samples have peak characteristic for cellulose I (card No. PDF-203-0289) located on $2\theta \approx 14^\circ$, 16° , 23° and 35° which are ascribed to the (101), $(10\bar{1})$, (002) and (040) crystallographic plane reflection, respectively [240–242]. The X-ray diffractograms of amorphous solids and lattice distortion show a wide peak, while solids with crystalline structure have sharper peaks indicating larger crystallites [243]. When the figure is examined, it is observed that the peaks at 14° , 16° and 35° are not sharp or not obvious. This is in accordance with high content of hemicellulose and lignin which contributes to amorphous phase [244]. However, according to the literature, the peak at 2θ around 22° corresponds to the 002 crystallographic plane of the cellulose I lattice, which is clearly observed in Figure 4.2, is an evidence of cellulose as a main component of all lignocellulosic bio-polymeric materials. Lignocellulosic materials are semi-crystalline materials and the tensile strength and elastic modulus have an evident relationship with its crystal content [239]. In this context, in order to support these results, crystallinity index values were calculated according to Equation (4.1) and given in Table 4.4.

$$CrI = \frac{I_{002} - I_{am}}{I_{002}} * 100\% \quad (4.1)$$

where I_{002} is the maximum intensity of diffraction of the (002) lattice peak at $2\theta = 22.5^\circ$, I_{am} is the intensity of diffraction contributing to the amorphous fraction, which is taken at a 2θ angle between 18° and 19° where the intensity is a minimum [245].

Table 4.4: Crystallinity Index of bio-polymeric materials

Bio-polymeric Admixture	Crystallinity Index
AKS	32.21 %
HKS	23.78 %
WKS	22.21 %
OS	21.77 %

According to Table 4.4, the bio-polymeric material with the highest crystallinity index was determined as the apricot kernel shells. This result supports the experimental results of the chemical structures of the biopolymeric materials given in Table 4.2. The increased crystallinity indicates that the lower amount of phenolic polymer and amorphous components, and as a result, stiffness and embrittlement of natural fiber were increased [239].

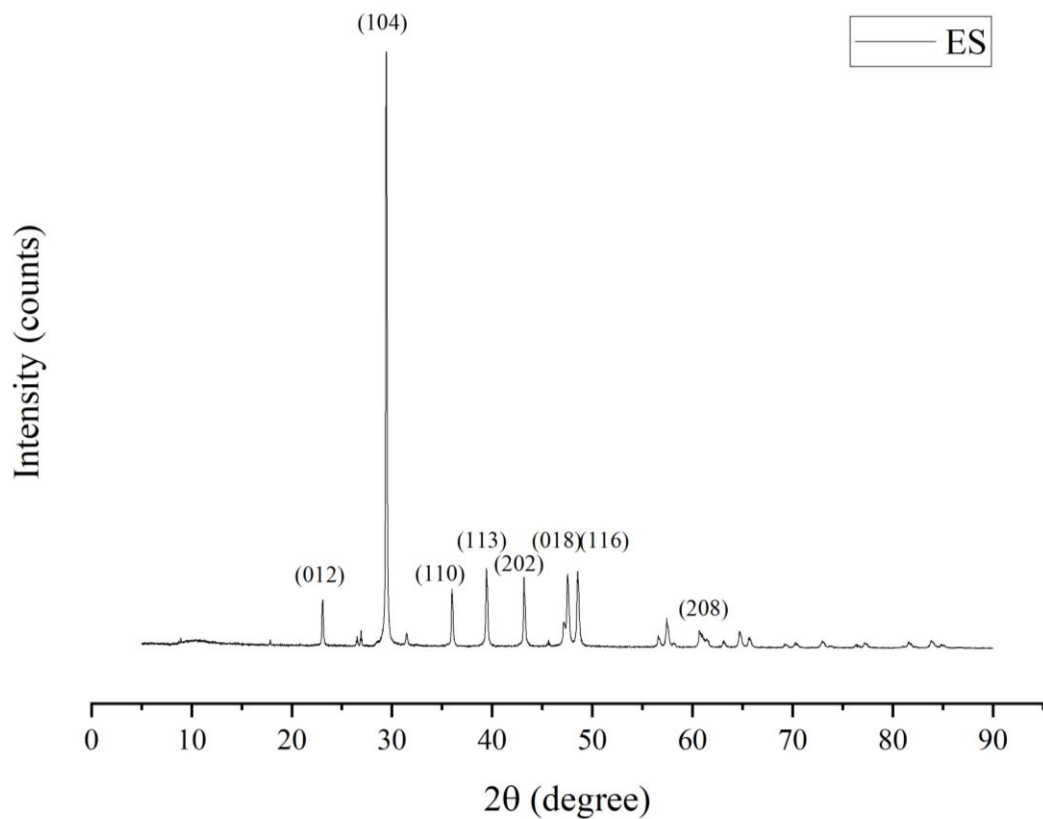


Figure 4.3: XRD pattern of ES.

The XRD characterizations of the eggshells are shown in Figure 4.3. The figure showed that the eggshell bio-polymeric admixture was composed of calcium carbonate, which revealed all diffraction peaks are matched to the crystalline calcite phase corresponds to JCPDS card no. (05-0586) [246]. The highest XRD diffraction peaks appear at $2\theta \approx 23^\circ$ (012), 29° (104), 36° (110), 39° (113), 43° (202), 47.5° (018) and 48.5° (116).

4.2.3 FT-IR Results of Bio-polymeric Admixtures

The FT-IR spectra of bio-polymeric admixtures were used to determine the vibrational frequency changes in the functional groups. The results of FT-IR analyze are shown in Figure 4.4 and Figure 4.5.

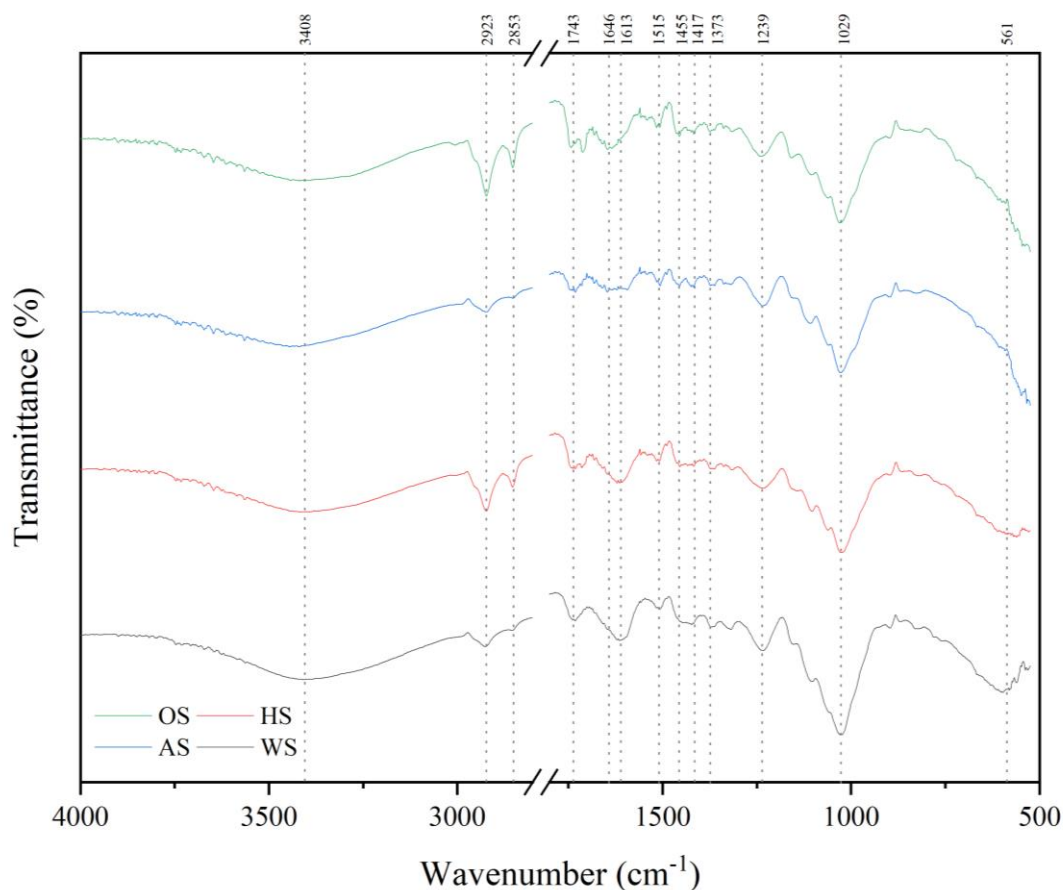


Figure 4.4: FT-IR spectrums of OS, AS, HS and WS

Figure 4.4 shows that all the bio-polymeric admixture types have similar peaks in the FTIR spectra but different intensities. Figure 4.4 shows broad peaks around 3408 cm^{-1} , which represents the OH (hydroxyl) functional groups with a minor contribution of NH functional group [247–250]. The broad peak observed at $3500\text{--}3100\text{ cm}^{-1}$ and around 1029 cm^{-1} in the spectra of the bio-polymeric admixture types corresponds to free OH in molecule and OH group forming hydrogen bonds of stretching groups of macro-molecular association [247,251,252]. The absorption band at 2923 cm^{-1} and 2853 cm^{-1} is related to asymmetric and symmetric stretching vibration of C–H bonds (CH_2 and CH_3 groups) [247–250,253]. In addition, The characteristic peak located at 1743 cm^{-1} and 1655 cm^{-1} is due to the carbonyl resulting from the hemicellulose structure and carboxyl C=O stretching vibrations [248,249,253,254]. Another small absorption peak at 1650 and 1613 cm^{-1} can be associated with the bending vibrations of H_2O molecules [247–249]. The amide I band at 1646 cm^{-1} results from the C=O stretching in the amides I, II, and III [253]. The small peaks observed at 1515 and 1455 cm^{-1} may be attributed to C=C stretching vibrations or asymmetric and symmetric stretching vibrations of ion carboxylic groups (1456 cm^{-1}) [248,250].

The IR region from 1500 to 800 cm^{-1} is commonly referred to as the “fingerprint” region, which includes bands corresponding to the vibrations of the C-O, C-C, C-H, and C-N bonds [253,255]. This region is, on the one hand, very rich in information, but, on the other hand, difficult to analyze due to its complexity. This area provides important information about organic compounds, such as sugars, alcohols, and organic acids, present in the sample [253]. The bands located at about 1417 cm^{-1} were attributed to carboxylate ion (COO^-) groups [250]. In addition, the absorption bands at 1373 cm^{-1} indicate the presence of the chemical functional groups, $-\text{CH}_3$, $-\text{CH}_2$ and $-\text{CH}$, which are characteristic for alkanes and alkyl groups, cellulose, hemicellulose, and lignin [247,253,254]. The peak at 1239 cm^{-1} is assigned to acetyl groups of lignin [251,256]. 1239 cm^{-1} deformation vibration of C=O and stretching formation of the $-\text{OH}$ of carboxylic acids and phenols [248,249]. The peak at 1029 cm^{-1} corresponds to the C–O band in the $-\text{OCH}_3$ groups of lignin [248,257]. The additional peak at around 561 cm^{-1} can be assigned to bending modes of aromatic compounds [258].

The peak at approximately 3000–3600 cm^{-1} is due to O–H stretching vibrations in cellulose [249]. As analyzing intensity degrees of 3000–3600 cm^{-1} band in Figure 4.4, it is observed that cellulose amount is higher in AS and HS than OS and WS, this observation also support the results given in Table 4.2. The 1745 cm^{-1} band corresponds to the stretching of the C=O ester carbonyl or carboxylic acid groups, which are characteristic of triglycerides and fatty acids [40]. As analyzing intensity degrees of around 1745 cm^{-1} band in Figure 4.4, it is observed that fatty acid amount is higher in OS and WS than HS and AS, this observation also support the results given in Table 4.2 (according to obviously higher amount of extractives of OS and WS). The peak at a wavelength of about 1600 cm^{-1} is known C = O asymmetric stretching resulting from aldehyde, ketone, and carboxylic acid groups. [254,259]. A shoulder peak observed at 1720–1740 cm^{-1} as the characteristic absorption peak of hemicellulose [260]. As analyzing intensity degrees of 1740 cm^{-1} band in Figure 4.4, it is observed that hemicellulose amount is higher in OS, this observation also support the results given in Table 4.2. Lignin was identified based on the benzene spectrum C=C at 1650 cm^{-1} [261]. As analyzing intensity degrees of 1650 cm^{-1} band in Figure 4.4, it is observed that lignin amount is higher in OS and WS than AS and HS, this observation also support the results given in Table 4.2.

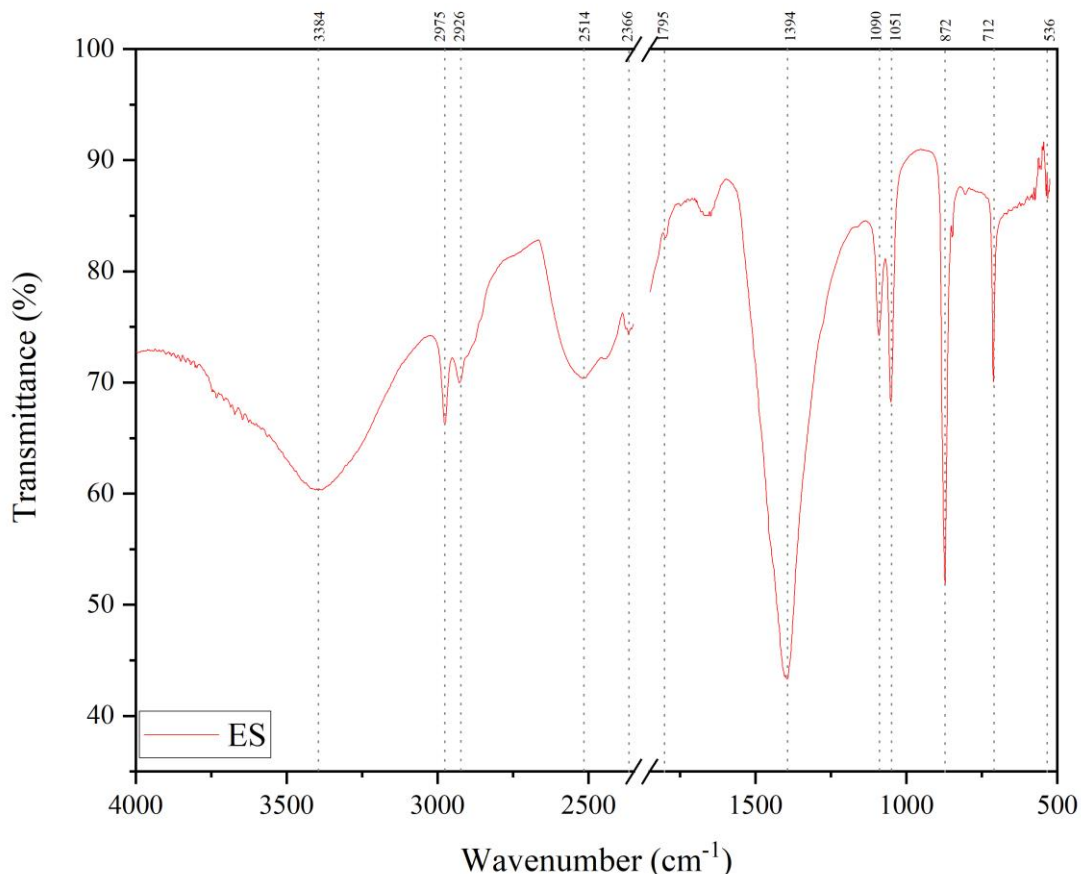


Figure 4.5: FT-IR spectrums of ES

FTIR analysis was applied to characterize the powdered eggshell bio-polymeric admixture sample. The analysis results were shown in Figure 4.5. The IR spectra demonstrated broad transmission bands at around 712, 872 cm^{-1} and 1394 cm^{-1} , which are attributed to absorption of CaCO_3 molecule. CaCO_3 was dominantly found as a main content in eggshell powder [262–265]. Also, the medium broadband at 2514 cm^{-1} indicates the presence of HCO_3^- for an eggshell [266]. The absorption that occurred around 1795 and 2975 cm^{-1} correspond to C=O from carbonate ion (CO_3^{2-}) [265]. Furthermore, the stretching vibration of the CO_3^{2-} group was eventually observed at 1051–1090 cm^{-1} [262,267], revealing that the natural base composition of eggshell absorbent was carbonate (CO_3^{2-}). Additionally, the bending band at 3384 cm^{-1} and 2514 cm^{-1} related to the presence of alcohol hydroxyl group (-OH) group and acidic hydrogen group (-OH) stretching, respectively [262,268–271]. Also, 3384 cm^{-1} can be associated with the H_2O molecules [272]. There was an evidence of a peak at about 712 cm^{-1} attributed to the Ca-O bond [262,263]. The bands at 2926 cm^{-1} represent C-H vibration, indicating the existence of the organic layers, built from amino acids, in

the eggshells [271]. Bands at 1795 and 1645 cm^{-1} correspond to C=O and carbonyl group stretching (amide), respectively [271,273].

4.2.4 SEM Image Results of Bio-polymeric Admixtures

SEM images of the bio-polymeric admixtures are shown in Figure 4.6-Figure 4.10 at 500x magnification.

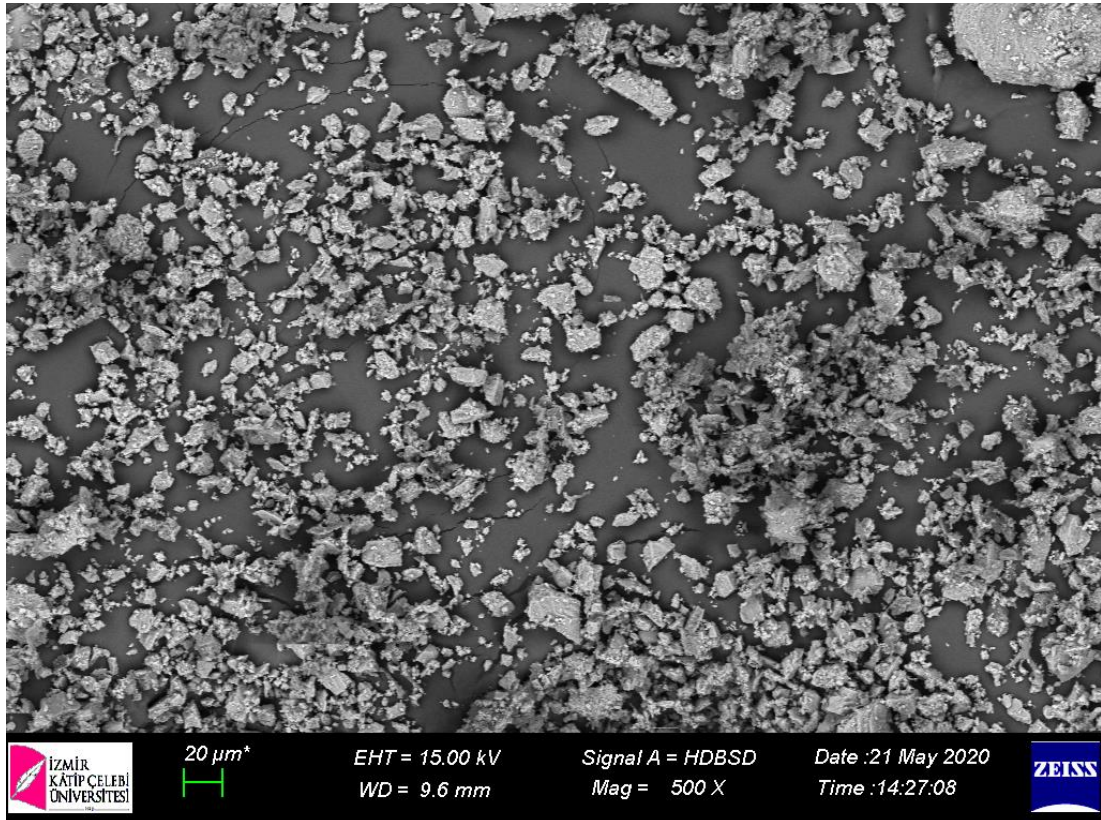


Figure 4.6: SEM micrograph of ES

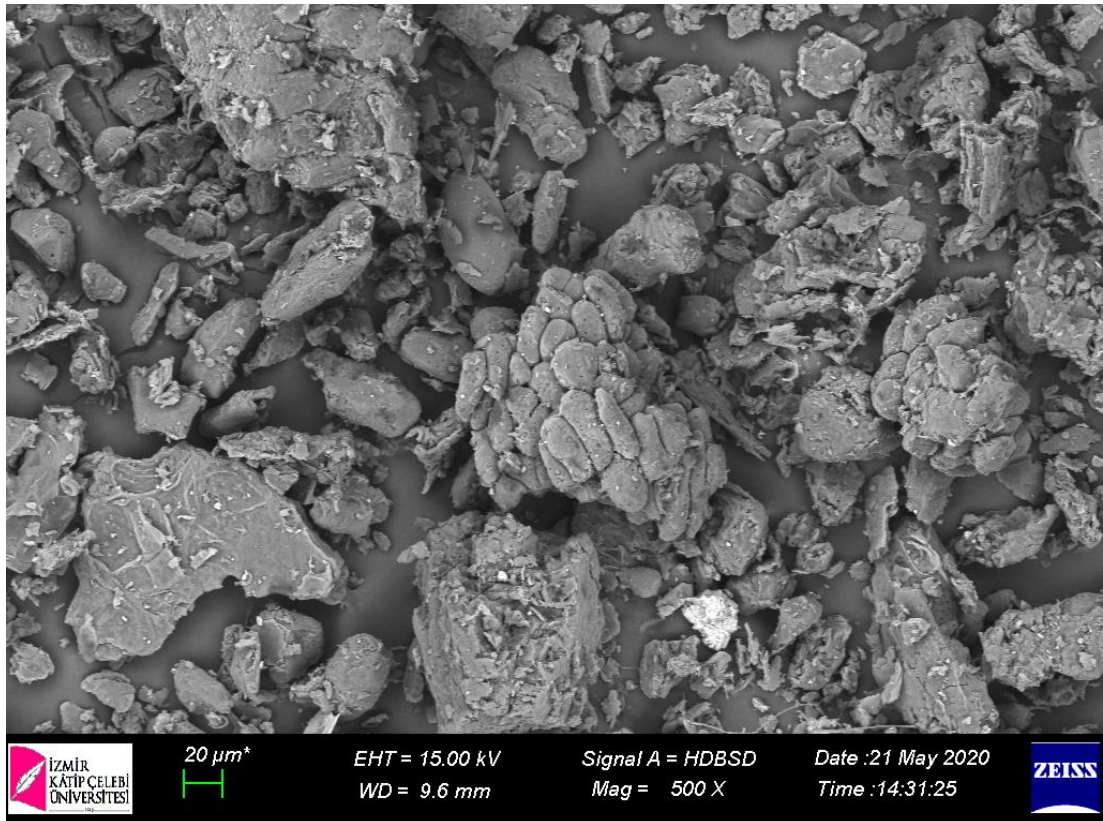


Figure 4.7: SEM micrograph of AKS

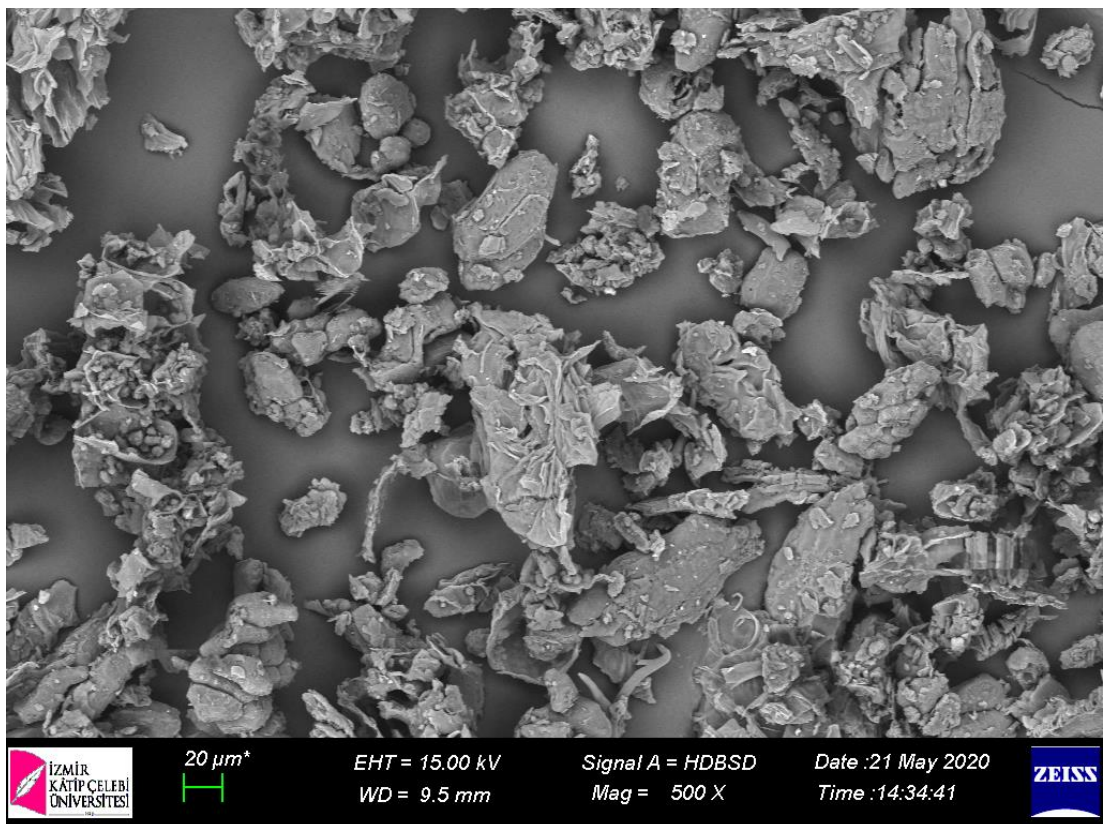


Figure 4.8: SEM micrograph of HKS

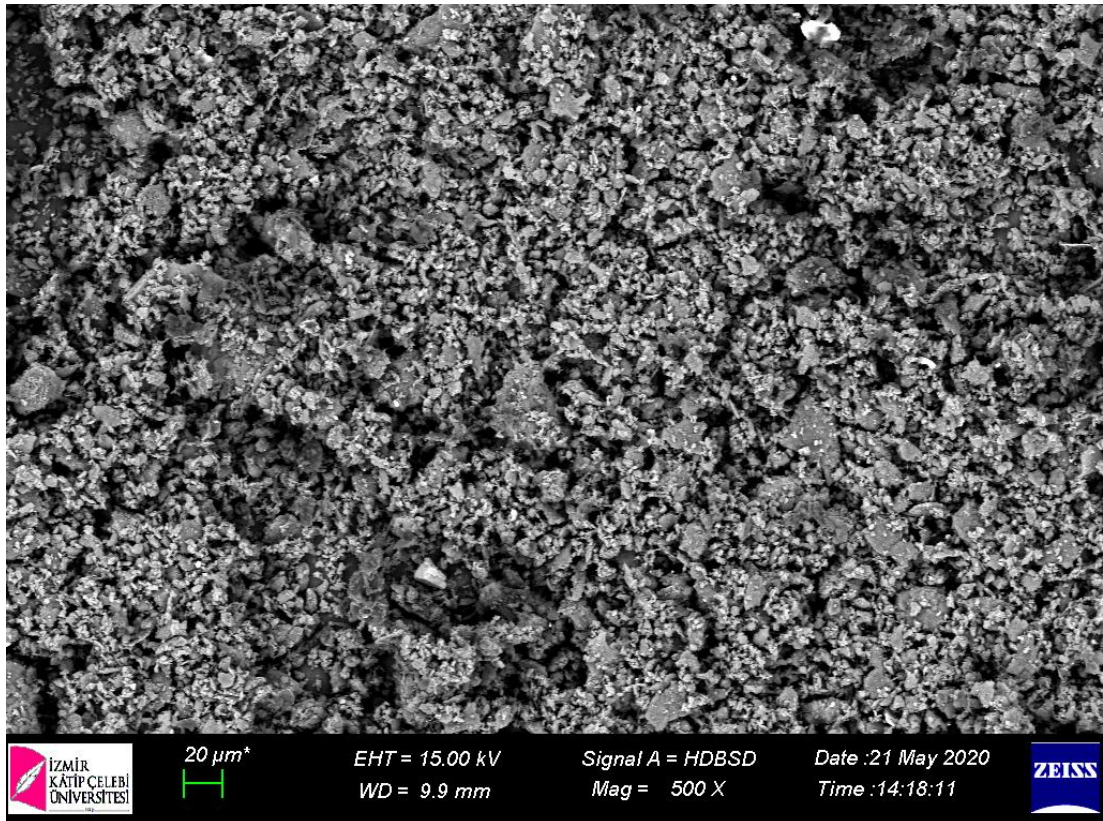


Figure 4.9: SEM micrograph of WKS

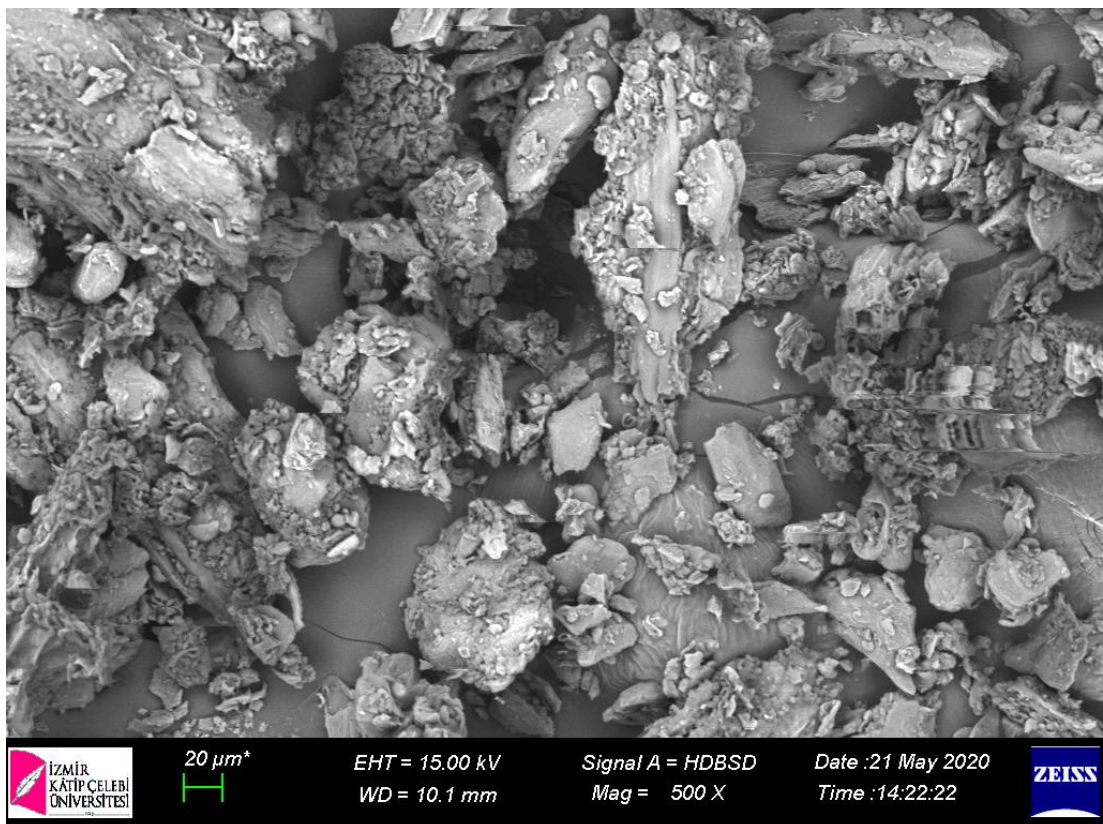


Figure 4.10: SEM micrograph of OS

It was observed from the SEM images, the bio-polymeric admixtures were characterized by the presence of irregular particles that tend to form larger agglomerates. When the SEM images of the bio-polymeric admixtures are examined, it is observed that the grains are in angular and rough structure. Considering this particle structure alone, it can be thought that it will reduce the workability properties of cement mortars in the first place. However, as will be discussed in more detail in the following sections, these materials can serve as good fillers in cement mortar. And even the extractive and lignin in lignocellulosic admixtures can be an improving factor on the workability.

The physical appearances of all the bio-polymeric admixtures used were quite different from each other (Figure 4.6-Figure 4.10). The microstructure of hazelnut kernel shell consisted of amorphous flakes, while the apricot kernel shells had lumpy granular structures and olive seed consisted of woody fibrous structure. According to Figure 4.6 and Figure 4.9, it seems that when the egg shell and walnut kernel shell are grinded, they become very fine grains almost to nano size. Also, As previously given in Table 4.2, the lignin amount is much higher in WKS compared to other lignocellulosic materials, while the holocellulose amount is relatively lower. Considering these conditions, it has been observed that lignocellulosic materials with low holocellulose content and high lignin content gain a more brittle and finer grain size structure when ground.

In addition, microstructure of the bio-polymeric admixtures used in this study and the same or similar materials used for different purposes in the literature were compared between Figure 4.11-Figure 4.15.

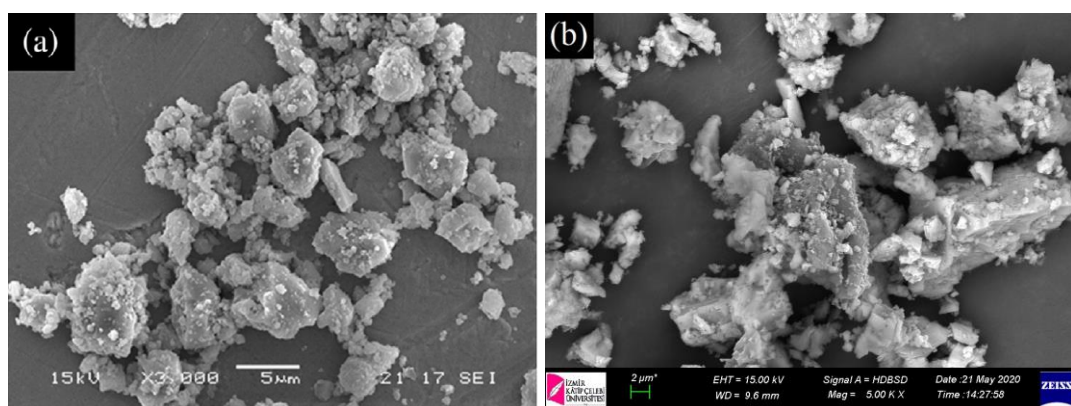


Figure 4.11: SEM micrographs of (a) limestone powder [274], (b) ES at 5000x magnification

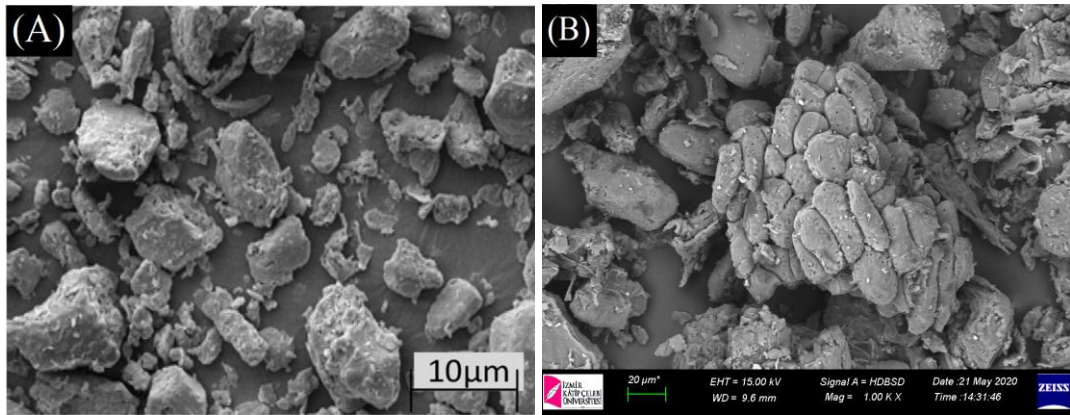


Figure 4.12: SEM micrographs of (A) apricot shell [275], (B) AKS at 5000x magnification

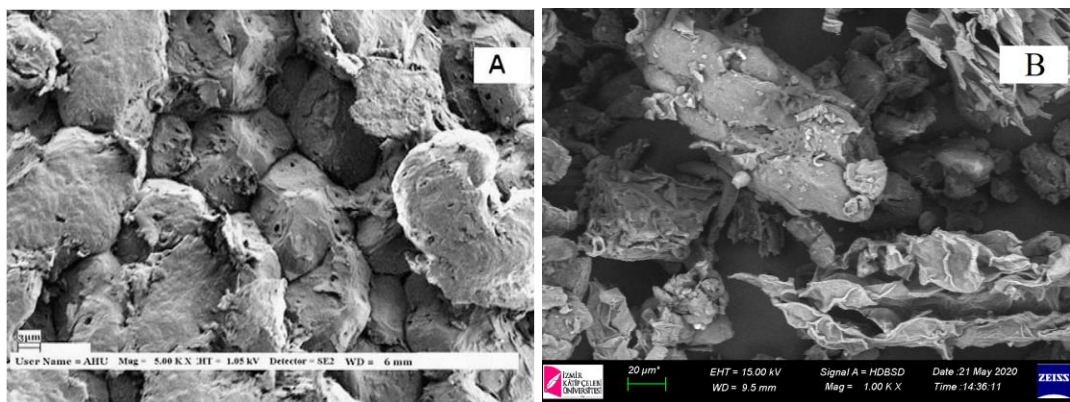


Figure 4.13: SEM micrographs of (A) hazelnut shell [276], (B) HKS at 5000x magnification

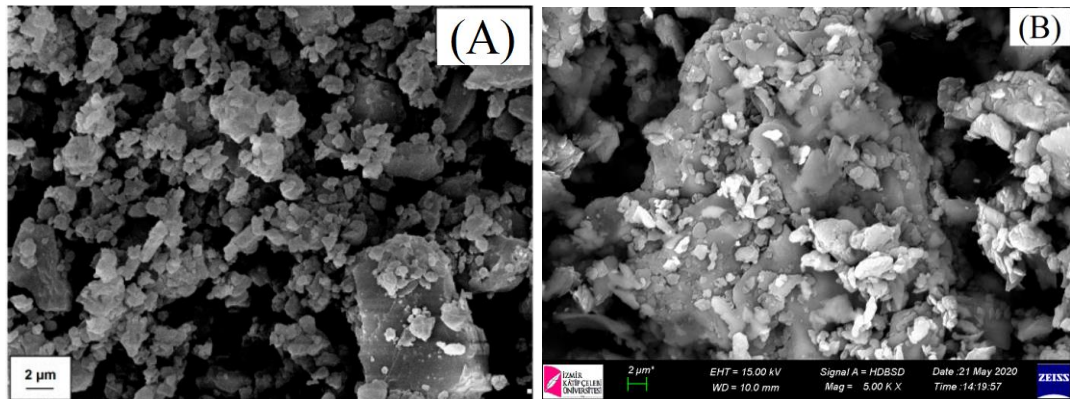


Figure 4.14: SEM micrographs of (A) lignin [277], (B) WKS at 5000x magnification

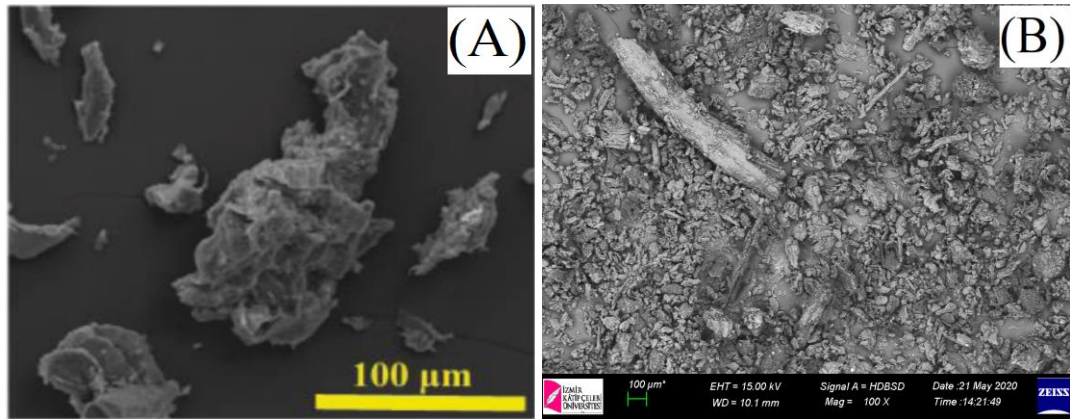


Figure 4.15: SEM micrographs of (A) hazelnut shell [278], (B) HKS at 5000x magnification

Figure 4.11 revealed that since the eggshell contains a very large proportion of calcium carbonate, it has almost the same grain shape and properties as powdered limestone. In Figure 4.12, it was determined that the ground apricot kernel shell used in this study and the ground apricot kernel shell used in the other studies in literature had similar grain shapes. A similar phenomenon also applies to the ground hazelnut kernel shell in Figure 4.13. Similar to the harmony of the grain properties of the egg shell due to the content affinity with the limestone, it can be easily observed from Figure 4.14 that the grain shape and properties of the ground walnut shells coincide with raw lignin due to the high lignin content of the ground walnut shells. Also, the layered and cracked surface of the ground olive seed is in agreement with other examples in the literature Figure 4.15.

4.2.5 Evaluation of the Characterization of Bio-polymeric

Admixtures

The detailed characterization study of ES, AKS, HKS, WKS, and OS bio-polymeric admixtures to be used in this thesis study was carried out with XRD, FT-IR and SEM analyzes. In addition, the amount of extractive, lignin, hemicellulose, and cellulose as chemical components of bio-polymeric additives in lignocellulosic structure were determined as percentages.

Many factors such as the way the lignocellulosic wastes are collected, the growing type of the mother plant and the growing shade play an important role in the chemical composition of the material. Therefore, the chemical content of each lignocellulosic additive was found to be different by the researchers. Therefore, the chemical structure

of bio-polymeric admixtures in four different lignocellulosic structures used in this study was experimentally determined. In waste lignocellulosic type biopolymeric additives, the highest extractive, lignin, hemicellulose and cellulose contents were determined in OS (18.39 ± 0.26 %), WKS (41.23 ± 1.14 %), HKS (31.73 ± 1.78 %), and AKS (37.92 ± 0.18 %), respectively. The lowest extractive, lignin, hemicellulose and cellulose contents were determined in AKS (3.81 ± 0.11 %), AKS (27.07 ± 0.19 %), WKS (20.58 ± 4.24 %), and OS (19.48 ± 1.22 %), respectively.

In XRD analysis, lignin, hemicellulose, and cellulose were determined, which supports the experimentally found chemical contents of lignocellulosic admixtures. Lignocellulosic admixtures were found as semicrystalline materials and the highest crystallinity index was found as 32.21 % with AKS, which had the highest alpha cellulose content. It was determined that the ES biopolymeric additive also consisted of a high amount of CaCO_3 , as a result of XRD analysis. FT-IR analyzes of biopolymeric additives also support the amount of substances found in the experimental content determination and XRD analysis results. OH groups, which are the main groups that provide water retention in cellulosic materials, were clearly seen in FT-IR analyzes. In addition, the high amount of lignin in the walnut kernel shell and fatty acids in the olive seed were also detected.

As can be observed, the bio-polymeric admixtures evaluated in this study are composite materials consisting of a combination of more than one substance. For this reason, each component can impart different properties to the mortar. Fatty acids in the composition of the extractives can add water repellency to the cement mortar. It is known that lignin is an important substance used for cement dispersion. Cellulose are used as water-retaining materials in cement mortars. In addition, calcium carbonate, which is found in high amounts in egg shells, is tried as a filling material in many studies. For this reason, it is important to understand the internal structure of biopolymeric admixtures in order to predict what kind of benefit they can provide to the cement mortar.

4.3 Effect of Bio-polymeric Admixtures on Composite Cement Mortars and Comparison with Some Chemical Admixtures

4.3.1 Fresh and Hardened Unit Weight of Mortars

Fresh and hardened unit weights of composite cement mortars are given in Table 4.5-

Table 4.8.

Table 4.5: Composite cement mortar mixture combinations with 0/45 μm grain size bio-polymeric admixtures

Mix code	Fresh Unit Weight (kg/m^3)	Hardened Unit Weight (kg/m^3)
R	2270	2204
ES0.2	2257	2231
ES0.35	2154	2116
ES0.5	2157	2130
ES1.0	2143	2124
ES1.5	2139	2109
AKS0.2	2232	2151
AKS0.35	2114	2095
AKS0.5	2073	2141
AKS1.0	2199	2105
AKS1.5	2118	2093
HKS0.2	2125	2079
HKS0.35	2111	2074
HKS0.5	2177	2111
HKS1.0	2095	2077
HKS1.5	2118	2076
WKS0.2	2069	2044
WKS0.35	2064	2011
WKS0.5	2041	2021

Table 4.5 (Continued): Composite cement mortar mixture combinations with 0/45 μm grain size bio-polymeric admixtures

Mix code	Fresh Unit Weight (kg/m^3)	Hardened Unit Weight (kg/m^3)
WKS1.0	2127	2074
WKS1.5	2158	2085
OS0.2	2015	1904
OS0.35	2014	1954
OS0.5	2021	1959
OS1.0	2078	2003
OS1.5	2133	2064

Table 4.6: Composite cement mortar mixture combinations with 0/125 μm grain size bio-polymeric admixtures

Mix code	Fresh Unit Weight (kg/m^3)	Hardened Unit Weight (kg/m^3)
R	2270	2204
ES0.2	2260	2246
ES0.35	2274	2236
ES0.5	2267	2247
ES1.0	2262	2193
ES1.5	2195	2181
AKS0.2	2264	2209
AKS0.35	2248	2194
AKS0.5	2227	2162
AKS1.0	2194	2167
AKS1.5	2183	2162
HKS0.2	2271	2199
HKS0.35	2198	2100
HKS0.5	2198	2105
HKS1.0	2170	2115
HKS1.5	2160	2111
WKS0.2	2148	2078

Table 4.6 (Continued): Composite cement mortar mixture combinations with 0/125 μm grain size bio-polymeric admixtures

Mix code	Fresh Unit Weight (kg/m^3)	Hardened Unit Weight (kg/m^3)
WKS0.35	2191	2101
WKS0.5	2141	2114
WKS1.0	2200	2135
WKS1.5	2258	2201
OS0.2	2077	1991
OS0.35	2052	2023
OS0.5	2088	2040
OS1.0	2183	2105
OS1.5	2183	2165

Table 4.7: Composite cement mortar mixture combinations with 125/250 μm grain size bio-polymeric admixtures

Mix code	Fresh Unit Weight (kg/m^3)	Hardened Unit Weight (kg/m^3)
R	2270	2204
ES0.2	2244	2168
ES0.35	2237	2092
ES0.5	2243	2156
ES1.0	2194	2134
ES1.5	2156	2017
AKS0.2	2291	2127
AKS0.35	2167	2122
AKS0.5	2277	2175
AKS1.0	2134	2195
AKS1.5	2285	2197
HKS0.2	2245	2188
HKS0.35	2136	2190
HKS0.5	2117	2187
HKS1.0	2182	2148
HKS1.5	2170	2068

Table 4.7 (Continued): Composite cement mortar mixture combinations with 125/250 μm grain size bio-polymeric admixtures

Mix code	Fresh Unit Weight (kg/m^3)	Hardened Unit Weight (kg/m^3)
WKS0.2	2248	2156
WKS0.35	2105	2168
WKS0.5	2236	2163
WKS1.0	2095	2079
WKS1.5	2093	2043
OS0.2	2168	2103
OS0.35	2088	2014
OS0.5	2077	1972
OS1.0	2059	2001
OS1.5	2052	2021

Table 4.8: Composite cement mortar mixture combinations with chemical admixtures

Mix code	Fresh Unit Weight (kg/m^3)	Hardened Unit Weight (kg/m^3)
R	2270	2204
CS0.2	2282	2251
CS0.35	2278	2238
CS0.5	2281	2247
CS1.0	2256	2223
CS1.5	2239	2204
PCE0.01	2296	2243
PCE0.025	2279	2198
PCE0.05	2196	2102
PCE0.1	2213	2178
PCE0.2	2391	2309
SMF0.05	2284	2238
SMF0.1	2268	2224
SMF0.2	2263	2214
SMF0.35	2381	2307

Table 4.8 (Continued): Composite cement mortar mixture combinations with chemical admixtures

Mix code	Fresh Unit Weight (kg/m ³)	Hardened Unit Weight (kg/m ³)
SMF0.5	2377	2288
TA0.03	2282	2205
TA0.05	2177	2166
TA0.1	2285	2178
TA0.2	2179	2166
TA0.35	2248	2230

As the unit volume mass results were examined, there was a slight decrease in the unit volume mass of the mortars when all other bio-polymeric materials were used as admixtures in the mortars, except for ES. In particular, as the grain size of the bio-polymeric admixtures increases, the decrease in the unit volume mass values of the mortars becomes more evident. The chemical composition of lignocellulosic materials includes fatty acids, lignin and cellulose. It has been determined in studies conducted by researchers that fatty acids have some air-entraining properties in cement-binding products [102]. In addition, it has been determined by researchers that lignin and cellulose additives have some air-entraining effect in cementitious products [277,279,280]. Results similar to the literature were also obtained in this thesis study and the unit volume mass values of the mortars in which bio-polymeric admixtures used were determined to be lower than the unit volume mass value of the reference mortar. This indicates that there is more void left in the mortar during the molding of the fresh mortars. Thus, bio-polymeric admixtures entrain some air in cementitious mortars. In the use of eggshell, the opposite effect is observed, and eggshell powder can fill the voids with its good filling feature [152]. Thus, no significant decrease was recorded in the unit volume mass values of the mortars produced with this admixture.

4.3.2 Flowability of Mortars

While preparing the cement mortar samples, the flow diameter values of the samples prepared in the flow table were determined depending on the bio-polymeric admixture particle size and usage rate. The flow diameter values of the test samples are given in Table 4.9. Flow diameters of fresh mortars depending on the bio-polymeric admixture

particle size and using rates in the mortar are shown in between Figure 4.16 and Figure 4.20.

Table 4.9: Flow diameter values of test specimens

Mix Code	Flow Diameters (mm)		
	0/45 μm	0/125 μm	125/250 μm
R	120.36	120.36	120.36
ES0.2	125.25	131.13	123.25
ES0.35	128.75	130.15	123.75
ES0.5	129.00	132.90	117.50
ES1.0	128.13	134.80	113.00
ES1.5	125.13	128.00	111.50
AKS0.2	130.00	143.29	116.00
AKS0.35	130.75	142.08	114.25
AKS0.5	131.75	140.81	114.00
AKS1.0	119.75	139.86	112.00
AKS1.5	114.00	121.10	110.00
HKS0.2	123.63	122.63	118.50
HKS0.35	132.00	122.79	116.50
HKS0.5	123.88	123.50	114.25
HKS1.0	117.25	121.83	111.50
HKS1.5	109.50	118.11	110.00
WKS0.2	138.13	163.80	118.00
WKS0.35	138.75	155.25	117.00
WKS0.5	139.63	152.94	112.50
WKS1.0	117.75	135.16	109.50
WKS1.5	104.00	127.85	105.00
OS0.2	137.50	149.17	135.50
OS0.35	147.00	157.76	136.00
OS0.5	141.50	159.06	141.50
OS1.0	131.00	146.61	144.00
OS1.5	112.75	126.51	129.25

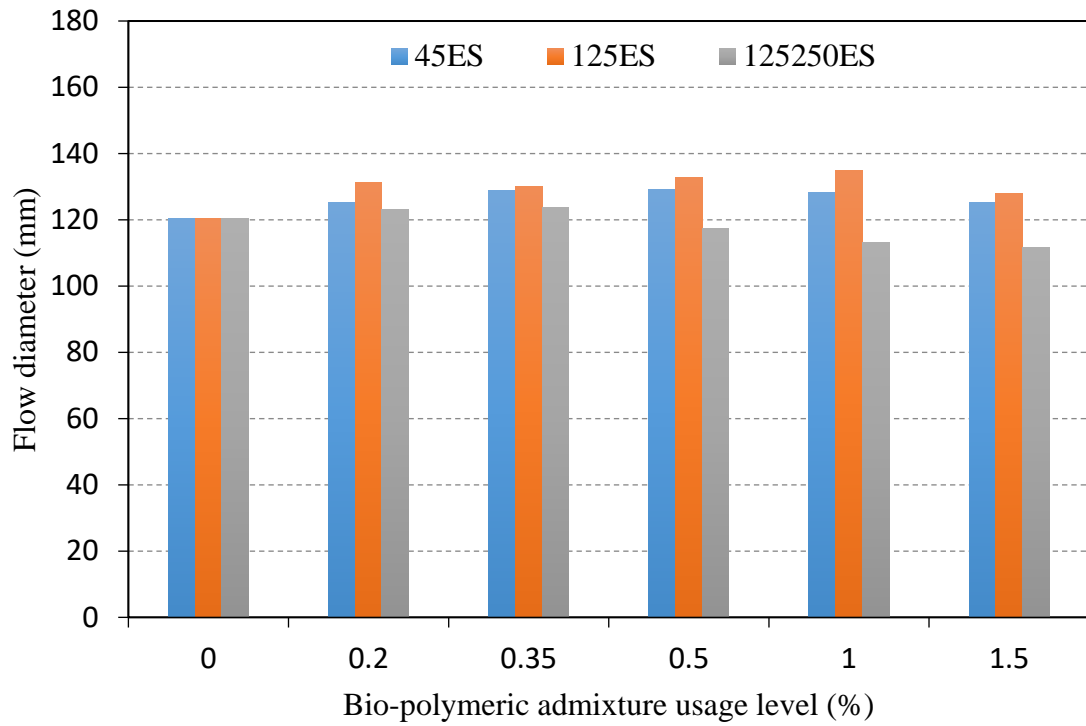


Figure 4.16: Flow diameters of ES admixed cement mortars

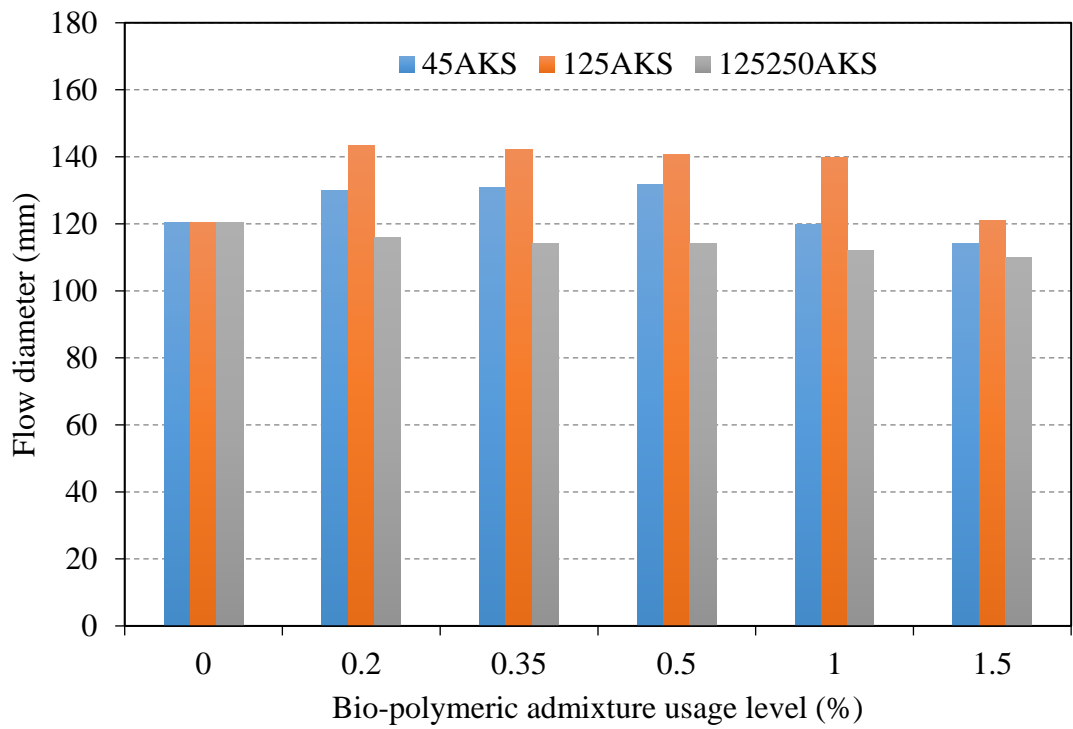


Figure 4.17: Flow diameters of AKS admixed cement mortars

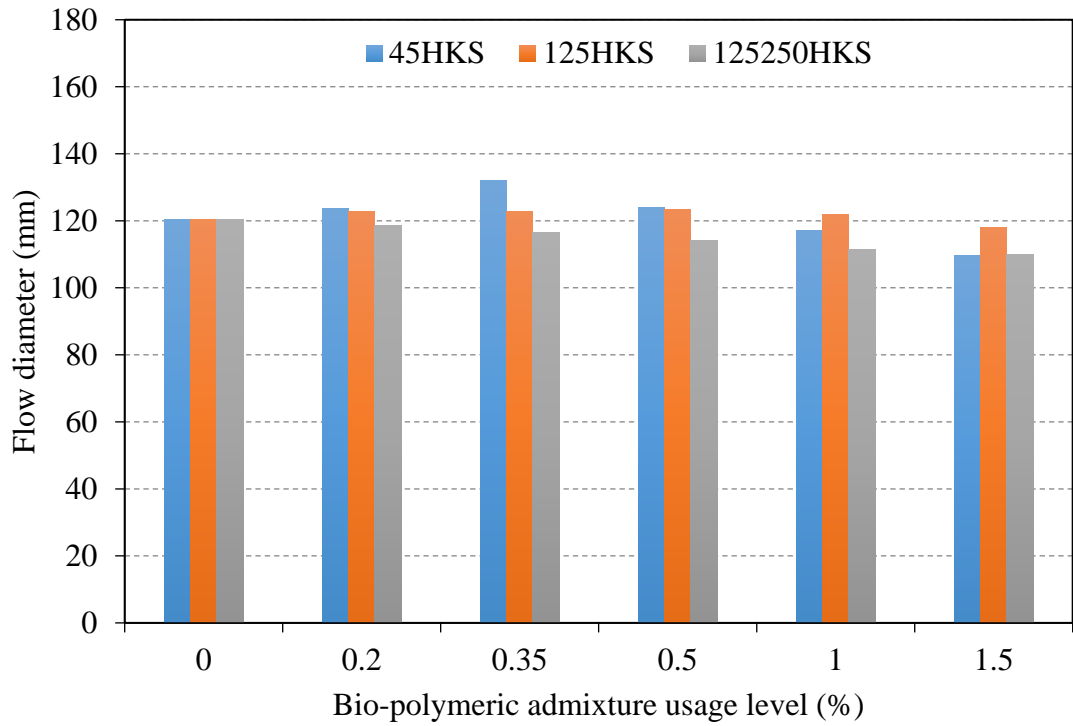


Figure 4.18: Flow diameters of HKS admixed cement mortars

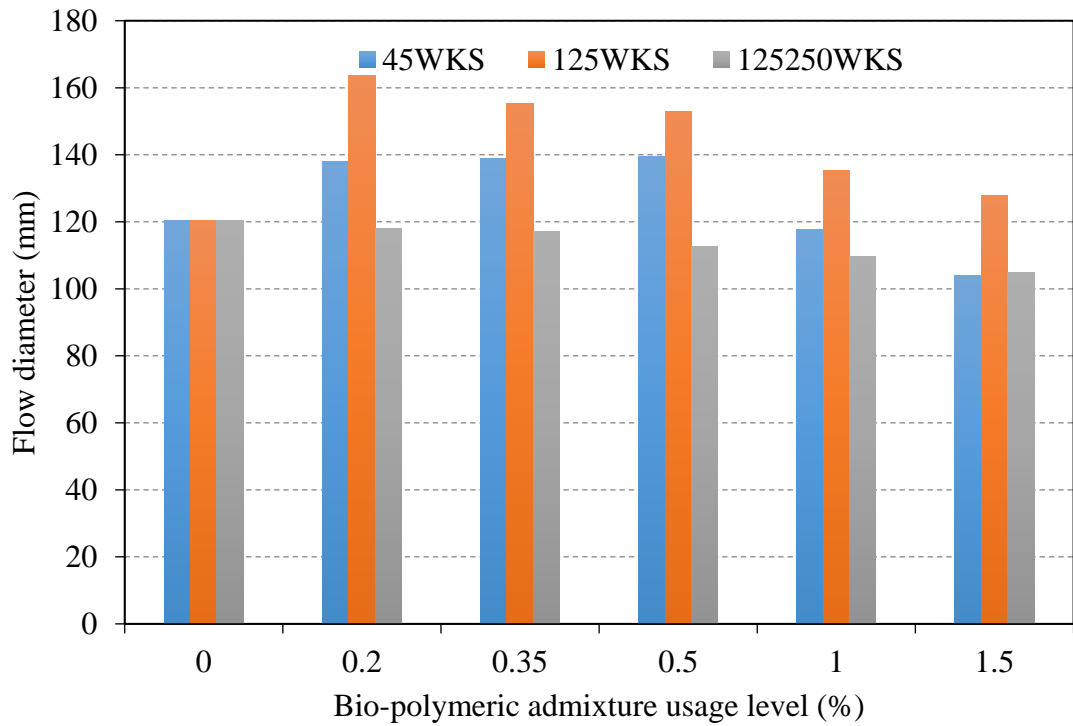


Figure 4.19: Flow diameters of WKS admixed cement mortars

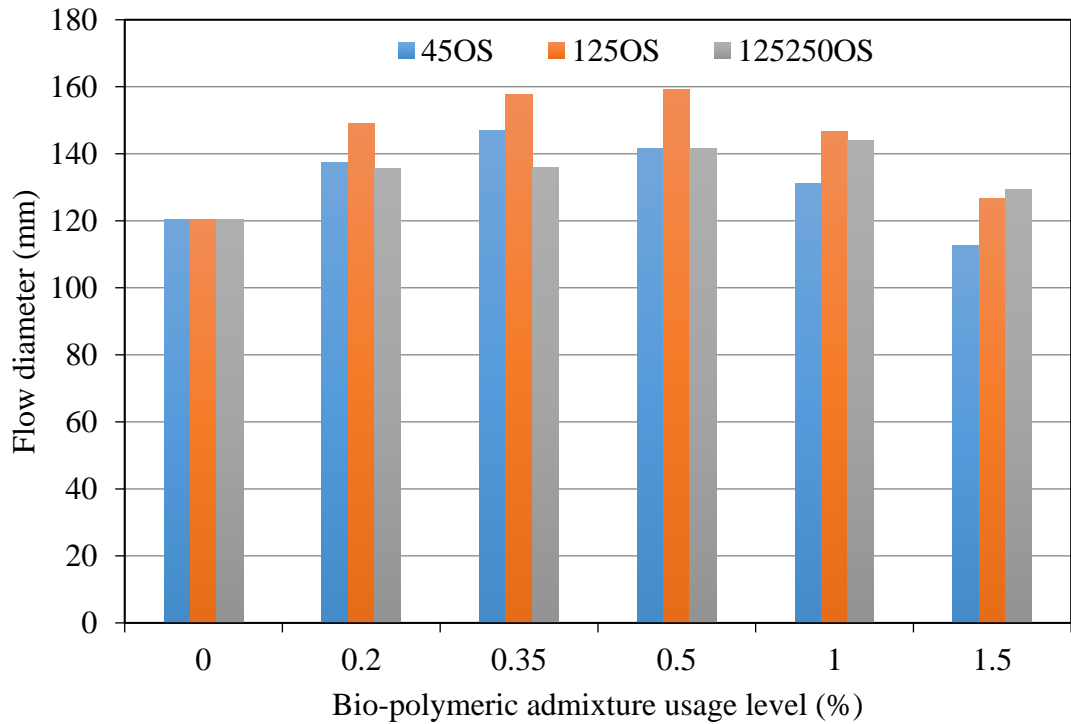


Figure 4.20: Flow diameters of OS admixed cement mortars

Analyzing the figures above, almost all fresh mortars samples with 0/45 μm and 0/125 μm grain size bio-polymeric admixtures exhibited a wider flow diameter over the flow table than flow diameter of reference mortar. The reason for this can be explained in two ways, firstly since all egg shell, apricot shell, hazelnut shell, walnut shell, and olive seed bio-polymeric admixtures were used as 0/45 and 0/125 μm , these admixtures may have gained filling feature in the cement mortar. According to Moosberg-Bustnes et al. [281] and Subaşı et al. [282] using filler materials finer than 0.125 mm is quite effective on the fresh state properties of concrete due to improving and maintaining the cohesion and segregation resistance of concrete and filling the intergranular voids between cement particles and improving the compactness of the concrete. Nehdi [283] stated that the workability can be obtained with the densest particle packing. Because, by this way, the adsorbed water will not only fill voids, it also will increase the thickness of the water layer around particles so decreasing in viscosity and improving in flow properties will occur. It is also known that lignin-derived plasticizers have a dispersing effect on cement particles. One of the main components of all bio-polymeric admixtures used in the experiments, except egg shell, is lignin (28.15% - 49.18 % by weight). The lignin, which is bound with cellulose and hemicellulose, can be released after the celluloses dissolved in alkaline environment and may show a dispersing effect on cement particles. On the other hand, it has been

determined by some researchers that some fatty acids, especially fatty acids in olive seeds (i.e. oleic and linoleic acid), have a dispersing effect on cement particles by electrostatic repulsion and steric effect [103,284].

Flow diameter of reference sample was 120.36 mm. When ES additive was used, the maximum improvement in flowability was determined as 12 % (125ES1.0). The flow diameter value of the 125AKS0.2 mixture improved by 19.05% compared to the flow diameter of the reference sample. Flow diameter value of the 45HKS0.35 mixture improved by 9.67 % compared to the flow diameter of the reference sample. The two admixtures that contributed the most to the cement mortar in terms of flowability were WKS with high lignin ratio and OS with high extractive ratio. When the grain size of these two admixtures is 0/125 μm like the others, the increase in flow diameters is greater. Compared to the reference mixture, 125WKS0.2 and 125OS0.5 improved the flow diameters by 36.09 % and 32.19 %, respectively. The general trend observed in the flowability of the mortars is an increase with the use of 0.2, 0.35 and 0.5 % bio-polymeric admixtures usage, and a decrease in the flow diameter of the mortars with the use of 1% and 1.5% bio-polymeric admixture. The general reason for this decrease is that the bio-polymeric admixtures grains are agglomerated.

When the graphs shown above are examined, when 125/250 μm particle size distribution is used, the flowability improving feature of bio-polymeric admixtures in mortars decreases. The reason for this is that the grain structure of the bio-polymeric admixtures is closer to the fiber structure in this grain size distribution.

The interaction of flow diameter values with the components that make up the chemical structure of the bio-polymeric admixtures are shown in Figure 4.21 - Figure 4.23.

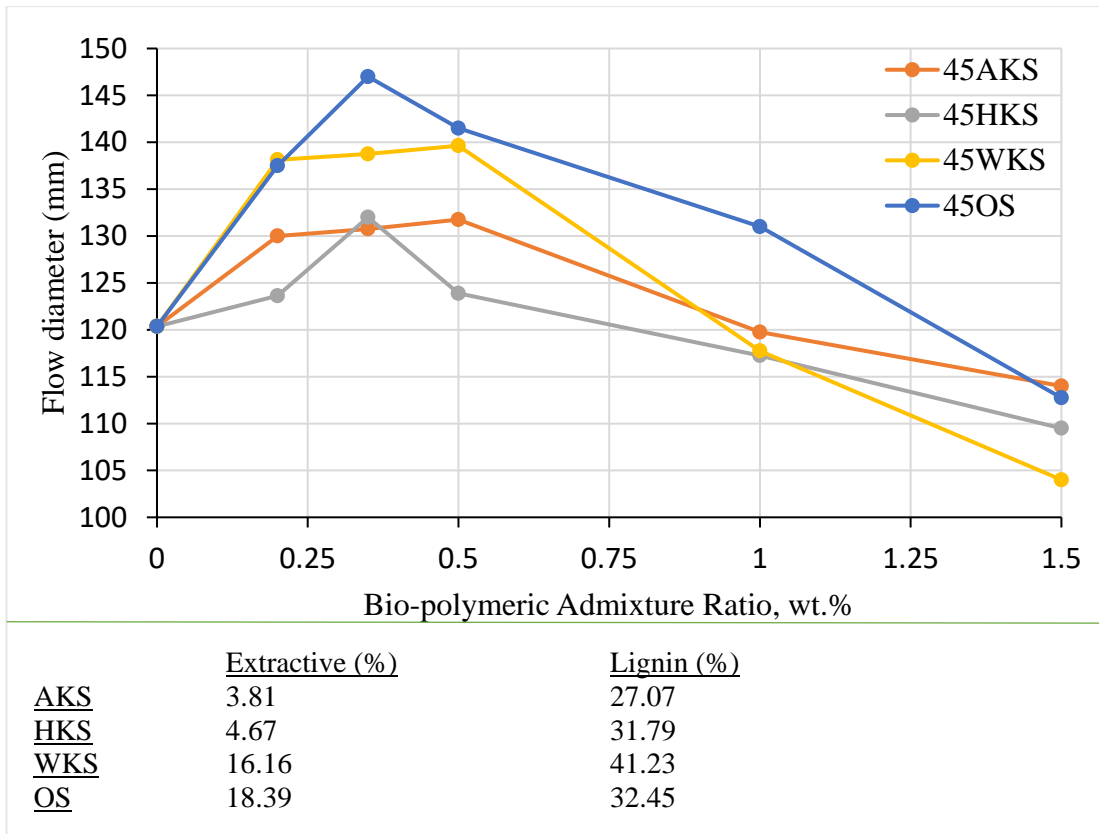


Figure 4.21: Relationship between chemical contents of 0/45 μm bio-polymeric admixture and flow diameter

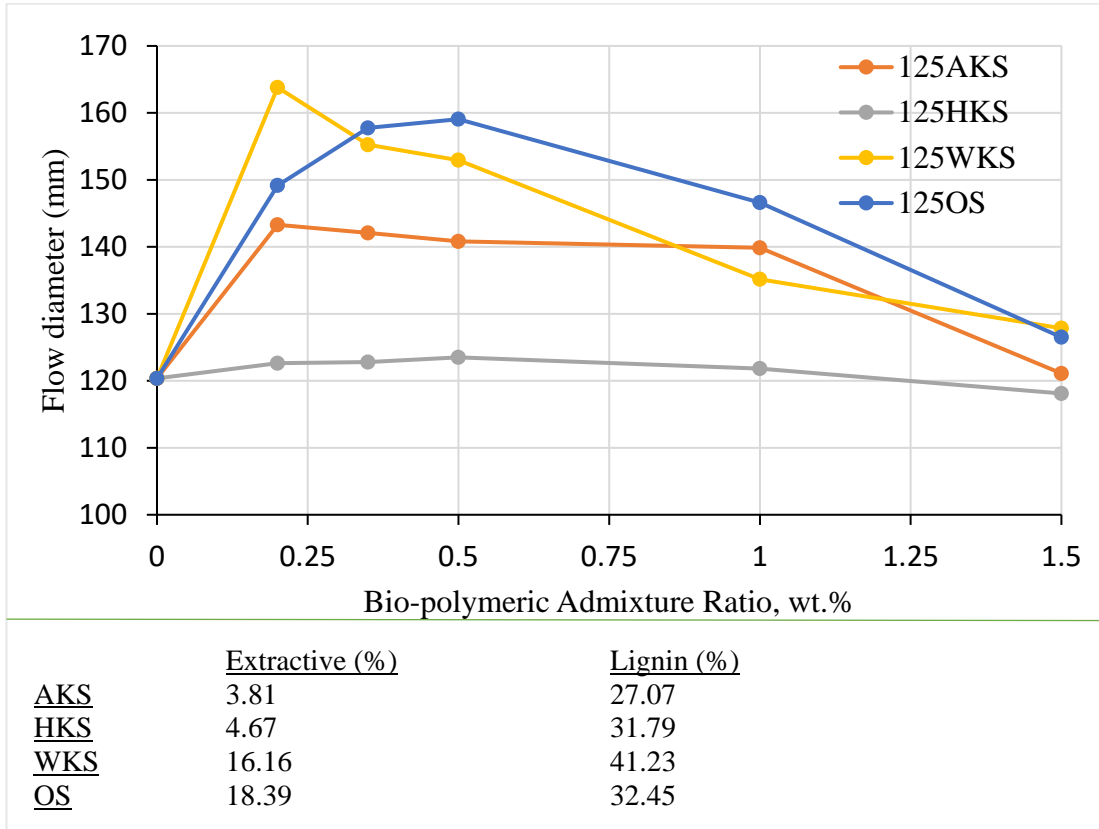


Figure 4.22: Relationship between chemical contents of 0/125 μm bio-polymeric admixture and flow diameter

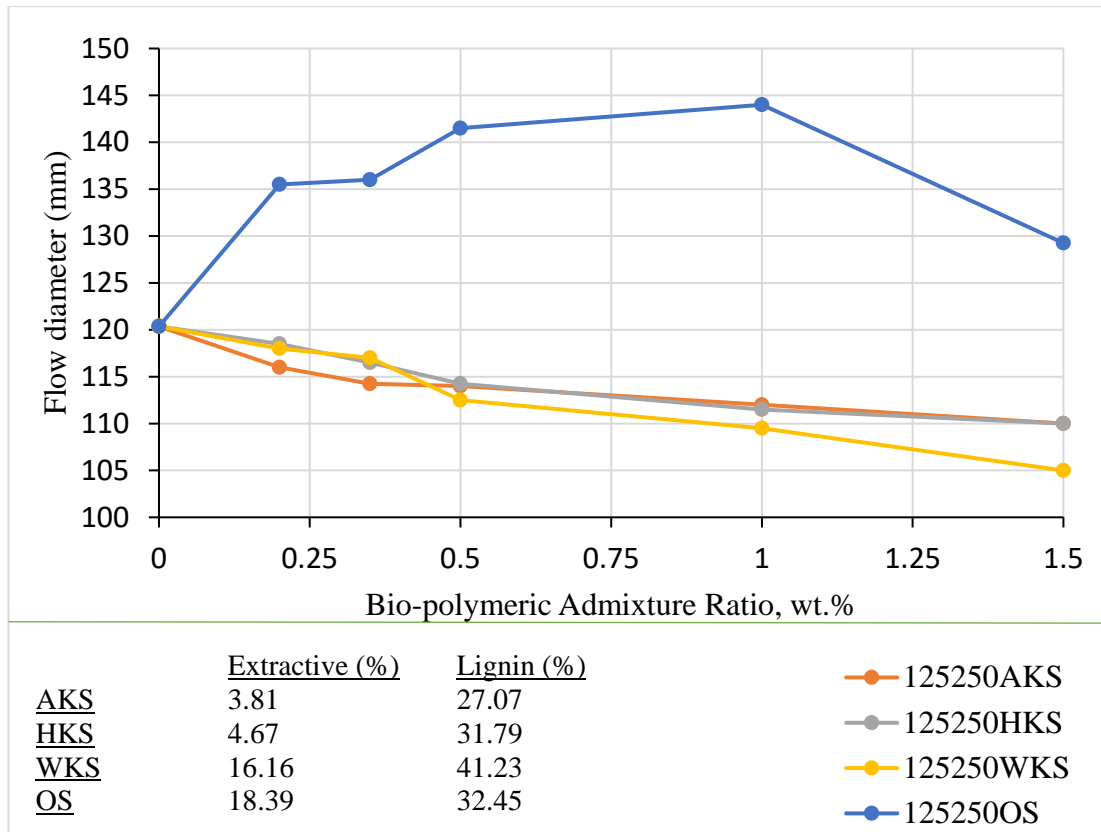


Figure 4.23: Relationship between chemical contents of 125/250 μm bio-polymeric admixture and flow diameter

According to Figure 4.21, Figure 4.22 and Figure 4.23, it was determined that the extractive and lignin content of bio-polymeric admixtures increased the flowability of the cement mortar. In addition, it was determined that bio-polymeric admixtures with higher extractive and lignin ratios had a greater plasticizing effect.

The sum of the extractive and lignin content is 57.39 % in the walnut shell, 50.84 % in the olive seed, 34.98 % in the hazelnut shell and 30.89 % in the apricot shell, respectively. Considering this information, as Figure 4.17 to Figure 4.20 is examined, the materials that increase flow diameter the most were WS and OS admixtures for all three dimensional fractions (0/45, 0/125 and 125/250 μm). When all the mixtures are taken into consideration, the grain size with the most flowability effect among all grain sizes was 0/125 μm . However, when admixtures with 0/45 and 125/250 μm grain distribution are used, the plasticizing effects of these admixtures are relatively reduced. When 0/45 μm particle size is used as bio-polymeric materials, water requirement increases because more bio-polymeric admixture particles enter the mortar compared to 0/125 μm particle distribution. Since the amount of water in the mixtures is kept constant, the increasing water demand cannot be met, and the plasticizer effect of 0/45

micron particle size admixtures is lower than 0/125 μm particle size admixtures. Similarly, low diameters of the mortars with bio-polymeric admixtures with a grain size of 125/250 microns are lower than the flow diameters of the mortars with bio-polymeric admixtures with a grain size of 0/125 μm . The reason for this is that when the bio-polymeric admixtures are ground in coarser sizes, the grain shapes turn into a more fibrous structure. Such fibrous grains increase the consistency of the mortar. Since the amount of water was kept constant, the consistency of the mortar was higher. Therefore, flow diameter was determined to be lower.

When the flow diameters of the eggshell added products were examined, it was determined that the flow diameters changed the very little compared to the control specimen (Figure 4.16).

Since it was determined that the bio-polymeric admixtures used in this thesis improved the flowability of the cement mortar, cement mortars were produced with two different superplasticizer admixture and their flowability was tested in order to compare this property of bio-polymeric admixtures. Test results are presented in Figure 4.24.

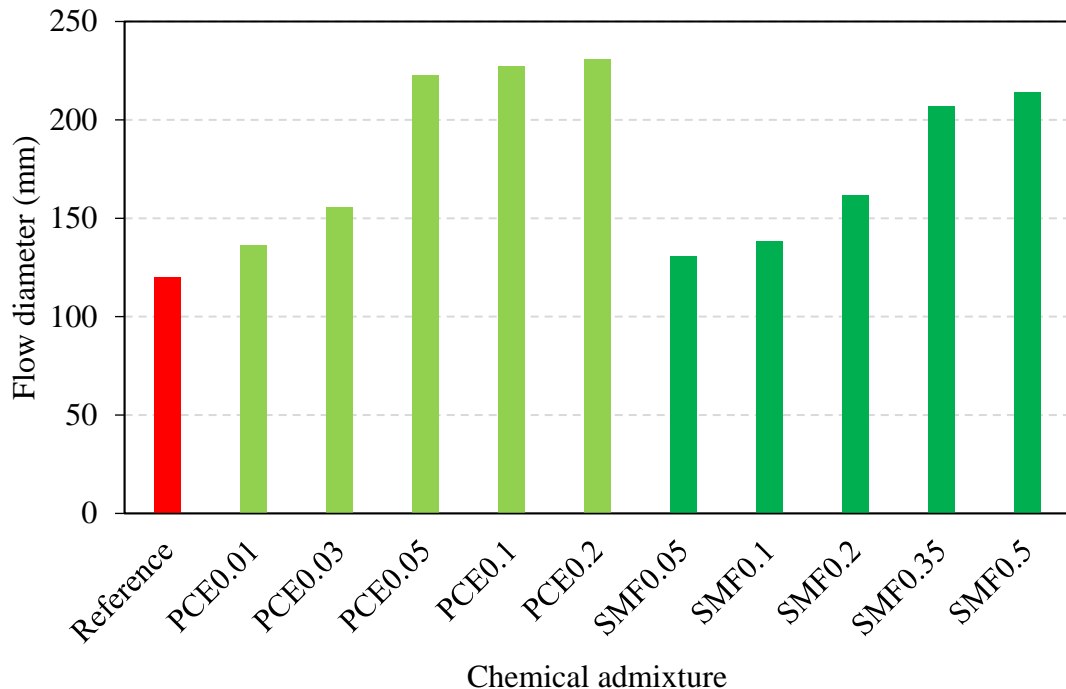


Figure 4.24: Flow diameters of PCE and SMF admixed cement mortars

When Figure 4.24 is examined in detail, as expected, superplasticizers significantly increased the flowability character of cement mortars. In the graph, the flow diameter of 120.36 mm belongs to the reference sample without any admixture. As it can be

understood from the coding of the figures, these chemicals were not used in cement mortars at such high rates as bio-polymeric admixtures, since the plasticizing feature of superplasticizers is very strong. When looking at the highest improving rates, the use of 0.2 wt.% of PCE in the mortar increased the flow diameter by 91.92 % compared to the reference mix. Similarly, the use of 0.5 wt.% of SMF increased the flow diameter by 77.89% compared to the reference mixture.

On the other hand, it can be concluded that instead of 0.03 wt.% polycarboxylate based superplasticizer or 0.20 wt.% melamine sulphionate based superplasticizer, 0.2 wt.% walnut shell powder or 0.50 wt.% ground olive seed can be used in mortars for which the flowability value is desired to improve. Thus, it has been determined that bio-polymeric admixtures can be used instead of superplasticizers by taking advantage of the fluidization feature of bio-polymeric admixtures up to a certain flow diameter value.

4.3.3 Setting Time of Mortars

The initial and final setting values of the test specimens are given in the Table 4.10. The setting time values of mortars depending on the bio-polymeric admixture particle size and the rate of use in the mortar are shown in between Figure 4.25 to Figure 4.29 below.

Table 4.10: Initial and final setting times of test specimens

Mix Code	Setting Times (min)					
	0/45 μm		0/125 μm		125/250 μm	
	Initial	Final	Initial	Final	Initial	Final
R	90	235	90	235	90	235
ES0.2	105	155	95	245	110	230
ES0.35	105	160	105	230	95	225
ES0.5	110	160	110	230	95	180
ES1.0	115	160	105	255	60	160
ES1.5	105	175	110	245	65	150
AKS0.2	70	140	165	295	115	190
AKS0.35	165	215	190	320	125	170

Table 4.10 (Continued): Initial and final setting times of test specimens

Mix Code	Setting Times (min)					
	0/45 μm		0/125 μm		125/250 μm	
	Initial	Final	Initial	Final	Initial	Final
AKS0.5	145	245	220	365	140	210
AKS1.0	95	265	220	415	95	215
AKS1.5	45	200	50	280	65	215
HKS0.2	100	175	160	220	90	205
HKS0.35	105	180	185	240	95	200
HKS0.5	125	205	170	295	90	180
HKS1.0	95	180	110	310	85	170
HKS1.5	50	155	100	300	45	140
WKS0.2	205	315	250	400	100	235
WKS0.35	220	325	260	525	95	235
WKS0.5	260	405	315	585	60	250
WKS1.0	95	345	85	395	40	155
WKS1.5	75	165	70	230	15	100
OS0.2	100	275	220	300	165	250
OS0.35	215	315	295	390	185	285
OS0.5	200	345	320	435	205	300
OS1.0	115	340	275	570	265	370
OS1.5	90	300	135	475	95	325

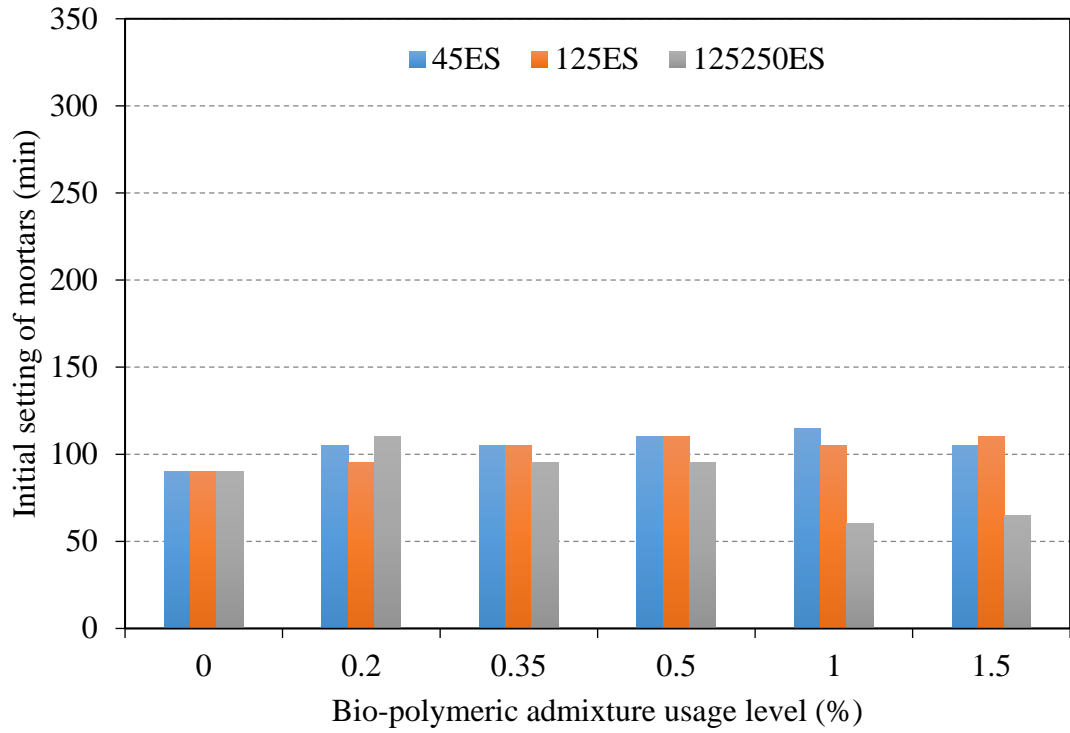


Figure 4.25: Initial setting times of ES admixed cement mortars

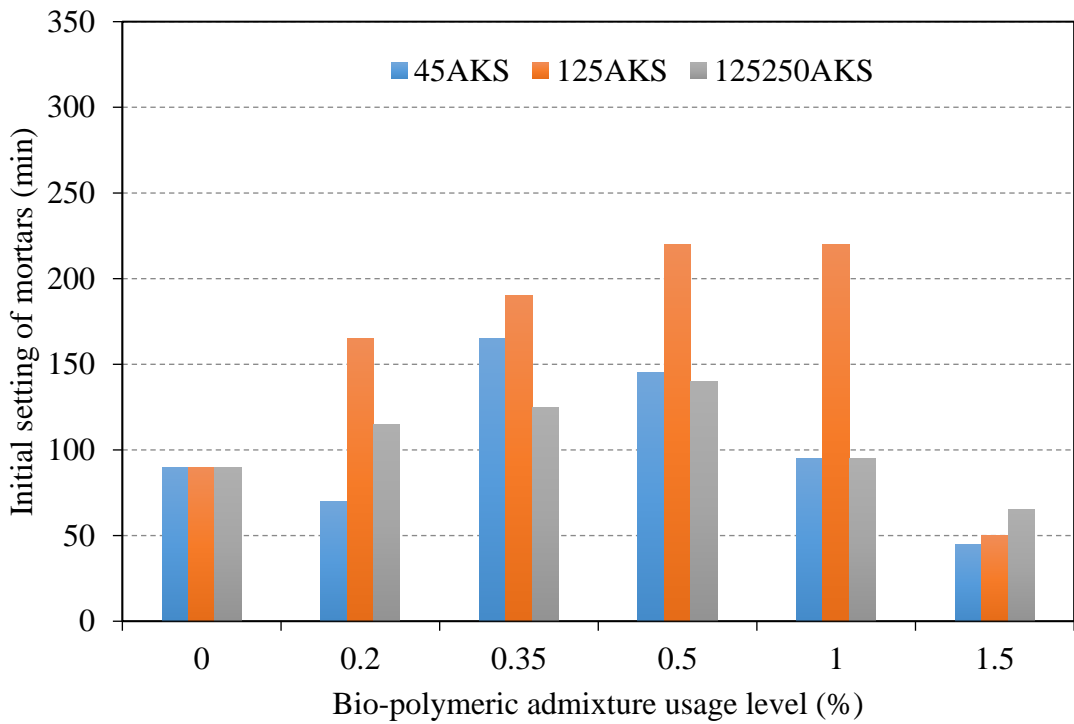


Figure 4.26: Initial setting times of AKS admixed cement mortars

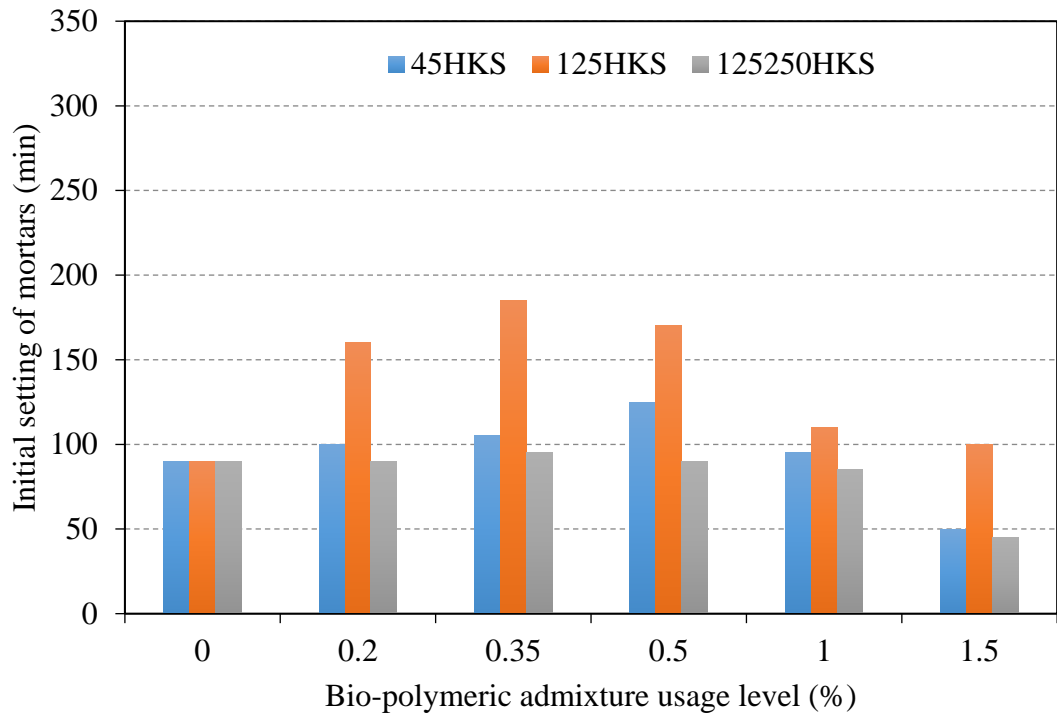


Figure 4.27: Initial setting times of HKS admixed cement mortars

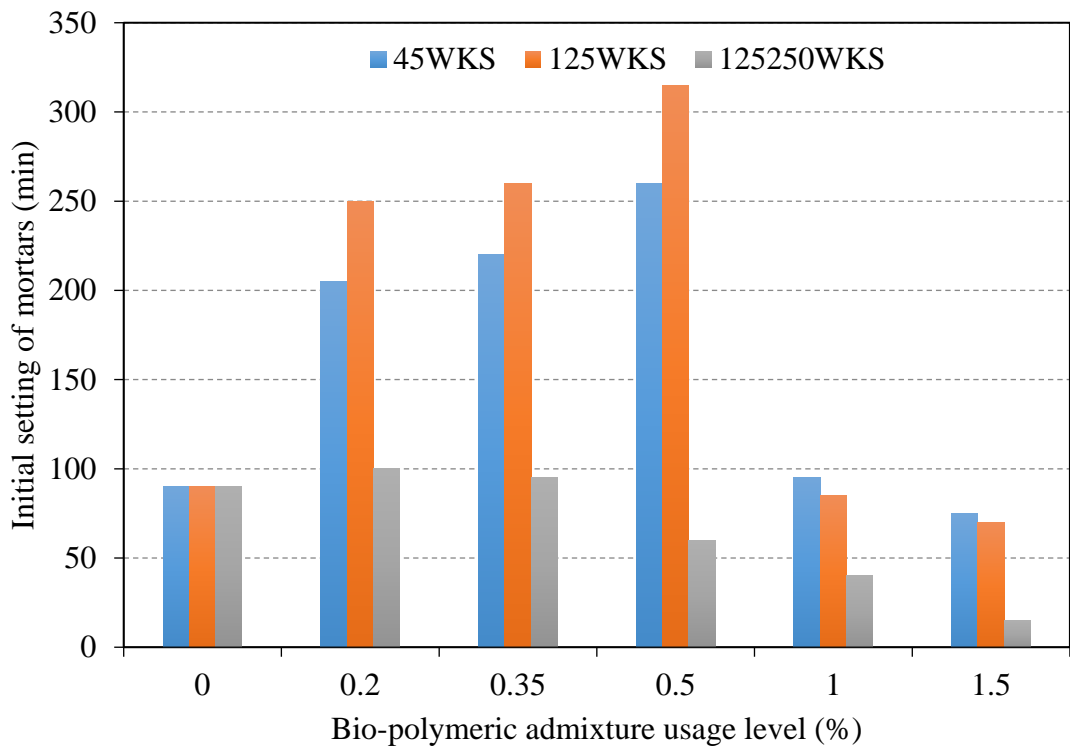


Figure 4.28: Initial setting times of WKS admixed cement mortars

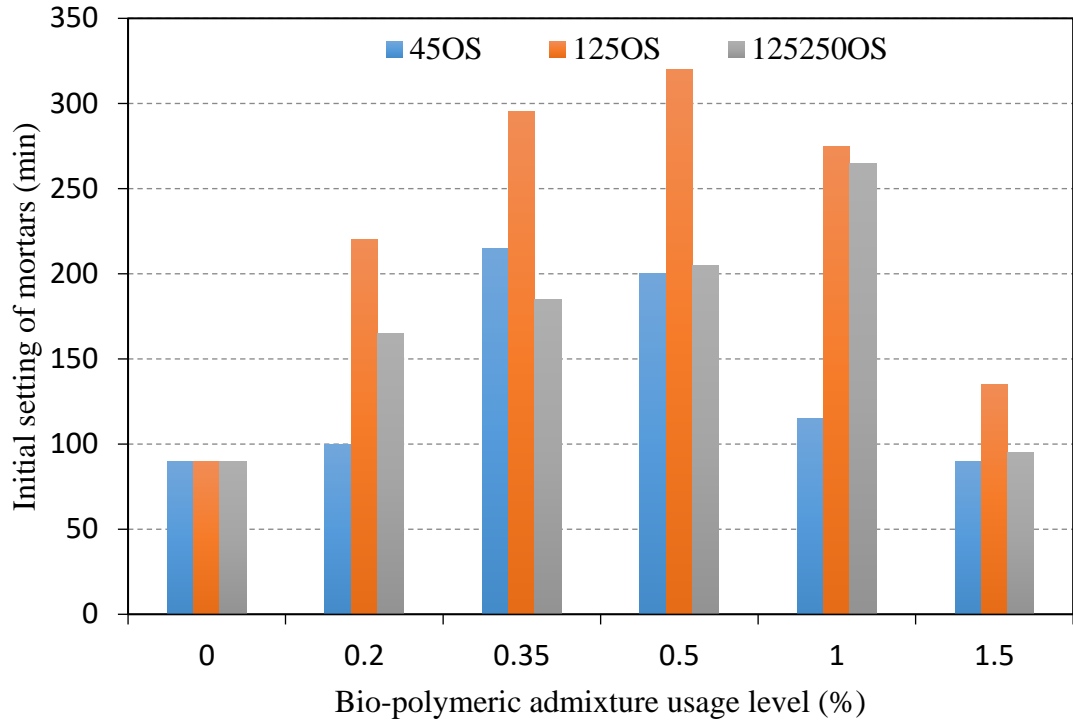


Figure 4.29: Initial setting times of OS admixed cement mortars

In above figures, the initial setting time of 90 minutes belongs to the control sample without any admixture addition to the mortars. Examining above figures from Figure 4.25 and Figure 4.29 together, all bio-polymeric admixtures have a delaying effect on initial final setting times of mortar samples, except egg shell powder. It is well known that polysaccharides such as cellulose and hemicellulose delay the setting time of cement. In addition, lignin slows cement hydration due to the sugar component and prolongs setting time. While the egg shell admixture caused a slight delay in the initial and final setting times of cement mortars.

Initial setting time of reference sample was 90 min. When ES admixture was used, comparing with reference sample, the maximum retarding in initial setting time was determined as 25 min (45ES1.0). The initial setting times of the 125AKS0.5 and 125AKS1.0 mixtures delayed by 130 min compared to the initial setting time of the reference sample. Initial setting time of the 125HKS0.2 mixture prolonged by 95 min compared to the initial setting time of the reference sample. The two admixtures that contributed the most to the cement mortar in terms of extension of initial setting time were WKS with high lignin ratio and OS with high extractive ratio. When the grain size of these two admixtures is 0/125 μm like the others, the increase in initial setting time is greater. Compared to the reference mixture, 125WKS0.5 and 125OS0.5

delayed the initial setting times by 250.00 % and 255.55 %, respectively. The general trend observed in the initial setting time of the mortars is an increase with the use of 0.2, 0.35 and 0.5 % bio-polymeric admixtures, and a decrease in the initial setting times of the mortars with the use of 1% and 1.5% bio-polymeric admixture. The general reason for this is the increase in the water requirement with the increase in the bio-polymeric admixture ratio and the fact that no water is added to the mortar due to the constant w/c ratio within the scope of the study, and the consistency of the fresh mortar is close to dry. In addition, the initial setting times of the mortars using bio-polymeric additives in the range of 0/45 μm , which can be considered as fine size, and the range of 125/250 μm , which can be considered as coarse size, were determined to be lower than the initial setting times of the mortars using bio-polymeric additives in the range of 0/125 μm . The reason for this is due to the loss of consistency of the mortar with the use of very fine or very coarse size bio-polymeric admixtures.

The interaction of initial setting times with the components that make up the chemical structure of the bio-polymeric admixtures are shown in Figure 4.30, Figure 4.31 and Figure 4.32.

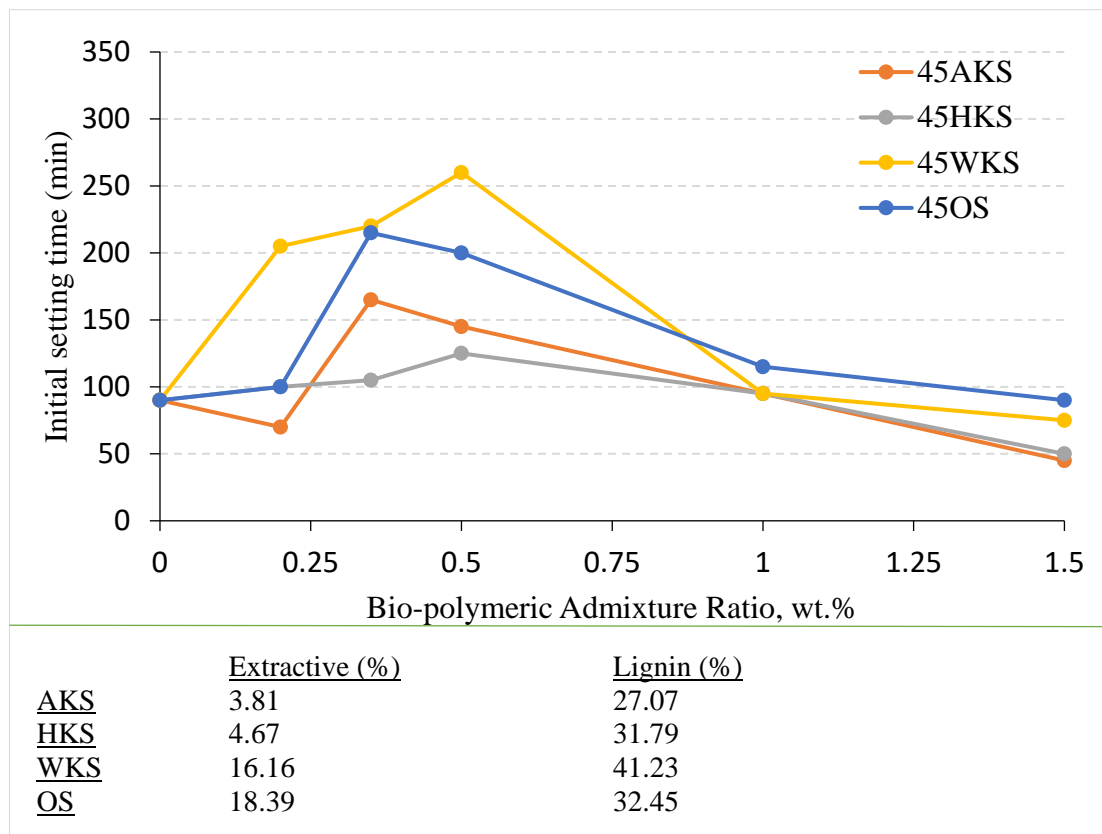


Figure 4.30: Relationship between chemical contents of 0/45 μm bio-polymeric admixture and initial setting time

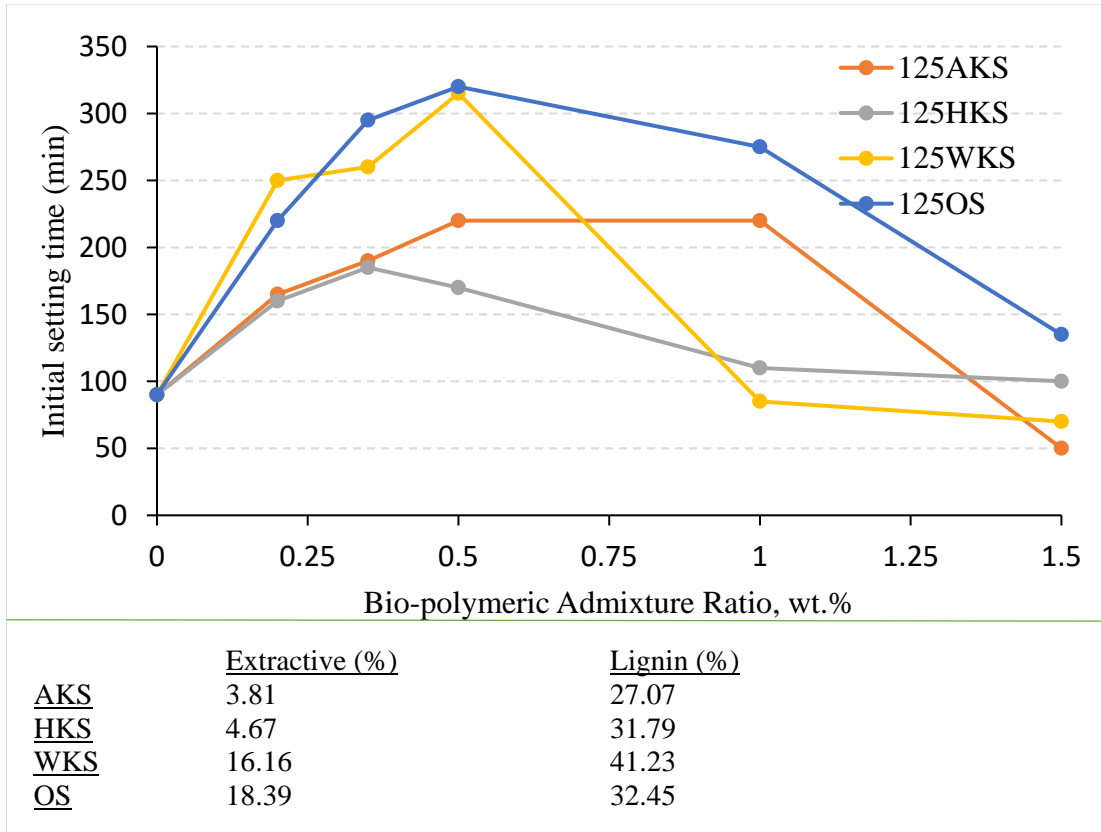


Figure 4.31: Relationship between chemical contents of 0/125 μm bio-polymeric admixture and initial setting time

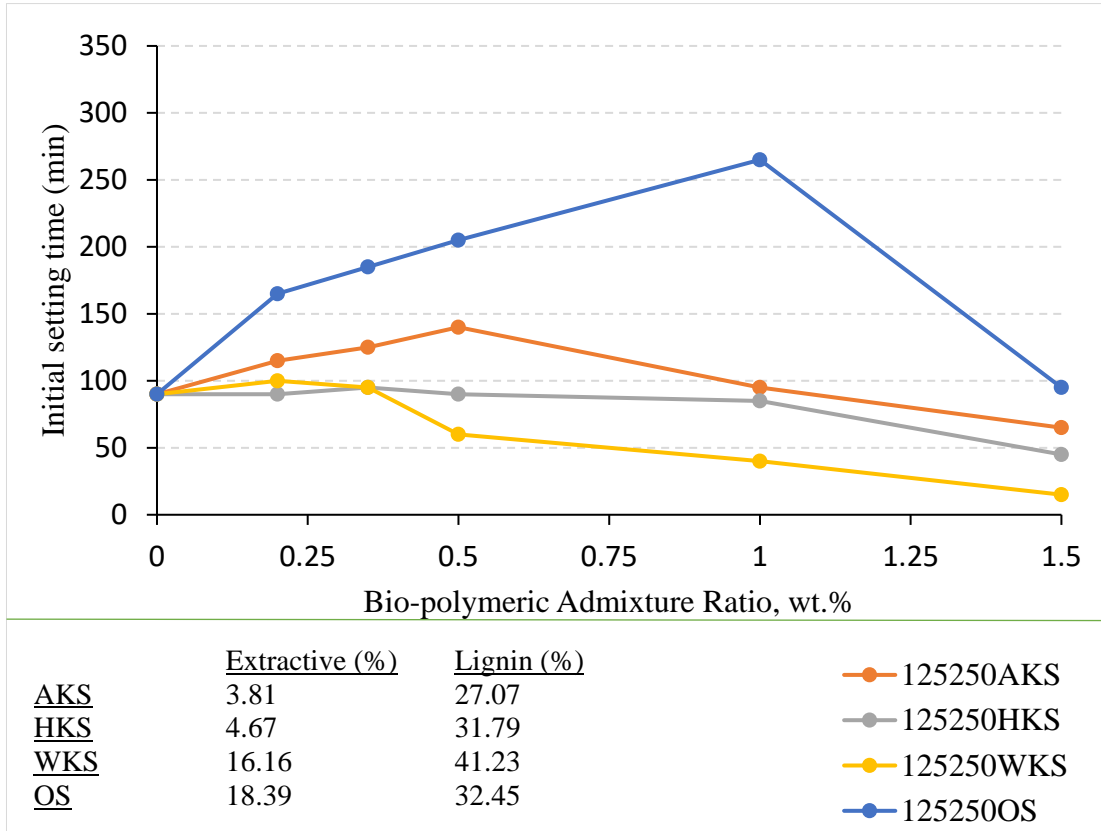


Figure 4.32: Relationship between chemical contents of 125/250 μm bio-polymeric admixture and initial setting time

According to Figure 4.30, Figure 4.31 and Figure 4.32, it was determined that the extractive and lignin content of bio-polymeric admixtures delayed the initial setting time of the cement mortar. In addition, it was determined that bio-polymeric admixture with higher extractive and lignin ratios had a greater set retarding effect. The sum of the extractive and lignin content is 57.39 % in the walnut shell, 50.84 % in the olive seed, 34.98 % in the hazelnut shell and 30.89 % in the apricot shell, respectively. Considering this information, when above figures between Figure 4.26 and Figure 4.29 are examined, the materials that delay the initial set the most were WS and OS admixtures for all three dimensional fractions (0/45, 0/125 and 125/250 μm). When all the mixtures are taken into consideration, the grain size with the most retarding effect among all grain sizes was 0/125 μm .

When 0/45 μm particle size is used as bio-polymeric materials, water requirement increases because more bio-polymeric admixture particles enter the mortar compared to 0/125 μm particle distribution. Since the amount of water in the mixtures is kept constant, the increasing water demand cannot be met, and the setting retardation feature of 0/45 μm particle size admixtures is lower than 0/125 μm particle size admixtures. In addition, very fine materials can agglomerate around the cement particles and slow down the hydration by cutting off the water content of the cement [285]. Similar to 0/45 μm particle size admixtures, the initial setting times of the mortars with bio-polymeric admixtures with a grain size of 125/250 μm are lower than the initial setting times of the mortars with bio-polymeric admixtures with a grain size of 0/125 μm . The reason for this is that when the bio-polymeric admixtures are ground in coarser sizes, the grain shapes turn into a more fibrous structure. Such fibrous grains increase the water requirement of the mortar. Since the amount of water was kept constant, the consistency of the mortar was higher. Therefore, the initial setting time was determined to be lower. When the initial setting times of the eggshell admixed mixtures were examined, it was determined that the initial setting delayed very little compared to the control specimen (Figure 4.25).

Since it was determined that the bio-polymeric admixtures used in this thesis have the ability to delay the initial setting times of the cement mortars, cement mortars were produced with a setting retarder admixture and their initial setting times were tested in order to compare this property of bio-polymeric admixtures. Test results are presented in Figure 4.33.

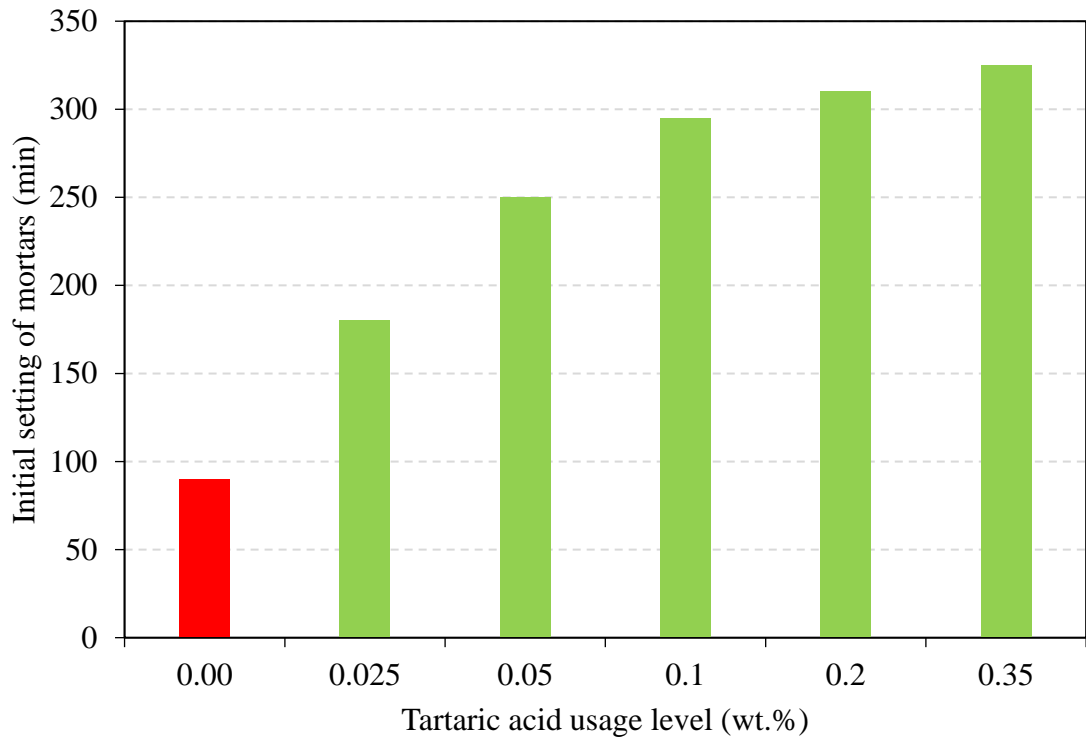


Figure 4.33: Initial setting times of TA admixed cement mortars

When Figure 4.33 is examined, tartaric acid, known and used as a set retarder, delayed the initial setting of fresh mortars for 235 minutes. When the figures are examined, it is easily noticed that the use of bio-polymeric admixtures has similar set retarding properties with tartaric acid. Also, it can be concluded that instead of up to 0.35 wt.% tartaric acid, 0/125 μm sized 0.50 wt.% walnut shell powder or 0.50 wt.% ground olive seed can be used in mortars for desired initial set delaying. Thus, it has been determined that bio-polymeric admixtures can be used instead of setting retarders by taking advantage of the slowing hydration feature of bio-polymeric admixtures up to a certain ratio.

The comparative representation of the final setting times for the mortars with each other is given in between Figure 4.34 to Figure 4.38. Also, in Figure 4.42, the effect of tartaric acid, which is used as a setting retarder, on the initial setting of the cement mortars produced in this study is presented.

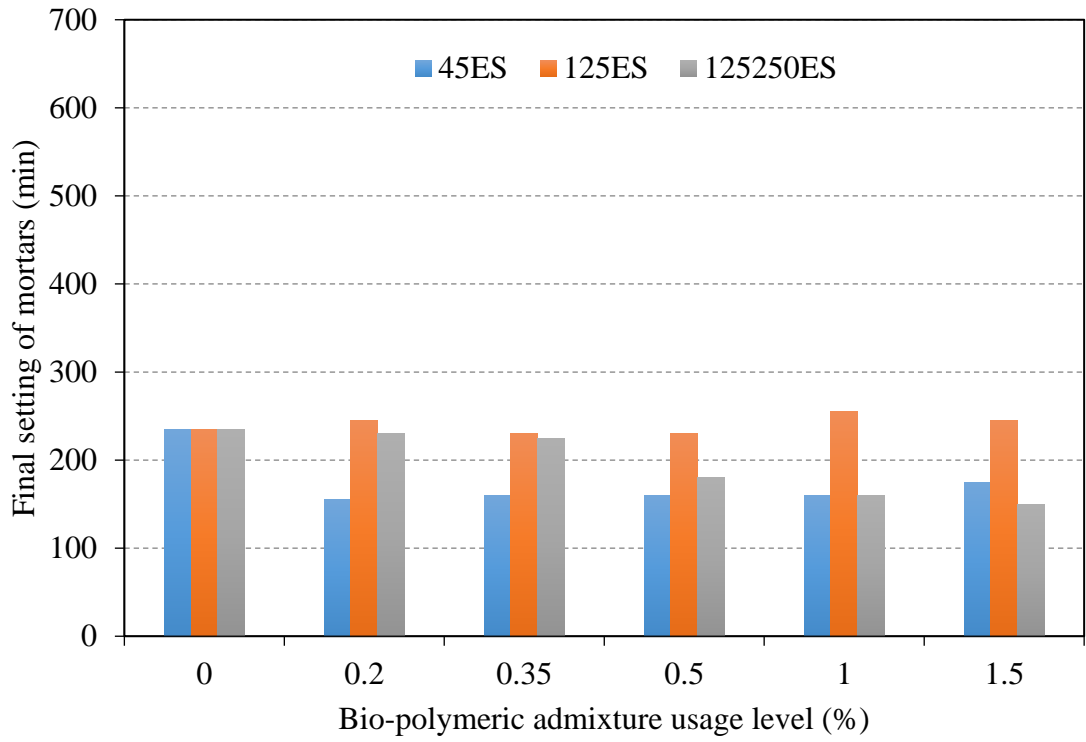


Figure 4.34: Final setting times of ES admixed cement mortars

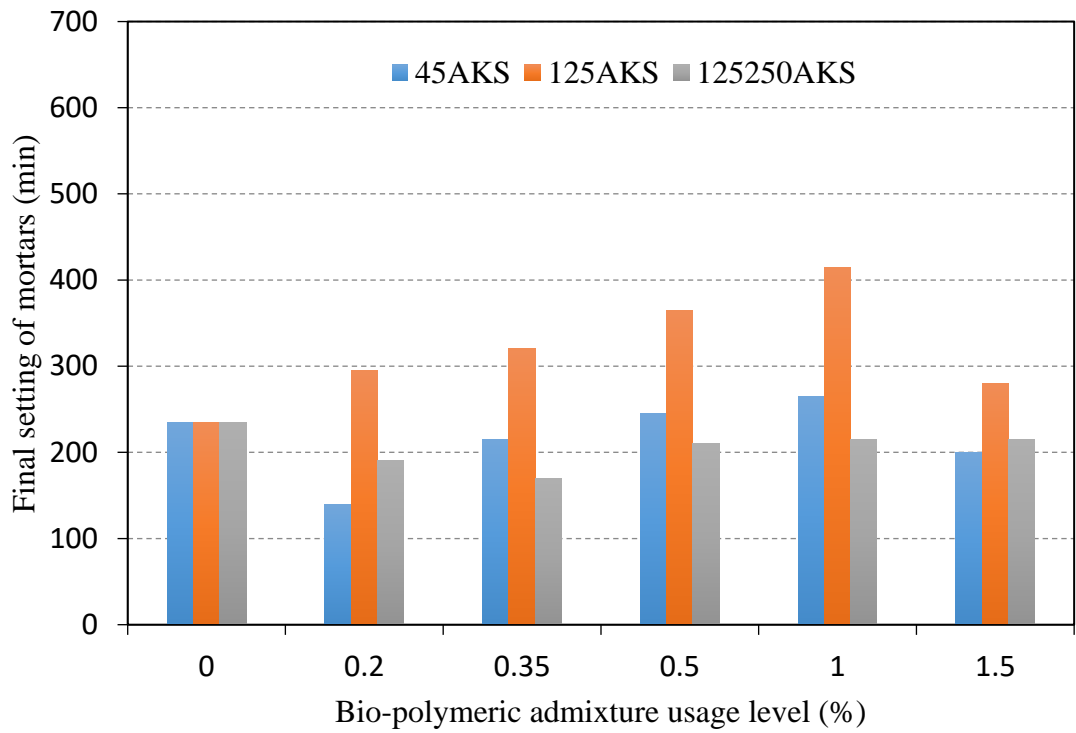


Figure 4.35: Final setting times of AKS admixed cement mortars

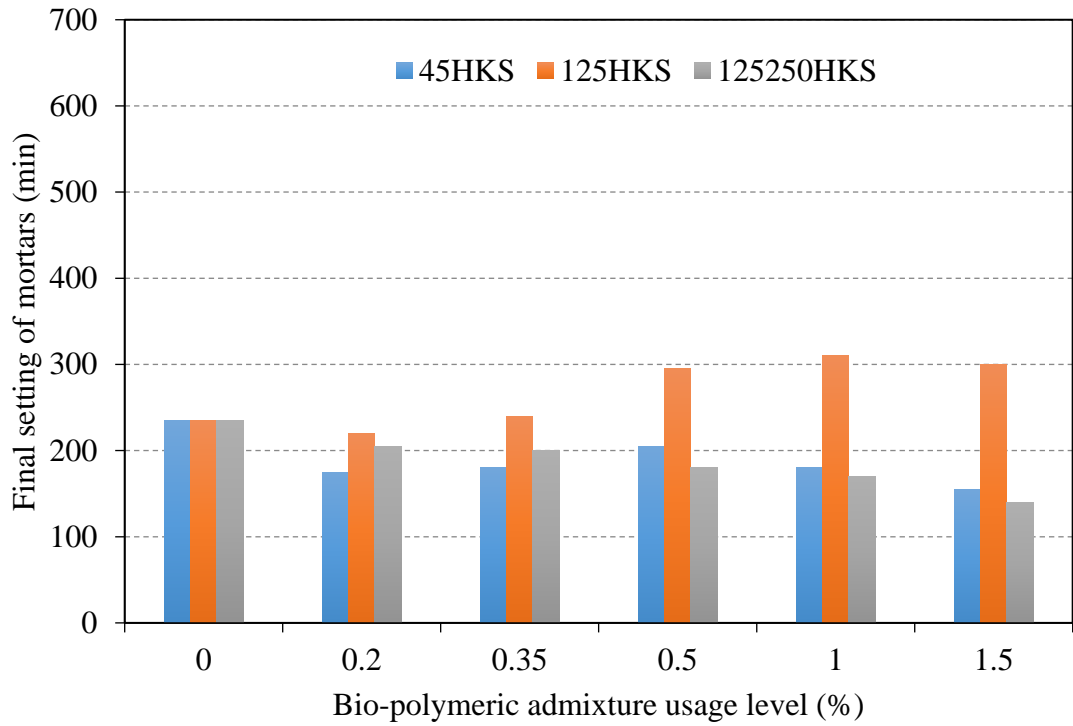


Figure 4.36: Final setting times of HKS admixed cement mortars

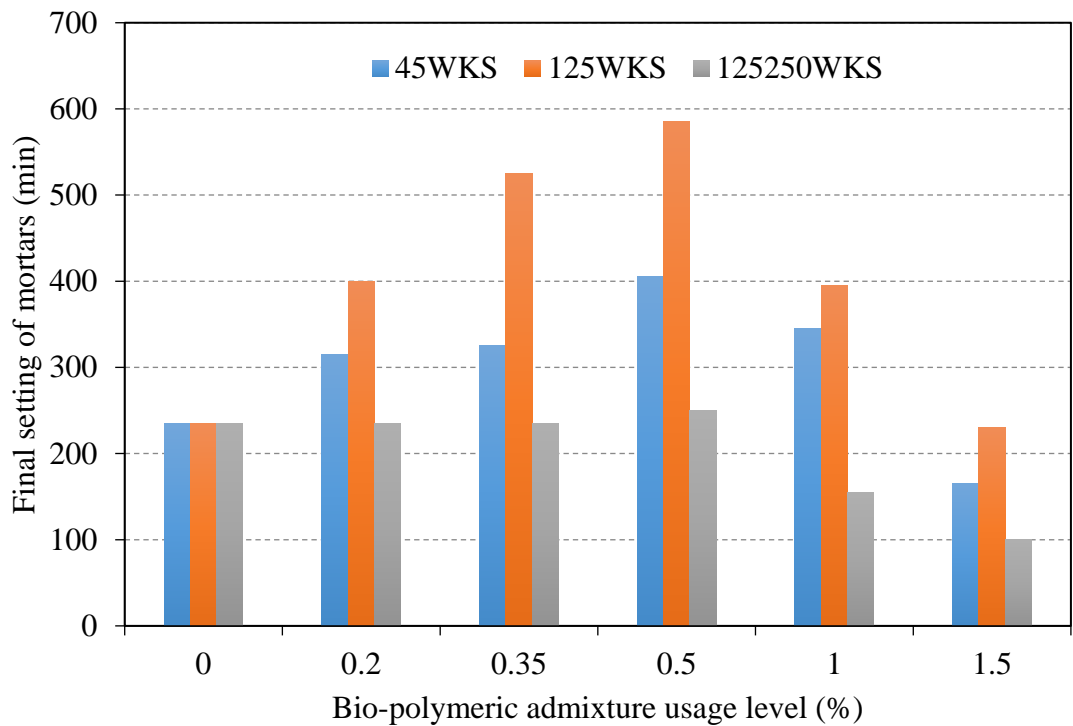


Figure 4.37: Final setting times of WKS admixed cement mortars

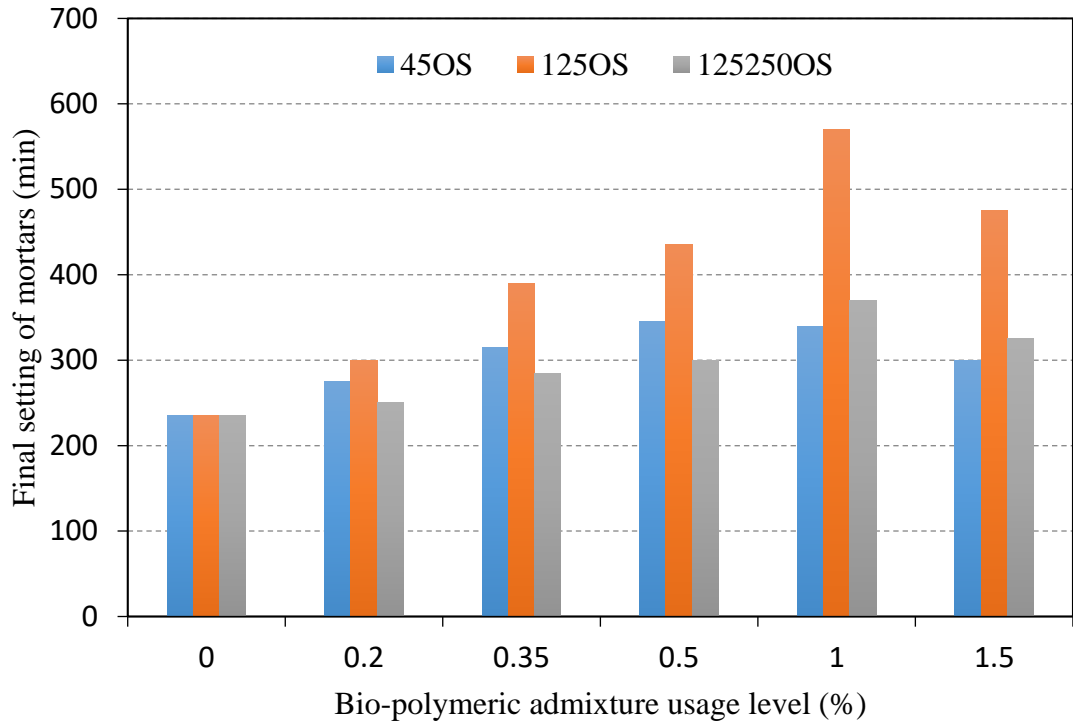


Figure 4.38: Final setting times of OS admixed cement mortars

Examining between Figure 4.34 and Figure 4.38 together, all bio-polymeric admixtures have a delaying effect on final setting times, except egg shell powder, of the specimens. It is well known that polysaccharides such as cellulose and hemicellulose delay the setting time of cement. In addition, lignin slows cement hydration due to the sugar component and prolongs setting time. While the egg shell admixture caused a slight delay in the initial, it showed an accelerating effect on final setting times of cement mortars. This phenomenon can be explained by addition of eggshell as the filler effect of the eggshell and extra calcium hydroxide for the formation of the secondary C-S-H gel [151,152]. It is seen that the eggshell admixture with 0/125 μm grain distribution does not cause a very significant change in the final setting times of the mortars. However, it has been determined that the final setting is considerably faster in the use of 0/45 and 125/250 μm admixtures compared to the control sample. The reason for this is that these grain sizes increase the internal friction and the water requirement of the mortars.

When Figure 4.35 to Figure 4.38 are examined, WS and OS were the bio-polymeric admixtures with the highest set retarding properties in the final setting times as well as in the initial setting times. In addition, when analyzed in terms of grain size, the grain size that delays the final setting time the most was determined as 0/125 μm . The reason

for this is that the 0/125 μm grain distribution in bio-polymeric admixtures has filling effect on the mortars at the optimum level and thus reduces the water demand.

The interaction of initial setting times with the components that make up the chemical structure of the bio-polymeric admixtures are shown in Figure 4.39, Figure 4.40 and Figure 4.41.

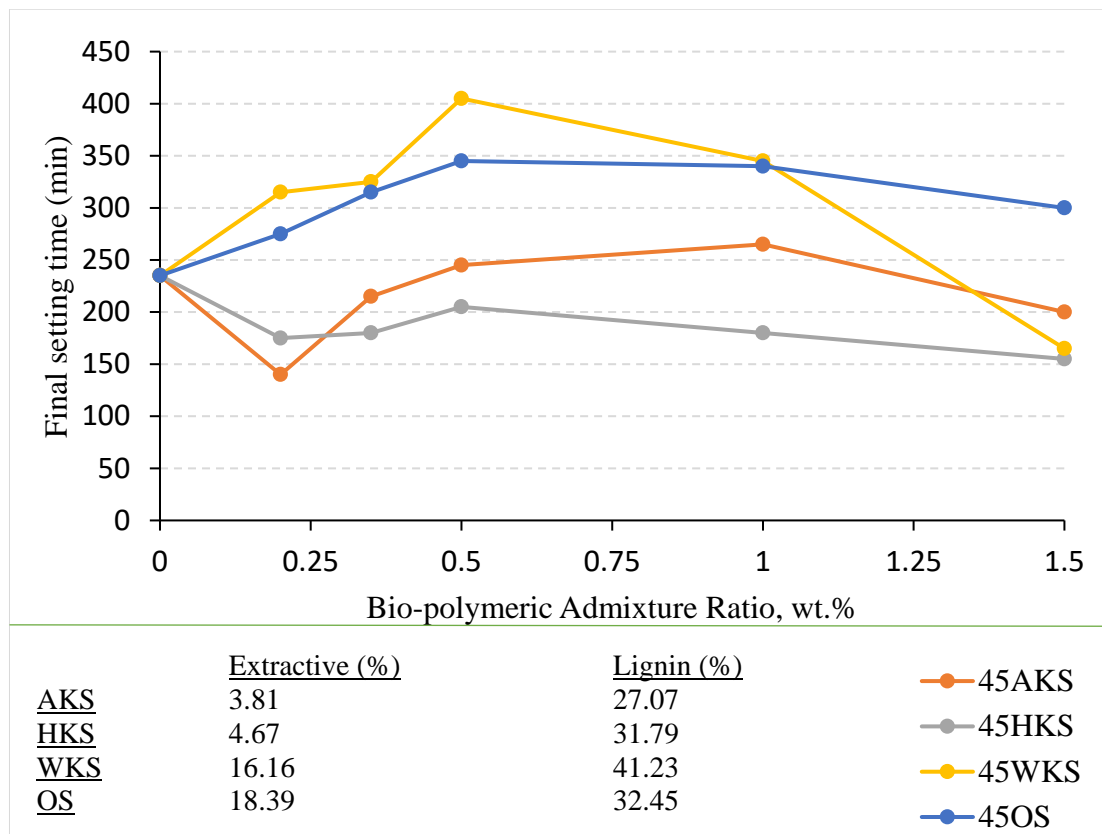


Figure 4.39: Relationship between chemical contents of 0/45 μm bio-polymeric admixture and final setting time

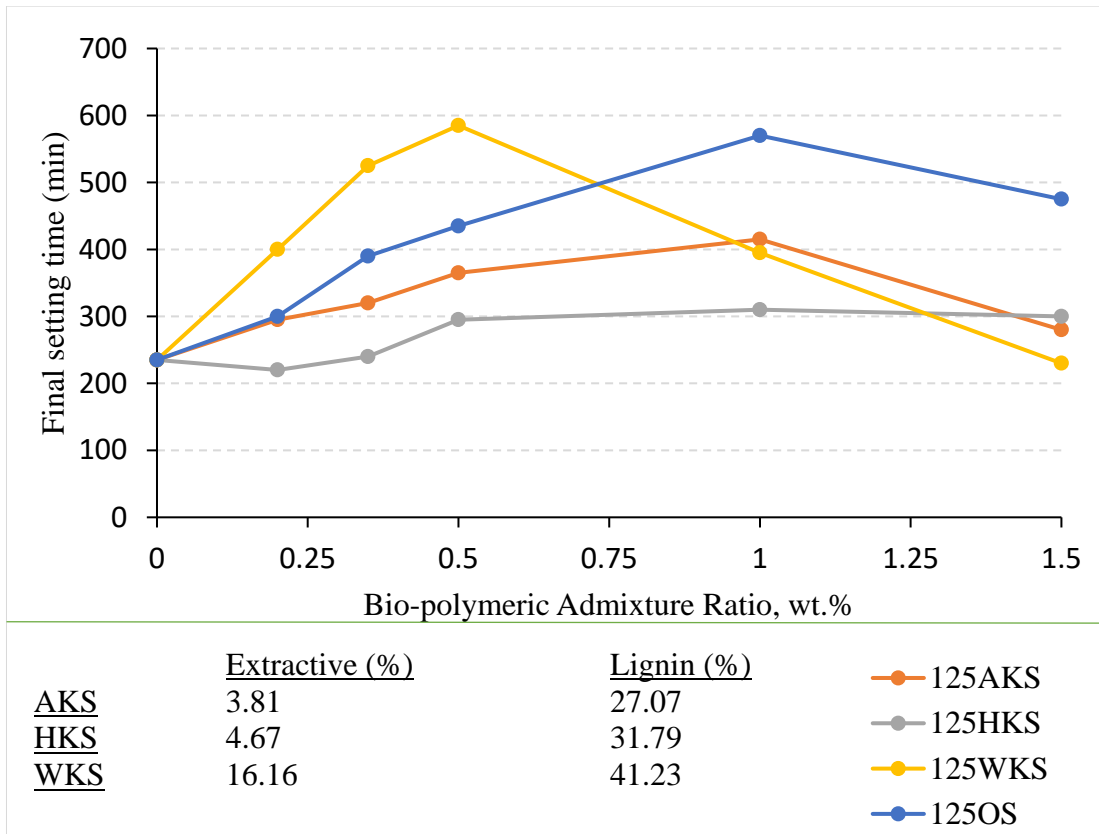


Figure 4.40: Relationship between chemical contents of 0/125 μm bio-polymeric admixture and final setting time

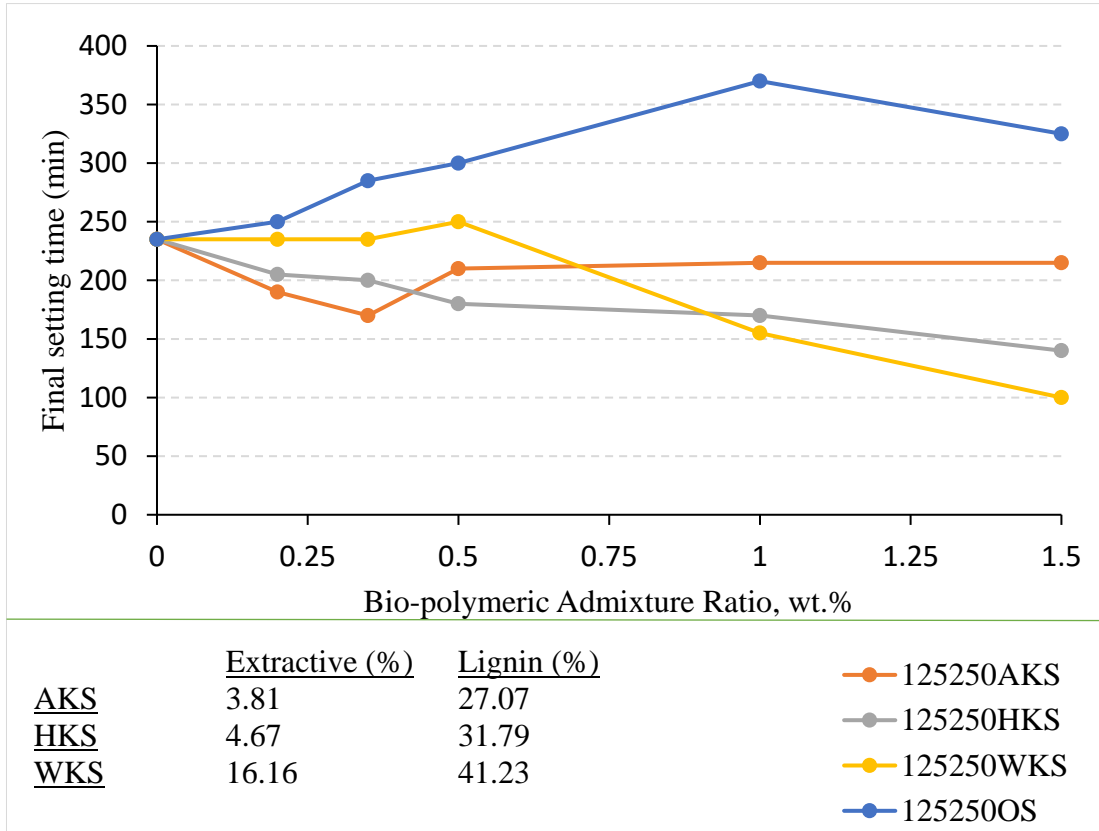


Figure 4.41: Relationship between chemical contents of 125/250 μm bio-polymeric admixture and final setting time

According to Figure 4.39, Figure 4.40 and Figure 4.41, it was determined that the extractive and lignin content of bio-polymeric admixtures delayed the final setting time of the cement mortar. In addition, it was determined that bio-polymeric admixture with higher extractive and lignin ratios had a greater set retarding effect. The sum of the extractive and lignin content is 57.39 % in the walnut shell, 50.84 % in the olive seed, 34.98 % in the hazelnut shell and 30.89 % in the apricot shell, respectively. Considering this information, when above figures between Figure 4.35 and Figure 4.38 are examined, the materials that delay the initial set the most were WS and OS admixtures for all three dimensional fractions (0/45, 0/125 and 125/250 μm). When all the mixtures are taken into consideration, the grain size with the most retarding effect among all grain sizes was 0/125 μm . It has been determined that the final setting time of the mortars and the initial setting times exhibit similar trends.

When 0/45 μm particle size is used as bio-polymeric materials, water requirement increases because more bio-polymeric admixture particles enter the mortar compared to 0/125 μm particle distribution. Since the amount of water in the mixtures is kept constant, the increasing water demand cannot be met, and the setting retardation feature of 0/45 μm particle size admixtures is lower than 0/125 μm particle size admixtures. In addition, very fine materials can agglomerate around the cement particles and slow down the hydration by cutting off the water content of the cement [285]. Similar to 0/45 μm particle size admixtures, the final setting times of the mortars with bio-polymeric admixtures with a grain size of 125/250 μm are lower than the final setting times of the mortars with bio-polymeric admixtures with a grain size of 0/125 μm . The reason for this was thought to be due to the fact that the grain shapes turn into a more fibrous structure when the biopolymeric additives are ground in larger sizes. Such fibrous grains increase the water requirement of the mortar. Since the amount of water was kept constant, the consistency of the mortar was higher. Therefore, the initial setting time was determined to be lower.

Since it was determined that the bio-polymeric admixtures used in this thesis have the ability to delay the initial and final setting times of the cement mortars, cement mortars were produced with a setting retarder admixture and their final setting times were tested in order to compare this property of bio-polymeric admixtures. Test results are presented in Figure 4.42.

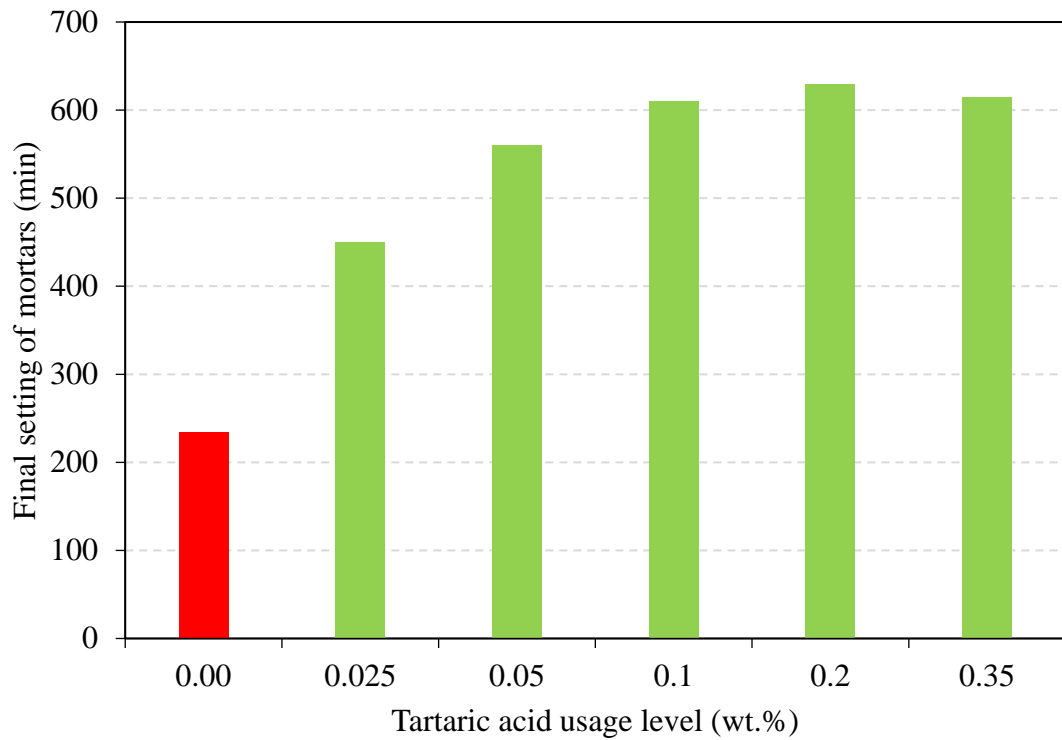


Figure 4.42: Final setting times of TA admixed cement mortars

When Figure 4.42 is examined, the final setting time of 235 minutes belongs to the reference sample without any admixture. As expected, the final setting values of the mortar increased with the addition of tartaric acid to the fresh mortar as the chemical admixture ratio increased. With the use of tartaric acid, the final setting time of cement mortars could be delayed up to 168.09%. The maximum set retardation was achieved by using 0.2 % tartaric acid by weight and the final setting of this test mortar was delayed for 395 minutes compared to the reference mortar.

According to figures between Figure 4.34 and Figure 4.38, it was observed that the ES admixture did not have a significant effect on the final setting values of the mortars. However, the effect of lignocellulosic bio-polymeric admixtures on the final setting of the mortars is obvious. When the highest amount of set retarding characteristics of bio-polymeric admixtures are examined, the final setting times of the 125AKS1.0 mixtures delayed by 180 min compared to the final setting time of the reference sample. Final setting time of the 125HKS1.0 mixture prolonged by 75 minutes compared to the final setting time of the reference sample. The two admixtures that contributed the most to the cement mortar in terms of extension of final setting time were WKS with high lignin ratio and OS with high extractive ratio. When the grain size of these two admixtures is 0/125 μm like the others, the increase in final setting time is greater. As

comparing to the reference mixture, 125WKS0.5 and 125OS1.0 delayed the initial setting times by 148.94 % and 142.55 %, respectively.

It can be concluded that instead of up to 0.10 wt.% tartaric acid, up to 0.50 wt.% 0/125 μm sized walnut shell powder or up to 1.0 wt.% ground olive seed can be used in mortars for desired final set delaying. Thus, it has been determined that bio-polymeric admixtures can be used instead of setting retarders by taking advantage of the slowing hydration feature of bio-polymeric admixtures up to a certain ratio.

4.3.4 Water Absorption of Mortars

The capillary water absorption and mass water absorption values of the test specimens are given in Table 4.11. The capillary water absorption values of mortars depending on the bio-polymeric admixture particle size and the rate of use in the mortar are shown in between Figure 4.43 to Figure 4.47 below.

Table 4.11: Water absorption values of test specimens

Mix Code	Water Absorption					
	0/45 μm		0/125 μm		125/250 μm	
	Capillary ($\text{g}/\text{cm}^2 \cdot \text{min}^{0.5}$)	Mass (%)	Capillary ($\text{g}/\text{cm}^2 \cdot \text{min}^{0.5}$)	Mass (%)	Capillary ($\text{g}/\text{cm}^2 \cdot \text{min}^{0.5}$)	Mass (%)
R	0.60	6.84	0.60	6.84	0.60	6.84
ES0.2	0.64	6.34	0.72	6.61	0.33	6.4
ES0.35	0.67	5.16	0.82	6.56	0.43	7.08
ES0.5	0.79	5.48	0.90	6.43	0.51	7.68
ES1.0	0.70	5.82	0.81	6.20	0.49	7.02
ES1.5	0.68	6.84	0.86	6.20	0.50	6.58
AKS0.2	0.61	4.32	0.41	6.59	0.38	7.34
AKS0.35	0.62	4.22	0.33	6.22	0.41	6.34
AKS0.5	0.62	4.18	0.32	6.06	0.42	5.44
AKS1.0	0.63	3.86	0.30	5.94	0.45	5.04
AKS1.5	0.83	3.44	0.31	5.93	0.46	4.6
HKS0.2	1.00	6.46	0.29	5.55	0.27	6.44
HKS0.35	0.79	5.32	0.23	4.99	0.34	6.00

Table 4.11 (Continued): Water absorption values of test specimens

Mix Code	Water Absorption					
	0/45 μm		0/125 μm		125/250 μm	
	Capillary ($\text{g}/\text{cm}^2 \cdot \text{min}^{0.5}$)	Mass (%)	Capillary ($\text{g}/\text{cm}^2 \cdot \text{min}^{0.5}$)	Mass (%)	Capillary ($\text{g}/\text{cm}^2 \cdot \text{min}^{0.5}$)	Mass (%)
HKS0.5	0.75	4.6	0.16	4.81	0.35	5.88
HKS1.0	0.61	3.26	0.15	3.66	0.38	4.52
HKS1.5	0.55	3.2	0.17	3.61	0.40	3.70
WKS0.2	0.50	3.82	0.48	6.23	0.44	6.80
WKS0.35	0.54	3.32	0.36	5.99	0.49	5.86
WKS0.5	0.60	2.88	0.27	6.03	0.53	5.78
WKS1.0	0.62	2.32	0.30	6.00	0.63	5.88
WKS1.5	0.65	2.12	0.33	5.98	0.67	6.28
OS0.2	0.54	3.14	0.21	4.81	0.55	6.12
OS0.35	0.52	2.92	0.13	4.65	0.56	4.52
OS0.5	0.49	2.44	0.10	4.55	0.57	3.62
OS1.0	0.44	2.38	0.10	3.3	0.57	3.32
OS1.5	0.34	2.18	0.15	2.29	0.55	2.80

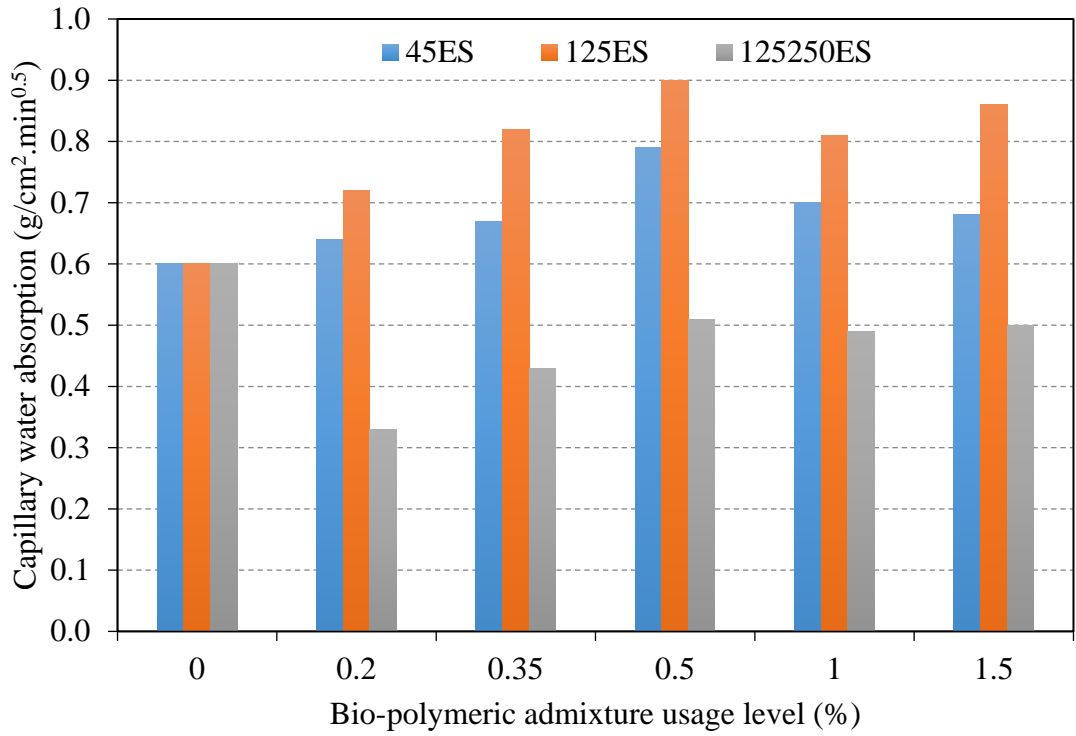


Figure 4.43: Capillary water absorption of ES admixed cement mortars

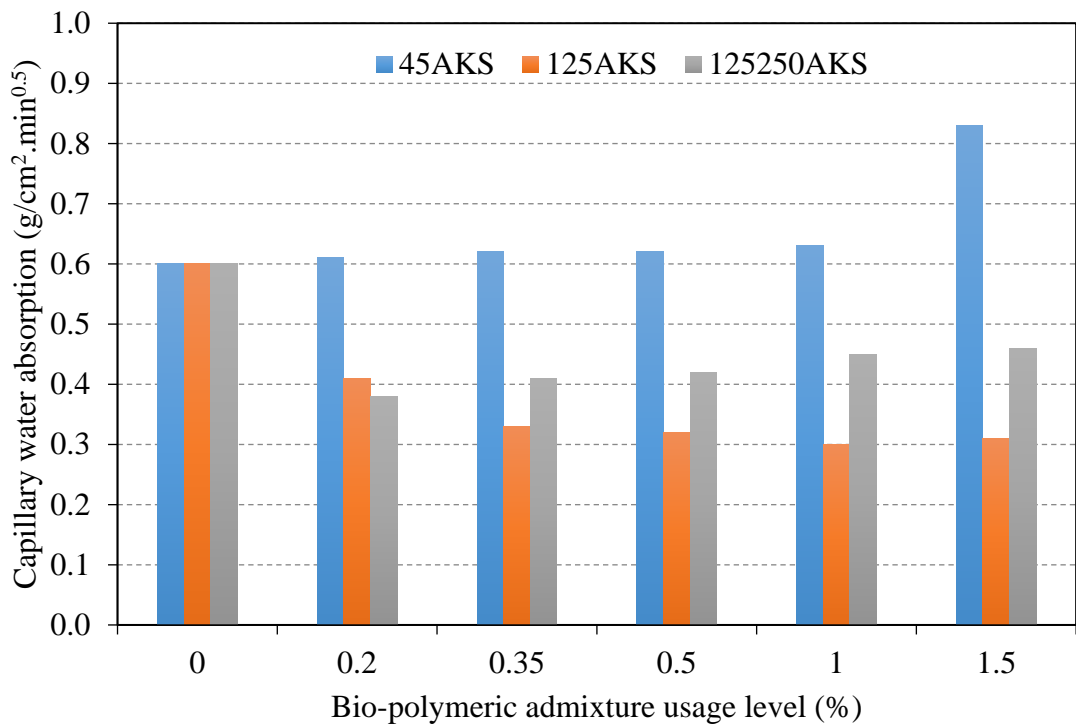


Figure 4.44: Capillary water absorption of AKS admixed cement mortars

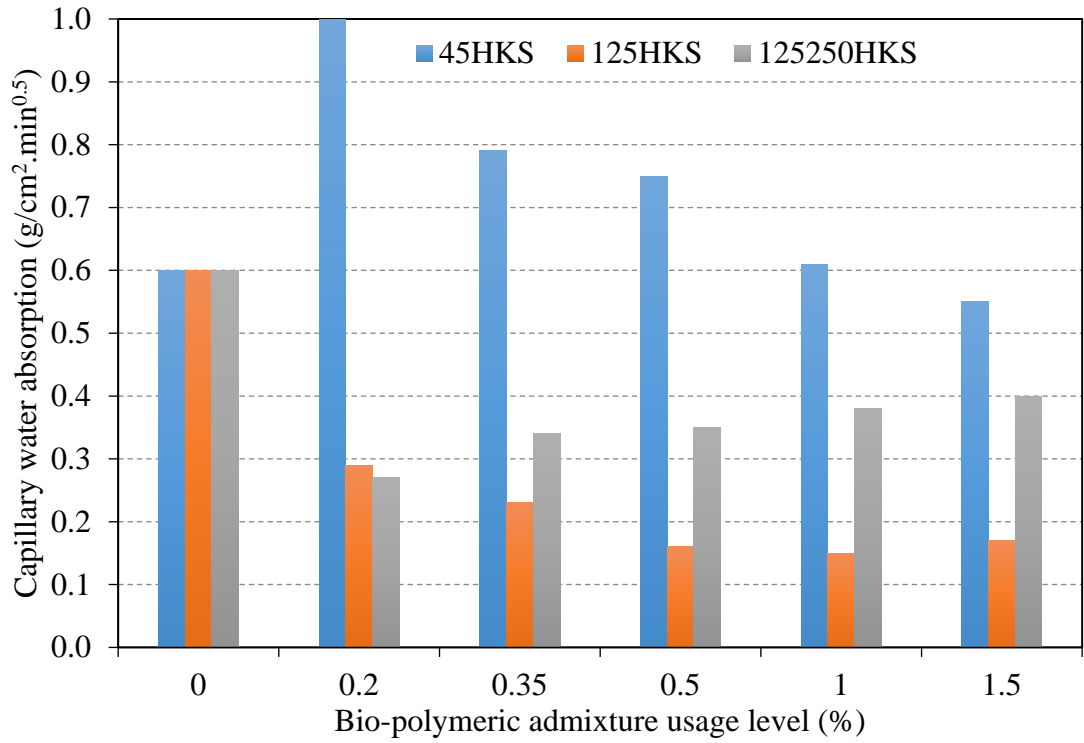


Figure 4.45: Capillary water absorption of HKS admixed cement mortars

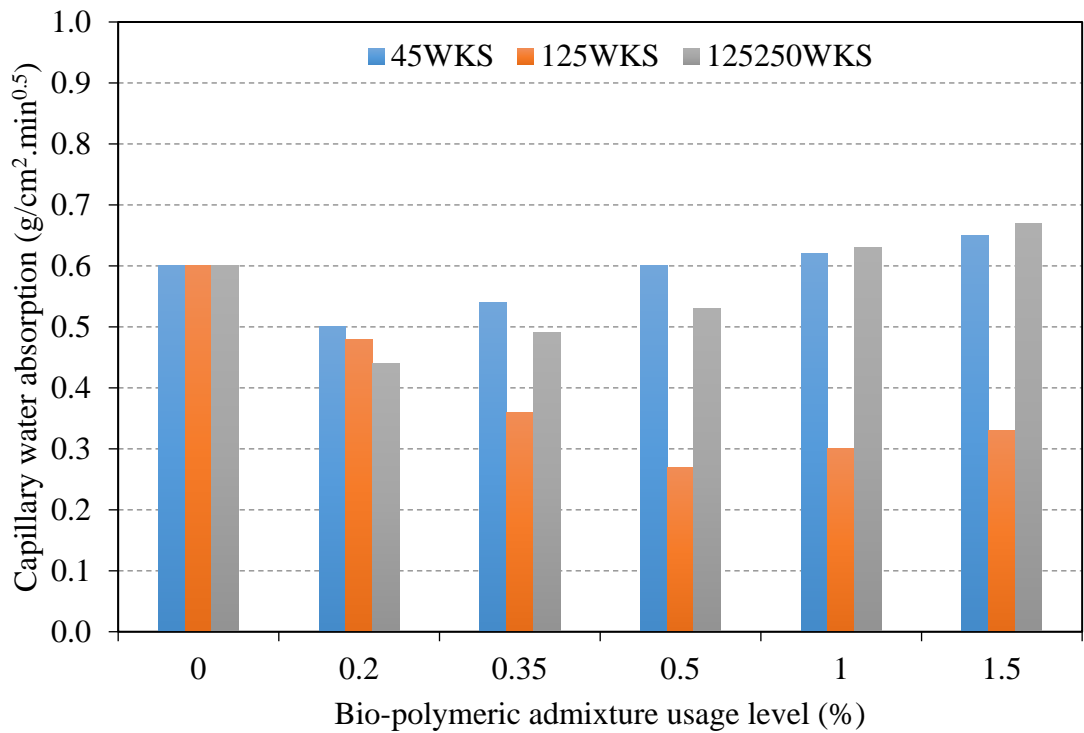


Figure 4.46: Capillary water absorption of WKS cement mortars

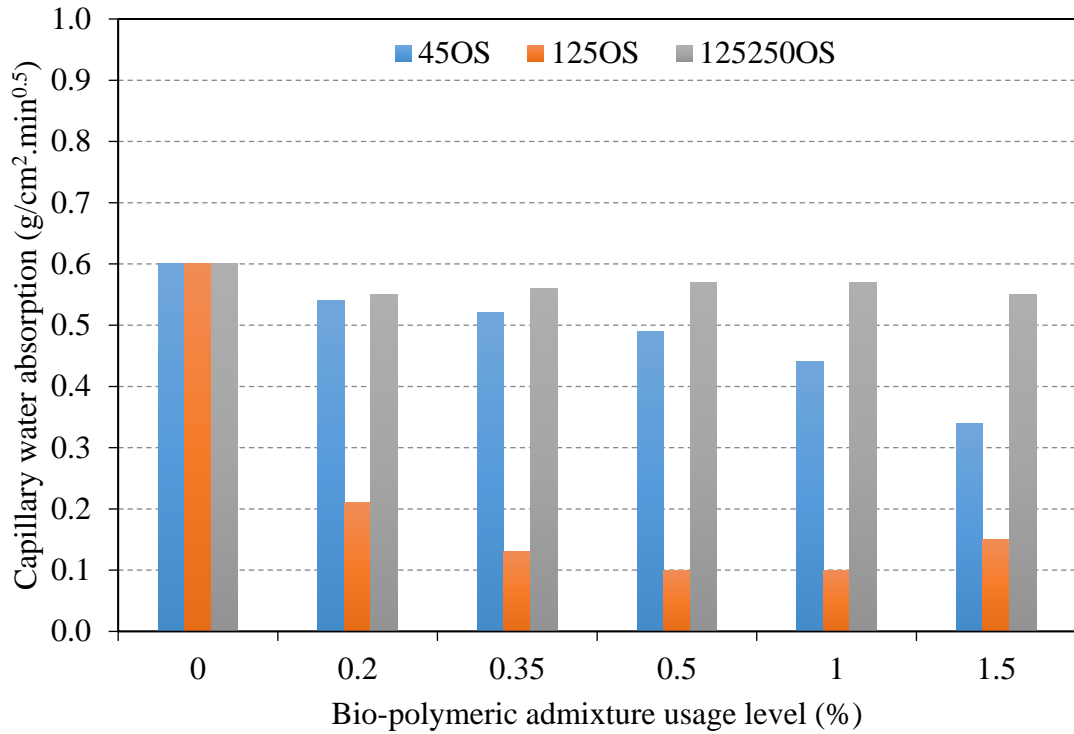


Figure 4.47: Capillary water absorption of OS admixed cement mortars

Analyzing the figures above, almost all mortar specimens with 0/125 μm grain size bio-polymeric admixtures exhibited a lower capillary absorption than capillary absorption of reference mortar. This showed that capillary voids in mortars can be reduced when an admixture of this particle size is used. It has been determined that capillary water absorption can be reduced up to 45% when 125/250 μm grain size ES additive is used. In the AKS additive, the most effective grain size was determined as 0/125 μm . In the mortars using this grain size, a decrease in capillary water absorption up to 48.33 % was observed. The use of HKS admixture in the size range of 0/45 μm increased the capillary water absorption considerably compared to the control specimen. However, for this admixture, the additive grain size of 0/125 μm was determined as ideal and it was determined that it could reduce the capillary water absorption up to 75% compared to the reference specimen. For the HKS admixture, the most effective particle size distribution was 0/125 μm . When WKS admixture with this grain size distribution is used, the capillary water absorption of the mortar can be reduced by 55 % compared to the reference mortar. OS admixture was the most effective bio-polymeric admixture that could reduce capillary water absorption. When all three grain sizes were used in mortars, the capillary water absorption of the mortar decreased. Again, the most effective particle size distribution for this admixture was

0/125 μm . Capillary water absorption of mortars with this grain size can be reduced up to 83.33%.

The interaction of capillary water absorption values with the components that make up the chemical structure of the bio-polymeric admixtures are shown in Figure 4.48, Figure 4.49 and Figure 4.50.

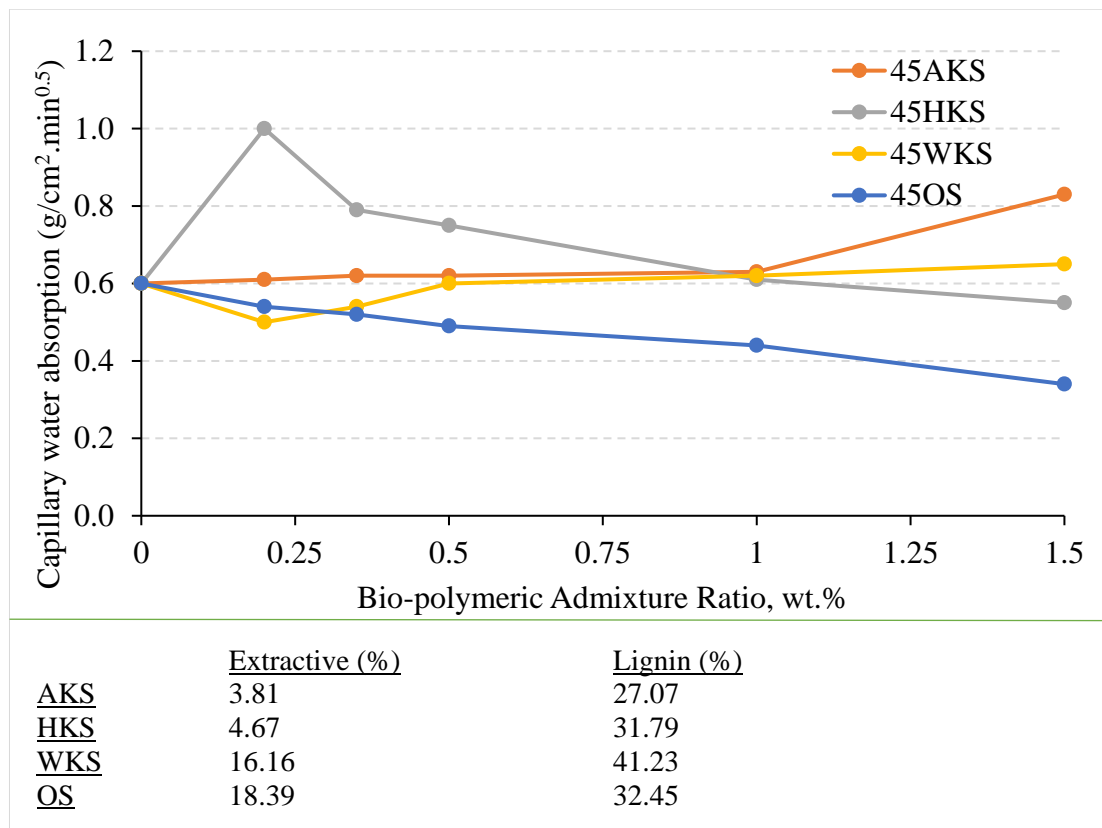


Figure 4.48: Relationship between chemical contents of 0/45 μm bio-polymeric admixture and capillary water absorption

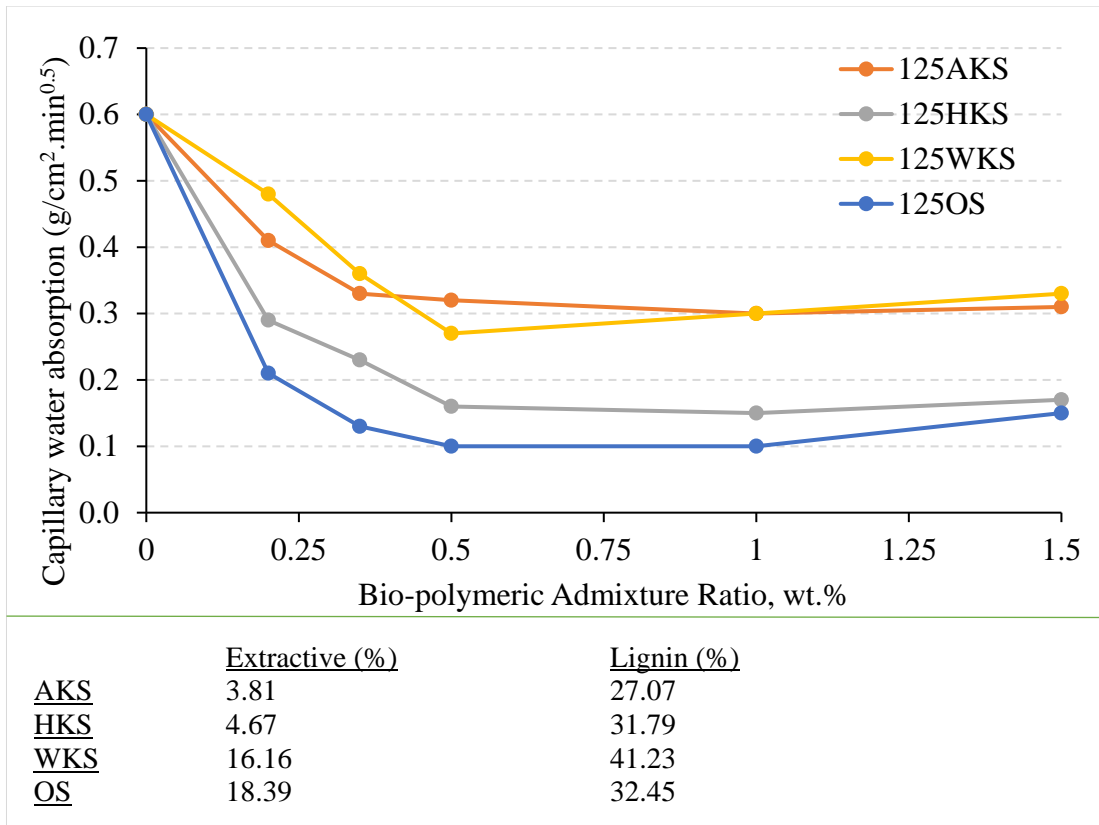


Figure 4.49: Relationship between chemical contents of 0/125 μm bio-polymeric admixture and capillary water absorption

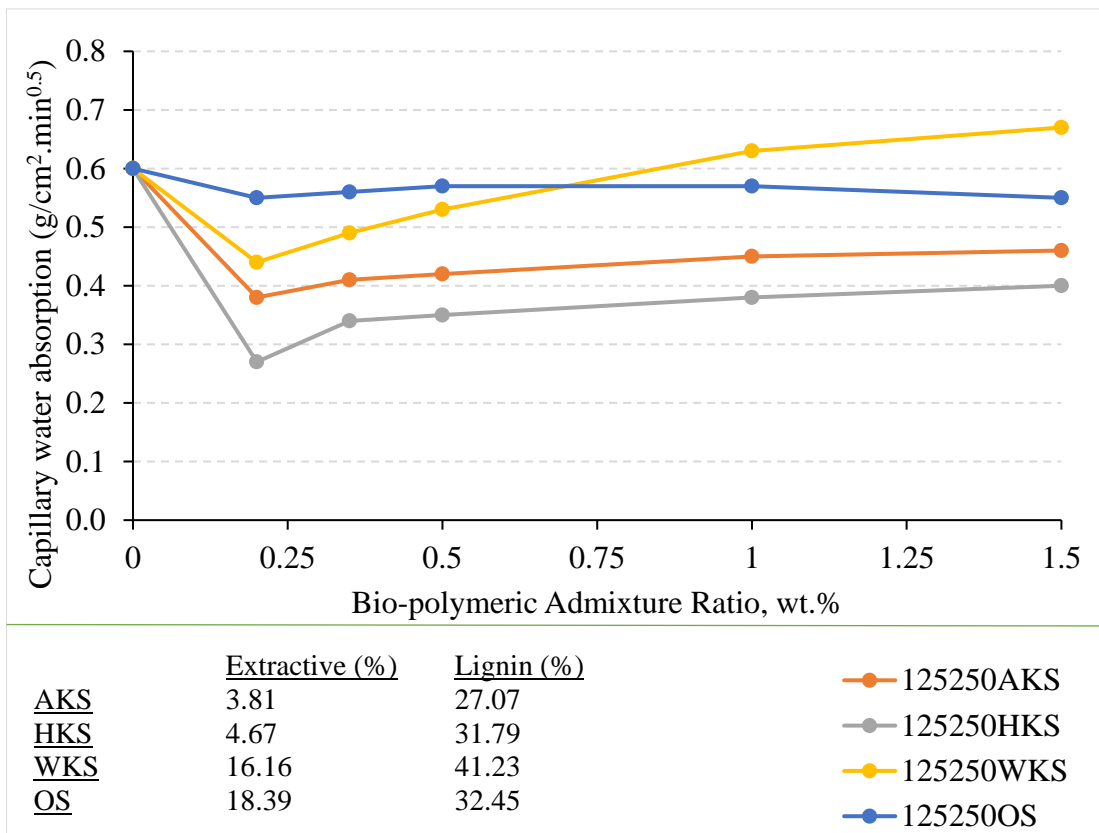


Figure 4.50: Relationship between chemical contents of 125/250 μm bio-polymeric admixture and capillary water absorption

According to Figure 4.48, Figure 4.49 and Figure 4.50, it was determined that the extractive and lignin content of bio-polymeric admixtures considerably improve water stability of the cement mortars. It is known that the fatty acids in the extractives are used as a water repellent in cement products [286,287]. In addition, lignin can reduce the water absorption characteristic of cement-bound materials thanks to its hydrophobic structure [288]. Similarly, it was determined that bio-polymeric admixture with higher extractive and lignin ratios had a greater water repellent effect. The sum of the extractive and lignin content is 57.39 % in the walnut shell, 50.84 % in the olive seed, 34.98 % in the hazelnut shell and 30.89 % in the apricot shell, respectively. Considering this information, when above figures between Figure 4.48 and Figure 4.50 are examined, the admixtures that have water repellent effect most were WS and OS admixtures for 0/45 μm and 0/125 μm grain size distributions. On the other hand, the grain sizes of lignocellulosic materials after grinding change the percentage of chemicals that make up the material. Queirós et al. [289] in their study on walnut, almond, and pine nut shells, it was determined that the extractive content of lignocellulosic materials increased slightly with the decrease in grain size, while the lignin ratios decreased slightly. Analyzing Figure 4.50, In this study, when admixtures with 125/250 μm grain size distribution, which can be considered as coarse size, are used, the opposite situation appears to be the case with the capillary water absorption results of mortars using other size admixtures in this study. On the other hand, when coarse particle size admixtures were used, lignin of AKS and HKS additives was released more, and extractives of WKS and OS additives remained less. Thus, AKS and HKS have become more effective in capillary water absorption in large sizes. Withal, when all the mixtures are taken into consideration, the grain size with the most water repellent effect among all grain sizes was 0/125 μm . Especially thanks to the fatty acids, triacylglycerols and high amount of lignin found in the olive seed, the water absorption values of 125OS series were further determined as the lowest capillary water absorbed series.

Since it was determined that the bio-polymeric admixtures used in this thesis have the ability to reduce capillary water absorption of cement mortars, cement mortars were produced with a water repellent admixture and its capillary water absorption was tested in order to compare this property of bio-polymeric admixtures. Test results are presented in Figure 4.51.

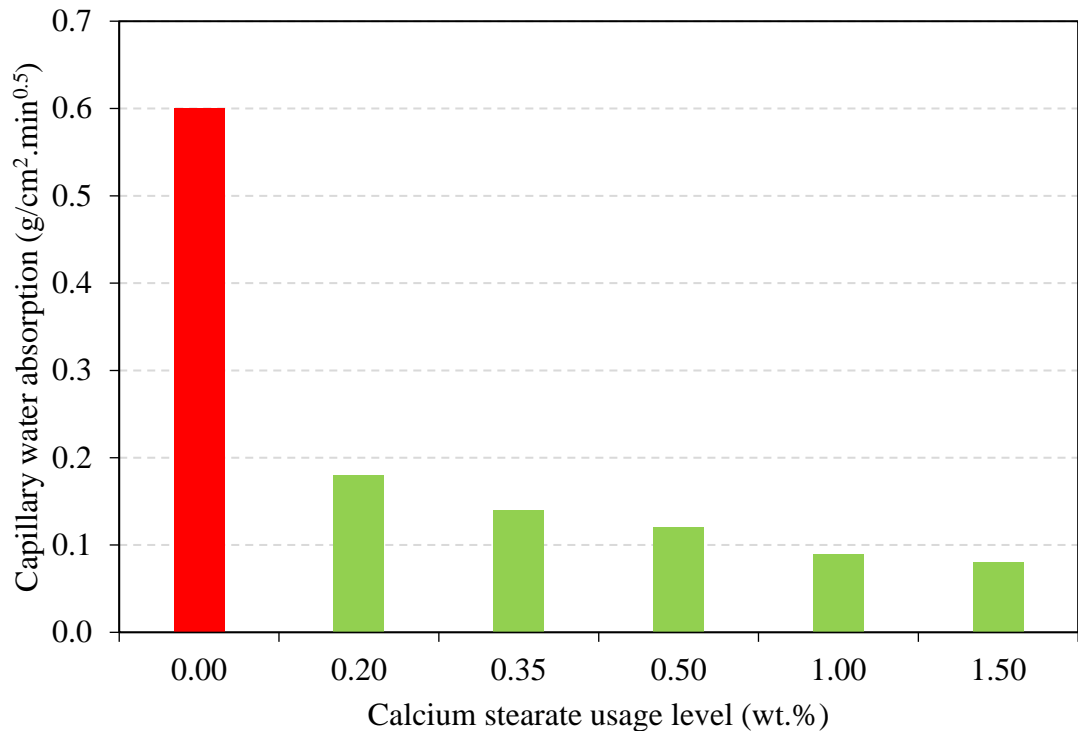


Figure 4.51: Capillary water absorption of CS admixed cement mortars

In Figure 4.51, the capillary water absorption value of $0.6 \text{ g/cm}^2\text{min}^{0.5}$ belongs to the reference sample without any admixture. When the figure examined, as expected, as the use of calcium stearate increases, the capillary water absorption values of the hardened mortars decrease. The reason for this decrease in water absorption is explained as follows; calcium stearate reacts with cement and water during hydration to form a wax-like component. This component creates a hydrophobic structure by covering capillary cavities and pores during evaporation. Thus, the water absorption characteristics of the samples are reduced [290,291].

Depending on the usage rate of the CS chemical admixture, up to 86.67% reduction in capillary water absorption was detected. Especially as a result of decreasing the capillary water absorption value, the use of hazelnut shell bio-polymeric admixture and olive seed bio-polymeric admixture has been shown to provide similar hydrophobicity to hardened cement mortars with the use of calcium stearate. Olive seed is rich in triacylglycerols and triacylglycerols have a hydrophobic nature [292]. Also, there are free fatty acids in the olive seed. This structure of olive seed adds hydrophobic property to cement mortar. Similarly, the high content of lignin and oil (about 6 %) in the hazelnut shell, which has hydrophobic properties, makes the hardened cement mortar more hydrophobic. Compared to the reference specimens,

capillary water absorption decreased by 75% in 125HKS1.0 mixture and 83.33 % in 125OS0.5 and 125OS1.0 mixtures. For this reason, in order to reduce the capillary water absorption values, instead of using up to 1% calcium stearate, 0.5% HKS and 1.0% OS additives can be used in mortars in 0/125 micron grain distribution, respectively.

In addition, the mass water absorption of all mortars was also measured. The water absorption values measured by immersion are given in between Figure 4.52 and Figure 4.56.

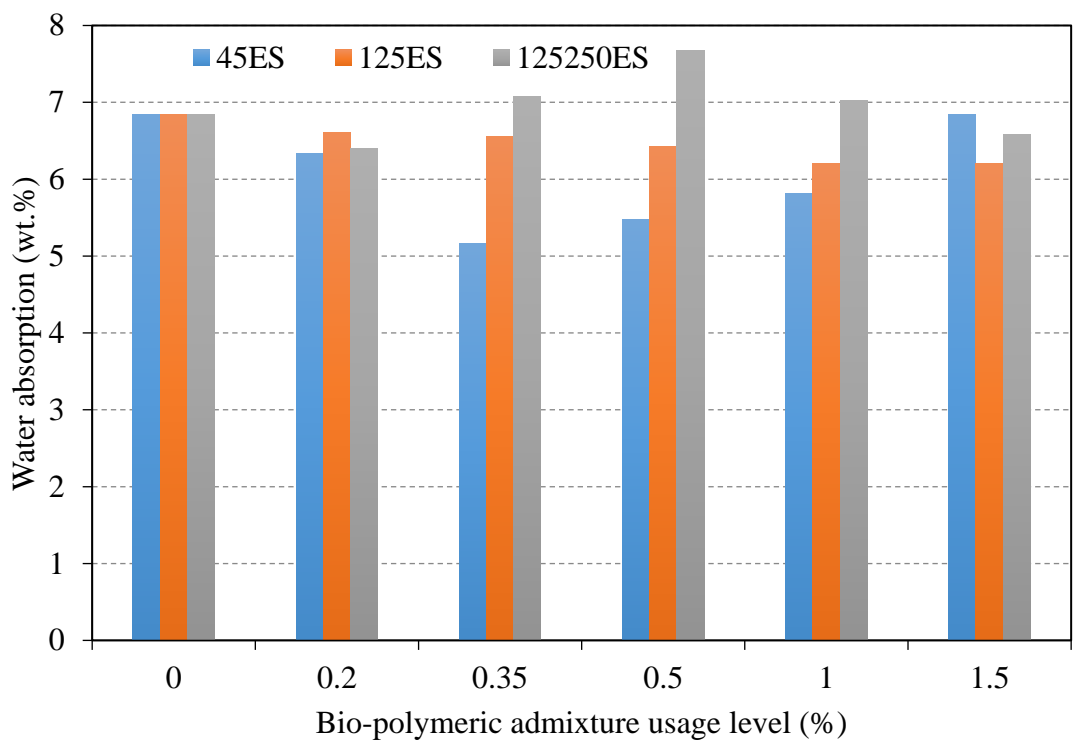


Figure 4.52: Mass water absorption of ES admixed cement mortars

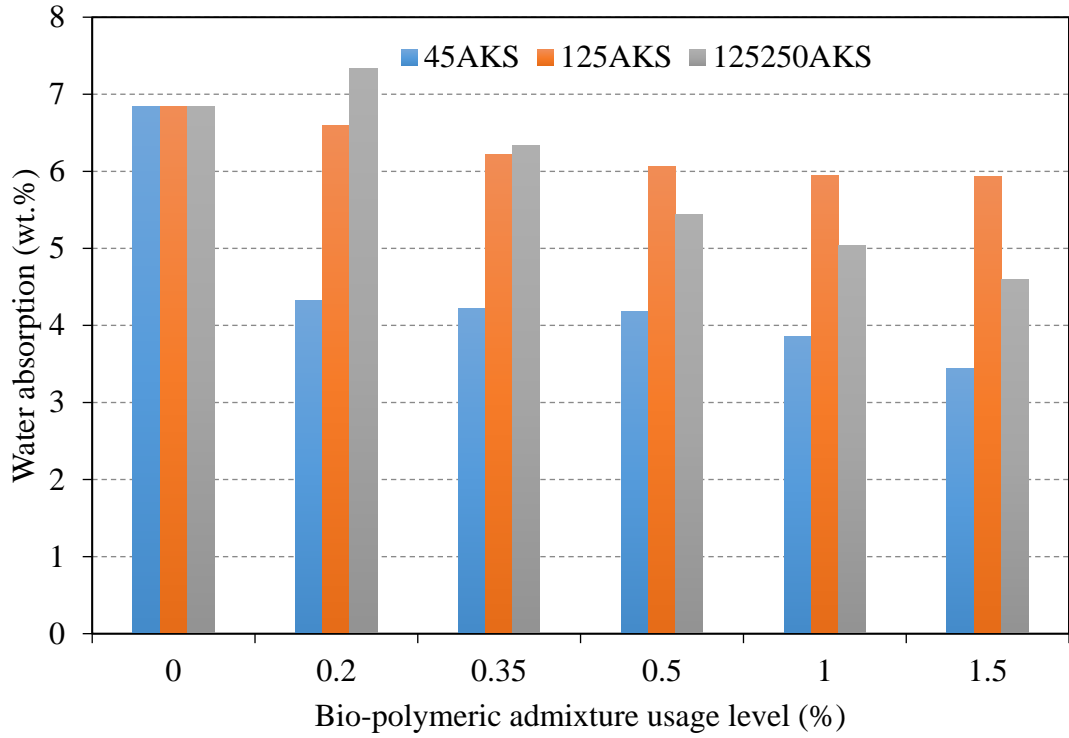


Figure 4.53: Mass water absorption of AKS admixed cement mortars

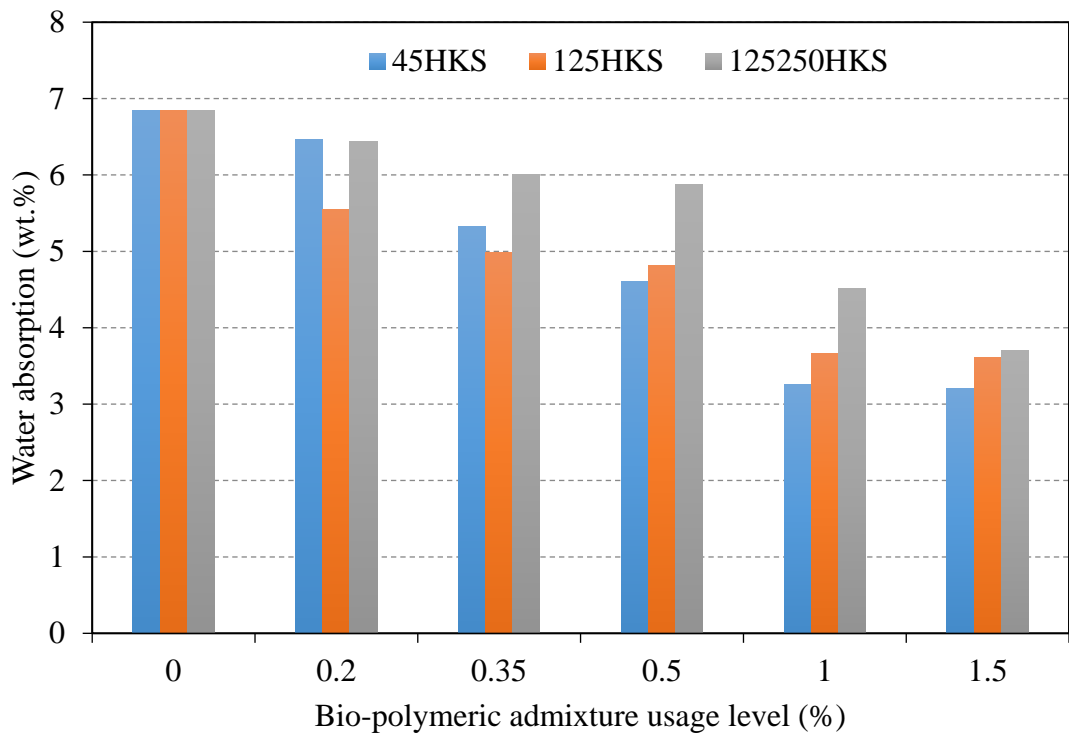


Figure 4.54: Mass water absorption of HKS admixed cement mortars

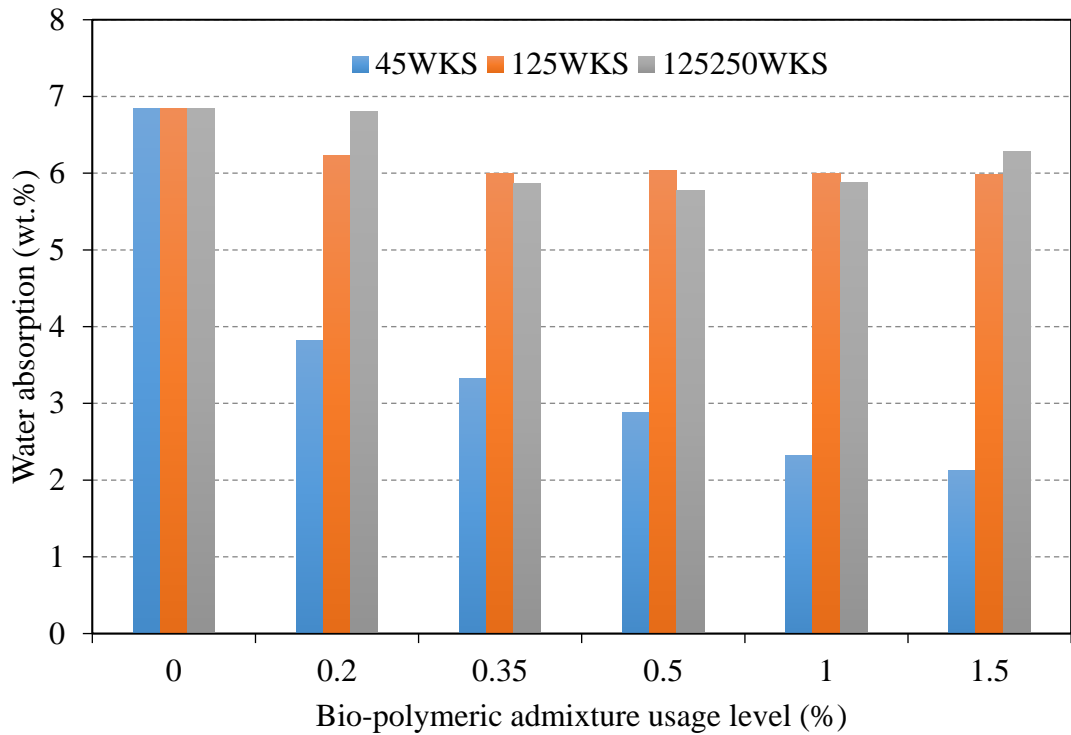


Figure 4.55: Mass water absorption of WKS admixed cement mortars

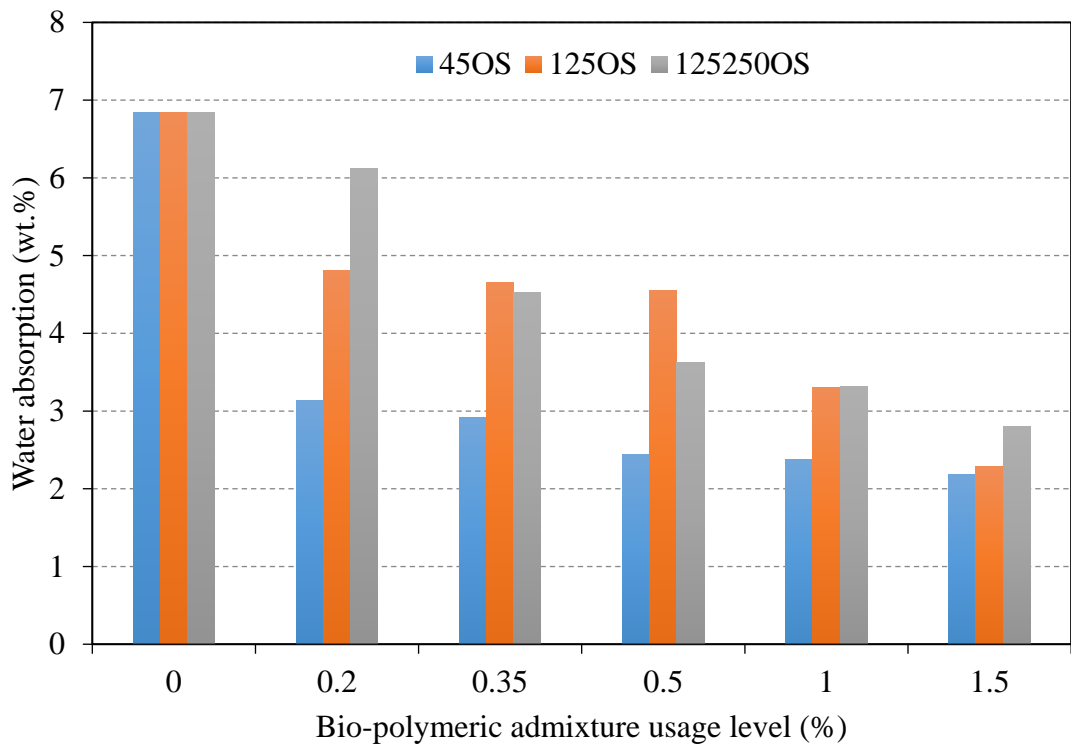


Figure 4.56: Mass water absorption of OS admixed cement mortars

When the graphs between Figure 4.52 and Figure 4.56 were examined, it was determined that the grain size of the used bio-polymeric admixture made a difference between the mass water absorption and capillary water absorption characteristics of cement mortars. Capillary water absorption values in the majority of cement mortars

were determined at the lowest level in the use of 0/125 μm admixtures. However, the lowest values of water absorption by mass (least absorbent) were observed in cement mortars where admixtures with 0/45 μm particle distribution were used. The reason for this is that when lignocellulosic materials are grounded in smaller grain sizes, the amount of extractive substance is released more. This feature is more evident in mass water absorption tests rather than capillary water absorption values. As expected, the water absorption values by mass of cement mortars with olive seed admixtures with higher extractive content were found to be the lowest for all the grain size fractions. In addition, the water absorption values by mass of the mortar specimens in which the WS admixture with 0/45 μm particle size distribution was used were determined to be quite low.

In particular, when fine size (0/45 μm) ES admixture is used, a reduction of up to 24.56 % in the water absorption characteristics of cement mortars has been determined. However, as the ES grain size increased, the water absorption properties of the mortars increased. Similar results were obtained in studies using eggshell powder and it was stated by researchers that very fine grained eggshell reduces the water absorption property of mortars [246,293]. One of the main reasons for the decrease in water absorption with ES admixture is filling the pores with ES and another is the reaction of ES with C_3S , thus reducing the pores. The water absorption value of the reference mixture was determined as 6.84 %. The lowest water absorption values in AKS, HKS, WKS and OS mixtures were exhibited in the 0/45 μm grain size distribution and were determined as 3.44, 3.20, 2.12, and 2.18%, respectively. It has been noted that as the usage rate of lignocellulose bio-polymeric admixtures increases, the water absorption values of the mortar decrease. The reason for this decrease is that more extractive is released in bio-polymeric additives used in lower sizes and these extractives add more hydrophobic properties to the mortar.

In addition, the interaction of mass water absorption values with the components that make up the chemical structure of the bio-polymeric admixtures are shown in Figure 4.57, Figure 4.58 and Figure 4.59.

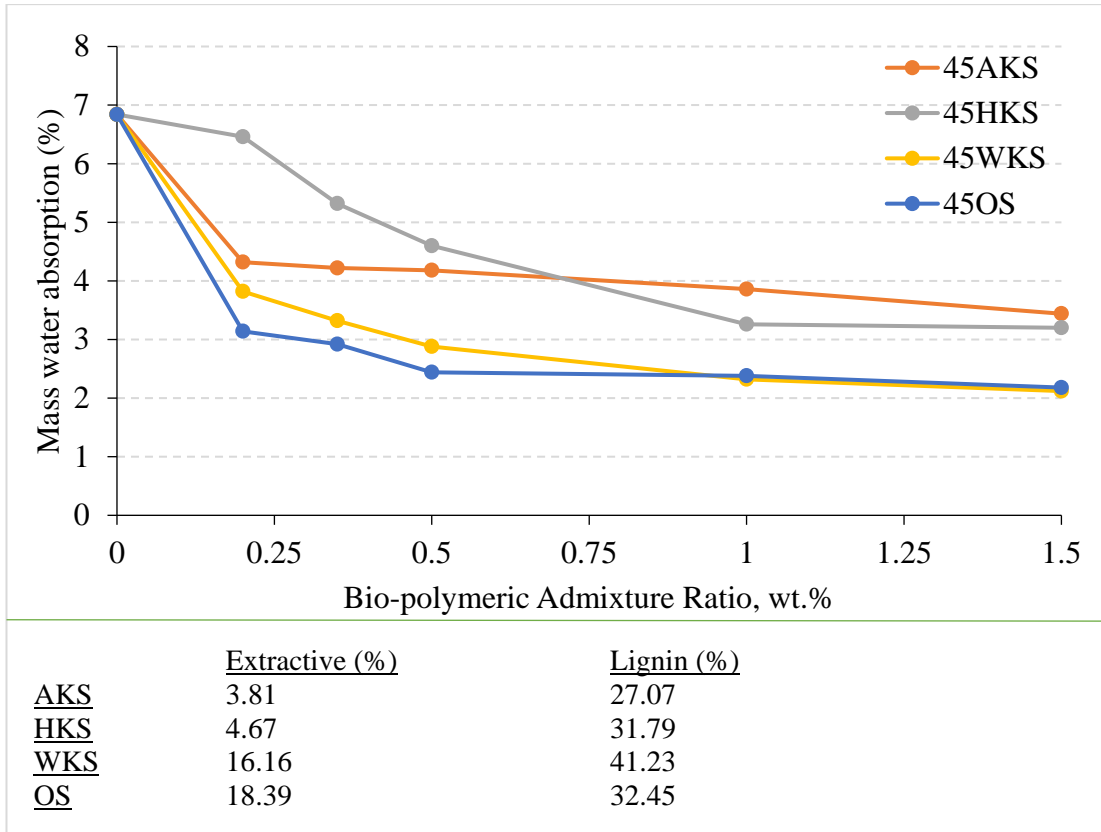


Figure 4.57: Relationship between chemical contents of 0/45 μm bio-polymeric admixture and mass water absorption

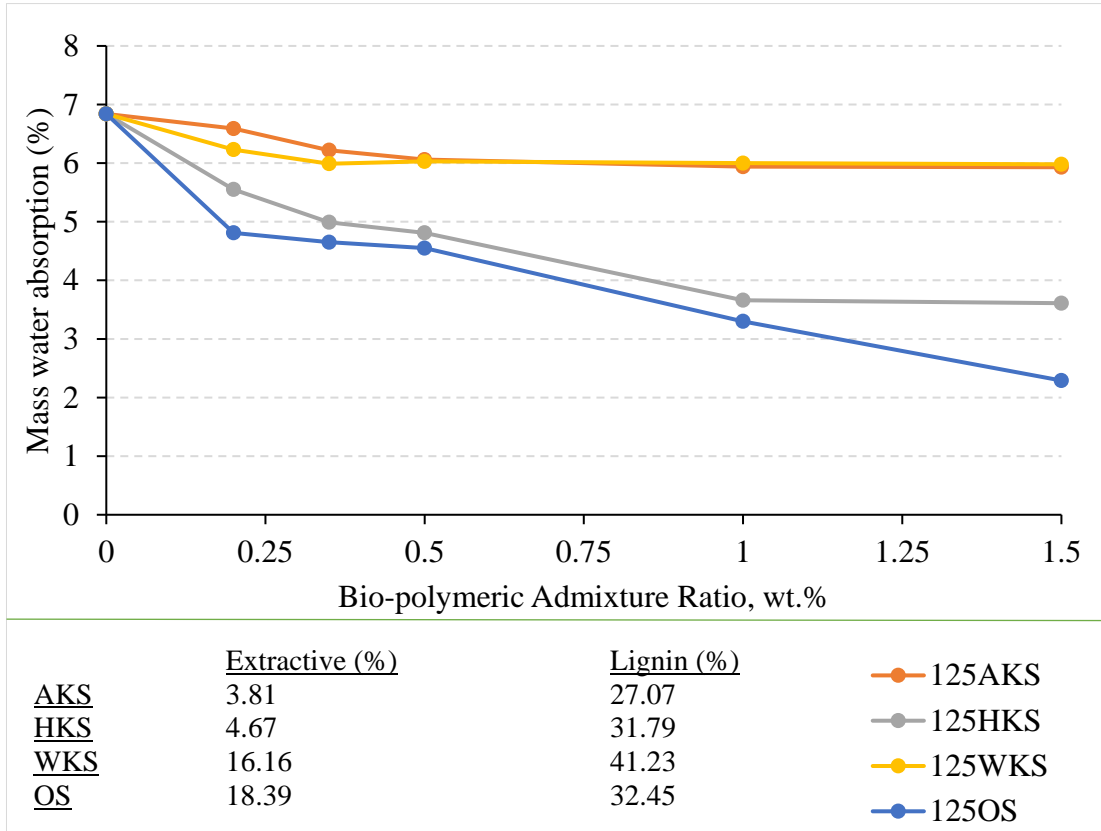


Figure 4.58: Relationship between chemical contents of 0/125 μm bio-polymeric admixture and mass water absorption

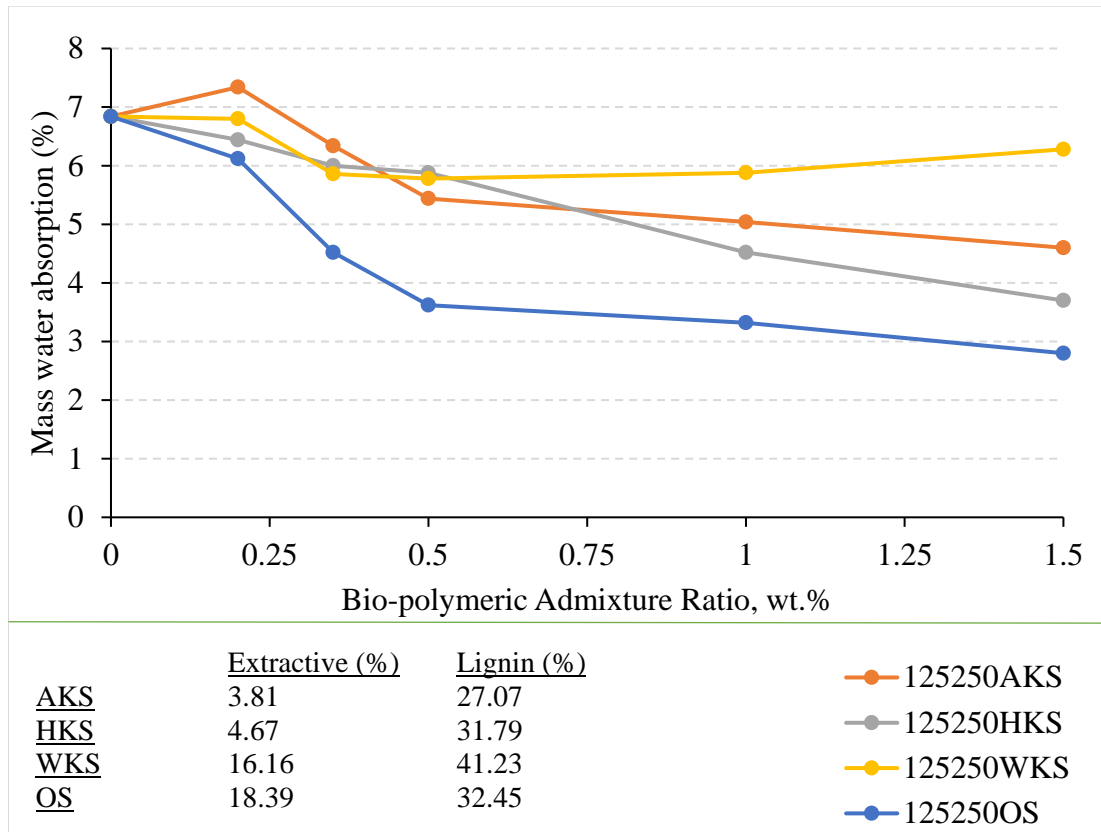


Figure 4.59: Relationship between chemical contents of 125/250 μm bio-polymeric admixture and mass water absorption

According to Figure 4.57, as mentioned before, WKS and OS additives with high extractive ratio can reduce the water absorption rate of the hardened mortar about 69 % when used in 0/45 μm size. When Figure 4.58 and Figure 4.59 are examined, the use of OS additives provided water repellency to the mortar in other grain sizes as well. According to Figure 4.57, Figure 4.58 and Figure 4.59, it was determined that the extractive and lignin content of bio-polymeric admixtures water absorption of the cement mortars. In addition, it was determined that bio-polymeric admixture with higher extractive ratios and finer particle size had a greater water repellency effect on cement mortars. When all the mixtures are taken into consideration, the grain size with the most retarding effect among all grain sizes was 0/45 μm .

Since it was determined that the bio-polymeric admixtures used in this study impart water repellency in the mortars, calcium stearate, a water-repellent agent, was added to the mortars in the same proportions in order to analyze comparatively this water repellency feature of bio-polymeric admixtures better, and then the water absorption values of the chemical admixed mortar were determined. The mass water absorption values of cement mortars with CS admixtures are represented in Figure 4.60.

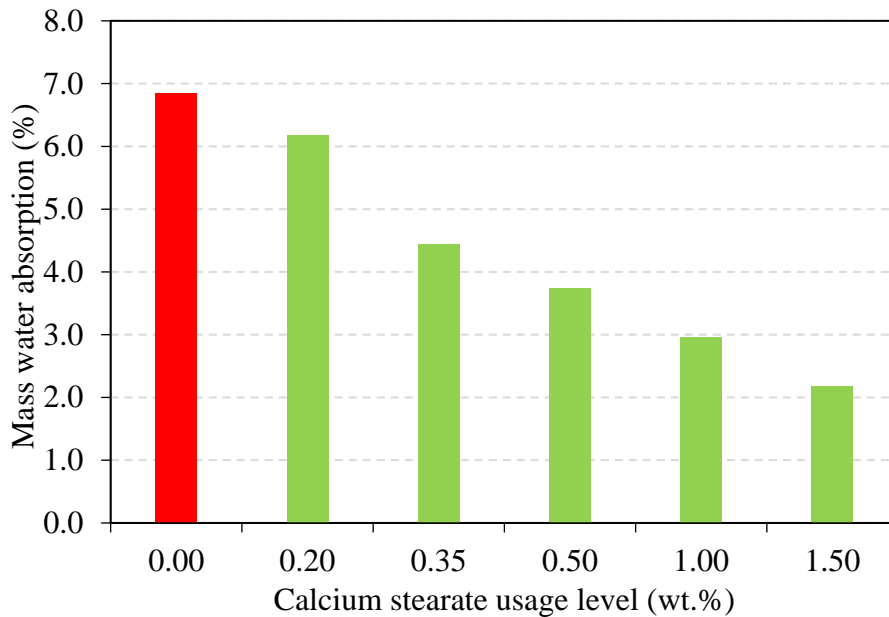


Figure 4.60: Capillary water absorption of CS admixed cement mortars

In Figure 4.60, the mass water absorption value of 6.84 % belongs to the reference sample without any admixture. As the use of calcium stearate increases, the mass water absorption values of the hardened mortars decrease. The reason for this decrease in water absorption is explained as follows; calcium stearate reacts with cement and water during hydration to form a wax-like component. This component creates a hydrophobic structure by covering capillary cavities and pores during evaporation. Thus, the water absorption characteristics of the samples are reduced [290,291]. Depending on CS chemical admixture, up to 68.27 % reduction in mass water absorption was detected. Especially as a result of decreasing the capillary water absorption value, the use of 0/45 μm grain size WKS and OS, 0/125 grain size HKS and OS, and 125/250 μm grain size bio-polymeric admixtures have been shown to provide similar hydrophobicity to hardened cement mortars with the use of calcium stearate. For this reason, in order to reduce the mass water absorption values, instead of using up to 1.5 % calcium stearate, 1.5% WKS and 1.5 % OS admixtures can be used in mortars in 0/45 μm grain size distribution. Also, 1.5% OS with 125/250 micron grain size can be used instead of 1.0 % CS to achieve similar water absorption by mass.

4.3.5 Compressive Strength of Mortars

The 7-, 28-, and 150-days compressive strength values of the test specimens are given in Table 4.12. The 28-days compressive strength values of mortars depending on the

bio-polymeric admixture particle size and the rate of use in the mortar are presented in between Figure 4.61 and Figure 4.65 below.

Table 4.12: Compressive strength values of test specimens

Mix Code	Compressive Strength (MPa)								
	0/45 μm			0/125 μm			125/250 μm		
	7- days	28- days	150- days	7- days	28- days	150- days	7- days	28- days	150- days
R	23.71	35.06	46.05	23.71	35.06	46.05	23.71	35.06	46.05
ES0.2	24.45	36.42	47.87	27.19	38.84	51.50	23.86	35.35	41.11
ES0.35	21.88	32.65	42.92	26.06	38.63	50.50	23.31	34.38	40.31
ES0.5	21.81	32.54	41.66	26.96	38.51	49.32	22.19	34.19	39.67
ES1.0	21.66	32.48	40.02	20.87	35.82	49.11	19.78	29.66	39.96
ES1.5	19.49	29.24	37.33	23.58	33.69	40.22	16.46	24.84	36.46
AKS0.2	22.74	34.09	44.95	24.49	34.99	47.89	23.28	35.55	46.47
AKS0.35	21.91	32.55	41.15	20.46	33.23	44.60	24.20	35.85	47.52
AKS0.5	21.45	32.48	40.52	22.40	32.36	40.50	24.11	35.99	47.53
AKS1.0	21.63	32.42	37.60	21.00	32.11	36.90	25.44	37.98	47.49
AKS1.5	19.35	29.11	37.54	21.70	31.48	35.01	25.49	38.72	48.78
HKS0.2	20.45	30.90	47.19	24.50	35.14	46.90	24.75	36.66	47.00
HKS0.35	21.60	31.38	45.13	18.20	26.93	38.25	24.45	36.63	46.59
HKS0.5	21.74	32.48	44.39	18.00	26.12	35.80	24.30	35.86	44.24
HKS1.0	21.39	31.82	41.06	18.69	26.70	35.90	23.83	34.90	40.18
HKS1.5	20.71	30.99	40.58	18.40	26.35	35.60	18.75	27.72	32.42
WKS0.2	19.98	29.90	37.52	19.13	27.33	34.23	23.73	34.88	44.34
WKS0.35	18.19	27.07	35.12	17.56	25.09	33.33	23.39	35.72	40.61
WKS0.5	19.28	28.63	34.45	18.75	26.78	35.10	23.38	35.56	39.90
WKS1.0	19.67	29.54	37.69	21.85	31.22	39.54	20.72	30.25	35.74
WKS1.5	20.34	30.50	40.40	24.47	34.95	41.59	17.82	25.79	30.82
OS0.2	13.20	19.44	22.68	13.30	19.01	29.00	19.35	29.15	33.23
OS0.35	14.77	22.04	29.63	16.10	23.22	33.00	15.48	23.10	31.44
OS0.5	15.71	22.64	29.89	16.80	24.30	36.50	13.22	19.73	25.08
OS1.0	17.56	26.34	38.57	20.41	29.15	39.67	14.25	21.67	24.42
OS1.5	19.66	29.34	40.59	20.78	29.68	51.00	15.30	22.44	29.82

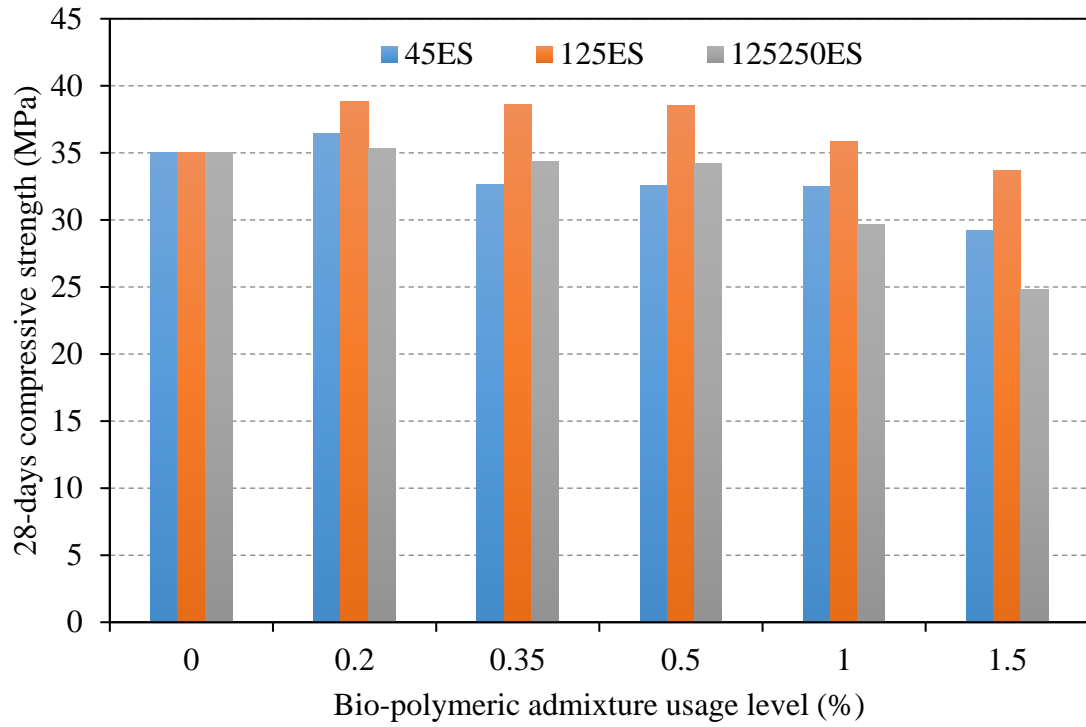


Figure 4.61: 28-days compressive strength of ES admixed cement mortars

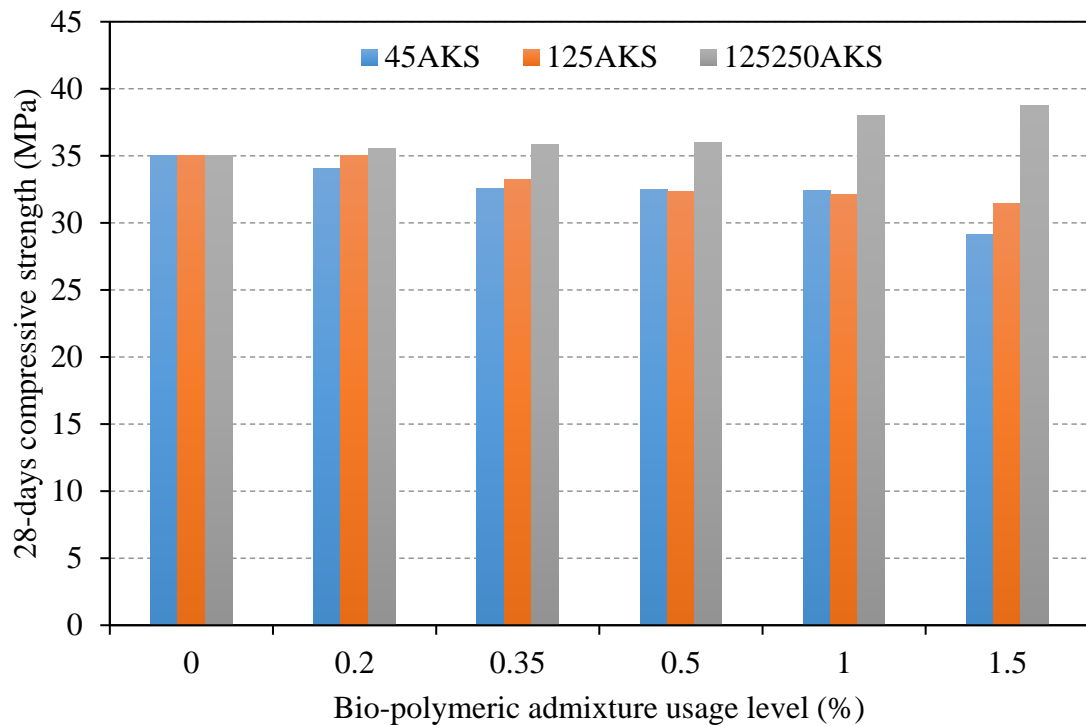


Figure 4.62: 28-days compressive strength of AKS admixed cement mortars

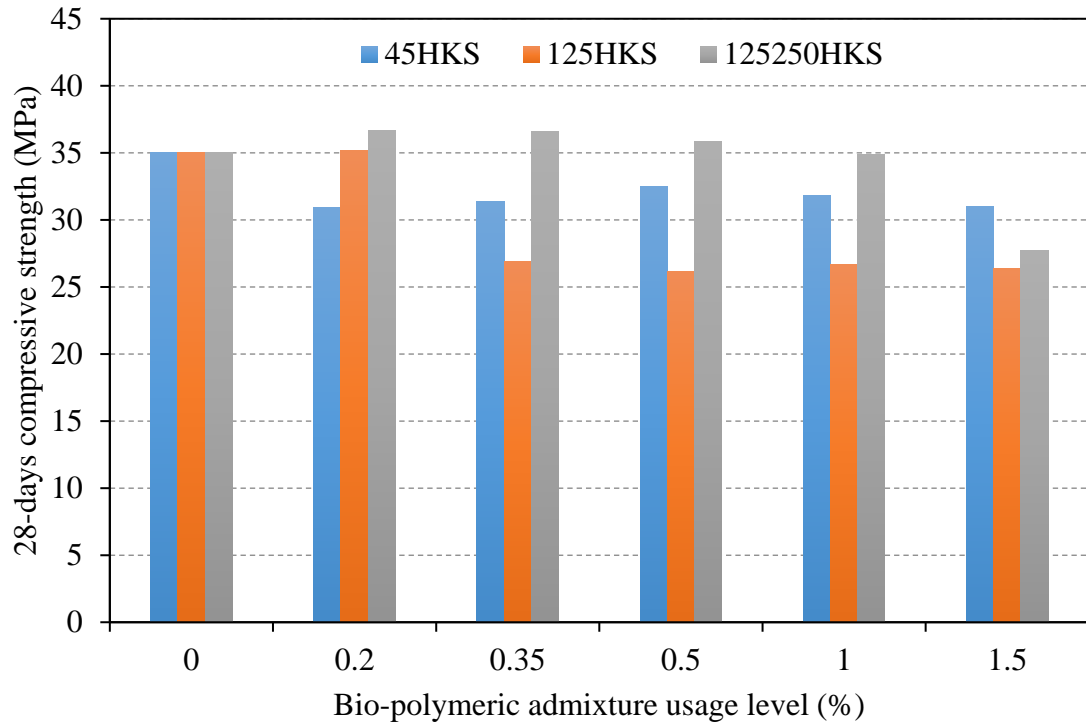


Figure 4.63: 28-days compressive strength of HKS admixed cement mortars

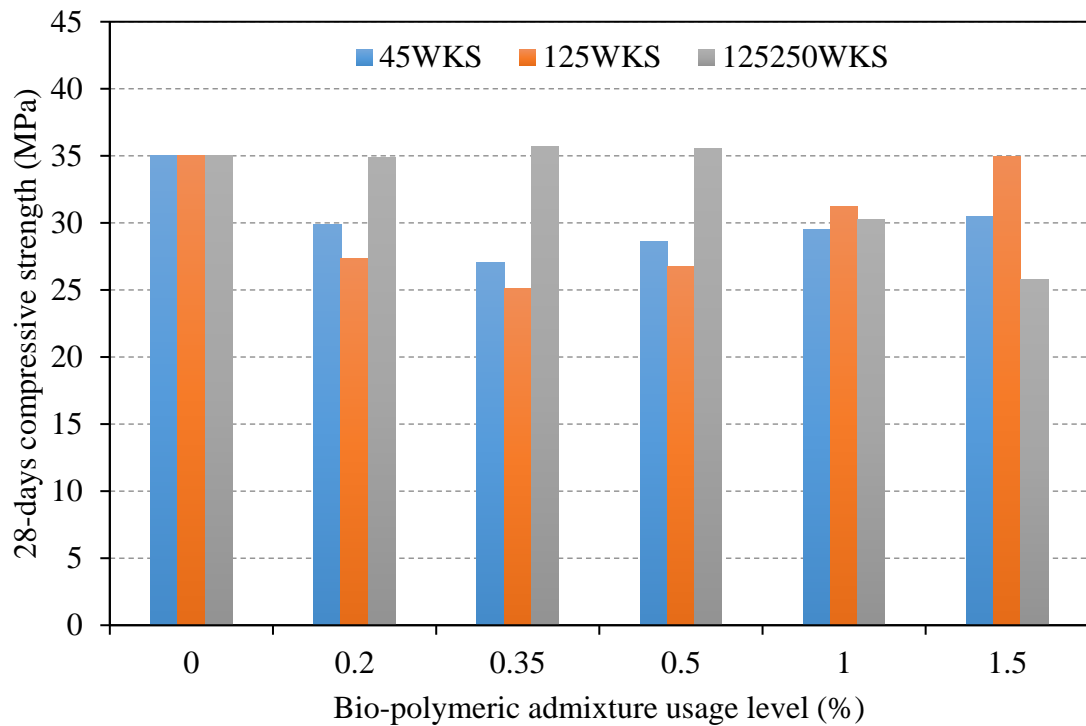


Figure 4.64: 28-days compressive strength of WKS admixed cement mortars

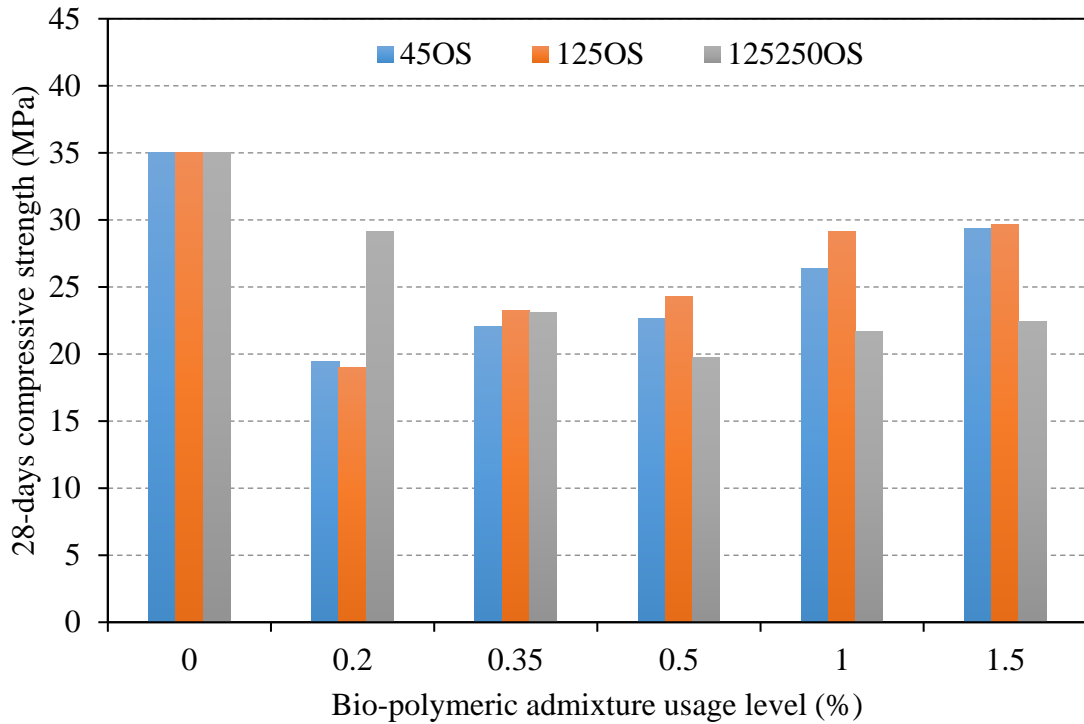


Figure 4.65: 28-days compressive strength of OS admixed cement mortars

Analyzing Figure 4.61, the compressive strength value of 35.06 MPa belongs to the control specimen without any admixture. It has been found that the use of 0/125 μm egg shell powder in cement mortar up to 1.0 % by mass improves the compressive strength. This increase in compressive strength can be explained as the filler effect of the eggshell and extra calcium hydroxide for the formation of the secondary C-S-H gel [152]. The literature results from previous studies indicate that the compressive strength of concrete and cement mortars generally increases with fine size ESP usage [294]. Hamada et al. [294] also concluded that the inclusion of small particle sizes of ESP has a better effect than large particles in terms of improving concrete properties. In this thesis study, similar mechanical properties were determined in mortars. Compressive strengths in the use of coarse size (125/250 μm) ES decreased up to 29.16 % compared to the reference sample. On the other hand, using 0.2 wt.% fine size (0/45 μm) ES improved 3.87%. The grain size that improved the compressive strength the most was the 0/125 μm range. ES used in this grain size improved the compressive strength of the cement mortar by 10.78, 10.18, 9.84, and 2.17 % at the usage rates of 0.2, 0.35, 0.5, and 1.0 wt.%, respectively. One reason why ES, which is used in a relatively thin size, improves the compressive strength of the mortar, is to obtain denser mortars by showing a filling effect. Also, fillers with small particle sizes improved the hydration of cement mortars and therefore accelerated the formation of

calcium silicate hydroxides [295]. It has been determined that the compressive strength decreases after the optimum ES utilization rate is exceeded for each grain size. The pattern agreed with past research on eggshell added cement mortars, and the relationship between percentage eggshell replacement and compressive strength can be said to be curvilinear [293].

When figures between Figure 4.62 and Figure 4.65 are examined, almost all hardened mortars samples with 125/250 μm grain size bio-polymeric admixtures exhibited a higher compressive strength than mortars produced with 0/45 and 0/125 μm bio-polymeric admixture mortars. The physical structure of lignocellulosic bio-polymeric admixtures used as coarse size (125/250 μm) in this study have the appearance of microfibers. For this reason, they have the potential to distribute the load by adopting the fiber feature in the mortar composition. Therefore, it has been determined that the compressive strength of the mortars in which these microfibers are used has improved up to a certain usage rate. Similar results were obtained in other studies using cellulose microfibers [296,297]. In this thesis study, especially with the use of 125/250 μm size AKS, 28-day compressive strength values of the mortars were improved by 1.40, 2.26, 2.64, 8.32, and 10.43 % at 0.2, 0.35, 0.5, 1.0, and 1.5% usage rates, respectively. Again, with the use of 125/250 μm size HKS, the 28-day compressive strength values of the mortars were improved by 4.57, 4.47 and 2.28 % at 0.2, 0.35 and 0.5% usage rates, respectively. In addition, with the use of 0.35 wt.% and 0.5 wt.% WKS, the compressive strength of the mortar increased by 1.87 % and 1.44 % compared to the reference mortar. This enhancement of compressive strength may be attributed to the higher fiber/matrix bond and to the fiber crack bridging efficiency [297,298]. Generally, it has been observed that the compressive strength decreases with the use of microfiber above 1.0 wt.%. This can be attributed to an increase in fiber contiguity and to difficulty in achieving good homogenization of the fresh mortar [297]. Considering the 28-day compressive strengths, it was determined that the OS admixture could not show the expected effect on this property. This is thought to be due to the high extractive content of OS, which slows down cement hydration considerably. In addition, since it adds hydrophobic properties to the mortar thanks to the fatty acids in it, hydration cannot develop sufficiently since enough water cannot be taken into the mortar during water curing.

Within the scope of this thesis, the amount of cellulose in the structure of bio-polymeric admixtures and accordingly the crystallinity index of the bio-polymeric admixtures was determined as the main parameters affecting the compressive strength of cement mortars. For this reason, the 28-days compressive strengths of the mortars and the cellulose amounts and crystallinity indexes of the bio-polymeric admixtures used in the cement mortar are shown in Figure 4.66, Figure 4.67 and Figure 4.68 comparatively.

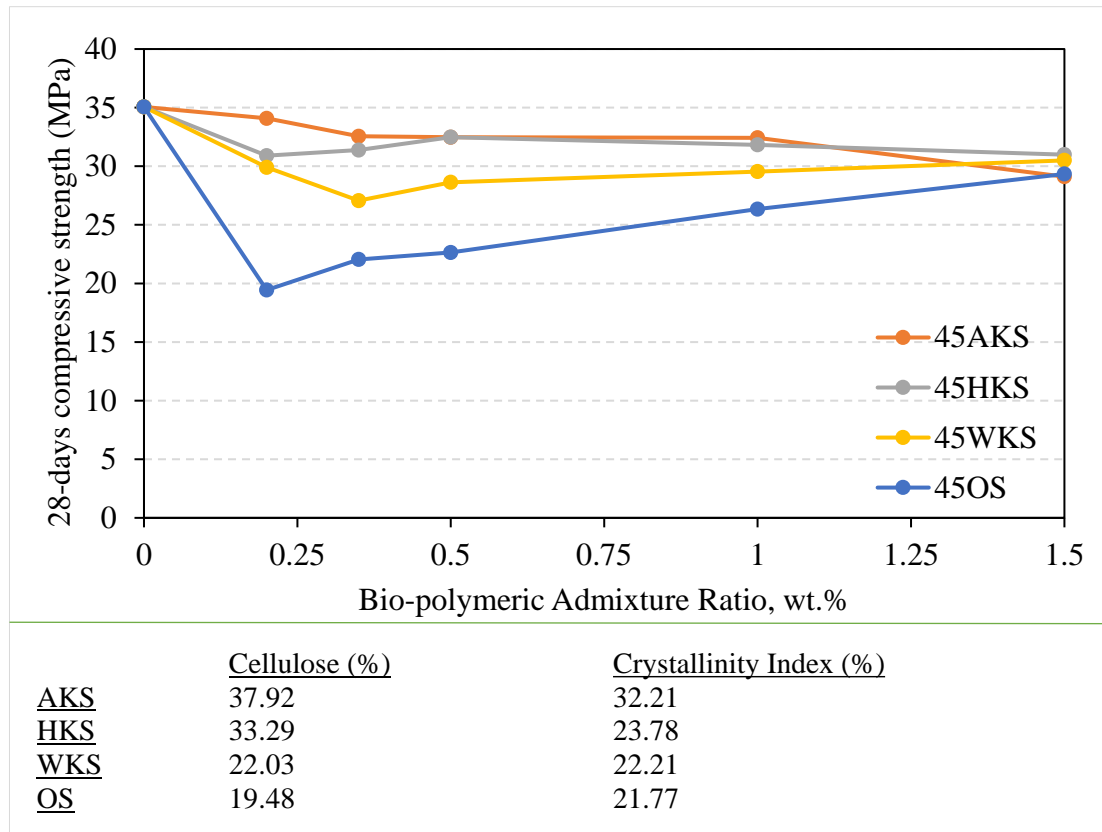


Figure 4.66: Relationship between chemical contents of 0/45 μm bio-polymeric admixture and 28-days compressive strength

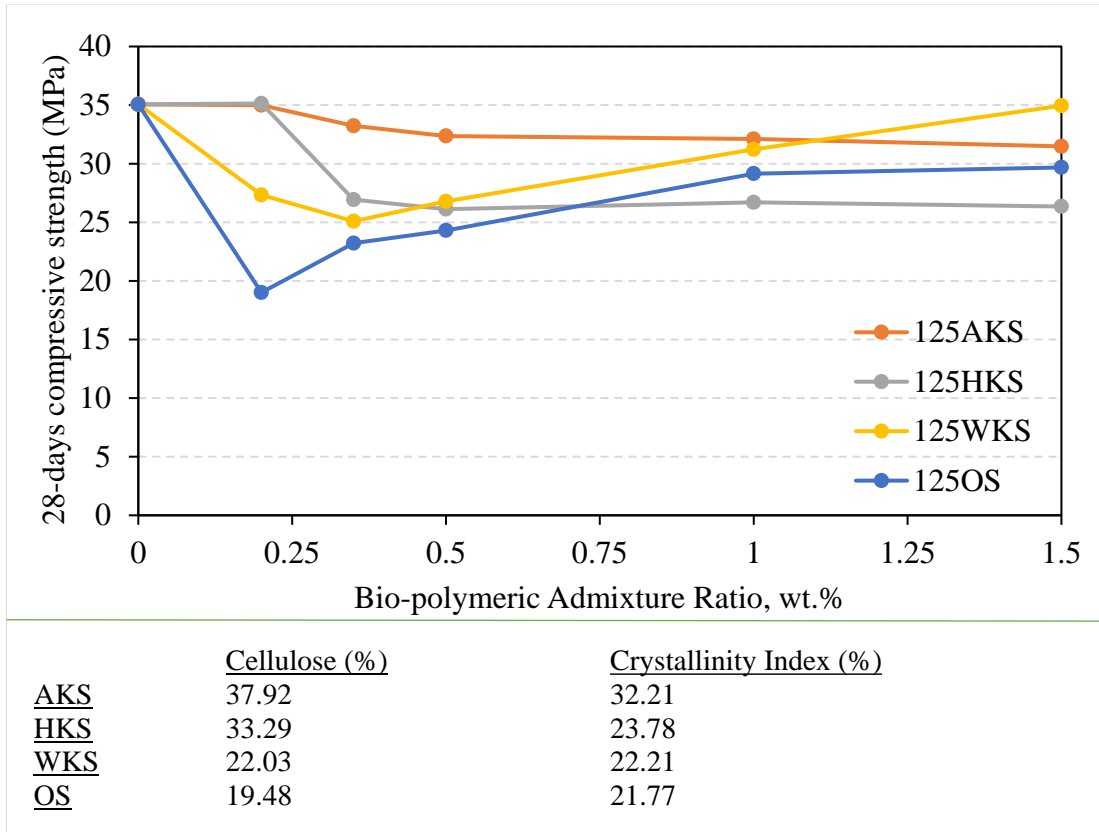


Figure 4.67: Relationship between chemical contents of 0/125 μm bio-polymeric admixture and 28-days compressive strength

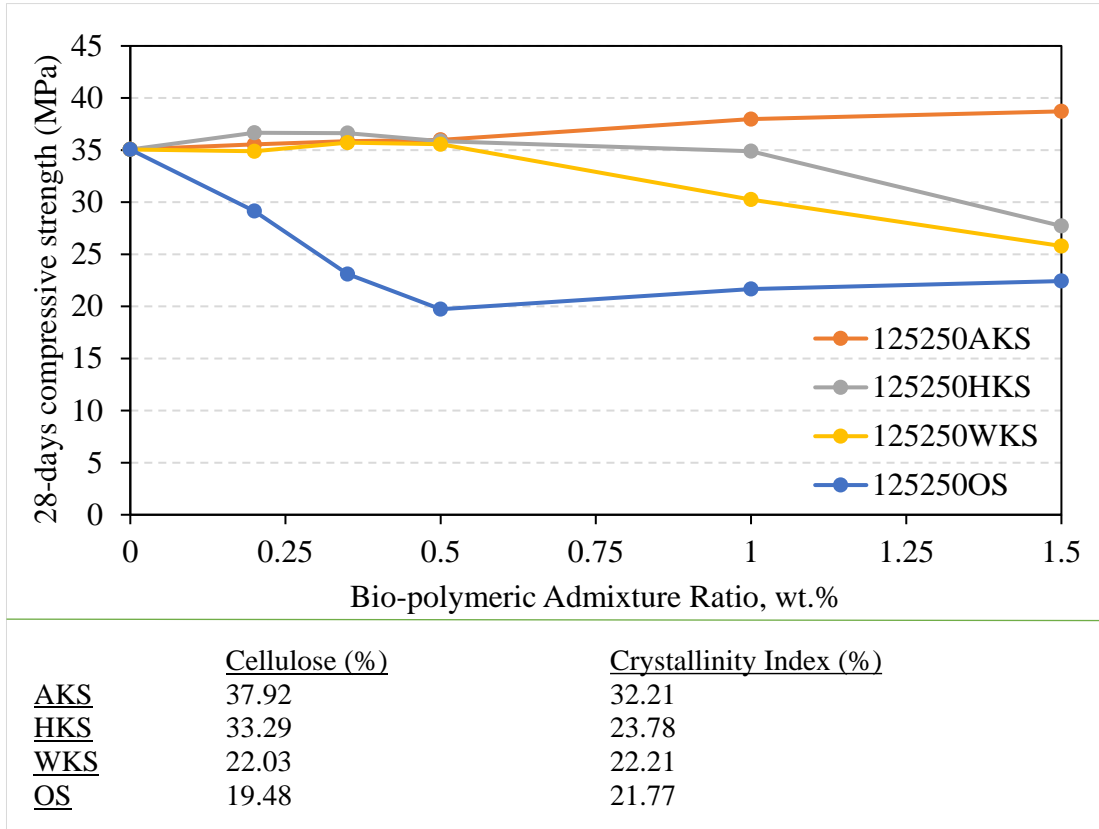


Figure 4.68: Relationship between chemical contents of 125/250 μm bio-polymeric admixture and 28-days compressive strength

According to Figure 4.66, Figure 4.67 and Figure 4.68, it was determined that the cellulose amount and crystallinity index of bio-polymeric admixtures considerably effect 28-days compressive strength of the cement mortars. It is known that cellulose fibers can improve mechanical behavior of cementitious material at μm scale and as well as nm, mm, and cm scale [299]. However, performance of cellulose fibers on cement mortars depends on several conditions such as the mixture formula, curing conditions and the fiber itself (fiber morphology, fiber amount, fiber length, fiber aspect ratio, etc.) [299–301]. In this thesis study, the particle size of the lignocellulosic bio-polymeric admixtures and the chemical content of the admixture are very effective on the compressive strength of the mortar. As mentioned before, 125/250 μm grain size distribution exhibited a more fibrous character, which was an improvement factor in the 28-day compressive strengths. On the other hand, when the effect of grain sizes on compressive strength is examined separately, the compressive strength of cement mortars with AKS admixture with high cellulose content and accordingly high crystallinity index has always been determined to be higher, and it is valid for all three grain size distributions. As it can be easily noticed when the graphs above are examined, the 28-day compressive strength of the OS admixed (which has the lowest cellulose content and the lowest crystallinity index) cement mortars was determined to be the lowest.

In addition, it is known that there is a direct proportionality between the unit volume mass of cementitious materials and the compressive strength. It is frequently determined by researchers that biopolymers, natural additives, fillers and fibers entrain some air in cementitious materials and increase the pore ratio in the matrix structure [102,126,194,296,297,302,303]. In this thesis, it has been determined that another factor affecting the compressive strength values of cement mortars is the unit volume mass values that decrease with the use of bio-polymeric admixtures. Therefore, the unit volume mass change of the mortars versus the compressive strength for each grain size distribution is graphically represented in Figure 4.69, Figure 4.70 and Figure 4.71.

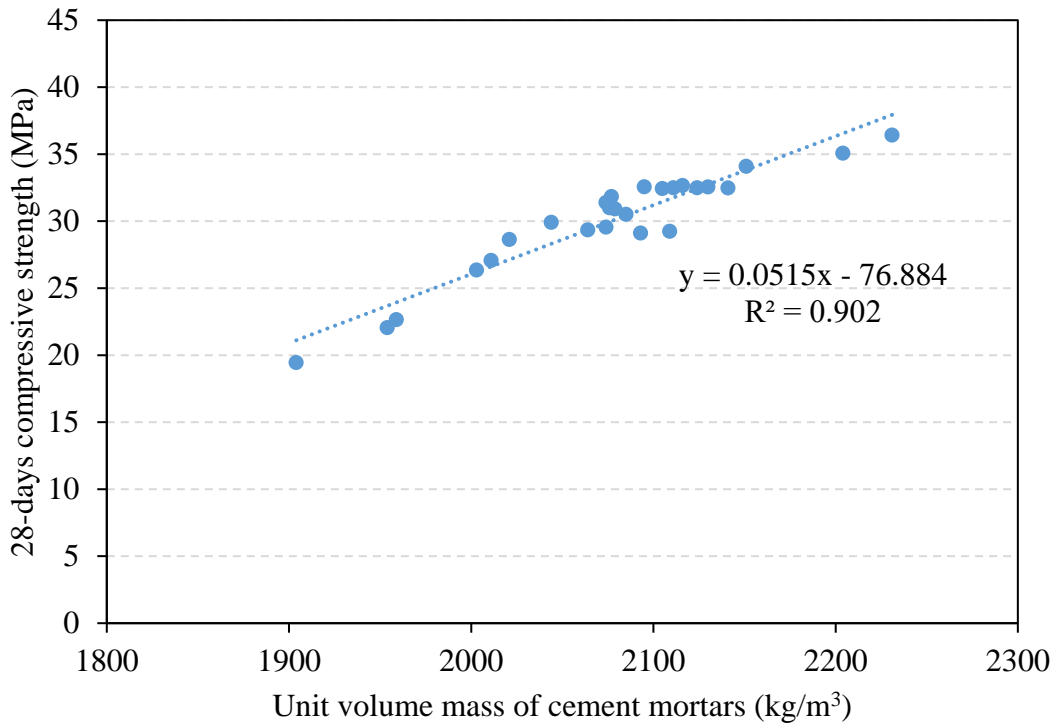


Figure 4.69: Relation between unit volume mass and 28-days compressive strength of mortars (0/45 μm)

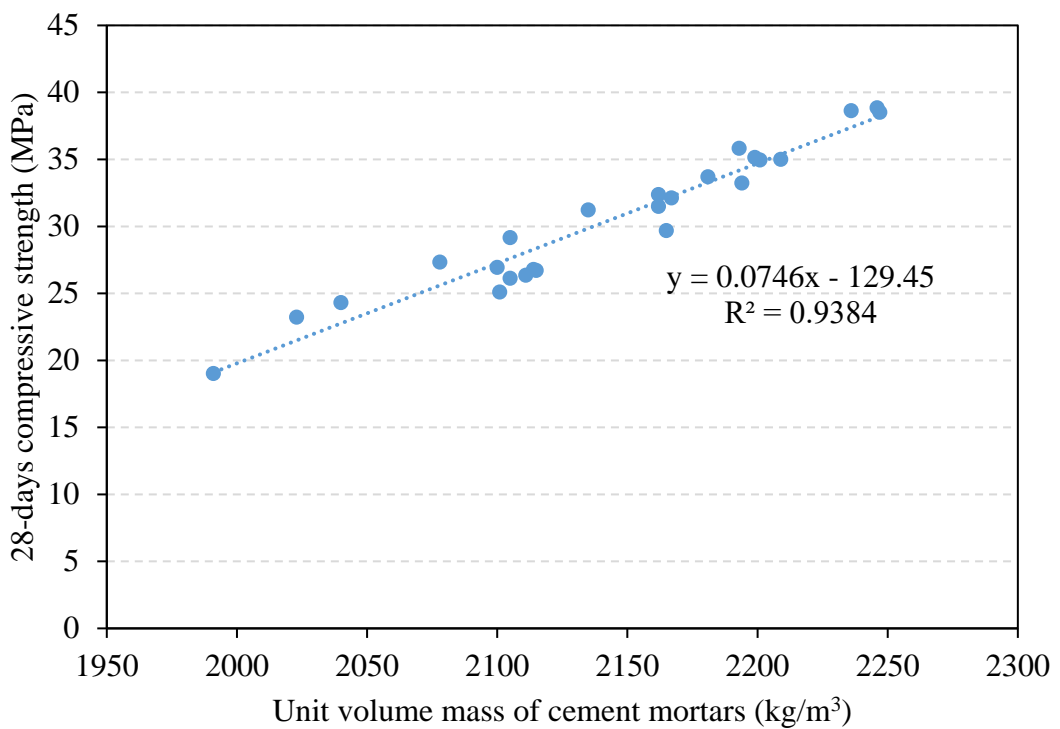


Figure 4.70: Relation between unit volume mass and 28-days compressive strength of mortars (0/125 μm)

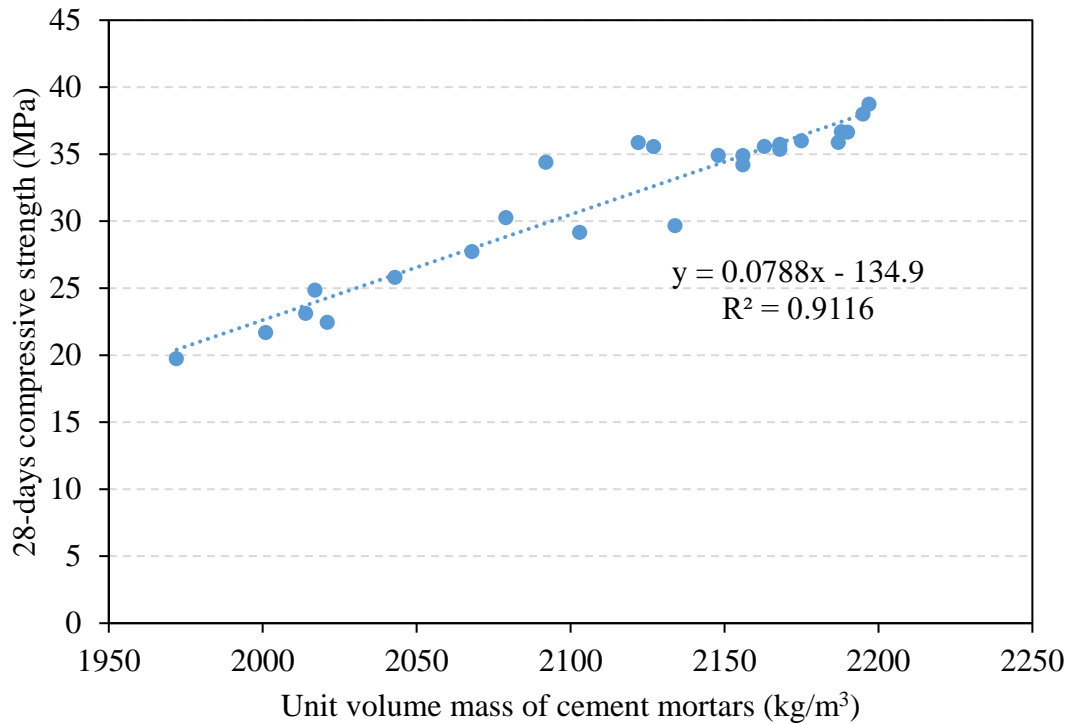


Figure 4.71: Relation between unit volume mass and 28-days compressive strength of mortars (125/250 μm)

When Figure 4.69, Figure 4.70 and Figure 4.71 are examined, it can be easily observed that there is a very strong correlation between the 28-day unit volume mass values and the 28-day pressure values of the mortars in which bio-polymeric additives are used in all three particle size distributions. The decrease in unit volume mass also causes a decrease in compressive strength values. It is not always advantageous to add more bio-polymeric admixtures to the cement mortar. Since the admixture increase increases the amount of air trapped in the fresh and hardened mortar and thus reduces the unit volume mass values, the optimum admixture usage rate in terms of compressive strength should not be exceeded. The compressive strength of all test mortar with 0/45 μm grain size admixtures remained below the compressive strength of the reference mortar, because of decreasing unit volume mass values. However, it has been observed that with the HKS admixture, it can reach up to 87% of the compressive strength of the reference sample. Optimum utilization rate of 0/125 μm grain size can be evaluated as 0.2% for AKS and HKS because the compressive strength of this series is similar to the reference mortar. Although there was a slight decrease in unit volume mass values at 125/250 μm grain size, the compressive strength of the test samples improved somewhat due to the conversion of the structure of the admixture to fibrous properties and thus, adding fiber crack bridging effect to mortars. While the optimum usage rate

for AKS admixture in 125/250 μm grain size is 1.5 wt.%, it can be evaluated as 0.5 wt.% for HKS and WKS admixtures.

In this thesis, 150-days compressive strengths were tested to determine the long-term strength of cement mortars. The changes in the 150-days compressive strength of cement mortars depending on the bio-polymeric admixture usage rate and admixture grain size are represented in Figure 4.72 - Figure 4.76 comparatively.

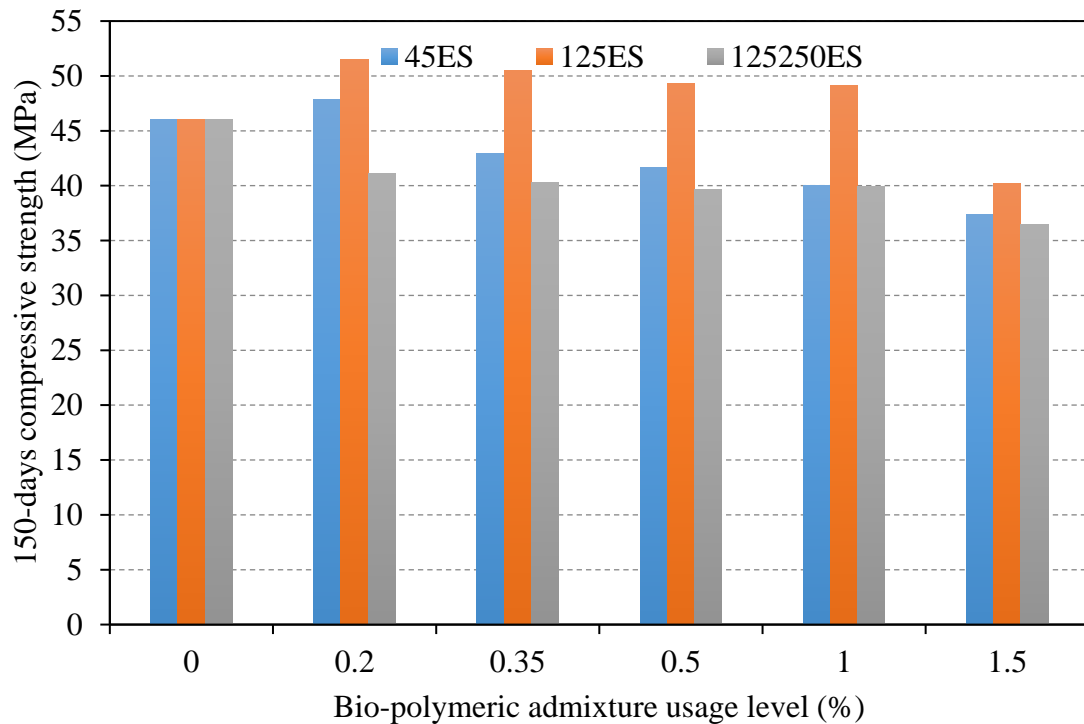


Figure 4.72: 150-days compressive strength of ES admixed cement mortars

Examining Figure 4.72, the 150-day compressive strength value of the reference mixture increased to 46.05 MPa. While the 28-day compressive strength of the reference sample was 35.06 MPa, there was a 31.35 % strength gain by the 150th day. Except for the use of 1.5% ES, it was determined that all samples with 0/125 μm grain size exhibited better compressive strength than the reference sample in the long term. The 28-day compressive strength values also showed a similar trend. When both 28-day and 150-day compressive strength values are considered, it is understood that the optimum grain size is 0/125 μm for ES bio-polymeric admixture once again. The compressive strengths of ES admixed mortars increased by 32.60, 30.73, 28.07, 37.10 and 19.38 % at 0.2, 0.35, 0.5, 1.0 and 1.5 wt.% usage rates, respectively, compared to their 28-day strengths. It has also been determined by other researchers that the compressive strength increases with the use of ES in later ages (90-days) and the

reason for this is stated as the progression of hydration [294,304]. The main reason for the increase in strength is that the high amount of calcium in the egg shell positively affects the development of hydration [305]. This component of egg shell reacts with the alumina phase in the cement to form carboaluminates and slows down the conversion of ettringites to sulfoaluminates. In addition, the egg shell contributes to the strength by increasing the C-S-H density [306]. However, the use of large size significantly reduces the reactivity of the eggshell.

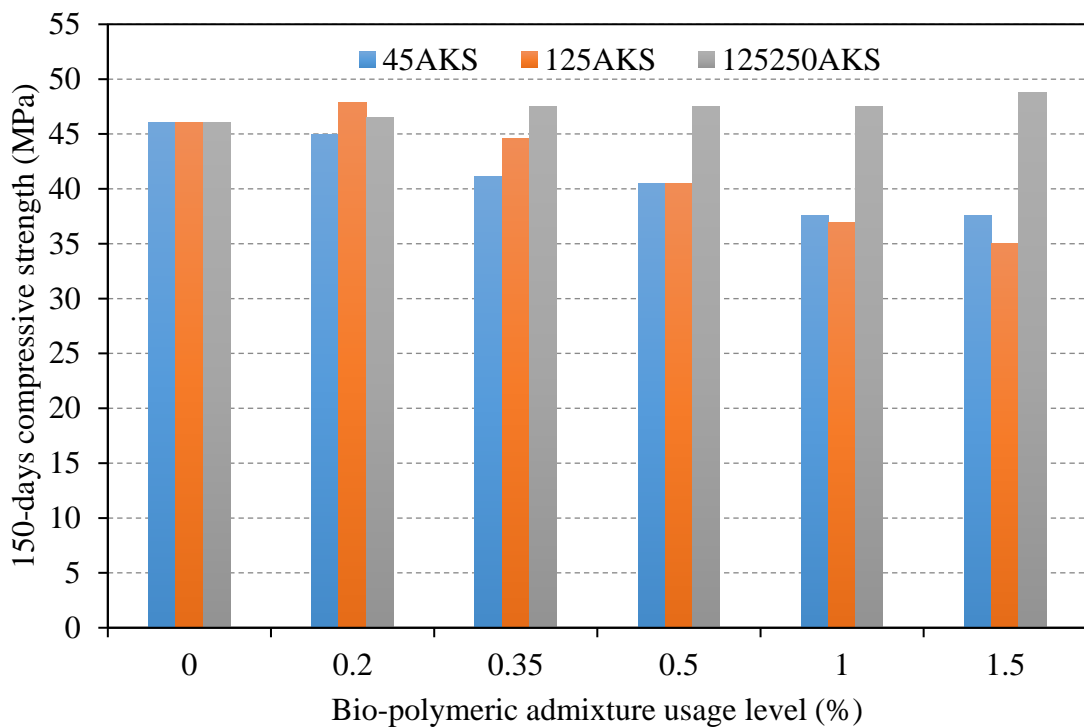


Figure 4.73: 150-days compressive strength of AKS admixed cement mortars

According to Figure 4.73, The 150-day compressive strength of the mortars using AKS admixture, in parallel with their 28-day compressive strength, reached higher compressive strength values than the reference mixture in the use of 125/250 μm grain size admixtures. Compared to the reference mortar, the use of 0.2, 0.35, 0.5, 1.0 and 1.5 wt.% 125/250 μm AKS admixture improved the compressive strength by 0.91, 3.19, 3.21, 3.12 and 5.92 %, respectively. In this study, it was stated that as the grain size of the admixture gets coarser, the grain structure gets closer to the fiber property. This fiber property improved both 28-day and 150-day compressive strengths. Other researchers have also determined that the long-term compressive strengths of mortars using natural fibers show values close to the reference sample [307].

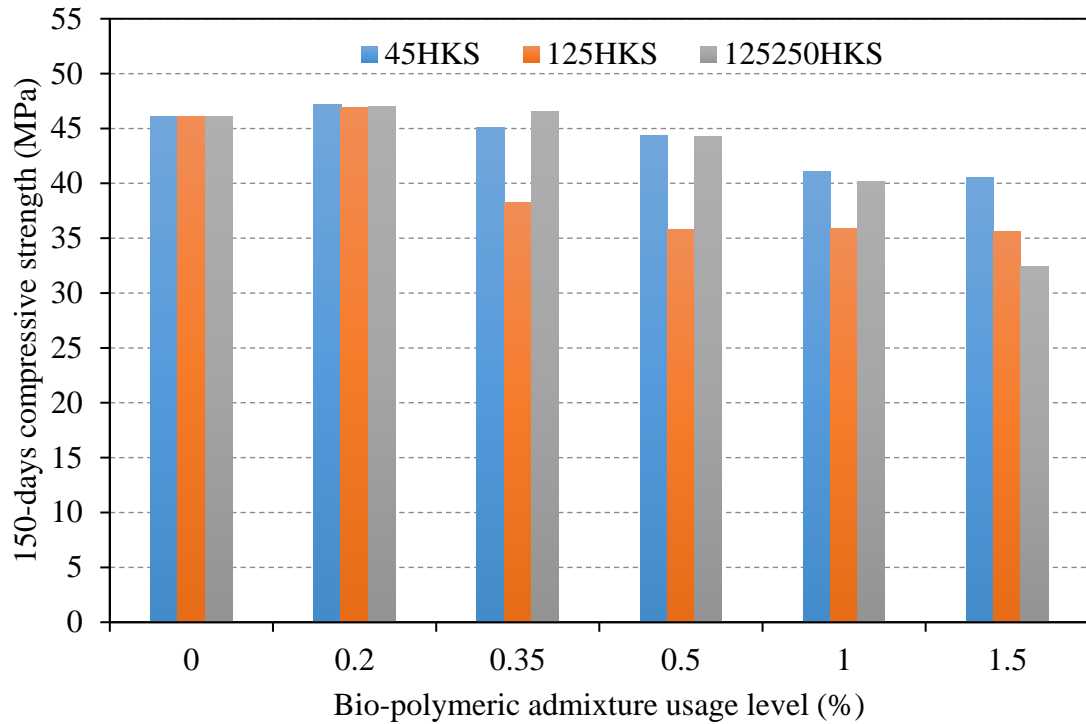


Figure 4.74: 150-days compressive strength of HKS admixed cement mortars

As can be observed from Figure 4.74, when the HKS admixture, which has a similar grain shape and similar chemical content to the AKS admixture, was used in low amounts, the 150-day compressive strength of the produced cement mortars was found to be close to the compressive strength of the reference mortar. When using 0.2 wt.% HKS additive for all three grain sizes, they improved the strength by an average of 2.12 % compared to the 150-day compressive strength of the reference sample. Similar results for the use of hazelnut shells have been found in previous studies by researchers [308]. Kalkan and Gündüz [308] revealed that 0/125 and 0/250 grain size waste hazelnut shells strengthened the matrix structure of cement mortars, when up to 0.35 wt.% utilization rate.

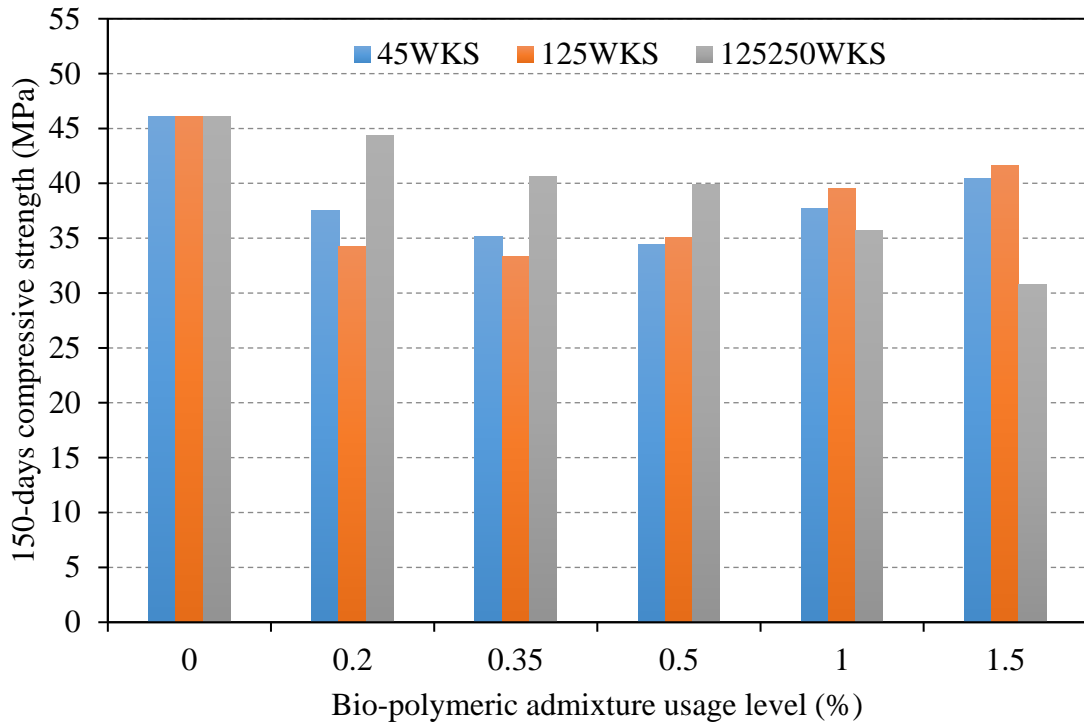


Figure 4.75: 150-days compressive strength of WKS admixed cement mortars

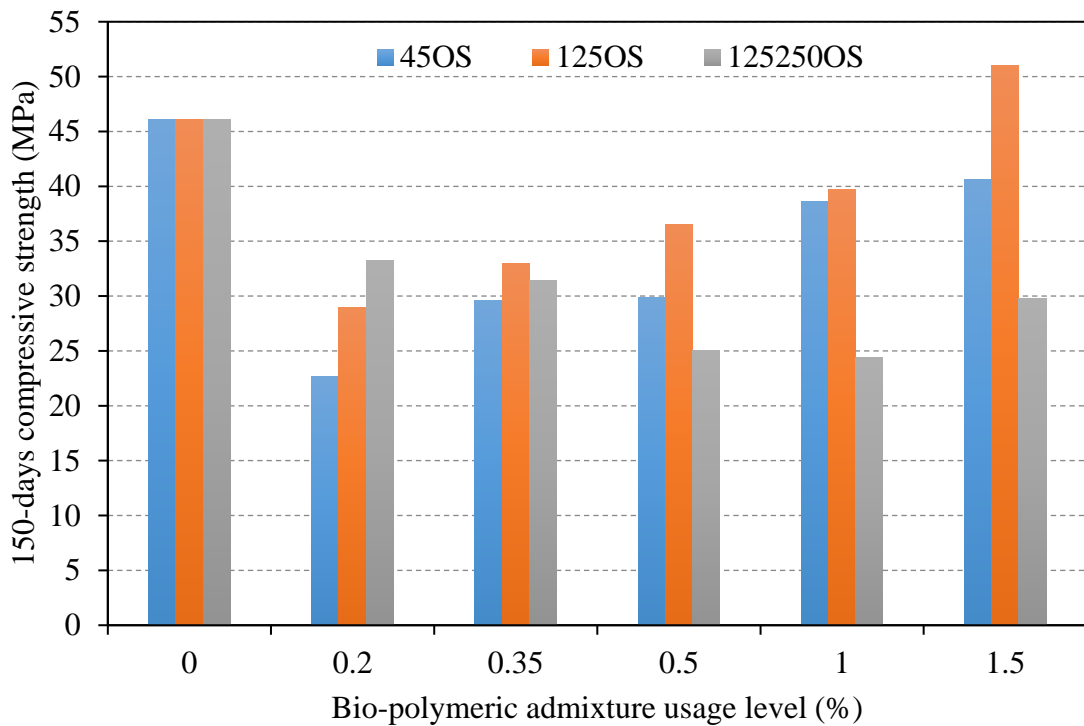


Figure 4.76: 150-days compressive strength of OS admixed cement mortars

Examination of Figure 4.75 and Figure 4.76 shows that the 150-days compressive strength values of WKS and OS admixed cement mortars yield a very different result than the compressive values of other mortars with other admixtures (ES, AKS, HKS).

In 45ES series, 150-day compressive strengths started to decrease with the use of admixtures more than 0.2 wt.%, which is the optimum usage rate in 45ES series. Similarly, the compressive strength of the 125ES series increased up to 1.0 wt.%, which is the optimum usage rate, and the compressive strength decreased in further use. A similar trend was observed for AKS and HKS admixtures, with strength increased up to 0.2 wt.%, the optimum ratio of 125AKS, and decreased 150-day compressive strength with further use. The optimum ratio was determined as 1.5 wt.% in the 125250AKS series, and the compressive strength increased until this ratio. While the optimum ratio was determined as 0.35 wt.% for 125250HKS series in cement mortars using HKS bio-polymeric admixtures, this ratio was determined as 0.2 wt.% in 45HKS and 125HKS series. As stated, the 150-day compressive strength of these three (ES, AKS, HKS) bio-polymeric admixtures increases compared to the reference mortar up to a certain admixture usage level, then the 150-day compressive strength values decrease if admixtures usage ratio above this optimum level are used. When Figure 4.75 and Figure 4.76 is examined, the 150-days compressive strength values of especially 45WKS, 125WKS, 45OS and 125OS have decreased sharply with the use of WKS and OS admixture, and the strengths have started to be regained with the increase in the use of bio-polymeric admixtures. With the addition of WKS or OS admixture to the cement mortar, the compressive strength decreases, and the strength increases again as the amount of admixture increases. This phenomenon is explained as, because WKS and OS provide superior hydrophobic properties to hardened mortar with high extractive substance content, hardened mortars cannot absorb enough water and hydration cannot develop during water curing. On the other hand, the high amount of pectin contained in the high extractive substance plays an important role in the hydration of cement in long-term ages and increases the compressive strength [111]. As the bio-polymeric admixture ratio increases, the pectin content included in the mortar increases, and this has been determined as a feature that improves hydration, which does not develop due to the hydrophobic feature in water curing phase. Pectin contained in the bio-polymeric admixtures react with calcium ions in alkaline environment and form a very stable “egg box” structure responsible of the decrease of Ca^{2+} concentration in lime-saturated solutions [209,309]. Also, pectin can trap calcium and thus acts as a growth inhibitor for CSH hydrates, which is the major hydration product of Portland cement [309]. In summary, the consumption of Ca^{2+} ions by the pectin in cement mortar enhanced the hydration of cement particles [111,310].

According to the results obtained in this thesis study, using low amounts of WKS and OS admixtures with high extractive content worsens the compressive strength due to the inability to absorb the water needed during water curing, providing high pectin addition to the mortar composition by using high rates of WKS and OS resolved the strength loss by promoting hydration by pectin Ca^{2+} interaction.

On the other hand, the chemical content of the biopolymeric additives and the changes in the 150-day compressive strength under the effect of grain size are graphically represented in Figure 4.77, Figure 4.78 and Figure 4.79.

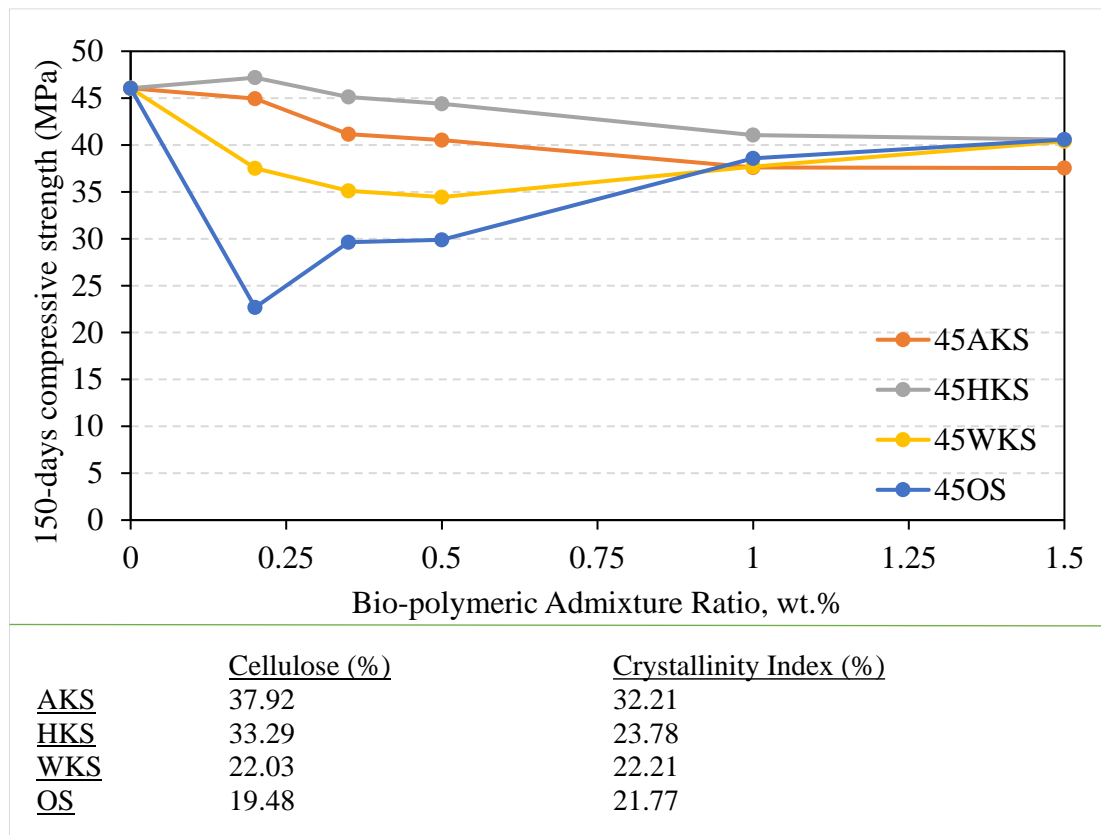


Figure 4.77: Relationship between chemical contents of 0/45 μm bio-polymeric admixture and 150-days compressive strength

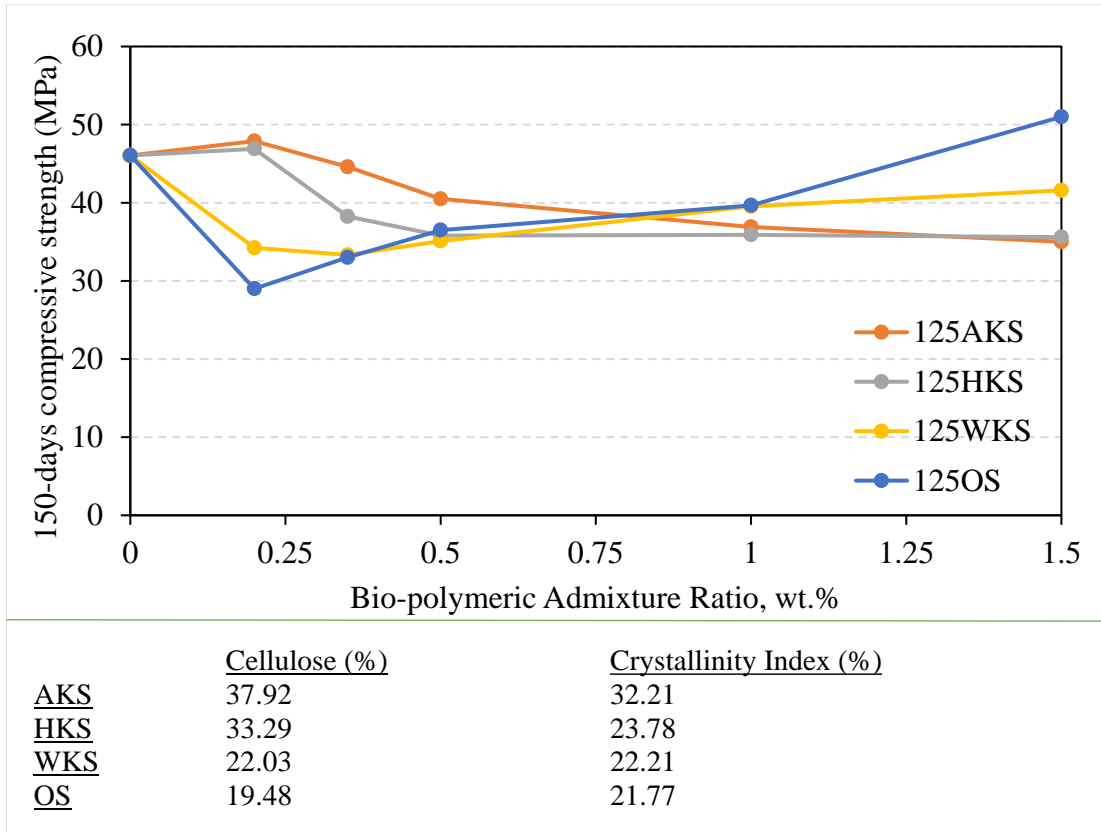


Figure 4.78: Relationship between chemical contents of 0/125 μm bio-polymeric admixture and 150-days compressive strength

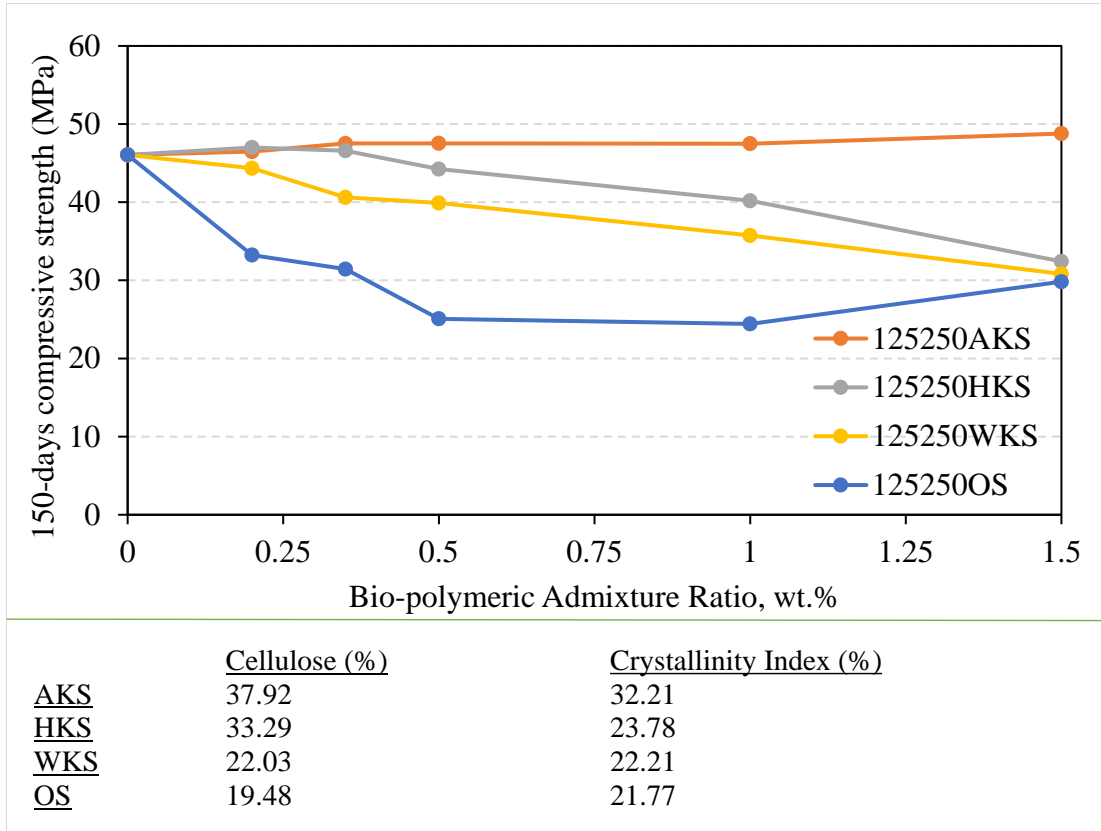


Figure 4.79: Relationship between chemical contents of 125/250 μm bio-polymeric admixture and 150-days compressive strength

When Figure 4.77, Figure 4.78 and Figure 4.79 are examined, it is concluded that although WKS and OS bio-polymeric admixtures have an improving effect on the compressive strength of pectin mortar at high usage rates, in general, the compressive strength of the mortars in which WKS and HKS admixtures with high cellulose ratio and crystallinity are used show higher performance. Especially from the point of waste evaluation, 125/250 μm AKS can be used easily in cementitious products without causing compressive strength loss.

It has been experienced by researchers that chemicals used to improve some properties of concrete and cementitious products can reduce the compressive strength of concrete or mortars [311–314]. To investigate the significance of the loss of compressive strength due to the use of bio-polymeric admixtures, the 28-days compressive strength of cement mortars with chemical admixtures (PCE, SMF, CS and TA) were used were also tested. The 28-day compressive strengths of chemical admixed mortars are given in the Table 4.13. In addition, the effect of the chemicals on the compressive strength is shown graphically in Figure 4.80.

Table 4.13: Compressive strength property of cement mortars with the use of chemical admixtures

Mix code	Compressive Strength (MPa)
R	35.06
CS0.2	30.76
CS0.35	28.91
CS0.5	27.28
CS1.0	26.35
CS1.5	23.12
PCE0.01	32.47
PCE0.025	32.18
PCE0.05	32.90
PCE0.1	32.62
PCE0.2	33.00
SMF0.05	34.20
SMF0.1	34.25

Table 4.13 (Continued): Compressive strength property of cement mortars with the use of chemical admixtures

Mix code	Compressive Strength (MPa)
SMF0.2	35.00
SMF0.35	34.68
SMF0.5	35.10
TA0.03	33.44
TA0.05	31.61
TA0.1	29.26
TA0.2	25.37
TA0.35	21.82

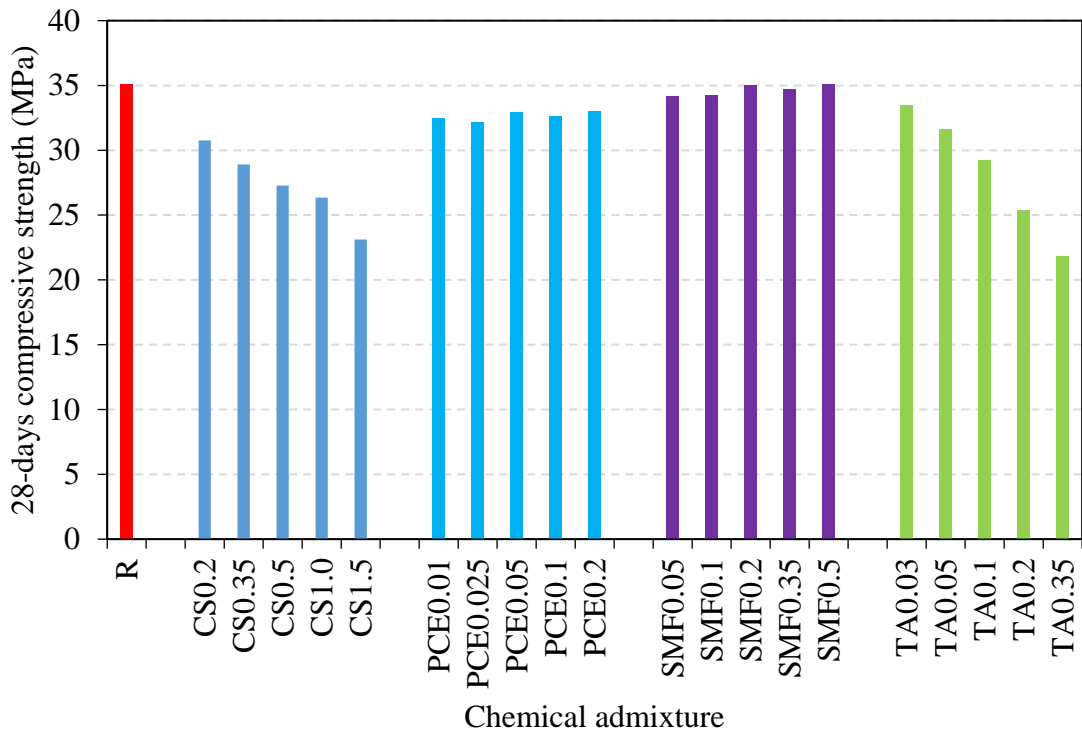


Figure 4.80: Compressive strength change of chemical admixed cement mortars

In this study, the proportions of chemicals added to the cement mortar were determined by considering the maximum usage rate suggested by the manufacturers producing the chemicals. As can be seen from Figure 4.80, the use of chemical additives in cement mortars produced with a constant water-cement ratio did not improve the compressive strength for any mortar series. On the contrary, the compressive strengths of most test mortars were adversely affected by the use of chemical admixtures. CS admixture can reduce the compressive strength of cement mortar up to 34.06 %. In addition, it has

been observed that the TA admixture can reduce the compressive strength up to 37.76 %. Since a constant water/cement ratio (0.50) was used in this study, water reducing admixtures worsened the compressive strength of cement mortars, apart from being an improving factor. PCE can reduce 28-day compressive strength by up to 8.21 % and SMF by up to 2.45 %.

4.3.6 Flexural Strength of Mortars

The 28-days flexural strength values of the test specimens are given in the Table 4.14. The 28-days flexural strength values of mortars depending on the bio-polymeric admixture particle size and the rate of use in the mortar are presented in between Figure 4.81 and Figure 4.85 below.

Table 4.14: Flexural strength values of test specimens

Mix Code	Flexural Strength (MPa)		
	0/45 μm	0/125 μm	125/250 μm
R	7.32	7.32	7.32
ES0.2	7.37	7.50	6.77
ES0.35	7.36	7.54	6.52
ES0.5	7.14	7.39	6.48
ES1.0	7.11	7.31	6.45
ES1.5	6.73	6.47	6.41
AKS0.2	5.58	6.85	7.33
AKS0.35	5.29	6.55	7.35
AKS0.5	4.81	6.53	7.39
AKS1.0	4.68	6.41	7.47
AKS1.5	4.74	5.81	7.56
HKS0.2	6.73	6.27	7.44
HKS0.35	6.69	6.15	7.41
HKS0.5	6.70	5.76	7.33
HKS1.0	6.32	5.68	6.74
HKS1.5	6.02	5.41	5.78

Table 4.14 (Continued): Flexural strength values of test specimens

Mix Code	Flexural Strength (MPa)		
	0/45 μm	0/125 μm	125/250 μm
WKS0.2	4.11	3.55	6.97
WKS0.35	4.40	3.50	6.79
WKS0.5	4.78	3.25	5.88
WKS1.0	4.79	5.58	5.26
WKS1.5	4.82	6.28	4.31
OS0.2	4.65	2.61	6.50
OS0.35	4.18	3.07	6.01
OS0.5	4.04	5.38	5.70
OS1.0	4.45	5.42	5.50
OS1.5	4.52	5.46	5.70

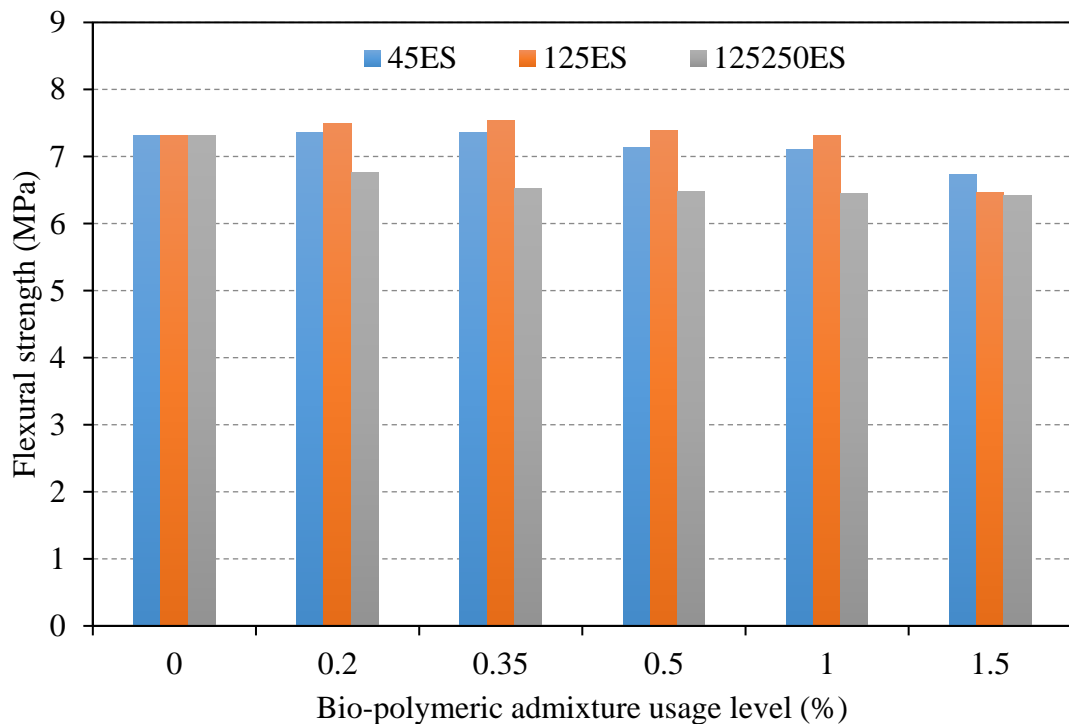


Figure 4.81: Flexural strength of ES admixed cement mortars

Figure 4.81 shows the flexural strength of egg shell admixed cement mortar obtained from flexural test. The optimum value of the 0/45 μm eggshell as bio-polymeric admixture for the flexural strength test was 0.35 wt.%. Eggshell 5% had the highest flexural strength at 1 day and 28 days. While the 28-day flexural strength of the

reference mortar was 7.32 MPa, the flexural strength increased to 7.36 when 0/45 μm ES was used at 0.35% by weight (45ES0.35). This grain size and utilization ratio increased the flexural strength by 0.55%. When the grain size is used as 0/125 μm , the highest strength increased to 7.54 MPa in the 125ES series. When 0.35 wt.% and 0/125 μm size ES used, it was able to increase the flexural strength by 3.01% compared to the reference mortar. However, the flexural strength of the mortars started to decrease in the use of ES above 0.35 wt.% for mortars using both grain sizes. Therefore, the optimum utilization rate for these two grain sizes is 0.35 wt.%. On the other hand, the use of 125/250 μm grain size ES reduced the flexural strength of the mortar in all from the lowest evaluation rate to the highest evaluation rate. It has been stated by the researchers that the flexural strengths of cementitious materials are increased up to a certain extent with the use of the egg shell as a replacement with cement or the use of the egg shell as a filling material [146,315,316]. Similarly, in this thesis study, when eggshell was used as a biopolymeric additive, the optimum rate for the improvement of flexural strength was found to be 0.35%.

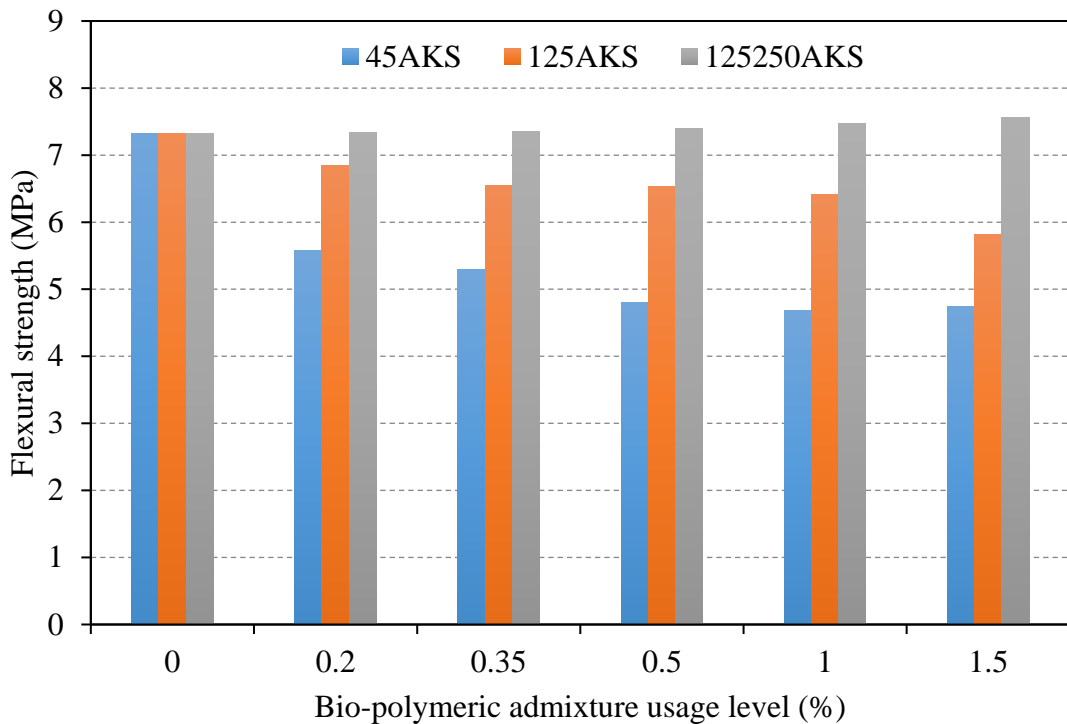


Figure 4.82: Flexural strength of AKS admixed cement mortars

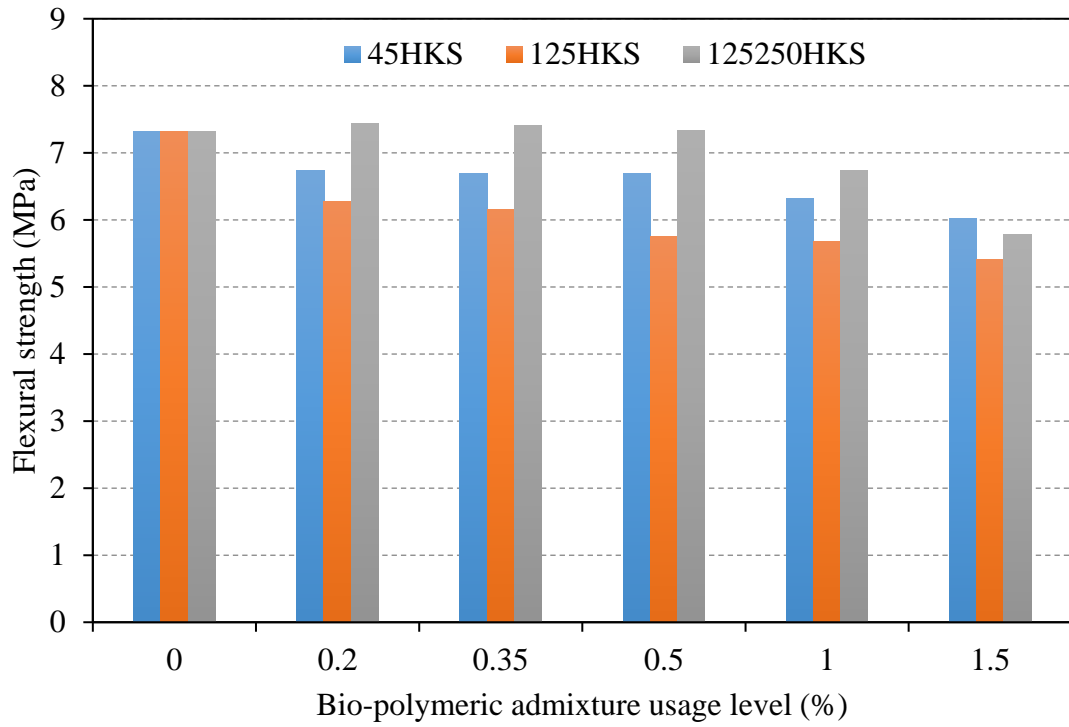


Figure 4.83: Flexural strength of HKS admixed cement mortars

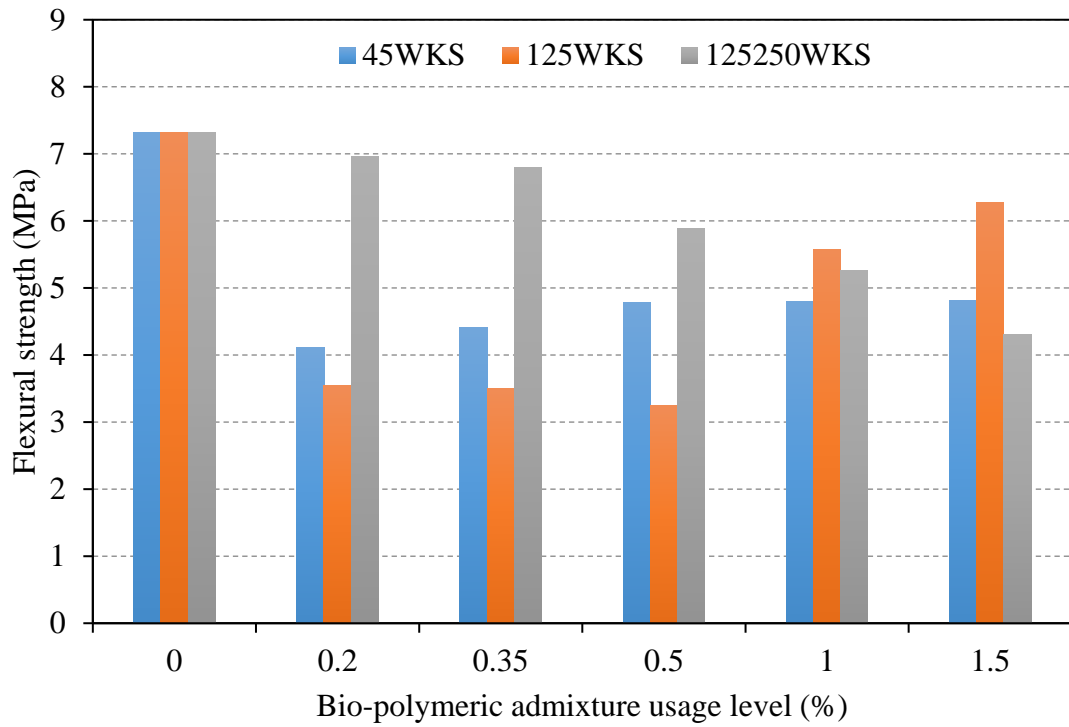


Figure 4.84: Flexural strength of WKS admixed cement mortars

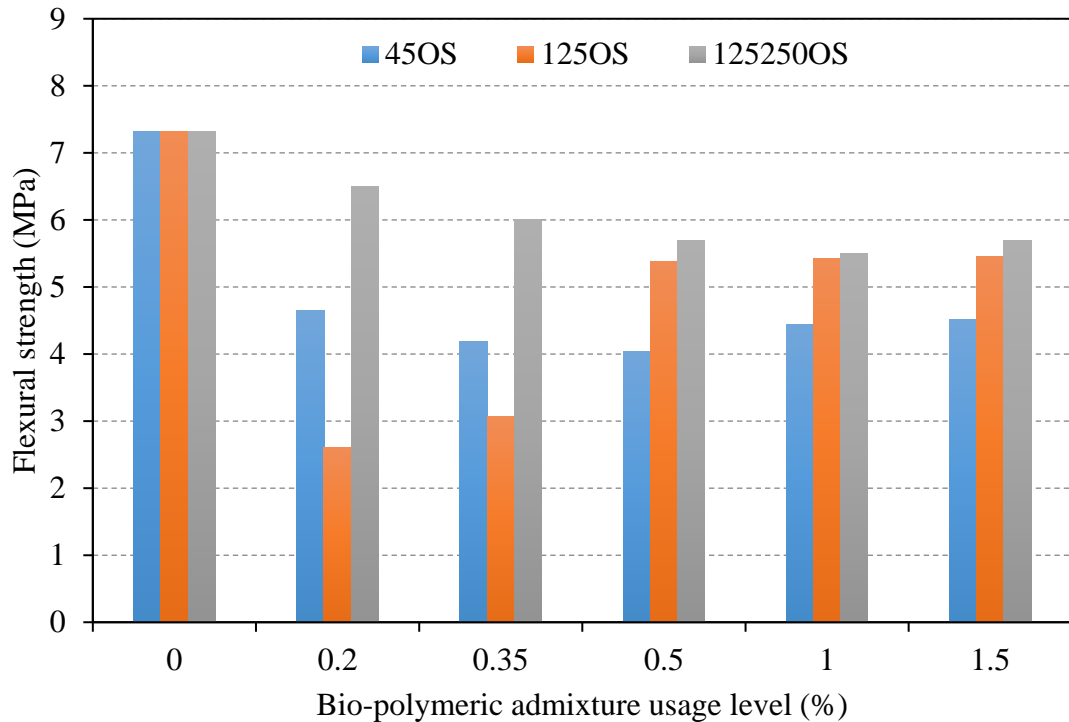


Figure 4.85: Flexural strength of OS admixed cement mortars

Lignocellulosic bio-polymeric admixtures used in coarse size (125/250 μm) within the scope of the study affected the flexural strength more positively than the bio-polymeric admixture used in 0/45 μm size and 0/125 μm size. In particular, with the use of AKS and HKS additives in 125/250 μm grain size, an increase was observed in the flexural strength of cement mortars, as well as the compressive strength. As can be seen from Figure 4.82, the use of AKS at 0.2, 0.35, 0.5, 1.0 and 1.5 wt.% and 125/250 μm grain size increased the flexural strength of the cement mortar by 0.17, 0.47, 0.96, 2.07 and 3.25 %, respectively, compared to the reference mortar. According to Figure 4.83, Similarly to AKS admixture, when the 125/250 μm grain size HKS admixture was used at 0.2, 0.35 and 0.5 wt.% ratios, it improved the flexural strength of the cement mortar by 1.65, 1.25 and 0.16 %, respectively. On the contrary, as can be observed from Figure 4.84 and Figure 4.85, WKS and OS additives with smaller cellulose content and crystallinity index contributed negatively to the flexural strength of the mortar. Similar results were also found for 28-day compressive strength values.

Within the scope of this thesis, the amount of cellulose in the structure of bio-polymeric admixtures and accordingly the crystallinity index of the bio-polymeric admixtures was determined as the main parameters affecting the flexural strength of cement mortars. For this reason, the 28-days flexural strengths of the mortars and the

cellulose amounts and crystallinity indexes of the bio-polymeric admixtures used in the cement mortar are shown in Figure 4.86, Figure 4.87 and Figure 4.88 comparatively.

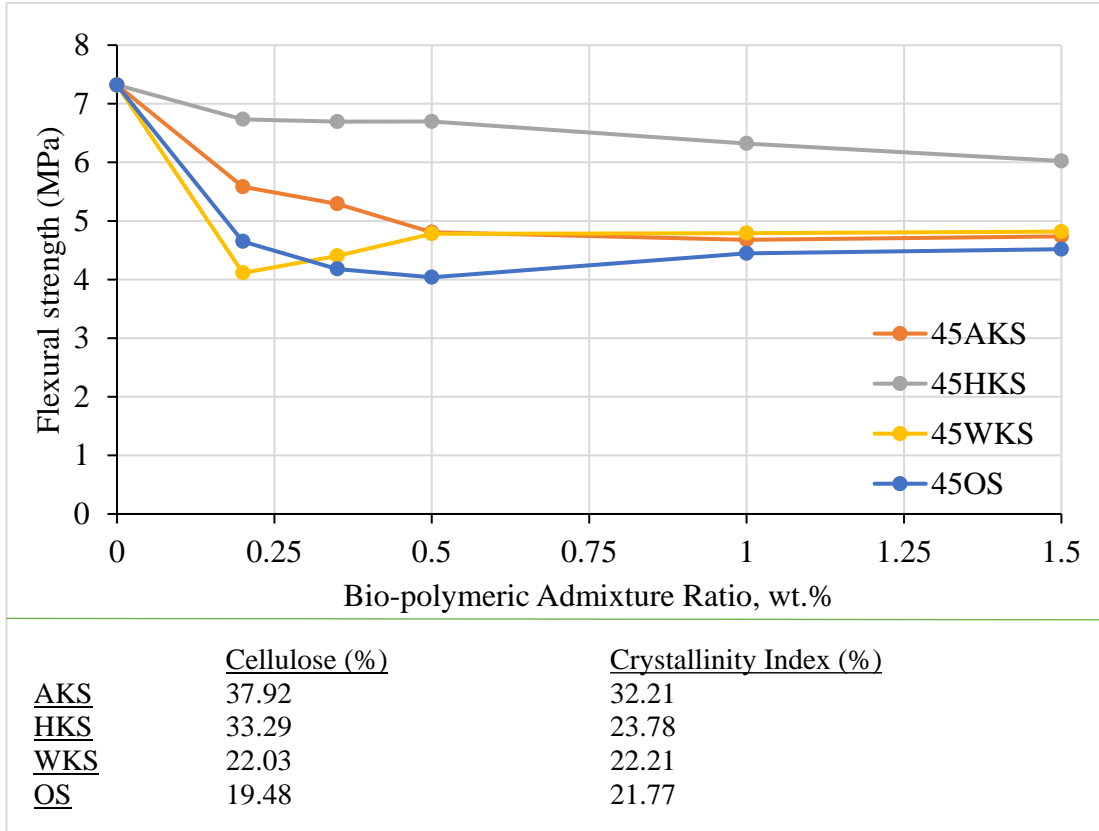


Figure 4.86: Relationship between chemical contents of 0/45 μ m bio-polymeric admixture and flexural strength

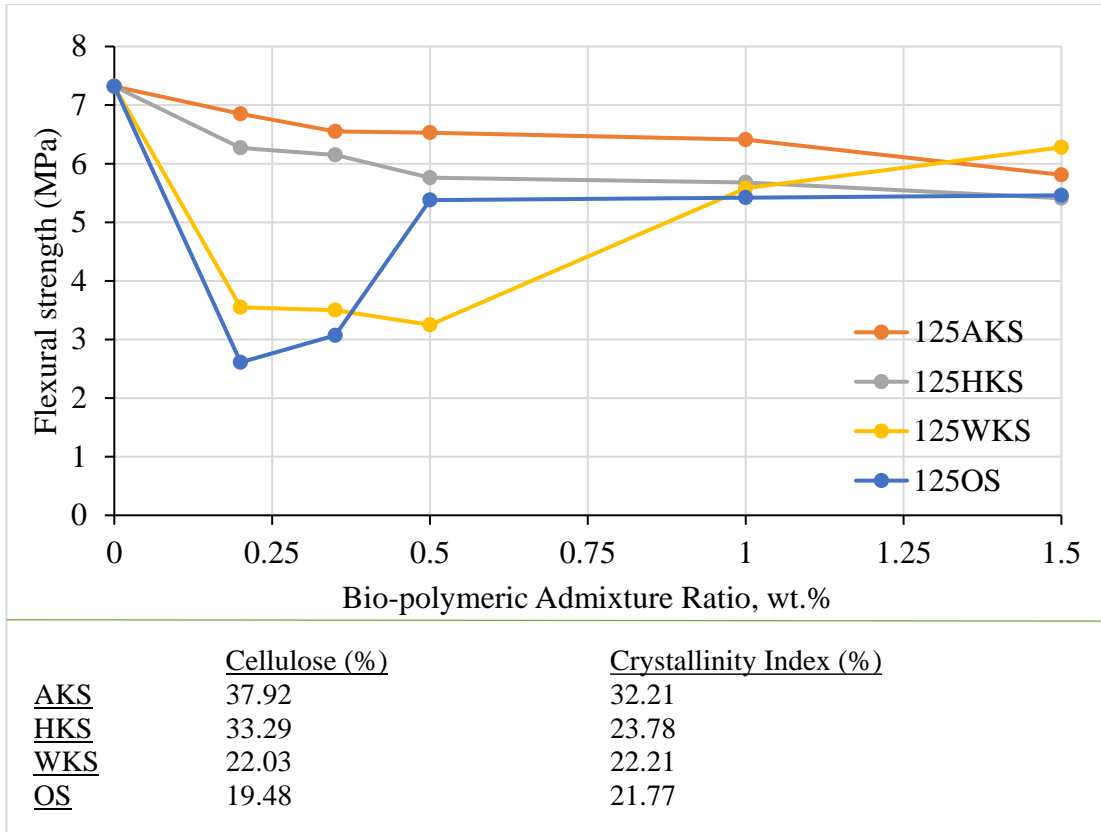


Figure 4.87: Relationship between chemical contents of 0/125 μm bio-polymeric admixture and flexural strength

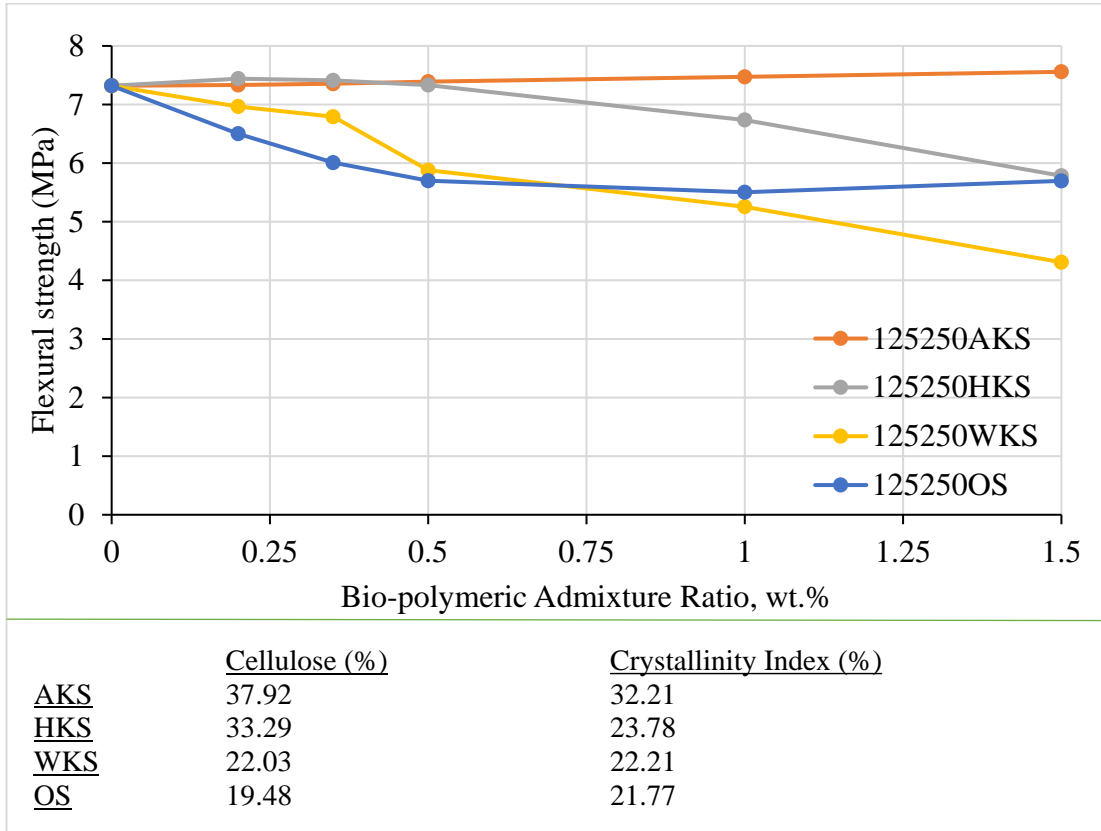


Figure 4.88: Relationship between chemical contents of 125/250 μm bio-polymeric admixture and flexural strength

When Figure 4.86, Figure 4.87 and Figure 4.88 are examined, it is concluded that although WKS and OS bio-polymeric admixtures have an improving effect on the flexural strength of pectin mortar at high usage rates, in general, the flexural strength of the mortars in which WKS and HKS admixtures with high cellulose ratio and crystallinity are used show higher performance. Especially from the point of waste evaluation, 125/250 μm AKS can be used easily in cementitious products without causing flexural strength loss.

4.3.7 Evaluation

It has been determined that bio-polymeric admixtures have significant effects on fresh and hardened mortar properties in cement mortars.

It has been observed that all five types of bio-polymeric admixtures can have a filling effect in mortars. It has been determined that the ES admixtures can slightly improve the fluidity of the mortar, thanks to the filling effect. The other 4 types of lignocellulosic bio-polymeric additives were able to improve the fluidity of the cement mortar thanks to both the filling effect and the lignin and extractives in their composition. In particular, WKS and OS admixtures were the two bio-polymeric admixtures that had the most positive effect on fluidity, thanks to their total extractive and lignin ratio. These two admixtures increased the flow diameter of the mortar by 36.09 % in 125WKS0.2 test mixture and by 32.15 % in 125OS0.5 mixture, respectively, compared to the reference mortar. When examined in terms of flowability, it was determined that the most effective particle size was 0/125 μm and the most effective admixture type was OS. On the other hand, it can be concluded that instead of 0.03 wt.% polycarboxylate based superplasticizer or 0.20 wt.% melamine sulphonate based superplasticizer, 0.2 wt.% walnut shell powder or 0.50 wt.% ground olive seed can be used in mortars for which the flowability value is desired to improve. In addition, PCE and SMF admixtures were used in cement mortars and the results were evaluated comparatively in order to better examine the potential of bio-polymeric admixtures to improve the fluidity property. It can be concluded that instead of 0.03 wt.% polycarboxylate based superplasticizer or 0.20 wt.% melamine sulphonate based superplasticizer, 0.2 wt.% walnut shell powder or 0.50 wt.% ground olive seed can be used in mortars for which the flowability value is desired to improve.

Considering the setting times of the cement mortars, although a balanced effect of the ES admixtures on the cement mortar could not be determined, it delayed the first set very slightly, and accelerated the final set when used in 0/45 μm and 125/250 μm sizes. The delay in the initial setting of the mortar is explained by the decreased water requirement due to the improved consistency, and accelerated final setting is explained by the positive effect of the on the hydration of the cement by the ES admixture. Lignocellulosic bio-polymeric admixtures, on the other hand, largely delayed the initial and final setting values of cement mortars due to the lignin and extractives contained in it. The highest setting retarding effect was determined in WKS and OS admixtures, which have high extractive and lignin content. The most effective grain size in retarding the setting was determined as 0/125 μm grain size distribution. In order to compare the set retarding properties of bio-polymeric admixtures, a separate batch of cement mortar mixture series was prepared using tartaric acid set retarder admixture. As a result, it has been observed that bio-polymeric admixtures can delay setting times as much as chemical admixtures. It can be concluded that instead of up to 0.10 wt.% TA, up to 0.50 wt.% 0/125 μm sized WKS or up to 1.0 wt.% ground OS can be used in mortars for desired final set delaying. Thus, it has been determined that bio-polymeric admixtures can be used instead of setting retarders by taking advantage of the slowing hydration feature of bio-polymeric admixtures up to a certain ratio.

It was observed that the capillary water absorption and mass water absorption values of the test mortars decreased especially with the use of bio-polymeric admixtures with a high extractive ratio. The fatty acids in the extractive materials contain stearic acids and fatty acids that can be used as the main raw material in cement water repellency chemicals. When stearates are used in cement-binding materials, they form wax-like components on the pore surfaces, giving the body a protective feature against water. For this reason, it was determined that OS admixture with especially high extractive content was a good water repellent agent in this study. In order to compare the water repellency of the bio-polymeric admixture, separate test specimens were prepared using calcium stearate. The water-repellent properties of bio-polymeric admixture mortars and CS added mortars were found to be close to each other. Depending on the usage rate of the CS chemical admixture, up to 68.27 % reduction in mass water absorption was detected. Especially as a result of decreasing the capillary water absorption value, the use of 0/45 μm grain size WKS and OS, 0/125 grain size HKS

and OS, and 125/250 μm grain size bio-polymeric admixtures have been shown to provide similar hydrophobicity to hardened cement mortars with the use of calcium stearate. For this reason, in order to reduce the mass water absorption values, instead of using up to 1.5 % calcium stearate, 1.5% WKS and 1.5 % OS admixtures can be used in mortars in 0/45 μm grain size distribution. Also, 1.5% OS with 125/250 μm grain size can be used instead of 1.0 % CS to achieve similar water absorption by mass.

When the mechanical properties of the test mortars were examined, it was determined that the ES admixture could improve the mechanical properties of the mortar by improving the hydration of the cement up to a certain usage rate in finer particle sizes. In the use of lignocellulosic bio-polymeric admixtures, the main parameter affecting the mechanical properties of the mortar is cellulose, which is one of the components that make up the bio-polymeric material. It has been found that AKS admixture with the highest cellulose content can improve the 28- and 150-day compressive strength and 28-day flexural strength of the cement mortar when used at 125/250 μm grain size. Furthermore, if the pectin ratio is high in the bio-polymeric admixture, it has been observed that the mechanical properties can improve depending on the admixture usage rate. However, it is observed that the mechanical properties can be reduced with the use of bio-polymeric admixture, except for the specific usage rate and particle size. On the other hand, there was also a decrease in the mechanical properties of the test samples in which chemical admixtures were used. Considering this situation, no obstacle has been identified for the use of bio-polymeric admixtures in cement mortar.

The main purpose of this type of chemical admixtures is to improve the physical properties of concrete and cementitious products rather than their mechanical properties. Similarly, the bio-polymeric admixtures used in this study were determined to improve the physical properties of the mortars rather than the mechanical properties. For example, it has been determined that calcium stearate, which is used to gain water repellency in cement mortars, can reduce the compressive strength of cement mortar up to 34.06 %. Similarly, OS bio-polymeric admixture used to improve water repellency can reduce the compressive strength of the mortar up to 45 %. However, it has been observed that both chemical and bio-polymeric admixtures provide similar water repellency performance in mortars when used in certain proportions.

In this thesis, it is suggested that bio-polymeric admixtures that can provide similar properties can be used instead of products used as chemical admixtures in cementitious materials. The rates at which bio-polymeric additives evaluated in this study can be used instead of chemical additives are given in between Table 4.15 and

Table 4.19.

Table 4.15: Comparison of superplasticizers and bio-polymeric admixtures on flowability

Bio-polymeric Admixture	Effect on Flowability	Equivalent Chemical Admixture
ES (0/45 μm)	Increase up to 7.18 % (0.5 wt.%)	0.0041 wt.% PCE 0.045 wt.% SMF
ES (0/125 μm)	Increase up to 12 % (1.0 wt.%)	0.0073 wt.% PCE 0.066 wt.% SMF
ES (125/250 μm)	-	-
AKS (0/45 μm)	Increase up to 9.46 % (0.5 wt.%)	0.0056 wt.% PCE 0.055 wt.% SMF
AKS (0/125 μm)	Increase up to 19.05 % (0.2 wt.%)	0.0122 wt.% PCE 0.0982 wt.% SMF
AKS (125/250 μm)	-	-
HKS (0/45 μm)	Increase up to 9.67 % (0.35 wt.%)	0.0057 wt.% PCE 0.0559 wt.% SMF
HKS (0/125 μm)	Increase up to 2.61 % (0.5 wt.%)	0.0011 wt.% PCE 0.0254 wt.% SMF
HKS (125/250 μm)	-	-
WKS (0/45 μm)	Increase up to 16.01 % (0.5 wt.%)	0.0101 wt.% PCE 0.0844 wt.% SMF
WKS (0/125 m)	Increase up to 36.09 % (0.2 wt.%)	0.0249 wt.% PCE 0.183 wt.% SMF
WKS (125/250 μm)	-	-
OS (0/45 μm)	Increase up to 22.13 % (0.35 wt.%)	0.0144 wt.% PCE 0.113 wt.% SMF
OS (0/125 μm)	Increase up to 32.15 % (0.5 wt.%)	0.0219 wt.% PCE 0.1625 wt.% SMF
OS (125/250 μm)	Increase up to 19.64 %	0.0127 wt.% PCE

(1.0 wt.%)

0.1012 wt.% SMF

Table 4.16: Comparison of set retarder and bio-polymeric admixtures on initial setting time

Bio-polymeric Admixture	Effect on Initial Setting Time	Equivalent Chemical Admixture
ES (0/45 μm)	Increase up to 27.78 % (1.0 wt.%)	0.0025 wt.% TA
ES (0/125 μm)	Increase up to 22.22 % (1.5 wt.%)	0.0006 wt.% TA
ES (125/250 μm)	-	-
AKS (0/45 μm)	Increase up to 88.33 % (0.35 wt.%)	0.0229 wt.% TA
AKS (0/125 μm)	Increase up to 144.44 % (1.0 wt.%)	0.0479 wt.% TA
AKS (125/250 μm)	Increase up to 55.56 % (0.5 wt.%)	0.0124 wt.% TA
HKS (0/45 μm)	Increase up to 38.39 % (0.5 wt.%)	0.0064 wt.% TA
HKS (0/125 μm)	Increase up to 105.56 % (0.35 wt.%)	0.0316 wt.% TA
HKS (125/250 μm)	-	-
WKS (0/45 μm)	Increase up to 188.89 % (0.5 wt.%)	0.0685 wt.% TA
WKS (0/125 m)	Increase up to 250 % (0.5 wt.%)	0.1022 wt.% TA
WKS (125/250 μm)	-	-
OS (0/45 μm)	Increase up to 138.89 % (0.35 wt.%)	0.0455 wt.% TA
OS (0/125 μm)	Increase up to 255.56 % (0.5 wt.%)	0.1058 wt.% TA
OS (125/250 μm)	Increase up to 194.44 % (1.0 wt.%)	0.0713 wt.% TA

Table 4.17: Comparison of set retarder and bio-polymeric admixtures on final setting time

Bio-polymeric Admixture	Effect on Final Setting Time	Equivalent Chemical Admixture
ES (0/45 μm)	-	-
ES (0/125 μm)	-	-
ES (125/250 μm)	-	-
AKS (0/45 μm)	-	-
AKS (0/125 μm)	Increase up to 76.6 % (1.0 wt.%)	0.0276 wt.% TA
AKS (125/250 μm)	-	-
HKS (0/45 μm)	-	-
HKS (0/125 μm)	Increase up to 31.91 % (1.0 wt.%)	0.0037 wt.% TA
HKS (125/250 μm)	-	-
WKS (0/45 μm)	Increase up to 72.34 % (0.5 wt.%)	0.0252 wt.% TA
WKS (0/125 m)	Increase up to 148.94 % (0.5 wt.%)	0.0746 wt.% TA
WKS (125/250 μm)	-	-
OS (0/45 μm)	Increase up to 46.81 % (0.5 wt.%)	0.0113 wt.% TA
OS (0/125 μm)	Increase up to 142.55 % (1.0 wt.%)	0.0699 wt.% TA
OS (125/250 μm)	Increase up to 57.45 % (1.0 wt.%)	0.017 wt.% TA

Table 4.18: Comparison of water repellent agent and bio-polymeric admixtures on capillary water absorption

Bio-polymeric Admixture	Effect on Capillary Water Absorption	Equivalent Chemical Admixture
ES (0/45 μm)	-	-
ES (0/125 μm)	-	-
ES (125/250 μm)	Decrease up to 45 % (0.2 wt.%)	0.1435 wt.% CS
AKS (0/45 μm)	-	-
AKS (0/125 μm)	Decrease up to 50.0 % (1.0 wt.%)	0.1666 wt.% CS

Table 4.18 (Continued): Comparison of water repellent agent and bio-polymeric admixtures on capillary water absorption

Bio-polymeric Admixture	Effect on Capillary Water Absorption	Equivalent Chemical Admixture
AKS (125/250 μm)	Decrease up to 36.67 % (0.2 wt.%)	0.1085 wt.% CS
HKS (0/45 μm)	-	-
HKS (0/125 μm)	Decrease up to 75 % (1.0 wt.%)	0.3192 wt.% CS
HKS (125/250 μm)	Decrease up to 75 % (0.2 wt.%)	0.1914 wt.% CS
WKS (0/45 μm)	Decrease up to 16.67 % (0.2 wt.%)	0.0359 wt.% CS
WKS (0/125 m)	Decrease up to 55 % (0.5 wt.%)	0.1914 wt.% CS
WKS (125/250 μm)	Decrease up to 26.67 % (0.2 wt.%)	0.0705 wt.% CS
OS (0/45 μm)	Decrease up to 76.47 % (1.5 wt.%)	0.1363 wt.% CS
OS (0/125 μm)	Decrease up to 83.33 % (1.0 wt.%)	0.4022 wt.% CS
OS (125/250 μm)	-	-

Table 4.19: Comparison of water repellent agent and bio-polymeric admixtures on mass water absorption

Bio-polymeric Admixture	Effect on Mass Water Absorption	Equivalent Chemical Admixture
ES (0/45 μm)	Decrease up to 24.56 % (0.35 wt.%)	0.2616 wt.% CS
ES (0/125 μm)	Decrease up to 9.36 % (1.0 wt.%)	0.1064 wt.% CS
ES (125/250 μm)	Decrease up to 6.43 % (0.2 wt.%)	0.0803 wt.% CS
AKS (0/45 μm)	Decrease up to 49.71 % (1.5 wt.%)	0.6784 wt.% CS
AKS (0/125 μm)	Decrease up to 13.30 % (1.5 wt.%)	0.1431 wt.% CS

Table 4.19 (Continued): Comparison of water repellent agent and bio-polymeric admixtures on mass water absorption

Bio-polymeric Admixture	Effect on Mass Water Absorption	Equivalent Chemical Admixture
AKS (125/250 μm)	Decrease up to 32.75 % (1.5 wt.%)	0.3653 wt.% CS
HKS (0/45 μm)	Decrease up to 53.22 % (1.5 wt.%)	0.7785 wt.% CS
HKS (0/125 μm)	Decrease up to 47.22 % (1.0 wt.%)	0.6183 wt.% CS
HKS (125/250 μm)	Decrease up to 45.91 % (1.5 wt.%)	0.5894 wt.% CS
WKS (0/45 μm)	Decrease up to 69.01 % (1.5 wt.%)	1.9385 wt.% CS
WKS (0/125 μm)	Decrease up to 12.57 % (1.5 wt.%)	0.1361 wt.% CS
WKS (125/250 μm)	Decrease up to 15.50 % (0.5 wt.%)	0.1645 wt.% CS
OS (0/45 μm)	Decrease up to 68.13 % (1.5 wt.%)	1.5131 wt.% CS
OS (0/125 μm)	Decrease up to 66.52 % (1.5 wt.%)	1.4372 wt.% CS
OS (125/250 μm)	Decrease up to 59.06 % (1.5 wt.%)	1.0131 wt.% CS

As a result of these studies, it was concluded that the most appropriate grain size was 0/125 μm for utilization of bio-polymeric admixtures in cement mortar. For this reason, XRD, SEM and durability analyzes of bio-polymeric admixture added cement mortars were performed on samples using 0/125 μm grain size bio-polymeric admixtures.

4.4 Microstructural Analysis and Mineralogical Development of Mortars

When the physical and mechanical properties of cement mortars with bio-polymeric admixtures were examined, it was determined that the optimum grain size for bio-polymeric admixtures affecting the mortar performance was 0/125 μm . For this reason,

SEM and EDS analyzes were performed to analyze the microstructure on 28-day test specimens of cement mortars using 0/125 μm size admixtures.

SEM analysis was carried out in order to investigate the microstructure and the hydration products formed in the mortar specimens. 28 days water cured specimens were used in the analysis. SEM analyses were carried out on fracture surfaces of the cement mortars. Scanning electron microscope analyses of reference cement mortar specimen is shown in Figure 4.89.

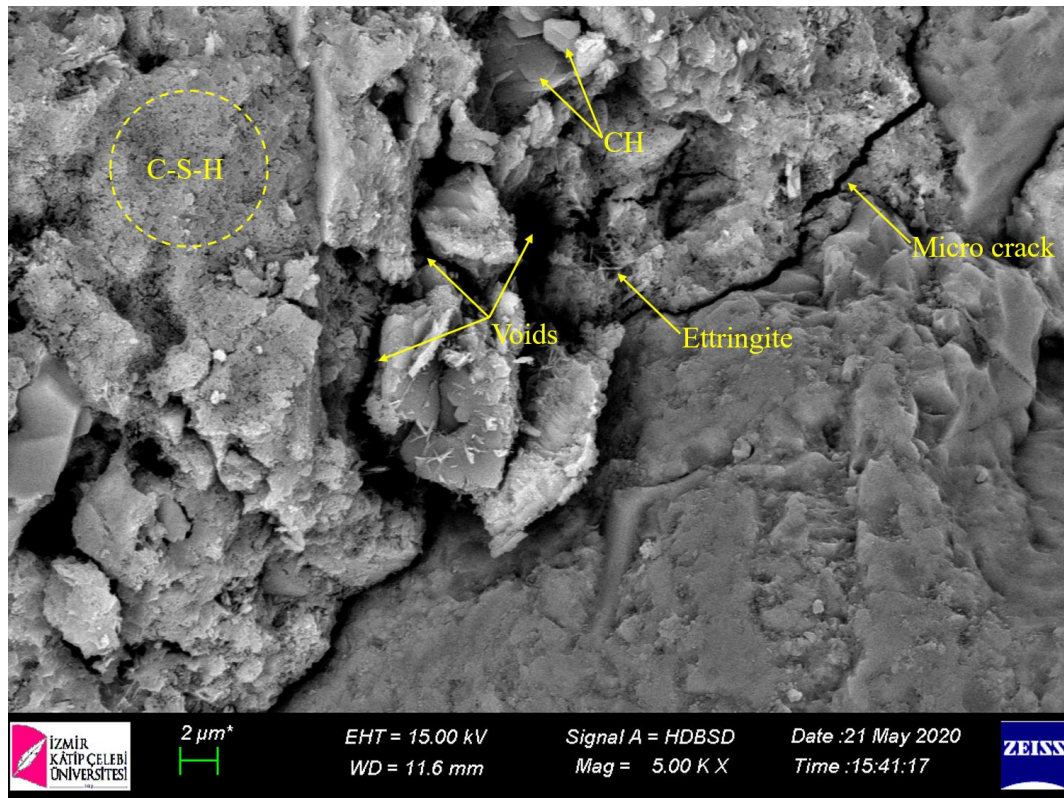


Figure 4.89: SEM micrograph of reference mortar.

Standard graded siliceous sand was used for all mixture combinations. When Figure 4.89 is examined, the microstructure of the reference specimen shows the formation of nearly amorphous and microcrystalline particles of calcium silicate hydrate phases as the dominant hydration products and plates like calcium hydroxide formation, needle like ettringite formation and also many of voids and micro-cracks, which low compact in the structure and reduces the mechanical strength of the cement mortar specimen.

Microstructure images of cement mortars with ES admixtures are shown in Figure 4.90 to Figure 4.94.

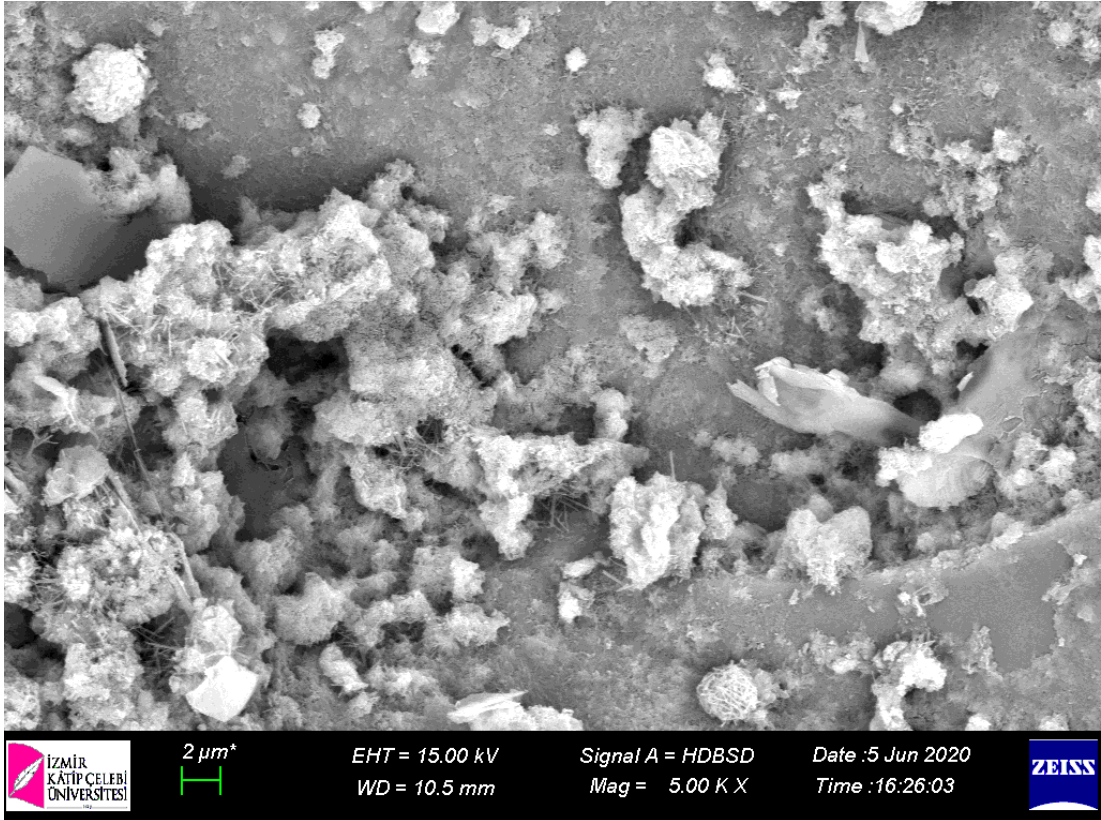


Figure 4.90: SEM micrograph of 0.2 wt.% ES admixed cement mortar

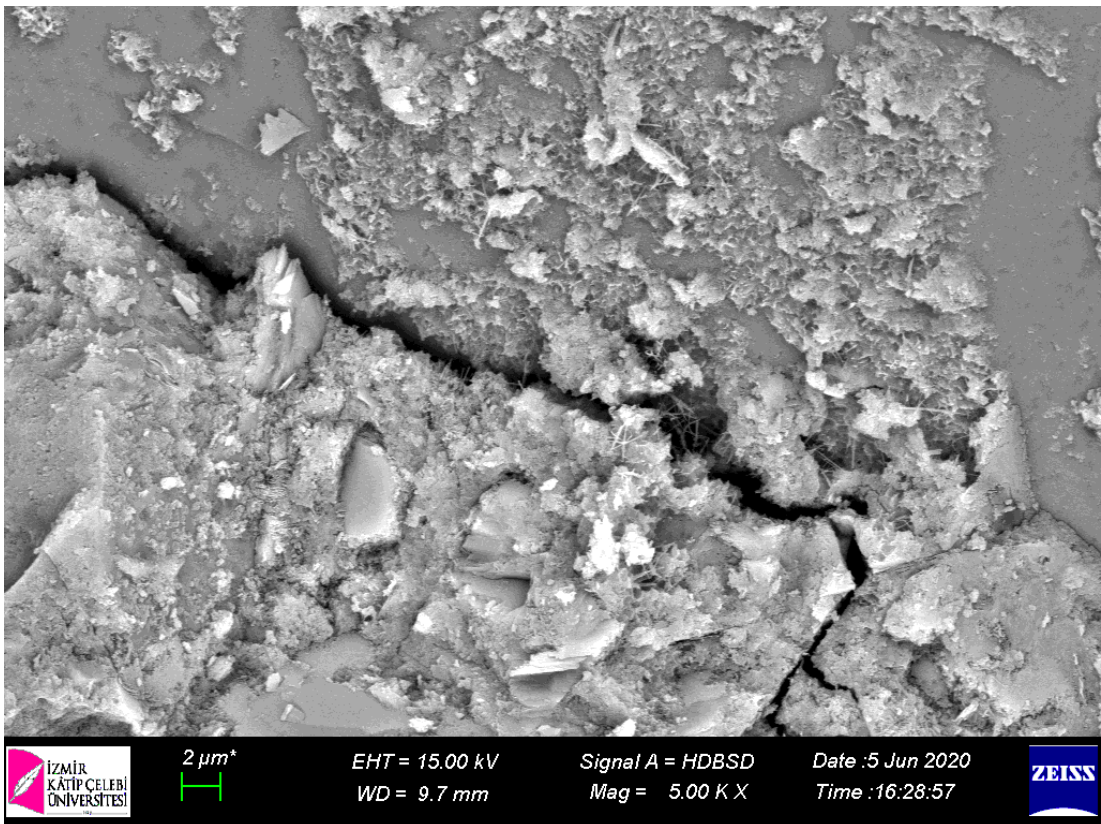


Figure 4.91: SEM micrograph of 0.35 wt.% ES admixed cement mortar

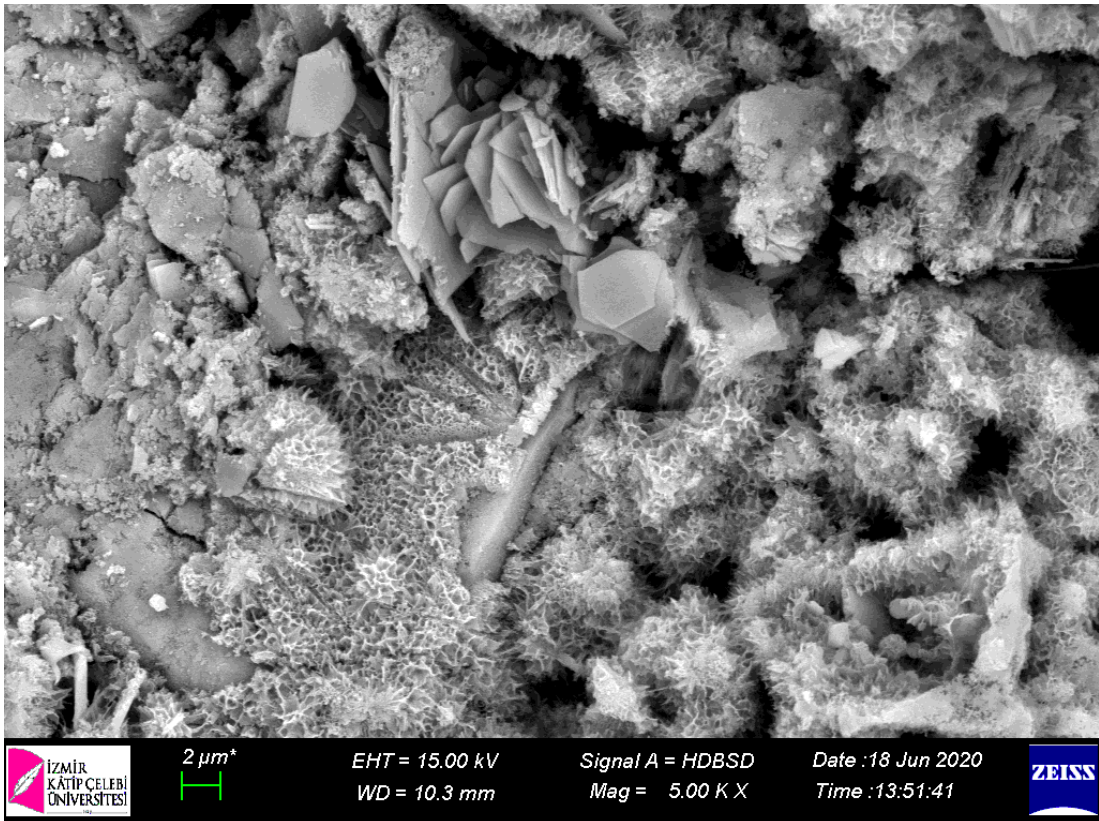


Figure 4.92: SEM micrograph of 0.5 wt.% ES admixed cement mortar

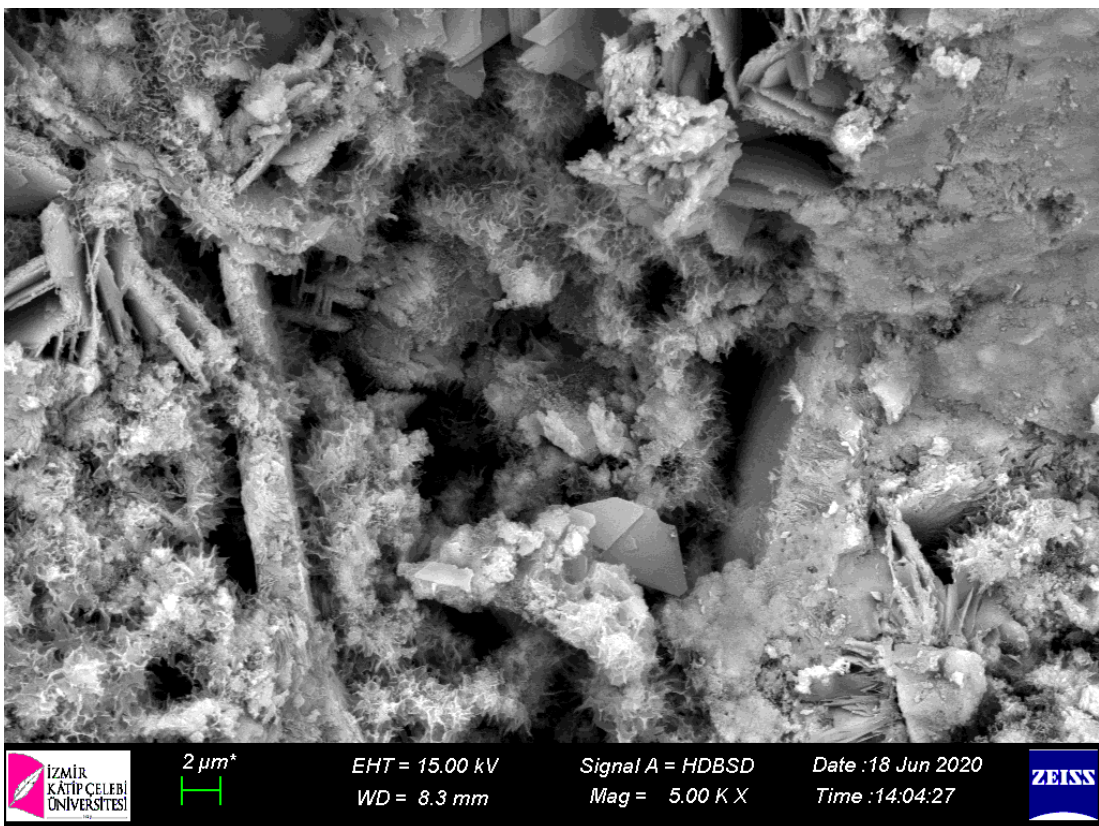


Figure 4.93: SEM micrograph of 1.0 wt.% ES admixed cement mortar

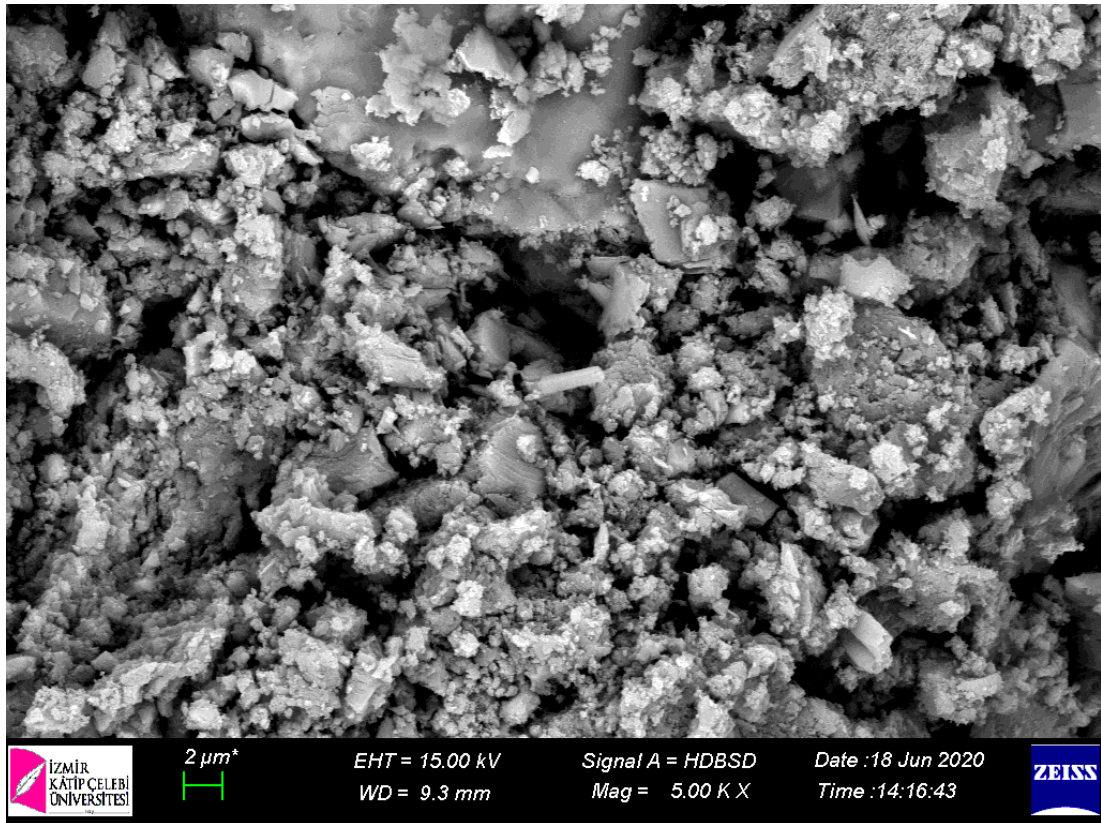


Figure 4.94: SEM micrograph of 1.5 wt.% ES admixed cement mortar

Above figures shows the SEM micrographs of tested cement mortars those produced with eggshell powder type bio-polymeric admixture. When examining Figure 4.90, Figure 4.91 and Figure 4.92 as in the egg shell added cement mortars, the low amount of eggshell admixture (up to 0.5 wt.%) created a denser and more compact structure in the matrix structure of the mortars. In this way, the compressive strength value of the mortar using this amount of admixtures has increased. However, it can be observed from Figure 4.93 and Figure 4.94, as the eggshell admixture ratio increased, the matrix structures of the mortars became looser and more pores. Thus, as the ES usage rate increased, the compressive strength of the mortars decreased. In addition, the denser matrix caused by the addition of almost nano size calcium carbonate could not provide available space for the formation of hydration products [317].

Microstructure images of cement mortars with AKS admixtures are shown in Figure 4.95 to Figure 4.99.

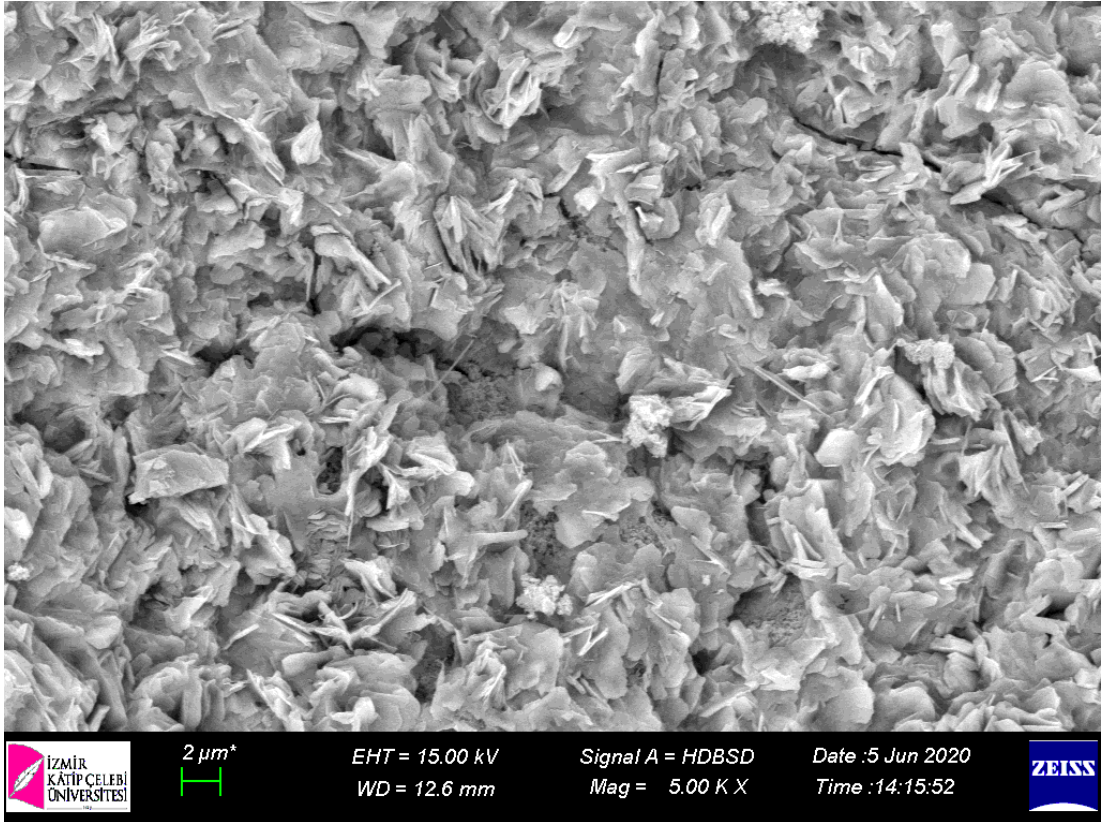


Figure 4.95: SEM micrograph of 0.2 wt.% AKS admixed cement mortar

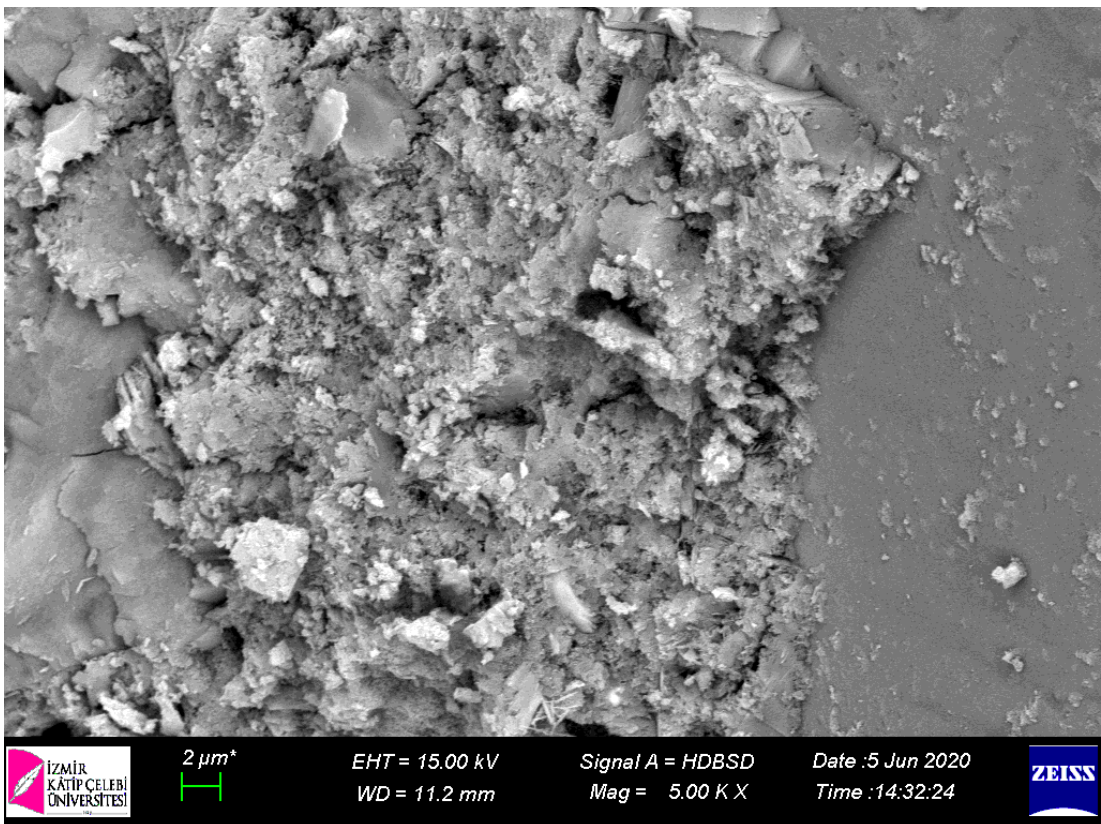


Figure 4.96: SEM micrograph of 0.35 wt.% AKS admixed cement mortar

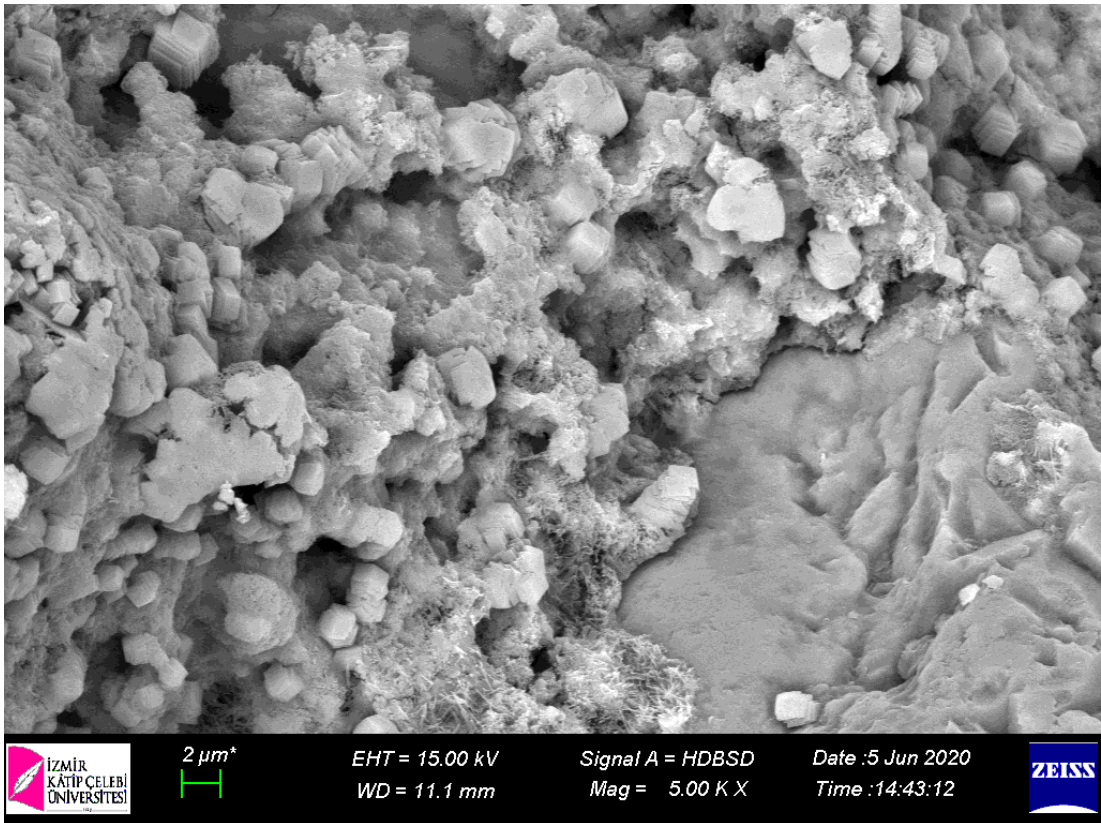


Figure 4.97: SEM micrograph of 0.5 wt.% AKS admixed cement mortar

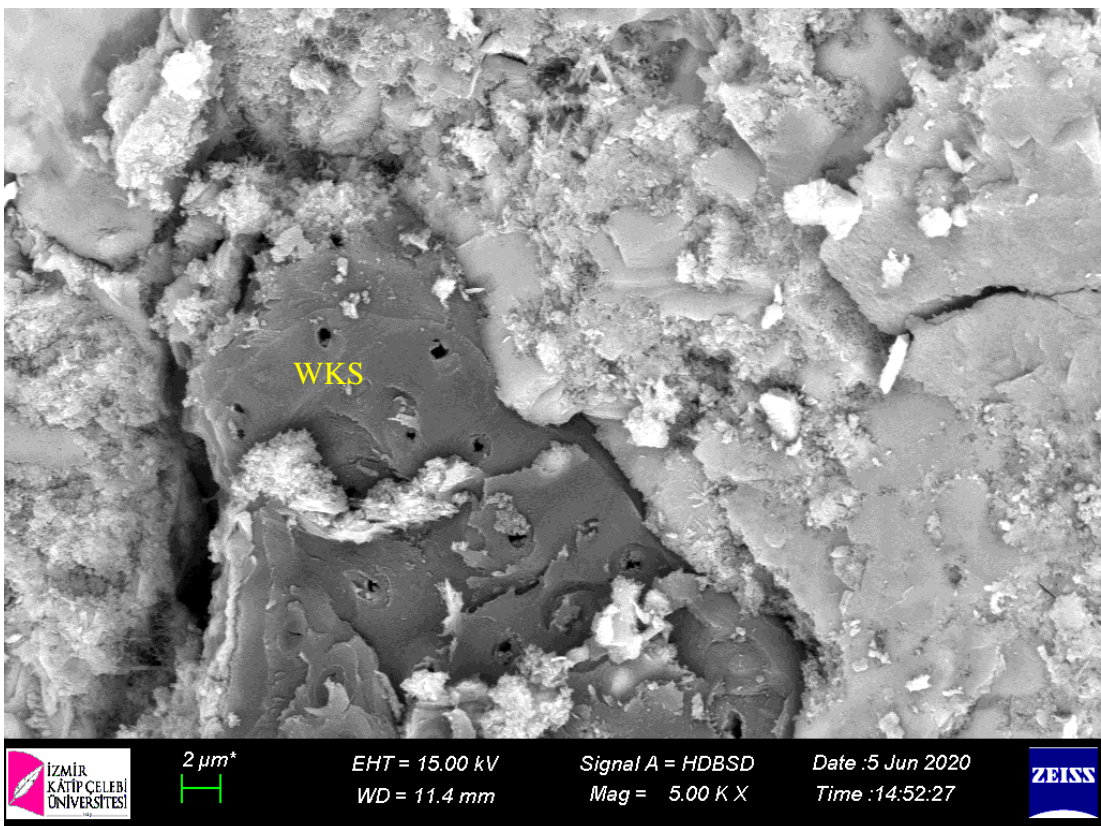


Figure 4.98: SEM micrograph of 1.0 wt.% AKS admixed cement mortar

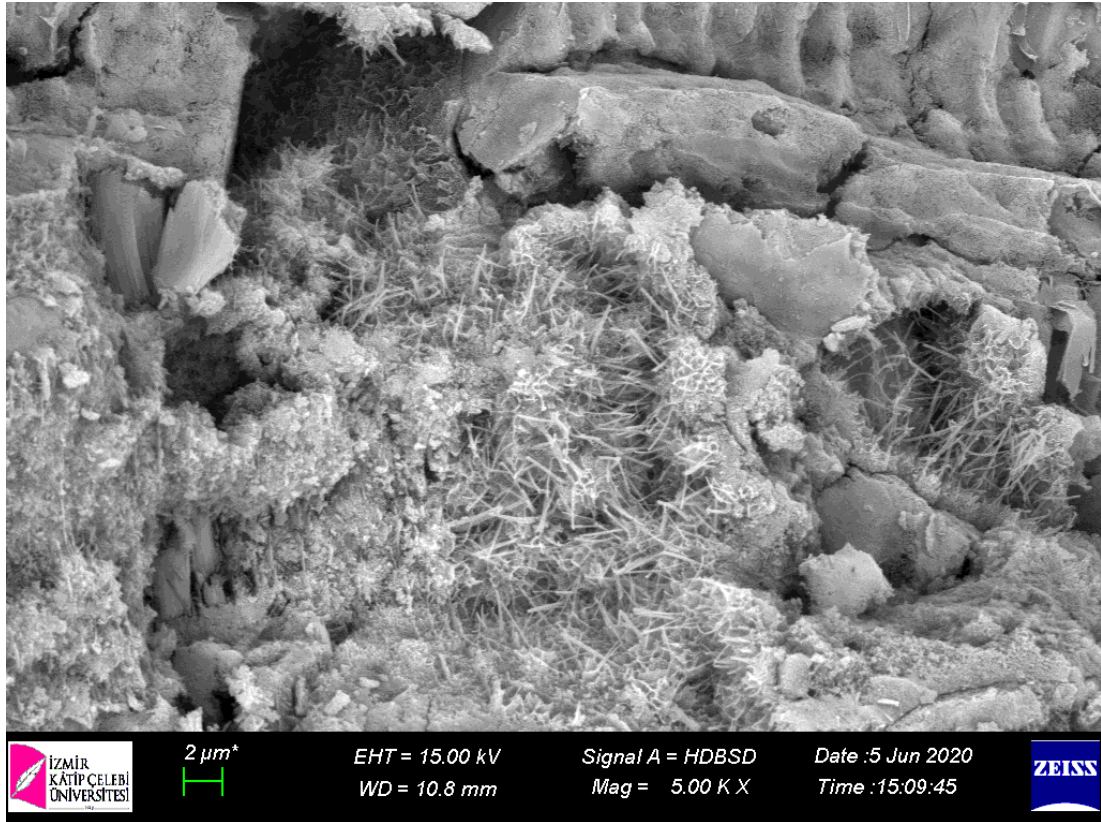


Figure 4.99: SEM micrograph of 1.5 wt.% AKS admixed cement mortar

Figure 4.95 shows that addition of apricot kernel shell powder as a bio-polymeric admixture makes the matrix structure more dense and compact. The reason why the compressive strength of the specimens using 0.2 wt.% AKS is higher than the compressive strength of the control specimen can be explained by this situation. However, it is observed from the above figures that there is a change in the amounts of hydration products with the increase in AKS usage rate. It is observed that cement mortars using more AKS have more CH (Figure 4.97) and ettringite (Figure 4.99) in their matrix structure. Although the formation of the CH mineral in the matrix structure indicates that hydration is progressing, these hydration products, which have lower strength compared to the CSH structure, are estimated to decrease the compressive strength of the mortar at high AS usage rates. The increase in the amount of portlandite formed in the matrix structure of the hardened mortars relative to the CSH structure causes a decrease in the compressive strength [318,319]. It has also been stated by other researchers that ettringite can form around cellulosic materials [320–322]. It is recommended to use pozzolanic additives to reduce the formation of this mineral [323]. Although the ITZ between the bio-polymeric additive particles and the cement matrix seems dense, it has been determined that the reason for the loss of compressive

strength of the mortar to some extent is due to air entrainment of the bio-polymeric additives into the mortar.

Microstructure images of cement mortars with AKS admixtures are shown in Figure 4.95 to Figure 4.104.

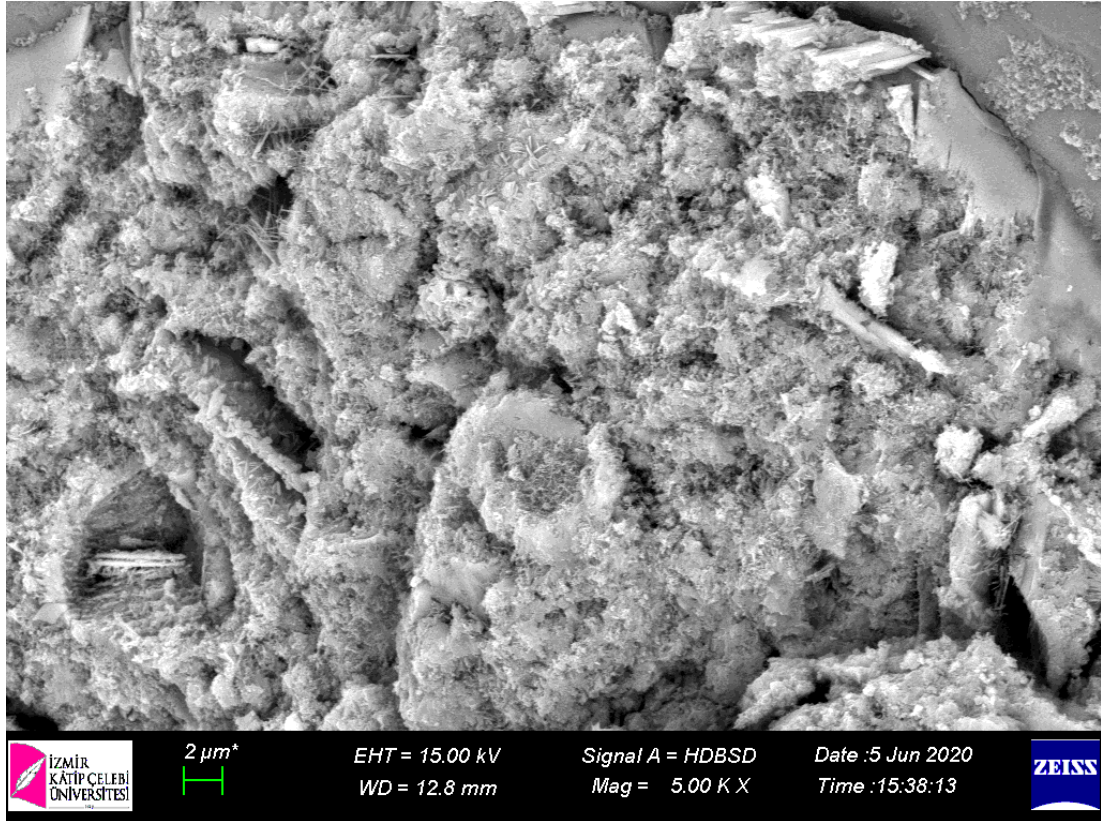


Figure 4.100: SEM micrograph of 0.2 wt.% HKS admixed cement mortar

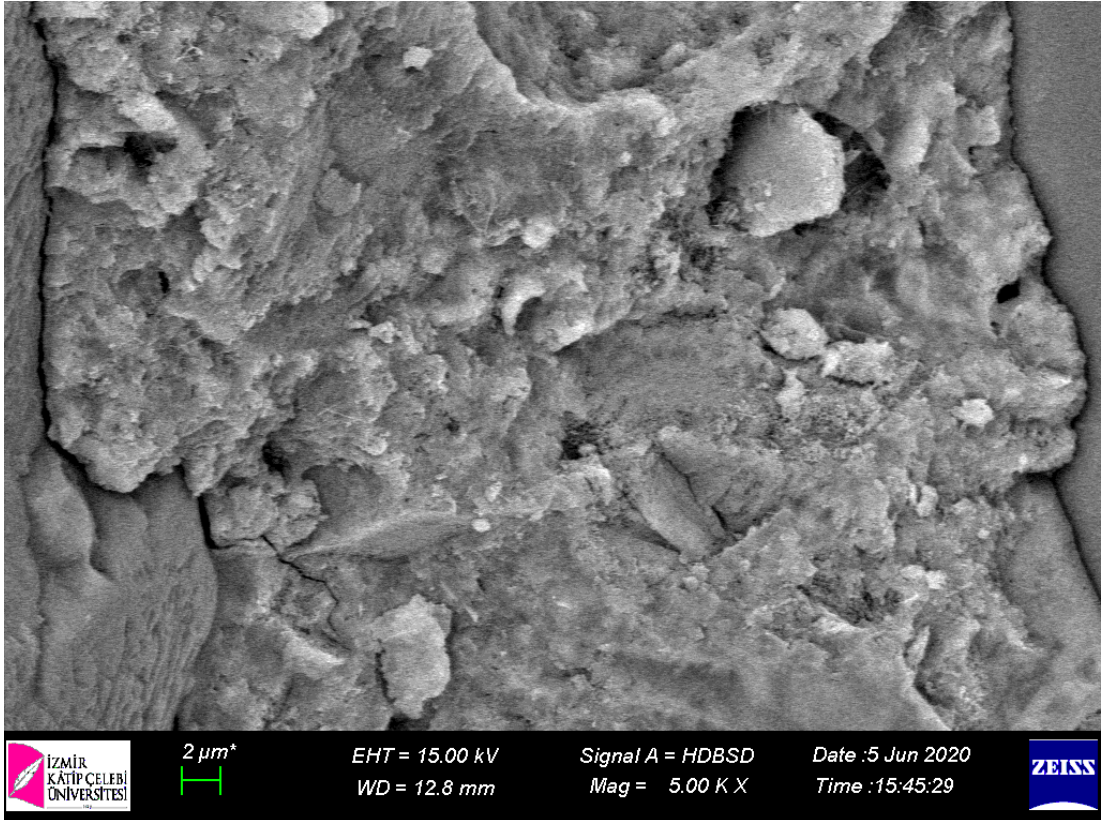


Figure 4.101: SEM micrograph of 0.35 wt.% HKS admixed cement mortar

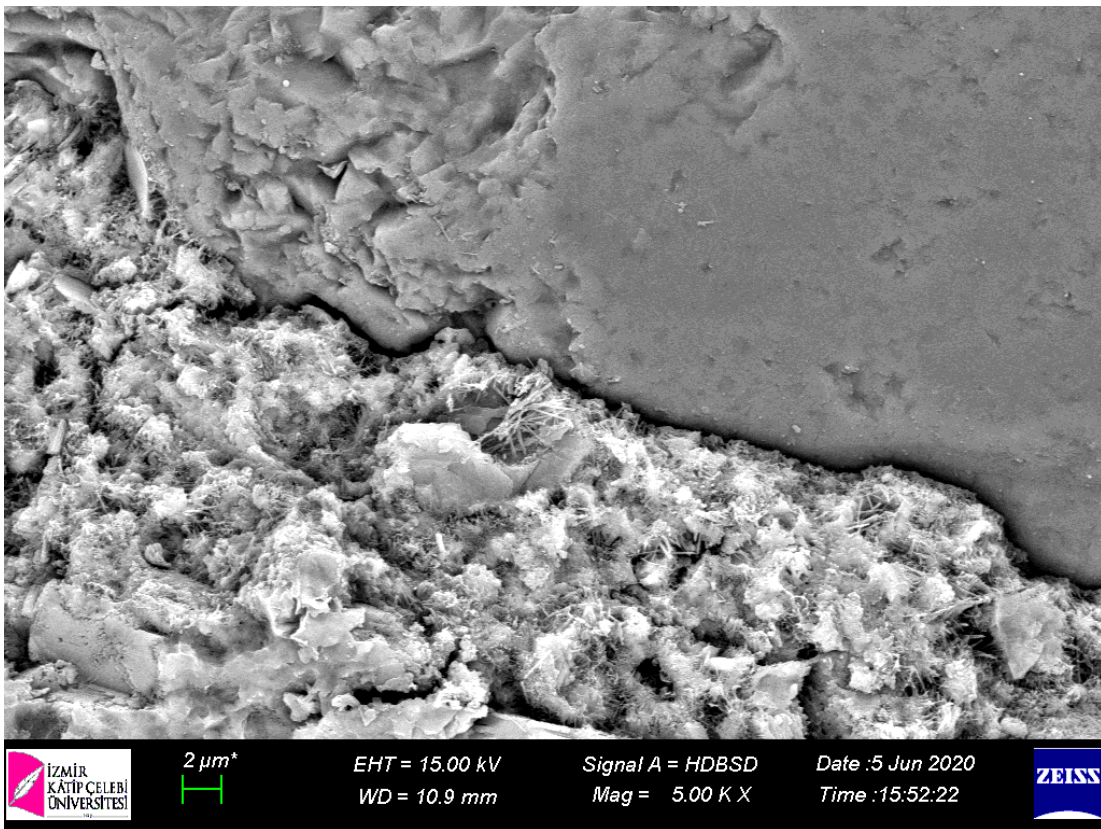


Figure 4.102: SEM micrograph of 0.5 wt.% HKS admixed cement mortar

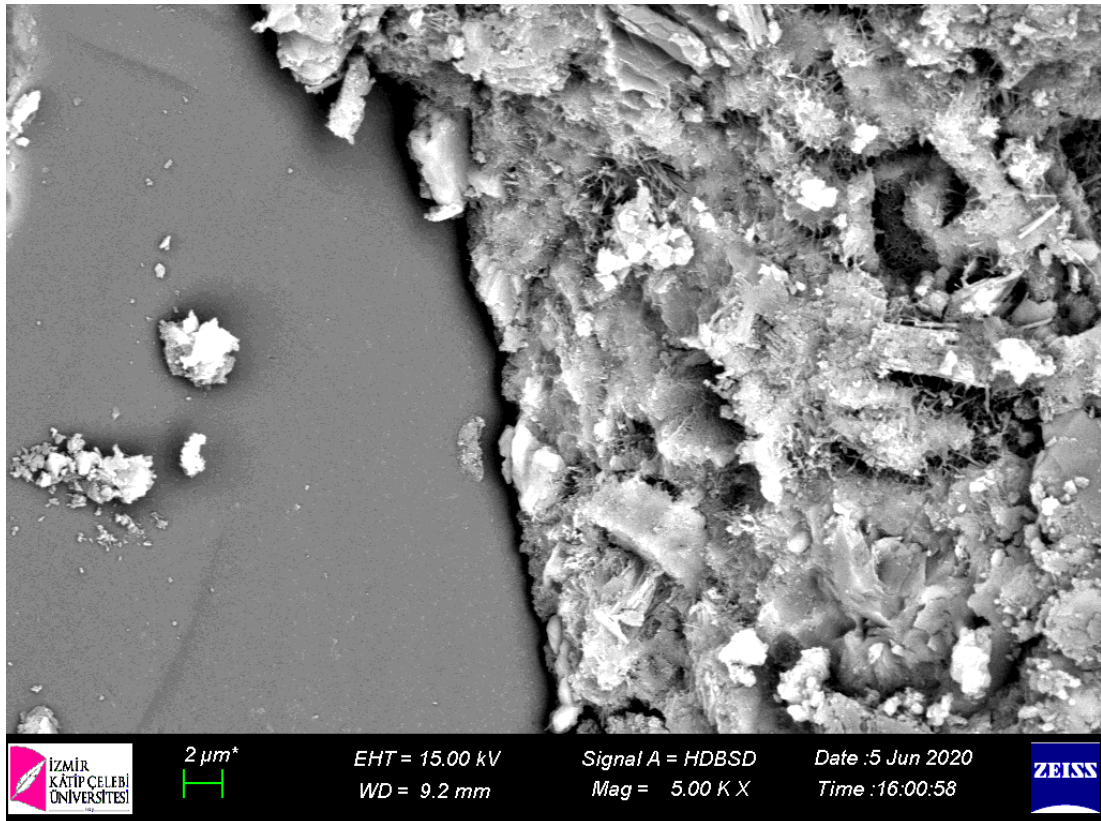


Figure 4.103: SEM micrograph of 1.0 wt.% HKS admixed cement mortar

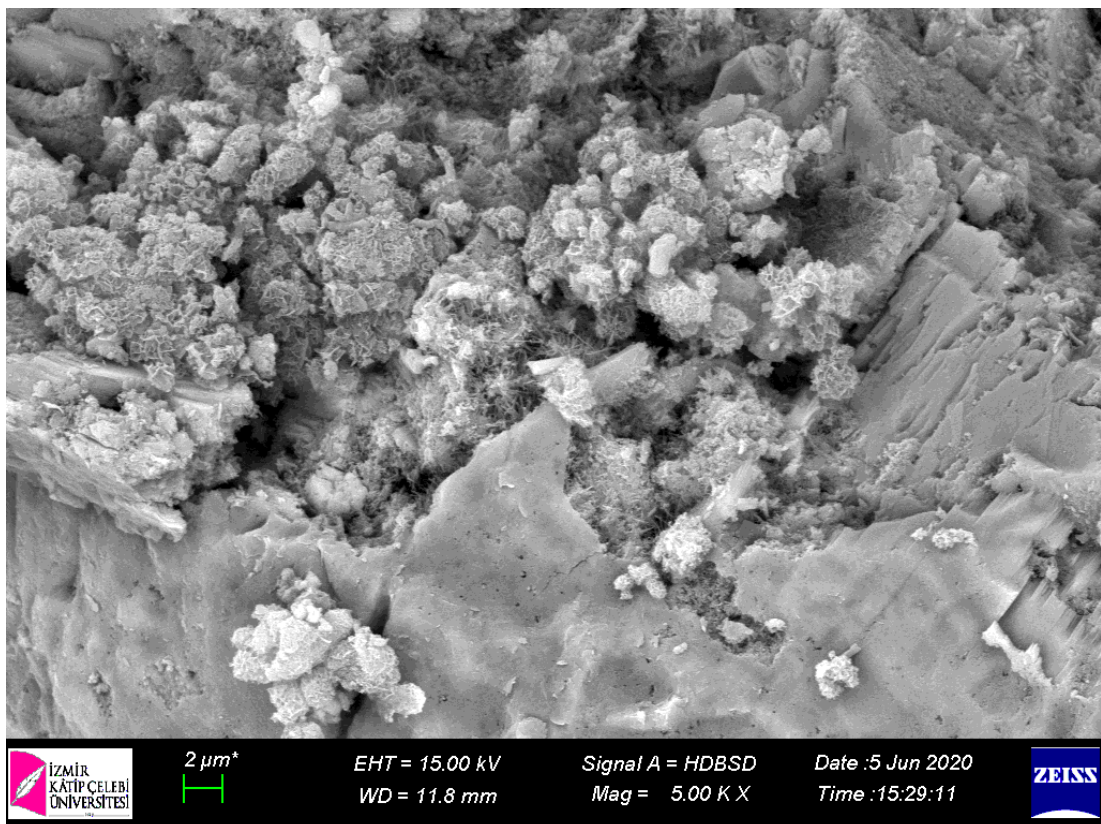


Figure 4.104: SEM micrograph of 1.5 wt.% HKS admixed cement mortar

Figure 4.100 to Figure 4.104 show the SEM micrographs of tested cement mortars those produced with hazelnut kernel shell powder type bio-polymeric admixture.

When examining above figures, as in the apricot kernel added cement mortars, the low amount of hazelnut kernel shell admixture (0.2 wt.%) created a denser and more compact structure in the matrix structure of the mortars. In this way, the compressive strength value of the mortar using this amount of additives has increased. However, it can be observed from Figure 4.101 to Figure 4.104, as the hazelnut kernel shell admixture ratio increased, the matrix structures of the mortars became looser and more porous. Thus, as the HS usage rate increased, the compressive strength of the mortars decreased.

Microstructure images of cement mortars with AKS admixtures are shown in Figure 4.95 to Figure 4.109.

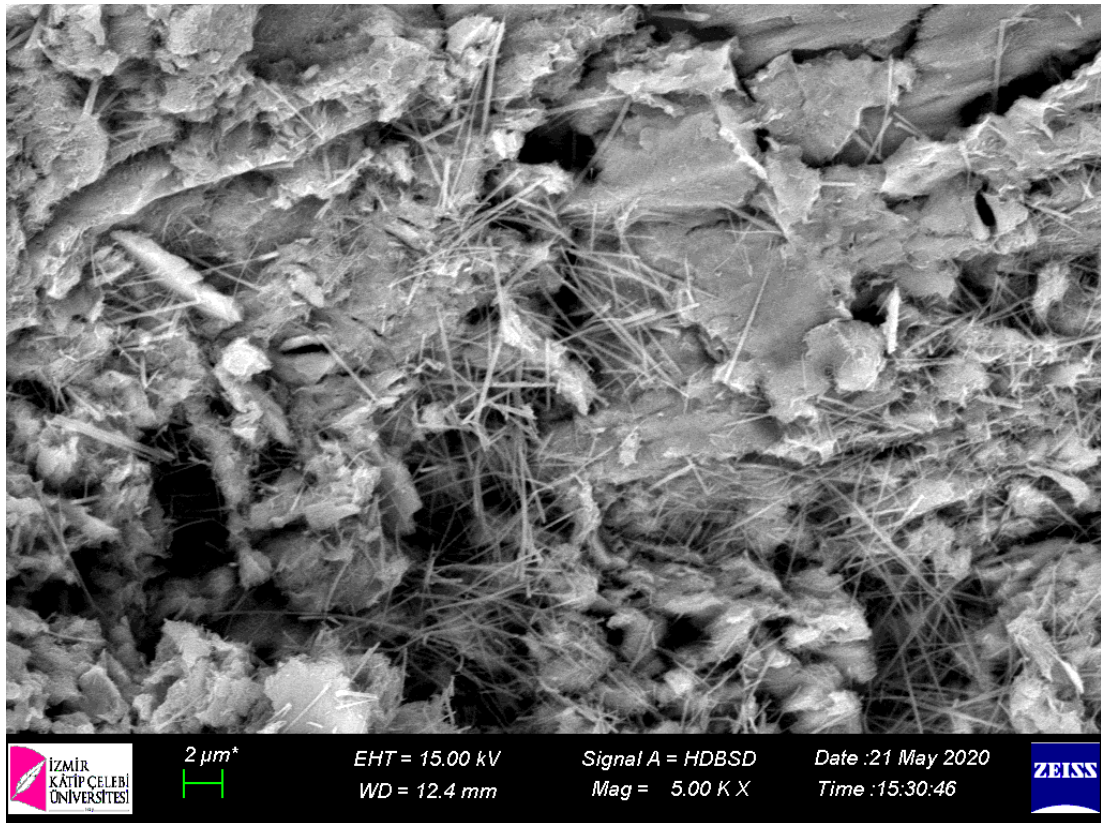


Figure 4.105: SEM micrograph of 0.2 wt.% WKS admixed cement mortar

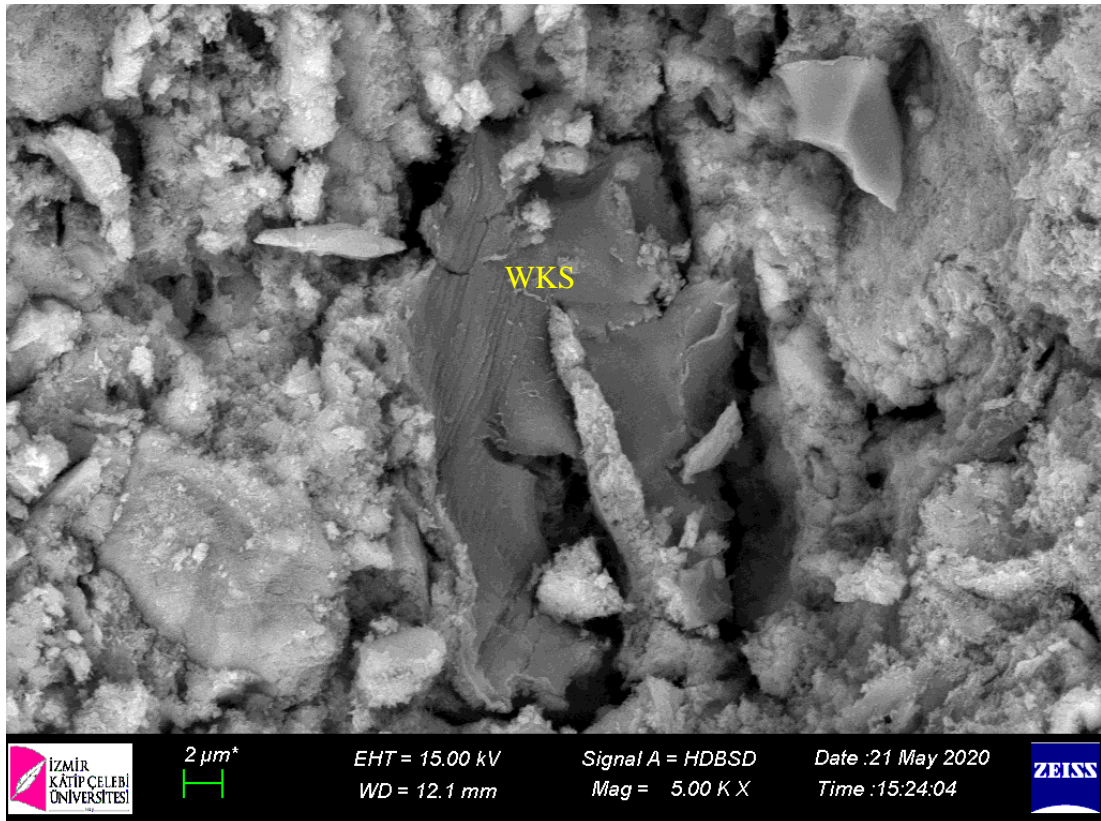


Figure 4.106: SEM micrograph of 0.35 wt.% WKS admixed cement mortar

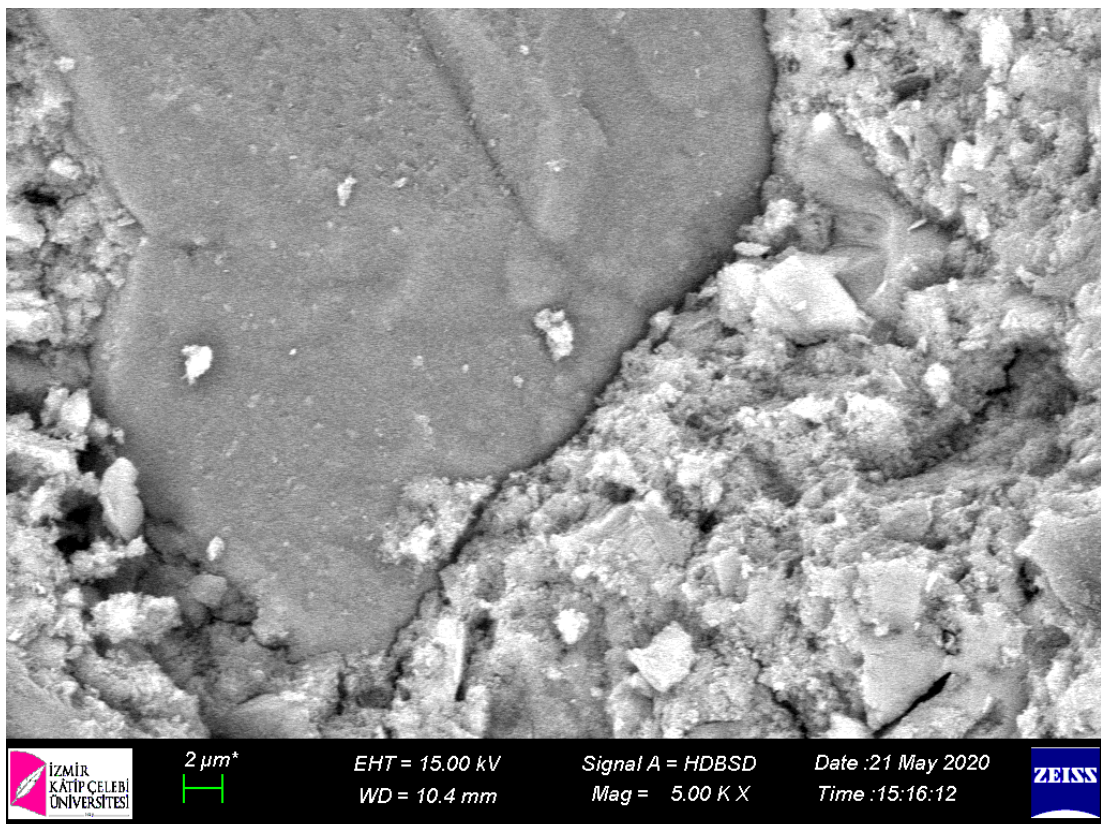


Figure 4.107: SEM micrograph of 0.5 wt.% WKS admixed cement mortar

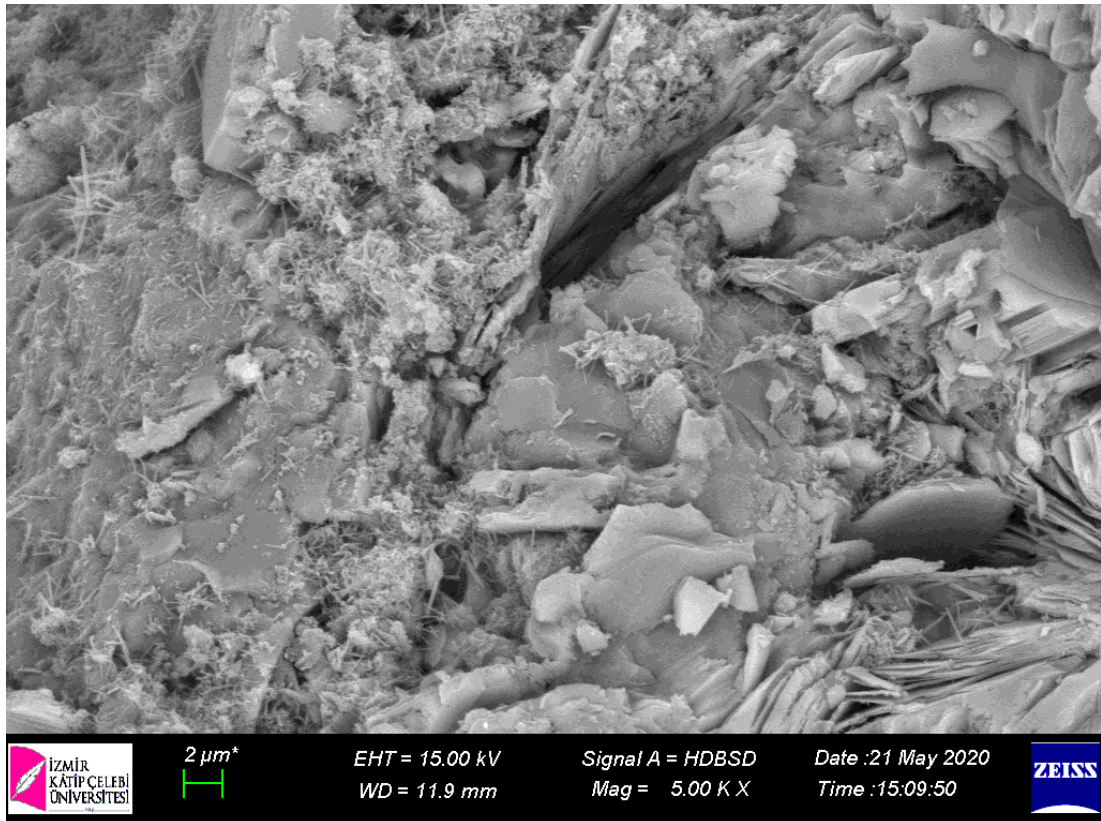


Figure 4.108: SEM micrograph of 1.0 wt.% WKS admixed cement mortar

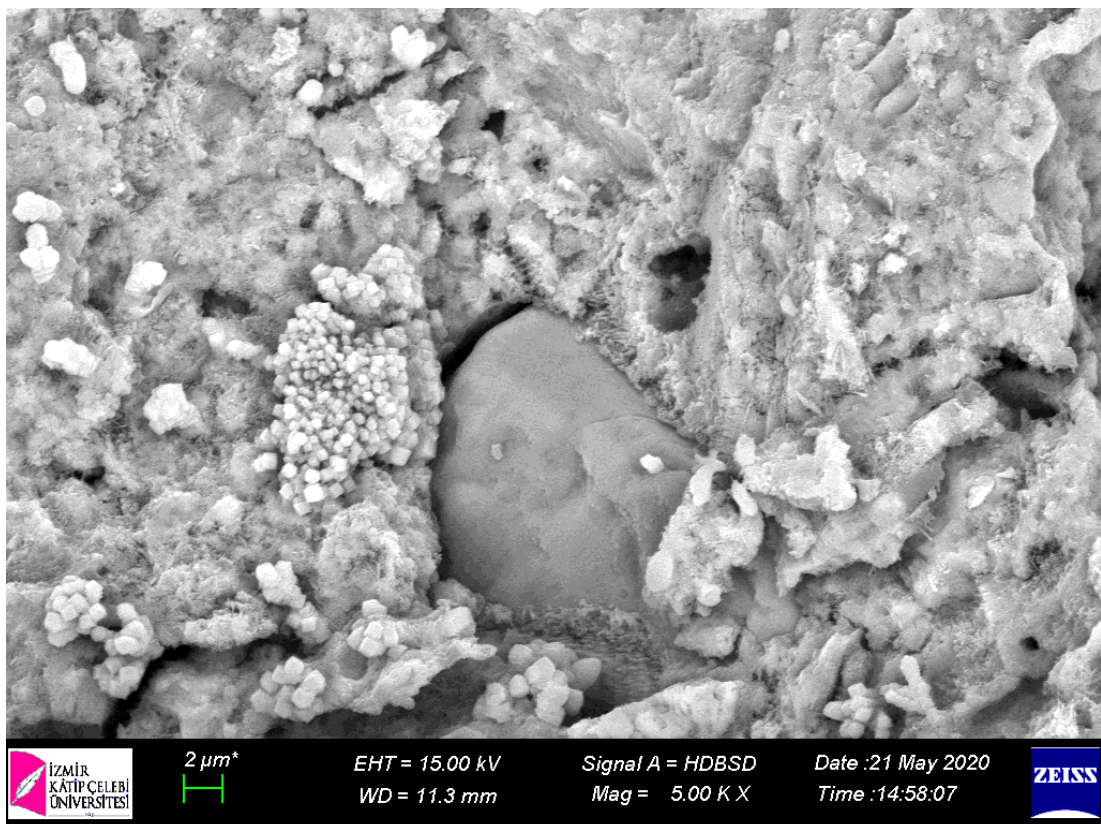


Figure 4.109: SEM micrograph of 1.5 wt.% WKS admixed cement mortar

According to Figure 4.105 and Figure 4.106, microstructures of cement mortars with WKS admixtures show a more porous and loose structure at low admixture utilization

rates in parallel with their 28-day compressive strength. It is observed from the Figure 4.107, Figure 4.108 and Figure 4.109 that there is a change in the observed amounts of hydration products with the increase in WKS usage rate. It is observed that cement mortars using more WKS have more CH and ettringite in their matrix structure, when it is used relatively low amounts. These hydration products, which have lower strength compared to the CSH structure, are estimated to decrease the compressive strength of the mortar at high AS usage rates. On the other hand, as a result of pectin bonding with calcium at higher usage rates, the formation of CH and ettringite decreased and the microstructure became denser.

Microstructure images of cement mortars with OS admixtures are shown in Figure 4.95 to Figure 4.114.

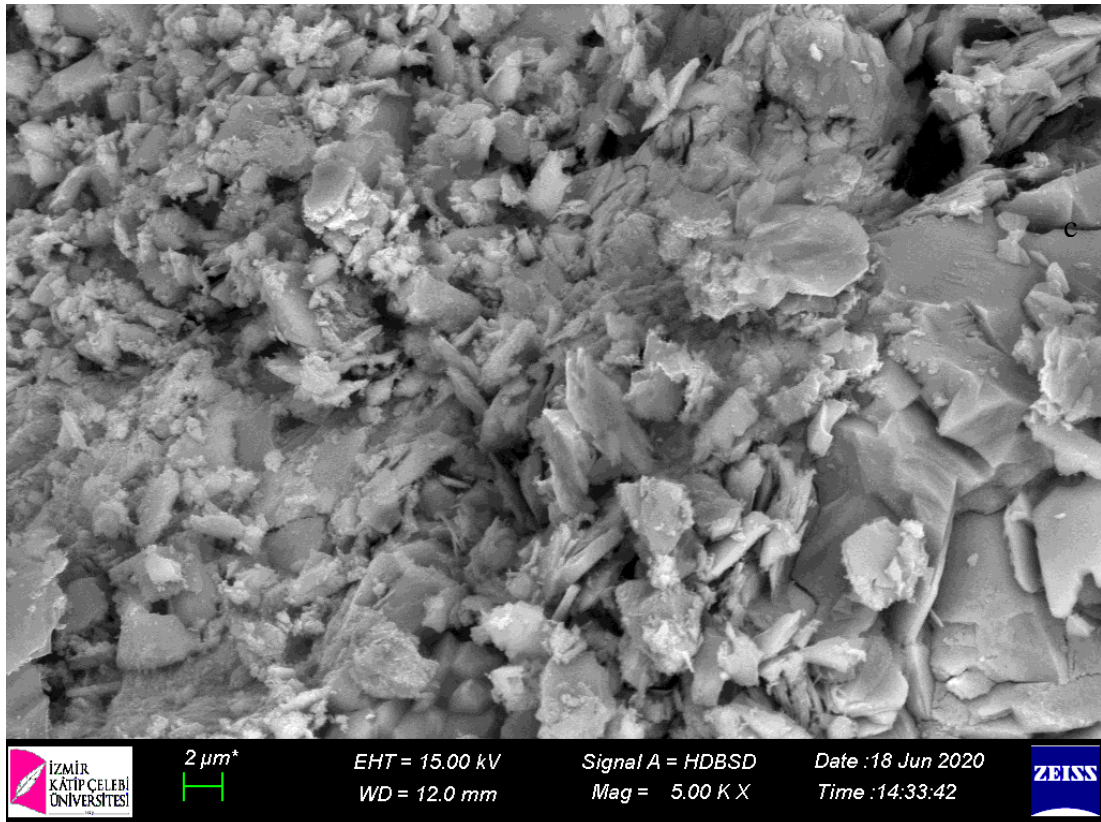


Figure 4.110: SEM micrograph of 0.2 wt.% OS admixed cement mortar

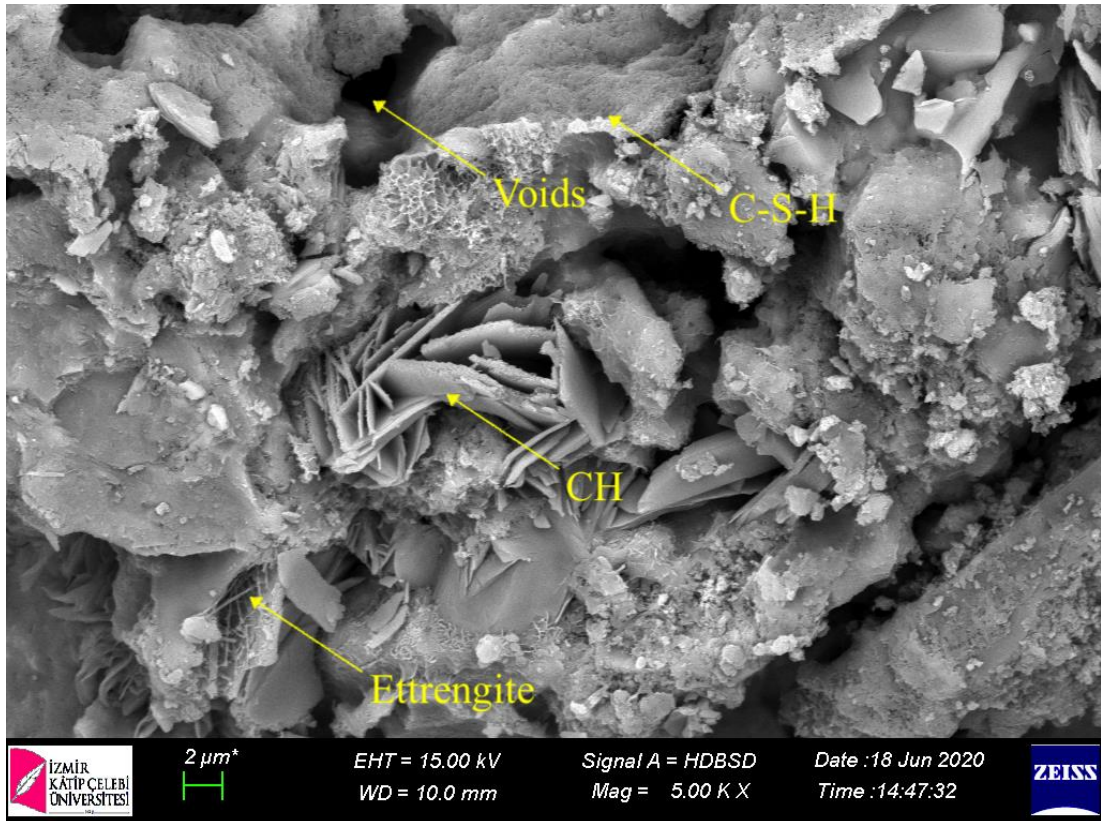


Figure 4.111: SEM micrograph of 0.35 wt.% OS admixed cement mortar

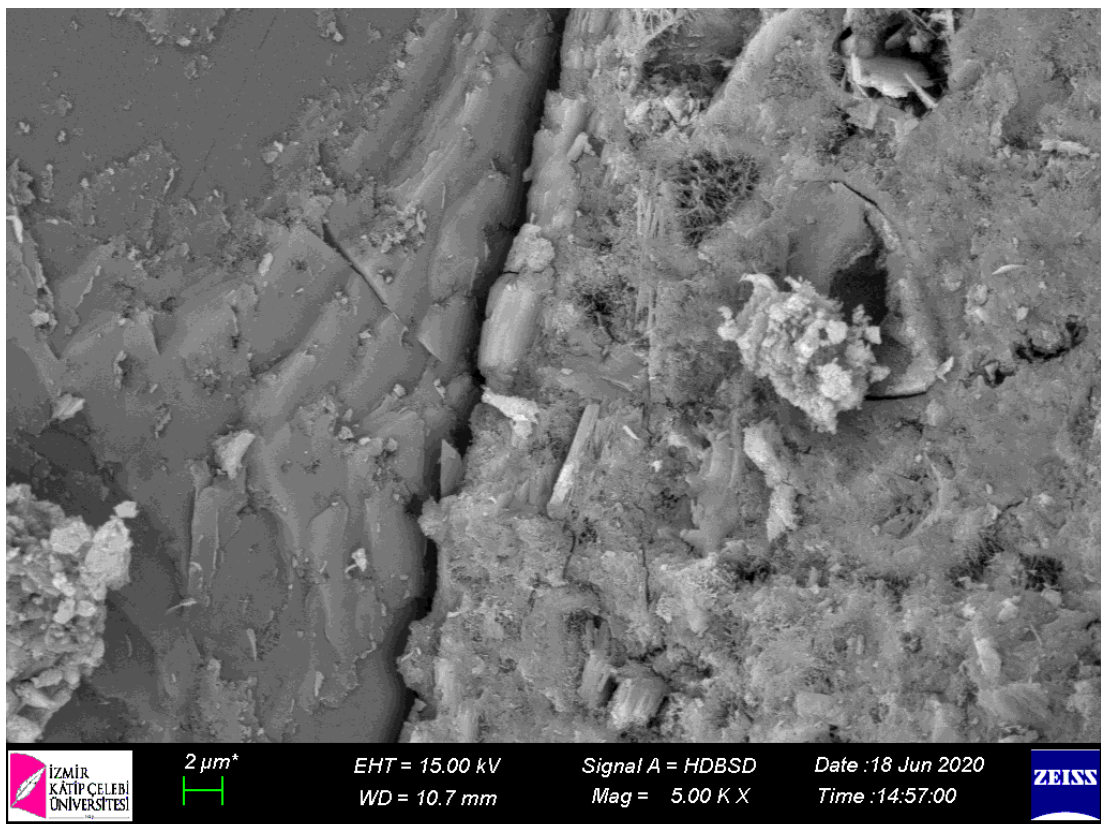


Figure 4.112: SEM micrograph of 0.5 wt.% OS admixed cement mortar

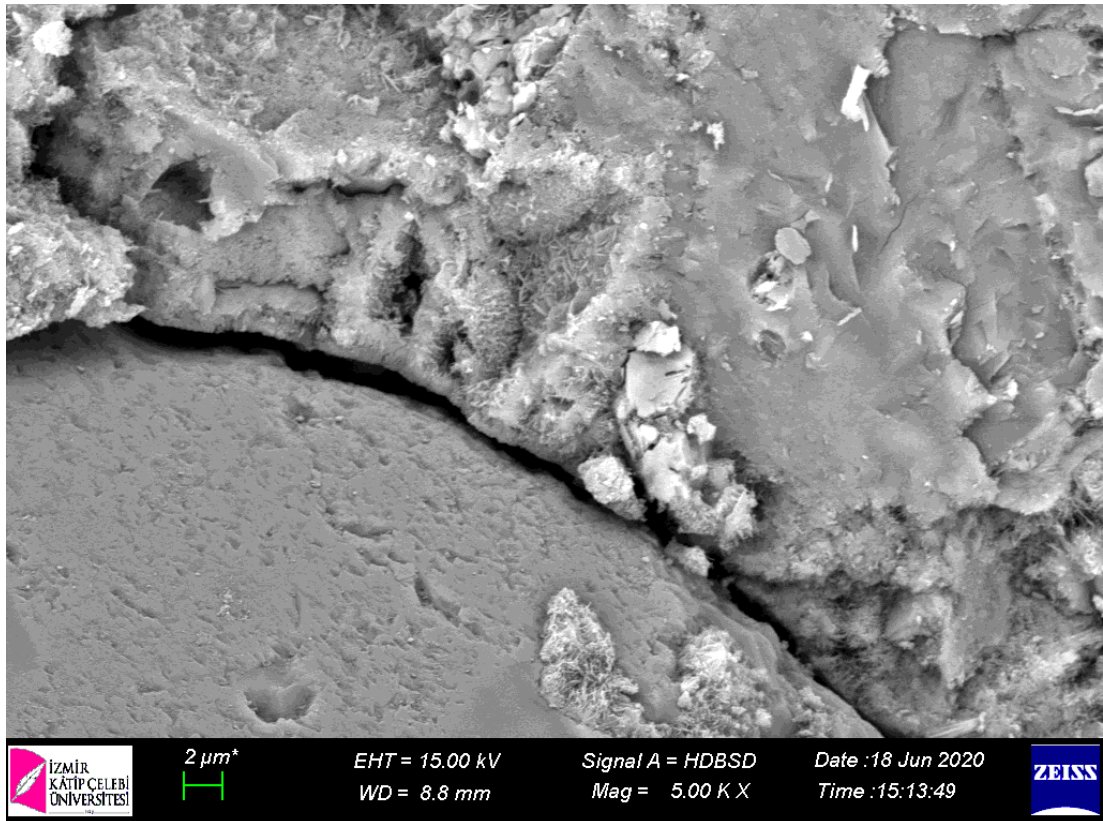


Figure 4.113: SEM micrograph of 1.0 wt.% OS admixed cement mortar

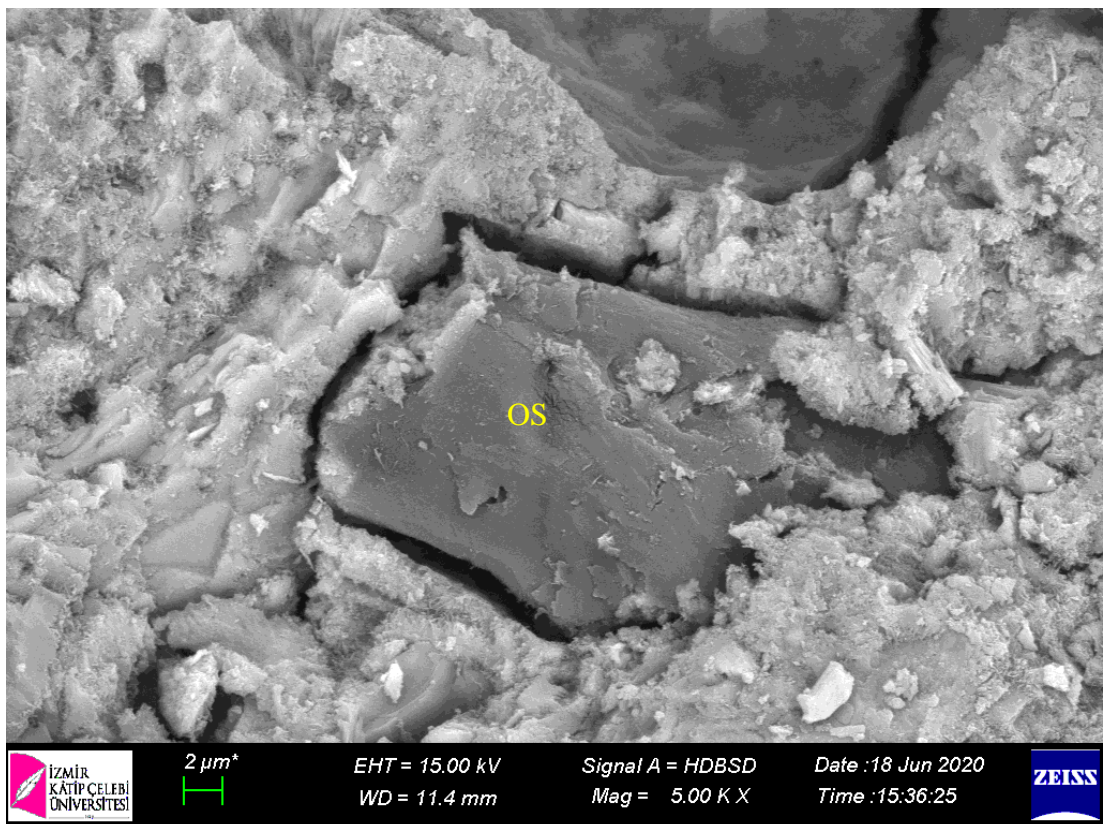


Figure 4.114: SEM micrograph of 1.5 wt.% OS admixed cement mortar

Figure 4.110 to Figure 4.114 demonstrates the cement mortars those produced with 0.2, 0.35, 0.5, 1.0 and 1.5 wt.% of 0/125 μm graded olive seed powder bio-polymeric

admixture, respectively. According to the figures, tested cement mortar specimens' matrix structure consists of calcium silicate hydrate phases as the dominant hydration products and plates like calcium hydroxide formation, needle like ettringite formation and also many of voids. When the 28-day compressive strength values of the olive seed admixed mortars were examined, it was determined that the compressive strength values of OS mortars below the compressive strength control sample (Figure 4.65). Although the hydration products are similar when SEM images are examined, the decrease in compressive strength can be explained by the fact that ITZ gained a looser structure in OS admixed mortars.

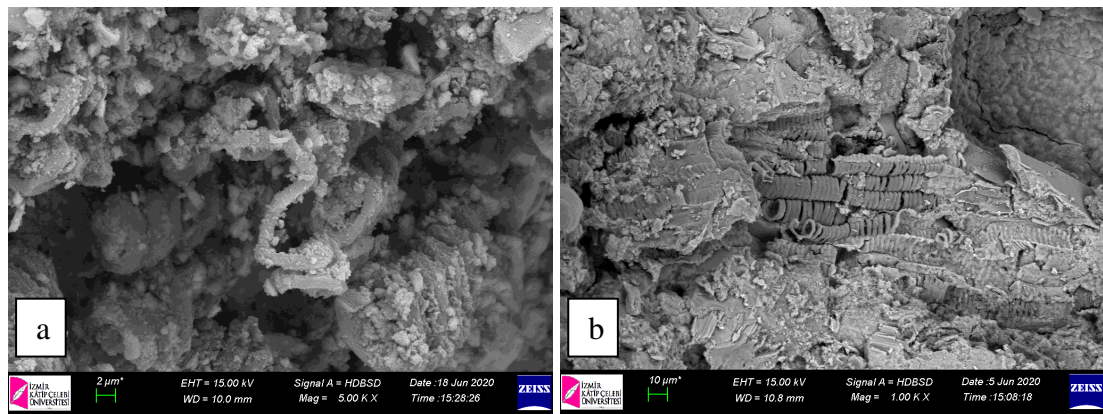


Figure 4.115: Shell fibers of OS (a) and AKS (b).

Figure 4.115 shows the fibers found in the shells of OS and AKS. The CH can be formed between the fibers during cement hydration and cause these fibers to mineralization. In this case, the fibers of the shells deteriorate, resulting in micro-voids between the fibers and loss of strength. To prevent this situation, it is recommended to use pozzolans together with lignocellulosic materials [239]. Therewithal, it is observed that the lignocellulosic materials used in this study can make a strong bond with the cement matrix.

Energy dispersive spectroscopy (EDS) instrument was used to evaluate the elemental analysis of tested cement mortars' matrix structures. EDS analysis results are represented in Table 4.20.

Table 4.20: EDS analysis of tested cement mortars.

Mortar	Si (Atomic %)	Ca (Atomic %)	O (Atomic %)	Si/Ca
Reference	8.93	22.50	71.54	0.40
125ES0.2	7.02	15.12	70.21	0.46
125ES0.35	6.37	14.76	64.15	0.43
125ES0.5	6.47	15.75	66.25	0.41
125ES1.0	6.00	14.29	72.39	0.42
125ES1.5	5.34	17.22	74.28	0.31
125AKS0.2	10.06	23.08	65.31	0.44
125AKS0.35	8.68	22.74	62.60	0.38
125AKS0.5	7.80	20.02	69.29	0.39
125AKS1.0	6.77	18.76	68.86	0.36
125AKS1.5	9.12	28.47	60.05	0.32
125HKS0.2	9.10	19.38	67.91	0.47
125HKS0.35	7.67	21.21	68.19	0.36
125HKS0.5	6.02	15.83	72.05	0.38
125HKS1.0	8.74	21.90	62.65	0.40
125HKS1.5	7.72	20.54	64.47	0.38
125WKS0.2	5.23	26.96	65.10	0.19
125WKS0.35	4.39	18.84	61.88	0.23
125WKS0.5	6.28	15.61	73.35	0.40
125WKS1.0	8.98	21.37	67.14	0.42
125WKS1.5	6.95	15.93	70.62	0.43
125OS0.2	9.15	10.19	71.69	0.90
125OS0.35	12.58	14.37	69.47	0.88
125OS0.5	9.25	29.52	60.75	0.31
125OS1.0	8.38	23.94	65.80	0.35
125OS1.5	6.98	19.29	66.97	0.36

When Table 4.20 is examined, the main elemental components of the matrix structure of the cement mortar samples were determined as Si and Ca. These two elements are also the main components of the CSH structure.

One very important characteristic of C–S–H is its variable composition, which is caused by defects and guest ions in its crystal structure. Several mechanisms have been

described to allow variation of Ca/Si, although doubts still remain at Ca/Si over 1.50 [324]. It is known that the Ca/Si ratio of the C–S–H varies due to missing bridging silica tetrahedra [325], charge compensation of terminal oxygen atoms by calcium rather than protons and by the likely presence of calcium in the interlayer [326,327]. The possible range of compositions is known for synthetic preparations. Solubility data in the CaO-SiO₂-H₂O system reports a Ca/Si in C–S–H which can vary from ≈ 0.67 up to ≈ 2.00 depending on the ionic activity of Si and Ca, generally with precipitation of portlandite occurring due to supersaturation of Ca with respect to the solid phase [326,328–331]. Pure C–S–H by most synthesis routes only exists for Ca/Si = 1.50 or less, with most attempts to form C–S–H with higher Ca/Si causing the co-precipitation of portlandite [64, 66, 67-69].

It was shown [217,332] that the composition of C–S–H measured in SEM-EDS – when represented as a scatter plot (e.g. Si/Ca– Al/Ca) – could be estimated by choosing the value with the least intermixing of C–S–H with CH or other phases rich in calcium [216]. Therefore, the EDS analysis was taken from a similar matrix structure for all cement mortar samples (Figure 4.116).

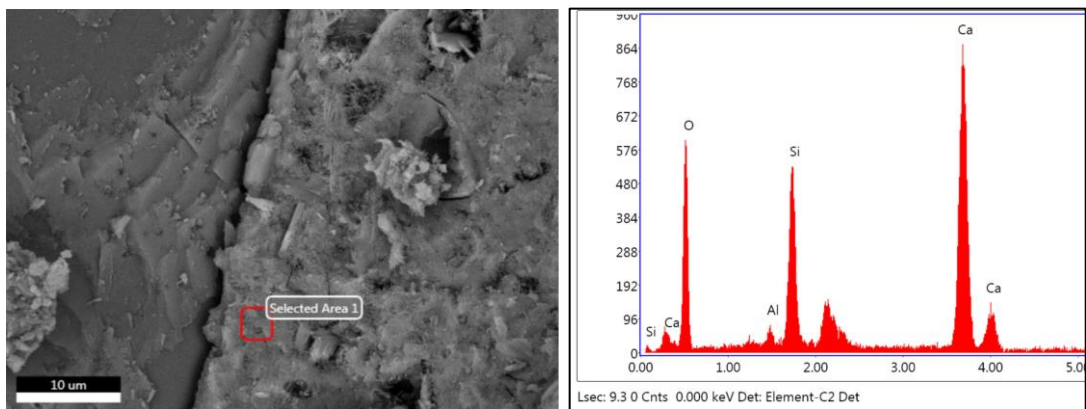


Figure 4.116: An example for EDS analysis (125OS0.5 specimen).

Furthermore, the relationship between the compressive strength of cement mortars containing bio-polymeric admixtures and the Si/Ca ratio is shown in the Figure 4.117 to Figure 4.121.

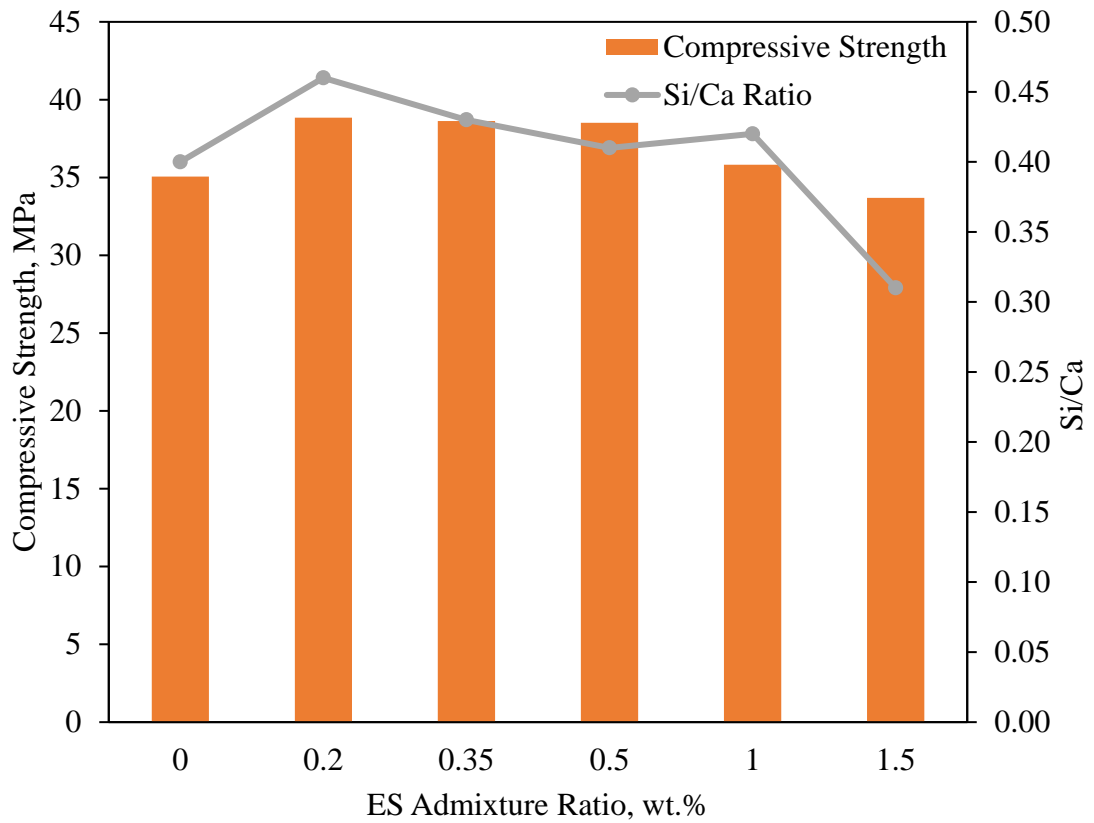


Figure 4.117: Relationship between Compressive strength and Si/Ca ratio of ES added cement mortars.

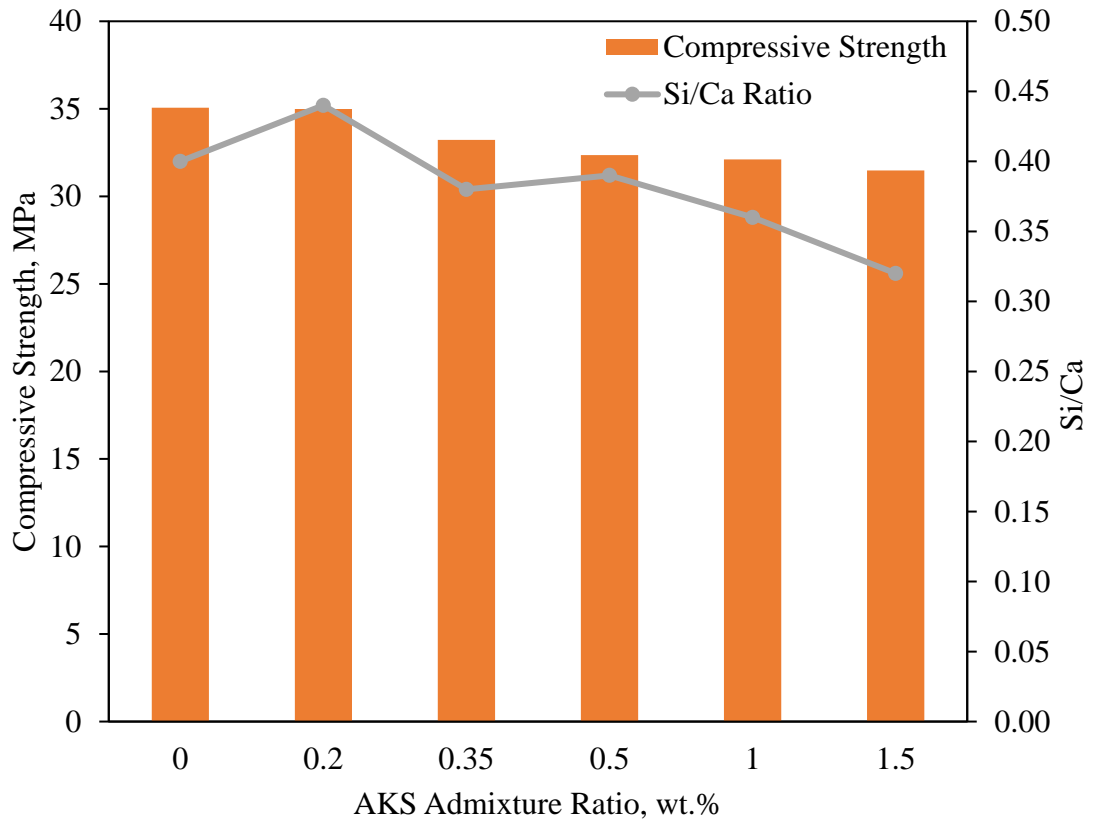


Figure 4.118: Relationship between compressive strength and Si/Ca ratio of AKS added cement mortars.

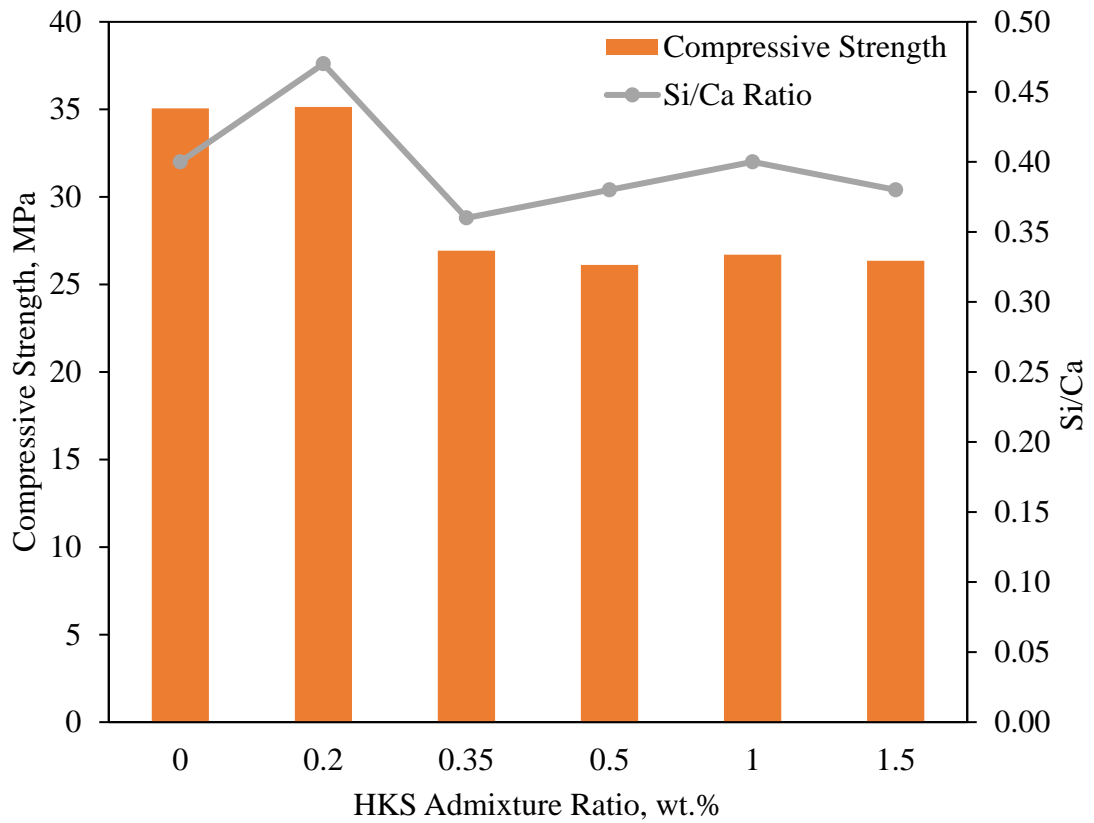


Figure 4.119: Relationship between compressive strength and Si/Ca ratio of HKS added cement mortars.

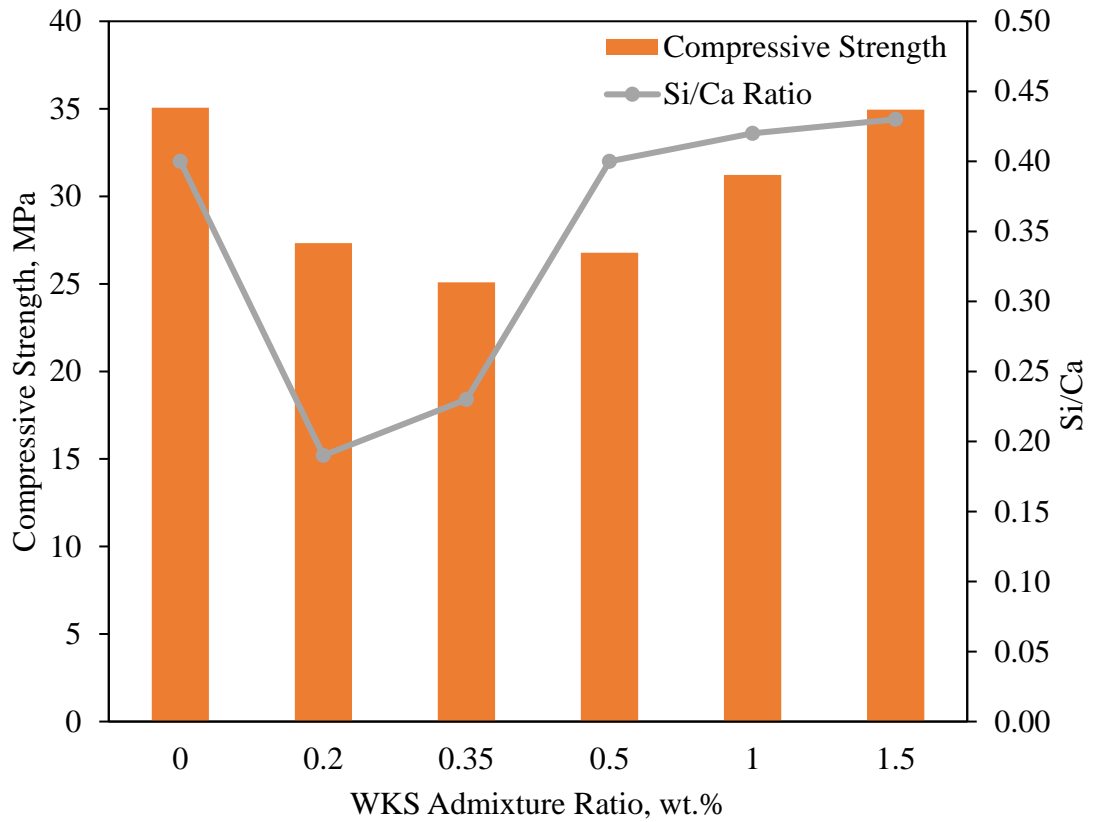


Figure 4.120: Relationship between compressive strength and Si/Ca ratio of WKS added cement mortars

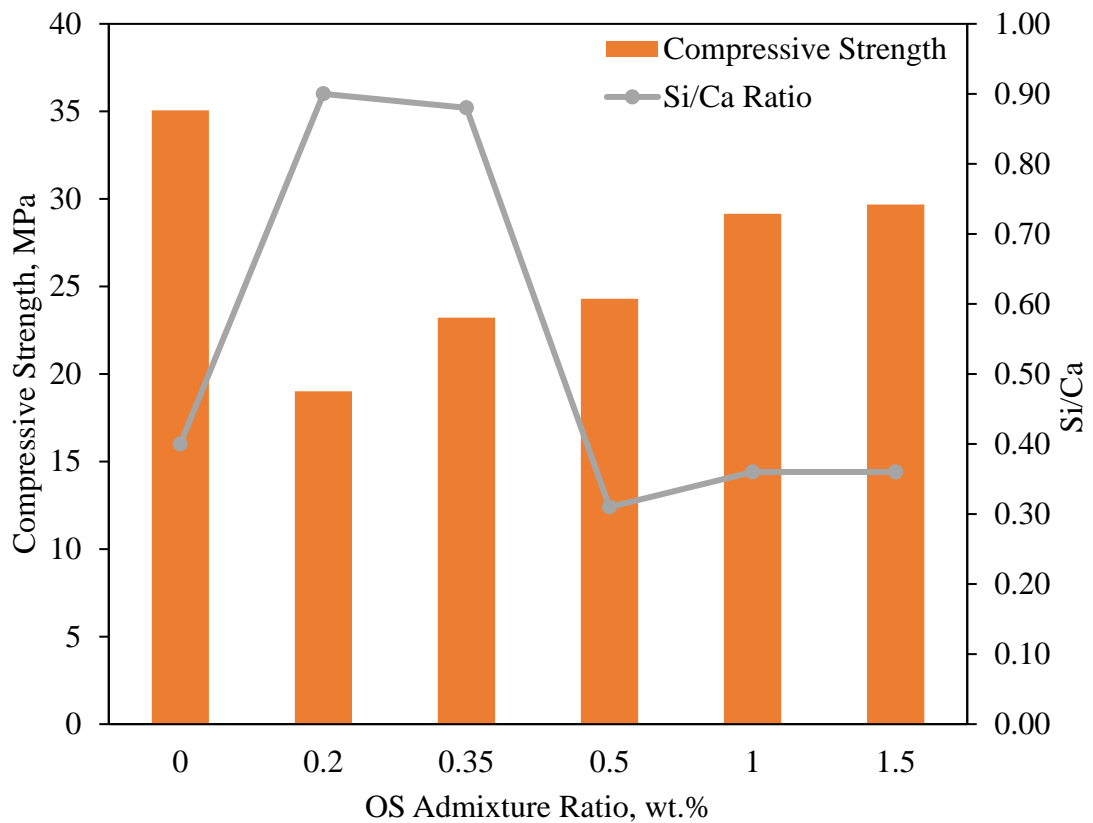


Figure 4.121: Relationship between compressive strength and Si/Ca ratio of OS added cement mortars.

As can be easily observed from Figure 4.117 to Figure 4.121, it has been determined that there is a direct proportionality between the compressive strength and the Si/Ca ratio. The compressive strength of the control mixture was determined as 35.06 MPa and the Si/Ca ratio was 0.40. In the test specimens, when the compressive strength of test specimens exceeds the compressive strength of the control mixture, the Si/Ca ratio of test specimens was higher than the Si/Ca ratio of the control mixture. In this relationship, only 125OS0.2 and 125OS0.35 coded samples deviated in the compressive strength and Si/Ca relationship (Figure 4.121). While the compressive strength of these samples decreased, a too much increase in Si/Ca ratio was observed. The reason that may be unhydrated cement particles on the matrix structure [239]. In this thesis study, it was determined that the cement matrix structure of the mortars with a Si/Ca ratio below 0.25 and above 0.80 had a relatively high number of unhydrated cement grains. For this reason, it can be concluded that the hydration of mortars with Si/Ca ratios below or above these limit values has not progressed as desired.

Furthermore, 28-day XRD analyzes of bio-polymeric admixture used cement pastes were performed to follow the hydration phases of the test mortars (between Figure

4.122 and Figure 4.126). Also, microstructural development of test pastes is represented in Appendix A as 3-, 7-, 28-, and 150-days XRD analysis.

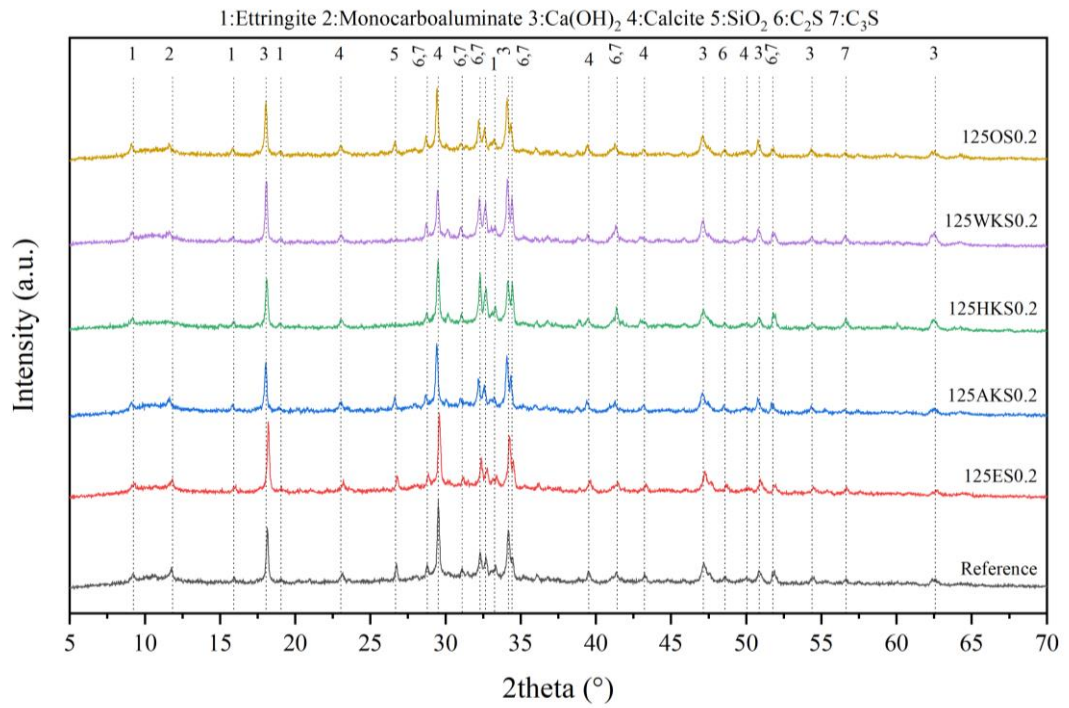


Figure 4.122: X-Ray Diffraction of 0.2 wt.% bio-polymeric admixture used cements pastes hydrated at 28-day

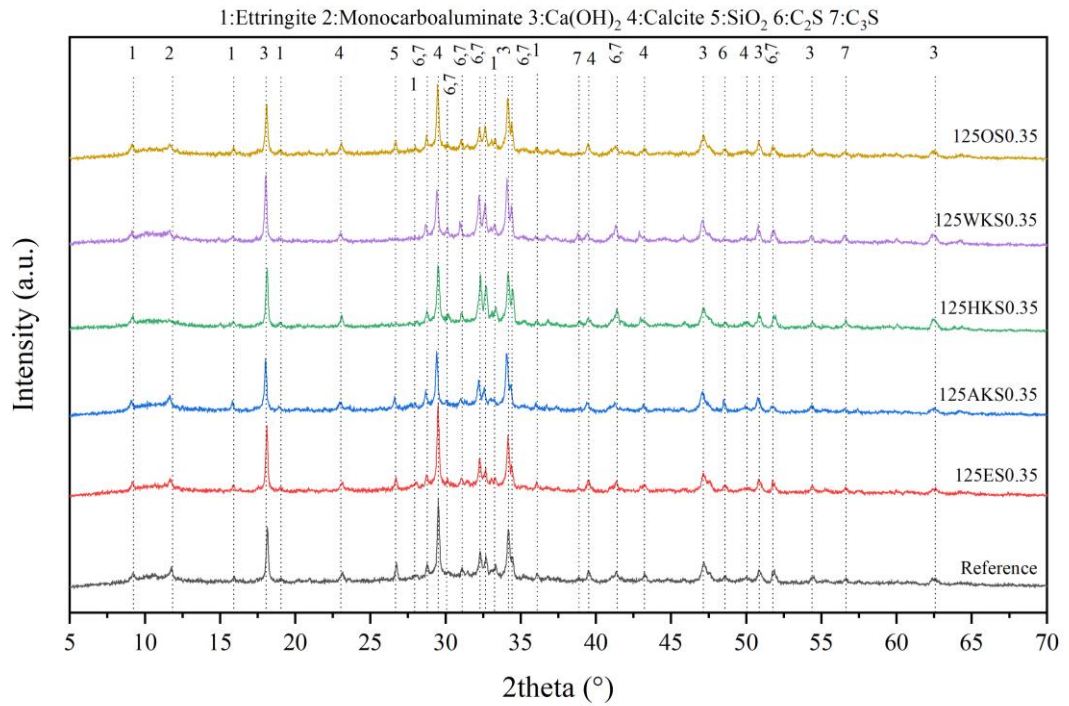


Figure 4.123: X-Ray Diffraction of 0.35 wt.% bio-polymeric admixture used cements pastes hydrated at 28-day

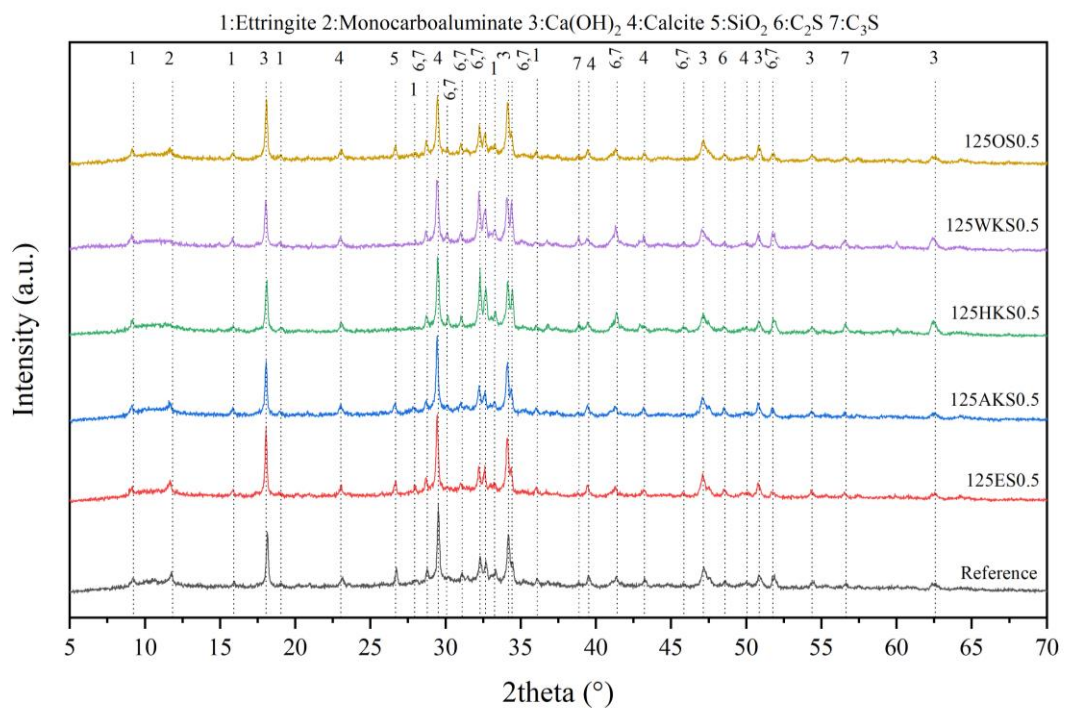


Figure 4.124: X-Ray Diffraction of 0.5 wt.% bio-polymeric admixture used cements pastes hydrated at 28-day

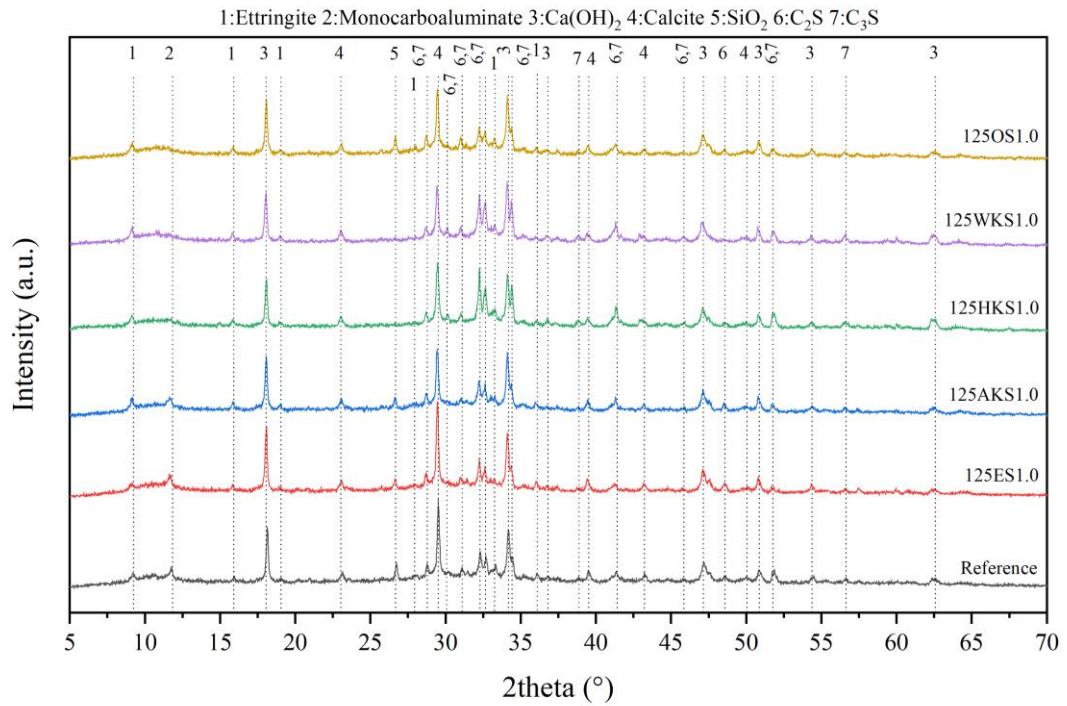


Figure 4.125: X-Ray Diffraction of 1.0 wt.% bio-polymeric admixture used cements pastes hydrated at 28-day

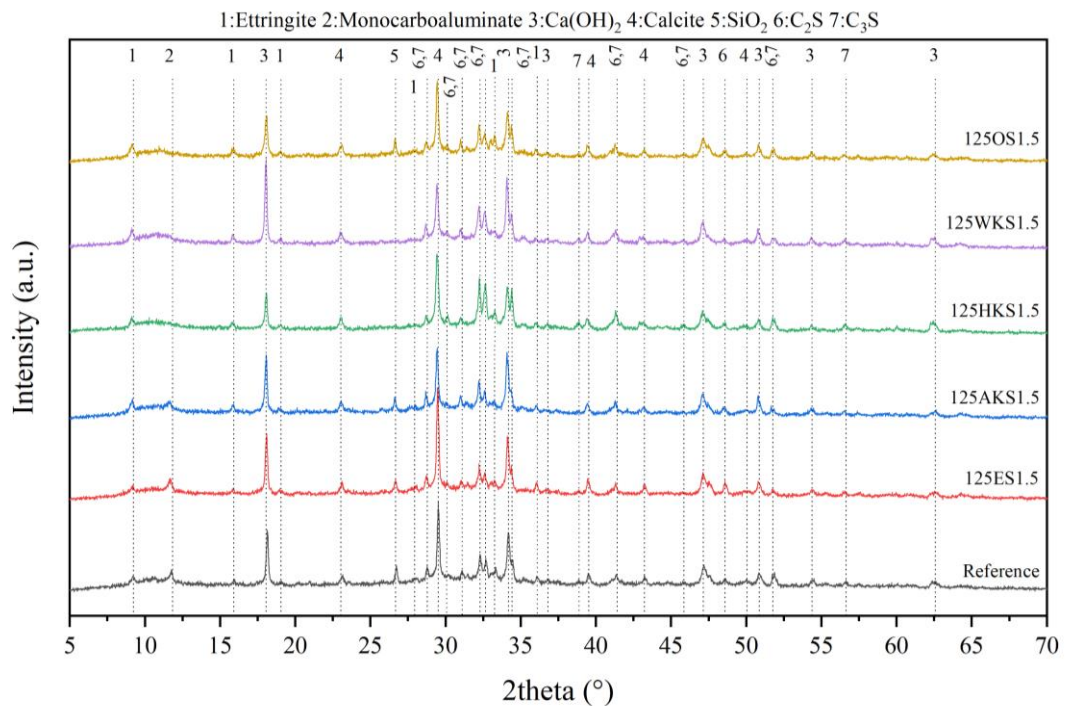


Figure 4.126: X-Ray Diffraction of 1.5 wt.% bio-polymeric admixture used cements pastes hydrated at 28-day

According to figures between Figure 4.122 and Figure 4.126, XRD phases of CEM I 42.5 R cement as reference paste showed expected hydration products, including calcium hydroxide (portlandite), ettringite, weakly crystalline C-S-H and unreacted

clinker phases (calcium silicates). The presence of calcium carbonate was attributed to the partial carbonation of the portlandite, especially with ES addition. It has been an established fact that finely ground calcium carbonate represents to a certain extent an active component during the hydration of Portland cement and the formation of calcium monocarboaluminate has been confirmed many times [333]. The monocarboaluminate phase almost disappeared, especially in high usage rates of WKS and OS admixtures with high extractive ratios. According to the XRD results, it can be said that a slight decrease in the intensity of ettringite peaks was observed with the use of bio-polymeric admixtures. Although, a considerable amount of Ca(OH)_2 is observed in all cases, in the use of low amount of OS admixture, a decrease in the intensity of Ca(OH)_2 peaks was detected. This is an indication that the hydration of these mixtures has not progressed sufficiently and as a result the compressive strength remains relatively low. On the other hand, the calcium-silicate hydration products did not present clear diffraction peaks, due to their semi-amorphous nature [334]. Besides, there is an overlapping of the peaks of the hydrated and anhydrous compounds. However, the peaks characterizing anhydrous calcium silicates are better expressed in the patterns of test pastes. Although the peak intensities of unhydrated cement particles are relatively higher at early ages, the peak intensity of unhydrated cement particles decreases in advancing ages with the use of bio-polymeric admixtures (see Appendix A). The reason why unhydrated cement grains are relatively dense at early ages can be explained by the fact that bio-polymeric admixtures both slow down the progress of hydration by reducing the water absorption of the mortar when water curing, and that very fine grained bio-polymeric admixtures cut the contact of the cement particle with the mixing water by being barrier by accumulation around the cement particles. However, it has been determined that the peak intensity of unhydrated cement grains may decrease with later ages. This can be explained by the fact that bio-polymeric admixtures provide the moisture required for hydration in later ages thanks to their superior water-retention ability, and the development of hydration products with pectin in its content. An increase in the intensity of calcite peaks was detected with the use of ES admixture. In addition, it has been observed that the quartz peak is almost disappeared in the XRD patterns of cement pastes in which HKS and WKS admixtures are used.

4.5 Durability of Cement Mortars

In this section, visual and mechanic changes cement mortar specimens, which are exposed to the effects of different chemical components and freezing and thawing, prepared without admixtures and with the addition of bio-polymeric admixtures in different proportions, are analyzed.

4.5.1 Resistance to Sulfate Effect

In order to determine the resistance of cement mortars to sulfate, cement mortars were subjected to 30 wetting-drying cycles in 5 wt.% magnesium sulfate solution as capillary absorption. In the interactions of $MgSO_4$ solution, it was observed that salt crystals, defined as $MgSO_4$ effloresce, were formed in large amounts on the specimen surfaces as well as crystallized $MgCO_3$ shell (Figure 4.127). This is particularly evident in reference mortar specimens. Figure 4.128 shows efflorescence on the sample surface at the 10th, 20th, and 30th wetting-dry cycles of the reference specimen. Figure 4.129 to Figure 4.133 shows the development of efflorescence on the surface of bio-polymeric admixed cement mortars.



Figure 4.127: $MgSO_4$ bloom in reference cement mortar samples

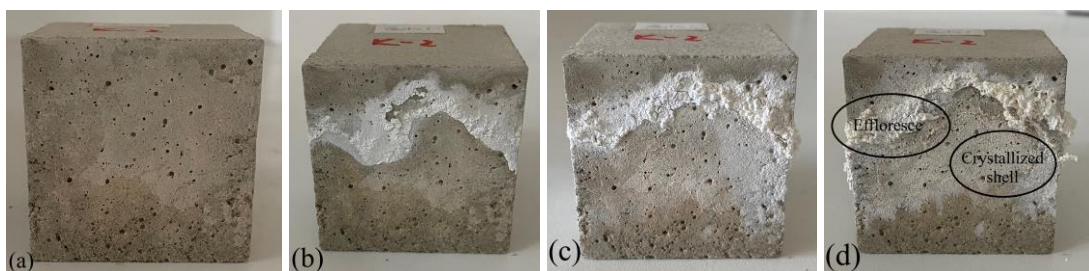


Figure 4.128: Salts formed on the surface of the reference mortar specimens after wetting-drying cycle, 0 cycle (a), 10 cycle (b), 20 cycle (c), 30 cycle (d)

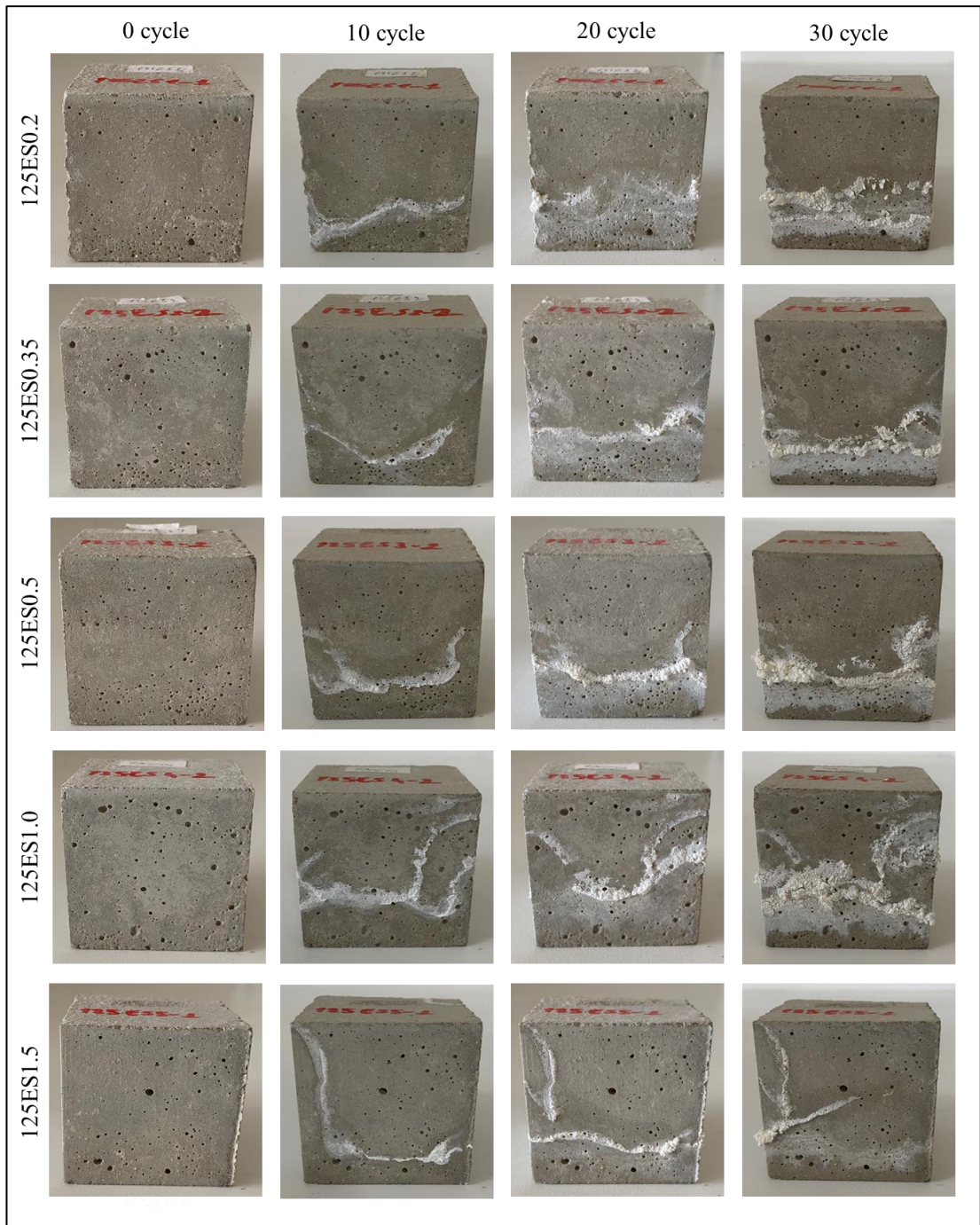


Figure 4.129: Salts formed on the surface of the 125ES mortar specimens after wetting-drying cycle

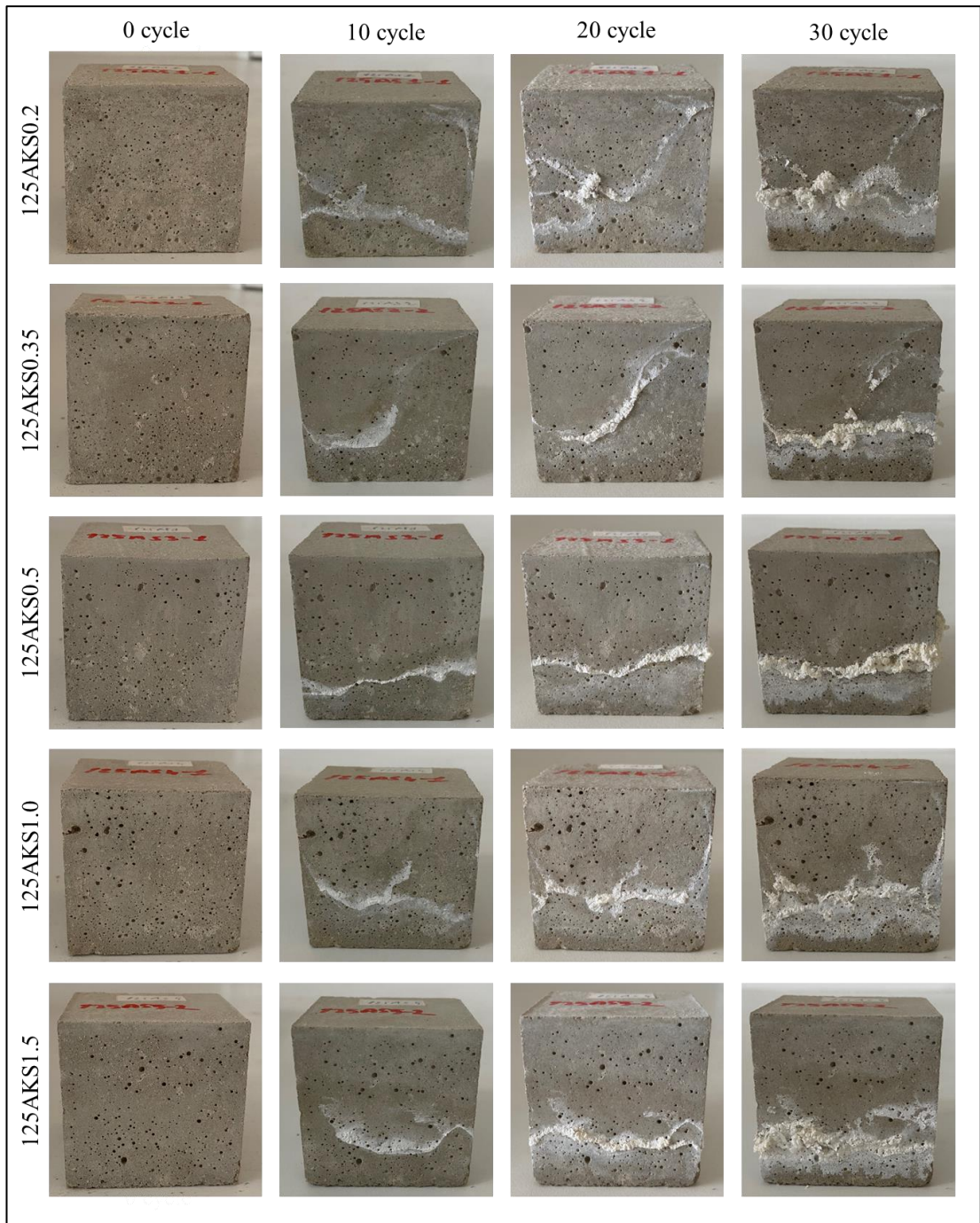


Figure 4.130: Salts formed on the surface of the 125AKS mortar specimens after wetting-drying cycle

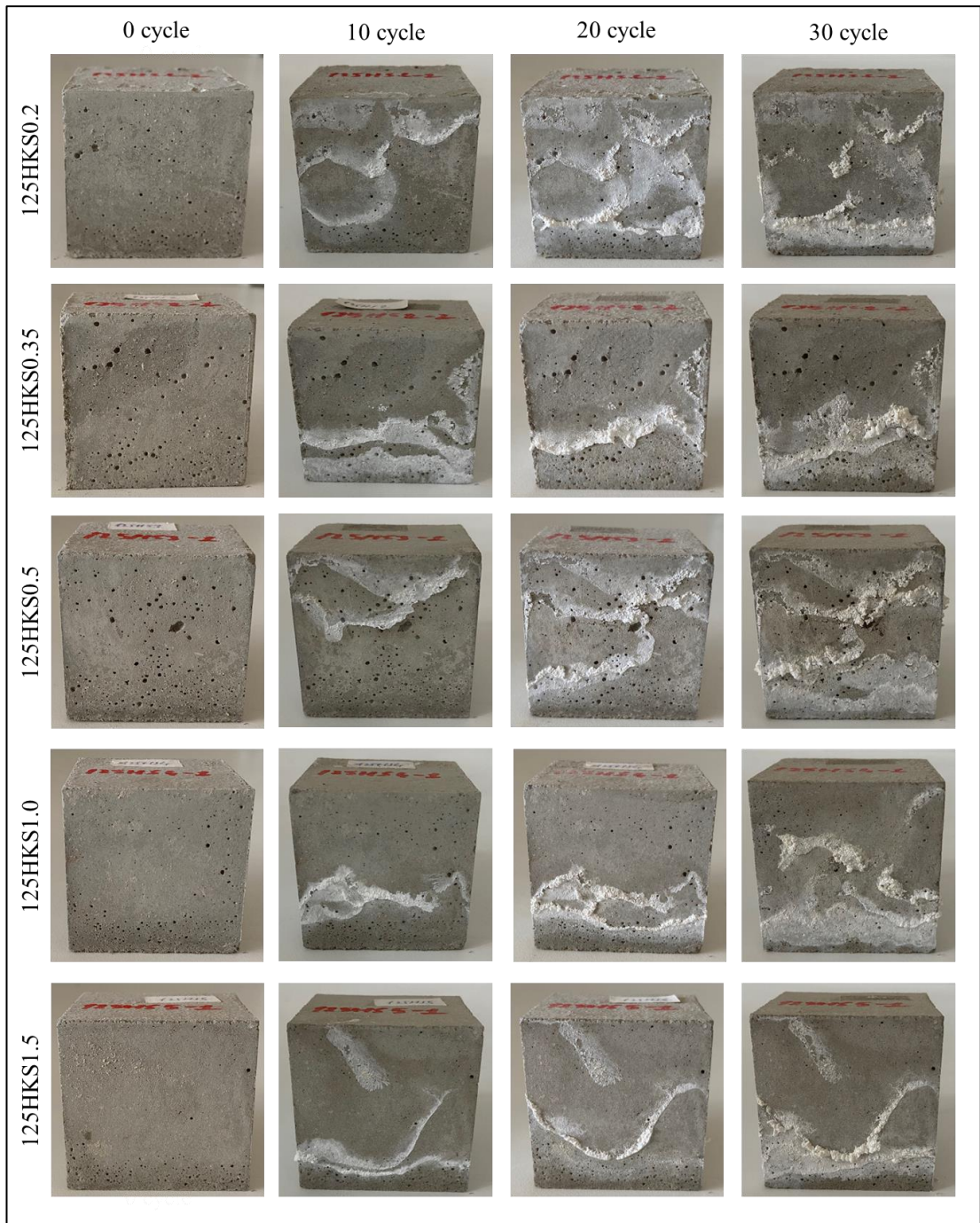


Figure 4.131: Salts formed on the surface of the 125HKS mortar specimens after wetting-drying cycle

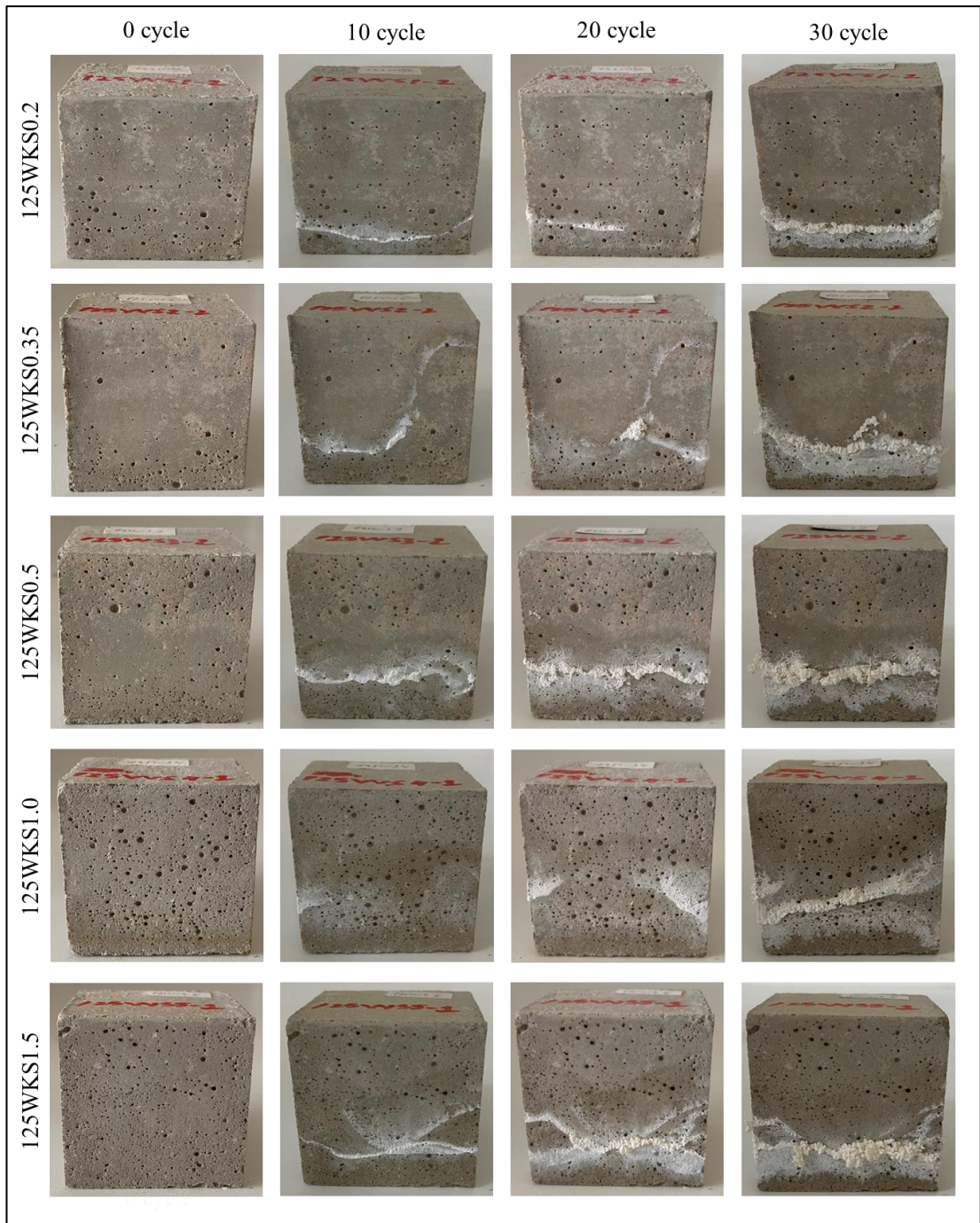


Figure 4.132: Salts formed on the surface of the 125WKS mortar specimens after wetting-drying cycle

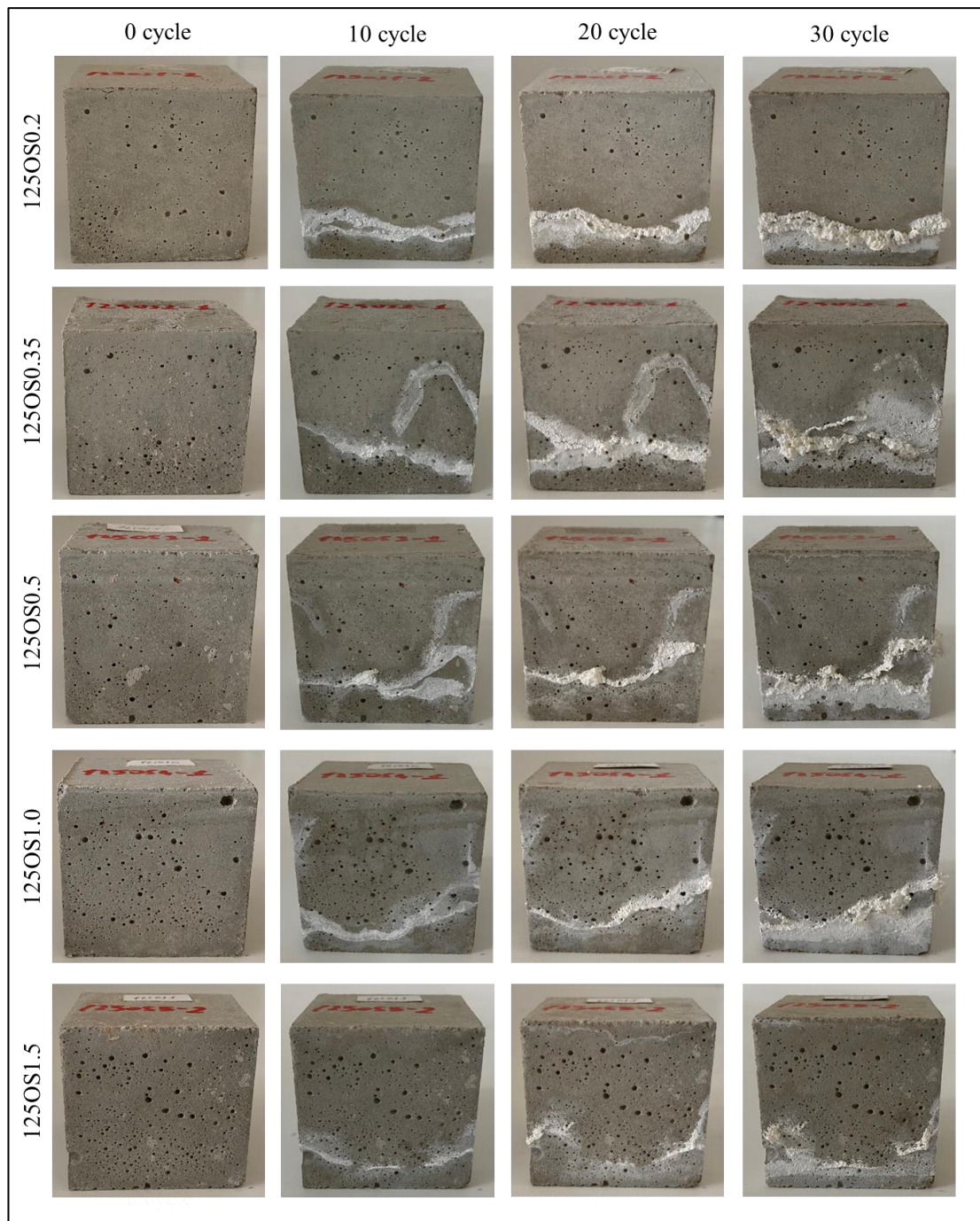


Figure 4.133: Salts formed on the surface of the 125WKS mortar specimens after wetting-drying cycle

Table 4.21 shows the compressive strength of composite cement mortars before and after magnesium sulfate effect by capillary action with 30 wet-dry cycle. The change in compressive strengths relative to the initial compressive strength of each test mortar is graphically shown in Figure 4.134.

Table 4.21: Compressive strength of mortar specimens after sulfate effect

Mortar	Compressive Strength (MPa)	
	0 wet-dry cycle	30 wet-dry cycle
Reference	40.62	43.04
125ES0.2	48.77	50.88
125ES0.35	43.34	45.44
125ES0.5	43.63	46.13
125ES1.0	43.36	46.01
125ES1.5	42.28	45.72
125AKS0.2	38.25	40.87
125AKS0.35	34.85	41.08
125AKS0.5	34.55	39.33
125AKS1.0	33.12	34.51
125AKS1.5	34.31	33.65
125HKS0.2	43.57	46.22
125HKS0.35	37.70	40.91
125HKS0.5	34.85	37.38
125HKS1.0	37.00	35.09
125HKS1.5	37.14	33.37
125WKS0.2	35.12	38.52
125WKS0.35	31.20	34.37
125WKS0.5	32.40	35.84
125WKS1.0	29.26	33.17
125WKS1.5	37.73	41.30
125OS0.2	24.17	27.16
125OS0.35	27.84	28.27
125OS0.5	28.97	30.81
125OS1.0	28.18	31.90
125OS1.5	30.63	34.38

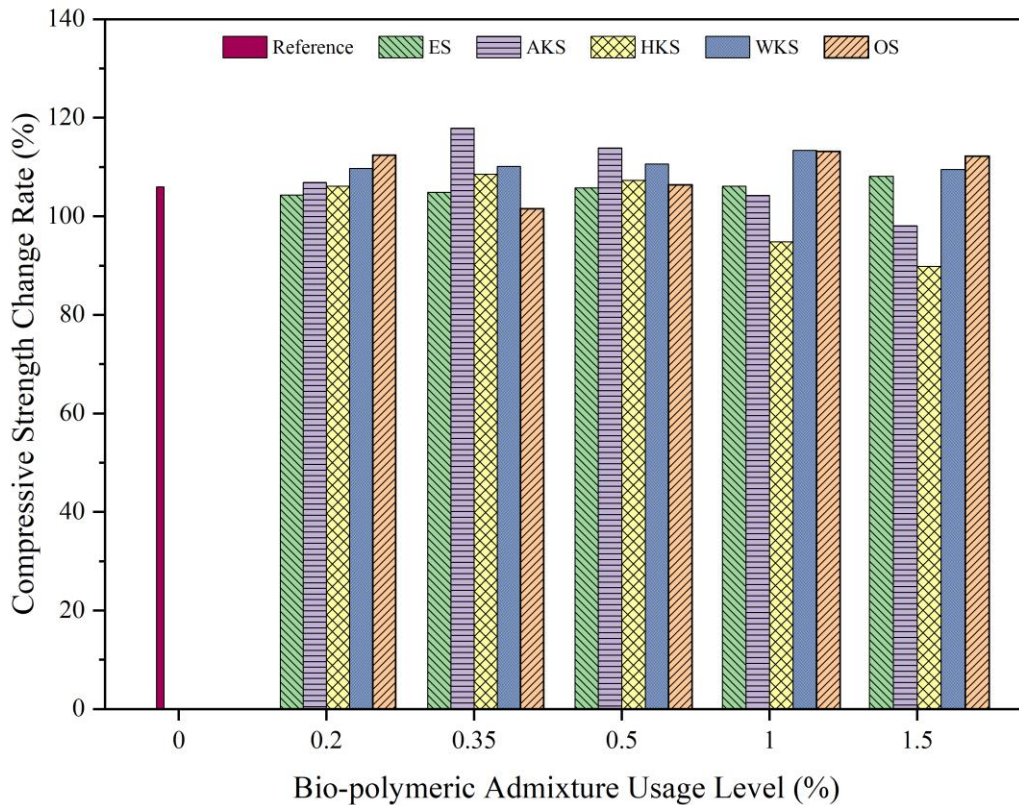


Figure 4.134: Rate of change in compressive strength relative to compressive strength before sulfate exposure

When Figure 4.134 is examined, it is observed that the reference mortar gained 5.95 % strength in 30 drying-wetting cycles. Similarly, it was determined that the mortar specimens with AKS admixtures gained strength up to 17.88 %. It has been observed that in HKS admixed mortars gain strength with low bio-polymeric admixtures, but their strength can decrease by 10.17 %, in 1 wt.% and 1.5 wt.% admixture usage levels. It has been determined that cement mortars with WKS and OS admixtures can gain strength up to 13 %. Due to the sulphate effect in cement mortars, it is expected that chemical reaction with hydration products of cement and sulphate will lead to deterioration in the mortars and a decrease in strength [335–337]. However, the degrading effect of sulfate on cementitious products can be more clearly demonstrated in longer test times. On the other hand, in this study, a 30-day test period was sufficient for the mortar specimens with high HKS admixtures to lose strength. In addition, the strength gain of the mortars using ES admixtures remained at a relatively lower level compared to the mortars using other admixtures. This shows that the strength gaining process of ES admixed mortars has ended, and when they are exposed to sulfate for a longer time, the strength loss phase will begin. According to Yu et al. [338], when cement mortars are exposed to the effect of sulfate, an increase in their strength can be

observed at 90 to 150 days of sulfate exposure. In strength gain stage, the primary reaction products, gypsum and ettringite, fill the pores and compact the microstructure, causing an increase in compressive strength. In strength loss stage, they overcame the pore limitation and the expanding tension sprouted. When the tensile strength exceeded the tensile strength of the mortar, microcracking developed and deteriorated the strength. Also, washing and consuming hydration products further weakened the cohesion [338]. In this thesis study, it has been determined that sulfate may deteriorate the mortar structures with ES and HKS admixtures with shorter interaction, while mortars using AKS, WKS and OS admixtures need to be exposed to sulfate for a longer period of time to deteriorate the structure. In this context, it can be said that AKS and WKS and OS admixtures increase the resistance to sulfate.

4.5.2 Resistance to Acid Effect

Another subject of study within the scope of this thesis is the analysis of the acid resistance characteristics of cement mortar specimens with bio-polymeric admixtures. Sulfuric acid solution was used in the analysis of the resistance of the mortars against acids. Such acids have a dissolving and disintegrating effect on CaCO₃-based building components. Compressive strength changes of mortar specimens used in the interaction analysis with acid solution in H₂SO₄ solution with pH=1 was experimentally investigated, and the results are given in Table 4.22. The change in compressive strengths relative to the initial compressive strength of each test mortar is graphically shown in Figure 4.135.

Table 4.22: Compressive strength of mortar specimens after acid effect

Mortar	Compressive Strength (MPa)	
	0 wet-dry cycle	30 wet-dry cycle
Reference	40.62	41.37
125ES0.2	48.77	43.59
125ES0.35	43.34	40.52
125ES0.5	43.63	41.30
125ES1.0	43.36	41.79
125ES1.5	42.28	40.60
125AKS0.2	38.25	39.62

Table 4.22 (Continued): Compressive strength of mortar specimens after acid effect

Mortar	Compressive Strength (MPa)	
	0 wet-dry cycle	30 wet-dry cycle
125AKS0.35	34.85	39.73
125AKS0.5	34.55	36.63
125AKS1.0	33.12	32.28
125AKS1.5	34.31	33.23
125HKS0.2	43.57	44.05
125HKS0.35	37.70	38.54
125HKS0.5	34.85	35.85
125HKS1.0	37.00	38.87
125HKS1.5	37.14	38.82
125WKS0.2	35.12	35.92
125WKS0.35	31.20	33.53
125WKS0.5	32.40	35.40
125WKS1.0	29.26	33.09
125WKS1.5	37.73	42.41
125OS0.2	24.17	24.71
125OS0.35	27.84	28.18
125OS0.5	28.97	29.67
125OS1.0	28.18	29.31
125OS1.5	30.63	33.08

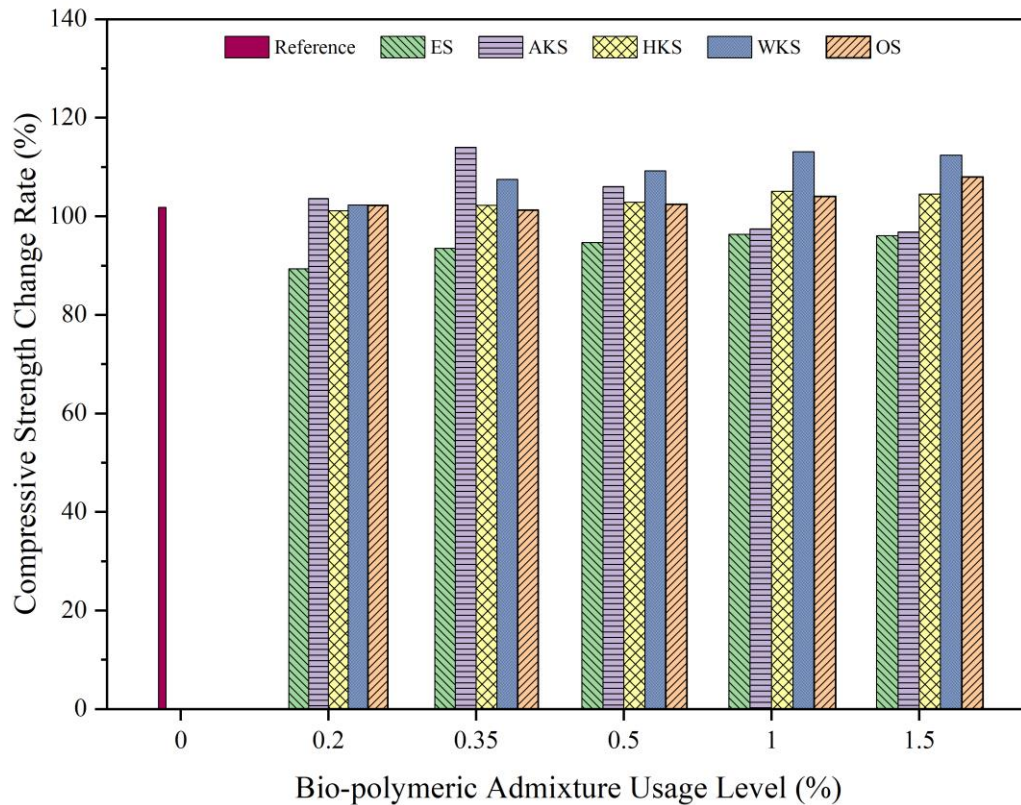


Figure 4.135: Rate of change in compressive strength relative to compressive strength before acid exposure

By reacting with calcium carbonate, sulfuric acid enables calcium carbonate to turn into gypsum and crystallize by taking two moles of water. It is also known that calcium hydroxide is the weakest component under the influence of acid [339]. According to Figure 4.135, the mixtures that had the most negative effect in the mortar specimens were cement mortars using ES admixtures. Since calcium hydroxide $\text{Ca}(\text{OH})_2$ is the most vulnerable element to acid attack, eggshell concrete suffers higher damage as eggshell powder increases the amount of said element in mortars [340]. Cement mortars with ES admixtures suffered a compressive strength loss of up to 10.62 % in 30 drying-wetting cycles with the effect of sulfuric acid. Similarly, it has been determined that the compressive strength of the cement mortars using AKS admixtures can decrease up to 3.14 % due to the acid effect as the admixture ratio increases. At the end of 30 cycles, the compressive strength of the mortars using HKS admixture increased by a maximum of 5.05 %. Similar to the specimens subjected to sulphate solution cycle, the compressive strengths of cement mortars with WKS and OS admixtures exposed to acid cycle increased by 13.10 % and up to 8 %. The compressive strength gain during the early capillary absorption period in pH=1 sulfuric acid solution could be attributed to a number of factors, which include continued

hydration of cement and formation of gypsum [341]. According to Chang et al. [341], cement-based test specimens generally require 56 days of acid interactions to lose their compressive strength. Even in their study, all test specimens had to be exposed to acid interaction for 168 days in order to record a decrease in compressive strength for all. The increase in compressive strength of the samples during the first period of acid solution interactions is probably due to the continued hydration of the cement and an early formation of gypsum and ettringite that will fill the pores of the mortar. However, further formation of gypsum and ettringite results in the dissolution of the cement paste in the acid solution, resulting in expansion leading to softening of the cement matrix followed by a decrease in the compressive strength of specimens. In this test study, mortars with HKS, WKS and OS admixtures could not pass to the second stage during the test period of 30 cycles. However, it was determined that AKS and ES admixed mortars lost their compressive strength in 30 cycles. Therefore, considering the exposure time to acid solution, it can be said that HKS, WKS and OS admixtures can make cement mortar comparatively more durable under the influence of acid solution. It is also known that water-repellent chemicals and fatty acids are used in mortars to reduce the effect of sulfate and acid attack [342]. In this thesis study, it was determined that especially the mortars with lower water absorption values performed better under the effect of acid and sulfate.

4.5.3 Resistance to Freeze-Thaw

Repeated freeze-thaw cycles can be detrimental to a porous and brittle material such as concrete. Under this type of influence, concrete can deteriorate rapidly by losing its strength and/or crumbling. From Figure 4.136 through Figure 4.141, visual changes on the surfaces of cement mortars exposed to 30 freeze-thaw cycles are presented. In Table 4.23, the initial compressive strengths and compressive strengths after 30 cycles of cement mortar specimens subjected to 30 freeze-thaw cycles are given. The change in compressive strengths relative to the initial compressive strength of each test mortar is graphically shown in Figure 4.146.

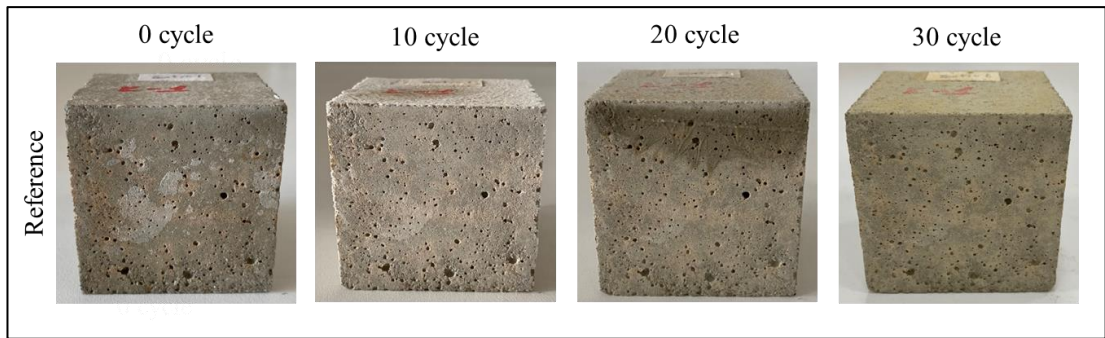


Figure 4.136: Reference specimens' appearance before and after freeze-thaw cycles

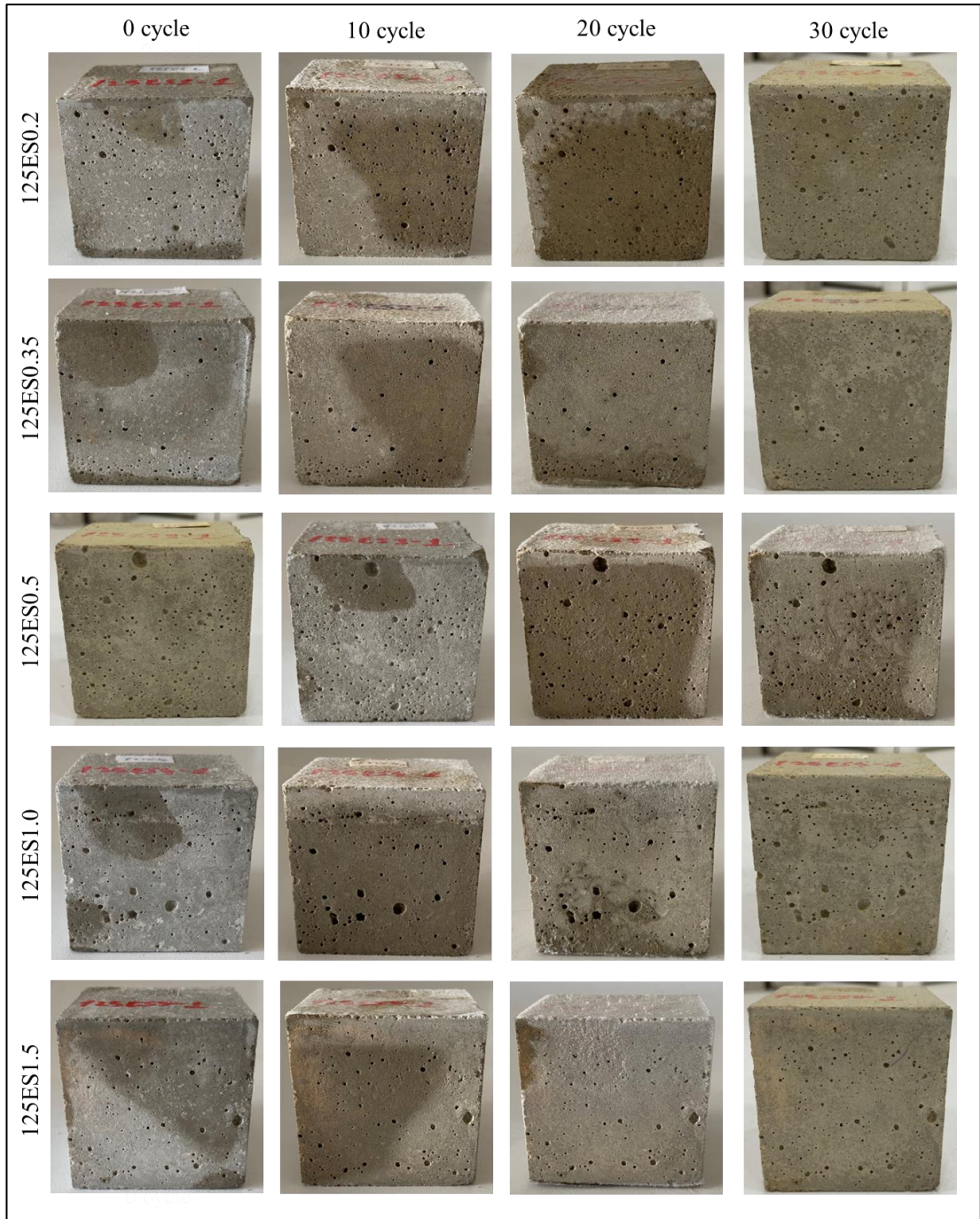


Figure 4.137: 125ES specimens' appearance before and after freeze-thaw cycles

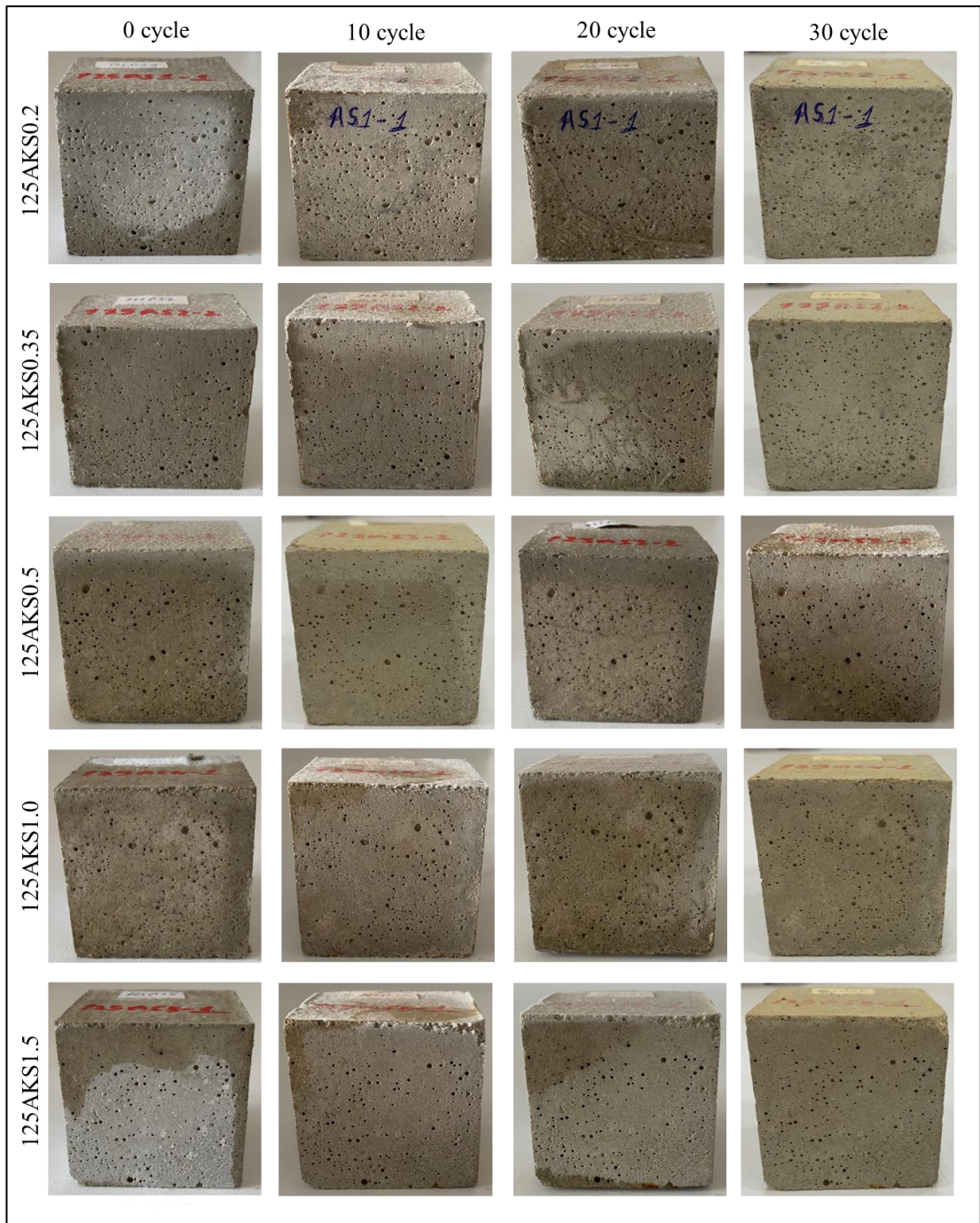


Figure 4.138: 125AKS specimens' appearance before and after freeze-thaw cycles

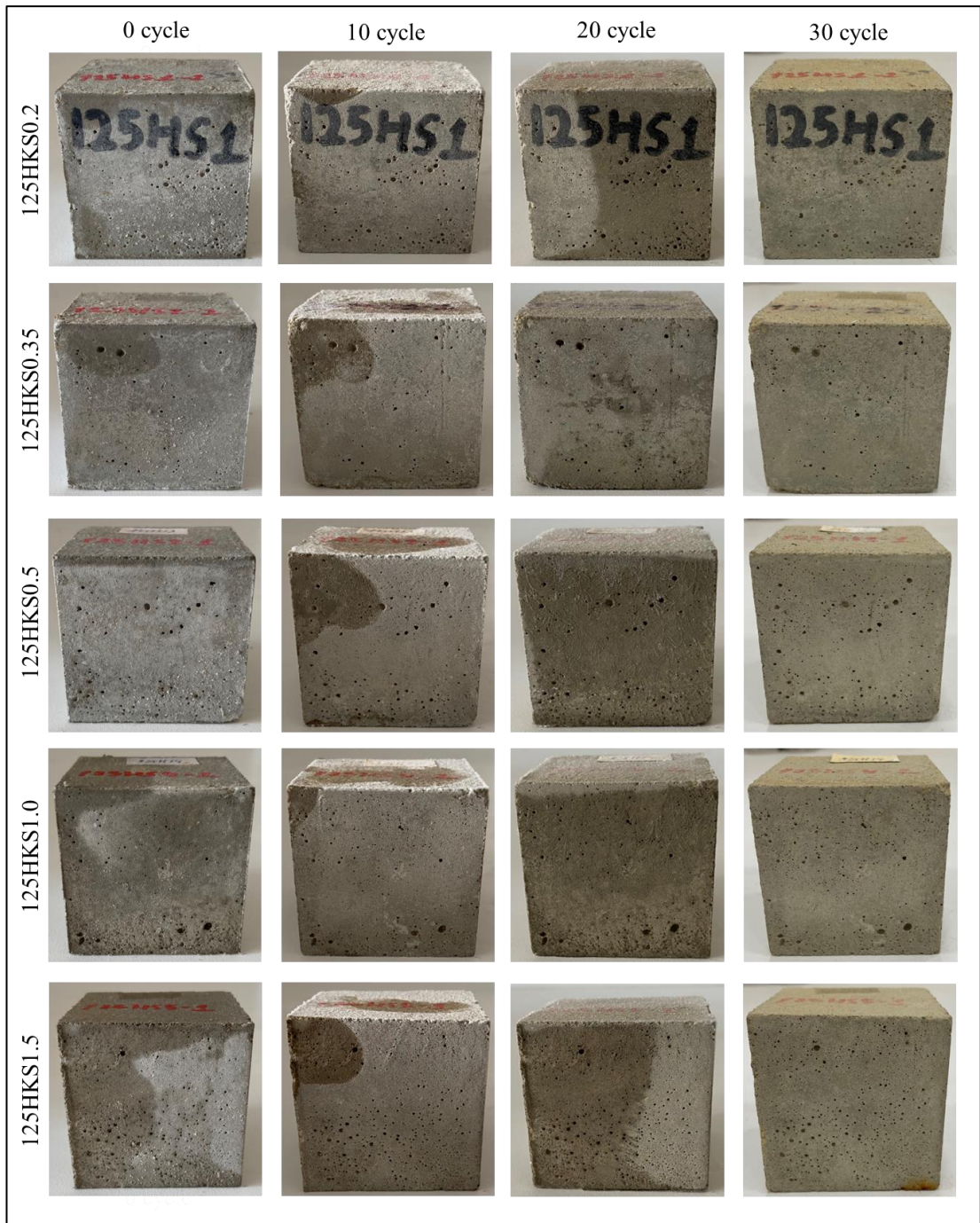


Figure 4.139: 125HKS specimens' appearance before and after freeze-thaw cycles

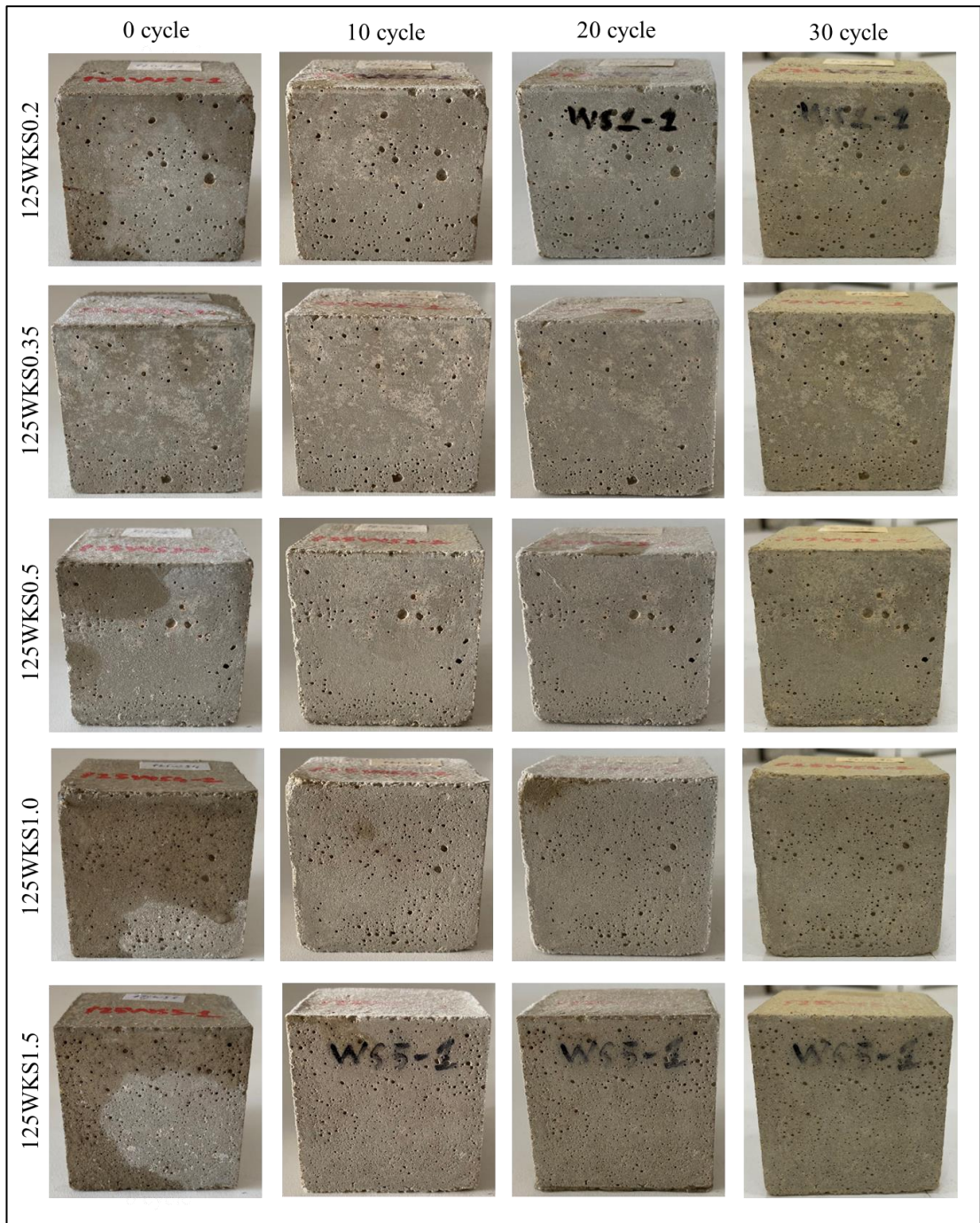


Figure 4.140: 125WKS specimens' appearance before and after freeze-thaw cycles

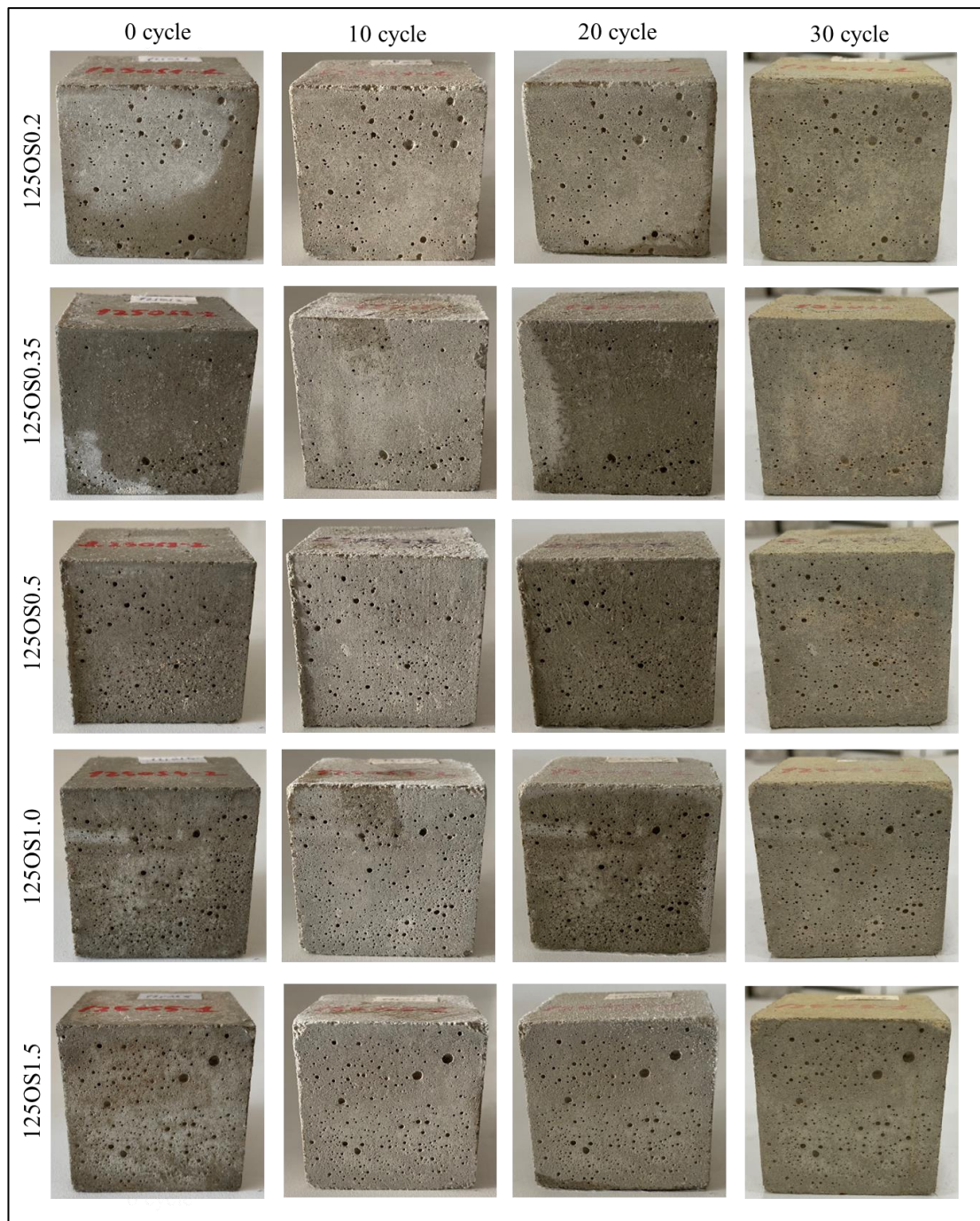


Figure 4.141: 125OS specimens' appearance before and after freeze-thaw cycles

The appearance of the tested specimens before and after completing 30 cycles of freeze-thaw action is shown between Figure 4.136 and Figure 4.141. Surface scaling and concrete pop-outs are the two signs of deterioration that are not clearly observed in any tested specimens. However, distinctive color changes were observed on the surface of many specimens. As the number of freeze-thaw cycles increases, surface scaling can be expected in these regions. However, cracks were detected on the surfaces of the reference mortars after 30 freeze-thaw cycles (Figure 4.142).

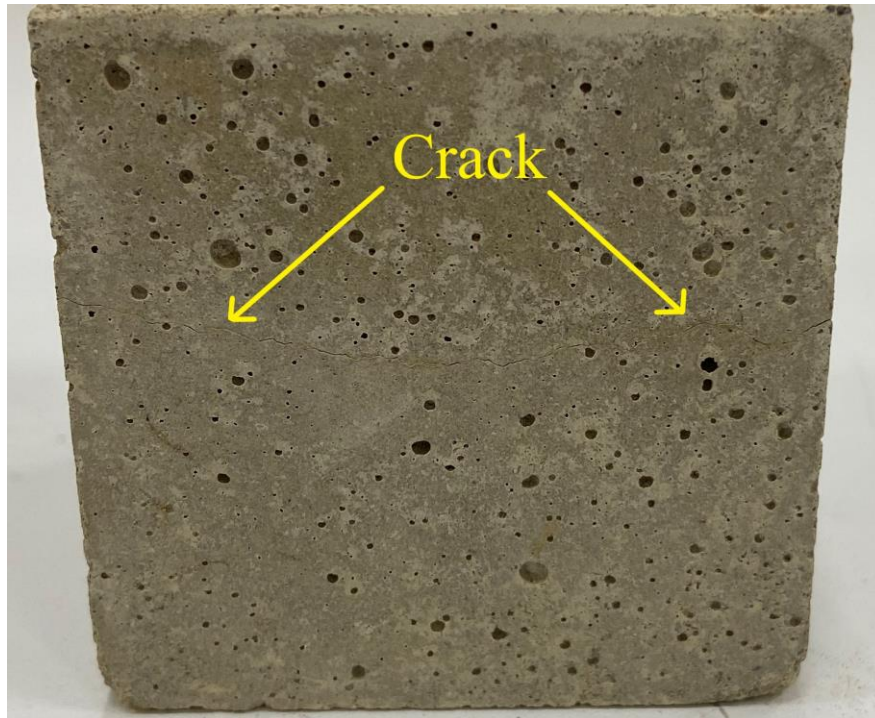


Figure 4.142: Freeze-thaw cracking on the surface of reference mortar

In addition, after 30 freeze-thaw, cracks were observed on the surfaces of the mortars using ES admixture and are shown in the Figure 4.143, Figure 4.144 and Figure 4.145.



Figure 4.143: Freeze-thaw cracking on the surface of 125ES02 mortar



Figure 4.144: Freeze-thaw cracking on the surface of 125ES0.5 mortar

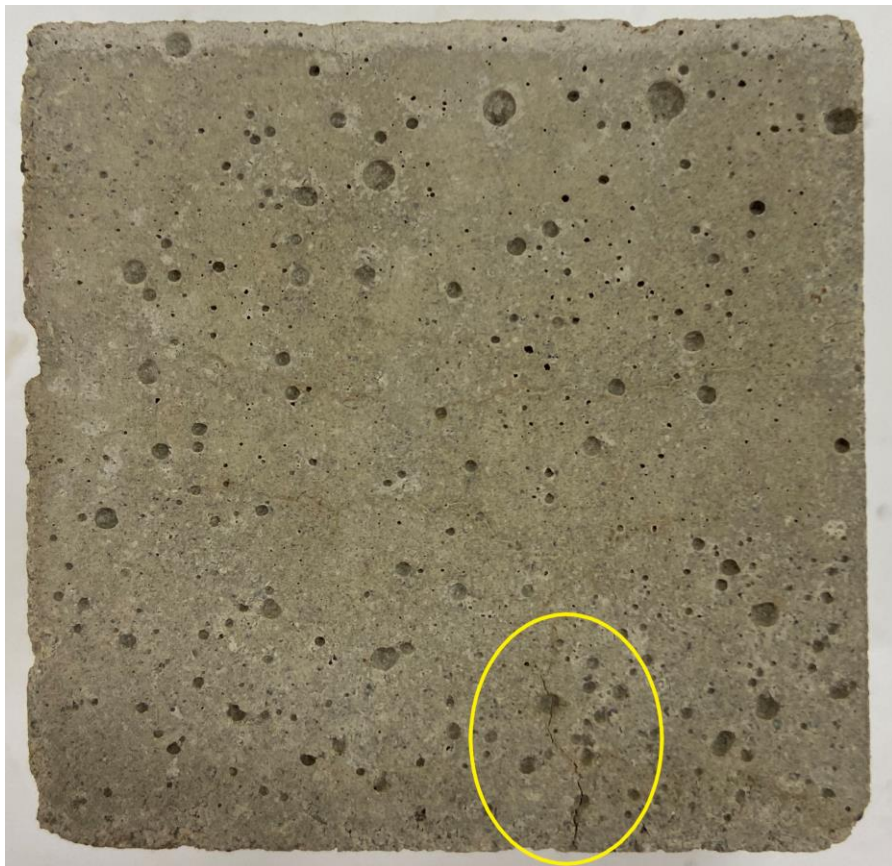


Figure 4.145: Freeze-thaw cracking on the surface of 125ES1.5 mortar

Table 4.23: Compressive strength of mortar specimens after freeze-thaw effect

Mortar	Compressive Strength (MPa)	
	0 freeze-thaw cycle	30 freeze-thaw cycle
Reference	40.62	30.26
125ES0.2	48.77	42.53
125ES0.35	43.34	38.08
125ES0.5	43.63	40.44
125ES1.0	43.36	42.34
125ES1.5	42.28	42.11
125AKS0.2	38.25	39.48
125AKS0.35	34.85	37.76
125AKS0.5	34.55	38.81
125AKS1.0	33.12	34.31
125AKS1.5	34.31	35.02
125HKS0.2	43.57	43.02
125HKS0.35	37.70	42.15
125HKS0.5	34.85	39.43
125HKS1.0	37.00	40.85
125HKS1.5	37.14	40.17
125WKS0.2	35.12	36.35
125WKS0.35	31.20	32.58
125WKS0.5	32.40	33.95
125WKS1.0	29.26	33.15
125WKS1.5	37.73	38.93
125OS0.2	24.17	25.87
125OS0.35	27.84	32.25
125OS0.5	28.97	31.81
125OS1.0	28.18	30.85
125OS1.5	30.63	31.63

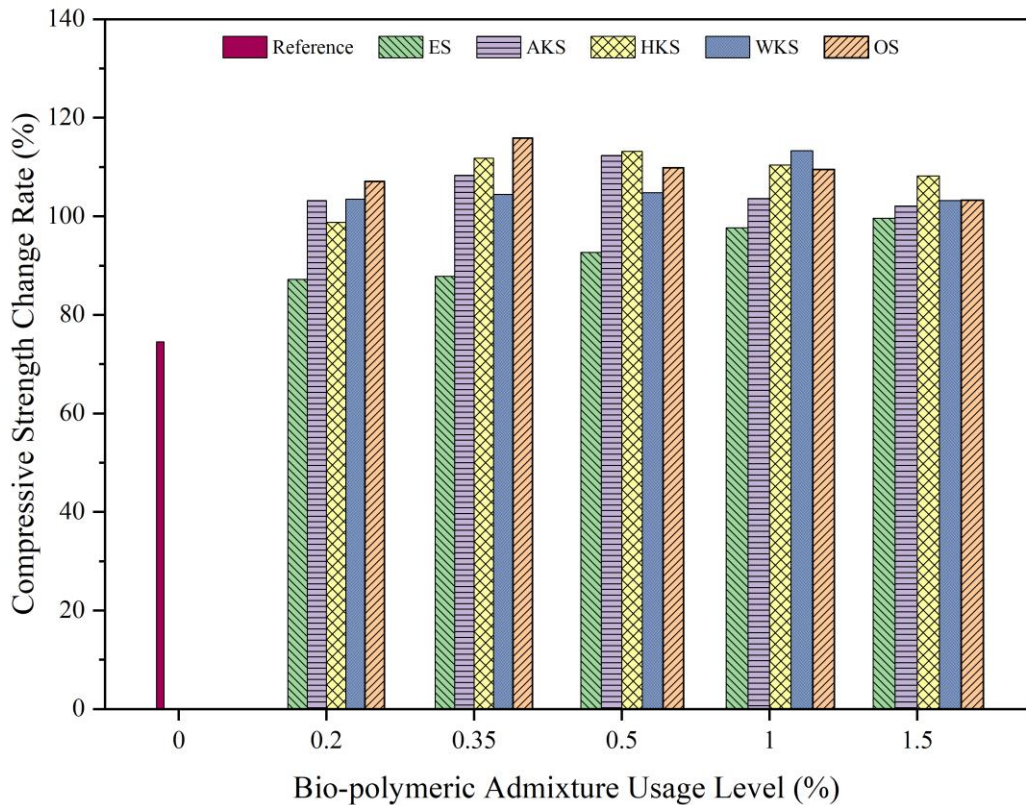


Figure 4.146: Rate of change in compressive strength relative to compressive strength before freeze-thaw cycles

According to Figure 4.146, the reference mortar lost 25.51 % of its initial compressive strength after 30 freeze-thaw cycles. The compressive strength of cement mortars with ES admixture, which have a relatively low porosity and a relatively high water absorption rate, also decreased up to 12.79 % at the end of 30 cycles. Water expands by 9% of its volume when frozen. When water begins to freeze in a capillary space, this expansion must be tolerated in the cement mortar. The magnitude of the hydraulic pressure created by the expansion of water when it freezes depends on the permeability of the cement paste, the degree of saturation, the distance to the nearest unfilled space and the freezing rate. If the hydraulic pressure exceeds the tensile strength of the cement paste at any point, it will cause local cracking. In repeated freezing and thawing cycles in a wet environment, during the thaw phase of the cycle, water enters the cracks and freezes again. A gradual deterioration occurs in each freeze-thaw cycle. Thus, the strength of the specimen decreases with the freeze-thaw cycle. In this way, it has been observed that the hydraulic pressure caused by the freezing expansion of water in the reference mortars decreases the strength of the mortar due to micro cracks in the mortar in the following cycles Figure 4.142.

In cement mortars in which AKS, HKS, WKS and OS admixtures are used, an average of 5.91, 8.45, 5.84 and 9.09 % strength increases were recorded after 30 freeze-thaw cycles, respectively. Wang et al. [343] noted that compressive strength of the graphite tailings cement mortar could increase in 25 freeze-thaw cycles. Liu et al. [344] stated that polycarboxylate cement mortars can gain strength after 25 freeze-thaw cycles. The decrease in strength of the mortars was recorded at freeze-thaw cycles higher than 25 cycles. The reason may be that the original pores inside the specimen were compacted by frost heave force in the early stage of freeze-thaw cycle, so that the strength increased [344]. Also, strength gain can be attributed to the interior of the mortar sample was still coagulating as the curing time was only 28 d, and the cement mortar was still in the healing phase. However, when compared with the reference specimens, while the reference samples lose strength, the strength of the bio-polymeric admixed specimens increased. This indicates that the lignocellulosic bio-polymeric admixtures have a significant positive effect on the freeze-thaw durability of the mortar. In addition, transforming the cement mortar into a more hydrophobic structure ensures that the mortar gains a more durable form in terms of freezing-thawing [345]. In this study, it was determined that the water absorption values of the mortars decreased with the use of lignocellulosic bio-polymeric admixtures. It has been observed that the compressive strength of the mortars, which absorb less water in the freeze-thaw cycle, is better after 30 cycles.

4.5.4 Evaluation of Durability of Cement Mortars

In this thesis, durability analyzes consisting of sulfate effect, acid effect and freeze-thaw effect on cement mortars using bio-polymeric additives were performed. In the durability evaluation of all three groups, it was determined that WKS and OS admixtures could add positive properties to the cement mortar. Due to the high extractive substance content of these admixtures, the hydrophobic feature added to the mortar improves its durability by reducing the absorption of harmful solutions to the mortar. Similarly, with these admixtures, the hydraulic pressure that may occur in freeze-thaw cycles decreases, as the mortar absorbs less water. A graphical

representation of the effect of each bio-polymeric admixture on each durability property is shown between Figure 4.147 and Figure 4.151.

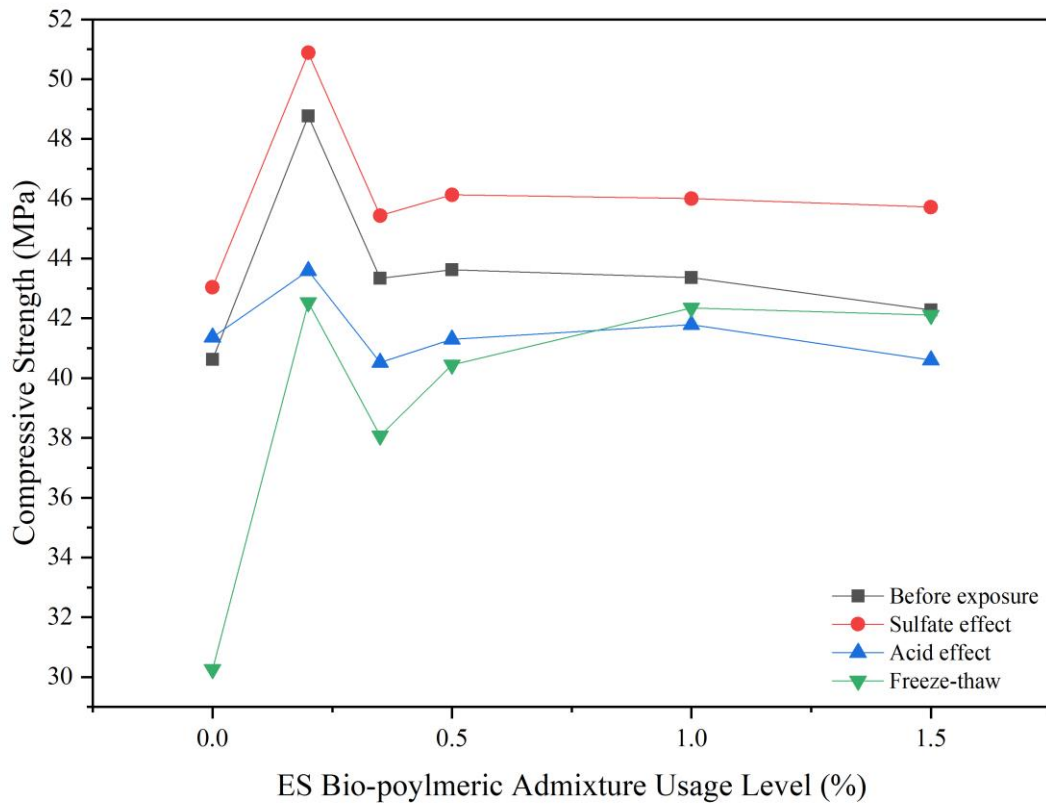


Figure 4.147: Compressive strength changes of cement mortars with ES admixture under different deteriorating effects

When Figure 4.147 is examined, it is observed that the compressive strength of cement mortars with 0 % admixture (reference mortar) after 30 freeze-thaw cycles is the lowest in ES added mortars. The compressive strengths of ES added mortars were below the reference strengths in 30 freeze-thaw, and 30 wetting-drying cycles under the influence of acid. This shows that ES admixture reduces the durability of the mortar against acid attack and freeze-thaw effect.

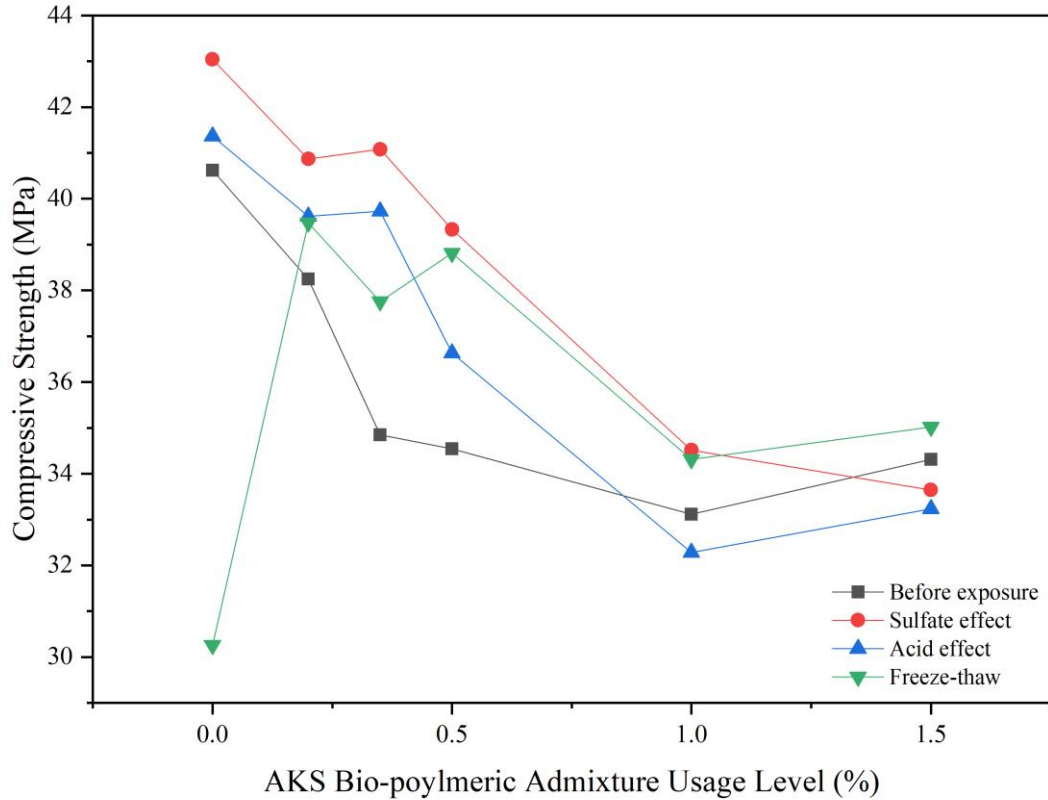


Figure 4.148: Compressive strength changes of cement mortars with AKS admixture under different deteriorating effects

When analyzing Figure 4.148, it can be concluded that the use of 1.5 wt.% AKS indicates that the mortar reduces its resistance to sulfate and acid attack. In addition, the use of 1 wt.% AKS negatively affects the resistance of the mortar against acid attack. The durability of cement mortars improved in 30 wetting-drying cycles under the effect of sulphate and acid, with relatively lower use of admixtures other than those mentioned above. Moreover, it has been found that all proportions of AKS admixture cement mortars improve freeze-thaw durability for 30 cycles. Therefore, AKS admixture can be evaluated in the composition of cement mortars, especially to increase the freeze-thaw resistance.

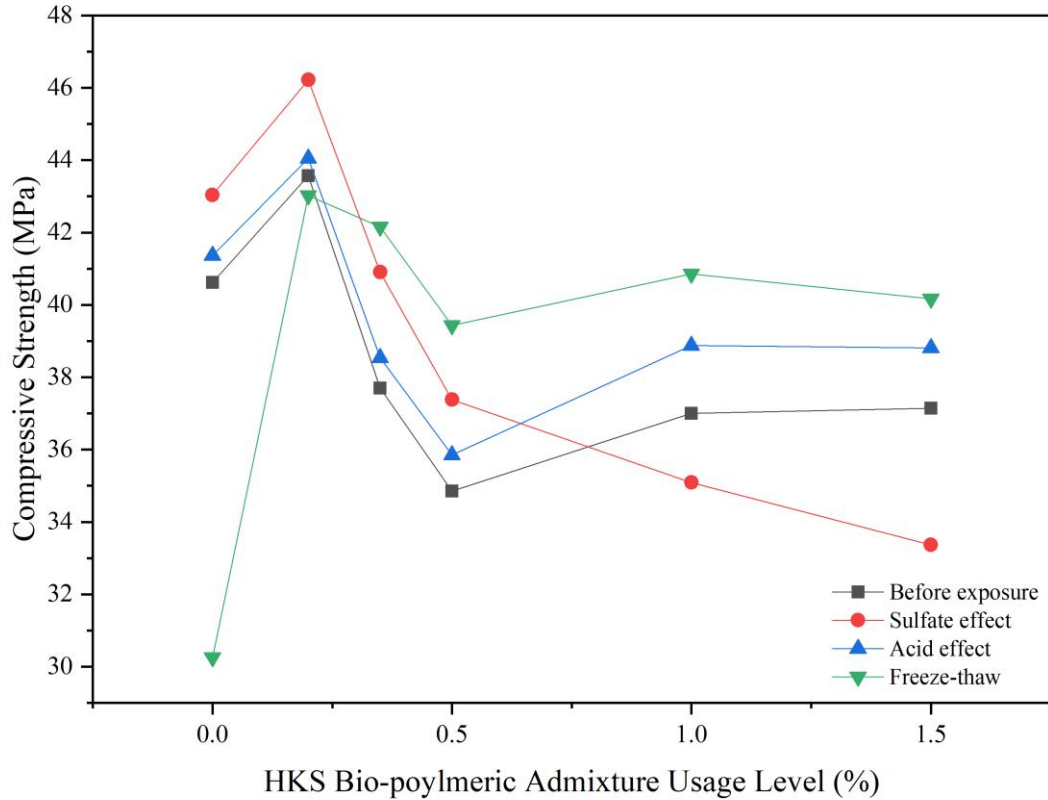


Figure 4.149: Compressive strength changes of cement mortars with HKS admixture under different deteriorating effects

Analyzing Figure 4.149, with the use of 1.0 wt.% and 1.5 w.t% of the HKS admixture, with 30 wetting-drying cycles under the effect of magnesium sulfate, the compressive strengths are lower than the compressive strength of the reference mortar. This means that the resistance of the reference mortar against sulphate is better than that of the cement mortar with high HKS usage. In addition, the use of a low amount of 0.2% reduced the compressive strength under freeze-thaw effect compared to the original compressive strength of the reference mortar. The compressive strength of any of the mortar series produced using HKS admixture remained below the original compressive strengths under the effect of acid solution. For this reason, it can be said that the HKS admixture provides the mortar resistance to sulfuric acid.

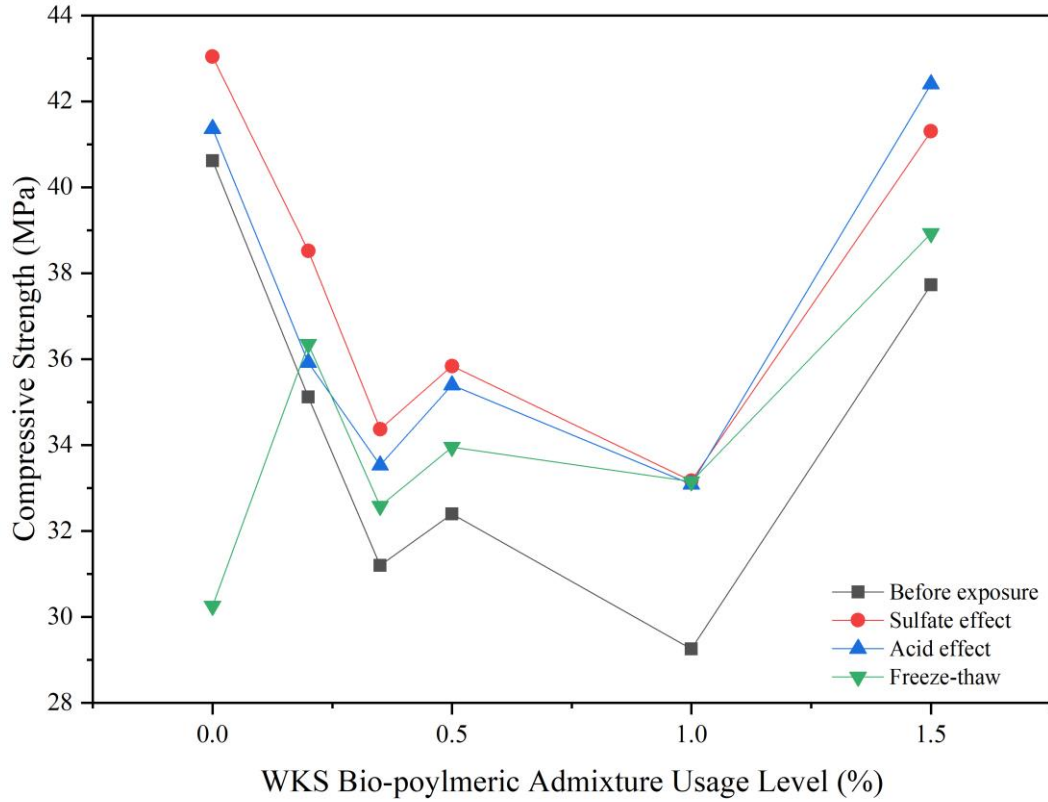


Figure 4.150: Compressive strength changes of cement mortars with WKS admixture under different deteriorating effects

According to the Figure 4.150, WKS admixture added superior durability to cement mortars in all three durability tests for 30 cycles for each. WKS admixed mortars gained strength after all three durability tests. For this reason, considering the number of 30 cycles, it can be said that the WKS admixture adds positive value to the mortar in all three effects.

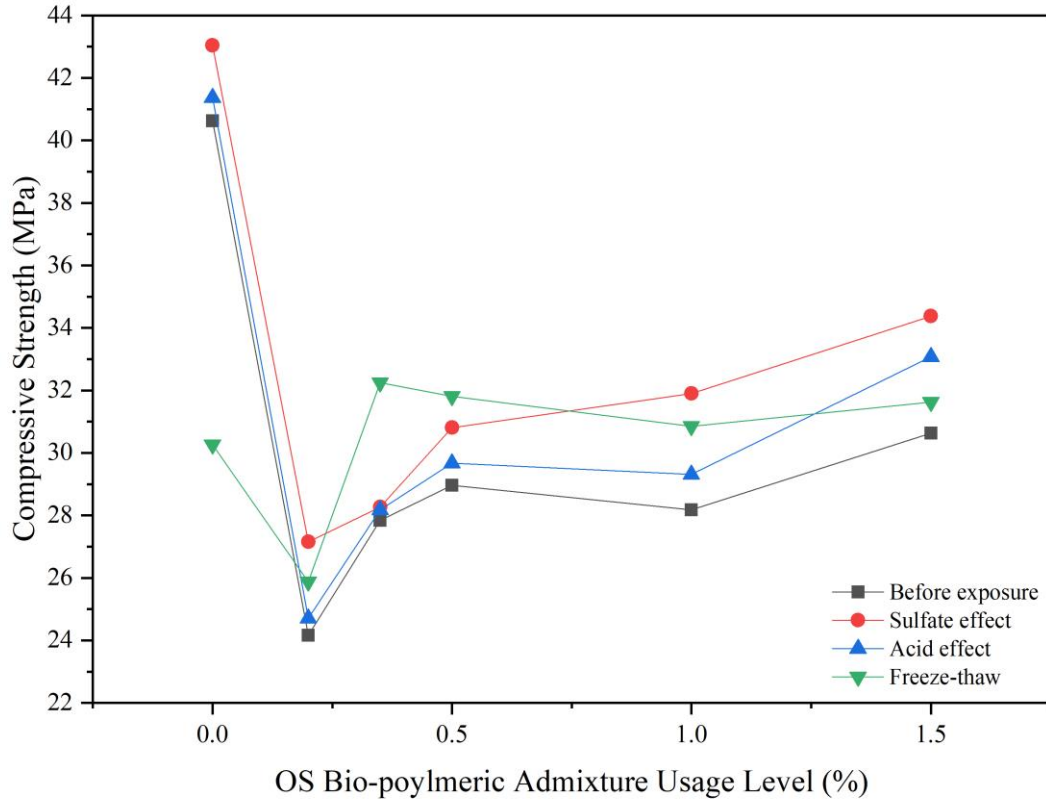


Figure 4.151: Compressive strength changes of cement mortars with OS admixture under different deteriorating effects

According to the Figure 4.151, OS admixture added superior durability to cement mortars in all three durability tests for 30 cycles for each. OS admixed mortars gained strength after all three durability tests. For this reason, considering the number of 30 cycles, it can be said that the OS admixture adds positive value to the mortar in all three effects.

It has been determined that ES admixture can improve the cement mortar against sulfate, AKS admixture against freezing-thawing, HKS admixture against acid, WKS and OS admixtures against all three, considering the number of 30 cycles under the effect of sulfate attack, acid attack and freeze-thaw.

On the other hand, 30 cycles were applied to the test specimens for all three durability analyses. In this number of cycles, higher compressive strengths than the original strength of many specimens were determined, that is, the specimens gained strength. However, it is recommended to extend the duration of the durability tests of bio-polymeric mortars and to test more wetting-drying or freeze-thawing cycles in order to determine in which number of cycles the test specimens begin to lose strength.

4.6 Optimization and Regression Analysis of Test Results

4.6.1 Grey Relational Grade

Flowability, setting times, water absorption, compressive strength and flexural strength parameter optimization was performed via grey relational grade, which is an analysis of a multiple performance characteristics. Optimization analyzes were analyzed in four sections. First, it identifies the best mix design for all of the results obtained as a result of the study. Second, it determines the best mix design in the fresh mortar properties. Third, it determines the best mix design for the hardened mortar properties (strength). Fourth and lastly, it specifies the most suitable mixture design according to the water absorptions known as the simplest durability test. Table 4.24 presents the parameters and their levels utilized in the experimental study, with three levels of grain size of bio-polymeric admixtures, five levels of bio-polymeric admixture type and six levels of usage rate of the bio-polymeric admixtures. Experimental test sequence is shown in the first stage of the optimization study, a multi-response optimization analysis was performed for eight different responses. Experimental test results are shown in Table 4.26.

Table 4.24: Test factors and levels

Factors	Symbol	Level 1	Level 2	Level 3	Level 4	Level 5	Level 6
Grain size (μm)	G	0/45	0/125	125/250			
Type	T	ES	AKS	HKS	WKS	OS	
Usage rate (wt.%)	U	0	0.2	0.35	0.5	1.0	1.5

Table 4.25: Experimental design

Experiment no	G	T	U
1	0/45	ES	0.00
2	0/45	ES	0.20
3	0/45	ES	0.35
4	0/45	ES	0.50
5	0/45	ES	1.00
6	0/45	ES	1.50
7	0/45	AKS	0.00
8	0/45	AKS	0.20
9	0/45	AKS	0.35
10	0/45	AKS	0.50
11	0/45	AKS	1.00
12	0/45	AKS	1.50
13	0/45	HKS	0.00
14	0/45	HKS	0.20
15	0/45	HKS	0.35
16	0/45	HKS	0.50
17	0/45	HKS	1.00
18	0/45	HKS	1.50
19	0/45	WKS	0.00
20	0/45	WKS	0.20
21	0/45	WKS	0.35
22	0/45	WKS	0.50
23	0/45	WKS	1.00
24	0/45	WKS	1.50
25	0/45	OS	0.00
26	0/45	OS	0.20
27	0/45	OS	0.35
28	0/45	OS	0.50
29	0/45	OS	1.00
30	0/45	OS	1.50
31	0/125	ES	0.00
32	0/125	ES	0.20
33	0/125	ES	0.35

Table 4.25 (Continued): Experimental design

Experiment no	G	T	U
34	0/125	ES	0.50
35	0/125	ES	1.00
36	0/125	ES	1.50
37	0/125	AKS	0.00
38	0/125	AKS	0.20
39	0/125	AKS	0.35
40	0/125	AKS	0.50
41	0/125	AKS	1.00
42	0/125	AKS	1.50
43	0/125	HKS	0.00
44	0/125	HKS	0.20
45	0/125	HKS	0.35
46	0/125	HKS	0.50
47	0/125	HKS	1.00
48	0/125	HKS	1.50
49	0/125	WKS	0.00
50	0/125	WKS	0.20
51	0/125	WKS	0.35
52	0/125	WKS	0.50
53	0/125	WKS	1.00
54	0/125	WKS	1.50
55	0/125	OS	0.00
56	0/125	OS	0.20
57	0/125	OS	0.35
58	0/125	OS	0.50
59	0/125	OS	1.00
60	0/125	OS	1.50
61	125/250	ES	0.00
62	125/250	ES	0.20
63	125/250	ES	0.35
64	125/250	ES	0.50
65	125/250	ES	1.00
66	125/250	ES	1.50

Table 4.25 (Continued): Experimental design

Experiment no	Experiment no	Experiment no	Experiment no
67	125/250	AKS	0.00
68	125/250	AKS	0.20
69	125/250	AKS	0.35
70	125/250	AKS	0.50
71	125/250	AKS	1.00
72	125/250	AKS	1.50
73	125/250	HKS	0.00
74	125/250	HKS	0.20
75	125/250	HKS	0.35
76	125/250	HKS	0.50
77	125/250	HKS	1.00
78	125/250	HKS	1.50
79	125/250	WKS	0.00
80	125/250	WKS	0.20
81	125/250	WKS	0.35
82	125/250	WKS	0.50
83	125/250	WKS	1.00
84	125/250	WKS	1.50
85	125/250	OS	0.00
86	125/250	OS	0.20
87	125/250	OS	0.35
88	125/250	OS	0.50
89	125/250	OS	1.00
90	125/250	OS	1.50

In the first stage of the optimization study, a multi-response optimization analysis was performed for eight different responses. Experimental test results are shown in Table 4.26.

Table 4.26: Experimental test results

Exp. No	28d CS (MPa)	150d CS (MPa)	28d FS (MPa)	Flow (mm)	Initial Set (min)	Final Set (min)	Capillary water abs. (g/cm ² .min ^{0.5})	Mass Water Abs. (%)
1	35.06	46.05	7.32	120.36	90.00	235.00	0.60	6.84
2	36.42	47.87	7.37	125.25	105.00	155.00	0.64	6.34
3	32.65	42.92	7.36	128.75	105.00	160.00	0.67	5.16
4	32.54	41.66	7.14	129.00	110.00	160.00	0.79	5.48
5	32.48	40.02	7.11	128.13	115.00	160.00	0.70	5.82
6	29.24	37.33	6.73	125.13	105.00	175.00	0.68	6.84
7	35.06	46.05	7.32	120.36	90.00	235.00	0.60	6.84
8	34.09	44.95	5.58	130.00	70.00	140.00	0.61	4.32
9	32.55	41.15	5.29	130.75	165.00	215.00	0.62	4.22
10	32.48	40.52	4.81	131.75	145.00	245.00	0.62	4.18
11	32.42	37.60	4.68	119.75	95.00	265.00	0.63	3.86
12	29.11	37.54	4.74	114.00	45.00	200.00	0.83	3.44
13	35.06	46.05	7.32	120.36	90.00	235.00	0.60	6.84
14	30.90	47.19	6.73	123.63	100.00	175.00	1.00	6.46
15	31.38	45.13	6.69	132.00	105.00	180.00	0.79	5.32
16	32.48	44.39	6.70	123.88	125.00	205.00	0.75	4.60
17	31.82	41.06	6.32	117.25	95.00	180.00	0.61	3.26
18	30.99	40.58	6.02	109.50	50.00	155.00	0.55	3.20
19	35.06	46.05	7.32	120.36	90.00	235.00	0.60	6.84
20	29.90	37.52	4.11	138.13	205.00	315.00	0.50	3.82
21	27.07	35.12	4.40	138.75	220.00	325.00	0.54	3.32
22	28.63	34.45	4.78	139.63	260.00	405.00	0.60	2.88
23	29.54	37.69	4.79	117.75	95.00	345.00	0.62	2.32
24	30.50	40.40	4.82	104.00	75.00	165.00	0.65	2.12
25	35.06	46.05	7.32	120.36	90.00	235.00	0.60	6.84
26	19.44	22.68	4.65	137.50	100.00	275.00	0.54	3.14
27	22.04	29.63	4.18	147.00	215.00	315.00	0.52	2.92
28	22.64	29.89	4.04	141.50	200.00	345.00	0.49	2.44
29	26.34	38.57	4.45	131.00	115.00	340.00	0.44	2.38
30	29.34	40.59	4.52	112.75	90.00	300.00	0.34	2.18
31	35.06	46.05	7.32	120.36	90.00	235.00	0.60	6.84

Table 4.26 (Continued): Experimental test results

Exp. No	28d CS (MPa)	150d CS (MPa)	28d FS (MPa)	Flow (mm)	Initial Set (min)	Final Set (min)	Capillary water abs. (g/cm ² .min ^{0.5})	Mass Water Abs. (%)
32	38.84	51.50	7.50	131.13	95.00	245.00	0.72	6.61
33	38.63	50.50	7.54	130.15	105.00	230.00	0.82	6.56
34	38.51	49.32	7.39	132.90	110.00	230.00	0.90	6.43
35	35.82	49.11	7.31	134.80	105.00	255.00	0.81	6.20
36	33.69	40.22	6.47	128.00	110.00	245.00	0.86	6.20
37	35.06	46.05	7.32	120.36	90.00	235.00	0.60	6.84
38	34.99	47.89	6.85	143.29	165.00	295.00	0.41	6.59
39	33.23	44.60	6.55	142.08	190.00	320.00	0.33	6.22
40	32.36	40.50	6.53	140.81	220.00	365.00	0.32	6.06
41	32.11	36.90	6.41	139.86	220.00	415.00	0.30	5.94
42	31.48	35.01	5.81	121.10	50.00	280.00	0.31	5.93
43	35.06	46.05	7.32	120.36	90.00	235.00	0.60	6.84
44	35.14	46.90	6.27	122.63	160.00	220.00	0.29	5.55
45	26.93	38.25	6.15	122.79	185.00	240.00	0.23	4.99
46	26.12	35.80	5.76	123.50	170.00	295.00	0.16	4.81
47	26.70	35.90	5.68	121.83	110.00	310.00	0.15	3.66
48	26.35	35.60	5.41	118.11	100.00	300.00	0.17	3.61
49	35.06	46.05	7.32	120.36	90.00	235.00	0.60	6.84
50	27.33	34.23	3.55	163.80	250.00	400.00	0.48	6.23
51	25.09	33.33	3.50	155.25	260.00	525.00	0.36	5.99
52	26.78	35.10	3.25	152.94	315.00	585.00	0.27	6.03
53	31.22	39.54	5.58	135.16	85.00	395.00	0.30	6.00
54	34.95	41.59	6.28	127.85	70.00	230.00	0.33	5.98
55	35.06	46.05	7.32	120.36	90.00	235.00	0.60	6.84
56	19.01	29.00	2.61	149.17	220.00	300.00	0.21	4.81
57	23.22	33.00	3.07	157.76	295.00	390.00	0.13	4.65
58	24.30	36.50	5.38	159.06	320.00	435.00	0.10	4.55
59	29.15	39.67	5.42	146.61	275.00	570.00	0.10	3.30
60	29.68	51.00	5.46	126.51	135.00	475.00	0.15	2.29
61	35.06	46.05	7.32	120.36	90.00	235.00	0.60	6.84
62	35.35	41.11	6.77	123.25	110.00	230.00	0.33	6.40

Table 4.26 (Continued): Experimental test results

Exp. No	28d CS (MPa)	150d CS (MPa)	28d FS (MPa)	Flow (mm)	Initial Set (min)	Final Set (min)	Capillary water abs. (g/cm ² .min ^{0.5})	Mass Water Abs. (%)
63	34.38	40.31	6.52	123.75	95.00	225.00	0.43	7.08
64	34.19	39.67	6.48	117.50	95.00	180.00	0.51	7.68
65	29.66	39.96	6.45	113.00	60.00	160.00	0.49	7.02
66	24.84	36.46	6.41	111.50	65.00	150.00	0.50	6.58
67	35.06	46.05	7.32	120.36	90.00	235.00	0.60	6.84
68	35.55	46.47	7.33	116.00	115.00	190.00	0.38	7.34
69	35.85	47.52	7.35	114.25	125.00	170.00	0.41	6.34
70	35.99	47.53	7.39	114.00	140.00	210.00	0.42	5.44
71	37.98	47.49	7.47	112.00	95.00	215.00	0.45	5.04
72	38.72	48.78	7.56	110.00	65.00	215.00	0.46	4.60
73	35.06	46.05	7.32	120.36	90.00	235.00	0.60	6.84
74	36.66	47.00	7.44	118.50	90.00	205.00	0.27	6.44
75	36.63	46.59	7.41	116.50	95.00	200.00	0.34	6.00
76	35.86	44.24	7.33	114.25	90.00	180.00	0.35	5.88
77	34.90	40.18	6.74	111.50	85.00	170.00	0.38	4.52
78	27.72	32.42	5.78	110.00	45.00	140.00	0.40	3.70
79	35.06	46.05	7.32	120.36	90.00	235.00	0.60	6.84
80	34.88	44.34	6.97	118.00	100.00	235.00	0.44	6.80
81	35.72	40.61	6.79	117.00	95.00	235.00	0.49	5.86
82	35.56	39.90	5.88	112.50	60.00	250.00	0.53	5.78
83	30.25	35.74	5.26	109.50	40.00	155.00	0.63	5.88
84	25.79	30.82	4.31	105.00	15.00	100.00	0.67	6.28
85	35.06	46.05	7.32	120.36	90.00	235.00	0.60	6.84
86	29.15	33.23	6.50	135.50	165.00	250.00	0.55	6.12
87	23.10	31.44	6.01	136.00	185.00	285.00	0.56	4.52
88	19.73	25.08	5.70	141.50	205.00	300.00	0.57	3.62
89	21.67	24.42	5.50	144.00	265.00	370.00	0.57	3.32
90	22.44	29.82	5.70	129.25	95.00	325.00	0.55	2.80

The normalized experimental test results are given in Table 4.30. While creating this table, 28-day compressive strength, 150-day compressive strength, 28-day flexural strength, flowability value, initial and final setting times were maximized according to

Equation (3.5). In the table, capillary water absorption and water absorption by mass are minimized using Equation (3.4). As examples, the calculation of the maximized and minimized values for 28-day compressive strength and mass water absorption of experiment 1 are $(35.06-19.01)/(38.84/19.01)=0.81$ and $(7.68-6.84)/(7.68-2.12)=0.15$.

Table 4.27: Comparability sequence of experimental test results

Exp. No	28d CS (MPa)	150d CS (MPa)	28d FS (MPa)	Flow (mm)	Initial Set (min)	Final Set (min)	Capillary water abs. (g/cm ² .min ^{0.5})	Mass Water Abs. (%)
1	0.81	0.81	0.95	0.27	0.25	0.28	0.44	0.15
2	0.88	0.87	0.96	0.36	0.30	0.11	0.40	0.24
3	0.69	0.70	0.96	0.41	0.30	0.12	0.37	0.45
4	0.68	0.66	0.92	0.42	0.31	0.12	0.23	0.40
5	0.68	0.60	0.91	0.40	0.33	0.12	0.33	0.33
6	0.52	0.51	0.83	0.35	0.30	0.15	0.36	0.15
7	0.81	0.81	0.95	0.27	0.25	0.28	0.44	0.15
8	0.76	0.77	0.60	0.43	0.18	0.08	0.43	0.60
9	0.68	0.64	0.54	0.45	0.49	0.24	0.42	0.62
10	0.68	0.62	0.44	0.46	0.43	0.30	0.42	0.63
11	0.68	0.52	0.42	0.26	0.26	0.34	0.41	0.69
12	0.51	0.52	0.43	0.17	0.10	0.21	0.19	0.76
13	0.81	0.81	0.95	0.27	0.25	0.28	0.44	0.15
14	0.60	0.85	0.83	0.33	0.28	0.15	0.00	0.22
15	0.62	0.78	0.82	0.47	0.30	0.16	0.23	0.42
16	0.68	0.75	0.83	0.33	0.36	0.22	0.28	0.55
17	0.65	0.64	0.75	0.22	0.26	0.16	0.43	0.79
18	0.60	0.62	0.69	0.09	0.11	0.11	0.50	0.81
19	0.81	0.81	0.95	0.27	0.25	0.28	0.44	0.15
20	0.55	0.51	0.30	0.57	0.62	0.44	0.56	0.69
21	0.41	0.43	0.36	0.58	0.67	0.46	0.51	0.78
22	0.49	0.41	0.44	0.60	0.80	0.63	0.44	0.86
23	0.53	0.52	0.44	0.23	0.26	0.51	0.42	0.96
24	0.58	0.61	0.45	0.00	0.20	0.13	0.39	1.00
25	0.81	0.81	0.95	0.27	0.25	0.28	0.44	0.15
26	0.02	0.00	0.41	0.56	0.28	0.36	0.51	0.82

Table 4.27 (Continued): Comparability sequence of experimental test results

Exp. No	28d CS (MPa)	150d CS (MPa)	28d FS (MPa)	Flow (mm)	Initial Set (min)	Final Set (min)	Capillary water abs. (g/cm ² .min ^{0.5})	Mass Water Abs. (%)
27	0.15	0.24	0.32	0.72	0.66	0.44	0.53	0.86
28	0.18	0.25	0.29	0.63	0.61	0.51	0.57	0.94
29	0.37	0.55	0.37	0.45	0.33	0.49	0.62	0.95
30	0.52	0.62	0.39	0.15	0.25	0.41	0.73	0.99
31	0.81	0.81	0.95	0.27	0.25	0.28	0.44	0.15
32	1.00	1.00	0.99	0.45	0.26	0.30	0.31	0.19
33	0.99	0.97	1.00	0.44	0.30	0.27	0.20	0.20
34	0.98	0.92	0.97	0.48	0.31	0.27	0.11	0.22
35	0.85	0.92	0.95	0.52	0.30	0.32	0.21	0.27
36	0.74	0.61	0.78	0.40	0.31	0.30	0.16	0.27
37	0.81	0.81	0.95	0.27	0.25	0.28	0.44	0.15
38	0.81	0.87	0.86	0.66	0.49	0.40	0.66	0.20
39	0.72	0.76	0.80	0.64	0.57	0.45	0.74	0.26
40	0.67	0.62	0.79	0.62	0.67	0.55	0.76	0.29
41	0.66	0.49	0.77	0.60	0.67	0.65	0.78	0.31
42	0.63	0.43	0.65	0.29	0.11	0.37	0.77	0.31
43	0.81	0.81	0.95	0.27	0.25	0.28	0.44	0.15
44	0.81	0.84	0.74	0.31	0.48	0.25	0.79	0.38
45	0.40	0.54	0.72	0.31	0.56	0.29	0.86	0.48
46	0.36	0.46	0.64	0.33	0.51	0.40	0.93	0.52
47	0.39	0.46	0.62	0.30	0.31	0.43	0.94	0.72
48	0.37	0.45	0.57	0.24	0.28	0.41	0.92	0.73
49	0.81	0.81	0.95	0.27	0.25	0.28	0.44	0.15
50	0.42	0.40	0.19	1.00	0.77	0.62	0.58	0.26
51	0.31	0.37	0.18	0.86	0.80	0.88	0.71	0.30
52	0.39	0.43	0.13	0.82	0.98	1.00	0.81	0.30
53	0.62	0.59	0.60	0.52	0.23	0.61	0.78	0.30
54	0.80	0.66	0.74	0.40	0.18	0.27	0.74	0.31
55	0.81	0.81	0.95	0.27	0.25	0.28	0.44	0.15
56	0.00	0.22	0.00	0.76	0.67	0.41	0.88	0.52
57	0.21	0.36	0.09	0.90	0.92	0.60	0.97	0.54

Table 4.27 (Continued): Comparability sequence of experimental test results

Exp. No	28d CS (MPa)	150d CS (MPa)	28d FS (MPa)	Flow (mm)	Initial Set (min)	Final Set (min)	Capillary water abs. (g/cm ² .min ^{0.5})	Mass Water Abs.(%)
58	0.27	0.48	0.56	0.92	1.00	0.69	1.00	0.56
59	0.51	0.59	0.57	0.71	0.85	0.97	1.00	0.79
60	0.54	0.98	0.58	0.38	0.39	0.77	0.94	0.97
61	0.81	0.81	0.95	0.27	0.25	0.28	0.44	0.15
62	0.82	0.64	0.84	0.32	0.31	0.27	0.74	0.23
63	0.78	0.61	0.79	0.33	0.26	0.26	0.63	0.11
64	0.77	0.59	0.78	0.23	0.26	0.16	0.54	0.00
65	0.54	0.60	0.78	0.15	0.15	0.12	0.57	0.12
66	0.29	0.48	0.77	0.13	0.16	0.10	0.56	0.20
67	0.81	0.81	0.95	0.27	0.25	0.28	0.44	0.15
68	0.83	0.83	0.95	0.20	0.33	0.19	0.69	0.06
69	0.85	0.86	0.96	0.17	0.36	0.14	0.66	0.24
70	0.86	0.86	0.97	0.17	0.41	0.23	0.64	0.40
71	0.96	0.86	0.98	0.13	0.26	0.24	0.61	0.47
72	0.99	0.91	1.00	0.10	0.16	0.24	0.60	0.55
73	0.81	0.81	0.95	0.27	0.25	0.28	0.44	0.15
74	0.89	0.84	0.98	0.24	0.25	0.22	0.81	0.22
75	0.89	0.83	0.97	0.21	0.26	0.21	0.73	0.30
76	0.85	0.75	0.95	0.17	0.25	0.16	0.72	0.32
77	0.80	0.61	0.83	0.13	0.23	0.14	0.69	0.57
78	0.44	0.34	0.64	0.10	0.10	0.08	0.67	0.72
79	0.81	0.81	0.95	0.27	0.25	0.28	0.44	0.15
80	0.80	0.75	0.88	0.23	0.28	0.28	0.62	0.16
81	0.84	0.62	0.84	0.22	0.26	0.28	0.57	0.33
82	0.83	0.60	0.66	0.14	0.15	0.31	0.52	0.34
83	0.57	0.45	0.54	0.09	0.08	0.11	0.41	0.32
84	0.34	0.28	0.34	0.02	0.00	0.00	0.37	0.25
85	0.81	0.81	0.95	0.27	0.25	0.28	0.44	0.15
86	0.51	0.37	0.79	0.53	0.49	0.31	0.50	0.28
87	0.21	0.30	0.69	0.54	0.56	0.38	0.49	0.57
88	0.04	0.08	0.62	0.63	0.62	0.41	0.48	0.73
89	0.13	0.06	0.58	0.67	0.82	0.56	0.48	0.78
90	0.17	0.25	0.62	0.42	0.26	0.46	0.50	0.88

The deviation sequence of experimental test results is given in Table 4.28. Deviation sequence is obtained by subtracting comparability sequence values from 1 in absolute value. As examples, the calculation of the deviation sequence values for 28-day compressive strength and mass water absorption of experiment 1 are $|1-0.81|=0.19$ and $|1-0.15|=0.85$.

Table 4.28: Deviation sequence of experimental test results

Exp. No	28d CS (MPa)	150d CS (MPa)	28d FS (MPa)	Flow (mm)	Initial Set (min)	Final Set (min)	Capillary water abs. (g/cm ² .min ^{0.5})	Mass Water Abs. (%)
1	0.19	0.19	0.05	0.73	0.75	0.72	0.56	0.85
2	0.12	0.13	0.04	0.64	0.70	0.89	0.60	0.76
3	0.31	0.30	0.04	0.59	0.70	0.88	0.63	0.55
4	0.32	0.34	0.08	0.58	0.69	0.88	0.77	0.60
5	0.32	0.40	0.09	0.60	0.67	0.88	0.67	0.67
6	0.48	0.49	0.17	0.65	0.70	0.85	0.64	0.85
7	0.19	0.19	0.05	0.73	0.75	0.72	0.56	0.85
8	0.24	0.23	0.40	0.57	0.82	0.92	0.57	0.40
9	0.32	0.36	0.46	0.55	0.51	0.76	0.58	0.38
10	0.32	0.38	0.56	0.54	0.57	0.70	0.58	0.37
11	0.32	0.48	0.58	0.74	0.74	0.66	0.59	0.31
12	0.49	0.48	0.57	0.83	0.90	0.79	0.81	0.24
13	0.19	0.19	0.05	0.73	0.75	0.72	0.56	0.85
14	0.40	0.15	0.17	0.67	0.72	0.85	1.00	0.78
15	0.38	0.22	0.18	0.53	0.70	0.84	0.77	0.58
16	0.32	0.25	0.17	0.67	0.64	0.78	0.72	0.45
17	0.35	0.36	0.25	0.78	0.74	0.84	0.57	0.21
18	0.40	0.38	0.31	0.91	0.89	0.89	0.50	0.19
19	0.19	0.19	0.05	0.73	0.75	0.72	0.56	0.85
20	0.45	0.49	0.70	0.43	0.38	0.56	0.44	0.31
21	0.59	0.57	0.64	0.42	0.33	0.54	0.49	0.22
22	0.51	0.59	0.56	0.40	0.20	0.37	0.56	0.14
23	0.47	0.48	0.56	0.77	0.74	0.49	0.58	0.04
24	0.42	0.39	0.55	1.00	0.80	0.87	0.61	0.00
25	0.19	0.19	0.05	0.73	0.75	0.72	0.56	0.85

Table 4.28 (Continued): Deviation sequence of experimental test results

Exp. No	28d CS (MPa)	150d CS (MPa)	28d FS (MPa)	Flow (mm)	Initial Set (min)	Final Set (min)	Capillary water abs. (g/cm ² .min ^{0.5})	Mass Water Abs.(%)
26	0.98	1.00	0.59	0.44	0.72	0.64	0.49	0.18
27	0.85	0.76	0.68	0.28	0.34	0.56	0.47	0.14
28	0.82	0.75	0.71	0.37	0.39	0.49	0.43	0.06
29	0.63	0.45	0.63	0.55	0.67	0.51	0.38	0.05
30	0.48	0.38	0.61	0.85	0.75	0.59	0.27	0.01
31	0.19	0.19	0.05	0.73	0.75	0.72	0.56	0.85
32	0.00	0.00	0.01	0.55	0.74	0.70	0.69	0.81
33	0.01	0.03	0.00	0.56	0.70	0.73	0.80	0.80
34	0.02	0.08	0.03	0.52	0.69	0.73	0.89	0.78
35	0.15	0.08	0.05	0.48	0.70	0.68	0.79	0.73
36	0.26	0.39	0.22	0.60	0.69	0.70	0.84	0.73
37	0.19	0.19	0.05	0.73	0.75	0.72	0.56	0.85
38	0.19	0.13	0.14	0.34	0.51	0.60	0.34	0.80
39	0.28	0.24	0.20	0.36	0.43	0.55	0.26	0.74
40	0.33	0.38	0.21	0.38	0.33	0.45	0.24	0.71
41	0.34	0.51	0.23	0.40	0.33	0.35	0.22	0.69
42	0.37	0.57	0.35	0.71	0.89	0.63	0.23	0.69
43	0.19	0.19	0.05	0.73	0.75	0.72	0.56	0.85
44	0.19	0.16	0.26	0.69	0.52	0.75	0.21	0.62
45	0.60	0.46	0.28	0.69	0.44	0.71	0.14	0.52
46	0.64	0.54	0.36	0.67	0.49	0.60	0.07	0.48
47	0.61	0.54	0.38	0.70	0.69	0.57	0.06	0.28
48	0.63	0.55	0.43	0.76	0.72	0.59	0.08	0.27
49	0.19	0.19	0.05	0.73	0.75	0.72	0.56	0.85
50	0.58	0.60	0.81	0.00	0.23	0.38	0.42	0.74
51	0.69	0.63	0.82	0.14	0.20	0.12	0.29	0.70
52	0.61	0.57	0.87	0.18	0.02	0.00	0.19	0.70
53	0.38	0.41	0.40	0.48	0.77	0.39	0.22	0.70
54	0.20	0.34	0.26	0.60	0.82	0.73	0.26	0.69
55	0.19	0.19	0.05	0.73	0.75	0.72	0.56	0.85
56	1.00	0.78	1.00	0.24	0.33	0.59	0.12	0.48
57	0.79	0.64	0.91	0.10	0.08	0.40	0.03	0.46

Table 4.28 (Continued): Deviation sequence of experimental test results

Exp. No	28d CS (MPa)	150d CS (MPa)	28d FS (MPa)	Flow (mm)	Initial Set (min)	Final Set (min)	Capillary water abs. (g/cm ² .min ^{0.5})	Mass Water Abs.(%)
58	0.73	0.52	0.44	0.08	0.00	0.31	0.00	0.44
59	0.49	0.41	0.43	0.29	0.15	0.03	0.00	0.21
60	0.46	0.02	0.42	0.62	0.61	0.23	0.06	0.03
61	0.19	0.19	0.05	0.73	0.75	0.72	0.56	0.85
62	0.18	0.36	0.16	0.68	0.69	0.73	0.26	0.77
63	0.22	0.39	0.21	0.67	0.74	0.74	0.37	0.89
64	0.23	0.41	0.22	0.77	0.74	0.84	0.46	1.00
65	0.46	0.40	0.22	0.85	0.85	0.88	0.43	0.88
66	0.71	0.52	0.23	0.87	0.84	0.90	0.44	0.80
67	0.19	0.19	0.05	0.73	0.75	0.72	0.56	0.85
68	0.17	0.17	0.05	0.80	0.67	0.81	0.31	0.94
69	0.15	0.14	0.04	0.83	0.64	0.86	0.34	0.76
70	0.14	0.14	0.03	0.83	0.59	0.77	0.36	0.60
71	0.04	0.14	0.02	0.87	0.74	0.76	0.39	0.53
72	0.01	0.09	0.00	0.90	0.84	0.76	0.40	0.45
73	0.19	0.19	0.05	0.73	0.75	0.72	0.56	0.85
74	0.11	0.16	0.02	0.76	0.75	0.78	0.19	0.78
75	0.11	0.17	0.03	0.79	0.74	0.79	0.27	0.70
76	0.15	0.25	0.05	0.83	0.75	0.84	0.28	0.68
77	0.20	0.39	0.17	0.87	0.77	0.86	0.31	0.43
78	0.56	0.66	0.36	0.90	0.90	0.92	0.33	0.28
79	0.19	0.19	0.05	0.73	0.75	0.72	0.56	0.85
80	0.20	0.25	0.12	0.77	0.72	0.72	0.38	0.84
81	0.16	0.38	0.16	0.78	0.74	0.72	0.43	0.67
82	0.17	0.40	0.34	0.86	0.85	0.69	0.48	0.66
83	0.43	0.55	0.46	0.91	0.92	0.89	0.59	0.68
84	0.66	0.72	0.66	0.98	1.00	1.00	0.63	0.75
85	0.19	0.19	0.05	0.73	0.75	0.72	0.56	0.85
86	0.49	0.63	0.21	0.47	0.51	0.69	0.50	0.72
87	0.79	0.70	0.31	0.46	0.44	0.62	0.51	0.43
88	0.96	0.92	0.38	0.37	0.38	0.59	0.52	0.27
89	0.87	0.94	0.42	0.33	0.18	0.44	0.52	0.22
90	0.83	0.75	0.38	0.58	0.74	0.54	0.50	0.12

Grey relation coefficient of experimental test results is shown in Table 4.29. Grey relation coefficient is calculated by Equation (3.8) with the “ ζ ” weight factor determined by the Analytical Hierarchy Method in this equation taken to be 0.10, 0.10, 0.10, 0.15, 0.15, 0.15, 0.15 and 0.10 for 28-day compressive strength, 150-day compressive strength, 28-day flexural strength, flowability value, initial setting time, final setting times, capillary water absorption and water absorption, respectively. As examples, the calculation of the grey relation coefficient values for 28-day compressive strength and mass water absorption of experiment 1 are $(0+0.10)/(0.19+0.10)=0.34$ and $(0+0.10)/(0.85+0.10)=0.11$.

Table 4.29: Grey relation coefficient of experimental test results

Exp. No	28d CS (MPa)	150d CS (MPa)	28d FS (MPa)	Flow (mm)	Initial Set (min)	Final Set (min)	Capillary water abs. (g/cm ² .min ^{0.5})	Mass Water Abs.(%)
1	0.34	0.35	0.67	0.17	0.17	0.17	0.21	0.11
2	0.45	0.44	0.72	0.19	0.18	0.14	0.20	0.12
3	0.24	0.25	0.71	0.20	0.18	0.15	0.19	0.15
4	0.24	0.23	0.54	0.20	0.18	0.15	0.16	0.14
5	0.24	0.20	0.52	0.20	0.18	0.15	0.18	0.13
6	0.17	0.17	0.37	0.19	0.18	0.15	0.19	0.11
7	0.34	0.35	0.67	0.17	0.17	0.17	0.21	0.11
8	0.29	0.31	0.20	0.21	0.15	0.14	0.21	0.20
9	0.24	0.22	0.18	0.21	0.23	0.16	0.21	0.21
10	0.24	0.21	0.15	0.22	0.21	0.18	0.21	0.21
11	0.24	0.17	0.15	0.17	0.17	0.19	0.20	0.24
12	0.17	0.17	0.15	0.15	0.14	0.16	0.16	0.30
13	0.34	0.35	0.67	0.17	0.17	0.17	0.21	0.11
14	0.20	0.40	0.37	0.18	0.17	0.15	0.13	0.11
15	0.21	0.31	0.36	0.22	0.18	0.15	0.16	0.15
16	0.24	0.29	0.37	0.18	0.19	0.16	0.17	0.18
17	0.22	0.22	0.29	0.16	0.17	0.15	0.21	0.33
18	0.20	0.21	0.24	0.14	0.14	0.14	0.23	0.34
19	0.34	0.35	0.67	0.17	0.17	0.17	0.21	0.11
20	0.18	0.17	0.13	0.26	0.28	0.21	0.25	0.25

Table 4.29 (Continued): Grey relation coefficient of experimental test results

Exp. No	28d CS (MPa)	150d CS (MPa)	28d FS (MPa)	Flow (mm)	Initial Set (min)	Final Set (min)	Capillary water abs. (g/cm ² .min ^{0.5})	Mass Water Abs.(%)
21	0.14	0.15	0.14	0.26	0.31	0.22	0.23	0.32
22	0.16	0.14	0.15	0.27	0.43	0.29	0.21	0.42
23	0.18	0.17	0.15	0.16	0.17	0.23	0.21	0.74
24	0.19	0.21	0.15	0.13	0.16	0.15	0.20	1.00
25	0.34	0.35	0.67	0.17	0.17	0.17	0.21	0.11
26	0.09	0.09	0.15	0.25	0.17	0.19	0.23	0.35
27	0.11	0.12	0.13	0.35	0.30	0.21	0.24	0.41
28	0.11	0.12	0.12	0.29	0.28	0.23	0.26	0.63
29	0.14	0.18	0.14	0.21	0.18	0.23	0.28	0.68
30	0.17	0.21	0.14	0.15	0.17	0.20	0.36	0.90
31	0.34	0.35	0.67	0.17	0.17	0.17	0.21	0.11
32	1.00	1.00	0.89	0.22	0.17	0.18	0.18	0.11
33	0.90	0.74	0.96	0.21	0.18	0.17	0.16	0.11
34	0.86	0.57	0.74	0.22	0.18	0.17	0.14	0.11
35	0.40	0.55	0.66	0.24	0.18	0.18	0.16	0.12
36	0.28	0.20	0.31	0.20	0.18	0.18	0.15	0.12
37	0.34	0.35	0.67	0.17	0.17	0.17	0.21	0.11
38	0.34	0.44	0.41	0.30	0.23	0.20	0.30	0.11
39	0.26	0.29	0.33	0.29	0.26	0.22	0.37	0.12
40	0.23	0.21	0.32	0.28	0.31	0.25	0.38	0.12
41	0.23	0.16	0.30	0.27	0.31	0.30	0.40	0.13
42	0.21	0.15	0.22	0.17	0.14	0.19	0.39	0.13
43	0.34	0.35	0.67	0.17	0.17	0.17	0.21	0.11
44	0.35	0.39	0.28	0.18	0.22	0.17	0.42	0.14
45	0.14	0.18	0.26	0.18	0.25	0.17	0.51	0.16
46	0.13	0.16	0.22	0.18	0.23	0.20	0.69	0.17
47	0.14	0.16	0.21	0.18	0.18	0.21	0.73	0.27
48	0.14	0.15	0.19	0.16	0.17	0.20	0.66	0.27
49	0.34	0.35	0.67	0.17	0.17	0.17	0.21	0.11
50	0.15	0.14	0.11	1.00	0.40	0.28	0.26	0.12
51	0.13	0.14	0.11	0.51	0.43	0.55	0.34	0.13
52	0.14	0.15	0.10	0.45	0.90	1.00	0.44	0.12

Table 4.29 (Continued): Grey relation coefficient of experimental test results

Exp. No	28d CS (MPa)	150d CS (MPa)	28d FS (MPa)	Flow (mm)	Initial Set (min)	Final Set (min)	Capillary water abs. (g/cm ² .min ^{0.5})	Mass Water Abs.(%)
53	0.21	0.19	0.20	0.24	0.16	0.28	0.40	0.13
54	0.34	0.23	0.28	0.20	0.15	0.17	0.37	0.13
55	0.34	0.35	0.67	0.17	0.17	0.17	0.21	0.11
56	0.09	0.11	0.09	0.38	0.31	0.20	0.55	0.17
57	0.11	0.13	0.10	0.60	0.65	0.27	0.82	0.18
58	0.12	0.16	0.19	0.65	1.00	0.33	1.00	0.19
59	0.17	0.20	0.19	0.34	0.50	0.83	1.00	0.32
60	0.18	0.85	0.19	0.19	0.20	0.40	0.73	0.77
61	0.34	0.35	0.67	0.17	0.17	0.17	0.21	0.11
62	0.36	0.22	0.39	0.18	0.18	0.17	0.37	0.11
63	0.31	0.20	0.32	0.18	0.17	0.17	0.29	0.10
64	0.30	0.20	0.31	0.16	0.17	0.15	0.25	0.09
65	0.18	0.20	0.31	0.15	0.15	0.15	0.26	0.10
66	0.12	0.16	0.30	0.15	0.15	0.14	0.25	0.11
67	0.34	0.35	0.67	0.17	0.17	0.17	0.21	0.11
68	0.38	0.36	0.68	0.16	0.18	0.16	0.33	0.10
69	0.40	0.42	0.70	0.15	0.19	0.15	0.30	0.12
70	0.41	0.42	0.74	0.15	0.20	0.16	0.30	0.14
71	0.70	0.42	0.85	0.15	0.17	0.16	0.28	0.16
72	0.94	0.51	1.00	0.14	0.15	0.16	0.27	0.18
73	0.34	0.35	0.67	0.17	0.17	0.17	0.21	0.11
74	0.48	0.39	0.80	0.17	0.17	0.16	0.44	0.11
75	0.47	0.37	0.77	0.16	0.17	0.16	0.36	0.13
76	0.40	0.28	0.68	0.15	0.17	0.15	0.35	0.13
77	0.33	0.20	0.38	0.15	0.16	0.15	0.33	0.19
78	0.15	0.13	0.22	0.14	0.14	0.14	0.31	0.26
79	0.34	0.35	0.67	0.17	0.17	0.17	0.21	0.11
80	0.33	0.29	0.46	0.16	0.17	0.17	0.28	0.11
81	0.39	0.21	0.39	0.16	0.17	0.17	0.26	0.13
82	0.38	0.20	0.23	0.15	0.15	0.18	0.24	0.13
83	0.19	0.15	0.18	0.14	0.14	0.14	0.20	0.13
84	0.13	0.12	0.13	0.13	0.13	0.13	0.19	0.12

Table 4.29 (Continued): Grey relation coefficient of experimental test results

Exp. No	28d CS (MPa)	150d CS (MPa)	28d FS (MPa)	Flow (mm)	Initial Set (min)	Final Set (min)	Capillary water abs. (g/cm ² .min ^{0.5})	Mass Water Abs.(%)
85	0.34	0.35	0.67	0.17	0.17	0.17	0.21	0.11
86	0.17	0.14	0.32	0.24	0.23	0.18	0.23	0.12
87	0.11	0.13	0.24	0.24	0.25	0.20	0.23	0.19
88	0.09	0.10	0.21	0.29	0.28	0.20	0.22	0.27
89	0.10	0.10	0.19	0.31	0.45	0.25	0.22	0.32
90	0.11	0.12	0.21	0.21	0.17	0.22	0.23	0.45

The gray relational grade and ranking for each experiment are given in Table 4.30. Also, illustrates the relationship between GRG and experimental numbers. Gray relational grade value is calculated by taking the average of the gray relation coefficient values of the relevant experimental series. As examples, the calculation of the grey relation grade of experiment 1 is $(0.34+0.67+0.17+0.17+0.17+0.35+0.21+0.11)/8=0.274$. Graphical representation of gray relations grades for the multiperformance is given in Figure 4.152.

Table 4.30: Gray relational grades and rankings for 8 different responses

Exp. No	Grey Relational Grade (GRG)	Rank
1	0.274	23
2	0.305	16
3	0.260	44
4	0.230	60
5	0.226	62
6	0.190	84
7	0.274	23
8	0.215	70
9	0.207	73
10	0.202	79
11	0.190	83
12	0.175	87
13	0.274	23
14	0.215	69

Table 4.30 (Continued): Gray relational grades and rankings for 8 different responses

Exp. No	Grey Relational Grade (GRG)	Rank
15	0.218	66
16	0.223	63
17	0.218	67
18	0.207	74
19	0.274	23
20	0.217	68
21	0.222	64
22	0.261	43
23	0.251	48
24	0.273	38
25	0.274	23
26	0.192	82
27	0.233	57
28	0.255	47
29	0.256	46
30	0.288	22
31	0.274	23
32	0.468	1
33	0.429	5
34	0.375	8
35	0.310	14
36	0.203	78
37	0.274	23
38	0.293	18
39	0.268	39
40	0.264	41
41	0.264	42
42	0.201	80
43	0.274	23
44	0.267	40
45	0.232	59
46	0.248	49
47	0.258	45

Table 4.30 (Continued): Gray relational grades and rankings for 8 different responses

Exp. No	Grey Relational Grade (GRG)	Rank
48	0.243	53
49	0.274	23
50	0.307	15
51	0.291	20
52	0.414	7
53	0.226	61
54	0.233	58
55	0.274	23
56	0.239	54
57	0.358	10
58	0.454	2
59	0.444	3
60	0.438	4
61	0.274	23
62	0.247	50
63	0.218	65
64	0.204	76
65	0.186	86
66	0.174	88
67	0.274	23
68	0.293	19
69	0.304	17
70	0.317	13
71	0.360	9
72	0.422	6
73	0.274	23
74	0.340	11
75	0.323	12
76	0.290	21
77	0.236	55
78	0.187	85
79	0.274	23
80	0.247	51

Table 4.30 (Continued): Gray relational grades and rankings for 8 different responses

Exp. No	Grey Relational Grade (GRG)	Rank
81	0.235	56
82	0.206	75
83	0.160	89
84	0.136	90
85	0.274	23
86	0.203	77
87	0.198	81
88	0.209	72
89	0.244	52
90	0.214	71

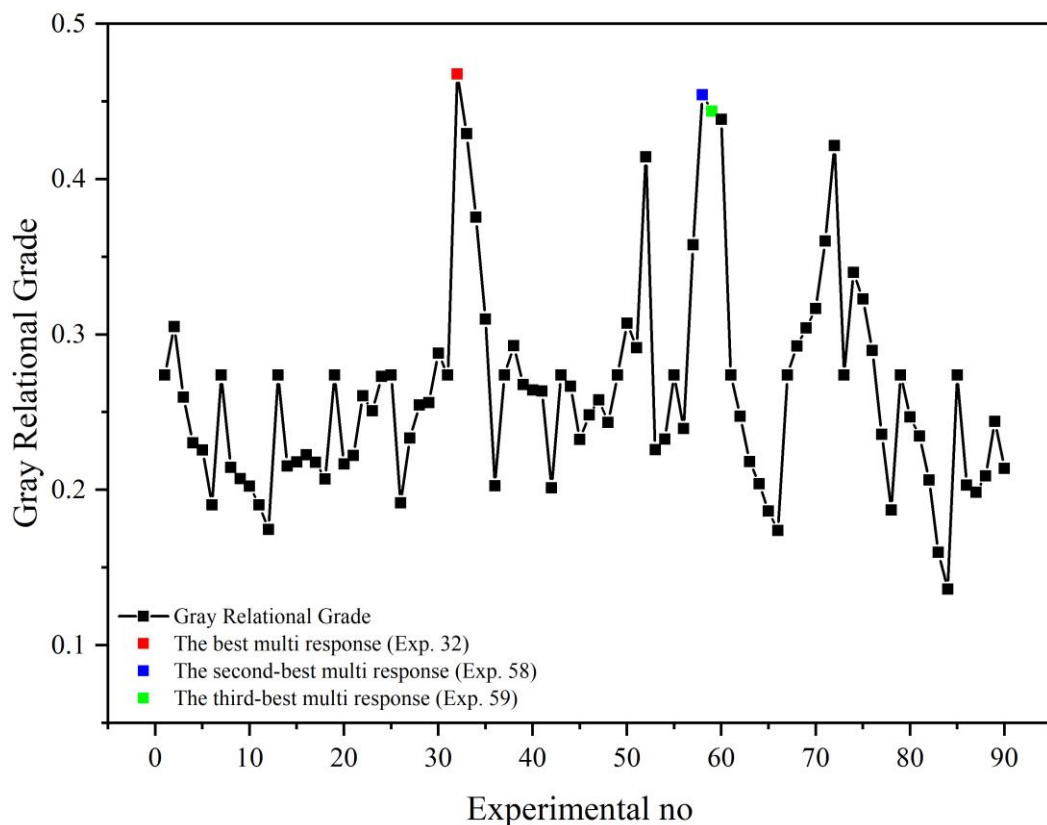


Figure 4.152: Gray relations grades for the multiperformance

The GRG and ranking for each experiment are given in Table 4.30. Furthermore, Figure 4.152 shows the gray relational degree graph for maximum 28-day compressive strength, 150-day compressive strength, 28-day flexural strength, flow diameter, initial and final setting times, and for minimum capillary water absorption and mass water

absorption. Gray relational grades that are higher signify that the corresponding experimental results are closer to ideal normalized values, i.e. that better multiple performance characteristics are indicated by higher gray relational grades [236,346]. Experiment 32 had the best multiple performance characteristics among all the experiments due to the fact that it had the highest gray relational grades. Thus, the optimal factor setting condition was G2T1U2 (Table 4.24, Table 4.25 and Figure 4.152). The second best experiment was determined as exp. no 58 (G2T5U4). The third best experiment was determined as exp. no 59 (G2T5U5). As a result of the evaluation of all the test results together with the condition of maximizing 6 responses and minimizing 2 responses, it was determined that the best mix could be with the use of 0.2 wt.% of 0/125 μm size ES. The other two best mixes are obtained by using 0.5 wt.% and 1.0 wt.% of 0/125 μm OS.

Furthermore, gray relational grade values for each level were calculated and represented in Table 4.31

Table 4.31: Average grey relational grade by level wise

Factors	Level 1	Level 2	Level 3	Level 4	Level 5	Level 6	Max-Min	Rank
G	0.237	0.303 ^a	0.251				0.066	1
T	0.269	0.266	0.251	0.250	0.280 ^a		0.030	3
U	0.274	0.270	0.266	0.277 ^a	0.255	0.239	0.038	2

^aOptimum level

Table 4.31 shows the average grey relational grade of each level. This could be calculated by taking average of each response from each level group in all levels. It is observed that higher level of GRG has very close and strong correlation with optimal value of inputs. The higher maximum-minimum value in Table 4.31 explicates the most important determining factor among the response. According to the table, G2, which is 0/125 μm grain size, is the optimum grain size. T5, which is OS type bio-polymeric admixture, is the optimum type of the bio-polymeric admixtures. Also, U4, which is 1 wt.% usage level, is the optimum usage level in this thesis. Moreover, according to the ranking in Table 4.31, the most important factor when evaluating the 8 different responses together as one, is grain size. The other two factors have lower influencing factor on maximizing 28-day compressive strength, 150-day compressive

strength, 28-day flexural strength, flow diameter, initial and final setting times, and minimizing capillary water absorption and mass water absorption.

Secondly, the results of fresh mortar properties of test mortars were optimized by following similar GRG application steps. Flow diameter value, initial setting time and final setting time of the mortars were taken into account as fresh mortar properties. While optimizing, the results of these features were tried to be maximized. The “ ζ ” weight factor was taken to be 0.34, 0.33 and 0.33 for flow diameter, initial setting time and final setting time, respectively. The gray relational grade and ranking for each experiment are given in Table 4.32. Graphical representation of gray relations grades for the multiperformance is given in Figure 4.153. Also, gray relational grade values for each level were calculated and represented in Table 4.33.

Table 4.32: Gray relational grades and rankings for fresh properties

Exp. No	Grey Relational Grade (GRG)	Rank
1	0.312	52
2	0.312	67
3	0.320	44
4	0.322	42
5	0.322	43
6	0.315	50
7	0.312	52
8	0.309	70
9	0.359	26
10	0.358	28
11	0.319	46
12	0.284	83
13	0.312	52
14	0.310	69
15	0.331	38
16	0.325	40
17	0.299	77
18	0.272	87
19	0.312	52
20	0.427	18

Table 4.32 (Continued): Gray relational grades and rankings for fresh properties

Exp. No	Grey Relational Grade (GRG)	Rank
21	0.444	14
22	0.518	8
23	0.338	34
24	0.274	86
25	0.312	52
26	0.363	25
27	0.470	11
28	0.444	13
29	0.369	23
30	0.316	48
31	0.312	52
32	0.338	35
33	0.335	37
34	0.344	31
35	0.353	30
36	0.335	36
37	0.312	52
38	0.416	19
39	0.432	17
40	0.464	12
41	0.482	9
42	0.313	51
43	0.312	52
44	0.341	32
45	0.358	27
46	0.364	24
47	0.339	33
48	0.327	39
49	0.312	52
50	0.685	5
51	0.686	4
52	0.868	1
53	0.391	21

Table 4.32 (Continued): Gray relational grades and rankings for fresh properties

Exp. No	Grey Relational Grade (GRG)	Rank
54	0.320	45
55	0.312	52
56	0.481	10
57	0.674	6
58	0.776	2
59	0.716	3
60	0.433	16
61	0.312	52
62	0.323	41
63	0.318	47
64	0.299	76
65	0.279	84
66	0.277	85
67	0.312	52
68	0.305	72
69	0.303	74
70	0.316	49
71	0.298	78
72	0.286	81
73	0.312	52
74	0.304	73
75	0.301	75
76	0.293	80
77	0.286	82
78	0.269	89
79	0.312	52
80	0.312	68
81	0.309	71
82	0.295	79
83	0.269	88
84	0.251	90
85	0.312	52
86	0.378	22

Table 4.32 (Continued): Gray relational grades and rankings for fresh properties

Exp. No	Grey Relational Grade (GRG)	Rank
87	0.399	20
88	0.434	15
89	0.527	7
90	0.354	29

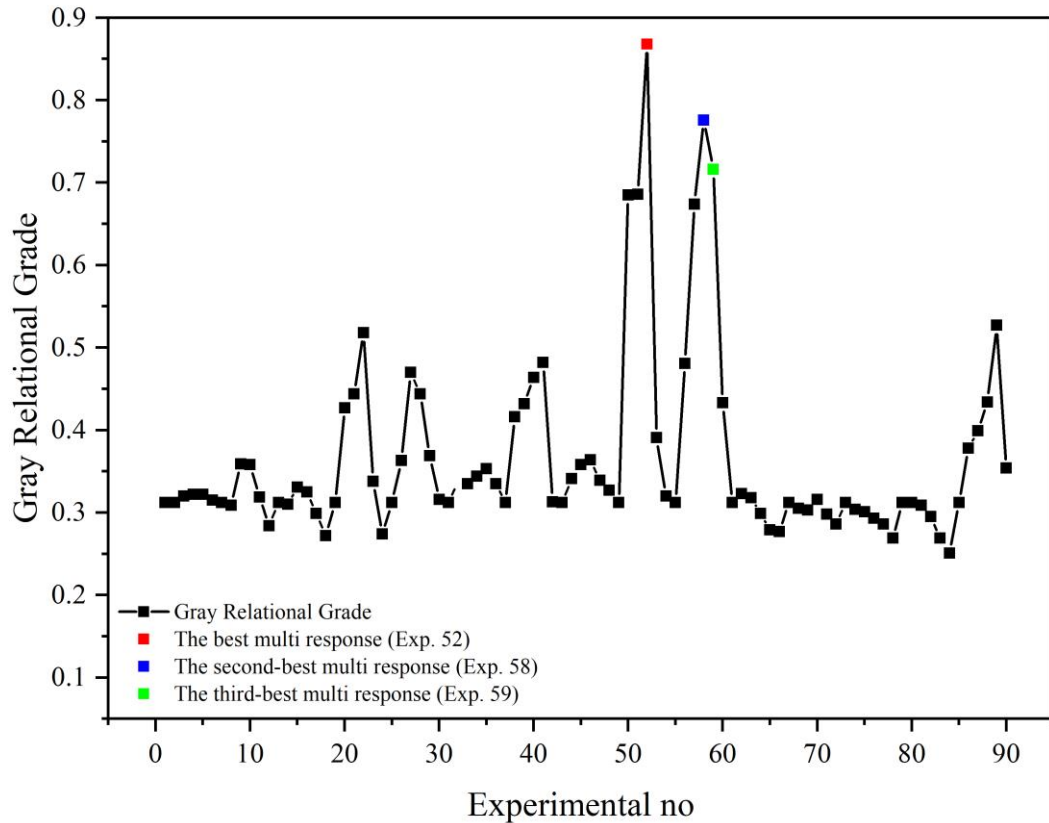


Figure 4.153: Gray relations grades for the multiperformance of fresh properties

Table 4.33: Average grey relational grade by level wise for fresh properties

Factors	Level 1	Level 2	Level 3	Level 4	Level 5	Level 6	Max-Min	Rank
G	0.343	0.438 ^a	0.318				0.119	3
T	0.318	0.343	0.314	0.407	0.448 ^a		0.134	1
U	0.312	0.374	0.403	0.428 ^a	0.372	0.308	0.120	2

^a Optimum level

According to Table 4.32 and Figure 4.153, experiment 52 is the optimum design in using bio-polymeric admixtures for cement mortars. Optimum mix for bio-polymeric admixture properties is G2T4U4, which is 0/125 μ m WKS with 0.5 wt.% usage level.

G2T4U4 mixture is the best solution for maximizing flow diameter, initial setting time and final setting time all together. Also, G2T5U4 and G2T5U5 can be considered as the other two options as maximizing flow diameter, initial setting time and final setting time. When the optimization is evaluated in terms of layer from

Table 4.33, optimum level for grain size is level 2 (0/125 μm), level 5 for bio-polymeric admixture type (OS), and level 4 for utilization level of bio-polymeric admixture (0.50 wt.%). It has been discussed in the previous sections that the effective parameter in increasing the fluidity of the mortars and prolonging the setting times depends on the amount of lignin and extractive substances in the structure of bio-polymeric admixtures. In the optimization phase, it is seen that bio-polymeric admixtures with higher lignin and extractive substances have a greater effect on the optimum use in improving the fresh properties of mortars. The most important factor affecting the fresh mortar properties was the bio-polymeric admixture type.

Thirdly, the results of hardened mortar properties (strength values) of test mortars were optimized by following similar GRG application steps. 28- and 150-day compressive strengths and 28-day flexural strength of the mortars were taken into account as hardened mortar properties. While optimizing, the results of these features were tried to be maximized. The “ ζ ” weight factor was taken to be 0.34, 0.33 and 0.33 for 28-day compressive strength, 150-day compressive strength and 28-day flexural strength, respectively. The gray relational grade and ranking for each experiment are given in Table 4.34. Graphical representation of gray relations grades for the multiperformance is given in Figure 4.154. Also, gray relational grade values for each level were calculated and represented in Table 4.35.

Table 4.34: Gray relational grades and rankings for hardened properties

Exp. No	Grey Relational Grade (GRG)	Rank
1	0.716	13
2	0.785	8
3	0.646	30
4	0.601	37
5	0.584	39
6	0.492	52
7	0.716	13

Table 4.34 (Continued): Gray relational grades and rankings for hardened properties

Exp. No	Grey Relational Grade (GRG)	Rank
8	0.544	46
9	0.472	55
10	0.450	58
11	0.427	64
12	0.394	71
13	0.716	13
14	0.603	36
15	0.575	42
16	0.581	41
17	0.512	50
18	0.481	54
19	0.716	13
20	0.385	73
21	0.357	78
22	0.375	76
23	0.400	69
24	0.427	63
25	0.716	13
26	0.289	89
27	0.305	87
28	0.305	86
29	0.373	77
30	0.410	66
31	0.716	13
32	0.988	1
33	0.954	2
34	0.891	4
35	0.786	7
36	0.541	47
37	0.716	13
38	0.686	29
39	0.581	40
40	0.529	49

Table 4.34 (Continued): Gray relational grades and rankings for hardened properties

Exp. No	Grey Relational Grade (GRG)	Rank
41	0.494	51
42	0.442	59
43	0.716	13
44	0.626	32
45	0.439	60
46	0.400	68
47	0.400	67
48	0.386	72
49	0.716	13
50	0.338	80
51	0.320	85
52	0.333	81
53	0.455	56
54	0.562	43
55	0.716	13
56	0.266	90
57	0.303	88
58	0.378	75
59	0.430	62
60	0.604	34
61	0.716	13
62	0.604	35
63	0.557	44
64	0.546	45
65	0.490	53
66	0.433	61
67	0.716	13
68	0.734	12
69	0.761	11
70	0.771	10
71	0.846	5
72	0.920	3
73	0.716	13

Table 4.34 (Continued): Gray relational grades and rankings for hardened properties

Exp. No	Grey Relational Grade (GRG)	Rank
74	0.789	6
75	0.776	9
76	0.712	28
77	0.585	38
78	0.396	70
79	0.716	13
80	0.645	31
81	0.610	33
82	0.539	48
83	0.410	65
84	0.330	83
85	0.716	13
86	0.453	57
87	0.378	74
88	0.331	82
89	0.328	84
90	0.355	79

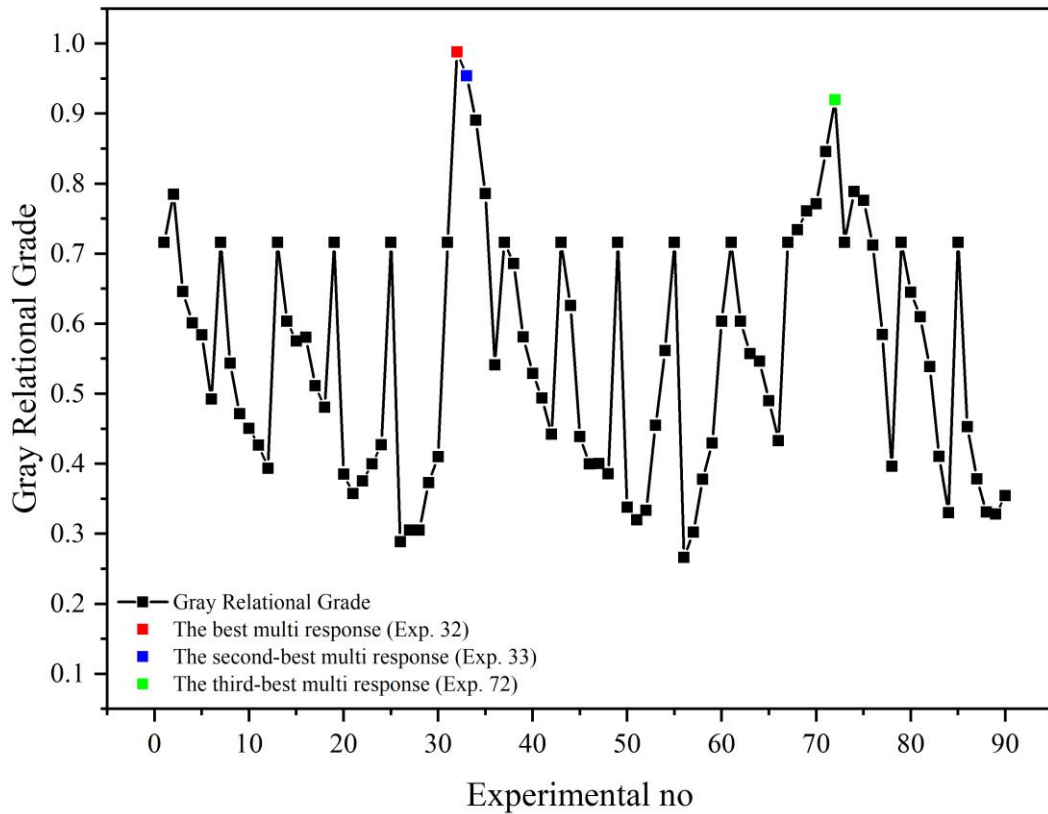


Figure 4.154: Gray relations grades for the multiperformance of hardened properties

Table 4.35: Average grey relational grade by level wise for hardened properties

Factors	Level 1	Level 2	Level 3	Level 4	Level 5	Level 6	Max-Min	Rank
G	0.512	0.557	0.596 ^a				0.084	3
T	0.669 ^a	0.662	0.578	0.480	0.425		0.244	1
U	0.716 ^a	0.582	0.536	0.516	0.501	0.478	0.238	2

^aOptimum level

According to Table 4.34 and Figure 4.154, experiment 32 is the optimum design in using bio-polymeric admixtures for cement mortars, when evaluated on a mixture basis. Optimum mix for bio-polymeric admixture properties is G2T1U2, which is 0/125 μm ES with 0.2 wt.% usage level. G2T1U2 mixture is the best solution for maximizing 28- and 150-day compressive strengths and 28-day flexural strength all together in a multiple performance basis. Also, G2T1U3 and G3T2U6 can be considered as the other two options as maximizing 28- and 150-day compressive strengths and 28-day flexural strength. When the optimization is evaluated in terms of layer performance from Table 4.35, optimum level for grain size is level 3 (125/250

μm), level 1 for bio-polymeric admixture type (ES), and level 1 for utilization level of bio-polymeric admixture (0.00 wt.%). In an optimization study where only the strength results are maximized, it is stated by the optimization results that it is more optimal not to use bio-polymeric admixture, since the use of other bio-polymeric admixtures, except for the use of eggshell, generally reduces the compressive and flexural strength of cement mortar. It has been discussed in the previous sections that the effective parameter in increasing the strength of the mortars depends on fiber-like structure of bio-polymeric admixtures. In the optimization phase, it is seen that lignocellulosic bio-polymeric admixtures with higher cellulose and fiber-like shape have a greater effect on the optimum use in improving the hardened properties of mortars. In addition, with the contribution of ES to hydration and thus its positive effect on strength, it is included in the best mixture in the optimization study. Also, the most important factor affecting the hardened mortar properties was again bio-polymeric admixture type.

Fourth and lastly, the optimization specifies the most suitable mixture design according to the water absorptions known as the simplest durability test. Capillary water absorption and mass water absorption of the mortars were taken into account as durability properties. While optimizing, the results of these features were tried to be minimized. The “ζ” weight factor was taken to be 0.60 and 0.40 and for capillary water absorption and mass water absorption, respectively. The gray relational grade and ranking for each experiment are given in Table 4.36. Graphical representation of gray relations grades for the multiperformance is given in Figure 4.155. Also, gray relational grade values for each level were calculated and represented in Table 4.37.

Table 4.36: Gray relational grades and rankings for durability properties

Exp. No	Grey Relational Grade (GRG)	Rank
1	0.420	67
2	0.423	66
3	0.454	58
4	0.419	82
5	0.425	64
6	0.401	84
7	0.420	67
8	0.508	48

Table 4.36 (Continued): Gray relational grades and rankings for durability properties

Exp. No	Grey Relational Grade (GRG)	Rank
9	0.512	46
10	0.514	45
11	0.533	36
12	0.526	40
13	0.420	67
14	0.357	90
15	0.425	65
16	0.463	57
17	0.588	23
18	0.609	20
19	0.420	67
20	0.571	24
21	0.600	21
22	0.632	16
23	0.713	10
24	0.748	6
25	0.420	67
26	0.618	18
27	0.649	14
28	0.727	9
29	0.754	4
30	0.833	2
31	0.420	67
32	0.398	85
33	0.381	88
34	0.372	89
35	0.392	86
36	0.384	87
37	0.420	67
38	0.484	50
39	0.526	39
40	0.536	34
41	0.549	30

Table 4.36 (Continued): Gray relational grades and rankings for durability properties

Exp. No	Grey Relational Grade (GRG)	Rank
42	0.544	32
43	0.420	67
44	0.567	26
45	0.621	17
46	0.676	12
47	0.753	5
48	0.742	7
49	0.420	67
50	0.469	53
51	0.520	42
52	0.562	28
53	0.547	31
54	0.533	35
55	0.420	67
56	0.642	15
57	0.708	11
58	0.739	8
59	0.827	3
60	0.922	1
61	0.420	67
62	0.522	41
63	0.465	56
64	0.427	63
65	0.446	61
66	0.454	59
67	0.420	67
68	0.479	51
69	0.490	49
70	0.515	44
71	0.520	43
72	0.536	33
73	0.420	67
74	0.550	29

Table 4.36 (Continued): Gray relational grades and rankings for durability properties

Exp. No	Grey Relational Grade (GRG)	Rank
75	0.528	37
76	0.528	38
77	0.570	25
78	0.614	19
79	0.420	67
80	0.468	54
81	0.477	52
82	0.467	55
83	0.438	62
84	0.417	83
85	0.420	67
86	0.451	60
87	0.510	47
88	0.566	27
89	0.592	22
90	0.656	13

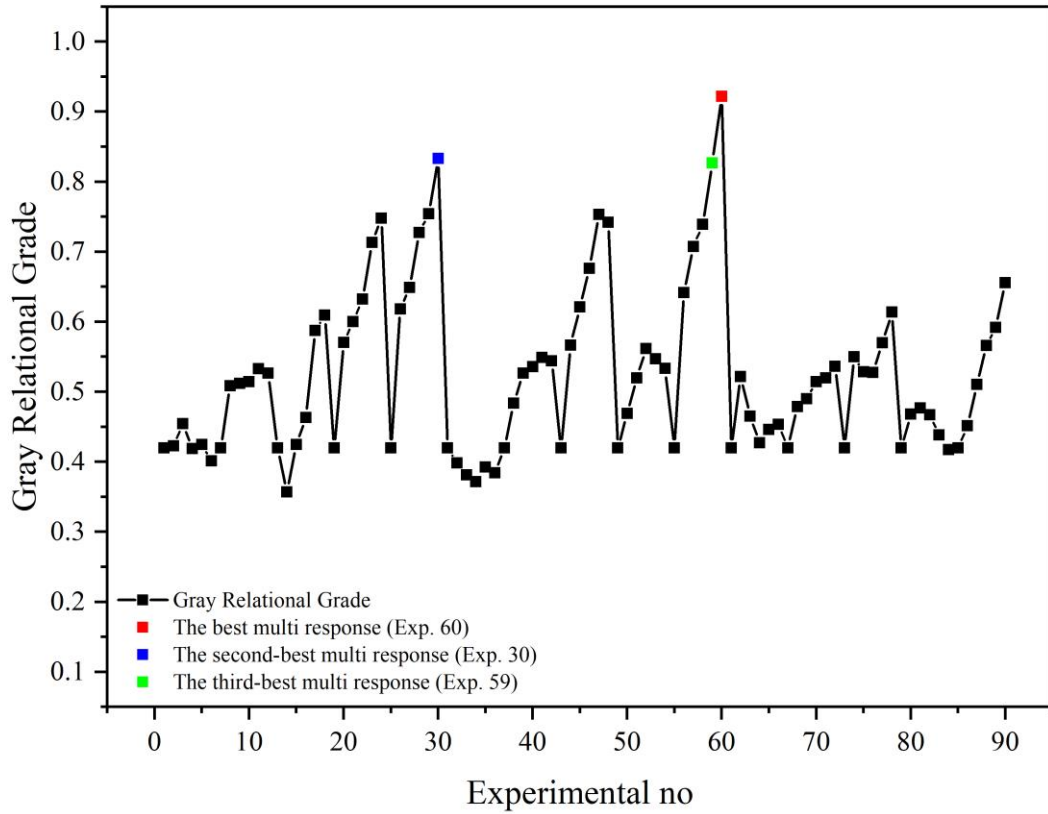


Figure 4.155: Gray relations grades for the multiperformance of durability properties

Table 4.37: Average grey relational grade by level wise for durability properties

Factors	Level 1	Level 2	Level 3	Level 4	Level 5	Level 6	Max-Min	Rank
G	0.537 ^a	0.550	0.493				0.057	3
T	0.423	0.502	0.547	0.523	0.636 ^a		0.213	1
U	0.420	0.500	0.525	0.543	0.576	0.595 ^a	0.175	2

^a Optimum level

According to Table 4.36 and Figure 4.155, experiment 60 is the optimum design in using bio-polymeric admixtures for cement mortars, when evaluated on a mixture basis. Optimum mix for bio-polymeric admixture properties is G2T5U6, which is 0/125 μ m OS with 1.5 wt.% usage level. G2T5U6 mixture is the best solution for minimizing capillary water absorption and mass water absorption all together in a multiple performance basis. Also, G1T5U6 and G2T5U5 can be considered as second and third options as minimizing capillary water absorption and mass water absorption. When the optimization is evaluated in terms of layer performance from Table 4.37, optimum level for grain size is level 1 (0/45 μ m), level 5 for bio-polymeric admixture type (OS), and level 6 for utilization level of bio-polymeric admixture (1.5 wt.%). It

has been discussed in the previous sections that the effective parameter in water repellent property of the mortars depends on extractive content of bio-polymeric admixtures. In the optimization phase, it is seen that lignocellulosic bio-polymeric admixtures with higher extractive content have a greater effect on the optimum use in improving the water repellency properties of mortars. In addition, with the contribution of OS to hydrophobicity, it is included in the best mixture in the optimization study. Also, the most important factor affecting the durability properties was again bio-polymeric admixture type.

4.6.2 Regression Analysis

All regression analyzes were performed using Wolfram Mathematica 12 software. The independent variables used in the regression analyzes are the extractive, lignin, hemicellulose and cellulose in the chemical structure of the lignocellulosic bio-polymeric admixtures, and the percent amount of use of bio-polymeric admixtures and the size of the bio-polymeric admixtures, a total of six independent variables.

Regression analysis is applied for modeling and analysis in the case of different variables having a relationship between one dependent variable and more than one independent variables [236]. Regression analysis was used in this thesis study to calculate the equations for prediction of 28-days compressive strength, 28-days flexural strength, 150-days compressive strength, flowability, initial and final setting times, and capillary and mass water absorption values. Equation predictions were formulated as described in Table 3.8. Table 4.38 and Table 4.39 shows the R-square values of predicted multiple regression equations for the output parameters. The R^2 values found via the second order multiple nonlinear rational (SONR) model equations were 90 %, 90 %, 91 %, 89 %, 93 %, 93 %, 89 %, and 97 % for 28-days compressive strength, 28-days flexural strength, 150-days compressive strength, flow diameter, initial setting time, final setting time, capillary water absorption, and mass water absorption, respectively. In addition, it is observed that the R-square and adjusted R-square values in the SONR model are quite close to each other. This shows that the terms in the SONR model have a high level of significance in the development of the model.

As can be seen in Appendix B, in regression analyzes established between only one independent variable and one dependent variable, it is observed that the regression formulas are parabolic curves of the third order. For this reason, R-square values of first order linear, trigonometric, and logarithmic regression models were found to be low. The most appropriate regression model was determined as SONR. SONR regression formulas developed for eight different dependent variables are shown in between Table 4.40 and Table 4.43.

Table 4.38: R-squares of regression models for 28-days compressive and flexural strength, 150-days compressive strength and flow diameter

Model	28-days Compressive Strength		28-days Flexural Strength		150-days Compressive Strength		Flow Diameter	
	R ²	R ² (adj.)	R ²	R ² (adj.)	R ²	R ² (adj.)	R ²	R ² (adj.)
L	0.46	0.41	0.46	0.41	0.32	0.25	0.34	0.28
LR	0.58	0.54	0.63	0.60	0.47	0.42	0.43	0.38
SON	0.58	0.54	0.59	0.55	0.55	0.51	0.71	0.68
SONR	0.90	0.89	0.90	0.89	0.91	0.90	0.89	0.88
FOTN	0.53	0.48	0.55	0.50	0.41	0.35	0.65	0.62
FOTNR	0.48	0.47	0.48	0.44	0.48	0.43	0.72	0.70
SOTN	0.58	0.54	0.62	0.58	0.44	0.38	0.69	0.66
SOTNR	0.71	0.69	0.80	0.78	0.65	0.62	0.82	0.81
FOLN	0.56	0.51	0.59	0.55	0.43	0.38	0.25	0.19
FOLNR	0.70	0.68	0.68	0.65	0.57	0.53	0.61	0.57
SOLN	0.58	0.54	0.64	0.60	0.43	0.38	0.65	0.62
SOLNR	0.77	0.74	0.85	0.84	0.66	0.62	0.88	0.86

Table 4.39: R-squares of regression models for initial and final setting times, and capillary and mass water absorption values

Model	Initial Setting Time		Final Setting Time		Capillary Water Absorption		Mass Water Absorption	
	R ²	R ² (adj.)	R ²	R ² (adj.)	R ²	R ² (adj.)	R ²	R ² (adj.)
L	0.22	0.14	0.26	0.19	0.10	0.02	0.62	0.58
LR	0.34	0.28	0.41	0.36	0.41	0.35	0.74	0.71
SON	0.71	0.68	0.75	0.73	0.74	0.72	0.83	0.81
SONR	0.93	0.92	0.93	0.92	0.89	0.88	0.97	0.97
FOTN	0.61	0.58	0.62	0.58	0.58	0.54	0.75	0.73
FOTNR	0.66	0.63	0.69	0.66	0.50	0.46	0.63	0.60
SOTN	0.66	0.63	0.62	0.58	0.60	0.56	0.77	0.74
SOTNR	0.77	0.75	0.80	0.78	0.77	0.74	0.85	0.83
FOLN	0.19	0.12	0.25	0.18	0.25	0.18	0.64	0.60
FOLNR	0.42	0.36	0.32	0.25	0.19	0.12	0.61	0.58
SOLN	0.52	0.47	0.54	0.50	0.59	0.56	0.76	0.74
SOLNR	0.79	0.77	0.79	0.78	0.87	0.85	0.89	0.88

A very good correlation was found between the predicted values and the experimental results for each dependent variable. Graphical representations of experimental values versus predicted values for each response are also shown in Appendix A.

Table 4.40: Regression equations for 28-days compressive strength and mass water absorption

Model	R ²	R ² (adj.)
$ \begin{aligned} Y = & (3439.87 + 187.254x_1 + 1.67957x_1^2 - 50721.4x_2 - 1436.24x_1x_2 + 179474x_2^2 + 1933.51x_3 \\ & + 67.2135x_1x_3 - 8126.74x_2x_3 + 249.129x_3^2 - 1323.57x_4 - 53.8944x_1x_4 + 12204.7x_2x_4 \\ & + 24.3025x_3x_4 - 54.3351x_4^2 - 1249.52x_5 - 44.3837x_1x_5 + 17388.1x_2x_5 + 131.172x_3x_5 \\ & - 112.483x_4x_5 - 152.81x_5^2 + 1977.37x_6 + 79.452x_1x_6 - 25224.3x_2x_6 + 81.1743x_3x_6 \\ & - 74.1582x_4x_6 + 10.7734x_5x_6 + 345.048x_6^2) / (-613.388 - 20.2872x_1 + 0.0469567x_1^2 \\ & - 985.623x_2 - 45.1284x_1x_2 + 5404.89x_2^2 + 43.3642x_3 + 2.08339x_1x_3 - 139.166x_2x_3 \\ & + 8.63384x_3^2 - 57.9153x_4 - 1.22451x_1x_4 + 305.646x_2x_4 + 1.00779x_3x_4 - 1.16155x_4^2 \\ & - 59.0393x_5 - 0.959694x_1x_5 + 598.924x_2x_5 + 4.88555x_3x_5 - 3.03235x_4x_5 - 4.34379x_5^2 \\ & + 38.8783x_6 + 2.44641x_1x_6 - 783.314x_2x_6 + 1.8355x_3x_6 - 1.83637x_4x_6 + 0.912508x_5x_6 \\ & + 10.7298x_6^2) \end{aligned} $	0.90	0.89
28-days Compressive Strength		
$ \begin{aligned} Y = & (-224994 - 3449.84x_1 + 3.99739x_1^2 + 102963x_2 + 116.999x_1x_2 + 5634.41x_2^2 + 169135x_3 \\ & - 107.509x_1x_3 - 9253.73x_2x_3 - 5830.56x_3^2 - 7652.22x_4 + 83.0613x_1x_4 + 3337.88x_2x_4 \\ & + 1822.08x_3x_4 - 821.585x_4^2 + 6784.44x_5 + 72.6773x_1x_5 - 1204.83x_2x_5 - 4292.57x_3x_5 \\ & + 683.531x_4x_5 + 703.935x_5^2 - 4507.93x_6 - 51.1916x_1x_6 - 3681.65x_2x_6 + 734.776x_3x_6 \\ & + 9.23535x_4x_6 - 30.674x_5x_6 - 376.5x_6^2) / (3188890 - 7256.76x_1 + 0.587333x_1^2 - 1325700x_2 \\ & + 22.122x_1x_2 + 2147.22x_2^2 - 492.096x_3 + 72.3564x_1x_3 + 11104.1x_2x_3 - 42496.5x_3^2 \\ & - 14248.3x_4 + 69.3933x_1x_4 + 14484.2x_2x_4 + 17679.7x_3x_4 - 2667.16x_4^2 + 30894.4x_5 \\ & + 674324x_1x_5 + 11943.1x_2x_5 + 4917.42x_3x_5 - 2615.26x_4x_5 + 598.108x_5^2 - 77681.3x_6 \\ & + 74.1489x_1x_6 + 13518.7x_2x_6 + 10486.1x_3x_6 - 1888.72x_4x_6 + 3354.4x_5x_6 - 1784.92x_6^2) \end{aligned} $	0.97	0.97
Mass Water Absorption		

Table 4.41: Regression equations for 28-days flexural strength and 150-days compressive strength

Model	R ²	R ² (adj.)
$ \begin{aligned} Y = & (-68669.7 + 880.817x_1 + 26.5214x_1^2 + 765674x_2 - 13549.4x_1x_2 + 380205x_2^2 - 9010.6x_3 \\ & - 1378.17x_1x_3 - 1360770x_2x_3 - 1917.16x_3^2 + 4655.02x_4 + 15.265x_1x_4 + 711247x_2x_4 \\ & - 494.057x_3x_4 + 234.036x_4^2 + 4230.27x_5 + 451.89x_1x_5 + 834940x_2x_5 - 585.714x_3x_5 \\ & + 552.05x_4x_5 + 491.154x_5^2 - 1505.51x_6 + 332.221x_1x_6 - 1051590x_2x_6 + 234.138x_3x_6 \\ & + 660.222x_4x_6 - 143.854x_5x_6 - 1218.94x_6^2) / (62431.8 - 3825.02x_1 + 3.69063x_1^2 - 107429x_2 \\ & - 2442.46x_1x_2 + 23271.6x_2^2 + 14540.2x_3 - 162.414x_1x_3 - 218839x_2x_3 - 971.79x_3^2 \\ & - 7434.68x_4 + 50.4862x_1x_4 + 118391x_2x_4 - 274.308x_3x_4 + 205.725x_4^2 + 7613.01x_5 \\ & + 107.692x_1x_5 + 140962x_2x_5 - 140.807x_3x_5 - 368.501x_4x_5 + 109.446x_5^2 - 465.215x_6 \\ & + 71.4693x_1x_6 - 167152x_2x_6 + 642.811x_3x_6 + 145.788x_4x_6 + 172.852x_5x_6 - 333.59x_6^2) \end{aligned} $	0.90	0.89
28-days Flexural Strength		
$ \begin{aligned} Y = & (13610.1 + 208.586x_1 - 0.185585x_1^2 + 8668.59x_2 - 395.662x_1x_2 - 17489.9x_2^2 - 2365.62x_3 \\ & + 62.6296x_1x_3 - 636.414x_2x_3 - 208.731x_3^2 + 574.597x_4 - 34.5159x_1x_4 + 3073.06x_2x_4 \\ & - 61.4614x_3x_4 + 16.403x_4^2 + 941.066x_5 - 33.3885x_1x_5 + 3356.34x_2x_5 - 82.5641x_3x_5 \\ & + 40.3363x_4x_5 + 46.4008x_5^2 + 656.979x_6 + 44.7037x_1x_6 - 4731.17x_2x_6 - 72.2174x_3x_6 \\ & + 38.8923x_4x_6 + 48.0312x_5x_6 - 0.829377x_6^2) / (-334.253 - 18.3645x_1 - 0.00450629x_1^2 \\ & + 543.738x_2 - 10.7815x_1x_2 - 673.767x_2^2 - 63.1433x_3 + 155017x_1x_3 - 46.1042x_2x_3 \\ & - 3.01669x_3^2 - 9.12862x_4 - 0.475995x_1x_4 + 80.8936x_2x_4 - 0.984784x_3x_4 + 0.670653x_4^2 \\ & - 2.57009x_5 - 0.459173x_1x_5 + 87.449x_2x_5 - 1.12333x_3x_5 + 0.902369x_4x_5 + 1.10551x_5^2 \\ & + 5.92065x_6 + 1.11446x_1x_6 - 101.725x_2x_6 - 1.82613x_3x_6 + 1.4018x_4x_6 + 1.93739x_5x_6 \\ & - 0.829377x_6^2) \end{aligned} $	0.91	0.90
150-days Compressive Strength		

Table 4.42: Regression equations for capillary water absorption and final setting time

Model	R ²	R ² (adj.)
$ \begin{aligned} Y = & (-138855 - 4787.97x_1 + 28.2444x_1^2 - 160867x_2 + 2032.41x_1x_2 + 11284.4x_2^2 + 6297.41x_3 \\ & - 168.026x_1x_3 - 5330.78x_2x_3 + 343.674x_3^2 + 6058.13x_4 - 99.0567x_1x_4 - 2723.29x_2x_4 \\ & + 528.145x_3x_4 - 36.5377x_4^2 + 284.372x_5 + 249.993x_1x_5 + 6586.37x_2x_5 - 972.736x_3x_5 \\ & - 189.244x_4x_5 - 145.325x_5^2 + 15739.8x_6 - 227.652x_1x_6 - 5985.85x_2x_6 + 1155.48x_3x_6 \\ & + 348.898x_4x_6 - 266.169x_5x_6 + 161.379x_6^2) / (238485 - 8304.8x_1 + 48.4009x_1^2 - 1204260x_2 \\ & + 3726.23x_1x_2 - 39053.4x_2^2 + 59370.5x_3 - 588.908x_1x_3 - 17597.6x_2x_3 + 334.185x_3^2 \\ & + 26740.4x_4 - 49.7157x_1x_4 + 10618.4x_2x_4 + 1637.89x_3x_4 - 225.666x_4^2 - 11188.2x_5 \\ & + 590.545x_1x_5 + 37915.8x_2x_5 - 1608.33x_3x_5 - 853.566x_4x_5 - 202.601x_5^2 + 27478.6x_6 \\ & - 554.887x_1x_6 - 15568x_2x_6 - 1225.02x_3x_6 + 174.021x_4x_6 - 458.192x_5x_6 + 612.134x_6^2) \end{aligned} $	0.89	0.88
<p>Capillary Water Absorption</p> $ \begin{aligned} Y = & (27923.9 + 3297.21x_1 + 3.87662x_1^2 - 305098x_2 - 241.264x_1x_2 + 168499x_2^2 + 2626.78x_3 - 59.7477x_1x_3 \\ & + 63882.1x_2x_3 - 347.624x_3^2 + 17.4423x_4 - 5.66259x_1x_4 - 30679.4x_2x_4 - 457.005x_3x_4 \\ & + 93.3256x_4^2 + 13600.1x_5 - 193.787x_1x_5 - 32570.1x_2x_5 - 405.402x_3x_5 + 560.526x_4x_5 \\ & + 676.903x_5^2 - 9561.53x_6 + 84.0343x_1x_6 + 43671x_2x_6 + 111.926x_3x_6 - 106.234x_4x_6 \\ & + 14.375x_5x_6 - 650.21x_6^2) / (-2092.81 - 19.0162x_1 + 0.045497x_1^2 - 1660.05x_2 \\ & + 0.0576435x_1x_2 + 1097.1x_2^2 - 63.0228x_3 + 0.20219x_1x_3 + 274.112x_2x_3 - 3.27844x_3^2 \\ & - 11.8656x_4 + 0.157096x_1x_4 - 122.765x_2x_4 - 0.656162x_3x_4 + 0.43838x_4^2 + 17.1178x_5 \\ & - 0.708491x_1x_5 - 190.318x_2x_5 + 1.58194x_3x_5 + 4.66536x_4x_5 + 3.05961x_5^2 - 69.1431x_6 \\ & + 0.732139x_1x_6 + 212.33x_2x_6 + 0.962745x_3x_6 + 1.01035x_4x_6 + 0.463121x_5x_6 - 2.01509x_6^2) \end{aligned} $	0.93	0.92
<p>Final Setting Time</p>		

Table 4.43: Regression equations for initial setting time and flow diameter

Model	R ²	R ² (adj.)
$ \begin{aligned} Y = & (-142111 + 155.747x_1 + 0.13641x_1^2 + 122699x_2 - 1043.62x_1x_2 + 30963.9x_2^2 - 4285.62x_3 \\ & + 197.85x_1x_3 - 36770.5x_2x_3 + 252.304x_3^2 + 2565.57x_4 - 111.935x_1x_4 + 20689.5x_2x_4 \\ & - 43.0678x_3x_4 - 12.2966x_4^2 + 776.691x_5 - 110.449x_1x_5 + 23576.4x_2x_5 + 133.023x_3x_5 \\ & - 33.7642x_4x_5 + 249.871x_5^2 + 2791.47x_6 + 188.364x_1x_6 - 34094.9x_2x_6 - 104.456x_3x_6 \\ & + 55.1829x_4x_6 - 177.254x_5x_6 - 40.3584x_6^2) / (677.549 - 35.9258x_1 + 0.048264x_1^2 \\ & - 372.359x_2 - 9.54159x_1x_2 + 2407.84x_2^2 - 41.4711x_3 + 1.73469x_1x_3 - 458.736x_2x_3 \\ & + 2.15762x_3^2 - 10.212x_4 - 0.42763x_1x_4 + 262.56x_2x_4 - 1.46736x_3x_4 + 1.29722x_4^2 \\ & - 33.0905x_5 - 0.939635x_1x_5 + 182.621x_2x_5 + 2.95767x_3x_5 + 0.0207125x_4x_5 + 2.61469x_5^2 \\ & - 36.651x_6 + 1.83662x_1x_6 - 354.377x_2x_6 - 1.3025x_3x_6 - 1.65348x_4x_6 + 0.0305166x_5x_6 \\ & + 1.19393x_6^2) \end{aligned} $	0.93	0.92
Initial Setting Time		
$ \begin{aligned} Y = & (715.537 + 157.547x_1 + 2.07374x_1^2 + 16775.9x_2 - 824.288x_1x_2 + 71655.2x_2^2 + 554.199x_3 \\ & - 160.119x_1x_3 + 7546.11x_2x_3 + 124.612x_3^2 - 220.862x_4 + 70.9093x_1x_4 - 2045.45x_2x_4 \\ & - 20.7888x_3x_4 - 10.053x_4^2 - 431.399x_5 + 112.589x_1x_5 - 8139.84x_2x_5 + 73.408x_3x_5 \\ & - 33.637x_4x_5 - 61.4349x_5^2 + 488.637x_6 - 140.403x_1x_6 + 9515.5x_2x_6 - 1.18652x_3x_6 \\ & - 2.7474x_4x_6 + 29.0192x_5x_6 + 58.1621x_6^2) / (-411.252 - 18.1724x_1 + 0.0190498x_1^2 \\ & - 674.461x_2 - 6.75459x_1x_2 + 687.167x_2^2 - 6.93971x_3 - 1.11698x_1x_3 + 60.5273x_2x_3 \\ & + 1.89393x_3^2 - 19.3401x_4 + 0.774007x_1x_4 - 5.51827x_2x_4 + 0.104844x_3x_4 + 0.292015x_4^2 \\ & - 23.3417x_5 + 1.07125x_1x_5 - 57.066x_2x_5 + 1.18024x_3x_5 - 0.0233187x_4x_5 - 0.213945x_5^2 \\ & - 11.1719x_6 - 0.926793x_1x_6 + 80.1587x_2x_6 - 0.350033x_3x_6 + 0.253618x_4x_6 + 0.713392x_5x_6 \\ & + 0.802453x_6^2) \end{aligned} $	0.89	0.88
Flow Diameter		

Where x_1 is maximum grain size of bio-polymeric admixture (μm), x_2 is usage rate of bio-polymeric admixture (%), x_3 is extractive content of any bio-polymeric admixture (%), x_4 is lignin content of any bio-polymeric admixture (%), x_5 is hemicellulose content of any bio-polymeric admixture (%) and x_6 is alpha cellulose content of any bio-polymeric admixture (%). Also, graphical representation of fitted values versus experimental values given in Appendix C.

Chapter 5

Conclusions

In this thesis, experimental studies were carried out on the evaluation of five different naturally occurring bio-polymeric admixtures in cementitious composite mortars. The results of the examination and analysis are interpreted, and the results are summarized below:

1. A comprehensive classification of biopolymers has been made. The components in the chemical structure of the bio-polymeric admixtures used in this study are cellulose, hemicellulose, lignin, fatty acids and proteins, which are in the class of natural biopolymers.
2. According to the results of the comprehensive literature review, egg shell, apricot kernel shell, hazelnut kernel shell, walnut kernel shell and olive seed used in this study were either carbonized and investigated in large sizes or as lightweight aggregates in their natural state in literature studies. The use of these materials in very fine grain sizes and low amounts for chemical/polymeric admixtures has been considered as a missing area in the literature.
3. In the beginning of the study a preliminary work was planned on several different bio-polymeric admixtures. With these admixtures, the compressive and flexural strengths of the cement mortar were determined. It was aimed to improve mechanical properties of composite cement mortars by using different bio-polymeric admixtures such as ground and sized corn cob, egg shell, walnut kernel shell, apricot kernel shell, olive pomace, mallow, hazelnut kernel shell, rice husk and olive seed. Most of these materials are leftovers from food production or household consumption. Cement mortars produced with corn cob powder and mallow powder were deformed during water curing, and their 28-

days compressive and flexural strength were found as unacceptable. Similarly, olive pomace admixture and rice husk powder were not evaluated in the study as it was below the strength expectations, and because it requires a lot of time and effort during the grinding phase. In the later stages of the study, egg shell, apricot kernel shell, hazelnut kernel shell, walnut kernel shell and olive seed were used.

On the other hand, rice husk powder, olive pomace powder, mallow powder and corn cob powder can be tested in cement mortars under different curing conditions after different grinding processes.

4. In the second phase of the study, characterization of five different bio-polymeric admixtures selected as a result of the preliminary study evaluations was made by chemical, XRD, FT-IR and SEM analyzes. It has been determined that the main components of lignocellulosic bio-polymeric admixtures are extractive, lignin, hemicellulose and cellulose. Extractive, lignin, hemicellulose and cellulose contents of AKS admixture are 3.81%, 27.07%, 31.19% and 37.92%, respectively. Extractive, lignin, hemicellulose and cellulose contents of HKS admixture are 4.67%, 31.79%, 31.73% and 33.29%, respectively. Extractive, lignin, hemicellulose and cellulose contents of WKS admixture are 16.16%, 41.23%, 20.58% and 22.03%, respectively. Extractive, lignin, hemicellulose and cellulose contents of AKS admixture are 18.39%, 32.45%, 29.67% and 19.48%, respectively. Fatty acids, lignin, hemicellulose and cellulose contents were determined in XRD and FT-IR examinations of these materials. High calcium carbonate content of the eggshell bio-polymeric admixture was determined during the characterization phase. It was observed from the SEM images, the bio-polymeric admixtures were characterized by the presence of irregular particles that tend to form larger agglomerates. When the SEM images of the bio-polymeric admixtures are examined, it is observed that the grains are in angular and rough structure.
5. In the third stage of the study, five different bio-polymeric admixtures were used in different proportions to improve some physical and mechanical properties of cementitious composite mortars. In addition, the effects of bio-polymeric admixtures on mortars were compared with the effects of cement chemicals on mortars.

As the unit volume mass results were examined, there was a slight decrease in the unit volume mass of the mortars when all other bio-polymeric materials were used as admixtures in the mortars, except for ES. It has been determined that fatty acids, lignin and cellulose additives have some air-entraining effect in cementitious mortars[277,279,280]. In the use of eggshell, the opposite effect is observed, and eggshell powder can fill the voids with its good filling feature. It was determined that the extractive and lignin content of bio-polymeric admixtures increased the flowability of the cement mortar. In addition, it was determined that bio-polymeric admixtures with higher extractive and lignin ratios had a greater plasticizing effect. Also, it was determined that the extractive and lignin content of bio-polymeric admixtures delayed the initial setting time of the cement mortar. In addition, it was determined that bio-polymeric admixture with higher extractive and lignin ratios had a greater set retarding effect.

It was determined that bio-polymeric admixture with higher extractive and lignin ratios had a greater water repellent effect.

It was determined that the cellulose amount and crystallinity index of bio-polymeric admixtures considerably effect 28-days compressive and flexural strength and 150-days compressive strength of the cement mortars. It has been observed that as the grain size of the biopolymeric additive increases, the mechanical properties can also improve due to the increase in fiber properties. Alos, high amount of pectin contained in the high extractive substance plays an important role in the hydration of cement in long-term ages and increases the compressive strength.

It has been determined that the bio-polymeric additives evaluated in this study can be used instead of cement chemicals at certain rates. They can be used in certain proportions instead of polycarboxylates and melamine sulfanates with their plasticizing properties, instead of tartaric acid with their setting retarding properties, instead of calcium stearate with their water-repellent properties.

In addition, according to the study findings, it was determined that the most effective particle size in bio-polymeric admixtures was 0/125 μm .

6. In the fourth phase of the study, XRD analyzes were carried out to examine the microstructure development of cement pastes on the 3rd, 7th, 28th and 150th days of the cement pastes with bio-polymeric admixtures. In addition, the matrix structure of the 28-day mortar samples was examined by SEM/EDS analyses. It has been determined that there is a direct proportionality between the compressive strength and the Si/Ca ratio. Cement matrix structure of the mortars with a Si/Ca ratio below 0.25 and above 0.80 had a relatively high number of unhydrated cement grains. The density of unhydrated cement phases at early ages was determined. This density continues in later ages due to the use of lignocellulosic bio-polymeric admixtures. However, looking at the long-term results, unhydrated cement grains decrease especially in materials with high pectin content.
7. In the fifth stage of the study, durability properties of mortars such as sulphate effect, acid effect and freeze-thaw effect were investigated. It has been determined that sulfate may deteriorate the mortar structures with ES and HKS admixtures with shorter interaction, while mortars using AKS, WKS and OS admixtures need to be exposed to sulfate for a longer period of time to deteriorate the structure. AKS and ES admixed mortars lost their compressive strength in 30 cycles under acid solution. Therefore, considering the exposure time to acid solution, it can be said that HKS, WKS and OS admixtures can make cement mortar comparatively more durable under the influence of acid solution. In addition, lignocellulosic bio-polymeric admixtures have a significant positive effect on the freeze-thaw durability of the mortar.
8. In the last stage of the study, the use of bio-polymeric admixtures in cementitious composite mortars was optimized. In addition, a regression formula was produced for each study output. According to the optimization analysis, it was determined that the best mix could be with the use of 0.2 wt.% of 0/125 μm size ES. The second and third best mixes are obtained by using 0.5 wt.% and 1.0 wt.% of 0/125 μm OS. In the production phase of the regression formula, the second order nonlinear rational expression was determined as the best option. R-square values of the regression formulas produced with this model were determined as high values between 0.89 and 0.97.

References

- [1] Thakur VK, Thakur MK. Handbook of Polymers for Pharmaceutical Technologies, Structure and Chemistry, vol. 1. John Wiley & Sons 2015.
- [2] Onar N. Biopolimerlerin Özellikleri ve Tekstil Aplikasyonlarında Kullanım Olanakları. In: I. Ulus. Tekst. Yardımcı Kimyasalları Kongresi. Bursa: 2002; P-5.
- [3] Stevens MP. Polymer Chemistry: An Introduction. Oxford univ. press New York 1999.
- [4] Lalit R, Mayank P, Ankur K. Natural fibers and biopolymers characterization: a future potential composite material. Strojnícky Časopis-Journal of Mechanical Engineering 2018; 68(1): 33–50.
- [5] Mohan S, Oluwafemi OS, Kalarikkal N, Thomas S, Songca SP. Biopolymers—application in nanoscience and nanotechnology. Recent Advances in Biopolymers. Croatia: InTech 2016: 47–72.
- [6] Hassan MES, Bai J, Dou D-Q. Biopolymers; definition, classification and applications. Egyptian Journal of Chemistry 2019; 62(9): 1725–1737.
- [7] Ekiert M, Młyniec A, Uhl T. The influence of degradation on the viscosity and molecular mass of poly (lactide acid) biopolymer. Diagnostyka 2015; 16(4): 63–70.
- [8] Othman SH. Bio-nanocomposite materials for food packaging applications: types of biopolymer and nano-sized filler. Agriculture and Agricultural Science Procedia 2014; 2: 296–303.
- [9] Jaszkiwicz A, Bledzki AK. Polymers from renewable raw materials—today and tomorrow. Humboldt College, Collegium Polonicum Frankfurt (Oder)/Slubice 2008: 13–15.
- [10] Araújo TR, Petkowicz CL de O, Cardoso VL, Coutinho Filho U, Vieira PA.

- Biopolymer production using fungus *mucor racemosus fresenius* and glycerol as substrate. *Polímeros* 2016; 26(2): 144–151.
- [11] Leathers TD. Biotechnological production and applications of pullulan. *Applied Microbiology and Biotechnology* 2003; 62(5–6): 468–473.
- [12] Gounga ME, Xu S-Y, Wang Z. Whey protein isolate-based edible films as affected by protein concentration, glycerol ratio and pullulan addition in film formation. *Journal of Food Engineering* 2007; 83(4): 521–530.
- [13] Rekha MR, Sharma CP. Pullulan as a promising biomaterial for biomedical applications: a perspective. *Trends Biomater Artif Organs* 2007; 20(2): 116–121.
- [14] Khan MS, Zhang X, You L, Fu X, Abbasi AM. Structure and bioactivities of fungal polysaccharides. *Polysaccharides: Bioactivity and Biotechnology* 2014: 1–14.
- [15] Cheba BA. Chitin and chitosan: marine biopolymers with unique properties and versatile applications. *Global Journal of Biotechnology & Biochemistry* 2011; 6(3): 149–153.
- [16] Khwaldia K, Arab-Tehrany E, Desobry S. Biopolymer coatings on paper packaging materials. *Comprehensive Reviews in Food Science and Food Safety* 2010; 9(1): 82–91.
- [17] Reddy N, Yang Y. Potential of plant proteins for medical applications. *Trends in Biotechnology* 2011; 29(10): 490–498.
- [18] Fahy E, Subramaniam S, Murphy RC, Nishijima M, Raetz CRH, Shimizu T, et al. Update of the lipid maps comprehensive classification system for lipids. *Journal of Lipid Research* 2009; 50(Supplement): S9–S14.
- [19] Subramaniam S, Fahy E, Gupta S, Sud M, Byrnes RW, Cotter D, et al. Bioinformatics and systems biology of the lipidome. *Chemical Reviews* 2011; 111(10): 6452–6490.
- [20] Mashaghi S, Jadidi T, Koenderink G, Mashaghi A. Lipid nanotechnology. *International Journal of Molecular Sciences* 2013; 14(2): 4242–4282.

- [21] Anneken DJ, Both S, Christoph R, Fieg G, Steinberner U, Westfechtel A. Fatty acids. Ullmann's Encyclopedia of Industrial Chemistry 2000.
- [22] Baker EA. Chemistry and Morphology of Plant Epicuticular Waxes. In: Linn. Soc. Symp. Ser. 1982.
- [23] Quideau S, Deffieux D, Douat-Casassus C, Pouységu L. Plant polyphenols: chemical properties, biological activities, and synthesis. *Angewandte Chemie International Edition* 2011; 50(3): 586–621.
- [24] Nonaka G. Isolation and structure elucidation of tannins. *Pure and Applied Chemistry* 1989; 61(3): 357–360.
- [25] Lu J, Tappel RC, Nomura CT. Mini-review: biosynthesis of poly (hydroxyalkanoates). *Journal of Macromolecular Science®, Part C: Polymer Reviews* 2009; 49(3): 226–248.
- [26] Sorrentino A, Gorrasi G, Vittoria V. Potential perspectives of bio-nanocomposites for food packaging applications. *Trends in Food Science & Technology* 2007; 18(2): 84–95.
- [27] Auras RA, Lim L-T, Selke SEM, Tsuji H. *Poly (Lactic Acid): Synthesis, Structures, Properties, Processing, and Applications*, vol. 10. John Wiley & Sons 2011.
- [28] Mitra BC. Environment friendly composite materials: biocomposites and green composites. *Defence Science Journal* 2014; 64(3): 244.
- [29] Tănase EE, Popa ME, Râpă M, Popa O. Preparation and characterization of biopolymer blends based on polyvinyl alcohol and starch. *Romanian Biotechnological Letters* 2015; 20(2): 10307.
- [30] Chong EJ, Phan TT, Lim IJ, Zhang YZ, Bay BH, Ramakrishna S, et al. Evaluation of electrospun pcl/gelatin nanofibrous scaffold for wound healing and layered dermal reconstitution. *Acta Biomaterialia* 2007; 3(3): 321–330.
- [31] Dziuba R, Kucharska M, Madej-Kiełbik L, Sulak K, Wiśniewska-Wrona M. Biopolymers and biomaterials for special applications within the context of the

circular economy. *Materials* 2021; 14(24): 7704.

- [32] Morin-Crini N, Lichtfouse E, Torri G, Crini G. Applications of chitosan in food, pharmaceuticals, medicine, cosmetics, agriculture, textiles, pulp and paper, biotechnology, and environmental chemistry. *Environmental Chemistry Letters* 2019; 17(4): 1667–1692.
- [33] Plank J. Applications of biopolymers in construction engineering. *Biopolymers Online* 2005.
- [34] Ventolà L, Vendrell M, Giraldez P, Merino L. Traditional organic additives improve lime mortars: new old materials for restoration and building natural stone fabrics. *Construction and Building Materials* 2011; 25(8): 3313–3318.
- [35] Chandra S, Aavik J. Influence of proteins on some properties of portland cement mortar. *International Journal of Cement Composites and Lightweight Concrete* 1987; 9(2): 91–94.
- [36] Gour KA, Ramadoss R, Selvaraj T. Revamping the traditional air lime mortar using the natural polymer–areca nut for restoration application. *Construction and Building Materials* 2018; 164: 255–264.
- [37] Pahlavan P, Manzi S, Sansonetti A, Bignozzi MC. Valorization of organic additions in restorative lime mortars: spent cooking oil and albumen. *Construction and Building Materials* 2018; 181: 650–658.
- [38] Fang S, Zhang K, Zhang H, Zhang B. A study of traditional blood lime mortar for restoration of ancient buildings. *Cement and Concrete Research* 2015; 76: 232–241.
- [39] Olivia M, Jingga H, Toni N, Wibisono G. Biopolymers to Improve Physical Properties and Leaching Characteristics of Mortar and Concrete: A Review. In: *IOP Conf. Ser. Mater. Sci. Eng.*, vol. 345. IOP Publishing 2018; 12028.
- [40] Mignon A, Snoeck D, D’Halluin K, Balcaen L, Vanhaecke F, Dubruel P, et al. Alginate biopolymers: counteracting the impact of superabsorbent polymers on mortar strength. *Construction and Building Materials* 2016; 110: 169–174.

- [41] Vikan HV. Rheology and reactivity of cementitious binders with plasticizers. 2005.
- [42] Chatterji J, Brenneis DC, Gray DW, Lebo SE, Dickman SL. Cement compositions and biodegradable dispersants therefor. 2000.
- [43] Colombo A, Geiker MR, Justnes H, Lauten RA, De Weerd K. On the effect of calcium lignosulfonate on the rheology and setting time of cement paste. *Cement and Concrete Research* 2017; 100: 435–444.
- [44] Payen A. Mémoire sur la composition du tissu propre des plantes et du ligneux. *Comptes Rendus* 1838; 7: 1052–1056.
- [45] Brongniart A, Pelouze TJ, Dumas AB. Rapport sur un mémoire de m. payen, relatif à la composition de la matière ligneuse. *CR Hebd Seances Acad Sci* 1839; 8: 51–53.
- [46] Klemm D, Heublein B, Fink H, Bohn A. Cellulose: fascinating biopolymer and sustainable raw material. *Angewandte Chemie International Edition* 2005; 44(22): 3358–3393.
- [47] Chen H. Chemical Composition and Structure of Natural Lignocellulose. In: *Biotechnol. Lignocellul.* Springer 2014; 25–71.
- [48] Kalkan ŞO, Gündüz L. Yeni Nesil Kompozit Harçlarda Polimer Kullanımları Üzerine Bir İnceleme. In: *Uluslararası Yapılarda Kimyasal Katkılar 5. Sempozyumu ve Sergisi.* Ankara: 2017; 253–266.
- [49] Ayırmis N, Kaymakci A, Ozdemir F. Physical, mechanical, and thermal properties of polypropylene composites filled with walnut shell flour. *Journal of Industrial and Engineering Chemistry* 2013; 19(3): 908–914.
- [50] Harika K, Sunitha K, Kumar PP, Maheshwar K, Rao MY. Basic concepts of cellulose polymers-a comprehensive review. *Archives of Pharmacy Practice* 2012; 3(3): 202.
- [51] Majee SB. *Emerging Concepts in Analysis and Applications of Hydrogels.* BoD–Books on Demand 2016.

- [52] Feller RL, Wilt MH. Evaluation of Cellulose Ethers for Conservation. Getty Publications 1991.
- [53] Company DC. Methocel cellulose ethers technical handbook. 2002.
- [54] Ruot B, Goto T, Pourchez J. Some Aspects of Cellulose Ethers and Latexes Influence on the Properties of Cement-Based Materials — Examples of Results Obtained within the CEReM. In: 7. Symp. Bras. Tecnol. Das Argamassas. 2007.
- [55] Khayat KH. Viscosity-enhancing admixtures for cement-based materials—an overview. *Cement and Concrete Composites* 1998; 20(2–3): 171–188.
- [56] Peschard A, Govin A, Grosseau P, Guilhot B, Guyonnet R. Effect of polysaccharides on the hydration of cement paste at early ages. *Cement and Concrete Research* 2004; 34(11): 2153–2158.
- [57] Betioli AM, Gleize PJP, Silva DA, John VM, Pileggi RG. Effect of hmc on the consolidation of cement pastes: isothermal calorimetry versus oscillatory rheometry. *Cement and Concrete Research* 2009; 39(5): 440–445.
- [58] Pourchez J, Peschard A, Grosseau P, Guyonnet R, Guilhot B, Vallée F. HPMC and hmc influence on cement hydration. *Cement and Concrete Research* 2006; 36(2): 288–294.
- [59] Pourchez J, Grosseau P, Guyonnet R, Ruot B. HEC influence on cement hydration measured by conductometry. *Cement and Concrete Research* 2006; 36(9): 1777–1780.
- [60] Ohama Y. Polymer-based admixtures. *Cement and Concrete Composites* 1998; 20(2–3): 189–212.
- [61] Patural L, Marchal P, Govin A, Grosseau P, Ruot B, Deves O. Cellulose ethers influence on water retention and consistency in cement-based mortars. *Cement and Concrete Research* 2011; 41(1): 46–55.
- [62] Li J-Y, Yeh A-I. Relationships between thermal, rheological characteristics and swelling power for various starches. *Journal of Food Engineering* 2001; 50(3): 141–148.

- [63] Herrero-Martínez JM, Schoenmakers PJ, Kok WT. Determination of the amylose–amylopectin ratio of starches by iodine-affinity capillary electrophoresis. *Journal of Chromatography A* 2004; 1053(1–2): 227–234.
- [64] Brown WH, Poon T. *Introduction to Organic Chemistry*. John Wiley & Sons 2016.
- [65] Tan H, Zheng X, Ma L, Huang H, Xia B. A study on the effects of starches on the properties of alkali-activated cement and the potential of starch as a self-degradable additive. *Energies* 2017; 10(7): 1048.
- [66] Mendes AC, Boesel LF, Reis RL. Degradation studies of hydrophilic, partially degradable and bioactive cements (hdbcs) incorporating chemically modified starch. *Journal of Materials Science: Materials in Medicine* 2012; 23(3): 667–676.
- [67] Shi C. *The preparation and performance of water-reducing retarder based on starch*. 2009.
- [68] Lü Z, Yu C, She W, Wu J, Wang T, Ran Q. Preparation and action mechanism of starch-based cement hydration heat regulating materials. 2016; 19: 625–630.
- [69] Zhang H, Wang W, Li Q, Tian Q, Li L, Liu J. A starch-based admixture for reduction of hydration heat in cement composites. *Construction and Building Materials* 2018; 173: 317–322.
- [70] Berninger T, Dietz N, Gonzalez Lopez O. Water-soluble polymers in agriculture: xanthan gum as eco-friendly alternative to synthetics. *Microbial Biotechnology* 2021; 14(5): 1881–1896.
- [71] Sakata N, Maruyama K, Minami M. 20 basic properties and effects of welan gum on self-consolidating concrete. *Production Methods and Workability of Concrete* 2004; 32: 237.
- [72] Connors Jr CW, Anderson MW. *Method of coating concrete and masonry surfaces*. 2016.
- [73] Annaamalai MGL, Maheswaran G, Ramesh N, Kamal C, Venkatesh G, Vennila

- P. Investigation of corrosion inhibition of welan gum and neem gum on reinforcing steel embedded in concrete. *International Journal of Electrochemical Science* 2018; 13: 9981–9998.
- [74] Jain N, Garg K, Karmakar NC, Palei SK. Guar Gum in Hydraulic Fracturing in Indian Shale Mines. In: Conference n.d.
- [75] Govin A, Bartholin M-C, Biasotti B, Giudici M, Langella V, Grosseau P. Effect of Guar Gum Derivatives on Fresh State Properties of Portland Cement-Based Mortars. In: *Concr. 2015/RILEM Week-27th Bienn. Natl. Conf. Concr. Inst. Aust. Conjunction with 69th RILEM Week. the Concrete Institute of Australia* 2015; 848-ā.
- [76] Govin A, Bartholin M-C, Biasotti B, Giudici M, Langella V, Grosseau P. Modification of water retention and rheological properties of fresh state cement-based mortars by guar gum derivatives. *Construction and Building Materials* 2016; 122: 772–780.
- [77] Radvand T, Toufigh V. Properties of concrete containing guar gum. *European Journal of Environmental and Civil Engineering* 2020: 1–17.
- [78] Lopes BM, Lessa VL, Silva BM, La Cerda LG. Xanthan gum: properties, production conditions, quality and economic perspective. *J Food Nutr Res* 2015; 54(3): 185–194.
- [79] Shekarforoush E, Faralli A, Ndoni S, Mendes AC, Chronakis IS. Electrospinning of xanthan polysaccharide. *Macromolecular Materials and Engineering* 2017; 302(8): 1700067.
- [80] Zhang J, Gao X, Yu L. Improvement of viscosity-modifying agents on air-void system of vibrated concrete. *Construction and Building Materials* 2020; 239: 117843.
- [81] Dursun Ç. Farklı Tip Biyopolimerlerin Çimento Harcı Mekanik ve Durabilite Özelliklerine Etkisi. Celal Bayar Üniversitesi, 2013.
- [82] (ANS) EP on FA and NS added to F, Mortensen A, Aguilar F, Crebelli R, Di

- Domenico A, Frutos MJ, et al. Re-evaluation of acacia gum (e 414) as a food additive. *EFSA Journal* 2017; 15(4): e04741.
- [83] Dauqan E, Abdullah A. Utilization of gum arabic for industries and human health. *American Journal of Applied Sciences* 2013; 10(10): 1270–1279.
- [84] Zhao C, Zhao Q, Zhang Y, Zhou M. The Effect of Gum Arabic on the Dispersion of Cement Pastes. In: *Proc. 11th Int. Congr. Appl. Mineral.* Springer 2015; 483–494.
- [85] Elinwa AU, Umar M. X-ray diffraction and microstructure studies of gum arabic-cement concrete. *Construction and Building Materials* 2017; 156: 632–638.
- [86] Zakka PW, Job OF, Anigbogu NA. Ecological selfcompacting concrete using gum arabic as a plasticizer. *West Africa Built Environment Research (WABER)* 2015: 10.
- [87] Elinwa AU, Abdulbasir G, Abdulkadir G. Gum arabic as an admixture for cement concrete production. *Construction and Building Materials* 2018; 176: 201–212.
- [88] Mbugua R, Wanjala R, Ndambuki J. Influence of gum acacia karroo on some mechanical properties of cement mortars and concrete. *International Journal of Civil, Environmental, Structural, Construction and Architectural Engineering* 2015; 9(11): 1369–1372.
- [89] Mbugua R, Salim R, Ndambuki J. Effect of gum arabic karroo as a water-reducing admixture in cement mortar. *Case Studies in Construction Materials* 2016; 5: 100–111.
- [90] Agulló E, Rodríguez MS, Ramos V, Albertengo L. Present and future role of chitin and chitosan in food. *Macromolecular Bioscience* 2003; 3(10): 521–530.
- [91] Chawla S, Kanatt S, Sharma A. 35. S. P. Chawla, S. R. Kanatt, & A. K. Sharma. (2014) “Chitosan.” *Polysaccharides*. Springer International Publishing, 2014. 1-24. In: 2014.

- [92] Demir A, Seventekin N. Kitin, kitosan ve genel kullanım alanları. *Tekstil Teknolojileri Elektronik Dergisi* 2009; 3(2): 92–103.
- [93] Pillai CKS, Paul W, Sharma CP. Chitin and chitosan polymers: chemistry, solubility and fiber formation. *Progress in Polymer Science* 2009; 34(7): 641–678.
- [94] Rinaudo M. Chitin and chitosan: properties and applications. *Progress in Polymer Science* 2006; 31(7): 603–632.
- [95] Lasheras-Zubiate M, Navarro-Blasco I, Fernández JM, Alvarez JI. Studies on chitosan as an admixture for cement-based materials: assessment of its viscosity enhancing effect and complexing ability for heavy metals. *Journal of Applied Polymer Science* 2011; 120(1): 242–252.
- [96] Ustinova Y V, Nikiforova TP. Cement compositions with the chitosan additive. *Procedia Engineering* 2016; 153: 810–815.
- [97] Susilowati PE, Rajiani NA, Hermawan H, Zaeni A, Sudiana IN. The Use Immobilized Bacteria-Alginate-Chitin for Crack Remediation. In: *IOP Conf. Ser. Earth Environ. Sci.*, vol. 299. IOP Publishing 2019; 12010.
- [98] Jisheng Y, Chengyin W, Honggan S, Haorong C. Application of chitin in concrete maintenance. *Chemical Industry Times* 1998; (3): 7.
- [99] Kaplan G, YILDIZEL SA, OZTURK AU. THE optimization of biopolymer additive cements on the behavior of freezing and thawing cycles. *European International Journal of Science and Technology* 2015; 4(7): 116–126.
- [100] Baishya P, Mandal M, Gogoi P, Maji TK. Natural polymer-based nanocomposites: a greener approach for the future. *Handbook of Composites from Renewable Materials, Nanocomposites: Science and Fundamentals* 2017; 7: 433.
- [101] Buckley HL, Touchberry CH, McKinley JP, Mathe ZS, Muradyan H, Ling H, et al. Renewable additives that improve water resistance of cellulose composite materials. *Journal of Renewable Materials* 2017; 5(1): 1–13.

- [102] Lagazzo A, Vicini S, Cattaneo C, Botter R. Effect of fatty acid soap on microstructure of lime-cement mortar. *Construction and Building Materials* 2016; 116: 384–390.
- [103] Albayrak AT, Yasar M, Gurkaynak MA, Gurgey I. Investigation of the effects of fatty acids on the compressive strength of the concrete and the grindability of the cement. *Cement and Concrete Research* 2005; 35(2): 400–404.
- [104] Karaipekli A, Sarı A. Preparation and characterization of fatty acid ester/building material composites for thermal energy storage in buildings. *Energy and Buildings* 2011; 43(8): 1952–1959.
- [105] Cellat K, Beyhan B, Güngör C, Konuklu Y, Karahan O, DüNDAR C, et al. Thermal enhancement of concrete by adding bio-based fatty acids as phase change materials. *Energy and Buildings* 2015; 106: 156–163.
- [106] Cellat K, Tezcan F, Beyhan B, Kardaş G, Paksoy H. A comparative study on corrosion behavior of rebar in concrete with fatty acid additive as phase change material. *Construction and Building Materials* 2017; 143: 490–500.
- [107] Wang R, Ren M, Gao X, Qin L. Preparation and properties of fatty acids based thermal energy storage aggregate concrete. *Construction and Building Materials* 2018; 165: 1–10.
- [108] Liston LC. Using mixtures of fatty acid methyl esters as phase change materials for concrete. 2015.
- [109] Liston LC, Farnam Y, Krafcik M, Weiss J, Erk K, Tao BY. Binary mixtures of fatty acid methyl esters as phase change materials for low temperature applications. *Applied Thermal Engineering* 2016; 96: 501–507.
- [110] Liu P, Feng C, Wang F, Gao Y, Yang J, Zhang W, et al. Hydrophobic and water-resisting behavior of portland cement incorporated by oleic acid modified fly ash. *Materials and Structures* 2018; 51(2): 38.
- [111] Hazarika A, Hazarika I, Gogoi M, Bora SS, Borah RR, Goutam PJ, et al. Use of a plant based polymeric material as a low cost chemical admixture in cement

- mortar and concrete preparations. *Journal of Building Engineering* 2018; 15: 194–202.
- [112] Chandra S, Eklund L, Villarreal RR. Use of cactus in mortars and concrete. *Cement and Concrete Research* 1998; 28(1): 41–51.
- [113] Woldemariam AM, Oyawa WO, Abuodha SO. The use of plant extract as shrinkage reducing admixture (sra) to reduce early age shrinkage and cracking on cement mortar. *International Journal of Innovation and Scientific Research* ISSN 2351-8014 Vol. 13 No. 1 Jan 2015; 2015: 136–144.
- [114] Parker K, Garancher J-P, Shah S, Fernyhough A. Expanded polylactic acid-an eco-friendly alternative to polystyrene foam. *Journal of Cellular Plastics* 2011; 47(3): 233–243.
- [115] Biron M. Renewable Plastics Derived From Natural Polymers. In: 2017; 115–154.
- [116] Sin LT, Rahmat AR, Rahman WAWA. 4 - Chemical Properties of Poly(Lactic Acid). In: Sin LT, Rahmat AR, Rahman WAWABT-PA (eds). *Plast. Des. Libr.* Oxford: William Andrew Publishing 2013; 143–176.
- [117] Sin LT, Rahmat AR, Rahman WAWA. 5 - Mechanical Properties of Poly(Lactic Acid). In: Sin LT, Rahmat AR, Rahman WAWABT-PA (eds). *Plast. Des. Libr.* Oxford: William Andrew Publishing 2013; 177–219.
- [118] Yu M, Yao J, Liang J, Zeng Z, Cui B, Zhao X, et al. Development of functionalized abamectin poly (lactic acid) nanoparticles with regulatable adhesion to enhance foliar retention. *RSC Advances* 2017; 7(19): 11271–11280.
- [119] Sayadi AA, Neitzert TR, Clifton GC. Feasibility of a biopolymer as lightweight aggregate in perlite concrete. *International Journal of Civil and Environmental Engineering* 2016; 10(6): 751–761.
- [120] Sayadi A, Neitzert TR, Clifton GC, Han MC. Assessment of vermiculite concrete containing bio-polymer aggregate. *International Journal of Civil and Environmental Engineering* 2016; 10(9): 1180–1187.

- [121] Sayadi A. Engineering properties of lightweight concrete containing poly-lactic acid. 2018.
- [122] Sayadi A, Neitzert TR, Clifton GC, Han MC, De Silva K. Ultra-lightweight concrete containing expanded poly-lactic acid as lightweight aggregate. *KSCE Journal of Civil Engineering* 2018; 22(10): 4083–4094.
- [123] Sayadi A, Neitzert TR, Clifton GC. Influence of poly-lactic acid on the properties of perlite concrete. *Construction and Building Materials* 2018; 189: 660–675.
- [124] Jagannathan P. THE study on the concrete by part cement with fly ash casein. *International Journal of Civil Engineering* 2017; 8(4).
- [125] Reddy AB, Manjula B, Sudhakar K, Sivanjineyulu V, Jayaramudu T, Sadiku ER. Polyethylene/other biomaterials-based biocomposites and bionanocomposites. *Polyethylene-Based Biocomposites Bionanocomposites* 2016: 279–314.
- [126] Jasiczak J, Zielinski K. Effect of protein additive on properties of mortar. *Cement and Concrete Composites* 2006; 28(5): 451–457.
- [127] WANG M, CHENG L. Preparation and performance of protein-concrete foaming agent from rapeseed meal [j]. *Fine Chemicals* 2011; 1.
- [128] YIN B, LIU C, HUO J, WEI J, LU Z, KONG Q. Preparation and performance measurement of animal protein foaming agent for concrete [j]. *New Building Materials* 2007; 7: 8–11.
- [129] Panesar DK. Cellular concrete properties and the effect of synthetic and protein foaming agents. *Construction and Building Materials* 2013; 44: 575–584.
- [130] Chinthapalli R, Skoczinski P, Carus M, Baltus W, de Guzman D, Käß H, et al. Biobased building blocks and polymers—global capacities, production and trends, 2018–2023. *Industrial Biotechnology* 2019; 15(4): 237–241.
- [131] Hataf N, Ghadir P, Ranjbar N. Investigation of soil stabilization using chitosan biopolymer. *Journal of Cleaner Production* 2018; 170: 1493–1500.

- [132] Fatehi H, Abtahi SM, Hashemolhosseini H, Hejazi SM. A novel study on using protein based biopolymers in soil strengthening. *Construction and Building Materials* 2018; 167: 813–821.
- [133] Aguilar R, Nakamatsu J, Ramírez E, Elgegren M, Ayarza J, Kim S, et al. The potential use of chitosan as a biopolymer additive for enhanced mechanical properties and water resistance of earthen construction. *Construction and Building Materials* 2016; 114: 625–637.
- [134] TS EN 196-2, Methods of Testing Cement- Part 2: Chemical Analysis of Cement. 2013.
- [135] ASTM C188-17, Standard Test Method for Density of Hydraulic Cement. West Conshohocken, PA: 2017.
- [136] TS EN 196-6, Methods of Testing Cement - Part 6: Determination of Fineness. 2020.
- [137] Institute TS. TS en 196–1 methods of testing cement-part 1: determination of strength. 2009.
- [138] TS 1247, Concrete Mixing, Casting and Maintenance Rules (under Normal Weather Conditions). 2018.
- [139] TS EN 1008, Mixing Water for Concrete - Specifications for Sampling, Testing and Assessing the Suitability of Water, Including Water Recovered from Processes in the Concrete Industry, as Mixing Water for Concrete. 2003.
- [140] Bishop M, Barron AR. Cement hydration inhibition with sucrose, tartaric acid, and lignosulfonate: analytical and spectroscopic study. *Industrial & Engineering Chemistry Research* 2006; 45(21): 7042–7049.
- [141] Hunton P. Research on eggshell structure and quality: an historical overview. *Brazilian Journal of Poultry Science* 2005; 7(2): 67–71.
- [142] Arias JL, Fernandez MS. Role of extracellular matrix molecules in shell formation and structure. *World's Poultry Science Journal* 2001; 57(4): 349–357.

- [143] Nys Y, Gautron J, Garcia-Ruiz JM, Hincke MT. Avian eggshell mineralization: biochemical and functional characterization of matrix proteins. *Comptes Rendus Palevol* 2004; 3(6–7): 549–562.
- [144] Gautron J, Hincke MT, Mann K, Panhéleux M, Bain M, McKee MD, et al. Ovocalyxin-32, a novel chicken eggshell matrix protein isolation, amino acid sequencing, cloning, and immunocytochemical localization. *Journal of Biological Chemistry* 2001; 276(42): 39243–39252.
- [145] Gowsika D, Sarankokila S, Sargunan K. Experimental investigation of egg shell powder as partial replacement with cement in concrete. *International Journal of Engineering Trends and Technology* 2014; 14(2): 65–68.
- [146] Dhanalakshmi M, Sowmya NJ, Chandrashekar A. A comparative study on egg shell concrete with partial replacement of cement by fly ash. *International Journal for Research in Applied Science and Engineering Technology (IJRASET)* 2015; 3(special issue 2): 12–20.
- [147] Karthick J, Jeyanthi R, Petchiyammal M. Experimental study on usage of egg shell as partial replacement for sand in concrete. *International Journal of Advanced Research in Education Technology* 2014; 1(1): 7–10.
- [148] Beraldo AL. Portland cement mortar composite with partial sand replacement by eggshell particles. *Open Journal of Inorganic Non-Metallic Materials* 2014; 4(04): 45.
- [149] Sivakumar M, Mahendran N. STRENGTH and permeability properties of concrete using fly ash (fa), rice husk ash (rha) and egg shell powder (esp). *Journal of Theoretical & Applied Information Technology* 2014; 66(1).
- [150] Kalkan Ş, Gündüz L. Evaluation of Physical And Mechanical Performance of A New Generation Composite Mortar Containing Eggshell Powder. 2017.
- [151] Yerramala A. Properties of concrete with eggshell powder as cement replacement. *The Indian Concrete Journal* 2014; 88(10): 94–105.
- [152] Yu TY, Ing DS, Choo CS. The effect of different curing methods on the

compressive strength of eggshell concrete. *Indian Journal of Science and Technology* 2017; 10(6): 1–4.

- [153] TÜİK. Stone Fruits, 1988-2019. 2019.
- [154] GÜNER M, VATANDAŞ M, DURSUN E. Bazı kayısı çeşitlerinde çekirdek kırılma karakteristiklerinin belirlenmesi. 1999.
- [155] Soleimani M, Kaghazchi T. Adsorption of gold ions from industrial wastewater using activated carbon derived from hard shell of apricot stones—an agricultural waste. *Bioresource Technology* 2008; 99(13): 5374–5383.
- [156] Manić N, Janković B, Pijović M, Waisi H, Dodevski V, Stojiljković D, et al. Apricot kernel shells pyrolysis controlled by non-isothermal simultaneous thermal analysis (sta). *Journal of Thermal Analysis and Calorimetry* 2020: 1–15.
- [157] Aljoumaa K, Tabeikh H, Abboudi M. Characterization of apricot kernel shells (*prunus armeniaca*) by ftir spectroscopy, dsc and tga. *Journal of the Indian Academy of Wood Science* 2017; 14(2): 127–132.
- [158] Wu F, Liu C, Zhang L, Lu Y, Ma Y. Comparative study of carbonized peach shell and carbonized apricot shell to improve the performance of lightweight concrete. *Construction and Building Materials* 2018; 188: 758–771.
- [159] Yang K, Gao Q, Tan Y, Tian W, Zhu L, Yang C. Microporous carbon derived from apricot shell as cathode material for lithium–sulfur battery. *Microporous and Mesoporous Materials* 2015; 204: 235–241.
- [160] Demiral I, Kul ŞÇ. Pyrolysis of apricot kernel shell in a fixed-bed reactor: characterization of bio-oil and char. *Journal of Analytical and Applied Pyrolysis* 2014; 107: 17–24.
- [161] Gezer I, Dođru M, Akay G. Gasification of apricot pit shells in a downdraft gasifier. *International Journal of Green Energy* 2009; 6(2): 218–227.
- [162] Yi Z, Yao J, Wang F, Chen H, Liu H, Yu C. Removal of uranium (vi) from aqueous solution by apricot shell activated carbon. *Journal of Radioanalytical and Nuclear Chemistry* 2013; 295(3): 2029–2034.

- [163] Cao J, Wu Y, Jin Y, Yilihan P, Yang S. Dynamic adsorption of anionic dyes by apricot shell activated carbon. *Desalination and Water Treatment* 2015; 53(11): 2990–2998.
- [164] Danish M, Hashim R, Ibrahim MNM, Sulaiman O. Optimization study for preparation of activated carbon from acacia mangium wood using phosphoric acid. *Wood Science and Technology* 2014; 48(5): 1069–1083.
- [165] Yildiz S, Emiroğlu M, Atalar O. Apricot pip shells used as aggregate replacement. *Journal of Civil Engineering and Management* 2012; 18(3): 318–322.
- [166] Wu F, Liu C, Sun W, Zhang L. Mechanical properties of bio-based concrete containing blended peach shell and apricot shell waste. *Materiali in Tehnologije* 2018; 52(5): 645–651.
- [167] Wu F, Yu Q, Liu C, Brouwers HJH, Wang L. Effect of surface treatment of apricot shell on the performance of lightweight bio-concrete. *Construction and Building Materials* 2019; 229: 116859.
- [168] Demirkaya E, Dal O, Yüksel A. Liquefaction of waste hazelnut shell by using sub-and supercritical solvents as a reaction medium. *The Journal of Supercritical Fluids* 2019; 150: 11–20.
- [169] 2016 Yılı Fındık Raporu. 2017.
- [170] Hazelnut Production. Rome: 2016.
- [171] Karagöz B. Yumurta kabuğu, antep fıstığı kabuğu, fındık kabuğu, pirinç kabuğu ve zeytin çekirdeğinden hazırlanan adsorbanların adsorpsiyon performansları. 2011.
- [172] Khushnood RA, Ahmad S, Restuccia L, Spoto C, Jagdale P, Tulliani J-M, et al. Carbonized nano/microparticles for enhanced mechanical properties and electromagnetic interference shielding of cementitious materials. *Frontiers of Structural and Civil Engineering* 2016; 10(2): 209–213.
- [173] FERRO LRGA. NANOPARTICLES FROM FOOD WASTE: A “GREEN”

FUTURE FOR TRADITIONAL BUILDING MATERIALS. In.: 9th Int. Conf. Fract. Mech. Concr. Concr. Struct. n.d.

- [174] Gürü M, Aruntaş Y, Tüzün FN, Bilici İ. Processing of urea-formaldehyde-based particleboard from hazelnut shell and improvement of its fire and water resistance. *Fire and Materials: An International Journal* 2009; 33(8): 413–419.
- [175] Demirbaş A, Aslan A. Effects of ground hazelnut shell, wood, and tea waste on the mechanical properties of cement. *Cement and Concrete Research* 1998; 28(8): 1101–1104.
- [176] TÜİK. Nuts, 1988-2019. 2019.
- [177] Martinez ML, Moiraghi L, Agnese M, Guzman C. Making and Some Properties of Activated Carbon Produced from Agricultural Industrial Residues from Argentina. In.: *Anales-Asociacion Quim. Argentina*, vol. 91. Fernando Garcia Cambeiro 2003; 103–108.
- [178] Li X, Cai Z, Winandy JE, Basta AH. Selected properties of particleboard panels manufactured from rice straws of different geometries. *Bioresource Technology* 2010; 101(12): 4662–4666.
- [179] Jahanban-Esfahlan A, Ostadrahimi A, Tabibiazar M, Amarowicz R. A comprehensive review on the chemical constituents and functional uses of walnut (*juglans spp.*) husk. *International Journal of Molecular Sciences* 2019; 20(16): 3920.
- [180] Cao J-S, Lin J-X, Fang F, Zhang M-T, Hu Z-R. A new absorbent by modifying walnut shell for the removal of anionic dye: kinetic and thermodynamic studies. *Bioresource Technology* 2014; 163: 199–205.
- [181] Pehlivan E, Altun T. Biosorption of chromium (vi) ion from aqueous solutions using walnut, hazelnut and almond shell. *Journal of Hazardous Materials* 2008; 155(1–2): 378–384.
- [182] Ding D, Zhao Y, Yang S, Shi W, Zhang Z, Lei Z, et al. Adsorption of cesium from aqueous solution using agricultural residue–walnut shell: equilibrium,

- kinetic and thermodynamic modeling studies. *Water Research* 2013; 47(7): 2563–2571.
- [183] Kim J-W, Sohn M-H, Kim D-S, Sohn S-M, Kwon Y-S. Production of granular activated carbon from waste walnut shell and its adsorption characteristics for Cu^{2+} ion. *Journal of Hazardous Materials* 2001; 85(3): 301–315.
- [184] Srinivasan A, Viraraghavan T. Removal of oil by walnut shell media. *Bioresource Technology* 2008; 99(17): 8217–8220.
- [185] Hilal NN, Sahab MF, Ali TKM. Fresh and hardened properties of lightweight self-compacting concrete containing walnut shells as coarse aggregate. *Journal of King Saud University-Engineering Sciences* 2020.
- [186] Cheng W, Liu G, Chen L. Pet fiber reinforced wet-mix shotcrete with walnut shell as replaced aggregate. *Applied Sciences* 2017; 7(4): 345.
- [187] Kamal I, Aryan Far Sherwani AA, Khalid A, Saadi I, Harbi A. Walnut shell for partial replacement of fine aggregate in concrete: modeling and optimization. *Journal of Civil Engineering Research* 2017; 7(4): 109–119.
- [188] 2018 YILI ZEYTİN VE ZEYTİNYAĞI RAPORU. 2019.
- [189] TÜİK. Olive Production, 1988-2019. 2019.
- [190] Çetinkaya E. Zeytin çekirdeğinden üretilen aktif karbonun baca gazı desülfürizasyonunda kullanılması. 2009.
- [191] Rodríguez G, Lama A, Rodríguez R, Jiménez A, Guillén R, Fernández-Bolaños J. Olive stone an attractive source of bioactive and valuable compounds. *Bioresource Technology* 2008; 99(13): 5261–5269.
- [192] Koutsomitopoulou AF, Bénézet JC, Bergeret A, Papanicolaou GC. Preparation and characterization of olive pit powder as a filler to pla-matrix bio-composites. *Powder Technology* 2014; 255: 10–16.
- [193] Alkheder S, Obaidat YT, Taamneh M. Effect of olive waste (husk) on behavior of cement paste. *Case Studies in Construction Materials* 2016; 5: 19–25.

- [194] La Rubia-García MD, Yebra-Rodríguez Á, Eliche-Quesada D, Corpas-Iglesias FA, López-Galindo A. Assessment of olive mill solid residue (pomace) as an additive in lightweight brick production. *Construction and Building Materials* 2012; 36: 495–500.
- [195] Barreca F, Fichera CR. Use of olive stone as an additive in cement lime mortar to improve thermal insulation. *Energy and Buildings* 2013; 62: 507–513.
- [196] Cuenca J, Rodríguez J, Martín-Morales M, Sánchez-Roldán Z, Zamorano M. Effects of olive residue biomass fly ash as filler in self-compacting concrete. *Construction and Building Materials* 2013; 40: 702–709.
- [197] Eisa A. Properties of concrete incorporating recycled post-consumer environmental wastes. *International Journal of Concrete Structures and Materials* 2014; 8(3): 251–258.
- [198] C618 A. Standard Specification for Coal Fly Ash and Raw or Calcined Natural Pozzolan for Use in Concrete. In: Am. Soc. Test. Mater. West Conshohocken Pennsylvania, USA 2008.
- [199] Institute TS. 197-1: 2012 cement—part 1: composition, specifications and conformity criteria for common cements. TSI, Ankara n.d.
- [200] Bezerra UT. Biopolymers with Superplasticizer Properties for Concrete. In: *Biopolym. Biotech Admixtures Eco-Efficient Constr. Mater.* Elsevier 2016; 195–220.
- [201] Plank J. Applications of biopolymers and other biotechnological products in building materials. *Applied Microbiology and Biotechnology* 2004; 66(1): 1–9.
- [202] Pacheco-Torgal F, Jalali S. Earth construction: lessons from the past for future eco-efficient construction. *Construction and Building Materials* 2012; 29: 512–519.
- [203] Corbett DB, Kohan N, Machado G, Jing C, Nagardeolekar A, Bujanovic BM. Chemical composition of apricot pit shells and effect of hot-water extraction. *Energies* 2015; 8(9): 9640–9654.

- [204] Uzuner S, Cekmecelioglu D. Hydrolysis of hazelnut shells as a carbon source for bioprocessing applications and fermentation. *International Journal of Food Engineering* 2014; 10(4): 799–808.
- [205] Soleimani M, Kaghazchi T. Agricultural waste conversion to activated carbon by chemical activation with phosphoric acid. *Chemical Engineering & Technology: Industrial Chemistry-Plant Equipment-Process Engineering-Biotechnology* 2007; 30(5): 649–654.
- [206] Wei L, Xu S, Zhang L, Zhang H, Liu C, Zhu H, et al. Characteristics of fast pyrolysis of biomass in a free fall reactor. *Fuel Processing Technology* 2006; 87(10): 863–871.
- [207] Yeganeh MM, Kaghazchi T, Soleimani M. Effect of raw materials on properties of activated carbons. *Chemical Engineering & Technology: Industrial Chemistry-Plant Equipment-Process Engineering-Biotechnology* 2006; 29(10): 1247–1251.
- [208] Aydoğmuş A. KİMYASAL MODİFİKASYON İŞLEMİNİN MÜZİK ALETLERİNİN SES TİNİSİ ÜZERİNE ETKİSİ. İzmir Katip Çelebi University, 2019.
- [209] Sedan D, Pagnoux C, Chotard T, Smith A, Lejolly D, Gloaguen V, et al. Effect of calcium rich and alkaline solutions on the chemical behaviour of hemp fibres. *Journal of Materials Science* 2007; 42(22): 9336–9342.
- [210] Wise LE, Karl HL. Cellulose and hemicellulose in pulp and paper science and technology. Earl LC, Editor 1962; 1.
- [211] TAPPI T. 203 cm-99 alpha-, beta-and gamma-cellulose in pulp. *Tappi Test Methods* 2009; 20(2): 1–5.
- [212] Turkish Standards Institution. TS EN 1015-6, Methods of Test for Mortar for Masonry - Part 7: Determination of Air Content of Fresh Mortar. Ankara: 2000.
- [213] Turkish Standards Institution. TS EN 1015-10, Methods of Test for Mortar for Masonry- Part 10: Determination of Dry Bulk Density of Hardened Mortar.

Ankara: 2001.

- [214] Standard A. C1437-13. Standard Test Method for Flow of Hydraulic Cement Mortar. ASTM, West Conshohocken, PA 2013.
- [215] Institute TS. TS en 196-3 çimento deney metotları-bölüm3: priz süresi ve hacim genleşme tayini. TS EN 2014: 193–196.
- [216] Rossen JE, Lothenbach B, Scrivener KL. Composition of c–s–h in pastes with increasing levels of silica fume addition. *Cement and Concrete Research* 2015; 75: 14–22.
- [217] Rossen JE, Scrivener KL. Optimization of sem-eds to determine the c–a–s–h composition in matured cement paste samples. *Materials Characterization* 2017; 123: 294–306.
- [218] ASTM C1012, Standard Test Method for Length Change of Hydraulic-Cement Mortars Exposed to a Sulfate Solution. West Conshohocken, PA: 2013.
- [219] Davraz M. ISPARTA KEÇİBORLU YÖRESİ DOĞAL AMORF SİLİKA OLUŞUMLARININ GELENEKSEL VE HAFİF BETON ENDÜSTRİLERİNDE KULLANILABİLİRLİĞİNİN ARAŞTIRILMASI. Süleyman Demirel Üniversitesi, 2004.
- [220] Vafaei M, Allahverdi A, Dong P, Bassim N. Acid attack on geopolymer cement mortar based on waste-glass powder and calcium aluminate cement at mild concentration. *Construction and Building Materials* 2018; 193: 363–372.
- [221] Allahverdi A, Skvara F. Sulfuric acid attack on hardened paste of geopolymer cements-part 1. mechanism of corrosion at relatively high concentrations. *Ceramics Silikaty* 2005; 49(4): 225.
- [222] Keleştemur O, Yıldız S, Gökçer B, Arıcı E. Statistical analysis for freeze–thaw resistance of cement mortars containing marble dust and glass fiber. *Materials & Design* 2014; 60: 548–555.
- [223] Wang W, Yang X, Huang S, Yin D, Liu G. Experimental study on the shear behavior of the bonding interface between sandstone and cement mortar under

freeze–thaw. *Rock Mechanics and Rock Engineering* 2020; 53(2): 881–907.

- [224] Elitaş C, ELEREN A, YILDIZ F, DOĞAN M. Gri İlişkisel Analiz İle Sigorta Şirketlerinin Performanslarının Belirlenmesi. In: 16. Finans Sempozyumu. Erzurum, Türkiye: 2012; 521–530.
- [225] Yılmaz E, Güngör F. Gri ilişkisel analiz yöntemine göre farklı sertliklerde optimum takım tutucusunun belirlenmesi. 2. Ulusal Tasarım İmalat ve Analiz Kongresi 2010: 1–8.
- [226] Çakmak Z, Baş M, Yıldırım E. Gri ilişkisel analiz ve uyum analizi ile bir işletmede karşılaşılan üretim hatalarının incelenmesi. Süleyman Demirel Üniversitesi İktisadi ve İdari Bilimler Fakültesi Dergisi 2012; 17(1): 123–142.
- [227] Sreenivasulu R, Rao CS. Application of grey relational analysis for surface roughness and roundness error in drilling of al 6061 alloy. *International Journal of Lean Thinking* 2012; 3(2): 67–78.
- [228] AYDOĞAN EK, ÖZMEN M. Stokastik çok kriterli karar vermede iki yeni yöntem: smaa-gri ilişkisel analiz ve smaa-dematel-gri ilişkisel analiz. *Journal of the Faculty of Engineering & Architecture of Gazi University* 2015; 30(4).
- [229] ARICI E, KELEŞTEMUR O. Gri ilişkisel analiz yöntemi ile tufal katkılı harçların basınç dayanımı ve porozitesinin optimizasyonu. *Politeknik Dergisi* 2021; 24(4): 1445–1452.
- [230] Panda A, Sahoo A, Rout R. Multi-attribute decision making parametric optimization and modeling in hard turning using ceramic insert through grey relational analysis: a case study. *Decision Science Letters* 2016; 5(4): 581–592.
- [231] Haq AN, Marimuthu P, Jeyapaul R. Multi response optimization of machining parameters of drilling al/sic metal matrix composite using grey relational analysis in the taguchi method. *The International Journal of Advanced Manufacturing Technology* 2008; 37(3): 250–255.
- [232] Tosun N. Determination of optimum parameters for multi-performance characteristics in drilling by using grey relational analysis. *The International*

Journal of Advanced Manufacturing Technology 2006; 28(5): 450–455.

- [233] Fung C-P. Manufacturing process optimization for wear property of fiber-reinforced polybutylene terephthalate composites with grey relational analysis. *Wear* 2003; 254(3–4): 298–306.
- [234] Tosun N, Pihtili H. The effect of cutting parameters on wire crater sizes in wire edm. *The International Journal of Advanced Manufacturing Technology* 2003; 21(10): 857–865.
- [235] Lo S-P. The application of an anfis and grey system method in turning tool-failure detection. *The International Journal of Advanced Manufacturing Technology* 2002; 19(8): 564–572.
- [236] Nas E, Altan Özbek N. Optimization of the machining parameters in turning of hardened hot work tool steel using cryogenically treated tools. *Surface Review and Letters* 2020; 27(05): 1950177.
- [237] Aziz MA, Paramasivam P, Lee SL. Prospects for natural fibre reinforced concretes in construction. *International Journal of Cement Composites and Lightweight Concrete* 1981; 3(2): 123–132.
- [238] Gram HE. Durability of natural fibres in concrete. *swedish cement and concrete research institute. CBI Research Fo* 1983; 1(83): 255.
- [239] Wei J, Meyer C. Sisal fiber-reinforced cement composite with portland cement substitution by a combination of metakaolin and nanoclay. *Journal of Materials Science* 2014; 49(21): 7604–7619.
- [240] Šoštarić T, Petrović M, Stojanović J, Marković M, Avdalović J, Hosseini-Bandegharai A, et al. Structural changes of waste biomass induced by alkaline treatment: the effect on crystallinity and thermal properties. *Biomass Conversion and Biorefinery* 2020: 1–11.
- [241] Sghaier AEO Ben, Chaabouni Y, Msahli S, Sakli F. Morphological and crystalline characterization of naoh and naocl treated agave americana l. fiber. *Industrial Crops and Products* 2012; 36(1): 257–266.

- [242] Gan S, Zakaria S, Chen RS, Chia CH, Padzil FNM, Moosavi S. Autohydrolysis processing as an alternative to enhance cellulose solubility and preparation of its regenerated bio-based materials. *Materials Chemistry and Physics* 2017; 192: 181–189.
- [243] Mittal A, Katahira R, Himmel ME, Johnson DK. Effects of alkaline or liquid-ammonia treatment on crystalline cellulose: changes in crystalline structure and effects on enzymatic digestibility. *Biotechnology for Biofuels* 2011; 4(1): 1–16.
- [244] Liao Z, Huang Z, Hu H, Zhang Y, Tan Y. Microscopic structure and properties changes of cassava stillage residue pretreated by mechanical activation. *Bioresource Technology* 2011; 102(17): 7953–7958.
- [245] Kim S, Holtzapple MT. Effect of structural features on enzyme digestibility of corn stover. *Bioresource Technology* 2006; 97(4): 583–591.
- [246] Jaber HA, Mahdi RS, Hassan AK. Influence of eggshell powder on the portland cement mortar properties. *Materials Today: Proceedings* 2020; 20: 391–396.
- [247] Khodadadi B, Bordbar M, Nasrollahzadeh M. Green synthesis of pd nanoparticles at apricot kernel shell substrate using salvia hydrangea extract: catalytic activity for reduction of organic dyes. *Journal of Colloid and Interface Science* 2017; 490: 1–10.
- [248] Ayala J, Fernandez B. Removal of zinc, cadmium and nickel from mining waste leachate using walnut shells. *Environment Protection Engineering* 2019; 45(2).
- [249] Kocaman S. Removal of methylene blue dye from aqueous solutions by adsorption on levulinic acid-modified natural shells. *International Journal of Phytoremediation* 2020; 22(8): 885–895.
- [250] Omri A, Ltaief HBH, Benzina M. Study of retention of silver ions onto activated carbon prepared from almond shell: approach for the treatment of liquid effluent from radiology. 2012.
- [251] Shah AH, Lia X, XUa XD, Wang S, BAia JW, Wang J, et al. Effect of alkali treated walnut shell (*juglansregia*) on high performance thermosets. study of

- curing behavior, thermal and thermomechanical properties. *Digest Journal of Nanomaterials and Biostructures* 2018; 13(3): 857–873.
- [252] Seki Y, Sarikanat M, Sever K, Durmuşkahya C. Extraction and properties of *ferula communis* (chakshir) fibers as novel reinforcement for composites materials. *Composites Part B: Engineering* 2013; 44(1): 517–523.
- [253] Durazzo A, Kiefer J, Lucarini M, Camilli E, Marconi S, Gabrielli P, et al. Qualitative analysis of traditional italian dishes: ftir approach. *Sustainability* 2018; 10(11): 4112.
- [254] Çelik YH, Yalcin R, Topkaya T, Başaran E, Kilickap E. Characterization of hazelnut, pistachio, and apricot kernel shell particles and analysis of their composite properties. *Journal of Natural Fibers* 2021; 18(7): 1054–1068.
- [255] Smith BC. *Infrared Spectra Interpretation. A Systematic Approach*. Boca Raton, FL, USA: CRC Press LLC 1999.
- [256] Liu W, Mohanty AK, Drzal LT, Askel P, Misra M. Effects of alkali treatment on the structure, morphology and thermal properties of native grass fibers as reinforcements for polymer matrix composites. *Journal of Materials Science* 2004; 39(3): 1051–1054.
- [257] Socrates G. *Infrared and Raman Characteristic Group Frequencies: Tables and Charts*. Chichester, West Sussex, England: Wiley 2001.
- [258] Farhan AM, Salem NM, Al-Dujaili AH, Awwad AM. Biosorption studies of cr (vi) ions from electroplating wastewater by walnut shell powder. *American Journal of Environmental Engineering* 2012; 2(6): 188–195.
- [259] Zhang W, Jiang S, Wang K, Wang L, Xu Y, Wu Z, et al. Thermogravimetric dynamics and ftir analysis on oxidation properties of low-rank coal at low and moderate temperatures. *International Journal of Coal Preparation and Utilization* 2015; 35(1): 39–50.
- [260] Yang K, Yang Z, Wu W, Gao H, Zhou C, Sun P, et al. Physicochemical properties improvement and structural changes of bamboo shoots (*phyllostachys*

- praecox f. prevernalis) dietary fiber modified by subcritical water and high pressure homogenization: a comparative study. *Journal of Food Science and Technology* 2020; 57(10): 3659–3666.
- [261] Darmawan S, Wistara NJ, Pari G, Maddu A, Syafii W. Characterization of lignocellulosic biomass as raw material for the production of porous carbon-based materials. *BioResources* 2016; 11(2): 3561–3574.
- [262] Torit J, Pihusut D. Phosphorus removal from wastewater using eggshell ash. *Environmental Science and Pollution Research* 2019; 26(33): 34101–34109.
- [263] Gergely G, Wéber F, Lukács I, Tóth AL, Horváth ZE, Mihály J, et al. Preparation and characterization of hydroxyapatite from eggshell. *Ceramics International* 2010; 36(2): 803–806.
- [264] Aldrich. *The Aldrich Library of FT-IR Spectra*. Milwaukee, WI, USA: 1997.
- [265] Anjaneyulu U, Sasikumar S. Bioactive nanocrystalline wollastonite synthesized by sol–gel combustion method by using eggshell waste as calcium source. *Bulletin of Materials Science* 2014; 37(2): 207–212.
- [266] Goli J, Sahu O. Development of heterogeneous alkali catalyst from waste chicken eggshell for biodiesel production. *Renewable Energy* 2018; 128: 142–154.
- [267] Vujcic D, Comic D, Zarubica A, Micic R, Boskovic G. Kinetics of biodiesel synthesis from sunflower oil over cao heterogeneous catalyst. *Fuel* 2010; 89(8): 2054–2061.
- [268] Boro J, Konwar LJ, Deka D. Transesterification of non edible feedstock with lithium incorporated egg shell derived cao for biodiesel production. *Fuel Processing Technology* 2014; 122: 72–78.
- [269] Farinella N V, Matos GD, Arruda MAZ. Grape bagasse as a potential biosorbent of metals in effluent treatments. *Bioresource Technology* 2007; 98(10): 1940–1946.
- [270] Ahmad M, Usman ARA, Lee SS, Kim S-C, Joo J-H, Yang JE, et al. Eggshell

and coral wastes as low cost sorbents for the removal of Pb^{2+} , Cd^{2+} and Cu^{2+} from aqueous solutions. *Journal of Industrial and Engineering Chemistry* 2012; 18(1): 198–204.

[271] Tizo MS, Blanco LA V, Cagas ACQ, Cruz BRB Dela, Encoy JC, Gunting J V, et al. Efficiency of calcium carbonate from eggshells as an adsorbent for cadmium removal in aqueous solution. *Sustainable Environment Research* 2018; 28(6): 326–332.

[272] Choudhary R, Koppala S, Swamiappan S. Bioactivity studies of calcium magnesium silicate prepared from eggshell waste by sol–gel combustion synthesis. *Journal of Asian Ceramic Societies* 2015; 3(2): 173–177.

[273] Coates J. *Interpretation of Infrared Spectra, a Practical Approach*. Chichester: John Wiley & Sons Ltd 2000.

[274] Thongsanitgarn P, Wongkeo W, Chaipanich A, Poon CS. Heat of hydration of portland high-calcium fly ash cement incorporating limestone powder: effect of limestone particle size. *Construction and Building Materials* 2014; 66: 410–417.

[275] Ali A, Ali S, Yu L, Liu H, Khalid S, Hussain A, et al. Preparation and characterization of starch-based composite films reinforced by apricot and walnut shells. *Journal of Applied Polymer Science* 2019; 136(38): 47978.

[276] Bakisgan C, Dumanli AG, Yürüm Y. Trace elements in turkish biomass fuels: ashes of wheat straw, olive bagasse and hazelnut shell. *Fuel* 2009; 88(10): 1842–1851.

[277] Ślosarczyk A, Klapiszewska I, Jędrzejczak P, Klapiszewski Ł, Jesionowski T. Biopolymer-based hybrids as effective admixtures for cement composites. *Polymers* 2020; 12(5): 1180.

[278] Demir F. Formation and characterization of mechanochemically generated free lignin radicals from olive seeds. *Turkish Journal of Chemistry* 2021; 45(2): 282–294.

[279] Pourchez J, Ruot B, Debayle J, Pourchez E, Grosseau P. Some aspects of

cellulose ethers influence on water transport and porous structure of cement-based materials. *Cement and Concrete Research* 2010; 40(2): 242–252.

- [280] Klapiszewski Ł, Klapiszewska I, Śłosarczyk A, Jesionowski T. Lignin-based hybrid admixtures and their role in cement composite fabrication. *Molecules* 2019; 24(19): 3544.
- [281] Moosberg-Bustnes H, Lagerblad B, Forsberg E. The function of fillers in concrete. *Materials and Structures* 2004; 37(2): 74.
- [282] Subaşı S, Öztürk H, Emiroğlu M. Utilizing of waste ceramic powders as filler material in self-consolidating concrete. *Construction and Building Materials* 2017; 149: 567–574.
- [283] Nehdi M. Microfiller effect on rheology, microstructure, and mechanical properties of high-performance concrete. 1998.
- [284] Ma B, Wang J, Li X, He C, Yang H. The influence of oleic acid on the hydration and mechanical properties of portland cement. *Journal of Wuhan University of Technology-Mater. Sci. Ed.* 2013; 28(6): 1177–1180.
- [285] Lertwattanaruk P, Suntijitto A. Properties of natural fiber cement materials containing coconut coir and oil palm fibers for residential building applications. *Construction and Building Materials* 2015; 94: 664–669.
- [286] Tkach E V, Semenov VS, Tkach SA, Rozovskaya TA. Highly effective water-repellent concrete with improved physical and technical properties. *Procedia Engineering* 2015; 111: 763–769.
- [287] Justnes H, Østnor TA, Barnils Vila N. Vegetable Oils as Water Repellents for Mortars. In: *Proc. 1st Int. Conf. Asian Concr. Fed. Chiang Mai.* 2004; 28–29.
- [288] Wei R, Sakai Y. Improving the properties of botanical concrete based on waste concrete, wood, and kraft lignin powder. *Powder Technology* 2022; 397: 117024.
- [289] Queirós CSGP, Cardoso S, Lourenço A, Ferreira J, Miranda I, Lourenço MJ V, et al. Characterization of walnut, almond, and pine nut shells regarding chemical

- composition and extract composition. *Biomass Conversion and Biorefinery* 2020; 10(1): 175–188.
- [290] Quraishi MA, Kumar V, Abhilash PP, Singh BN. Calcium stearate: a green corrosion inhibitor for steel in concrete environment. *J. Mater. Environ. Sci* 2011; 2(4): 365–372.
- [291] Maryoto A, Sthenly Gan B, Intang Setyo Hermanto N, Setijadi R. Effect of calcium stearate in the mechanical and physical properties of concrete with pcc and fly ash as binders. *Materials* 2020; 13(6): 1394.
- [292] Tada H, Takamura M, Kawashiri M. Genomics of hypertriglyceridemia. *Advances in Clinical Chemistry* 2020; 97: 141–169.
- [293] Wei CB, Othman R, Ying CY, Jaya RP, Ing DS, Mangi SA. Properties of mortar with fine eggshell powder as partial cement replacement. *Materials Today: Proceedings* 2021; 46: 1574–1581.
- [294] Hamada HM, Tayeh BA, Al-Attar A, Yahaya FM, Muthusamy K, Humada AM. The present state of the use of eggshell powder in concrete: a review. *Journal of Building Engineering* 2020; 32: 101583.
- [295] Soroka I, Setter N. The effect of fillers on strength of cement mortars. *Cement and Concrete Research* 1977; 7(4): 449–456.
- [296] Mohamed MAS, Ghorbel E, Wardeh G. Valorization of micro-cellulose fibers in self-compacting concrete. *Construction and Building Materials* 2010; 24(12): 2473–2480.
- [297] Krobba B, Bouhicha M, Kenai S, Courard L. Formulation of low cost eco-repair mortar based on dune sand and stipa tenacissima microfibers plant. *Construction and Building Materials* 2018; 171: 950–959.
- [298] Soliman AM, Nehdi ML. Effect of natural wollastonite microfibers on early-age behavior of uhpc. *Journal of Materials in Civil Engineering* 2012; 24(7): 816–824.
- [299] Zhang Y, Jiao Z, Deng L, Xie L, He B, Liang Q, et al. Comparison of the tensile

behaviour enhancement of cement paste incorporated with μm - and mm -scale cellulose fibres at the early curing age. *Construction and Building Materials* 2022; 322: 126452.

- [300] Li VC, Liang E. Fracture processes in concrete and fiber reinforced cementitious composites. *Journal of Engineering Mechanics* 1986; 112(6): 566–586.
- [301] Afroughsabet V, Biolzi L, Ozbakkaloglu T. High-performance fiber-reinforced concrete: a review. *Journal of Materials Science* 2016; 51(14): 6517–6551.
- [302] Gwon S, Choi YC, Shin M. Effect of plant cellulose microfibers on hydration of cement composites. *Construction and Building Materials* 2021; 267: 121734.
- [303] Ou Z, Xiao Y, Wang J, Ma B, Jiang L, Jian S. Analysis of air voids evolution in cement pastes admixed with non-ionic cellulose ethers. *Journal of Wuhan University of Technology-Mater. Sci. Ed.* 2018; 33(4): 915–923.
- [304] Al-Safy RA. Experimental investigation on properties of cement mortar incorporating eggshell powder. *Journal of Engineering and Sustainable Development* 2015; 19(6): 198–209.
- [305] Chandrasekaran V, Vasanth M, Thirunavukkarasu S. Experimental investigation of partial replacement of cement with glass powder and eggshell powder ash in concrete. *Civ. Eng. Res. J* 2018; 5: 1–9.
- [306] Lauch K-S, Dieryck V, Pollet V. The use of ternary cements to reduce the environmental impact of concrete. *RILEM Technical Letters* 2016; 1: 88–93.
- [307] Ribeiro B, Yamashiki Y, Yamamoto T. A study on mechanical properties of mortar with sugarcane bagasse fiber and bagasse ash. *Journal of Material Cycles and Waste Management* 2020; 22(6): 1844–1851.
- [308] KALKAN ŞO, GÜNDÜZ L. Effect of Waste Hazelnut Shell Powder on The Technical Properties of Cement Mortars. In: 13th Int. Congr. Adv. Civ. Eng. Izmir: 2018; 1–8.
- [309] Sedan D, Pagnoux C, Smith A, Chotard T. Mechanical properties of hemp fibre reinforced cement: influence of the fibre/matrix interaction. *Journal of the*

European Ceramic Society 2008; 28(1): 183–192.

- [310] Shanmugavel D, Selvaraj T, Ramadoss R, Raneri S. Interaction of a viscous biopolymer from cactus extract with cement paste to produce sustainable concrete. *Construction and Building Materials* 2020; 257: 119585.
- [311] Ozturk AU, Baradan B. A comparison study of porosity and compressive strength mathematical models with image analysis. *Computational Materials Science* 2008; 43(4): 974–979.
- [312] Ondova M, Stevulova N, Estokova A. The study of the properties of fly ash based concrete composites with various chemical admixtures. *Procedia Engineering* 2012; 42: 1863–1872.
- [313] Xiaowei Z, Chunxia L, Junyi S. Influence of tartaric acid on early hydration and mortar performance of portland cement-calcium aluminate cement-anhydrite binder. *Construction and Building Materials* 2016; 112: 877–884.
- [314] Nemati Chari M, Naseroleslami R, Shekarchi M. The impact of calcium stearate on characteristics of concrete. *Asian Journal of Civil Engineering* 2019; 20(7): 1007–1020.
- [315] Ing DOHS, Choo CS. Eggshell Powder: Potential Filler in Concrete. In: *Malaysian Tech. Univ. Conf. Eng. Technol.* 2014.
- [316] Parthasarathi N, Prakash M, Satyanarayanan KS. Experimental study on partial replacement of cement with egg shell powder and silica fume. *Rasayan Journal of Chemistry* 2017; 10(2): 442–449.
- [317] Cao M, Ming X, He K, Li L, Shen S. Effect of macro-, micro- and nano-calcium carbonate on properties of cementitious composites-a review. *Materials* 2019; 12(5).
- [318] Bachtiar E, Djamaluddin R, Sampebulu V. Microstructure characteristics of self compacting concrete using sea water. *International Journal of Applied Engineering Research* 2014; 9(22): 18087–18095.
- [319] Hranice C. The effect of water ratio on microstructure and composition of the

- hydration products of portland cement pastes. *Ceramics– Silikáty* 2002; 46(4): 152–158.
- [320] Pizzol VD, Mendes LM, Savastano Jr H, Frías M, Davila FJ, Cincotto MA, et al. Mineralogical and microstructural changes promoted by accelerated carbonation and ageing cycles of hybrid fiber–cement composites. *Construction and Building Materials* 2014; 68: 750–756.
- [321] Booya E, Ghaednia H, Das S, Pande H. Durability of cementitious materials reinforced with various kraft pulp fibers. *Construction and Building Materials* 2018; 191: 1191–1200.
- [322] Tonoli GHD, Rodrigues Filho UP, Savastano Jr H, Bras J, Belgacem MN, Lahr FAR. Cellulose modified fibres in cement based composites. *Composites Part A: Applied Science and Manufacturing* 2009; 40(12): 2046–2053.
- [323] Wei J, Meyer C. Degradation mechanisms of natural fiber in the matrix of cement composites. *Cement and Concrete Research* 2015; 73: 1–16.
- [324] Richardson IG. Tobermorite/jennite-and tobermorite/calcium hydroxide-based models for the structure of csh: applicability to hardened pastes of tricalcium silicate, β -dicalcium silicate, portland cement, and blends of portland cement with blast-furnace slag, metakaolin,. *Cement and Concrete Research* 2004; 34(9): 1733–1777.
- [325] Yu P, Kirkpatrick RJ, Poe B, McMillan PF, Cong X. Structure of calcium silicate hydrate (c-s-h): near-, mid-, and far-infrared spectroscopy. *Journal of the American Ceramic Society* 1999; 82(3): 742–748.
- [326] Nonat A, Lecoq X. The Structure, Stoichiometry and Properties of CSH Prepared by C 3 S Hydration Under Controlled Condition. In: *Nucl. Magn. Reson. Spectrosc. Cem. Mater.* Springer 1998; 197–207.
- [327] Nonat A. The structure and stoichiometry of csh. *Cement and Concrete Research* 2004; 34(9): 1521–1528.
- [328] Taylor HFW. *Cement Chemistry*, vol. 2. Thomas Telford London 1997.

- [329] Chen JJ, Thomas JJ, Taylor HFW, Jennings HM. Solubility and structure of calcium silicate hydrate. *Cement and Concrete Research* 2004; 34(9): 1499–1519.
- [330] Cong X, Kirkpatrick RJ. ²⁹Si mas nmr study of the structure of calcium silicate hydrate. *Advanced Cement Based Materials* 1996; 3(3–4): 144–156.
- [331] Greenberg SA, Chang TN. Investigation of the colloidal hydrated calcium silicates. ii. solubility relationships in the calcium oxide-silica-water system at 25. *The Journal of Physical Chemistry* 1965; 69(1): 182–188.
- [332] Rossen JE. *Composition and Morphology of CASH in Pastes of Alite and Cement Blended with Supplementary Cementitious Materials*. EPFL 2014.
- [333] Ipavec A, Gabrovšek R, Vuk T, Kaučič V, Maček J, Meden A. Carboaluminate phases formation during the hydration of calcite-containing portland cement. *Journal of the American Ceramic Society* 2011; 94(4): 1238–1242.
- [334] Kontoleonos F, Tsakiridis P, Marinos A, Katsiotis N, Kaloidas V, Katsioti M. Dry-grinded ultrafine cements hydration. physicochemical and microstructural characterization. *Materials Research* 2013; 16(2): 404–416.
- [335] Lothenbach B, Bary B, Le Bescop P, Schmidt T, Leterrier N. Sulfate ingress in portland cement. *Cement and Concrete Research* 2010; 40(8): 1211–1225.
- [336] Çavdar A, Yetgin Ş. Investigation of mechanical and mineralogical properties of mortars subjected to sulfate. *Construction and Building Materials* 2010; 24(11): 2231–2242.
- [337] Zhou Y, Li M, Sui L, Xing F. Effect of sulfate attack on the stress–strain relationship of frp-confined concrete. *Construction and Building Materials* 2016; 110: 235–250.
- [338] Yu X, Chen D, Feng J, Zhang Y. Behavior of mortar exposed to different exposure conditions of sulfate attack. *Ocean Engineering* 2018; 157: 1–12.
- [339] Durning TA, Hicks MC. Using microsilica to increase concrete’s resistance to aggressive chemicals. *Concrete International* 1991; 13(3): 42–48.

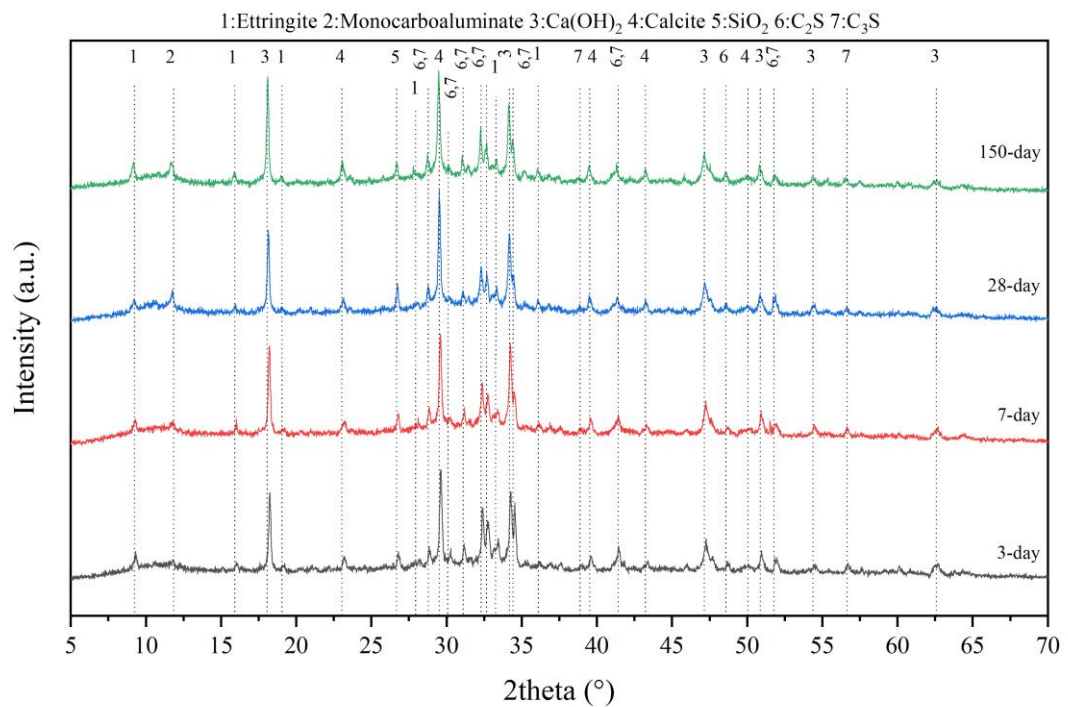
- [340] Chong BW, Othman R, Ramadhansyah PJ, Doh SI, Li X. Properties of concrete with eggshell powder: a review. *Physics and Chemistry of the Earth, Parts A/B/C* 2020; 120: 102951.
- [341] Chang Z-T, Song X-J, Munn R, Marosszeky M. Using limestone aggregates and different cements for enhancing resistance of concrete to sulphuric acid attack. *Cement and Concrete Research* 2005; 35(8): 1486–1494.
- [342] Jo BW, Sikandar MA, Chakraborty S, Baloch Z. Investigation of the acid and sulfate resistance performances of hydrogen-rich water based mortars. *Construction and Building Materials* 2017; 137: 1–11.
- [343] Wang Z-R, Li B, Liu H-B, Zhang Y-X, Qin X. Degradation characteristics of graphite tailings cement mortar subjected to freeze-thaw cycles. *Construction and Building Materials* 2020; 234: 117422.
- [344] Liu T, Zhang C, Zhou K, Tian Y. Freeze-thaw cycling damage evolution of additive cement mortar. *European Journal of Environmental and Civil Engineering* 2021; 25(11): 2089–2110.
- [345] Wang W, Wang S, Yao D, Wang X, Yu X, Zhang Y. Fabrication of all-dimensional superhydrophobic mortar with enhanced waterproof ability and freeze-thaw resistance. *Construction and Building Materials* 2020; 238: 117626.
- [346] Kalyon A, Günay M, Özyürek D. Application of grey relational analysis based on taguchi method for optimizing machining parameters in hard turning of high chrome cast iron. *Advances in Manufacturing* 2018; 6(4): 419–429.

Appendices

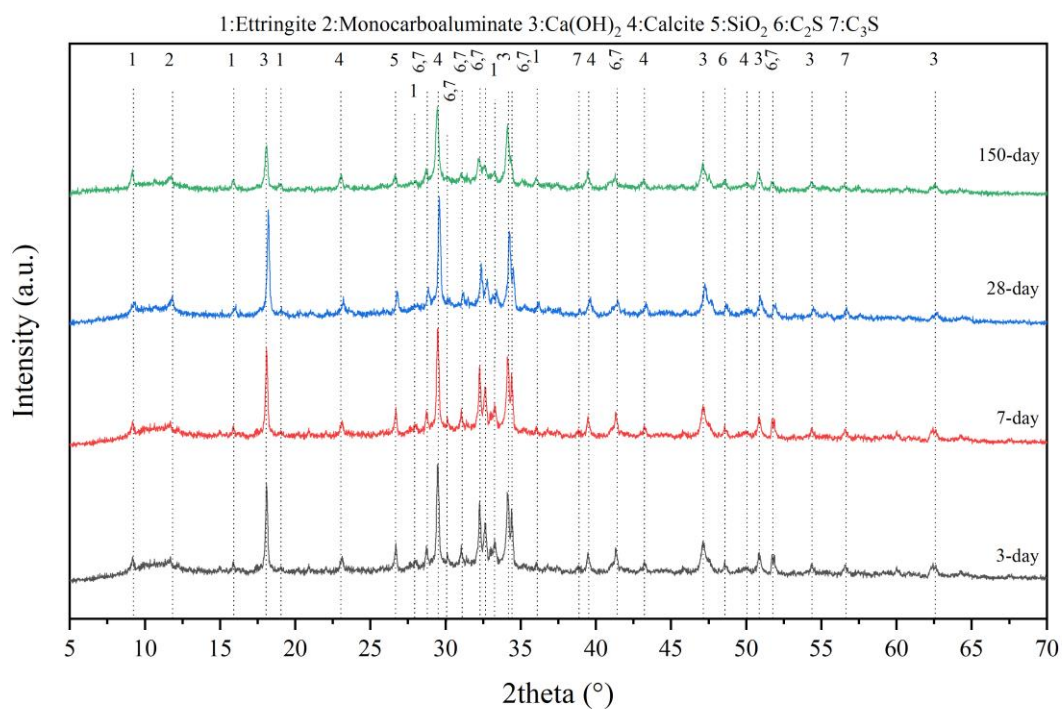
Appendix A

Graphical Representation of XRD

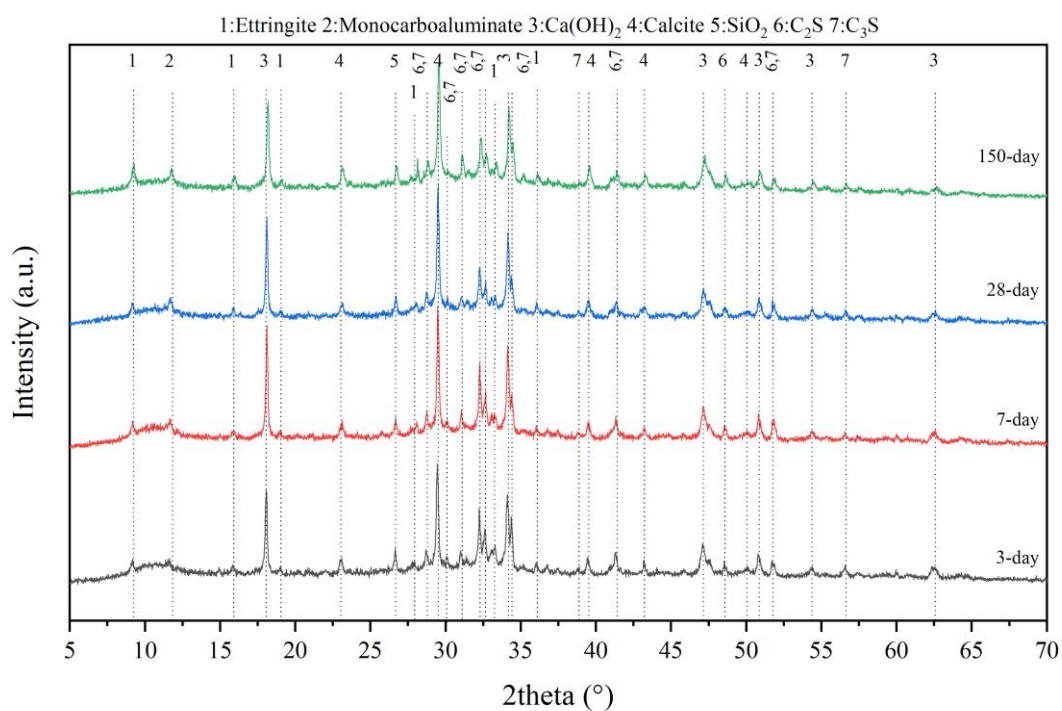
Analysis



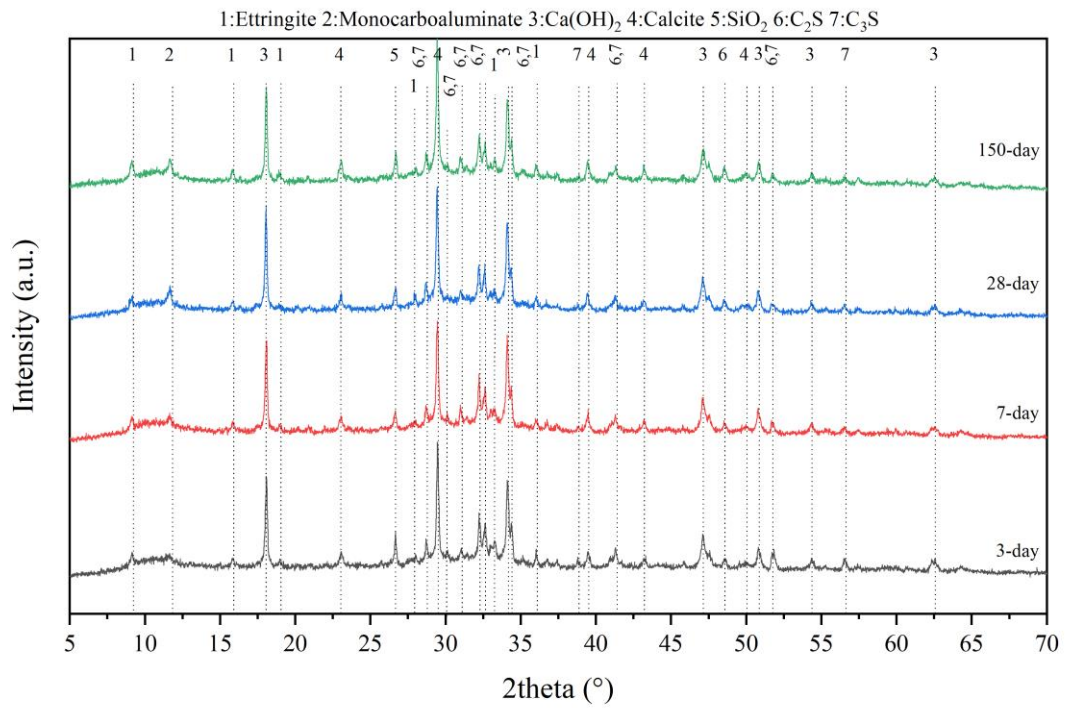
Appendix A.1: Mineralogical development of reference paste



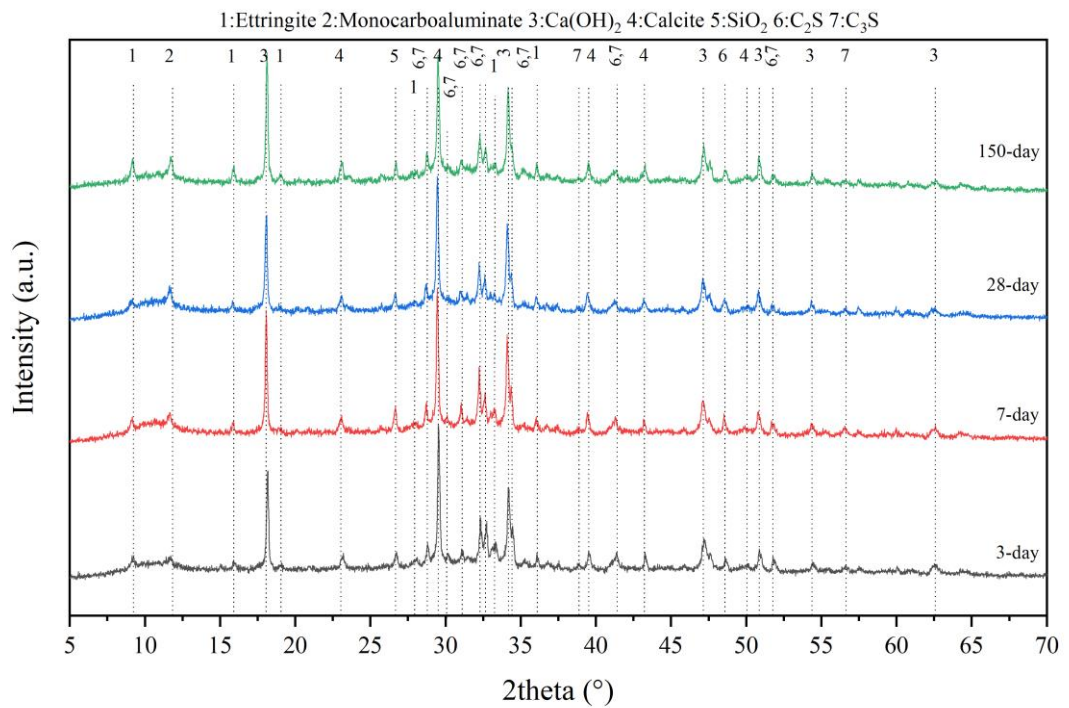
Appendix A.2: Mineralogical development of 125ES0.2



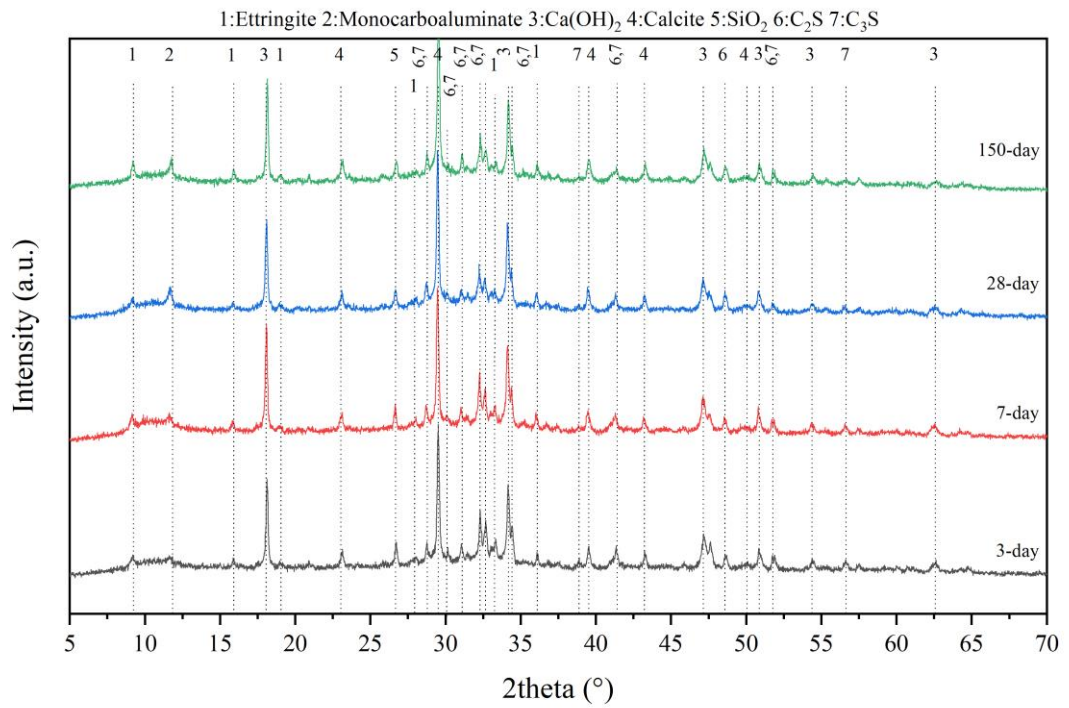
Appendix A.3: Mineralogical development of 125ES0.35



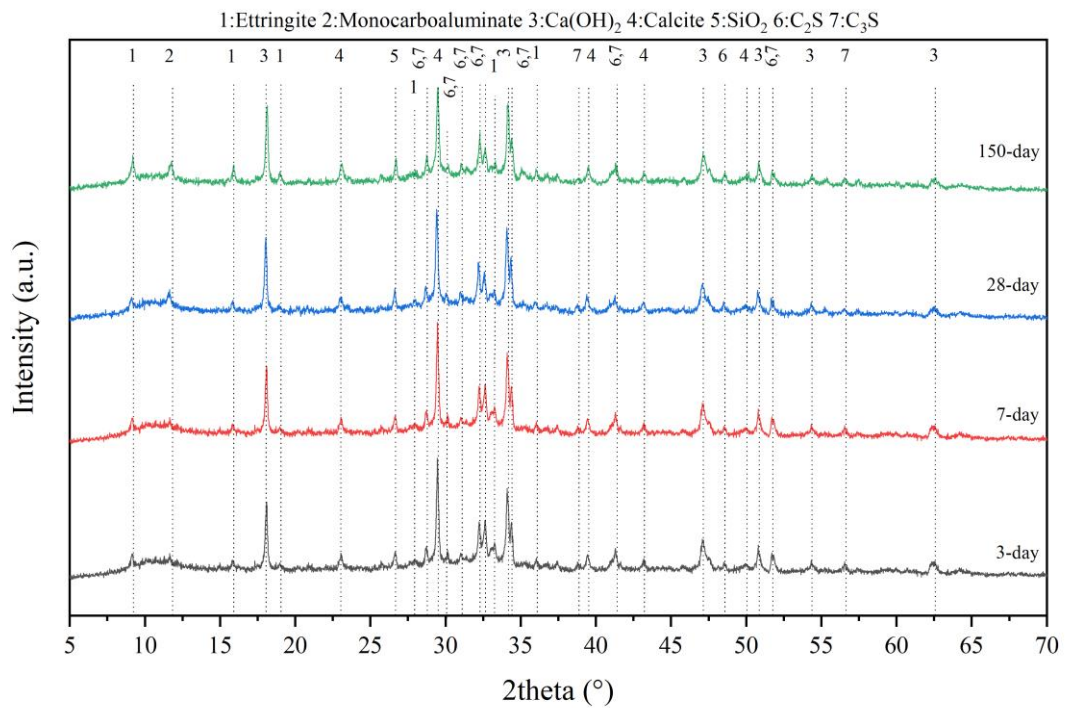
Appendix A.4: Mineralogical development of 125ES0.5



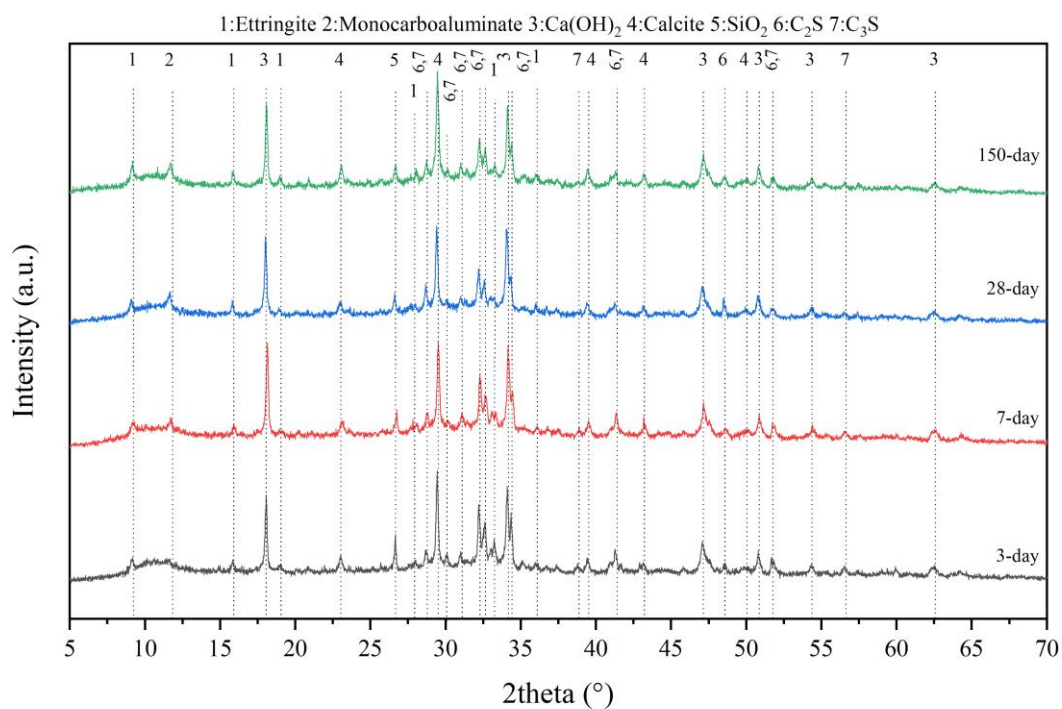
Appendix A.5: Mineralogical development of 125ES1.0



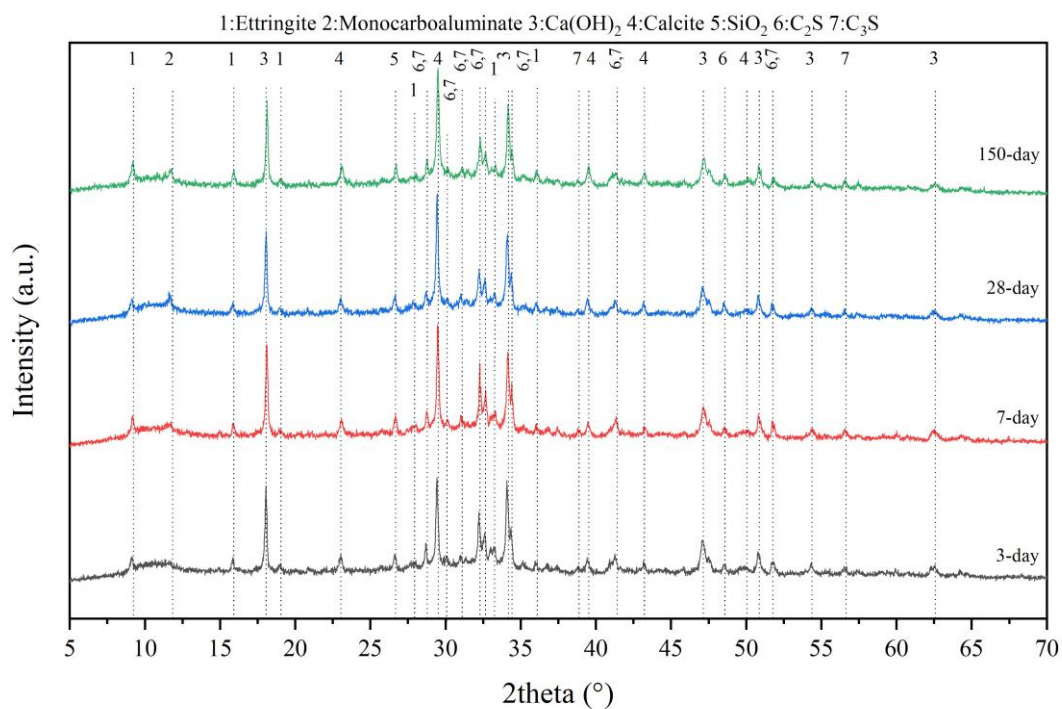
Appendix A.6: Mineralogical development of 125ES1.5



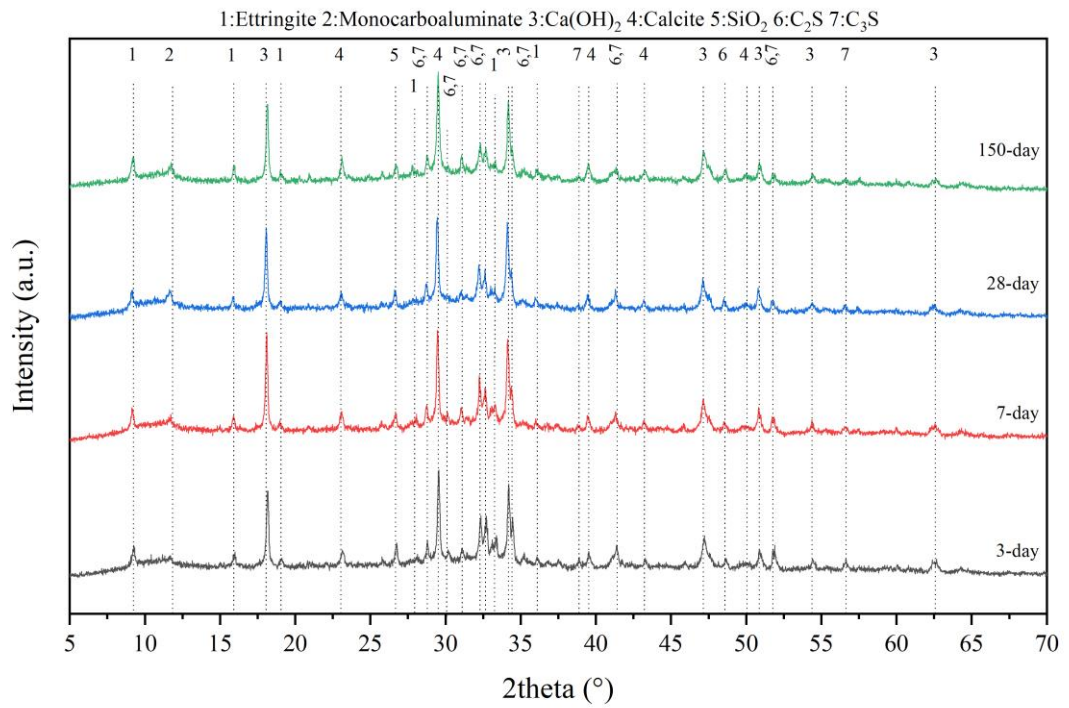
Appendix A.7: Mineralogical development of 125AKS0.2



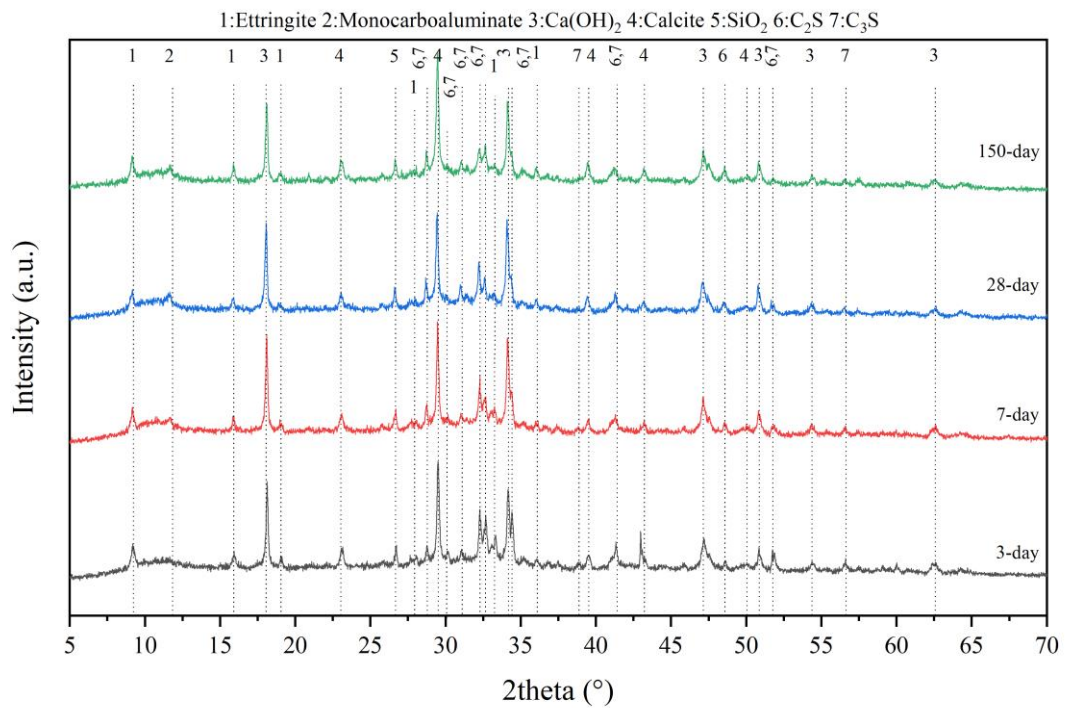
Appendix A.8: Mineralogical development of 125AKS0.35



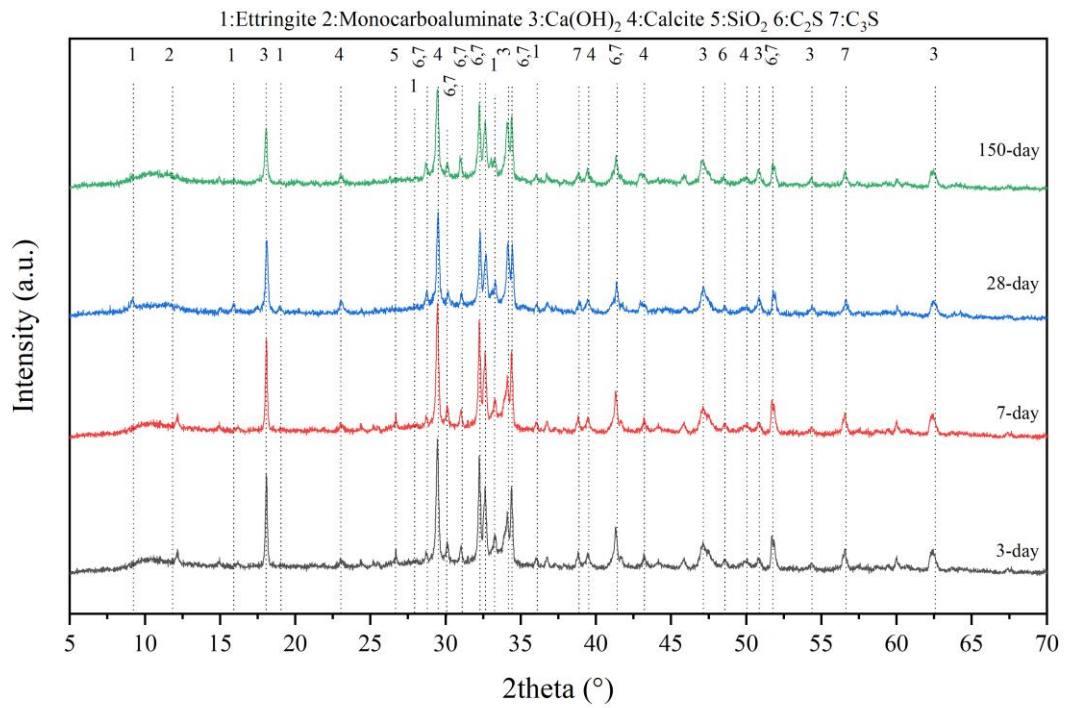
Appendix A.9: Mineralogical development of 125AKS0.5



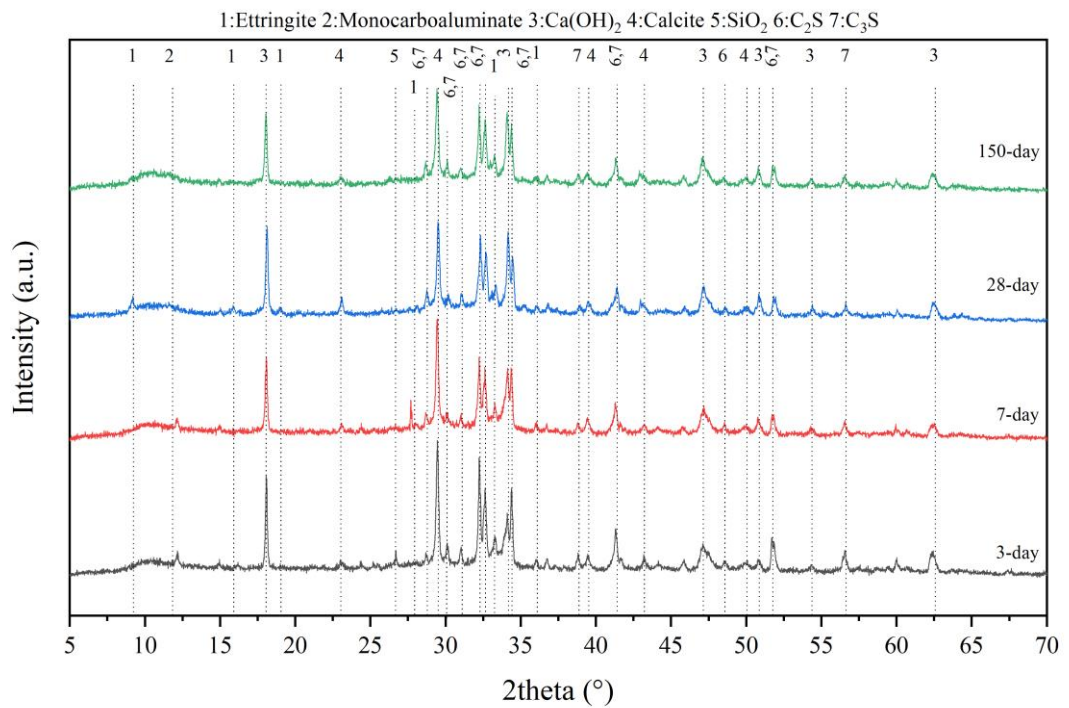
Appendix A.10: Mineralogical development of 125AKS1.0



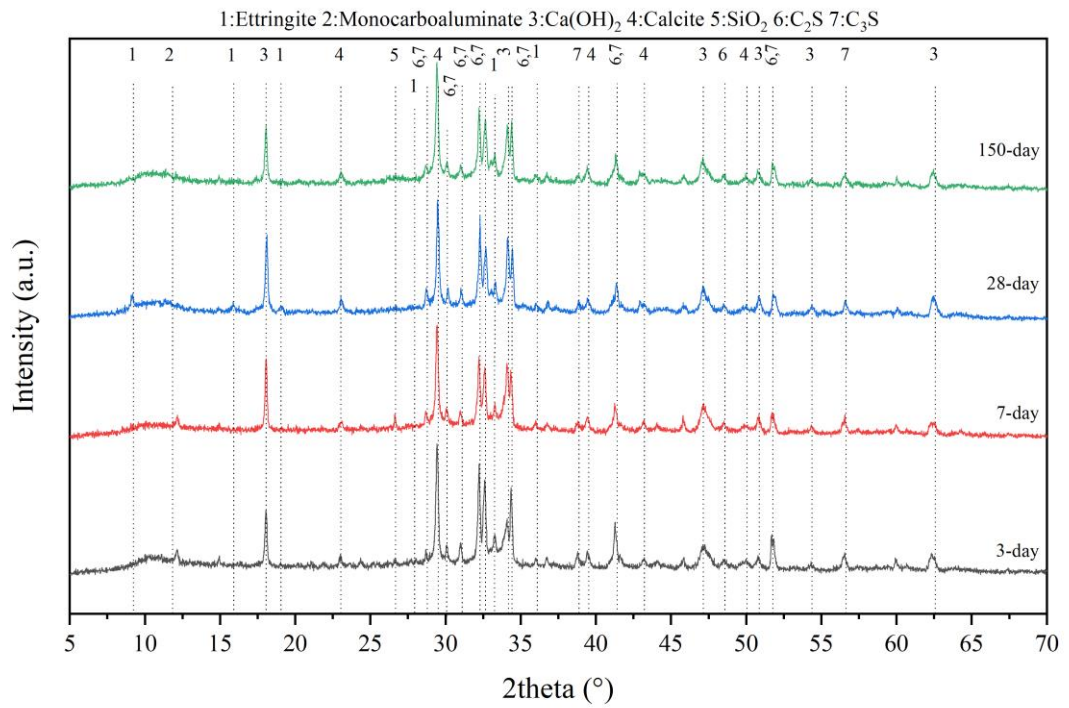
Appendix A.11: Mineralogical development of 125AKS1.5



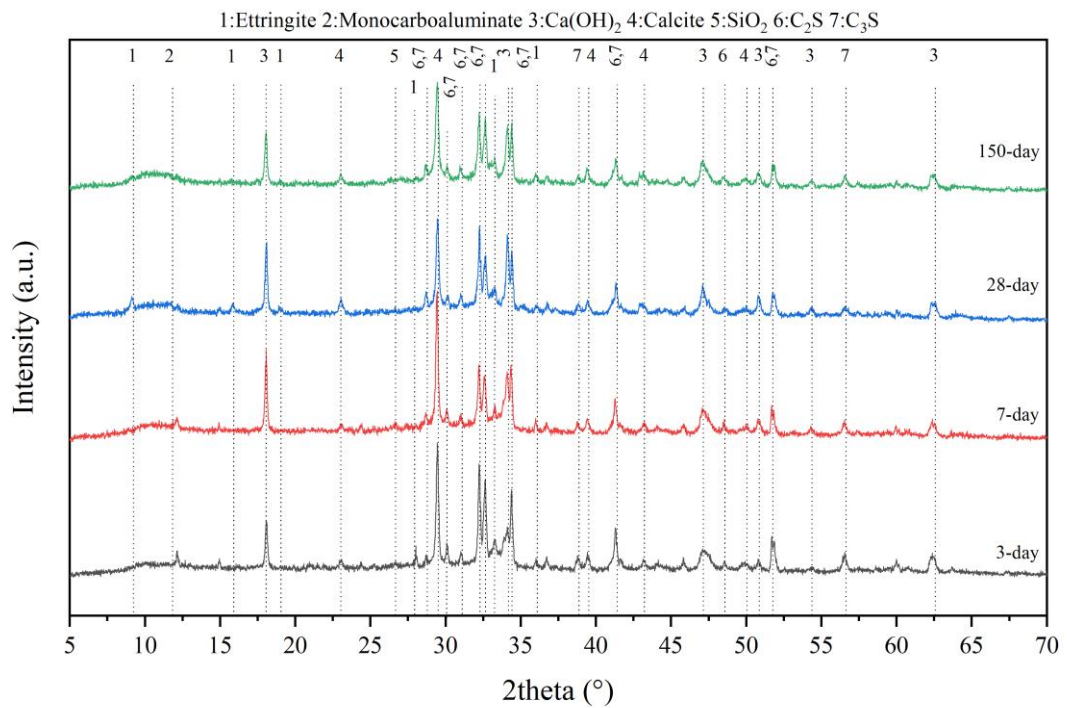
Appendix A.12: Mineralogical development of 125HKS0.2



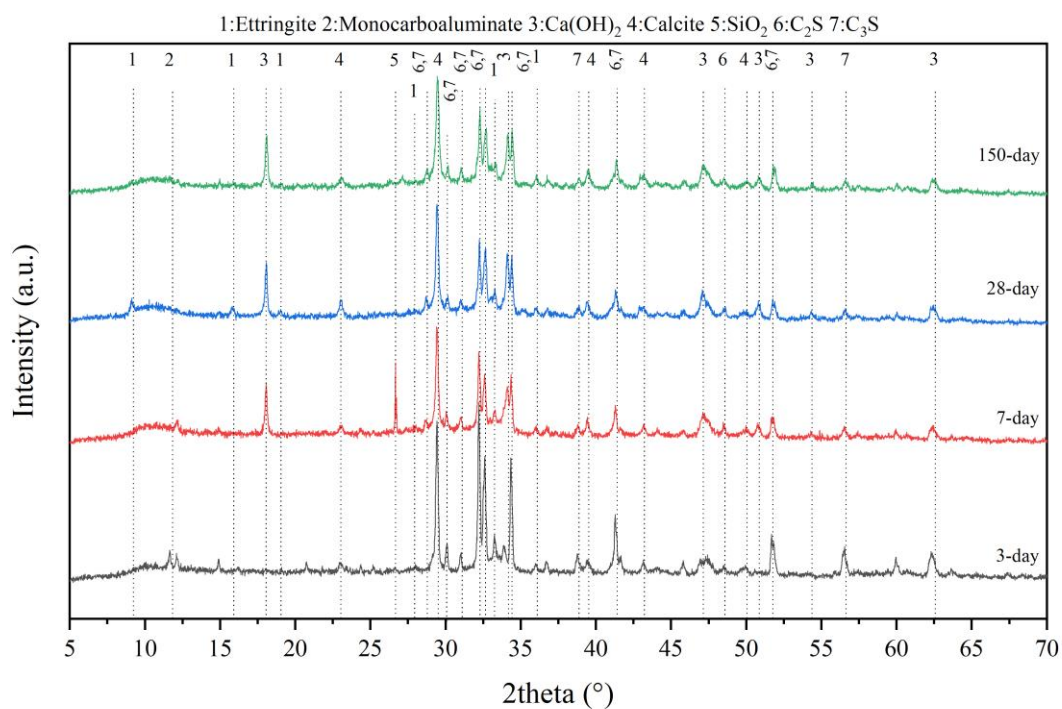
Appendix A.13: Mineralogical development of 125HKS0.35



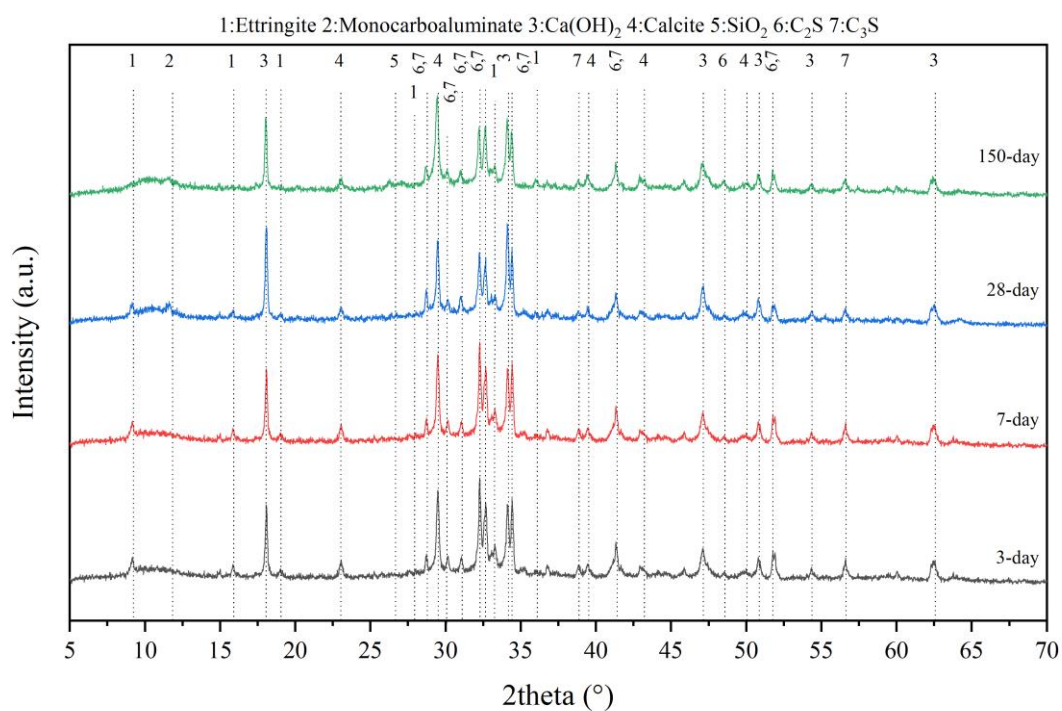
Appendix A.14: Mineralogical development of 125HKS0.5



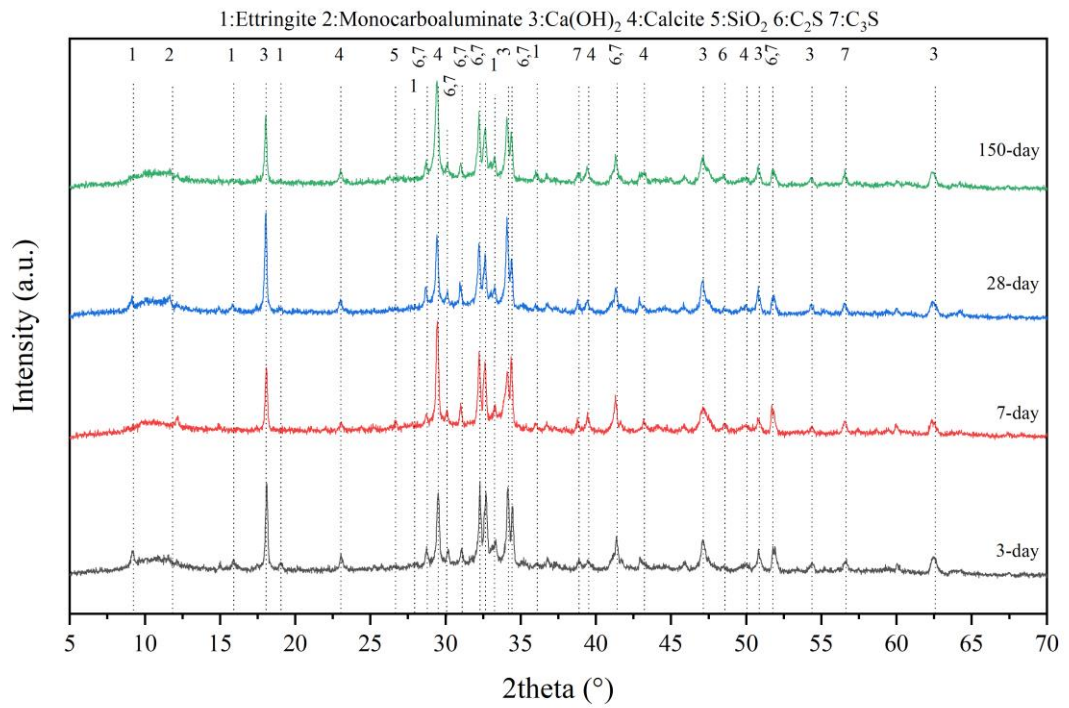
Appendix A.15: Mineralogical development of 125HKS1.0



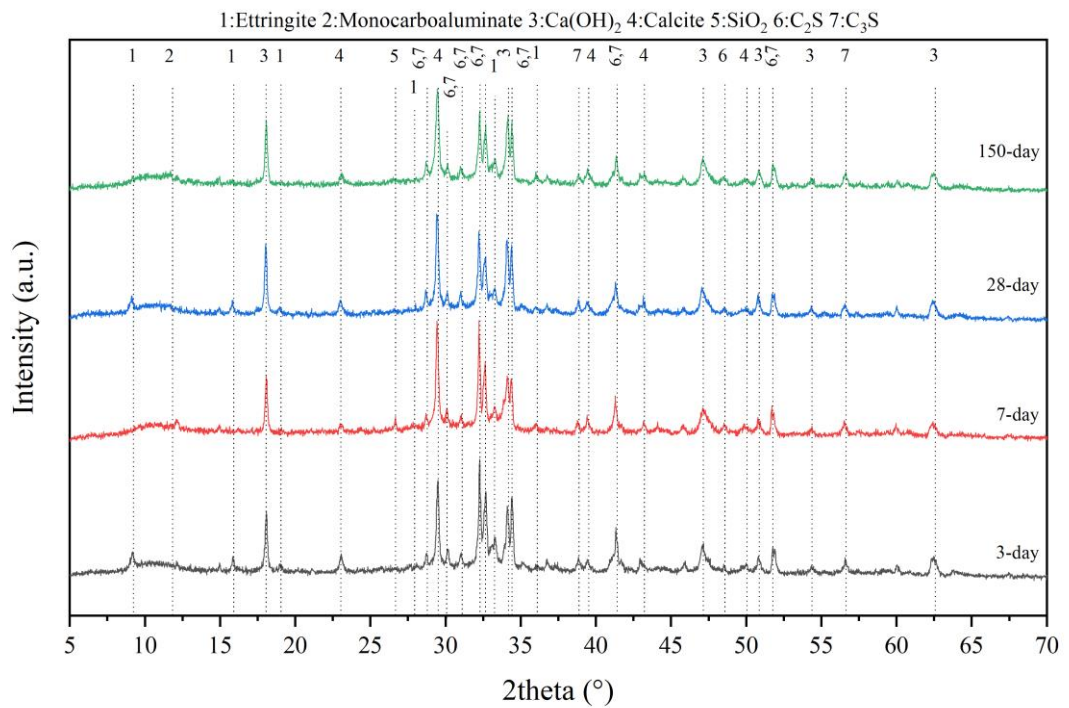
Appendix A.16: Mineralogical development of 125HKS1.5



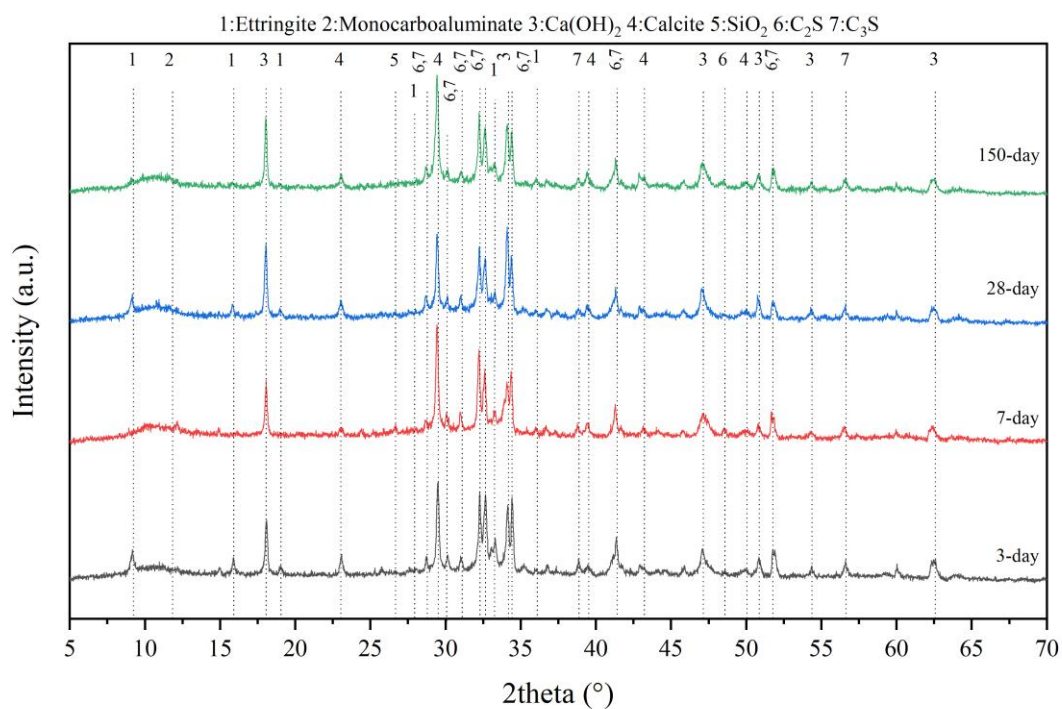
Appendix A.17: Mineralogical development of 125WKS0.2



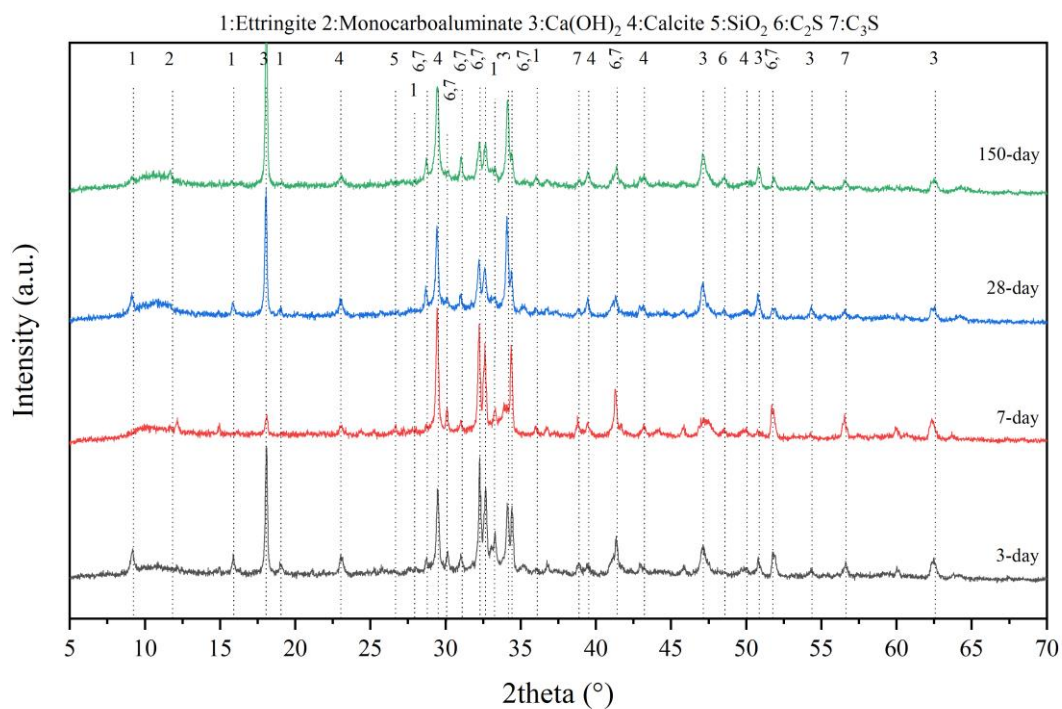
Appendix A.18: Mineralogical development of 125WKS0.35



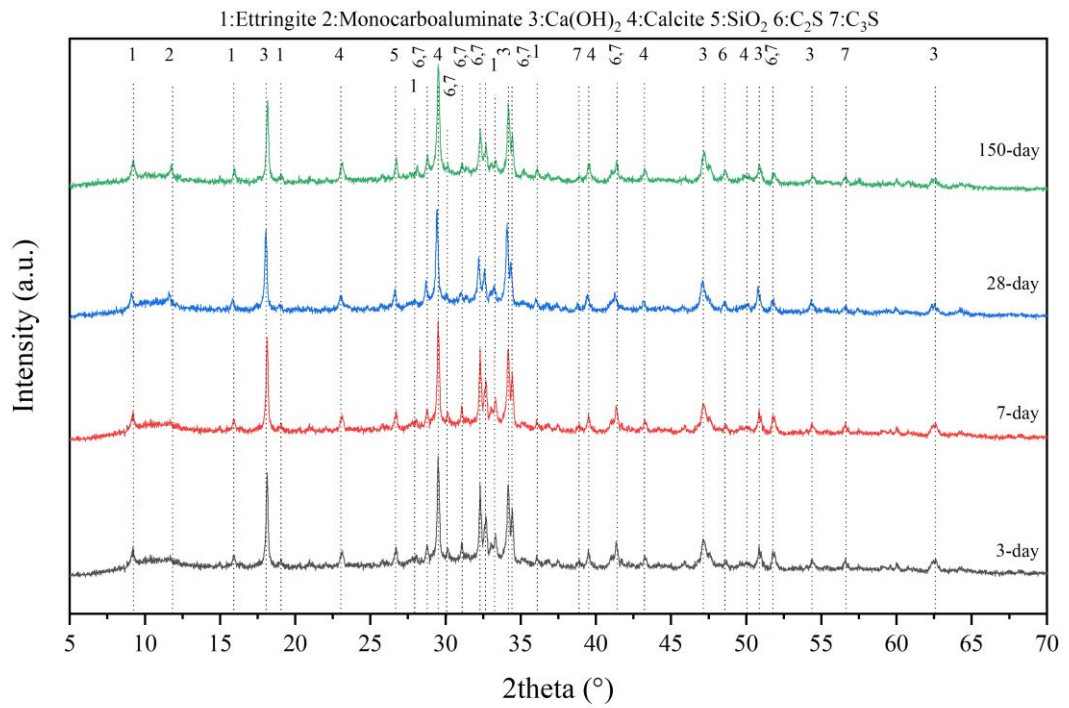
Appendix A.19: Mineralogical development of 125WKS0.5



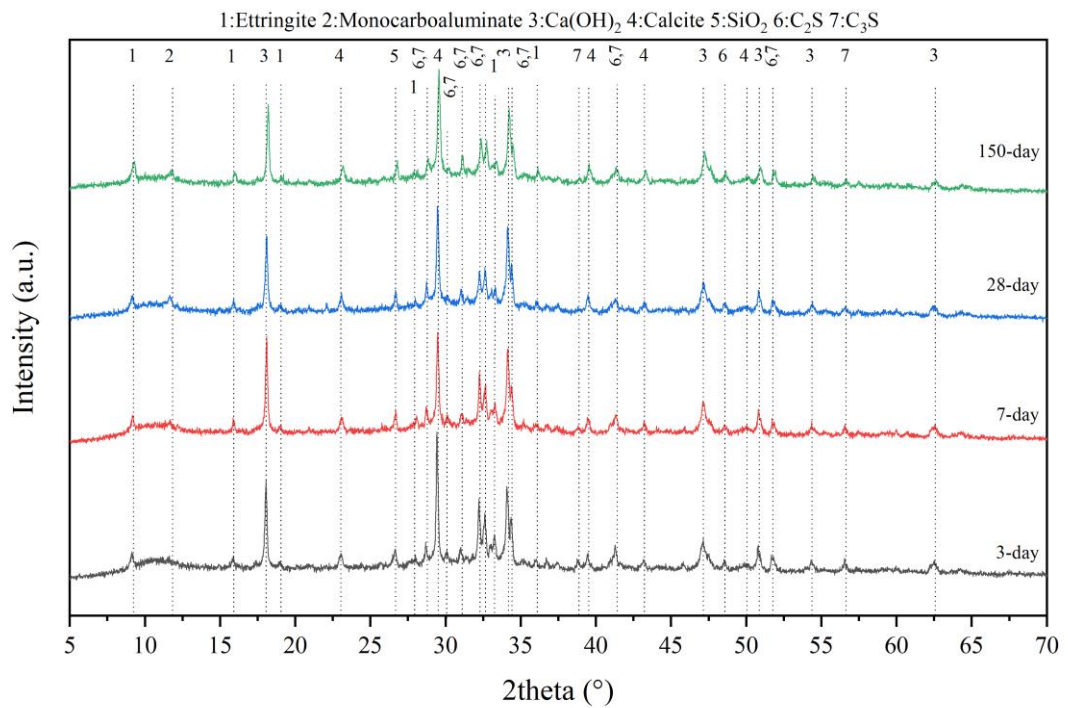
Appendix A.20: Mineralogical development of 125WKS1.0



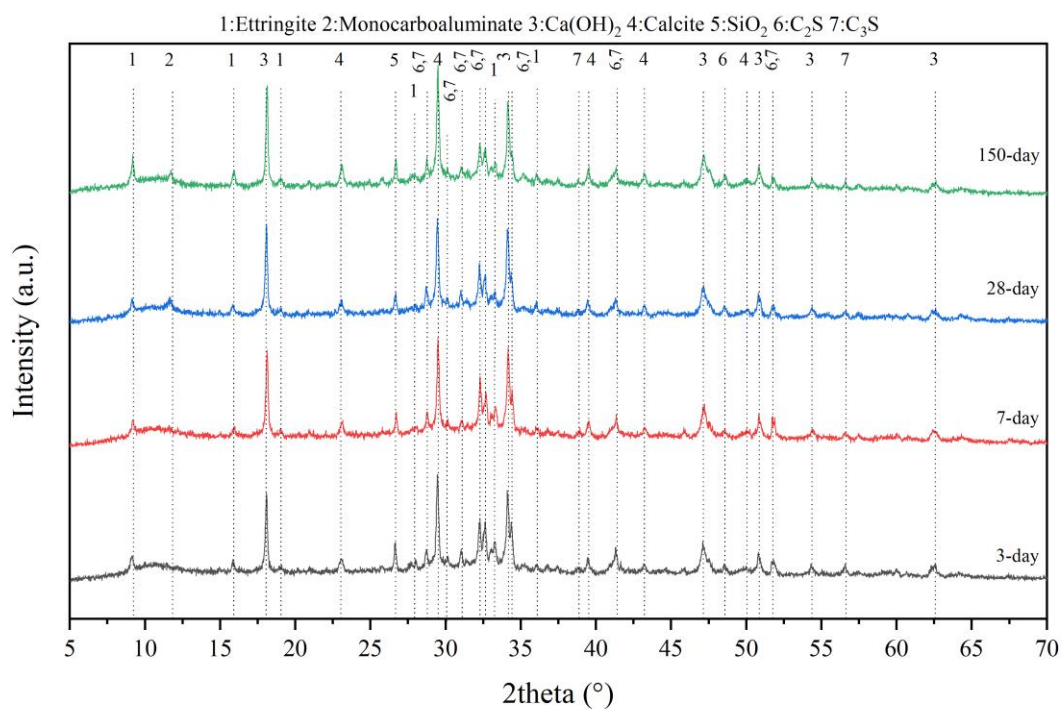
Appendix A.21: Mineralogical development of 125WKS1.5



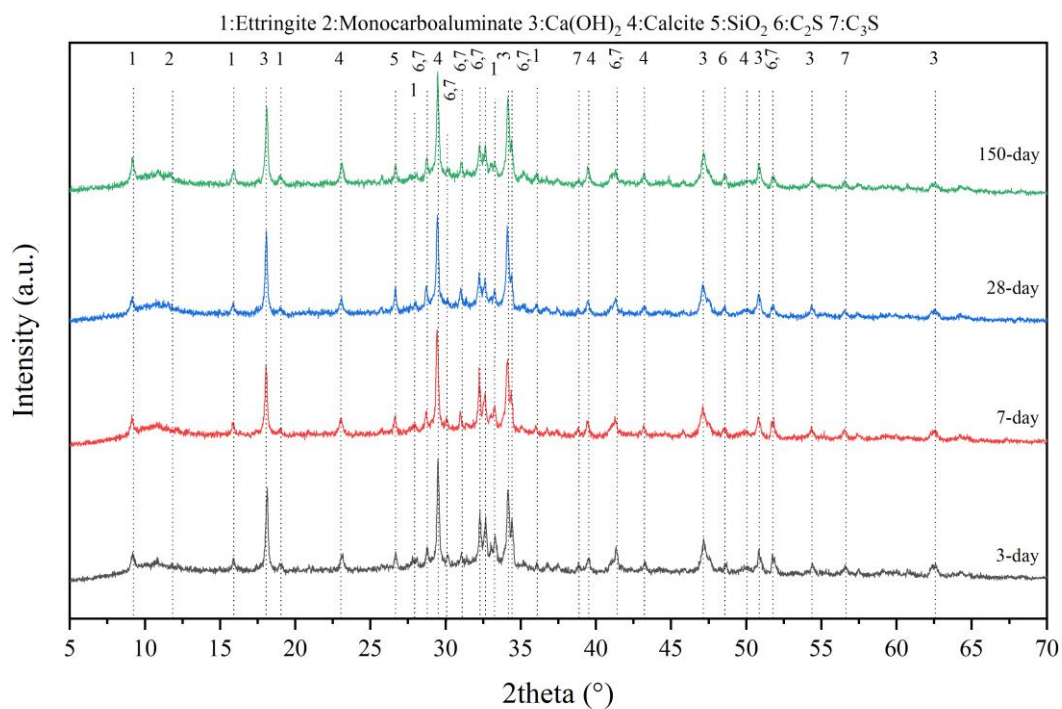
Appendix A.22: Mineralogical development of 125OS0.2



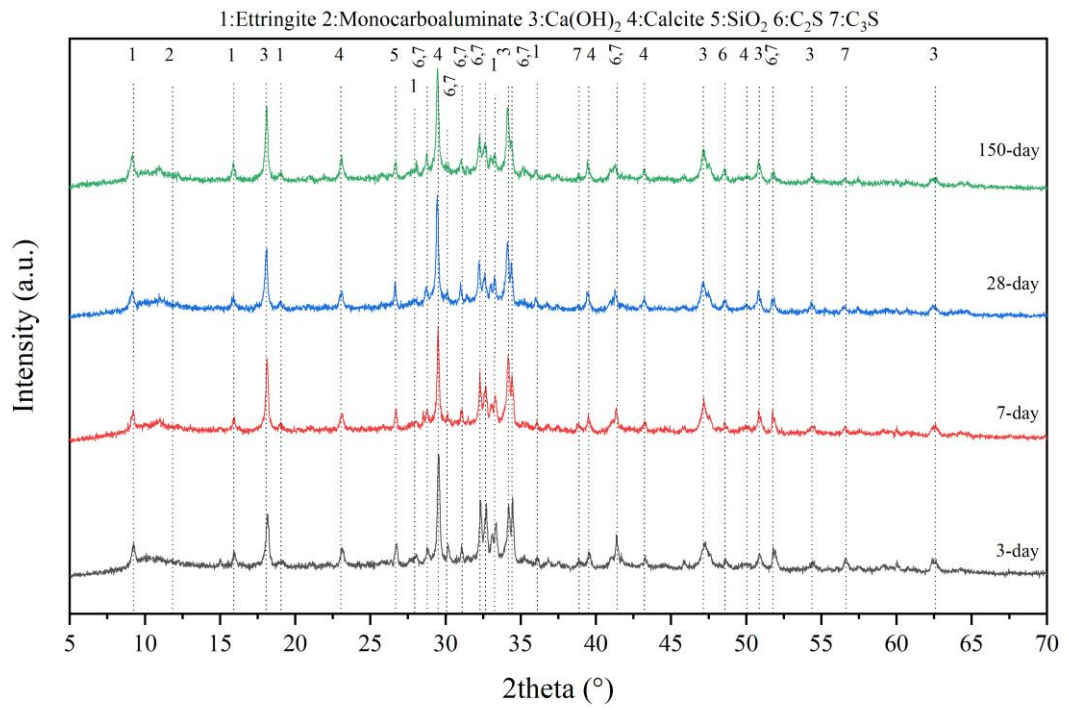
Appendix A.23: Mineralogical development of 125OS0.35



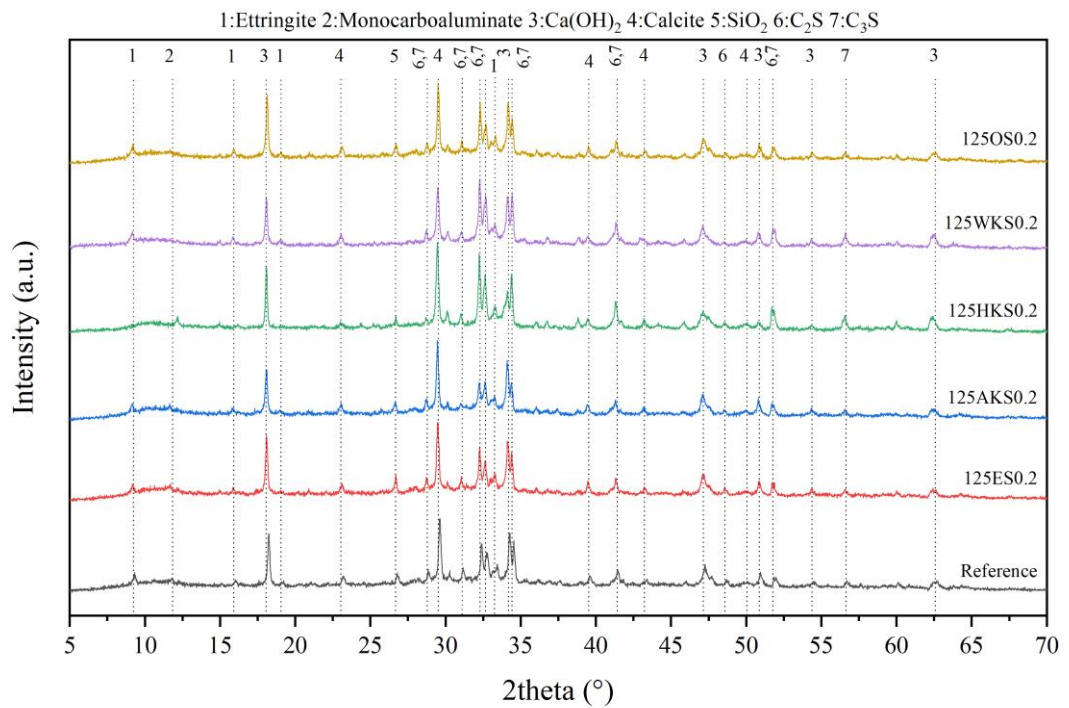
Appendix A.24: Mineralogical development of 125OS0.5



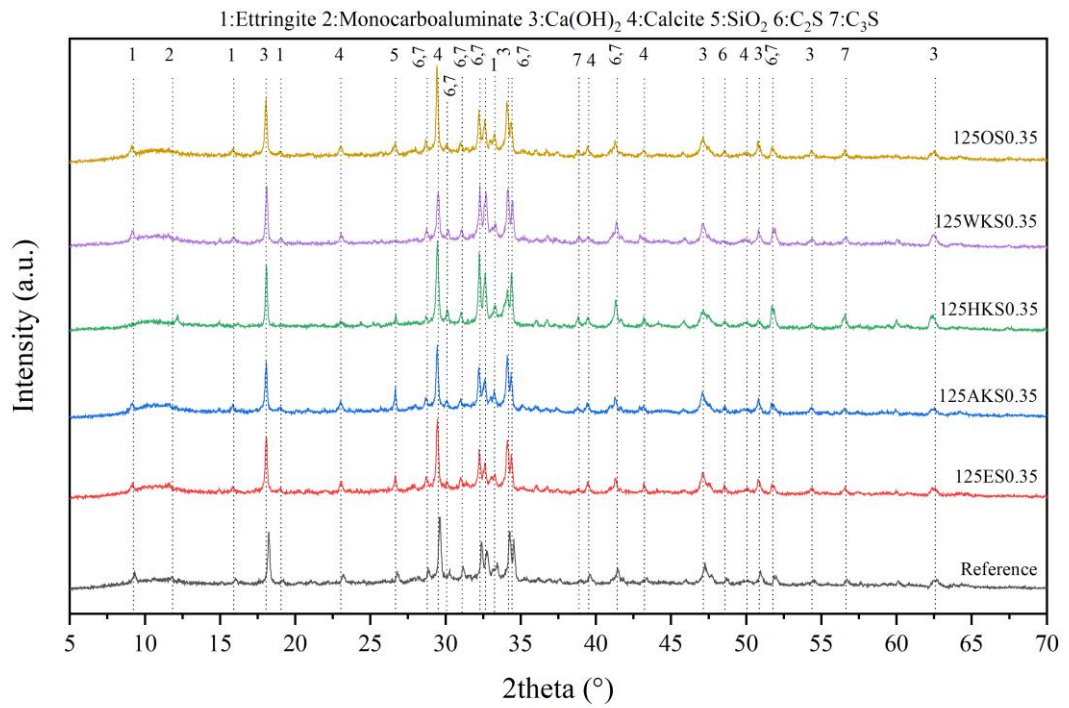
Appendix A.25: Mineralogical development of 125OS1.0



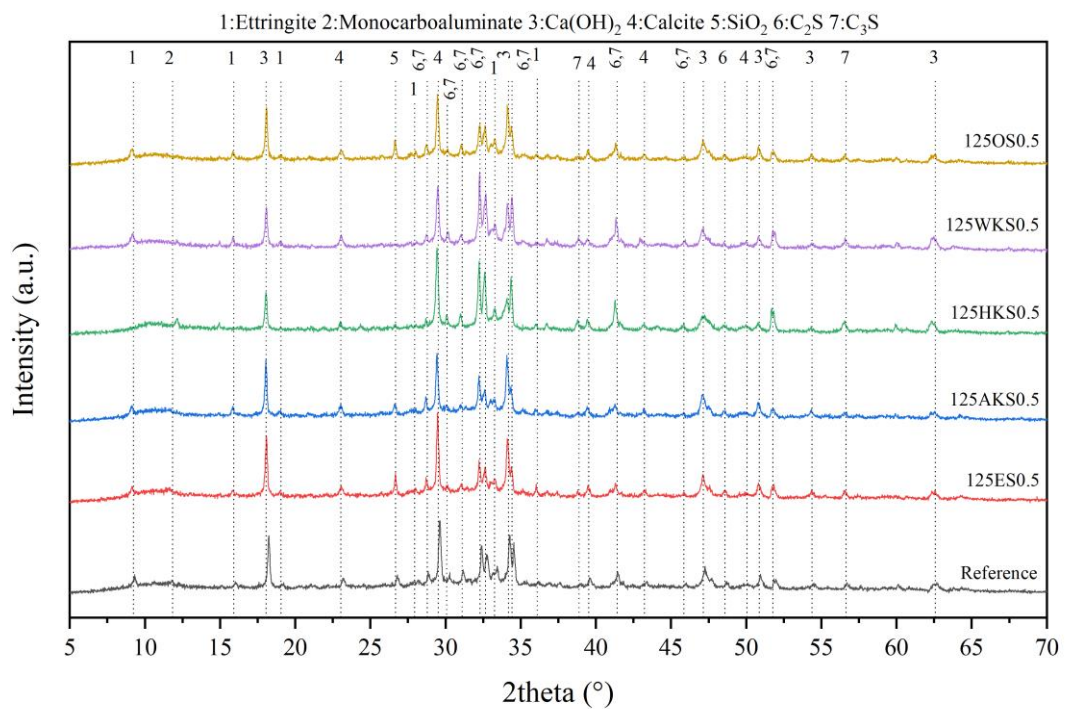
Appendix A.26: Mineralogical development of 125OS1.5



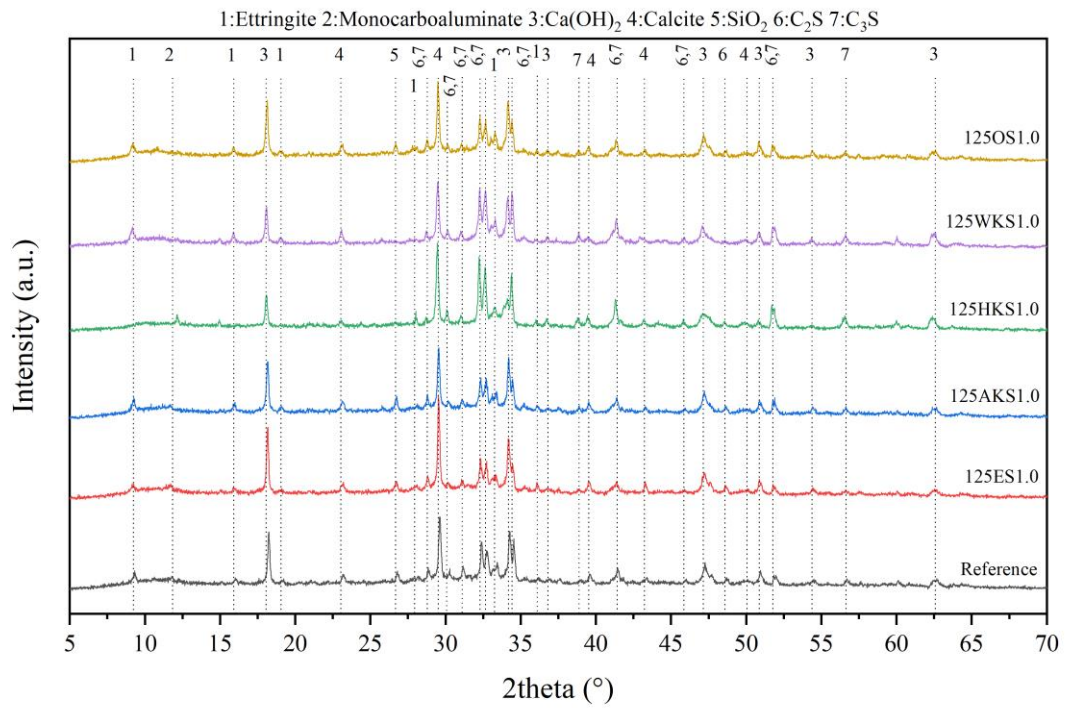
Appendix A.27: XRD patterns of test pastes with 0.2 wt.% bio-polymeric admixtures at 3-days of curing



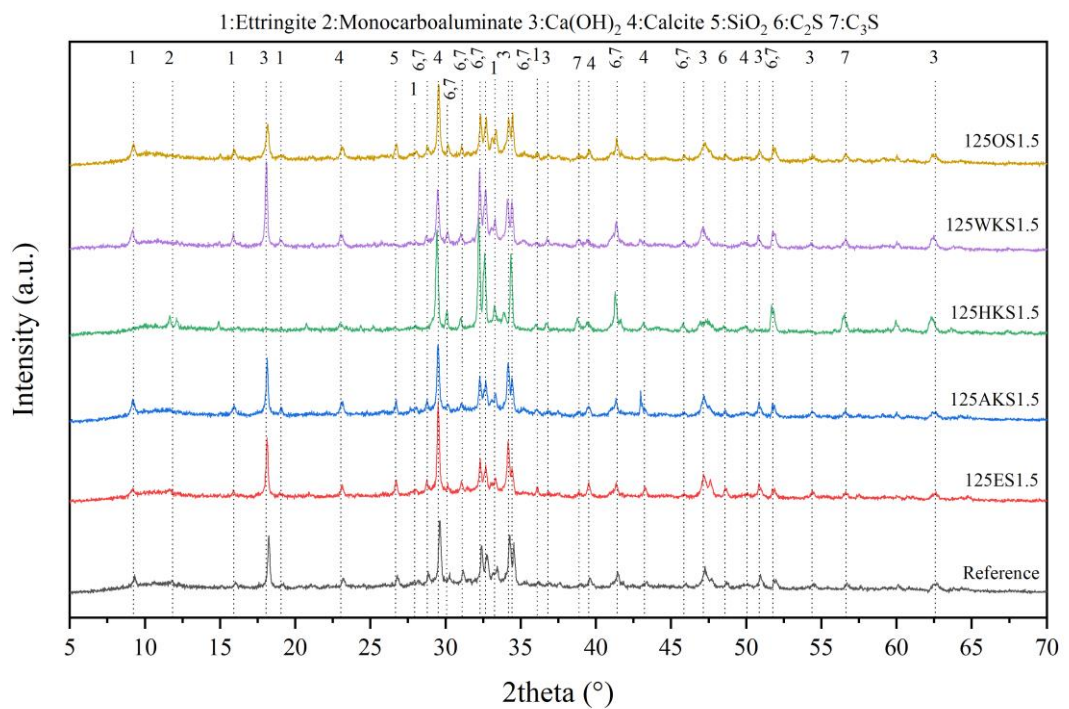
Appendix A.28: XRD patterns of test pastes with 0.35 wt.% bio-polymeric admixtures at 3-days of curing



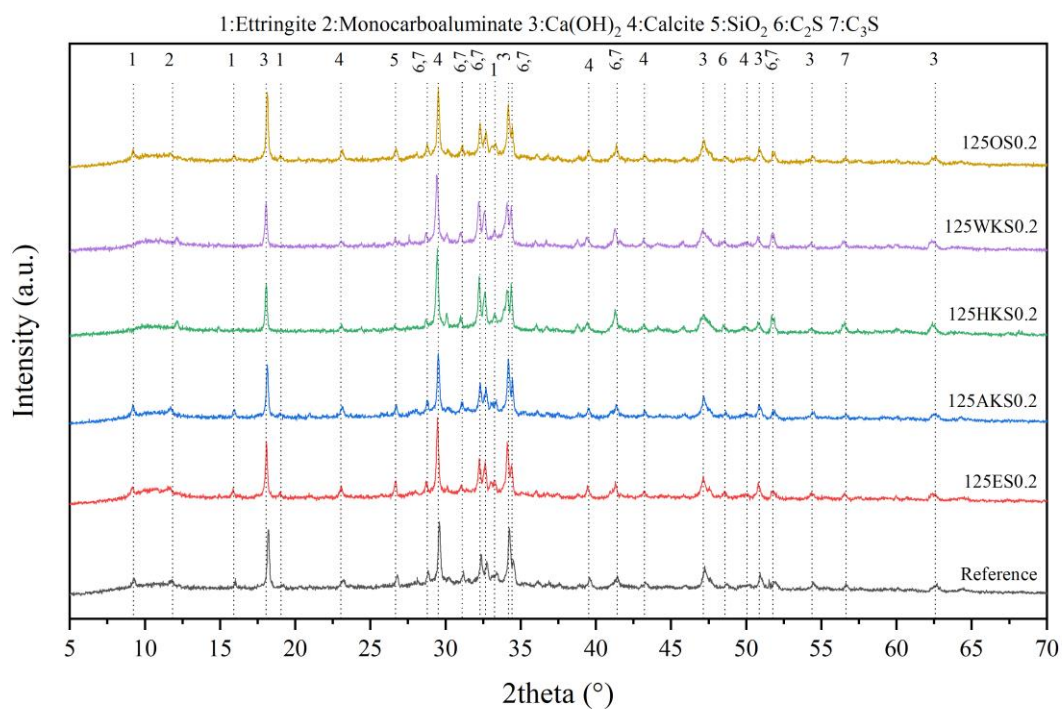
Appendix A.29: XRD patterns of test pastes with 0.5 wt.% bio-polymeric admixtures at 3-days of curing



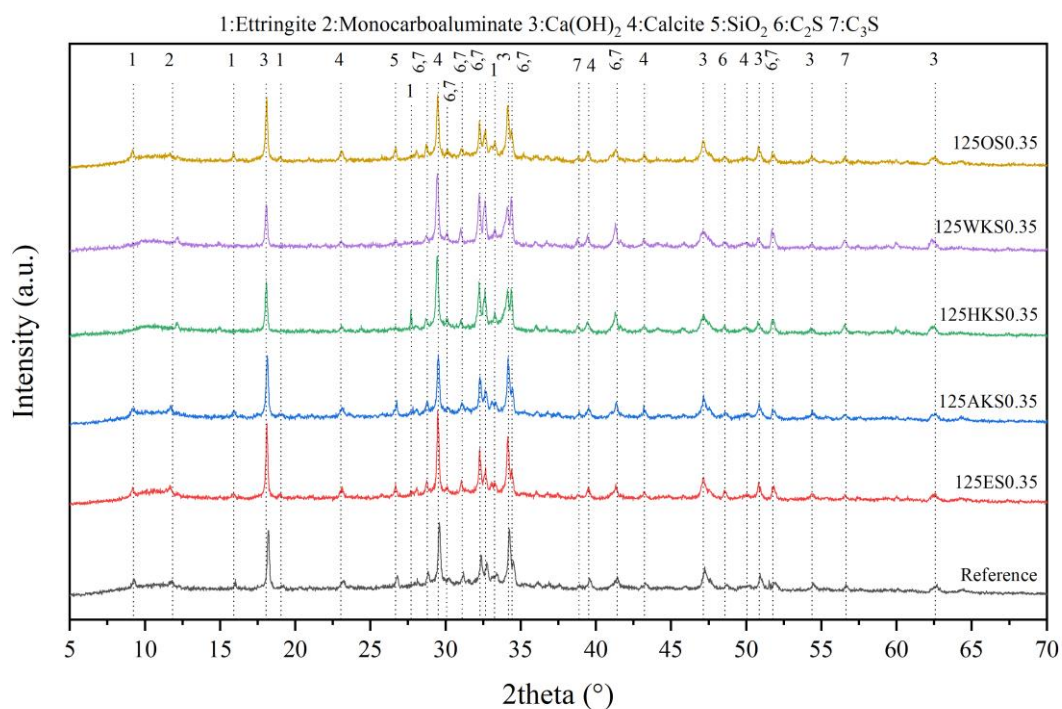
Appendix A.30: XRD patterns of test pastes with 1.0 wt.% bio-polymeric admixtures at 3-days of curing



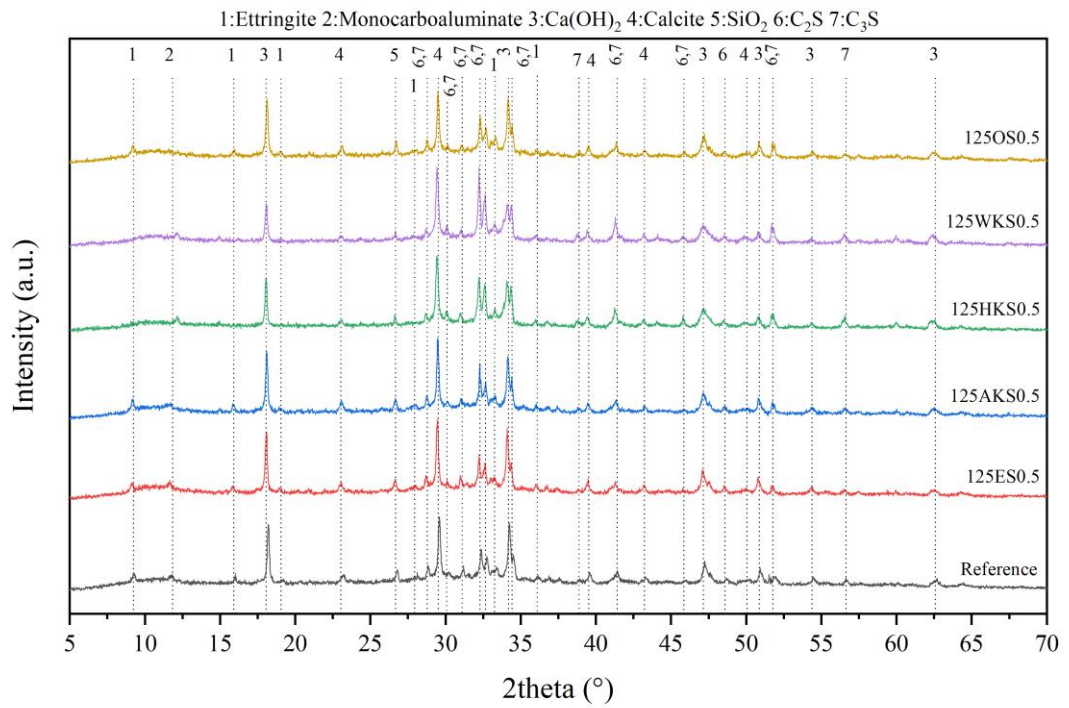
Appendix A.31: XRD patterns of test pastes with 1.5 wt.% bio-polymeric admixtures at 3-days of curing



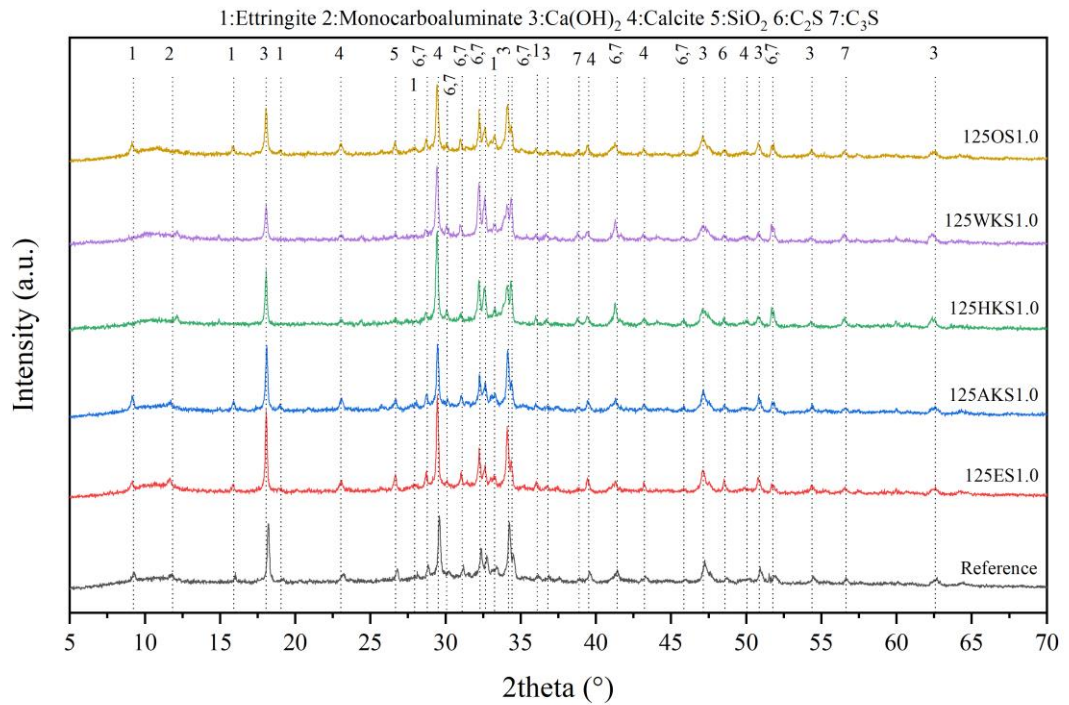
Appendix A.32: XRD patterns of test pastes with 0.2 wt.% bio-polymeric admixtures at 7-days of curing



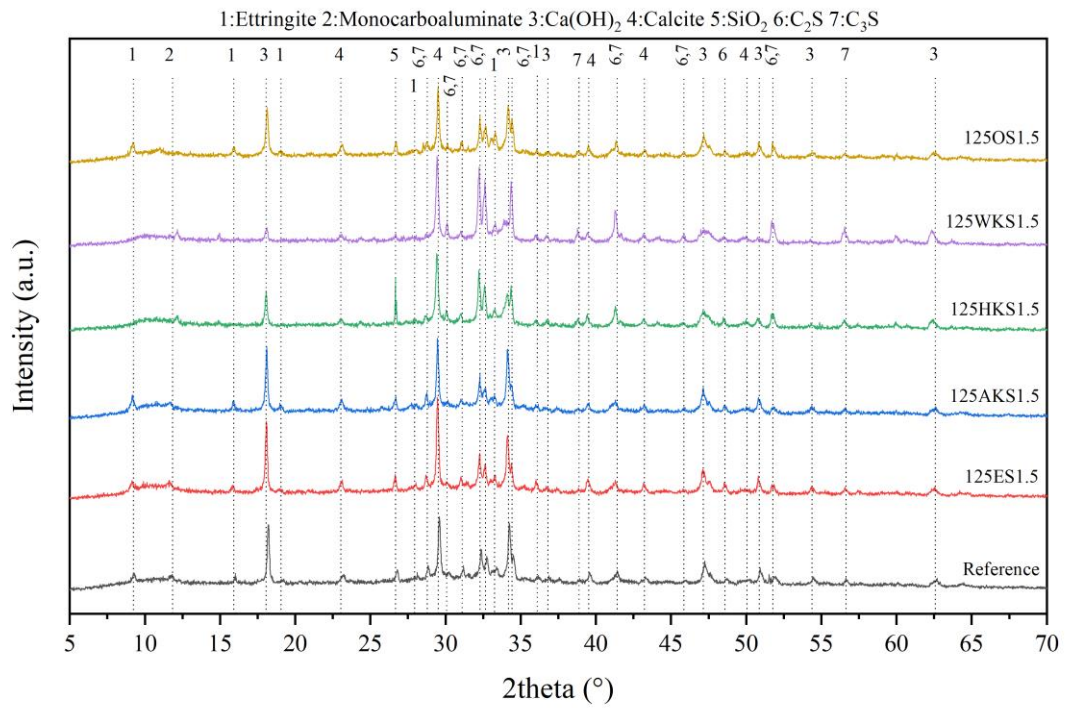
Appendix A.33: XRD patterns of test pastes with 0.35 wt.% bio-polymeric admixtures at 7-days of curing



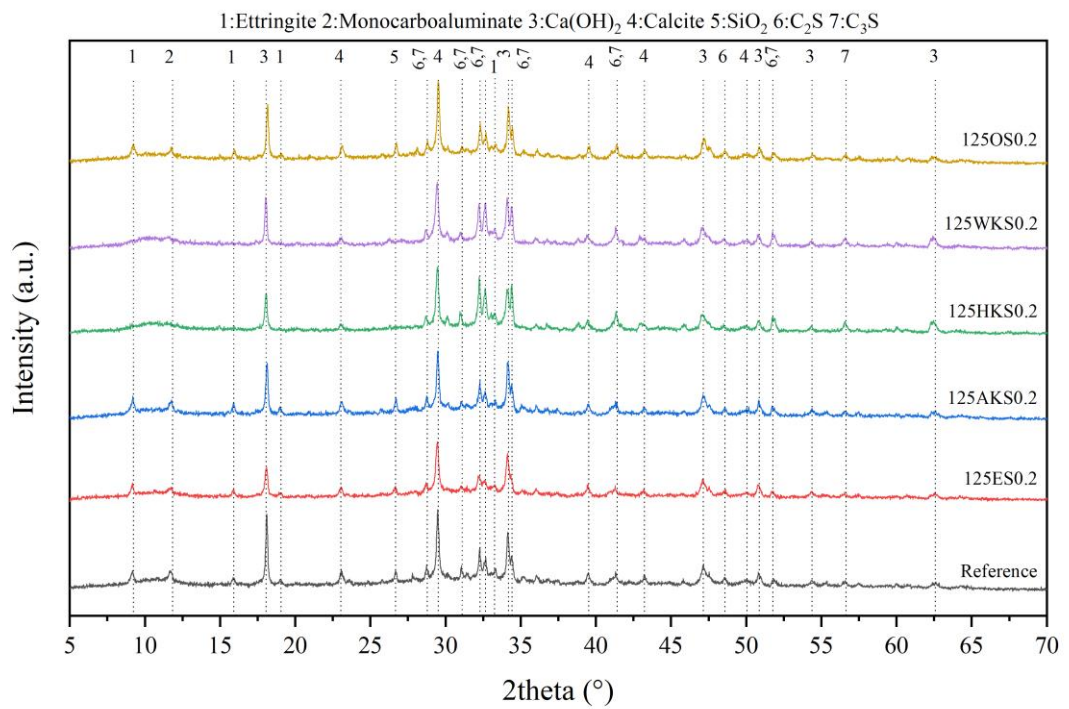
Appendix A.34: XRD patterns of test pastes with 0.5 wt.% bio-polymeric admixtures at 7-days of curing



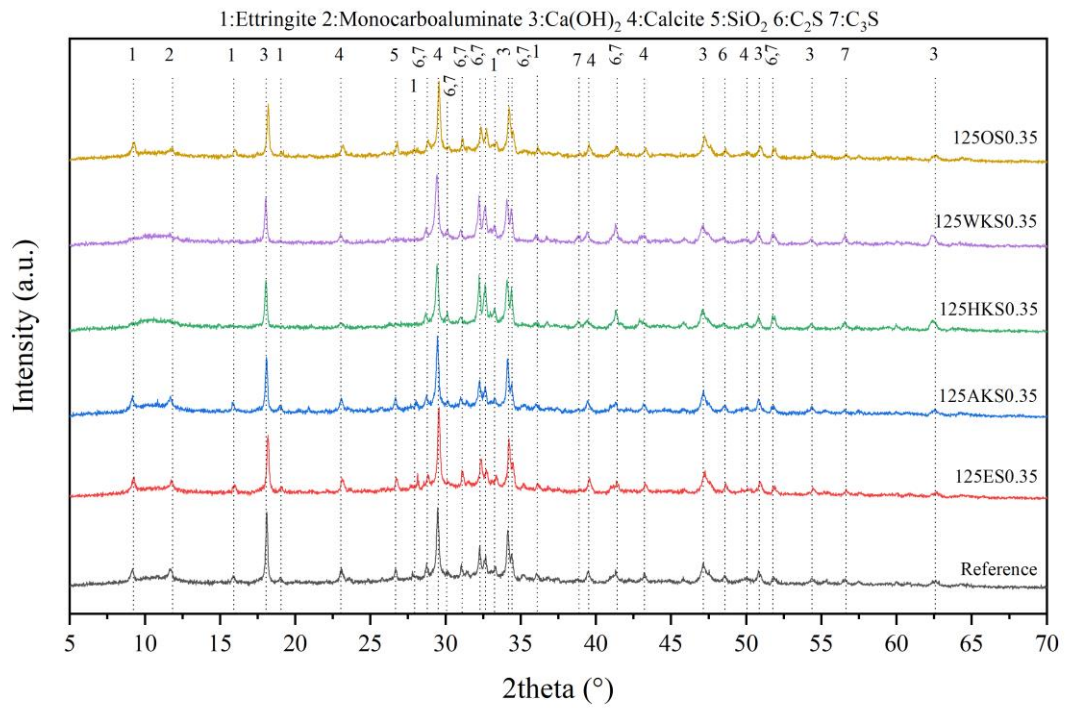
Appendix A.35: XRD patterns of test pastes with 1.0 wt.% bio-polymeric admixtures at 7-days of curing



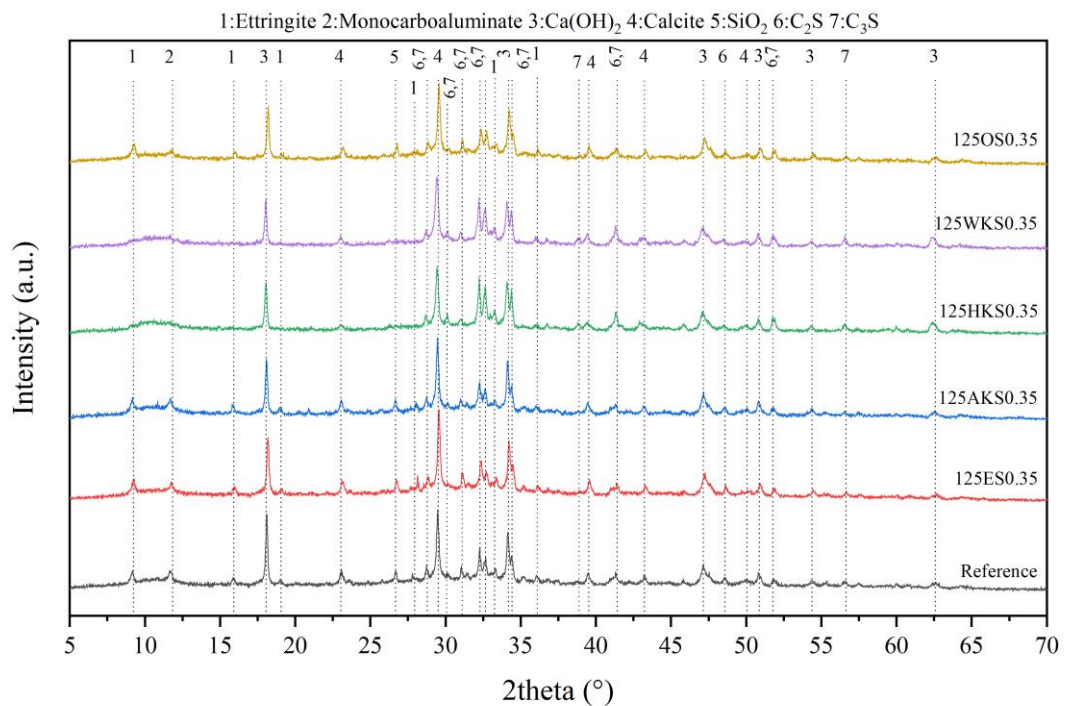
Appendix A.36: XRD patterns of test pastes with 1.5 wt.% bio-polymeric admixtures at 7-days of curing



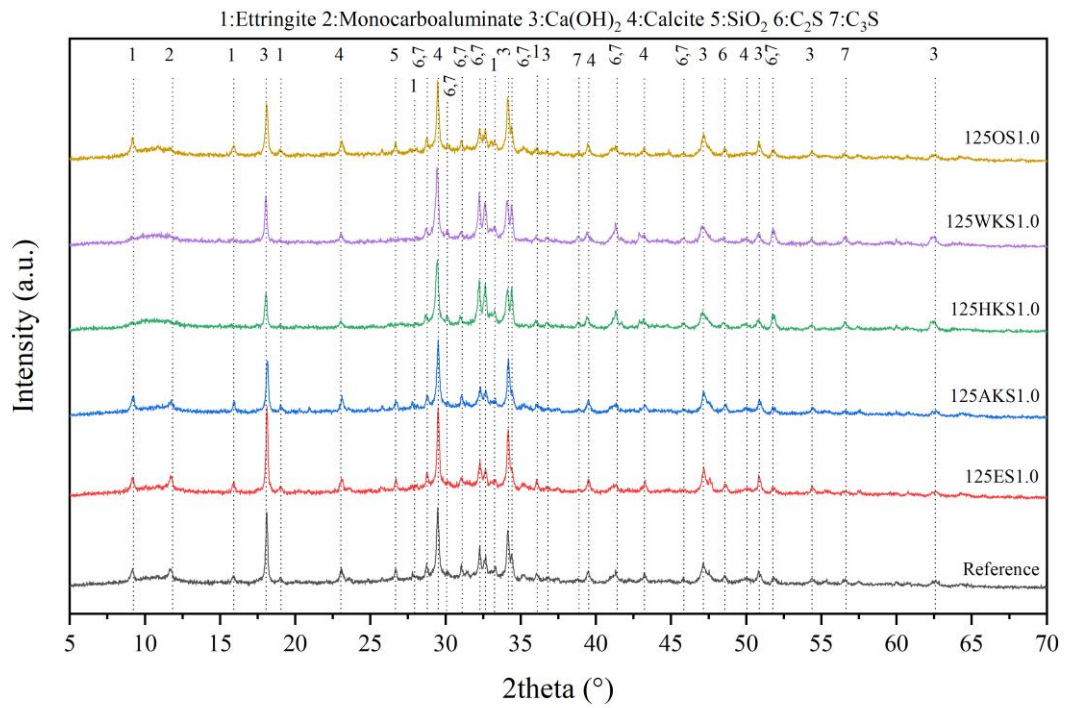
Appendix A.37: XRD patterns of test pastes with 0.2 wt.% bio-polymeric admixtures at 150-days of curing



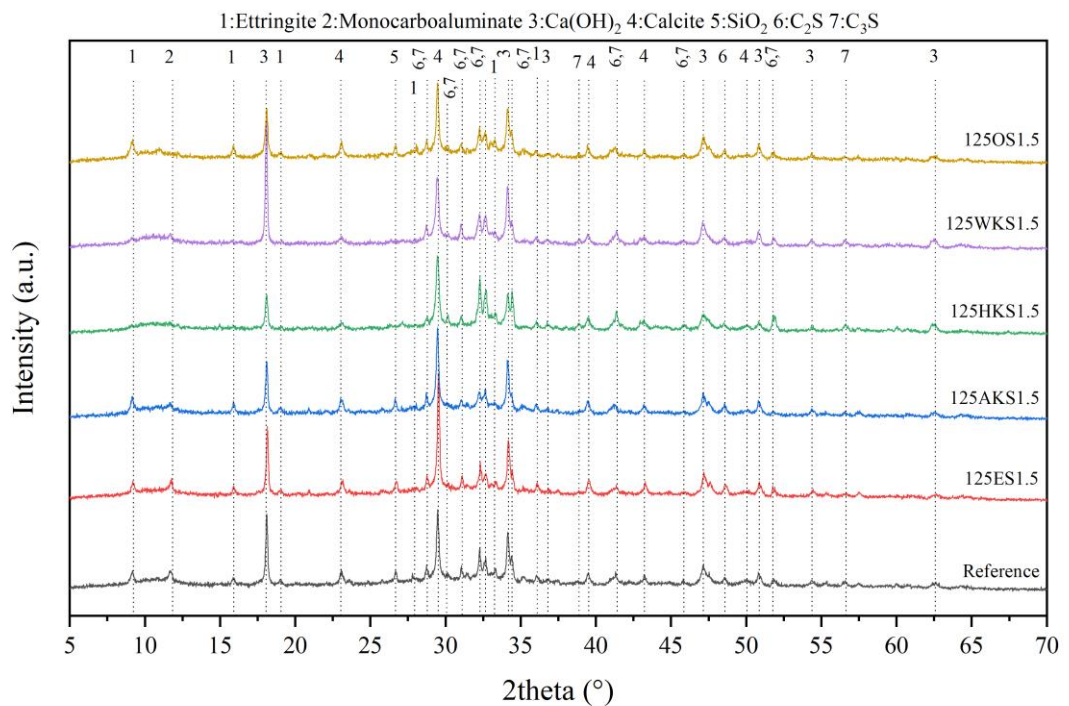
Appendix A.38: XRD patterns of test pastes with 0.35 wt.% bio-polymeric admixtures at 150-days of curing



Appendix A.39: XRD patterns of test pastes with 0.5 wt.% bio-polymeric admixtures at 150-days of curing



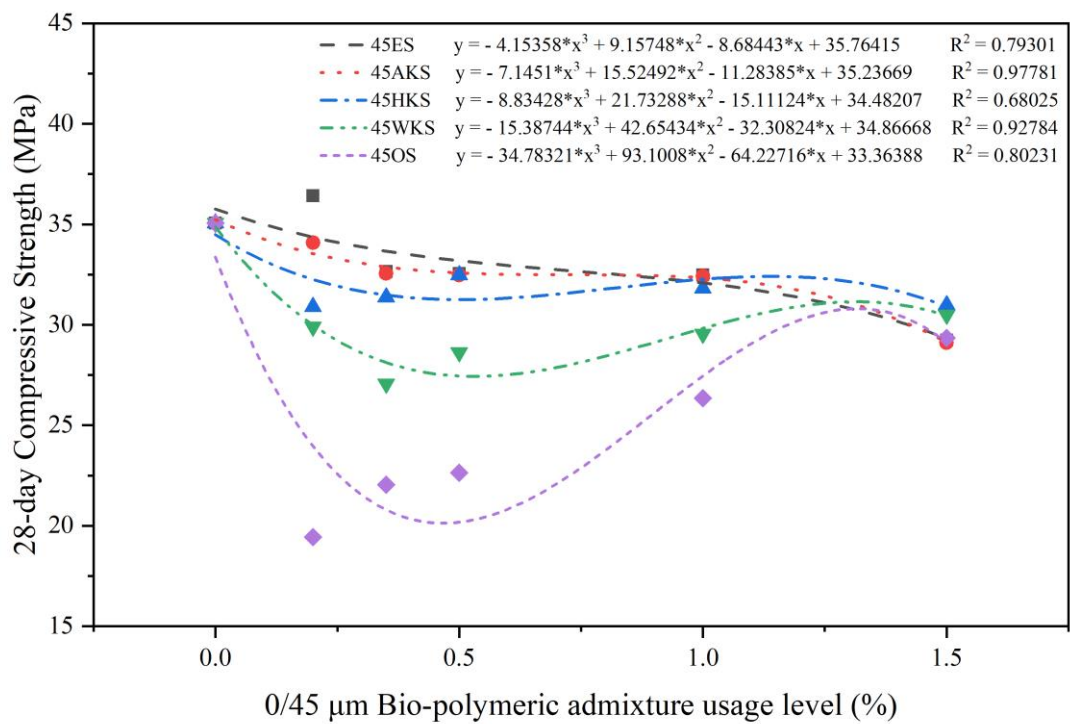
Appendix A.40: XRD patterns of test pastes with 1.0 wt.% bio-polymeric admixtures at 150-days of curing



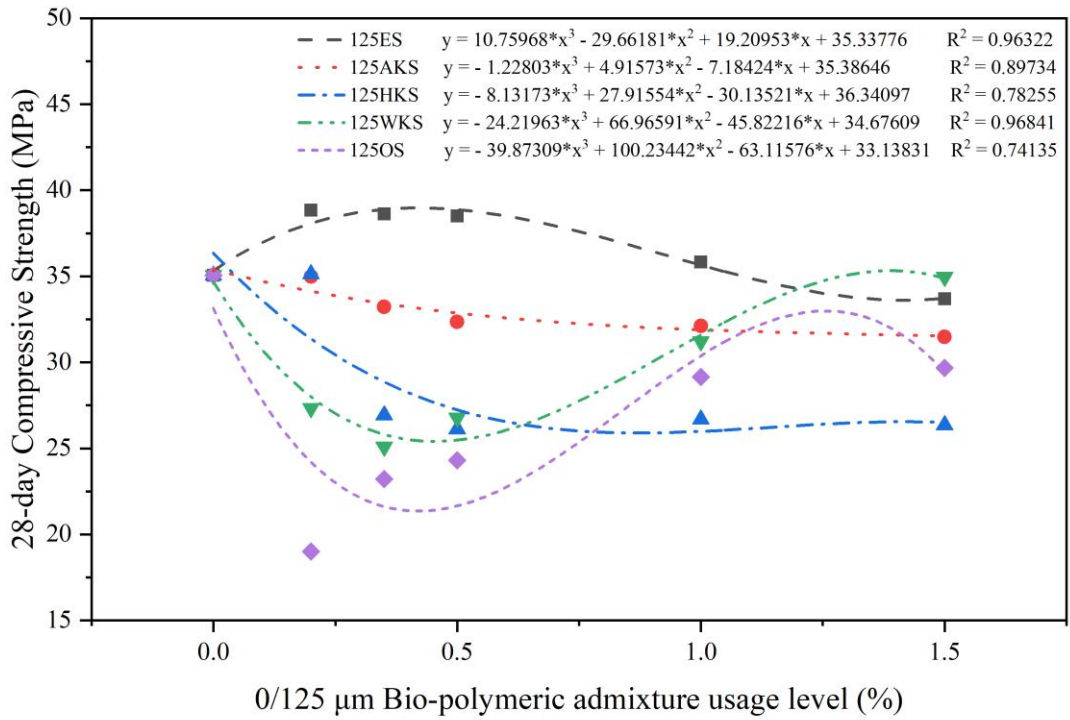
Appendix A.41: XRD patterns of test pastes with 1.5 wt.% bio-polymeric admixtures at 150-days of curing

Appendix B

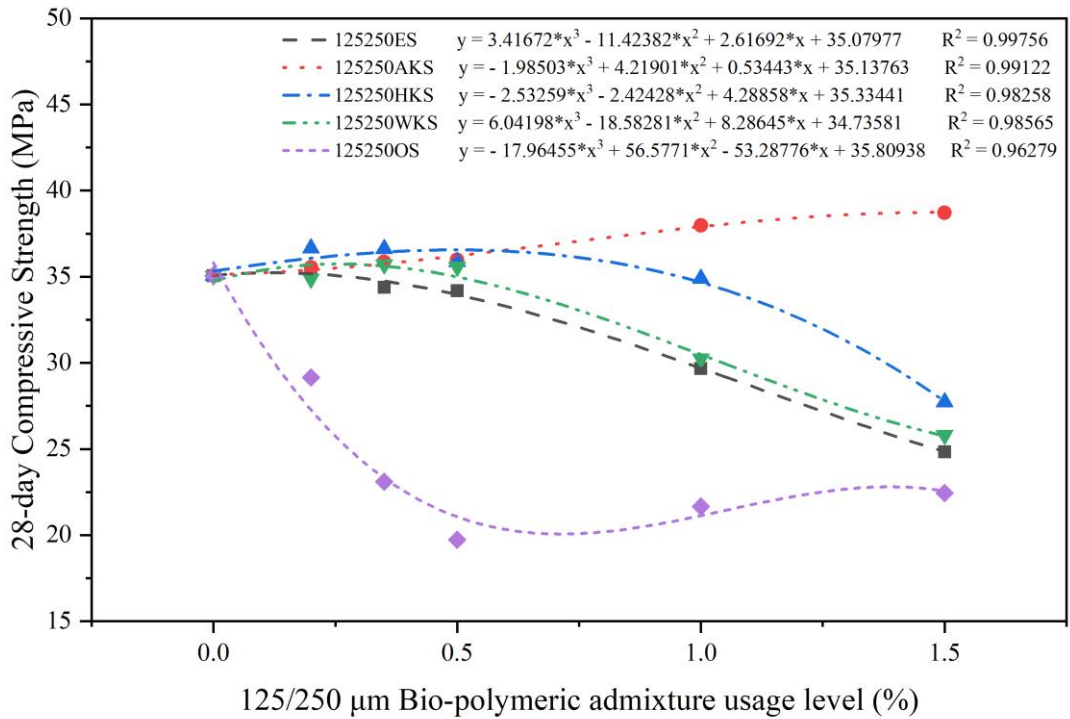
Graphical Representation of Research Findings



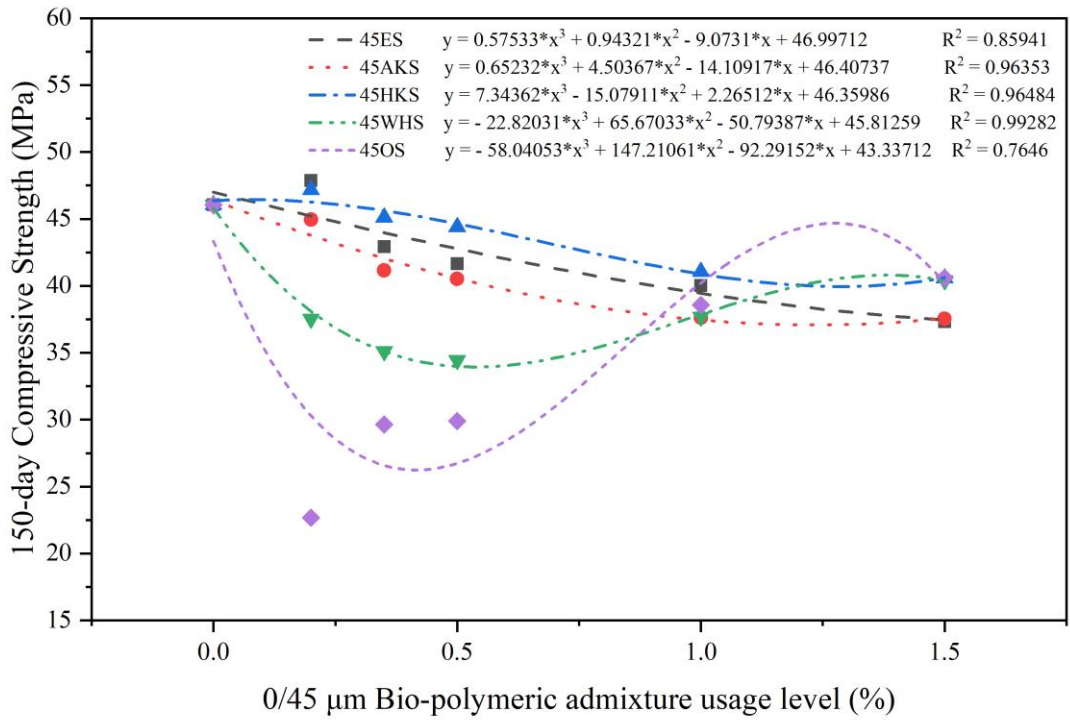
Appendix B.1: 28-day compressive strength versus 0/45 μm bio-polymeric admixture usage



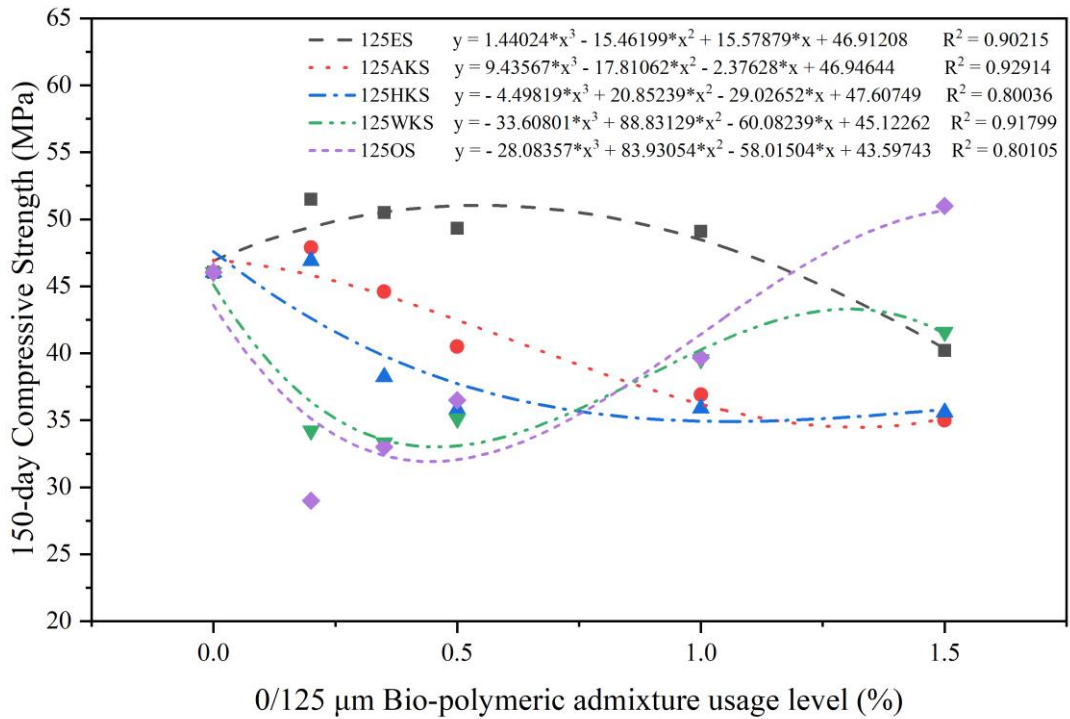
Appendix B.2: 28-day compressive strength versus 0/125 µm bio-polymeric admixture usage



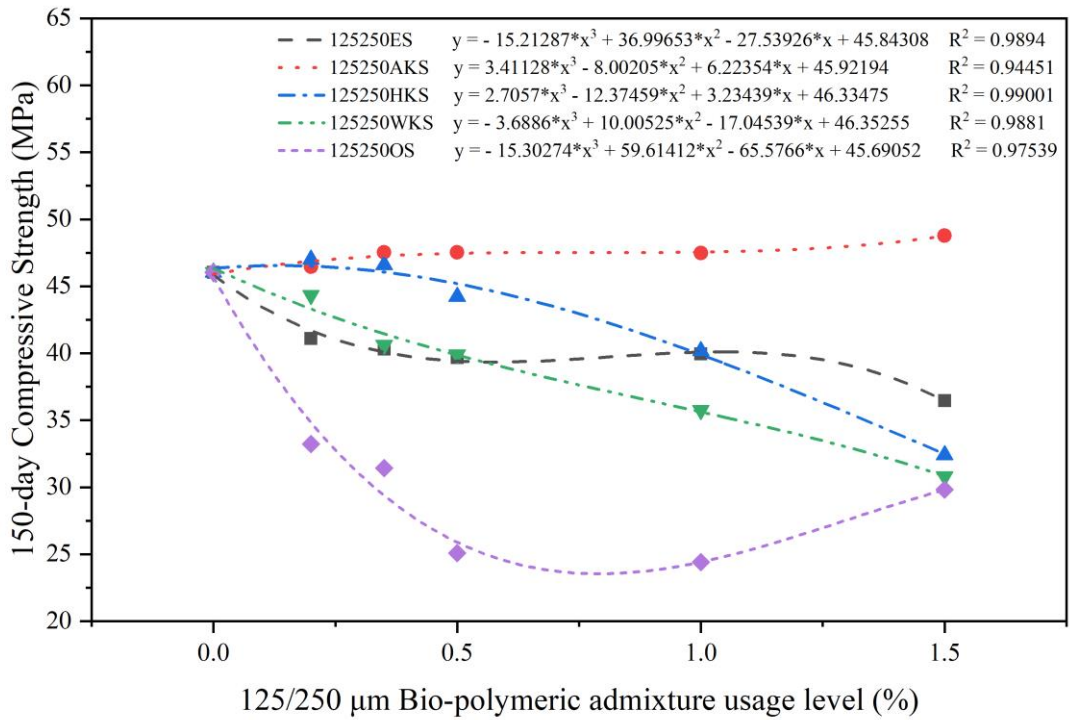
Appendix B.3: 28-day compressive strength versus 125/250 µm bio-polymeric admixture usage



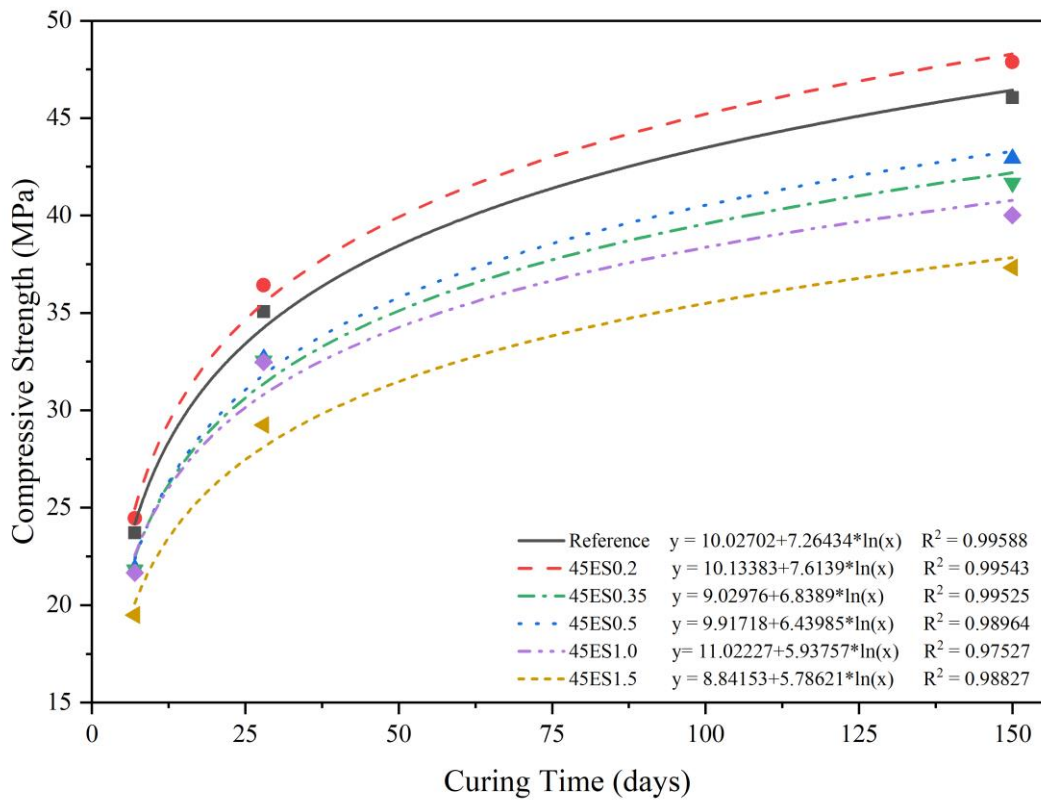
Appendix B.4: 150-day compressive strength versus 0/45 μm bio-polymeric admixture usage



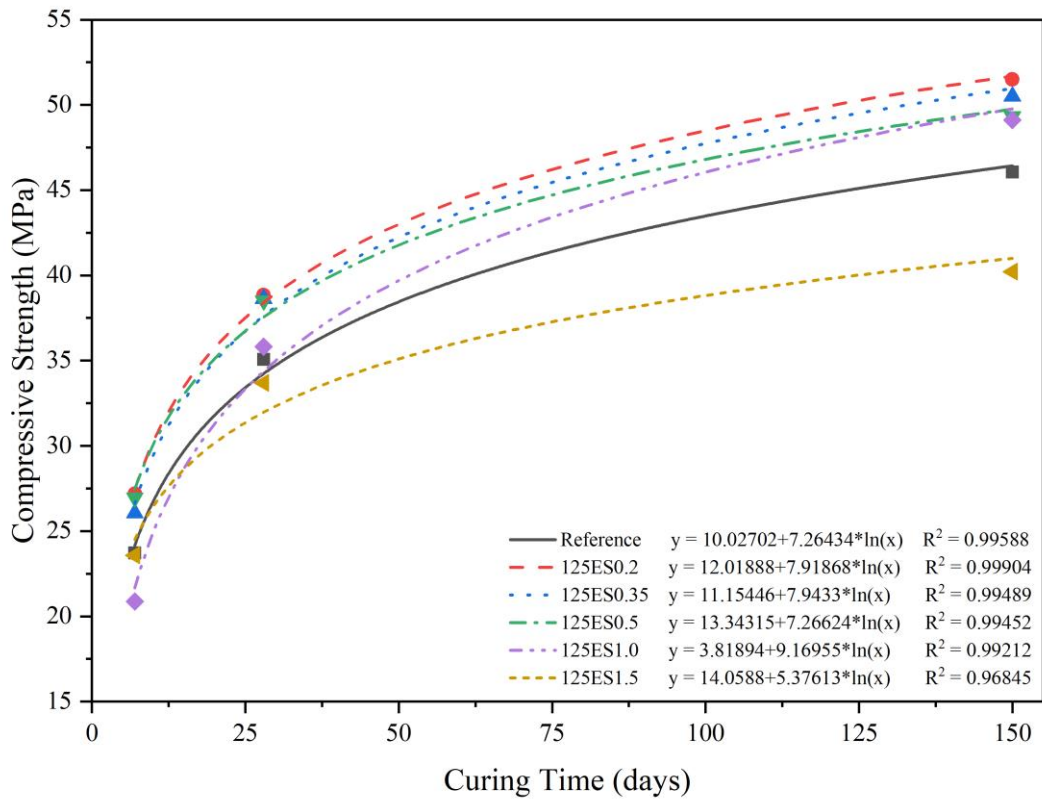
Appendix B.5: 150-day compressive strength versus 0/125 μm bio-polymeric admixture usage



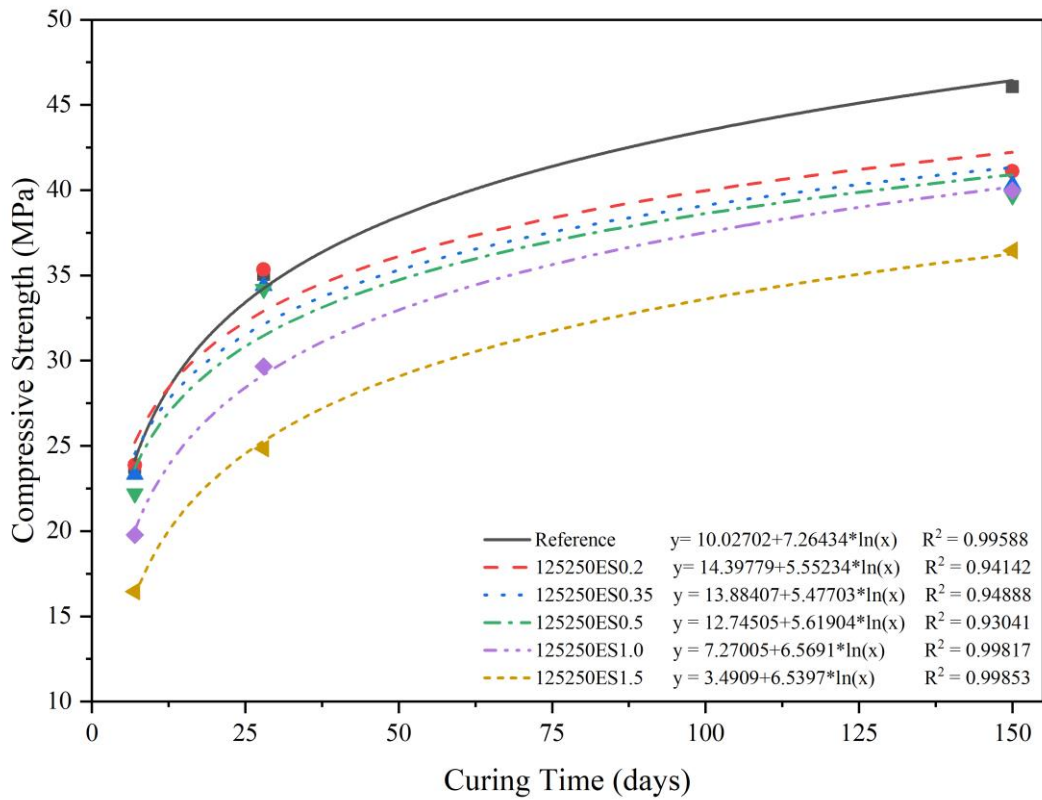
Appendix B.6: 150-day compressive strength versus 125/250 µm bio-polymeric admixture usage



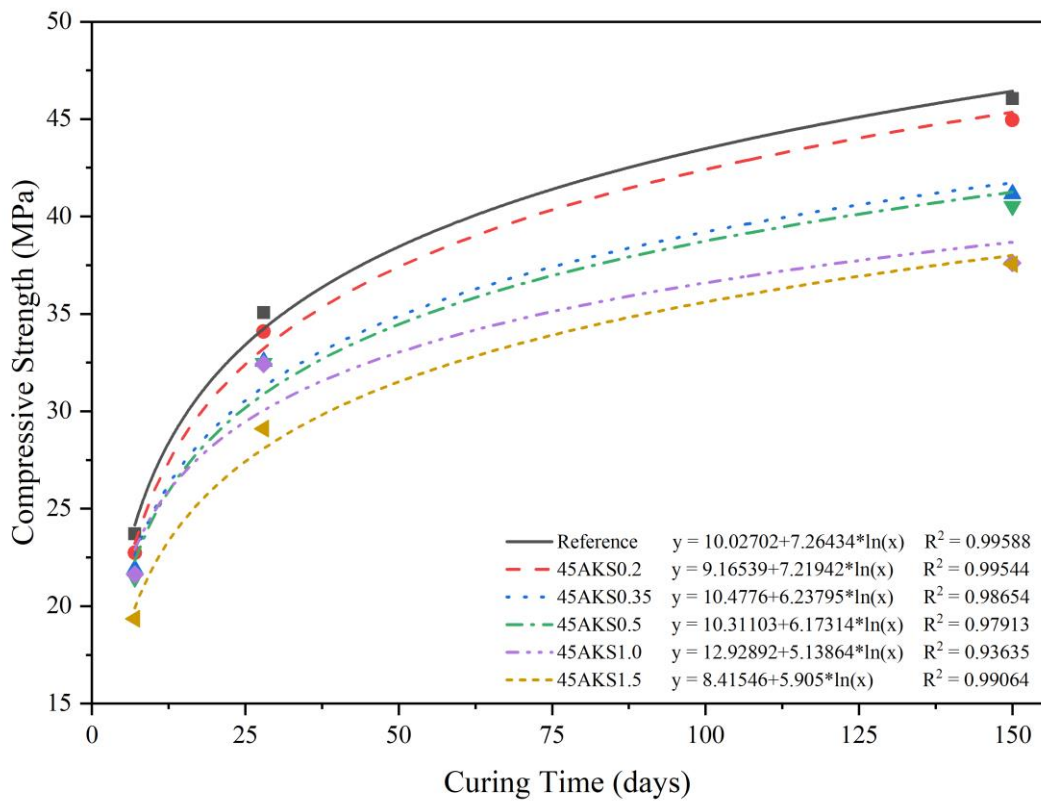
Appendix B.7: Compressive strength development of 45ES series



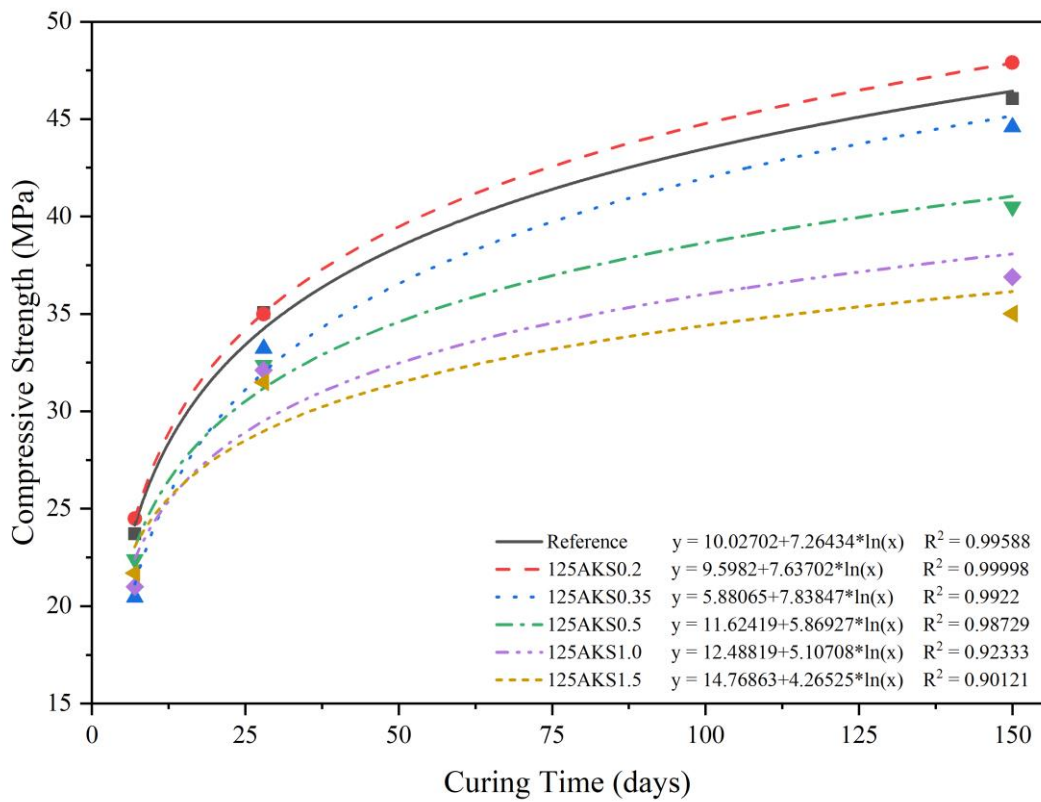
Appendix B.8: Compressive strength development of 125ES series



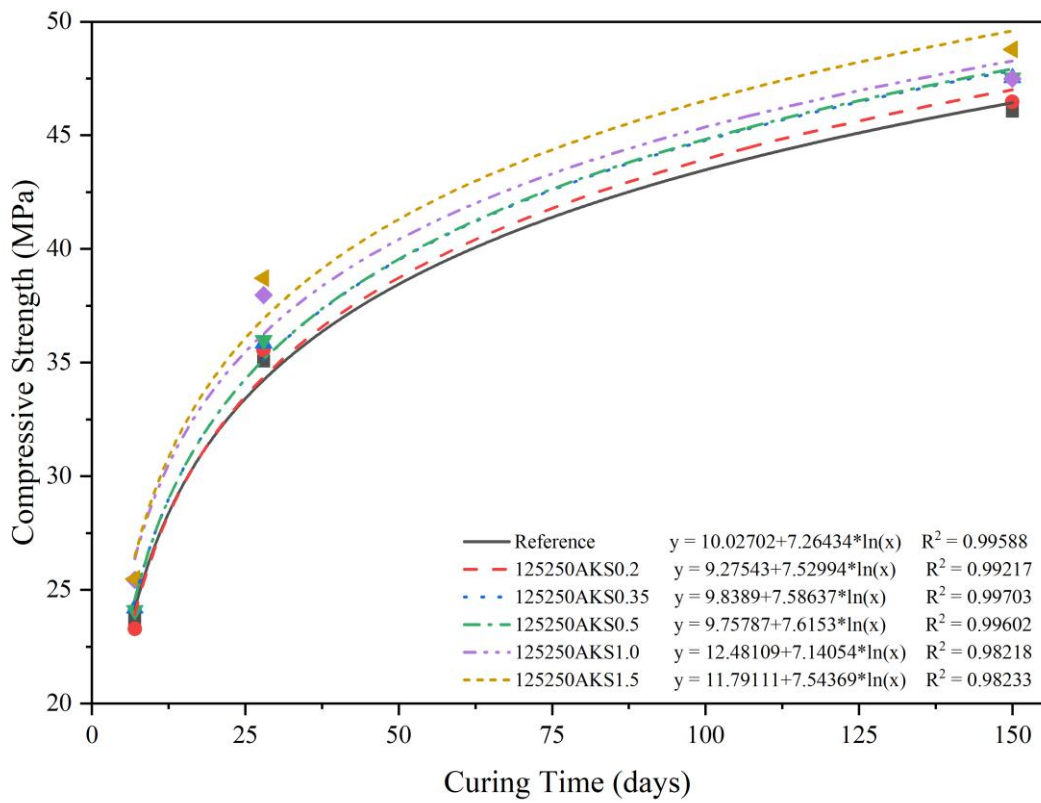
Appendix B.9: Compressive strength development of 125250ES series



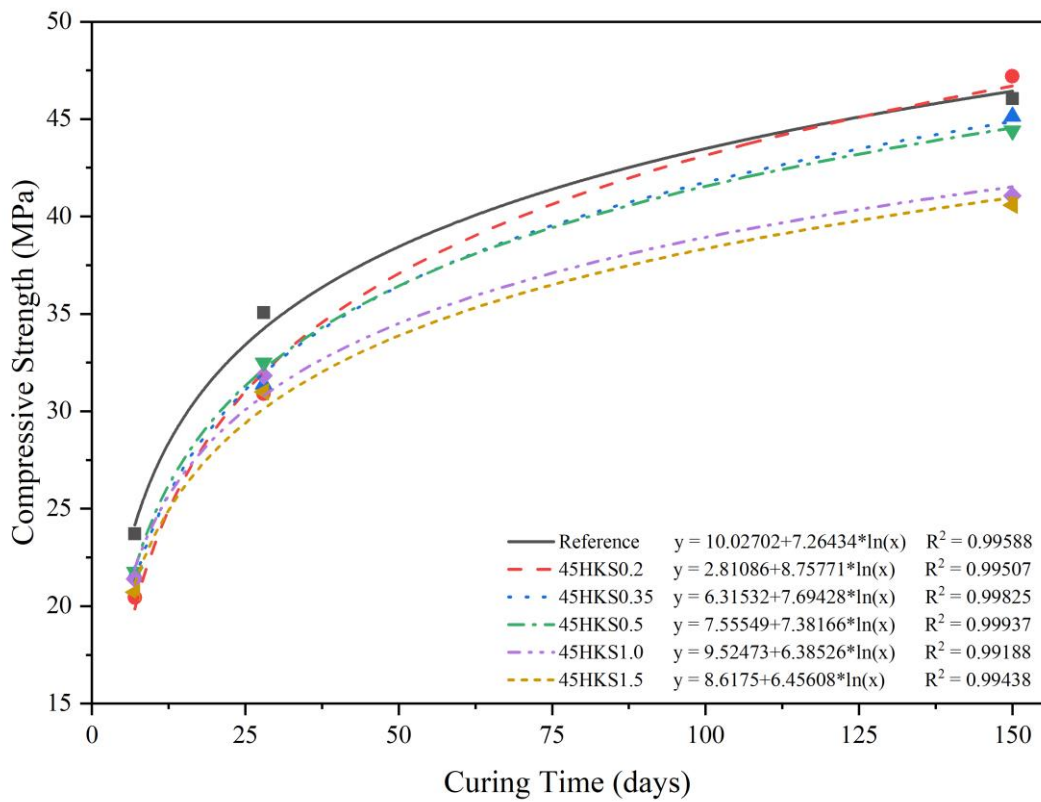
Appendix B.10: Compressive strength development of 45AKS series



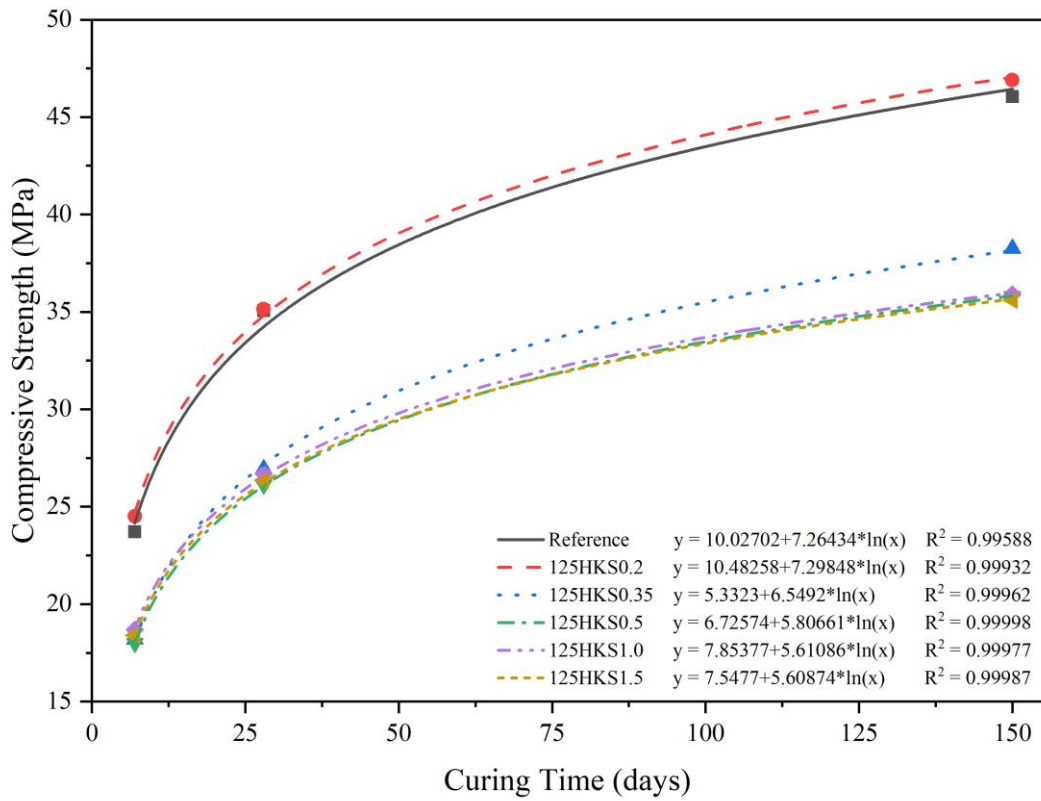
Appendix B.11: Compressive strength development of 125AKS series



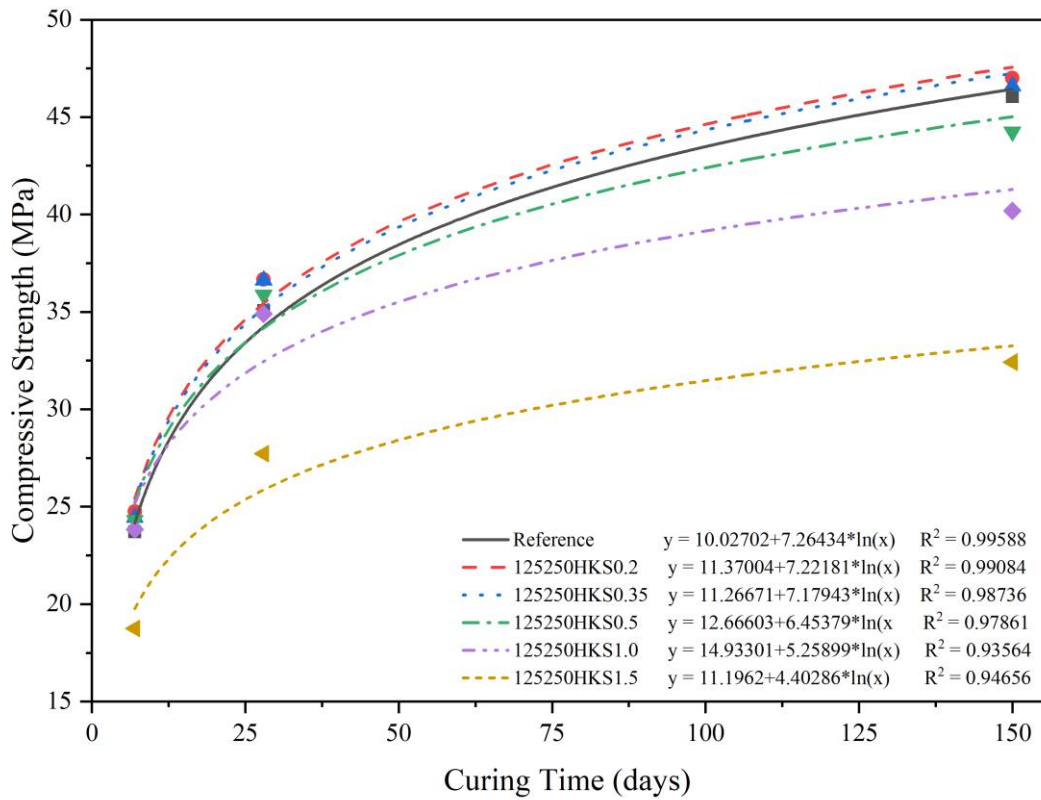
Appendix B.12: Compressive strength development of 125250AKS series



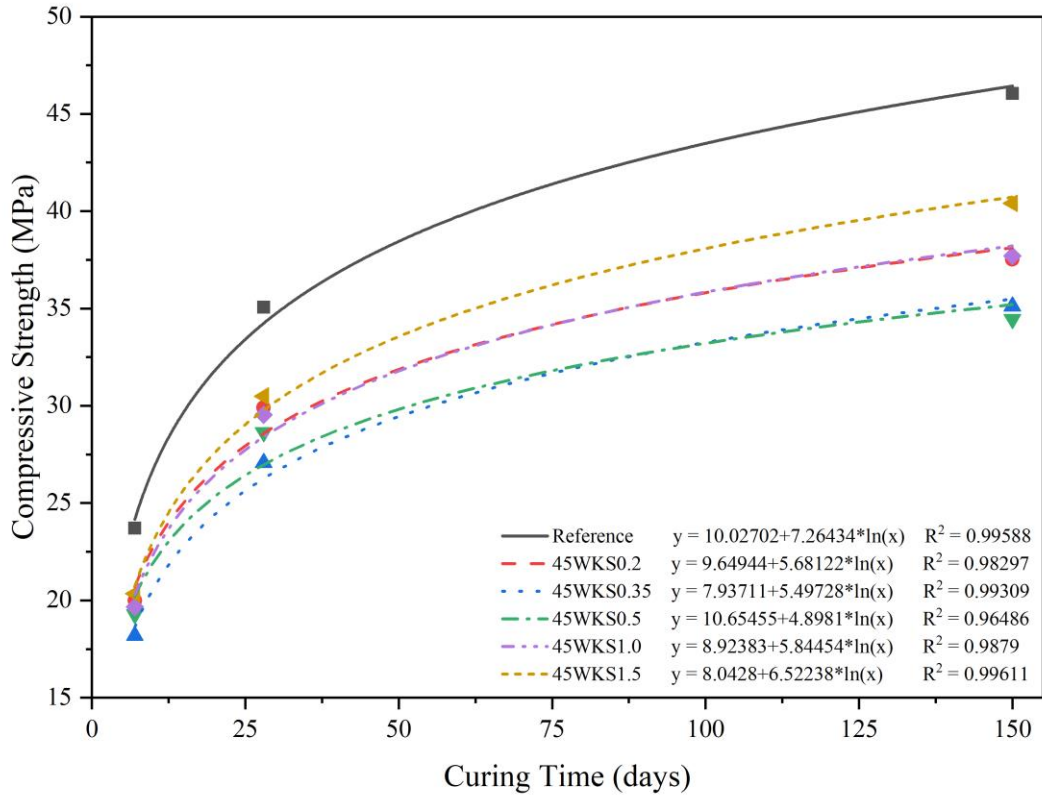
Appendix B.13: Compressive strength development of 45HKS series



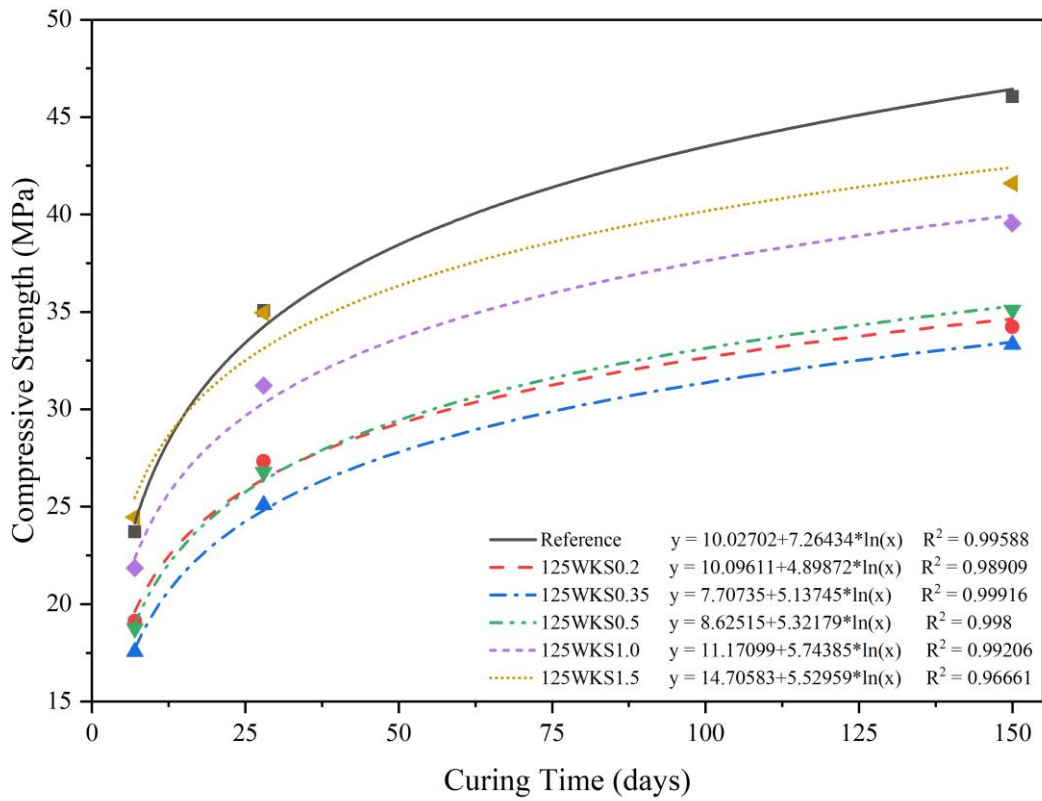
Appendix B.14: Compressive strength development of 125HKS series



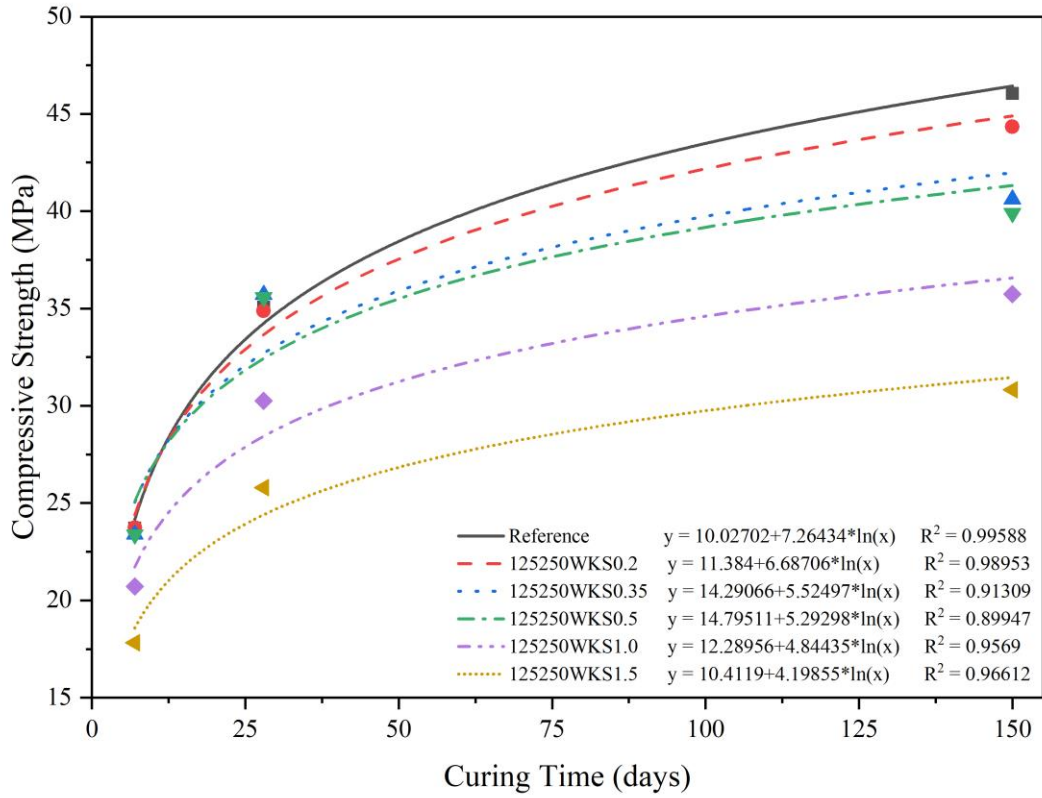
Appendix B.15: Compressive strength development of 125250HKS series



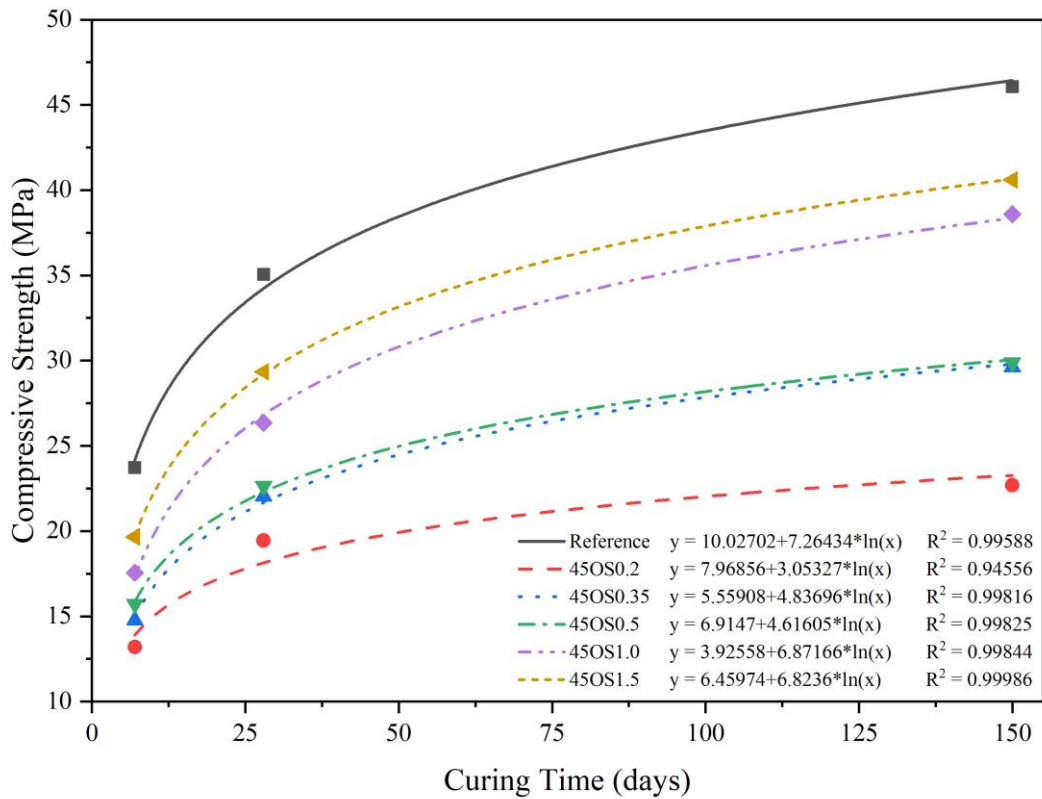
Appendix B.16: Compressive strength development of 45WKS series



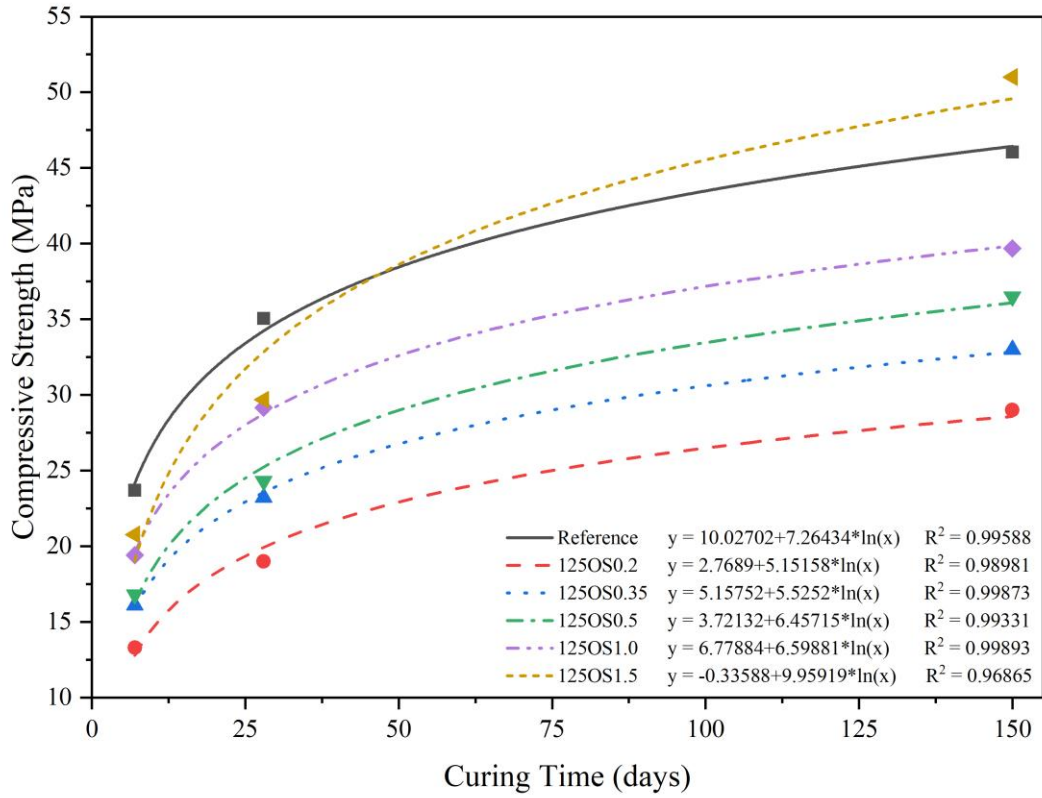
Appendix B.17: Compressive strength development of 125WKS series



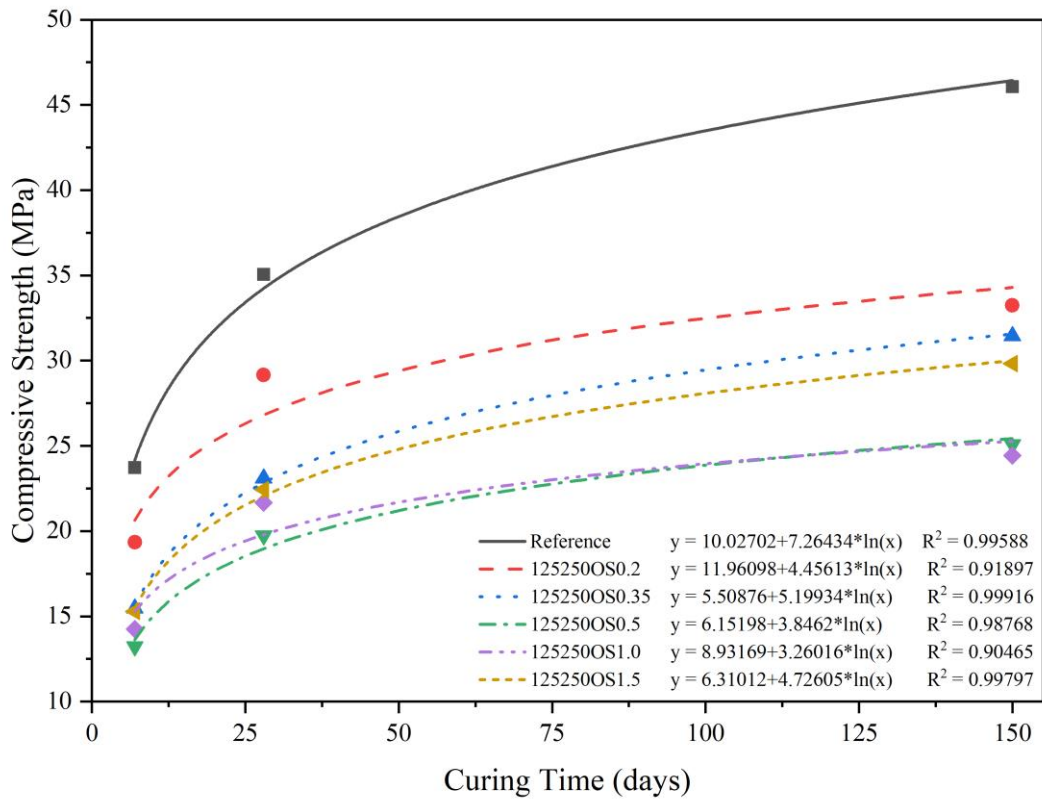
Appendix B.18: Compressive strength development of 125250WKS series



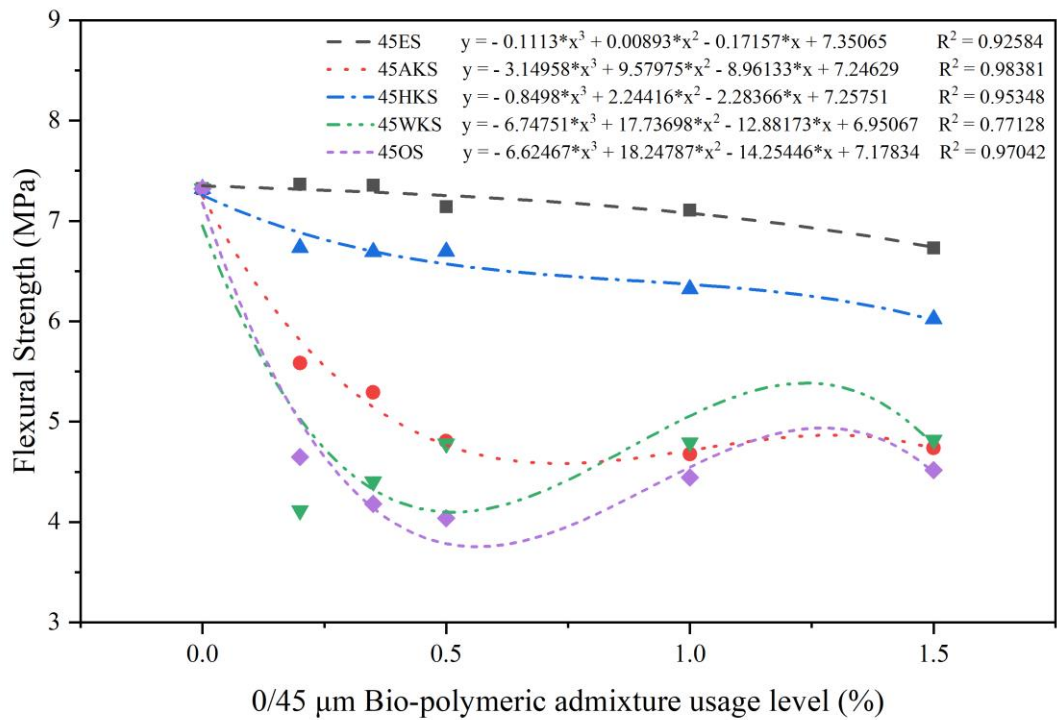
Appendix B.19: Compressive strength development of 45OS series



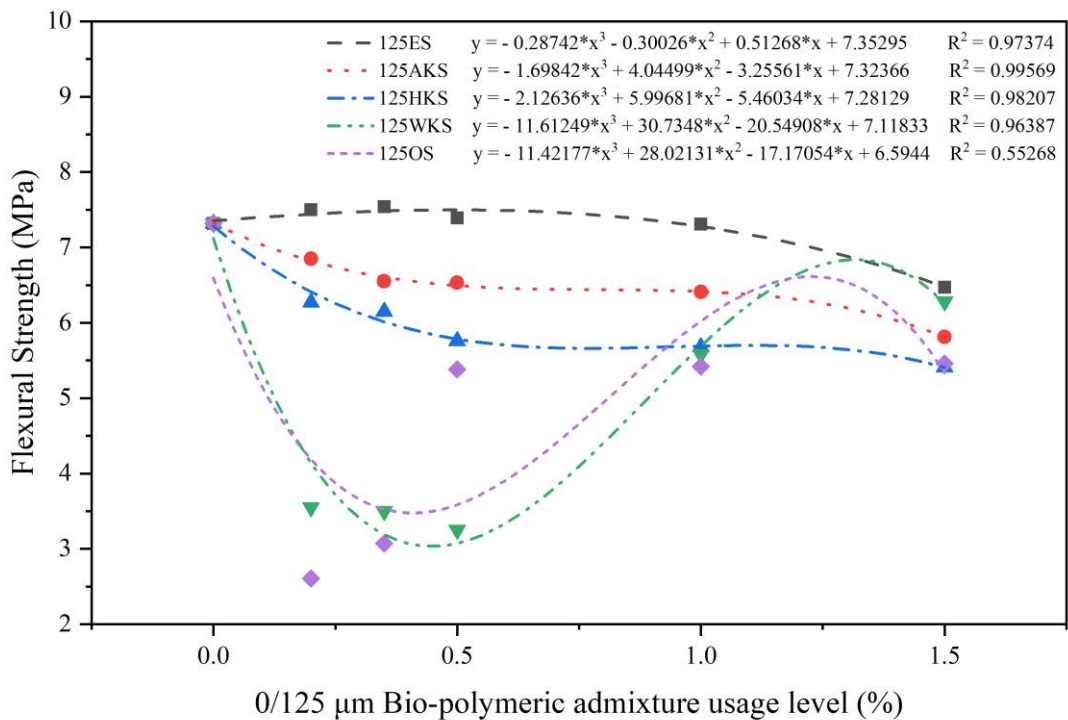
Appendix B.20: Compressive strength development of 125OS series



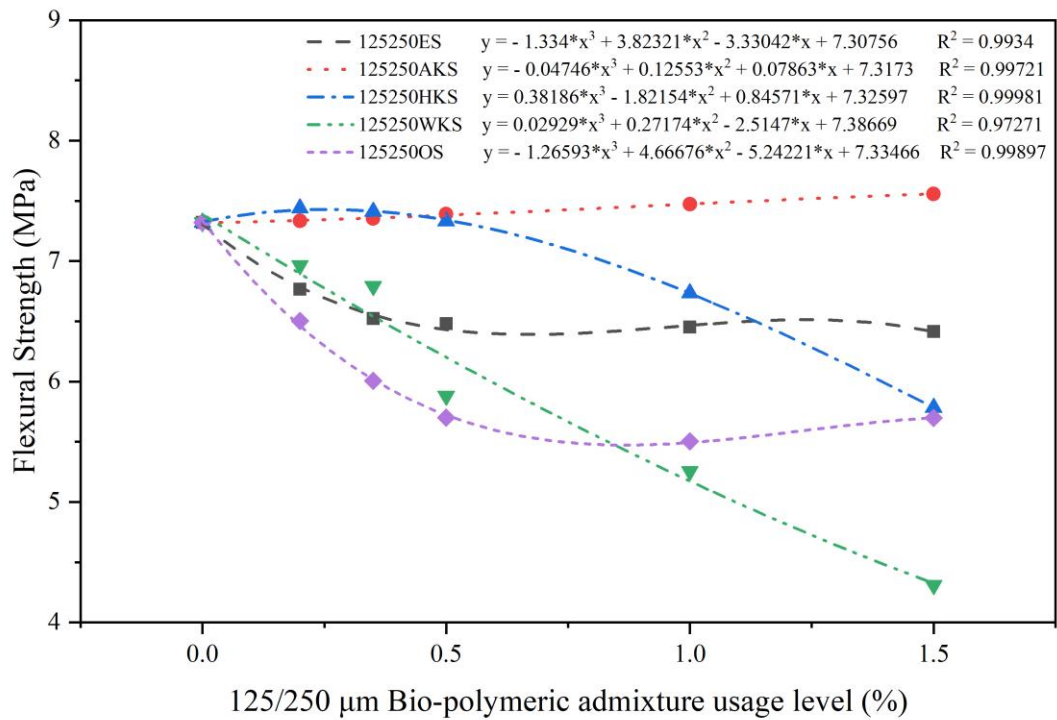
Appendix B.21: Compressive strength development of 125250OS series



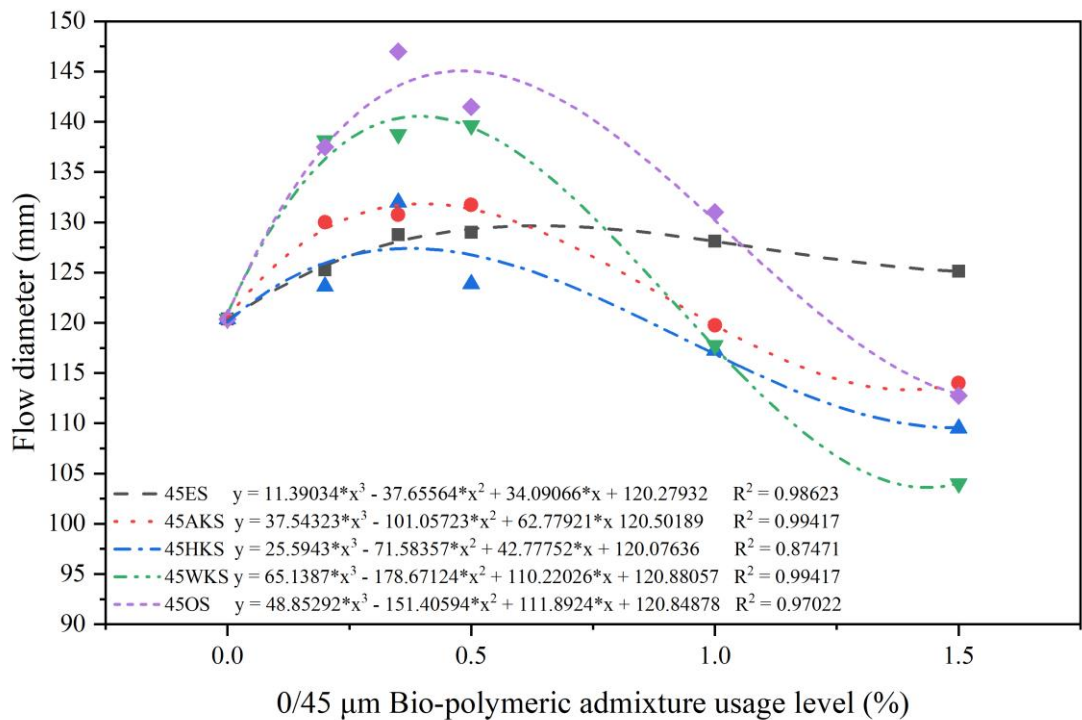
Appendix B.22: 28-day flexural strength versus 0/45 μm bio-polymeric admixture usage



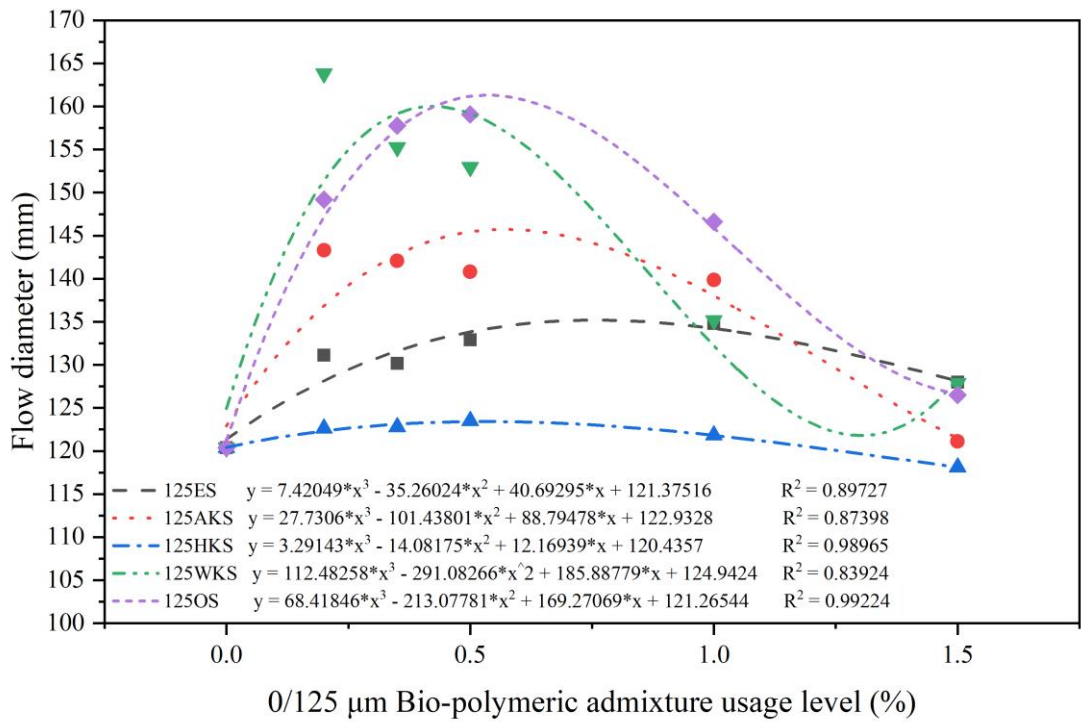
Appendix B.23: 28-day flexural strength versus 0/125 μm bio-polymeric admixture usage



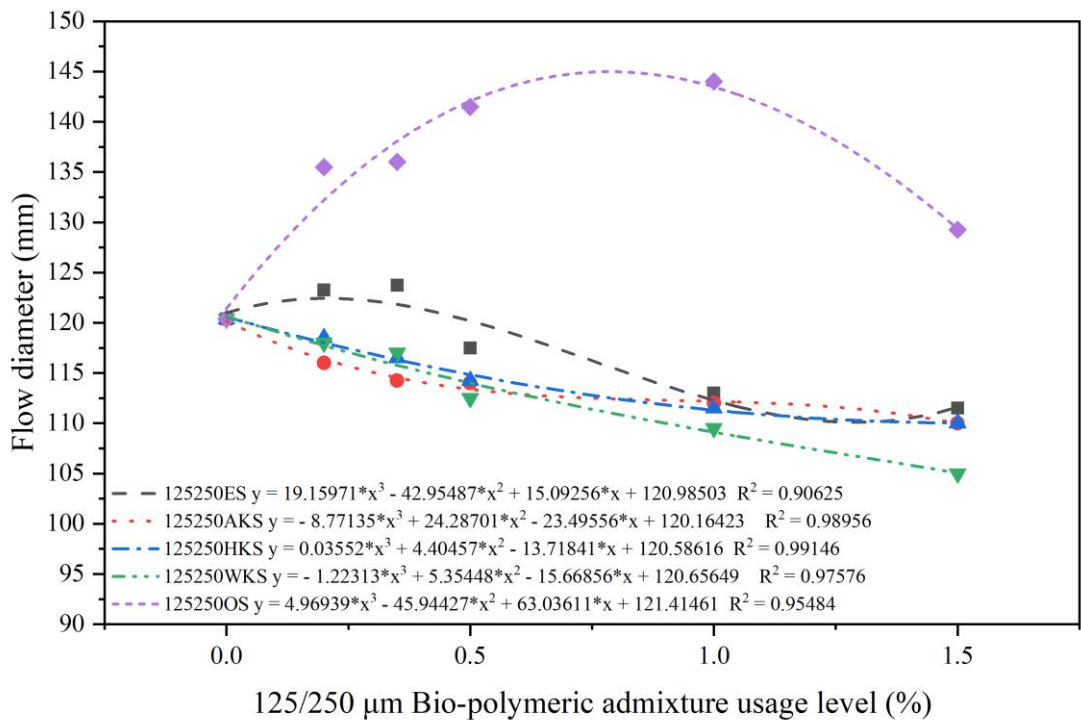
Appendix B.24: 28-day flexural strength versus 125/250 µm bio-polymeric admixture usage



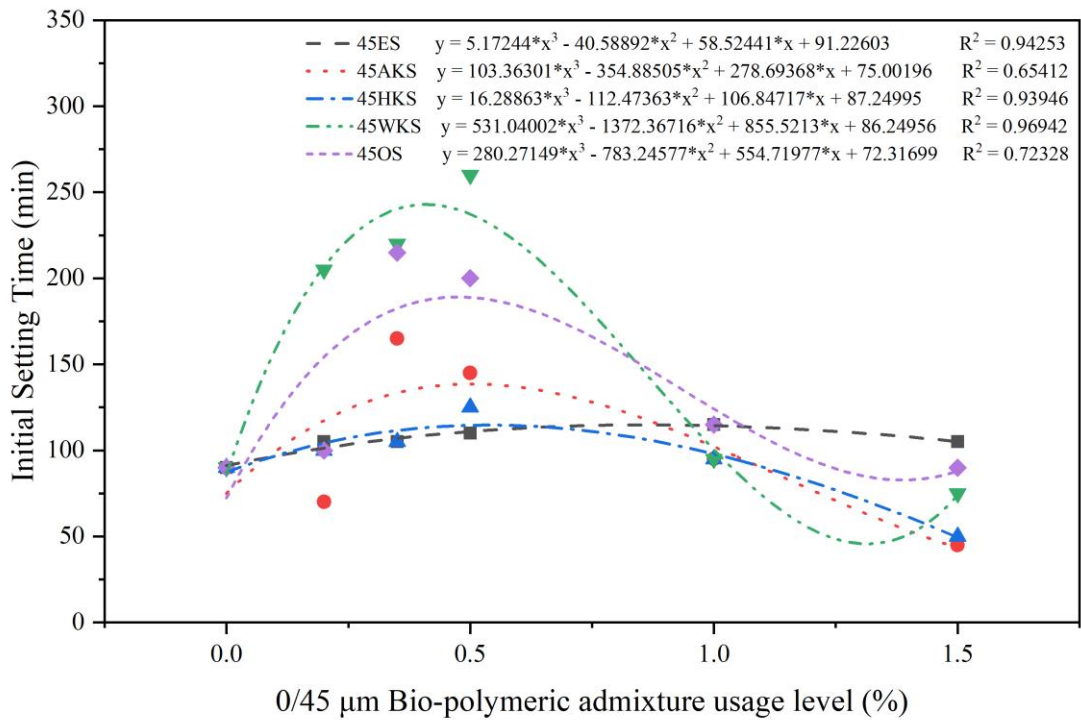
Appendix B.25: Flow diameters versus 0/45 µm bio-polymeric admixture usage



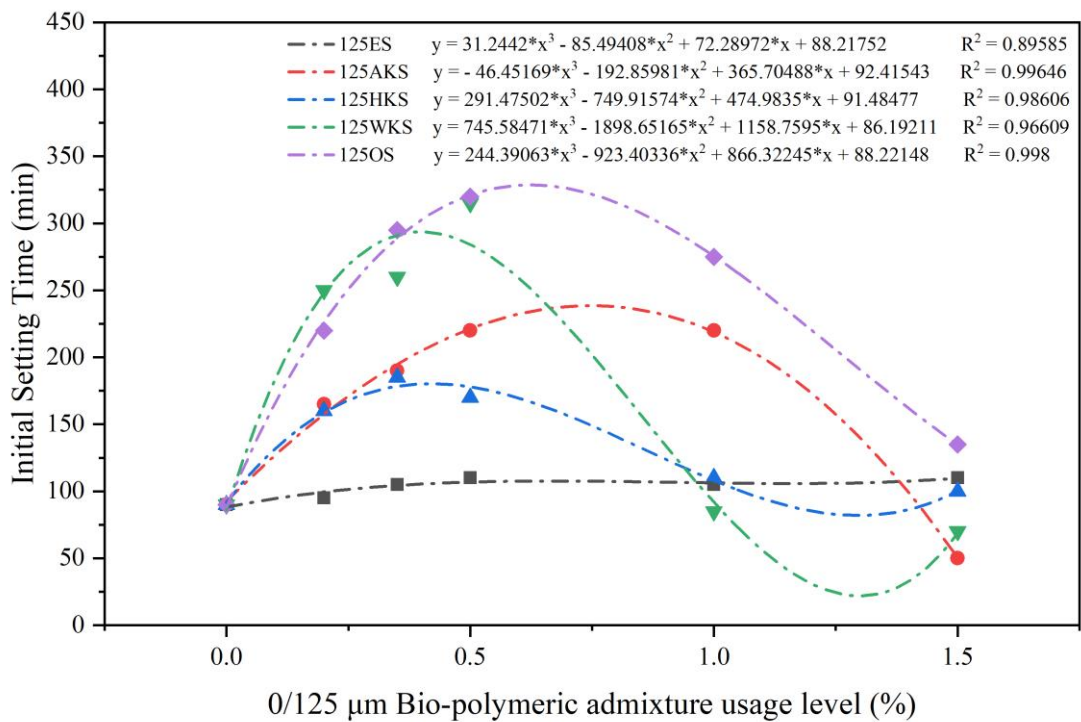
Appendix B.26: Flow diameters versus 0/125 µm bio-polymeric admixture usage



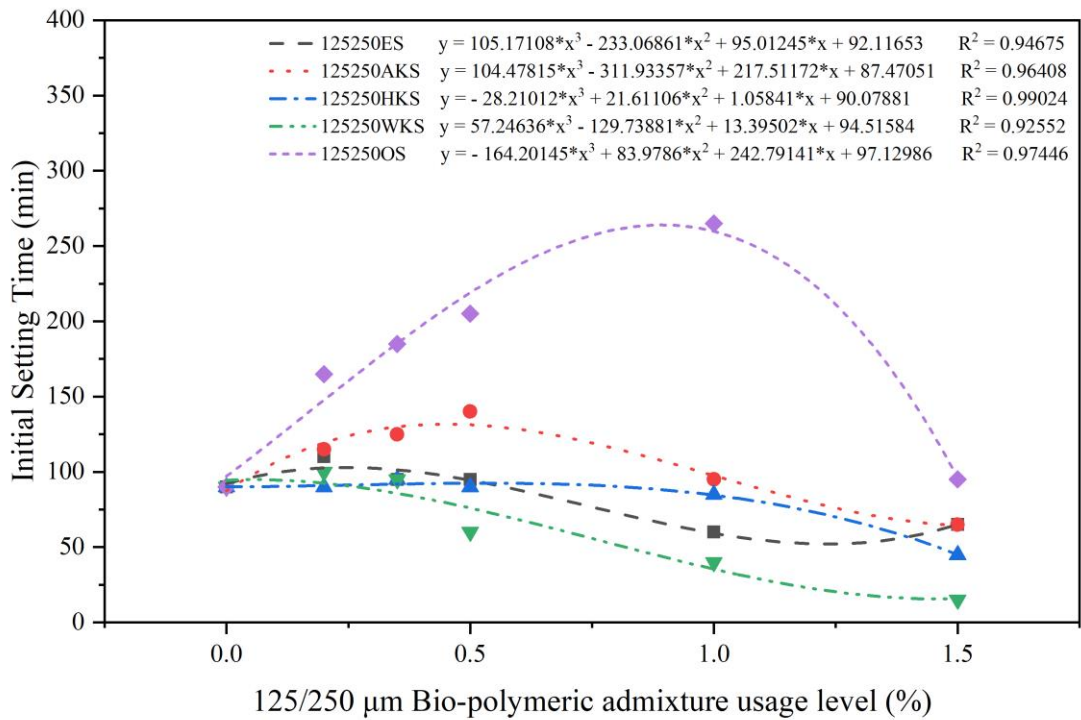
Appendix B.27: Flow diameters versus 125/250 µm bio-polymeric admixture usage



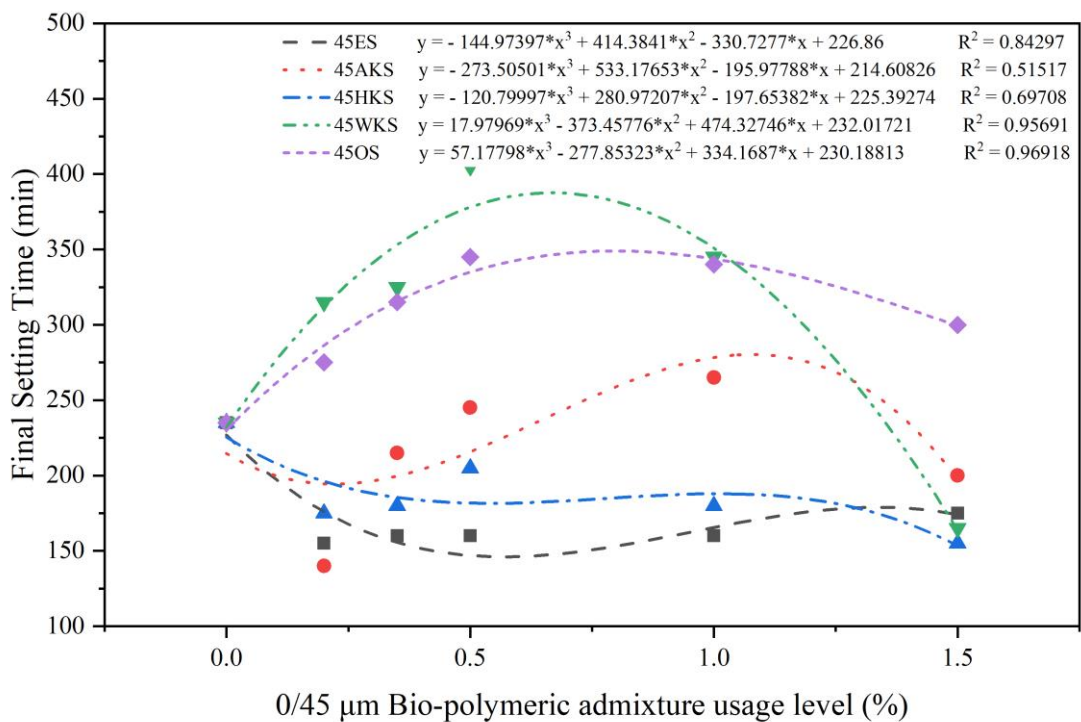
Appendix B.28: Initial setting times versus 0/45 µm bio-polymeric admixture usage



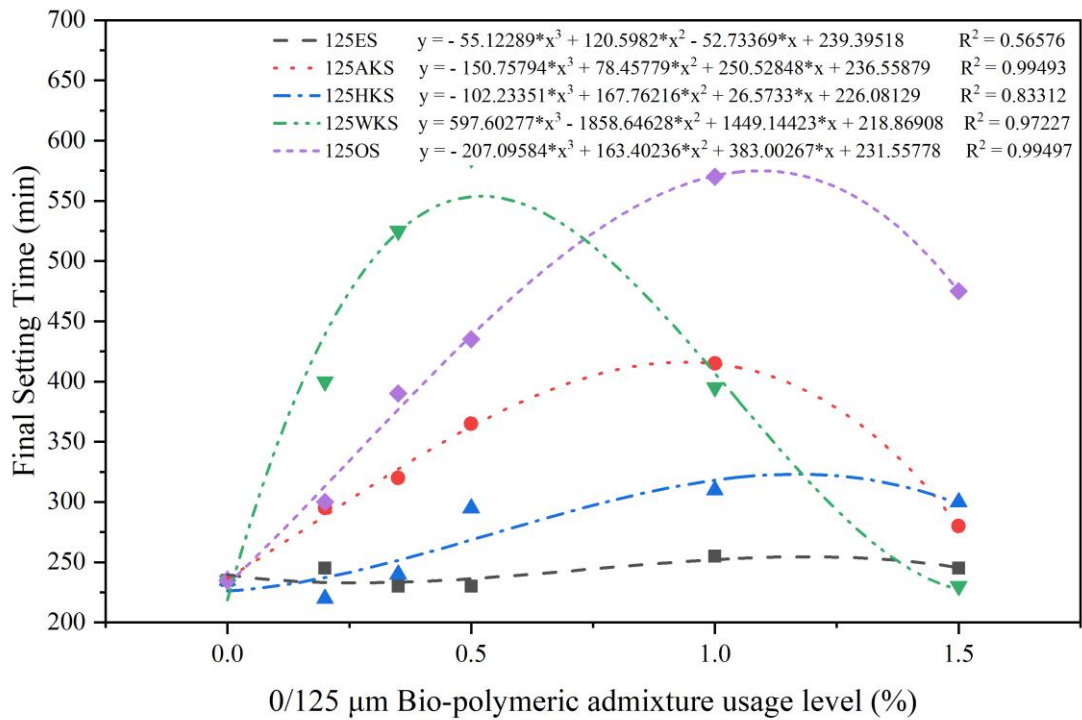
Appendix B.29: Initial setting times versus 0/125 µm bio-polymeric admixture usage



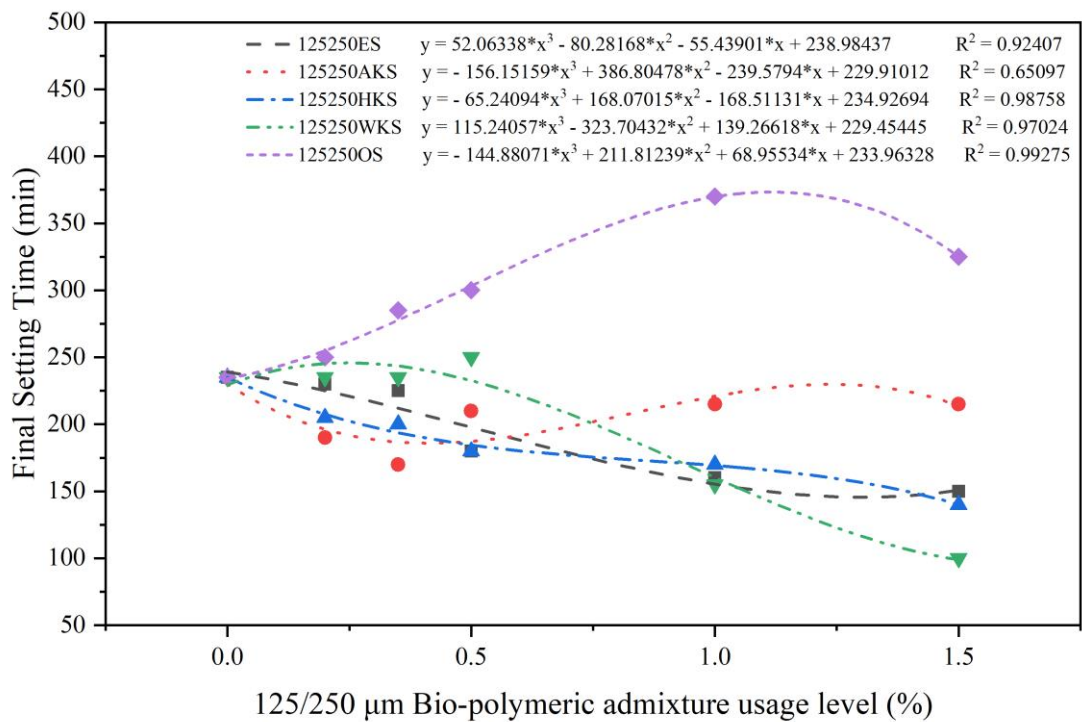
Appendix B.30: Initial setting times versus 125/250 µm bio-polymeric admixture usage



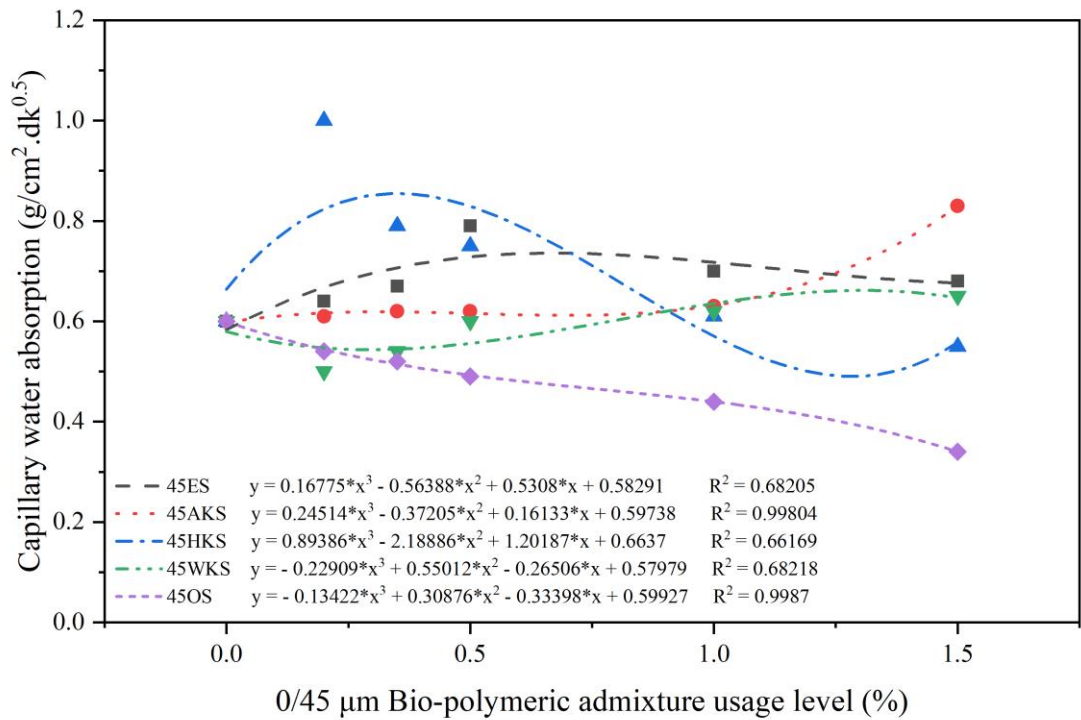
Appendix B.31: Final setting times versus 0/45 µm bio-polymeric admixture usage



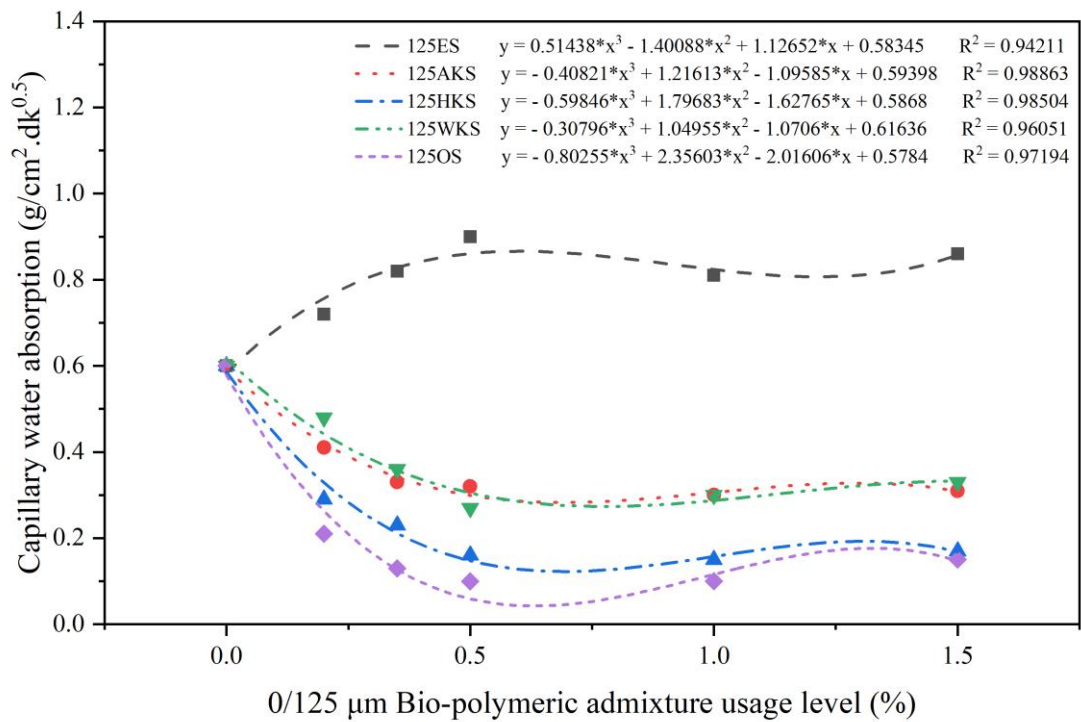
Appendix B.32: Final setting times versus 0/125 µm bio-polymeric admixture usage



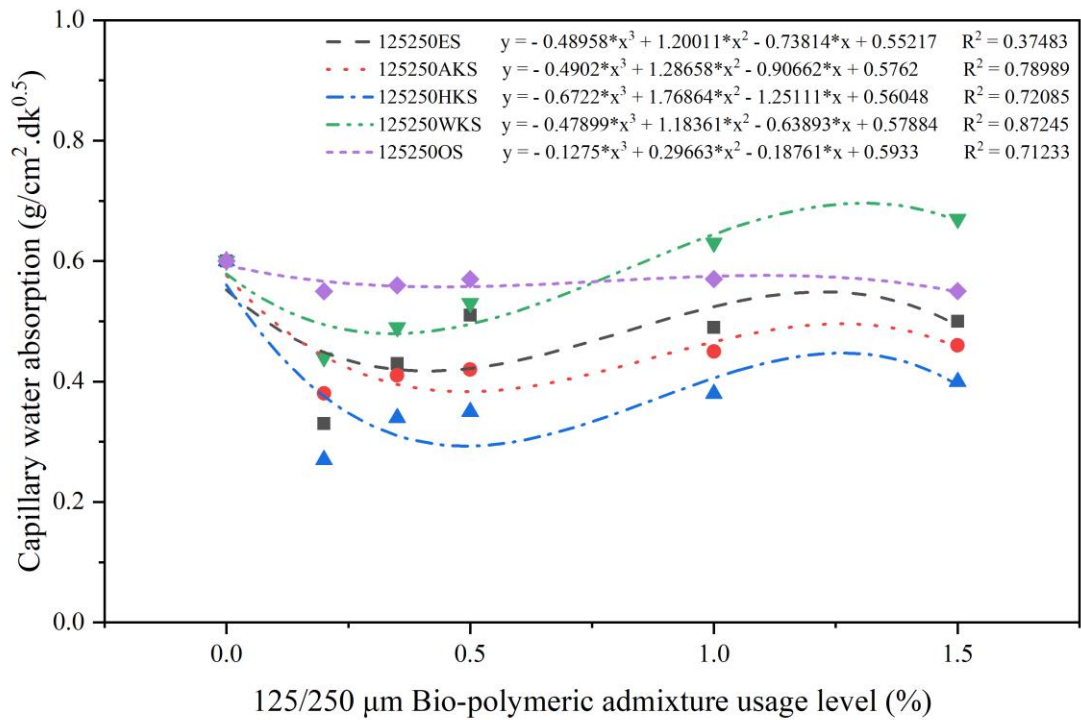
Appendix B.33: Final setting times versus 125/250 µm bio-polymeric admixture usage



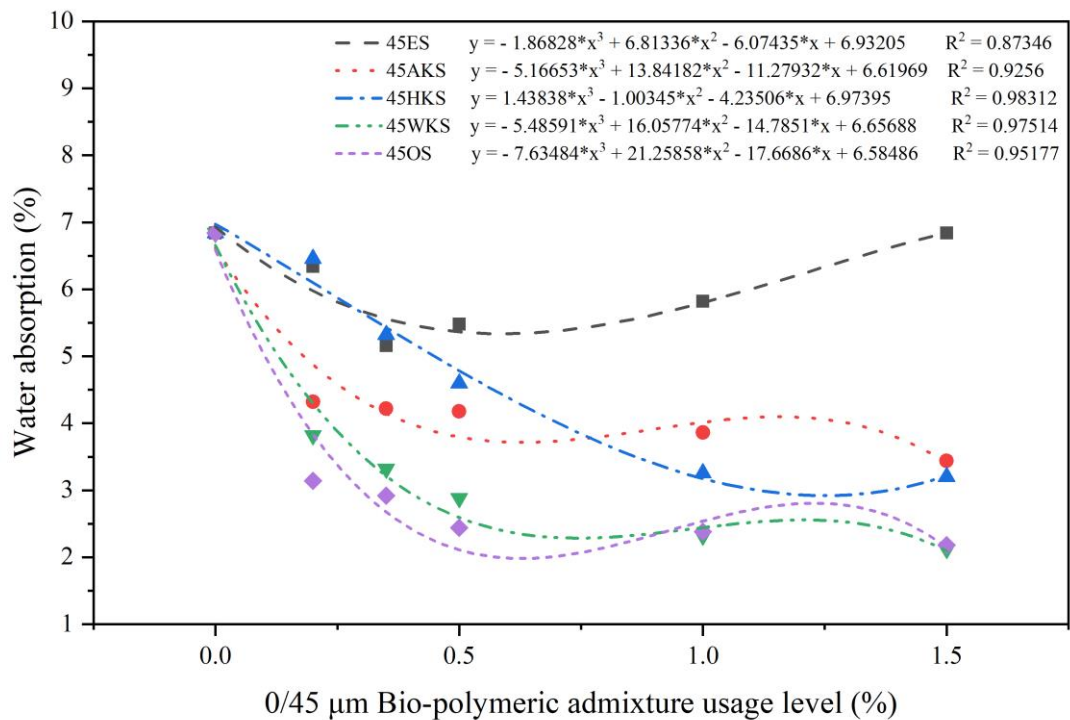
Appendix B.34: Capillary water absorption versus 0/45 µm bio-polymeric admixture usage



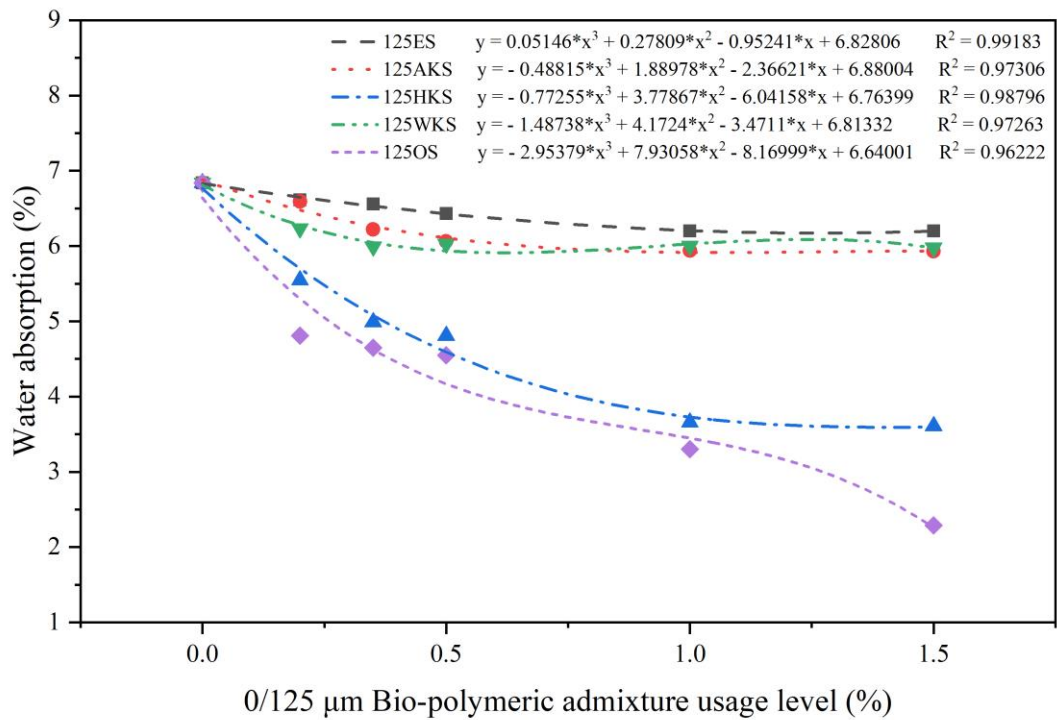
Appendix B.35: Capillary water absorption versus 0/125 µm bio-polymeric admixture usage



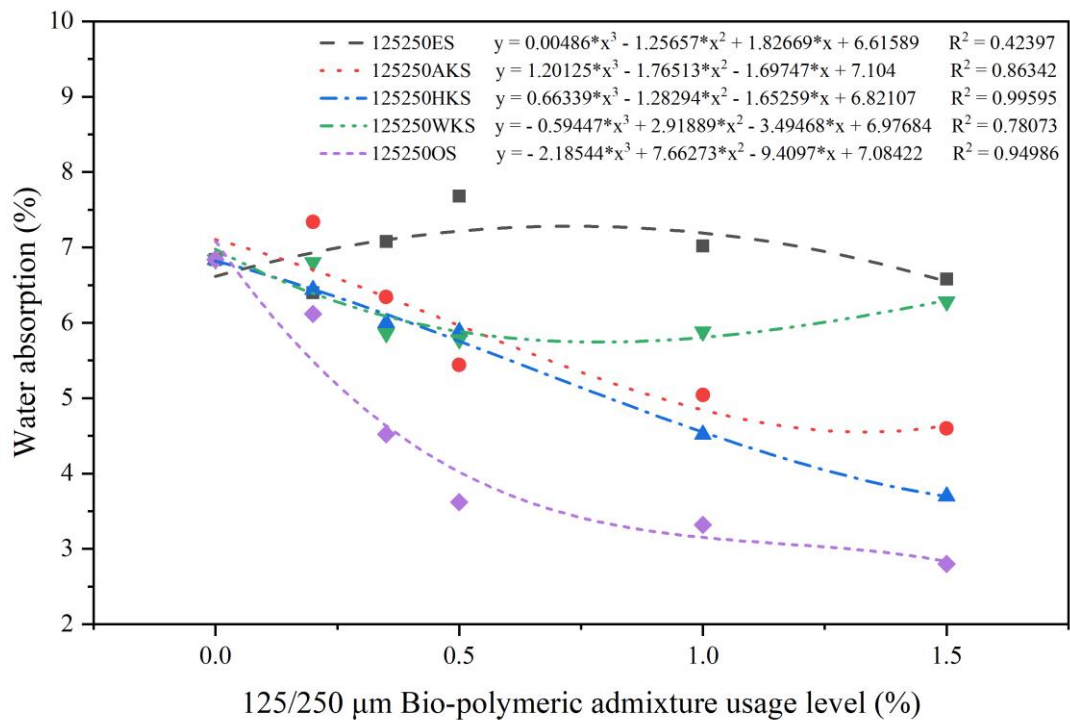
Appendix B.36: Capillary water absorption versus 125/250 µm bio-polymeric admixture usage



Appendix B.37: Mass water absorption versus 0/45 µm bio-polymeric admixture usage



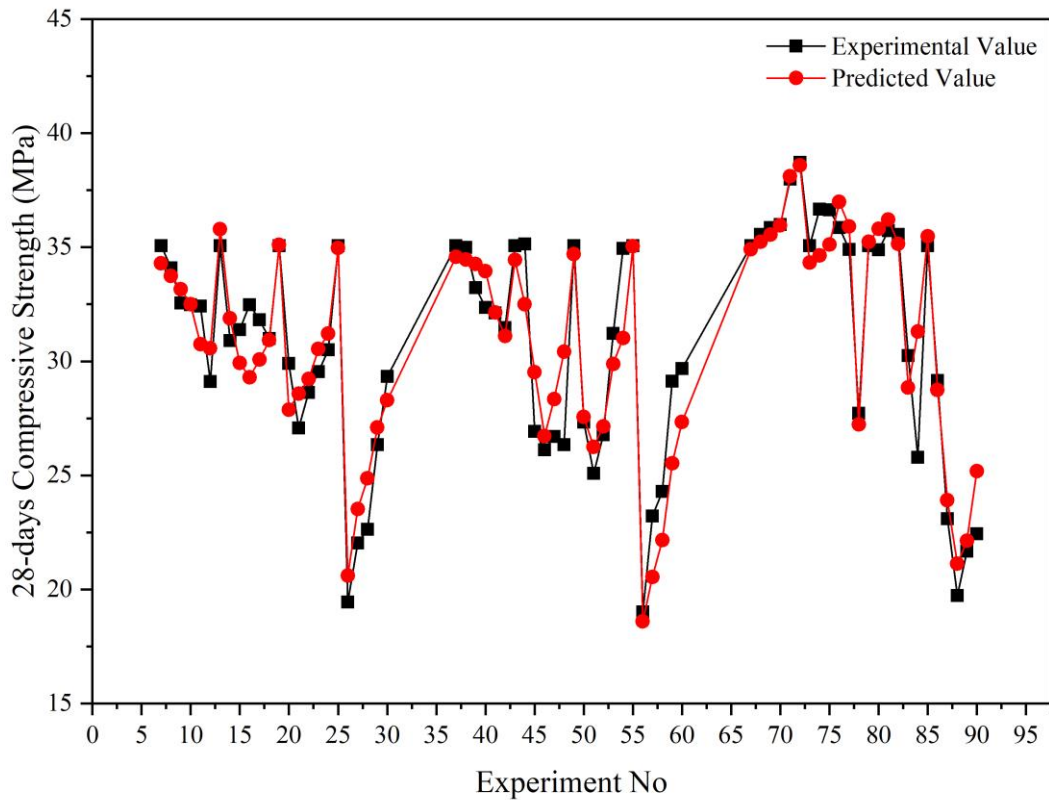
Appendix B.38: Mass water absorption versus 0/125 μm bio-polymeric admixture usage



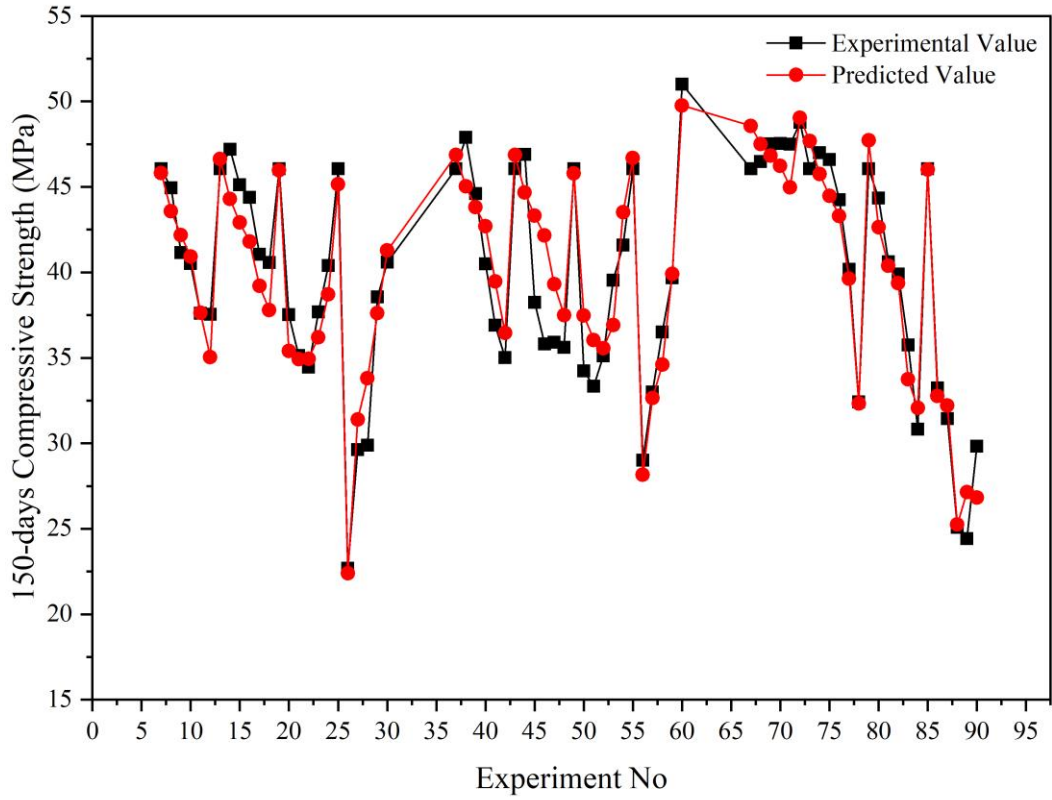
Appendix B.39: Mass water absorption versus 125/250 μm bio-polymeric admixture usage

Appendix C

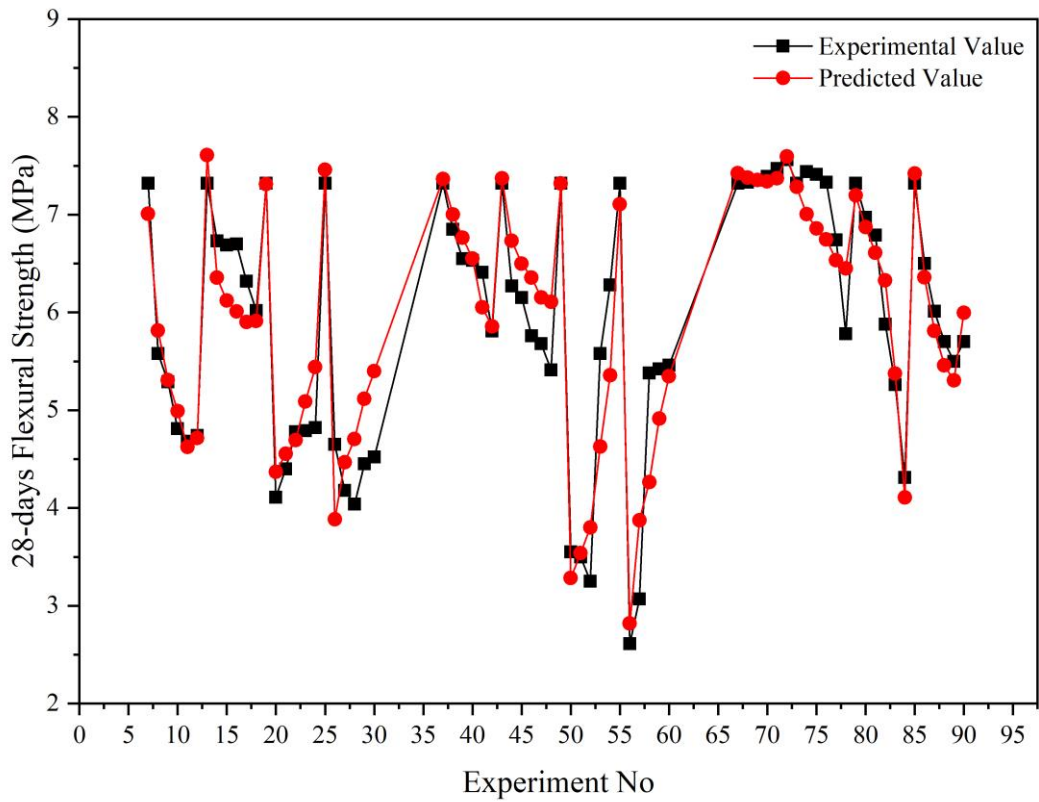
Graphical Representation of Fitted Values of Regression Analysis



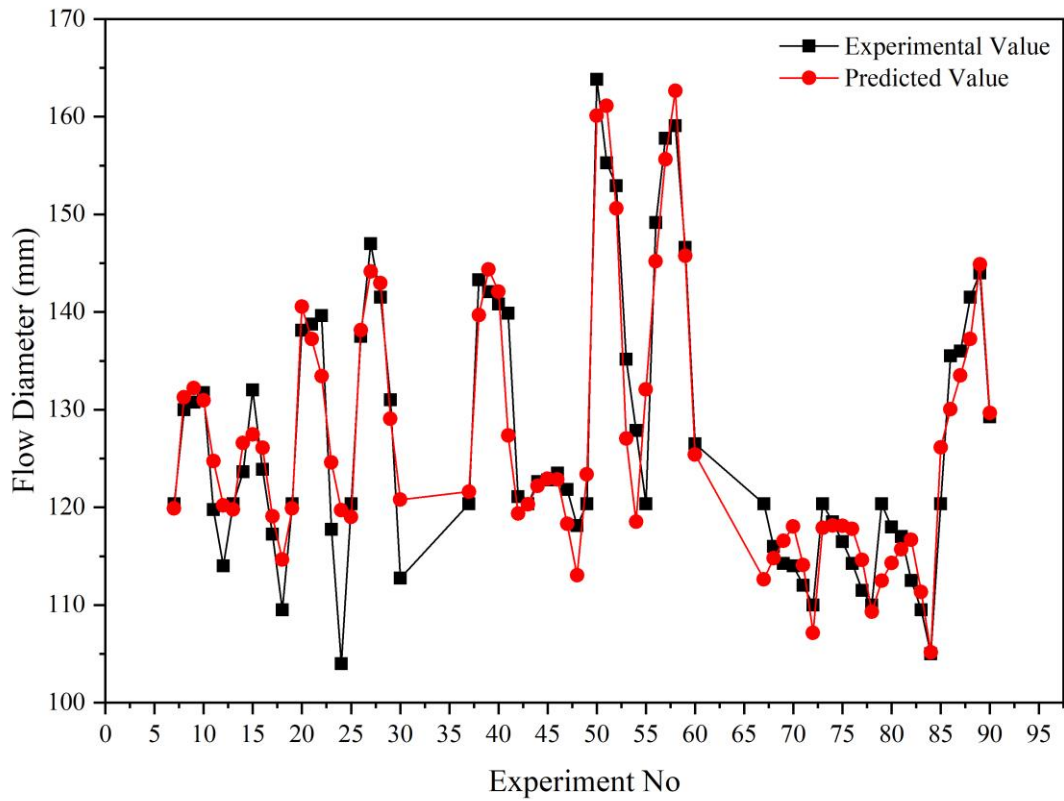
Appendix C.1: Experimental versus predicted values of 28-days compressive strength



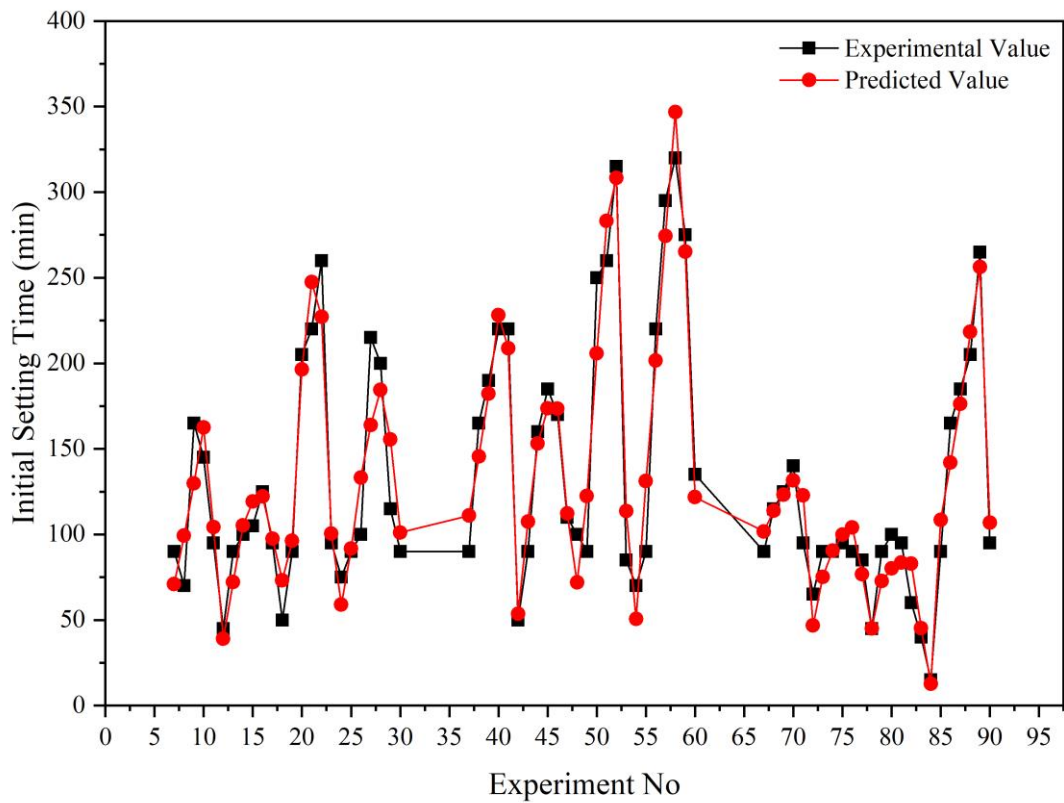
Appendix C.2: Experimental versus predicted values of 150-days compressive strength



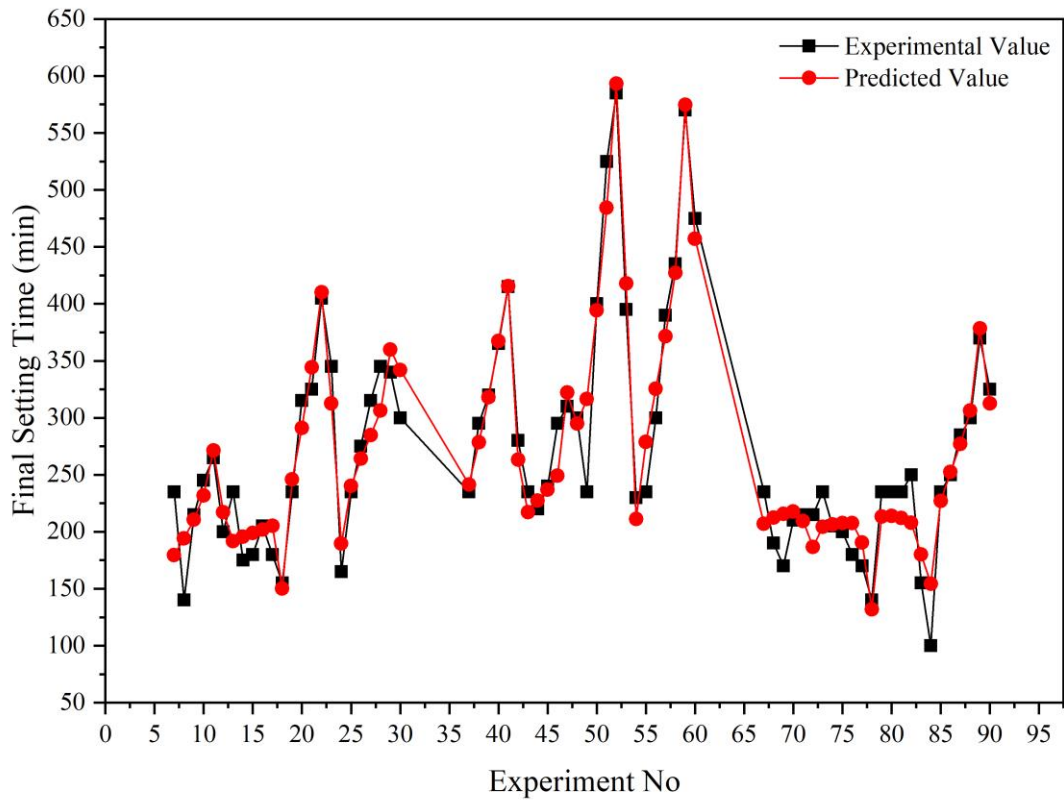
Appendix C.3: Experimental versus predicted values of 28-days flexural strength



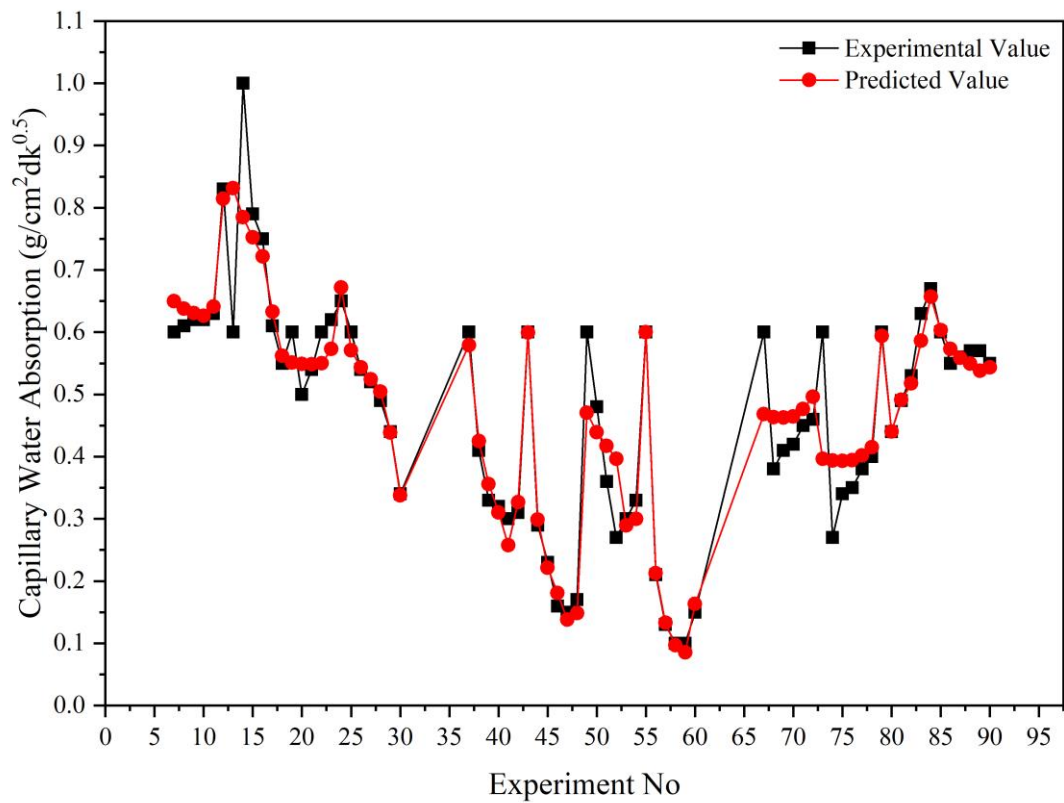
Appendix C.4: Experimental versus predicted values of flow diameter



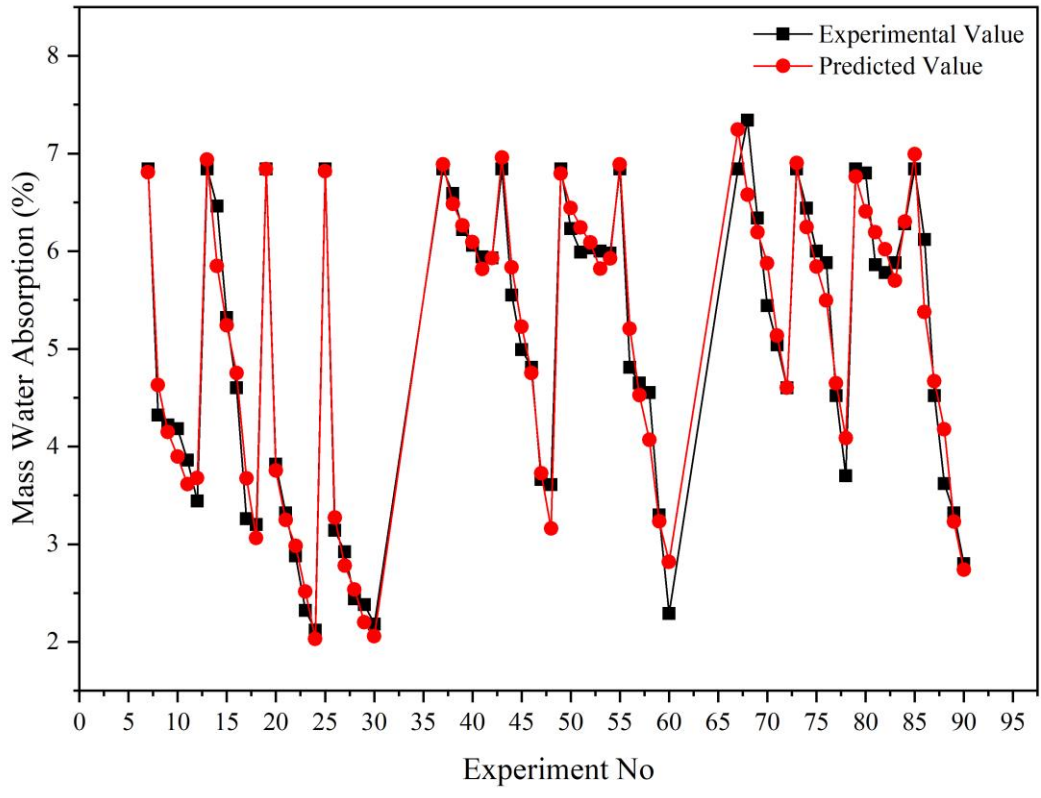
Appendix C.5: Experimental versus predicted values of initial setting time



Appendix C.6: Experimental versus predicted values of final setting time



Appendix C.7: Experimental versus predicted values of capillary water absorption



Appendix C.8: Experimental versus predicted values of mass water absorption

Curriculum Vitae

Name Surname : Şevket Onur KALKAN

Education:

2007–2012 Cyprus International University, Dept. of Civil Eng.
2015–2017 İzmir Kâtip Çelebi University, Dept. of Civil Eng. (Msc.)
2017-2022 İzmir Kâtip Çelebi University, Dept. of Civil Eng. (PhD)

Work Experience:

07/2012 – 01/2014 Hitit İnşaat San. Tic. LTD. ŞTİ.

Publications (if any):

1. Kalkan Şevket Onur, Yavaş Ahmet, Güler Saadet, Torman Kayalar Merve, Sütçü Mücahit, Gündüz Lütfullah (2022). An Experimental Approach to A Cementitious Lightweight Composite Mortar Using Synthetic Wollastonite. Construction And Building Materials, 341, Doi: 10.1016/J.Conbuildmat.2022.127911
2. Yavaş Ahmet, Kalkan Şevket Onur, Güler Saadet, Şahin Gökçe Nur, Gündüz Lütfullah (2022). A Novel Gypsum-Based Lightweight Composite: A Combined Investigation of Technical and Self-Cleaning Properties. Journal Of the Australian Ceramic Society, Doi: 10.1007/S41779-022-00756-9
3. Kalkan Şevket Onur, Gündüz Lütfullah, Isker Münir (2021). A Comparative Analysis on The Effects of Pumice, Tuff And Conventional Aggregates On Energy Efficiency Performance In New Generation Composite Mortars. Arabian Journal of Geosciences, 14(929), 1-8., Doi: 10.1007/S12517-021-07292-Z (Yayın No: 7139260)
4. Gündüz Lütfullah, Kalkan Şevket Onur (2020). Lightweight Cellular Hollow Concrete Blocks Containingvolcanic Tuff Powder, Expanded Clay and Diatomite Fornon-Load Bearing Walls. Teknik Dergi, 31(6), 10291-10313., Doi: <https://dx.doi.org/10.18400/Tekderg.426034> (Yayın No: 6680007)
5. Uzun Ertuğrul Türker, Güçü İlker, Arslan Tolga, Kalkan Şevket Onur (2019). Retrofitting Of Masonry Structures Considering the Architectural Perspective: A Case Study In Foca, Izmir. Iop Conference Series: Materials Science and Engineering, 471, Doi: 10.1088/1757-899x/471/2/022003 (Yayın No: 4850991)
6. Gündüz Lütfullah, Kalkan Şevket Onur (2019). A Technical Evaluation on The Determination of Thermal Comfortparametric Properties Of Different Originated Expanded And Exfoliated Aggregates. Arabian Journal of Geosciences, 12(4), 1-4., Doi: [Doi: Doi.Org/10.1007/S12517-019-4301-8](https://doi.org/10.1007/S12517-019-4301-8) (Yayın No: 5755897)
7. Gündüz Lütfullah, Kalkan Şevket Onur (2019). Use OfRice Husk Ash As Strength-Enhancing Additive In Lightweightcementitious Composite Mortars. Iop Conference

Series: Materials Science and Engineering, 471, 1-11., Doi: Doi:10.1088/1757-899x/471/3/032046

8. Gündüz Lütfullah, Kalkan Şevket Onur, Isker Münir (2018). Effects Of Using Cement-Bonded Particle Boards with A Composite Component In Terms Of Acoustic Performance In Outdoor Noise Barriers. The Eurasia Proceedings of Science, Technology, Engineering Mathematics, 4, 246-255.

9. Gündüz Lütfullah, Kalkan Şevket Onur, Isker Münir, Hacıoğlu Sibel, Altınyollar Özge (2018). Effect Of Different Wood Flake Chip Species on The Characteristic Features of Cement-Bonded Particle Boards. Düzce Üniversitesi Bilim Ve Teknoloji Dergisi, 6(3), 686-695.

10. Kalkan Şevket Onur, Gündüz Lütfullah (2018). Effect Of Porous Aggregate Size on The Techno-Mechanical Properties of Cementless Lightweight Mortars. El-Cezeri Fen Ve Mühendislik Dergisi, 5(1), 168-175., Doi: 10.31202/Ecjse.354569

11. Gündüz Lütfullah, Kalkan Şevket Onur, Isker Münir (2018). A Technical Analysis on The Effect of Exfoliated Vermiculite Aggregate on Thermal Comfort Parameters Of Composite Mortars For Insulation Purposes. 3rd International Energy Engineering Congress, 706-722.

12. Gündüz Lütfullah, Kalkan Şevket Onur, Isker Münir (2018). A Technical Analysis on The Use of Pvac Acrylic Ester Terpolymer Type In Composite Mortars For Insulation. International Conference on Innovative Engineering Applications, 222-230.

13. Gündüz Lütfullah, Kalkan Şevket Onur (2018). Investigation of the Effect Of Fine Grained Tuff On The Performance Of Foam Concrete. International Conference on Innovative Engineering Applications, 214-221.

14. Gündüz Lütfullah, Kalkan Şevket Onur, Isker Münir, Mocan Cavit, Hacıoğlu Sibel (2018). Effect Of Different Curing Conditions on The Technical Properties Of Inorganic-Bonded Fiber Composites. 13th International Congress on Advances In Civil Engineering

15. Kalkan Şevket Onur, Gündüz Lütfullah (2018). Effect Of Waste Hazelnut Shell Powder on The Technical Properties Of Cement Mortars. 13th International Congress on Advances In Civil Engineering.

16. Kalkan Şevket Onur, Gündüz Lütfullah (2018). Açılmış Vermikülit Agregaların Kompozit Yapılı Siva Harçlarında Harcin Termal Özelliklerine Etkisi. 3. Uluslararası Mühendislik Mimarlık Ve Tasarım Kongresi, 225-226.

17. Gündüz Lütfullah, Kalkan Şevket Onur, Isker Münir (2018). Lif Çimento Levhaların Gürültü Bariyeri Olarak Kullanımı Üzerine Bir Değerlendirme. 3. Uluslararası Mühendislik, Mimarlık Ve Tasarım Kongresi

18. Kalkan Şevket Onur, Gündüz Lütfullah (2018). The Effect of Different Pozzolanic Additives on Physical and Mechanical Properties Of The New Generation Composite Horasan Mortars. European Conference on Science, Art Culture, 235-241.

19. Gündüz Lütfullah, Kalkan Şevket Onur (2018). Yapısal Restorasyon Harçlarında Kıtık Boyutlarının Harcın Teknik Özelliklerine Etkisinin İncelenmesi. European Conference on Science, Art Culture, 243-251.
20. Gündüz Lütfullah, Kalkan Şevket Onur (2017). Tarihi-Eski Yapıların Onarımı Amaçlı Yeni Nesil Kompozit Harçların Kullanımı Üzerine Bir İnceleme. 6th International Symposium on Conservation and Consolidation of Historical Structures.
21. Gündüz Lütfullah, Kalkan Şevket Onur, İsker Münir, Güreli Bengi, Hacıoğlu Sibel (2017). Farklı Su İtici Ajanların İnorganik Bağlı Lifli Kompozit Levhalarda Hidrofobik Özelliğe Etkisi. Chemical Admixtures on Structures 5th International Symposium and Exhibition, 317-334.
22. Kalkan Şevket Onur, Gündüz Lütfullah (2017). Yeni Nesil Kompozit Harçlarda Polimer Kullanımları Üzerine Bir İnceleme. Chemical Admixtures on Structures 5th International Symposium and Exhibition, 253-268.
23. Kalkan Şevket Onur, Gündüz Lütfullah (2017). Hafif Agregali Kompozit Harçların Hidrofobluk Özelliğinin Geliştirilmesinde Biopolimer Katkı Kullanımı Üzerine Bir İnceleme. Chemical Admixtures on Structures 5th International Symposium and Exhibition, 269-286.
24. Gündüz Lütfullah, Kalkan Şevket Onur, Garip Dağlı Elvan (2017). Sivi Kür Malzemelerinin Taze Betonun Teknik Performansına Etkileri Üzerine Bir Analiz. Chemical Admixtures on Structures 5th International Symposium and Exhibition, 435-448.
25. Gündüz Lütfullah, Kalkan Şevket Onur, İsker Münir, Güreli Orhan Bengi, Hacıoğlu Sibel (2017). An Analysis on The Use of Fibrous Natural Rocks In Inorganic-Bonded Fiber Composites. Applied Sciences'17, 47-58.
26. Kalkan Şevket Onur, Gündüz Lütfullah (2017). Evaluation Of Physical and Mechanical Performance of A New Generation Composite Mortar Containing Eggshell Powder. Applied Sciences'17, 59-68.
27. Gündüz Lütfullah, Kalkan Şevket Onur (2017). Influence Of Different Lightweight Aggregate Types on Technical Properties of Non-Load Bearing Foam Concrete Masonry Units. Applied Sciences'17, 35-48.
28. Gündüz Lütfullah, Kalkan Şevket Onur (2017). Influence Of Elevated Temperature on The Strength Properties of Lightweight Concrete Masonry Units Prepared with Pumice Aggregates. Icaie International Conference on Advances and Innovations In Engineering, 390-397.
29. Gündüz Lütfullah, Kalkan Şevket Onur, Aydoğdu Namık Kemal (2016). İzmir-Alaçatı Taşının Kuru Karışım Hafif Beton Agregası Olarak Kullanılabilirliği Üzerine Teknik Bir Analiz. 8. Uluslararası Kırmataş Sempozyumu.
30. Gündüz Lütfullah, Kalkan Şevket Onur (2016). Diatomit Agregaların Çimento Esaslı Hafif Harç Özelliklerinin Gelişimine Etkisi. 8. Uluslararası Kırmataş Sempozyumu.

31. Kalkan Şevket Onur, Gündüz Lütfullah (2016). A Study on The Usage of Denim Waste As Reinforcement Element In Composite Mortars On Exterior Building Applications. 12th International Congress on Advantages In Civil Engineering
32. Gündüz Lütfullah, Kalkan Şevket Onur (2016). Evaluation Of Exfoliated Vermiculate Aggregates to Produce New Generation Composite Mortars In Environmentally Sustainable Buildings. 3. International Architectural Design Conference on Design and Nature
33. Kalkan Şevket Onur, Gündüz Lütfullah (2015). Dış Cephe Mimari Uygulamalarda Yeni Nesil Kompozit Bileşenli Harçların Teknik Değerlendirmesi Üzerine Bir Çalışma. 1. Uluslararası Mühendislik Mimarlık Ve Tasarım Kongresi.
34. Academic Works In The Fields Of Science, Culture And Art 2018 Fall, Bölüm Adı:(An Approach To The Use Of Lightweight Concrete Masonry Block Members With Pumice Aggregat In Different Geometric Design Features In Cyprus Climate Conditions) (2018)., Kalkan Şevket Onur, Gündüz Lütfullah, Isker Münir, Gece Kitaplığı, Editör:Bozdoğan Ali Musa, Kaya Latif Gürkan, Arapgirlioğlu Hasan, Atik Atilla, Basım Sayısı:1, Isbn:978-605-288-877-3, (Book Chapte).
35. Gündüz Lütfullah, Kalkan Şevket Onur, Özgüven Ahmet (2020). Genleşmiş Kil Agregaların Teknik Özelliklerinin Karşılaştırılması Üzerine Bir Çalışma: Ankara Kalecik Bölgesi Örneği. Hazır Beton, 1, 65-72. (Kontrol No: 6679931)
36. Gündüz Lütfullah, Kalkan Şevket Onur, Ertan Ferruh (2017). Mikronize Edilmiş İzmir-Alaçatı Alapetra Taşının Yalıtımlı Kompozit Dolgu Harci Üretiminde Kullanımı Üzerine Bir İnceleme / An Investigation on The Use Of Micronized Izmir-Alacati Alapetra Stone In The Production Of Insulating Composite Filling Mortar. Celal Bayar Üniversitesi Fen Bilimleri Dergisi, 13(2), 503-514., Doi: 10.18466/Cbayarfbe.319931 (Kontrol No: 3584033)
37. Gündüz Lütfullah, Kalkan Şevket Onur, Özgüven Ahmet (2017). Genleşmiş Kil Agregaların Teknik Özelliklerinin Karşılaştırılması Üzerine Bir Çalışma: Ankara Kalecik Bölgesi Örneği. Hazır Beton Kongresi, 1, 468-477.
38. Gündüz Lütfullah, Kalkan Şevket Onur (2017). Pirinç Kabuğu Külünün Çimentolu Hafif Kompozit Harçlarda Dayanım Arttırıcı Katkı Olarak Kullanılması Üzerine Teknik Bir İnceleme. Hazır Beton Kongresi 2017, 575-585.